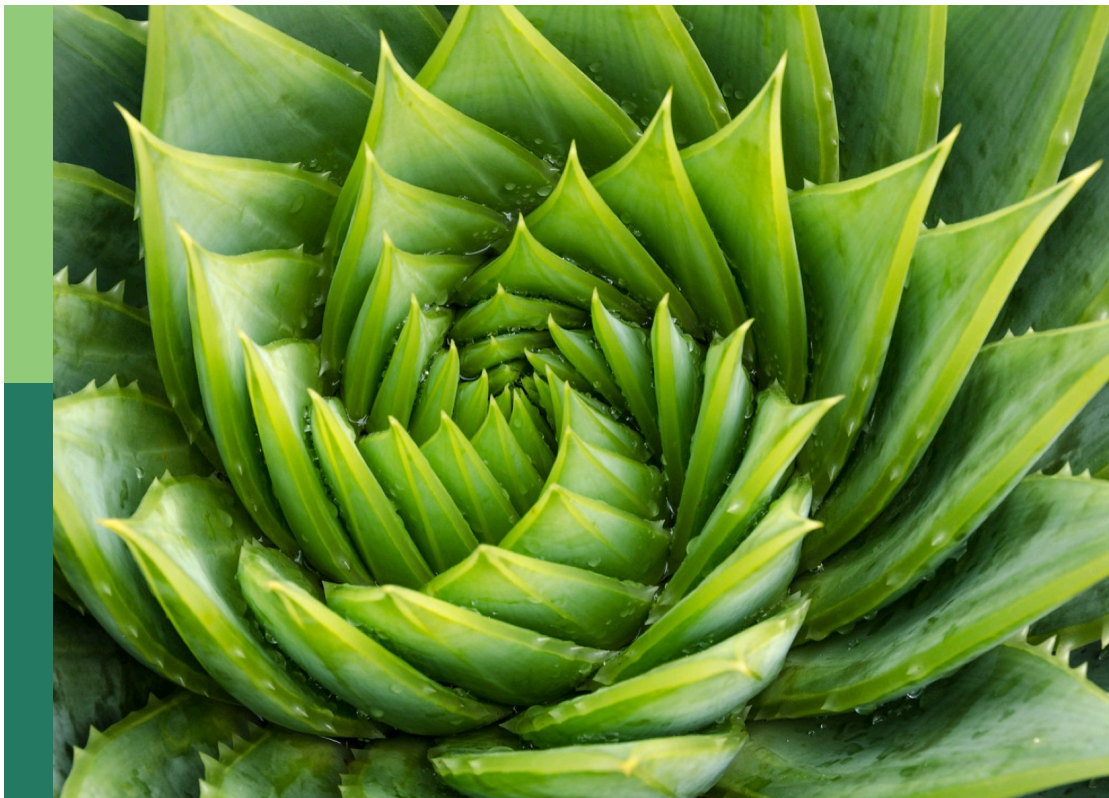
frontiers | Research Topics

Salinity and drought stress in plants: Understanding physiological, biochemical and molecular responses

Edited by
Muhammad Waseem, PingWu Liu
and Mehtab Muhammad Aslam

Published in
Frontiers in Plant Science



FRONTIERS EBOOK COPYRIGHT STATEMENT

The copyright in the text of individual articles in this ebook is the property of their respective authors or their respective institutions or funders. The copyright in graphics and images within each article may be subject to copyright of other parties. In both cases this is subject to a license granted to Frontiers.

The compilation of articles constituting this ebook is the property of Frontiers.

Each article within this ebook, and the ebook itself, are published under the most recent version of the Creative Commons CC-BY licence. The version current at the date of publication of this ebook is CC-BY 4.0. If the CC-BY licence is updated, the licence granted by Frontiers is automatically updated to the new version.

When exercising any right under the CC-BY licence, Frontiers must be attributed as the original publisher of the article or ebook, as applicable.

Authors have the responsibility of ensuring that any graphics or other materials which are the property of others may be included in the CC-BY licence, but this should be checked before relying on the CC-BY licence to reproduce those materials. Any copyright notices relating to those materials must be complied with.

Copyright and source acknowledgement notices may not be removed and must be displayed in any copy, derivative work or partial copy which includes the elements in question.

All copyright, and all rights therein, are protected by national and international copyright laws. The above represents a summary only. For further information please read Frontiers' Conditions for Website Use and Copyright Statement, and the applicable CC-BY licence.

ISSN 1664-8714
ISBN 978-2-8325-3764-0
DOI 10.3389/978-2-8325-3764-0

About Frontiers

Frontiers is more than just an open access publisher of scholarly articles: it is a pioneering approach to the world of academia, radically improving the way scholarly research is managed. The grand vision of Frontiers is a world where all people have an equal opportunity to seek, share and generate knowledge. Frontiers provides immediate and permanent online open access to all its publications, but this alone is not enough to realize our grand goals.

Frontiers journal series

The Frontiers journal series is a multi-tier and interdisciplinary set of open-access, online journals, promising a paradigm shift from the current review, selection and dissemination processes in academic publishing. All Frontiers journals are driven by researchers for researchers; therefore, they constitute a service to the scholarly community. At the same time, the *Frontiers journal series* operates on a revolutionary invention, the tiered publishing system, initially addressing specific communities of scholars, and gradually climbing up to broader public understanding, thus serving the interests of the lay society, too.

Dedication to quality

Each Frontiers article is a landmark of the highest quality, thanks to genuinely collaborative interactions between authors and review editors, who include some of the world's best academicians. Research must be certified by peers before entering a stream of knowledge that may eventually reach the public - and shape society; therefore, Frontiers only applies the most rigorous and unbiased reviews. Frontiers revolutionizes research publishing by freely delivering the most outstanding research, evaluated with no bias from both the academic and social point of view. By applying the most advanced information technologies, Frontiers is catapulting scholarly publishing into a new generation.

What are Frontiers Research Topics?

Frontiers Research Topics are very popular trademarks of the *Frontiers journals series*: they are collections of at least ten articles, all centered on a particular subject. With their unique mix of varied contributions from Original Research to Review Articles, Frontiers Research Topics unify the most influential researchers, the latest key findings and historical advances in a hot research area.

Find out more on how to host your own Frontiers Research Topic or contribute to one as an author by contacting the Frontiers editorial office: frontiersin.org/about/contact

Salinity and drought stress in plants: Understanding physiological, biochemical and molecular responses

Topic editors

Muhammad Waseem — Hainan University, China

PingWu Liu — Hainan University, China

Mehtab Muhammad Aslam — The Chinese University of Hong Kong, China

Citation

Waseem, M., Liu, P., Aslam, M. M., eds. (2023). *Salinity and drought stress in plants: Understanding physiological, biochemical and molecular responses*. Lausanne: Frontiers Media SA. doi: 10.3389/978-2-8325-3764-0

Table of contents

05 Editorial: Salinity and drought stress in plants: understanding physiological, biochemical and molecular responses
Muhammad Waseem, Pingwu Liu and Mehtab Muhammad Aslam

08 Ion absorption, distribution and salt tolerance threshold of three willow species under salt stress
Xin Ran, Xiaoxi Huang, Xiao Wang, Haiyong Liang, Yanchao Wang, Jiajing Li, Zihan Huo, Bingxiang Liu and Changming Ma

24 Genomic insights of the *WRKY* genes in kenaf (*Hibiscus cannabinus* L.) reveal that *HcWRKY44* improves the plant's tolerance to the salinity stress
Meixia Chen, Zeyuan She, Mohammad Aslam, Ting Liu, Zerong Wang, Jianmin Qi and Xiaoping Niu

40 Drought-responsive WRKY transcription factor genes *IgWRKY50* and *IgWRKY32* from *Iris germanica* enhance drought resistance in transgenic *Arabidopsis*
Jingwei Zhang, Dazhuang Huang, Xiaojie Zhao, Man Zhang, Qian Wang, Xueyan Hou, Dongliu Di, Beibei Su, Shaokun Wang and Pai Sun

58 Structure, development, and the salt response of salt bladders in *Chenopodium album* L.
Yigong Zhang, Ayibaiheremu Mutailifu and Haiyan Lan

69 Effects of limited water supply on metabolite composition in tomato fruits (*Solanum lycopersicum* L.) in two soils with different nutrient conditions
Yangmin X. Kim, Su Young Son, Seulbi Lee, Yejin Lee, Jwakyung Sung and Choong Hwan Lee

78 Integrative proteomic and physiological analyses of the molecular response to dessication-stress in *Auricularia fibrillifera*
Hao Guo, Xingwei Xiong, Yiqin Wang, Huaizhi Tian, Suqin Zhang and Guangdong Geng

93 Grafting enhances plants drought resistance: Current understanding, mechanisms, and future perspectives
Le Yang, Linchao Xia, Yi Zeng, Qingquan Han and Sheng Zhang

110 Insights into the regulation of wild soybean tolerance to salt-alkaline stress
Xiaoxi Cai, Bowei Jia, Mingzhe Sun and Xiaoli Sun

129 Integrative transcriptomic and TMT-based proteomic analysis reveals the mechanism by which *AtENO2* affects seed germination under salt stress
Yu Wu, Huimin Liu, Jie Bing and Genfa Zhang

147 Short-term severe drought influences root volatile biosynthesis in eastern white pine (*Pinus strobus L*)
Umashankar Chandrasekaran, Siyeon Byeon, Kunhyo Kim, Seo Hyun Kim, Chan Oh Park, Ah reum Han, Young-Sang Lee and Hyun Seok Kim

161 The miR169b/NFYA1 module from the halophyte *Halostachys caspica* endows salt and drought tolerance in *Arabidopsis* through multi-pathways
Jieyun Ji, Youling Zeng, Suwei Zhang, Fangyuan Chen, Xianfei Hou and Qiang Li

176 Grain yield and quality of wheat are improved through post-flowering foliar application of zinc and 6- benzylaminopurine under water deficit condition
Mohammad Javad Zarea and Nasrin Karimi

192 Selenium seed priming enhanced the growth of salt-stressed *Brassica rapa* L. through improving plant nutrition and the antioxidant system
Saber Hussain, Shakil Ahmed, Waheed Akram, Guihua Li and Nasim Ahmad Yasin

205 Photosynthetic activity and metabolic profiling of bread wheat cultivars contrasting in drought tolerance
Abdul Ghaffar, Nadeem Hussain, Rahaf Ajaj, Suzan Marwan Shahin, Hussan Bano, Muhammad Javed, Ayesha Khalid, Memoona Yasmin, Kausar Hussain Shah, Muhammad Zaheer, Muhammad Iqbal, Zafar Ullah Zafar and Habib-ur-Rehman Athar

221 Association mapping unravels the genetics controlling seedling drought stress tolerance in winter wheat
Matías Schierenbeck, Ahmad M. Alqudah, Samar G. Thabet, Ulrike Lohwasser, María Rosa Simón and Andreas Börner

234 Drought stress tolerance mechanisms and their potential common indicators to salinity, insights from the wild watermelon (*Citrullus lanatus*): A review
Goitseone Malambane, Kelebogile Madumane, Lesego T. Sewelo and Utlwang Batlang

255 Genome-wide analysis of long non-coding RNAs in sugar beet (*Beta vulgaris* L.) under drought stress
Chunlei Zou, Zhiqiang Guo, Shanshan Zhao, Jishuai Chen, Chunlai Zhang and Haoran Han

270 Changes in the morphology traits, anatomical structure of the leaves and transcriptome in *Lycium barbarum* L. under salt stress
Xiao-Cui Yao, Li-Fang Meng, Wang-Li Zhao and Gui-Lian Mao

frontiers | Frontiers in Plant Science

TYPE Editorial
PUBLISHED 09 October 2023
DOI 10.3389/fpls.2023.1277859

Check for updates

OPEN ACCESS

EDITED AND REVIEWED BY
Manuel Nieves-Cordones,
Spanish National Research Council (CSIC), Spain

*CORRESPONDENCE
Muhammad Waseem
m.waseem.botanist@gmail.com
Pingwu Liu
hnulpw@hainanu.edu.cn

RECEIVED 15 August 2023
ACCEPTED 08 September 2023
PUBLISHED 09 October 2023

CITATION
Waseem M, Liu P and Aslam MM (2023) Editorial: Salinity and drought stress in plants: understanding physiological, biochemical and molecular responses. *Front. Plant Sci.* 14:1277859. doi: 10.3389/fpls.2023.1277859

COPYRIGHT
© 2023 Waseem, Liu and Aslam. This is an open-access article distributed under the terms of the Creative Commons Attribution License (CC BY). The use, distribution or reproduction in other forums is permitted, provided the original author(s) and the copyright owner(s) are credited and that the original publication in this journal is cited, in accordance with accepted academic practice. No use, distribution or reproduction is permitted which does not comply with these terms.

Editorial: Salinity and drought stress in plants: understanding physiological, biochemical and molecular responses

Muhammad Waseem[1,2,3]*, Pingwu Liu[1,2,3]* and Mehtab Muhammad Aslam[4,5]

[1]Sanya Nanfan Research Institute of Hainan University, Sanya, China, [2]Sanya Nanfan Research Institute, Fang Zhiyuan Academician Team Innovation Center of Hainan Province, Sanya, China, [3]Key Laboratory of Tropical Horticultural Crop Quality Regulation, College of Horticulture, Hainan University, Haikou, Hainan, China, [4]School of Life Sciences and State Key Laboratory of Agrobiotechnology, The Chinese University of Hong Kong, Shatin, China, [5]College of Agriculture, Food and Natural Resources (CAFNR), Division of Plant Sciences & Technology, University of Missouri, Columbia, MO, United States

KEYWORDS

drought stress, salinity stress, food security, stress tolerance, plant breeding, plant physiology, omics

Editorial on the Research Topic
Salinity and drought stress in plants: understanding physiological, biochemical and molecular responses

1 Introduction

The foremost abiotic stresses, such as salinity and drought, are major limiting factors that hamper agricultural productivity worldwide (Waadt et al., 2022). Both of these stresses can induce several physiological, morphological, and metabolic changes through various mechanisms, ultimately impacting plant growth, development, and final productivity. The influence of salinity/drought stresses is further exacerbated by global climatic changes affecting the frequency and magnitude of occurrence of these stresses (Parihar et al., 2015). In the current scenario, the development of groundbreaking strategies for sustainable crop production is crucial in order to effectively mitigate the challenges presented by salinity and drought stresses (Rajput et al., 2021). Against this backdrop, significant progress has been made in decoding the key characteristics of salinity and drought stress, including their underlying physiological, biochemical, and molecular bases; such findings have greatly assisted in breeding of stress-tolerant crops (Kumar et al., 2023). However, our understanding of the accumulated knowledge regarding salinity/drought tolerance remains a persistent challenge (Zhang et al., 2022). The key challenges encompass (i) evolution of salinity/drought resistance, (ii) key genes in genetic and regulatory mechanisms at the transcriptional and posttranscriptional level, (iii) transfer of accumulated knowledge from laboratory to field for sustainable production, and (iv) biochemical alterations and metabolic adjustments to avoid cellular damage. To address these challenges, it is imperative to establish research initiatives that aim to target the

combined effects of salinity and drought stresses. Such research should focus on exploration at the genetic, molecular, biochemical, and physiological levels for the development of sustainable agriculture in the era of climate change.

2 Genome-wide functional analysis

Genome-wide gene functional analysis is a valuable tool for identifying key stress-related genes, which can then be characterized to better understand how plants are adapted to salinity and drought. Osmotic stress tolerance is primarily mediated by abscisic acid (ABA), and plants achieve osmotic stress tolerance through both ABA-dependent and ABA-independent mechanisms. Recently, researchers have highlighted the role of WRKY transcription factors in enhancing salinity and drought tolerance in plants through ABA-mediated regulation. For instance, in Kenaf (*Hibiscus cannabinus* L.), Chen et al. report that *HcWRKY44*, among 46 WRKY genes, acts as positive regulator of salinity tolerance through ABA-mediated regulation. Likewise, in *Iris germanica*, two WRKY genes (*IgWRKY50* and *IgWRKY32*) play a role in regulating the ABA signal transduction pathway and controlling stomatal aperture to improve drought tolerance (Zhang et al.). These studies offer a comprehensive understanding of WRKY genes, their potential in the development of plants with tolerance to salinity/drought stresses, and their utmost important in breeding and production of stress-tolerant crop varieties.

3 Integrated high-throughput approaches

Functional analysis relies on high-throughput techniques. For instance, Yao et al. performed transcriptome analysis to uncover the molecular mechanism behind leaf thickening under salinity stress in the halophytic plant *Lycium barbarum*. Their study identified a total of 3572 DEGs, among which expansin protein *EXLA2* acts as a positive regulator of palisade tissue thickness in *L. barbarum* leaves. In another study, Wu et al. uncovered the role of a glycolytic enzyme enolase 2 (ENO2) in seed germination under salt stress in Arabidopsis. They integrated transcriptomic and TMT-based proteomic approaches, revealing an array of salt stress-responsive genes in *AtENO2* mutant (*eno2*$^{-}$) and wild-type Arabidopsis. Their study shows that GAPA1/GAPB interacts with *AtENO2* to regulate seed germination under salinity stress, which could be leveraged to enhance plant tolerance to saline environments.

Water scarcity can limit soil nutrient solubilization and mineralization, affecting nutrient kinetics at the soil–root interface and resulting in impairments to leaf morphology and reduced stomatal conductance. To address this challenge, screening of agricultural crop germplasm could be conducted using integrated high-throughput techniques in order to develop crops with desirable traits. Kim et al. conducted a study on the quality and nutrition of tomato fruit under water stress with varying nutrient status. By using integrated GC-TOF-MS and UHPLC-LTQ-Orbitrap-MS approaches, they found that water stress shifted the primary metabolites of tomato fruits in different ways in soils with different nutrient conditions. On this basis, considering the nutritional quality of tomato fruit (particularly in relation to sugars and amino acids), the authors do not recommend propagation of tomatoes in water-deficient soils with surplus nutrients.

Shifting to another context, *Auricularia fibrillifera*, the third most widely cultivated mushroom and a common traditional Chinese food and medicine enriched in melanin, folate, and biotin, was studied by Guo et al. under desiccation stress. The focus was on transcriptomes and proteomes of fruit bodies under exposure to desiccation stress, rehydration, and regular watering. The research revealed that proteomics data aligned with transcriptomic data, particularly in pathways related to antibiotic biosynthesis, biosynthesis of biotin and folate, and amnio acid biosynthesis. This study provides valuable insights into desiccation tolerance in *A. fibrillifera*.

4 ncRNAs as emerging regulators of salinity/drought stress tolerance

Non-coding RNAs (ncRNAs) are emerging regulators of various biological processes, including stress tolerance (Waseem et al., 2021; Waseem et al., 2022; Aslam et., 2022). Zou et al. report 32017 long non-coding RNAs (lncRNAs) in *Beta vulgaris*, revealing 386 differentially expressed lncRNAs, including two significantly expressed lncRNAs (TCONS_00038334/TCONS_00055787) in response to drought. They also identified 42 lncRNAs as potential miRNA target mimics. In another study, Ji et al. showed that that the miR169b/NFYA1 module in the halophyte *Halostachys capsica* enhances salinity and drought tolerance by enhancing ABA biosynthesis, modulating ABA signal transduction pathways, and maintaining ROS homeostasis.

5 Exploration of underlying salinity/drought tolerance mechanisms

In the current era of global climatic change, the relationship between climate and crop yield is evolving, especially for global food security crops such as wheat. Drought directly impacts wheat production. Ghaffar et al. conducted a study evaluating agronomic adaptions for drought tolerance using Pakistan's wheat germplasm. They investigated 40 local wheat cultivars for various properties, including growth, pigmentation, and ROS accumulation capacity. Ghaffar et al. successfully identified drought-tolerant (Barani-83/Blue silver) and drought-sensitive (FSD-08/Lasani-08) cultivars. Another approach to enhancing drought stress in winter wheat involves foliar application of Zinc (Zn). Zarea and Karimi show that combing the foliar application of Zn with 6-Benzylaminopurine (6-BAP) promotes growth and improves drought tolerance, preventing grain yield reduction in winter wheat.

We appreciate the contribution by Schierenbeck et al., who conducted a quantitative trait nucleotide (QTN) analysis of a diverse winter wheat panel (261 accessions) under drought stress. The authors successfully identified a QTN, TraesCS2D02G133900, that may play a

role in controlling shoot and coleoptile length. This study highlights the significance of genetics factors in response to drought in wheat, offering insights for wheat adaptation and improvement.

Ran et al. performed a comparative analysis of salinity tolerance in three willow species, *Salix matsudana*, *S. gordejevii*, and *S. linearistipularis*. Their study revealed that *S. linearistipularis* is salt-sensitive and could be planted as an indicative plant for salinity. Meanwhile, Zhang et al. identified the formation of accessory structures, in the form of salt bladders, in *Chenopodium album*. These structures serve as an adaptive measure to prevent salt sensitivity in this plant. Additionally, Chandrasekaran et al. found that, under drought stress, *Pinus strobus* shifts carbon partitioning toward biosynthesis of volatile organic compounds (VOCs), particularly monoterpene synthesis. Lastly, Hussain et al. demonstrated that selenium seed priming in *Brassica rapa* mitigates salinity stress by activating stress-responsive genes and improving the ROS system.

On the basis of this comprehensive collection of research on the topic at hand, various invaluable insights into salinity and drought resistance have accumulated. We hope that this accumulated knowledge will assist with and pave the path for new studies and breeding programs aiming to develop salinity- and drought-resilient crops. To achieve a better understanding of salinity and drought tolerance in plants, a holistic approach involving integrated variety improvement, theoretical research, and field management is required. We sincerely appreciate the efforts and significant contributions of the authors, editors, and peer reviewers whose efforts and significant contributions have made this Research Topic possible. We hope that our readers will uncover valuable information within this Research Topic collection and identify potential collaborators in this critical area.

Author contributions

MW: Conceptualization, Supervision, Validation, Writing – original draft. PL: Writing – review & editing. MMA: Writing – review & editing.

Acknowledgments

We thank the authors of the papers published in this Research Topic for their valuable contributions and the referees for their rigorous review.

Conflict of interest

The authors declare that the research was conducted in the absence of any commercial or financial relationships that could be construed as a potential conflict of interest.

Publisher's note

All claims expressed in this article are solely those of the authors and do not necessarily represent those of their affiliated organizations, or those of the publisher, the editors and the reviewers. Any product that may be evaluated in this article, or claim that may be made by its manufacturer, is not guaranteed or endorsed by the publisher.

References

Aslam, M. M., Waseem, M., Xu, W., Ying, L., Zhang, J., and Yuan, W. (2022). Global identification of white lupin lncRNAs reveals their role in cluster roots under phosphorus deficiency. *Int. J. Mol. Sci.* 23 (16), 9012. doi: 10.3390/ijms23169012

Kumar, R., Sagar, V., Verma, V. C., Kumari, M., Gujjar, R. S., Goswami, S. K., et al. (2023). Drought and salinity stresses induced physio-biochemical changes in sugarcane: an overview of tolerance mechanism and mitigating approaches. *Front. Plant Sci.* 14, 1225234. doi: 10.3389/fpls.2023.1225234

Parihar, P., Singh, S., Singh, R., Singh, V. P., and Prasad, S. M. (2015). Effect of salinity stress on plants and its tolerance strategies: a review. *Environ. Sci. pollut. Res. Int.* 22, 4056–4075. doi: 10.1007/s11356-014-3739-1

Rajput, V. D., Minkina, T., Kumari, A., Harish,, Singh, V. K., Verma, K. K., et al. (2021). Coping with the challenges of abiotic stress in plants: new dimensions in the field application of nanoparticles. *Plants (Basel)* 10 (6), 1221. doi: 10.3390/plants10061221

Waseem, M., Liu, Y., and Xia, R. (2021). Long non-coding RNAs, the dark matter: an emerging regulatory component in plants. *Int. J. Mol. Sci.* 22 (1), 86. doi: 10.3390/ijms22010086

Waseem, M., Yang, X., Aslam, M. M., Li, M., Zhu, L., et al. (2022). Genome-wide identification of long non-coding RNAs in two contrasting rapeseed (Brassica napus L.) genotypes subjected to cold stress. *Environ. Exp. Bot.* 201, 104969.

Waadt, R., Seller, C. A., Hsu, P. K., Takahashi, Y., Munemasa, S., and Schroeder, J. I. (2022). Plant hormone regulation of abiotic stress responses. *Nat. Rev. Mol. Cell Biol.* 23, 680–694. doi: 10.1038/s41580-022-00479-6

Zhang, H., Sun, X., and Dai, M. (2022). Improving crop drought resistance with plant growth regulators and rhizobacteria: Mechanisms, applications, and perspectives. *Plant Commun.* 3, 100228. doi: 10.1016/j.xplc.2021.100228

frontiers | Frontiers in Plant Science

TYPE Original Research
PUBLISHED 02 August 2022
DOI 10.3389/fpls.2022.969896

Check for updates

OPEN ACCESS

EDITED BY
Muhammad Waseem,
Hainan University, China

REVIEWED BY
Shah Fahad,
The University of Haripur, Pakistan
Mohammad Shah Jahan,
Sher-e-Bangla Agricultural University, Bangladesh

*CORRESPONDENCE
Bingxiang Liu
proser211@126.com
Changming Ma
machangming@126.com

†These authors have contributed equally to this work and share first authorship

SPECIALTY SECTION
This article was submitted to Plant Abiotic Stress, a section of the journal Frontiers in Plant Science

RECEIVED 15 June 2022
ACCEPTED 14 July 2022
PUBLISHED 02 August 2022

CITATION
Ran X, Huang X, Wang X, Liang H, Wang Y, Li J, Huo Z, Liu B and Ma C (2022) Ion absorption, distribution and salt tolerance threshold of three willow species under salt stress. *Front. Plant Sci.* 13:969896. doi: 10.3389/fpls.2022.969896

COPYRIGHT
© 2022 Ran, Huang, Wang, Liang, Wang, Li, Huo, Liu and Ma. This is an open-access article distributed under the terms of the Creative Commons Attribution License (CC BY). The use, distribution or reproduction in other forums is permitted, provided the original author(s) and the copyright owner(s) are credited and that the original publication in this journal is cited, in accordance with accepted academic practice. No use, distribution or reproduction is permitted which does not comply with these terms.

Ion absorption, distribution and salt tolerance threshold of three willow species under salt stress

Xin Ran[1†], Xiaoxi Huang[1†], Xiao Wang[1], Haiyong Liang[1], Yanchao Wang[2], Jiajing Li[1], Zihan Huo[1], Bingxiang Liu[1,3]* and Changming Ma[1]*

[1]Department of Forest Cultivation, College of Forestry, Hebei Agricultural University, Baoding, China, [2]College of Bioscience and Engineering, Xingtai University, Xingtai, China, [3]Hebei Urban Forest Health Technology Innovation Center, Baoding, China

To investigate the response mechanism and salt tolerance threshold of three willow seedlings (*Salix matsudana, Salix gordejevii, Salix linearistipularis*), the absorption, transport and distribution of salt ions (Na^+, K^+, Ca^{2+}) were studied under hydroponic conditions with different salt concentrations (CK, 171, 342, 513, and 684 mm) and treatment times (1, 3, 5, 8, 11, and 15 days). *Salix linearistipularis* has the weakest ability to maintain its apparent shape, while *Salix matsudana* has the strongest ability. The three plants have a certain Na^+ interception ability, and the interception abilities of *Salix matsudana* and *Salix gordejevii* are higher than that of *Salix linearistipularis*. The leaf $S_{AK,\ Na}$ of *Salix linearistipularis* were higher than those of *Salix matsudana* and *Salix gordejevii*. The leaf selection ability was the highest, and the selection ability of the root system was the lowest in *Salix linearistipularis*. The long-term low salt concentration and the short-term high salt concentration can increase the root and leaf salinity. *Salix matsudana* grows more stably in a long-term high-salt stress environment, and *Salix gordejevii* grows stably in a short-term high-salt stress environment. However, *Salix linearistipularis* is more suitable for planting as an indicative plant because of its sensitivity to salt stress. The root Na^+ content of *Salix matsudana* and *Salix gordejevii* was 34.21 mg/g, which was the maximum root retention capacity. Once the accumulation of Na^+ content in roots exceeds this value, the rejection capacity of roots is broken through, and the selective ion absorption capacity will rapidly become weak, which easily leads to the death of plants.

KEYWORDS

ion absorption, NaCl stress, salt tolerance mechanism, *Salix matsudana*, *Salix gordejevii*, *Salix linearistipularis*, transport and distribution, threshold

Introduction

Soil salinization poses a serious threat to sustainable agricultural production and ecological balance (Litalien and Zeeb, 2020; Fahad et al., 2021b,e). It is predicted that by 2050, nearly 50% of the world's arable land will be salinized, which will be a huge threat to sustainable agricultural development and food security (Butcher et al., 2016). Soil salinity, as a major abiotic stress factor, seriously inhibits the growth and development of plants (Fahad et al., 2015b; Zhu et al., 2020). It is also considered a physiological drought phenomenon (Hasan et al., 2021). To achieve sustainable development of saline soil agriculture, people can only choose two methods: one from the soil itself affected by salt and the other comes from the plants themselves (Shao et al., 2019). Many scholars have also taken different measures for the improvement of saline-alkali land. For example, they installed hidden pipes to drain water (Ayars et al., 2006; Feng et al., 2017) or used gypsum as a soil conditioner to improve the soil (Zhao et al., 2019; Sheikh et al., 2022). However, studies have shown that planting saline-alkali-tolerant plants has the advantages of low investment, wide application and strong sustainability. Therefore, biological treatment has become the optimal measure for the improvement and utilization of saline-alkali lands (Djanaguiraman et al., 2006; Li et al., 2009).

Regarding the research on salt-tolerant plants, scholars mostly use hydroponics to study the growth and physiological characteristics of plants under different concentrations (Li et al., 2021), ion distribution (Rabiei et al., 2020) and the mechanism of salt tolerance (Bian and Lu, 2022). Salt stress affects plant growth and development in two ways: osmotic stress and ion imbalance. The former results in a decrease in chloroplast photosynthetic rate and CO_2 concentration, and a limitation of stomata (Wang et al., 2018; Ma et al., 2022). The latter can lead to unstable inflow and outflow of Na^+, K^+, and Ca^{2+} in cells (Yang and Guo, 2018; Zhang et al., 2022). Currently, many scholars have examined the effects of salt stress on the growth of different plants at different levels from different disciplines (such as ecology, phytophysiology, and molecular biology of the cell). They also discussed the mechanism of salt damage to plants (Aghaleh et al., 2011; Fahad et al., 2020; Hou et al., 2021) and noticed plant responses to salt stress (Fahad et al., 2015a; Karunasinghe et al., 2020; Kim et al., 2020; Shu et al., 2020; Altaf et al., 2021; Wu et al., 2022). Willow is a general term for Salix and Chosenia tree species in the Salicaceae family. It has the characteristics of fast growth, cold resistance, drought resistance, salinity resistance and pollution resistance. It also has ecological, timber and biomass energy value (Warmiński et al., 2021). Regarding the salt tolerance of willow, studies have mostly focused on root vigor, growth, salt tolerance, plant phenotype, physiological substances, and molecular biology. They observed a series of phenomena under salt stress, including root activity, plant growth index, and plant height decrease with increasing stress (Sui, 2006; Markus-Michalczyk et al., 2014; Tian and Li, 2018; Feng et al., 2020; Zhang et al., 2021). However, studies on the salt distribution on plant roots and leaves and salt tolerance thresholds are still not in-depth and systematic (Maggio et al., 2007; Kurunc et al., 2020; Banakar et al., 2022). Moreover, there are few studies on the growth and physiological characteristics of salt-tolerant plants at different times. What are the ion-selective absorption characteristics of different willow roots and leaves and the threshold for breaking the ion balance? What are the responses and correlations of Na^+, K^+, and Ca^{2+} (or ratios) of roots and leaves of different varieties of willow to salt stress? Do different willows resist salt stress through the same salt adaptation mechanism?

To explore the above problems, this paper selected three species of willow (*Salix matsudana*, *Salix gordejevii*, *Salix linearistipularis*) as experimental materials under the condition of greenhouse hydroponics. First, the effects of salt stress on plant growth and Na^+, K^+, and Ca^{2+} uptake, transport and distribution in root and leaf tissues were studied. Second, the correlation between salt ions and their ratios was analyzed, and the differences in salt tolerance mechanisms were discussed. Finally, the salt tolerance thresholds of the three willow trees were fitted according to the above data. This study provides new insights for the analytical evaluation of salt tolerance of willow and lays a foundation for further development of salt tolerance breeding strategies.

Materials and methods

Experimental materials

The experiment was performed in the artificial climate chamber of the West Campus of Hebei Agricultural University (115°25′ E, 38°48′ N), Nanshi District, Baoding City, Hebei Province. According to the existing research, when the light intensity is 1,000 $\mu mol \cdot m^{-2} \cdot s^{-1}$, the growth and photosynthetic capacity of plants are the best (Liu et al., 2013, 2022; Gerona et al., 2019; Zhu H. L. et al., 2019; Zhang G .C. et al., 2020; Ma et al., 2022). There are also many scholars who keep the relative humidity at 50–70% when setting up the experiments. Therefore, according to the existing research and the actual situation, we set the corresponding parameters of the climate chamber. The set temperature of the climate chamber was 28°C/25°C (light/dark). The LED cold light source controlled the light intensity at 1,000 $\mu mol \cdot m^{-2} \cdot s^{-1}$, the photoperiod was 14 h/10 h (light/dark), and the relative humidity was 60%.

The experimental materials were collected from the germplasm resource nursery of Jinshatan Forest Farm. In early spring of 2020, annual cuttings of 3 willow species *Salix*

matsudana, *Salix gordejevii,* and *Salix linearistipularis* were collected before germination. They were basically uniform, robust and free of pests and diseases. After harvesting, they were stored in a freezer at 0°C. On June 26, 2020, a water culture experiment was conducted in the artificial climate chamber. The middle two-thirds of the branches were selected and cut into 20 cm cuttings. The uppermost bud was 0.5–1 cm from the top of the cuttings. The upper cut was a flat cut, and the lower cut was an oblique cut. Sufficient cuttings of the three species of willows were placed in the clean water for natural growth and routine management. On July 15, when their growth reached the treatment requirement (the average root length was approximately 5 cm), the seedlings with basically uniform roots were selected for stress treatment.

Experimental design

The experimental materials were placed in a 55 cm × 38 cm × 15 cm (length × width × height) plastic box for water culture (**Figure 1**). We refer to the articles of some scholars who set the salt concentration between 100 and 700 mM. In addition, we also converted the salt concentration into international units according to the formula (Gao et al., 2022; Ni et al., 2022). Studies have found that a certain concentration of Hoagland nutrient solution has a good promotion effect on seedling growth of plants (Zobolo and Khumalo, 2017). When setting up experiments on the effects of salt stress on plants, some scholars take 1/2 Hoagland solution as the base solution and then add the corresponding concentration of salt (Regni et al., 2019). Therefore, we decided to use this method to set the salt concentration. Hydroponic solutions with NaCl concentrations of 171, 342, 513, and 684 mM were prepared based on 1/2 Hoagland complete nutrient solution, and 1/2 Hoagland complete nutrient solution was used as the control (pH 7.2). Each treatment was repeated 3 times, and 10 seedlings of each species were directly placed in the solution, with more than half of the height drowning in the solution. The nutrient solution was changed every 5 days during their growth. In order to prevent excessive accumulation of salt, we took out the seedlings and carefully rinsed off the residual salt from the roots with clean water before changing the nutrient solution. 1/2 Hoagland's complete nutrient solution includes: $NH_4H_2PO_4$ 57.5 mg, $FeSO_4$ 15 mg, $Ca(NO_3)_2{\cdot}4H_2O$ 472.5 mg, $MgSO_4$ 246.5 mg, $NaFeC_{10}H_{12}N_2O_8{\cdot}3H2O$ 30 mg, $CuSO_4$ 0.05 mg, H_3BO_3 2.86 mg, $H_8MoN_2O_4$ 0.02 mg, $Na_2B_4O_7{\cdot}10H_2O$ 4.5 mg, $MnSO_4$ 2.13 mg, $ZnSO_4$ 0.22 mg, K_2SO_4 303.5 mg.

We randomly selected three seedlings with even growth vigor on the 1st, 3rd, 5th, 8th, 11th, and 15th days of the stress test for the observation of various growth physiological indexes. The measurement of each index was repeated for 3 times, and the growth status was observed and recorded 1 week after the end of the experiment.

Measured indices and methods

Root and leaf phenotypic records

Following salt stress treatment, plants at different salt concentrations were taken out of the hydroponic tank intact at the indicated times. To avoid damaging the root system, rinse the solution with running water. After drying, the plants were placed in the EPSEN v700 (Seiko Epson Corporation, Japan) scanner for scanning. During the period, the camera was used to slightly adjust the position of the root to avoid overlapping and crossing of the root system. Scanned photographs of intact plants are used as final analysis images and are saved in TIFF format. A picture of the shape change of the plant under salt stress can be obtained.

Ion contents in roots and leaves, ion selective absorption and transport ratio

The method for ion content determination was slightly modified compared to the methods proposed by Yang (2010) and Meng et al. (2020). The sample was first baked at 105°C for 30 min and then dried at 70–80°C to a constant weight. After it was ground into powder, the fixed mass was weighed. After 30 ml of deionized water was added, the sample was shaken well and placed in a boiling water bath for 2 h. After cooling, the sample was filtered and diluted to 50 ml. The Na^+, K^+, and Ca^{2+} contents were determined by the atomic absorption method. By reference to the methods proposed by Yang et al. (2003), Xia et al. (2018), and Zhang et al. (2018), the following formula was used to calculate the selective absorption and transport coefficients of ions X (K^+ and Ca^{2+}) by roots and leaves, where ion absorption coefficient according to the Eqs. 1 and ion transport coefficient according to the Eqs. 2. In the formula, the K^+ content was mg/L, and the Ca^{2+} content was 230 mg/L in the medium (culture solution). The larger the value of $SA_{X,Na}$, the stronger the root system's ability to inhibit Na^+ and promote × absorption. The higher the $ST_{X,Na}$ value is, the stronger the root inhibition capacity of Na^+ and promotion of × transport to leaves is. "Medium" refers to the medium (such as soil, culture medium, etc.) in which plant roots grow.

$$SA_{X,Na} = \text{Root}\left(X|Na^+\right)/\text{Medium}\left(X|Na^+\right) \quad (1)$$

$$STX_{X,Na} = \text{Leaf}\left(X|Na^+\right)/\text{Root}\left(X|Na^+\right) \quad (2)$$

Data processing

Excel and Origin were used to fit the response curve data. SPSS 18.0 data processing software was used for statistical analysis, and the least significant difference (LSD) method was used to check the significance of the difference when the *P*-value was less than 0.05.

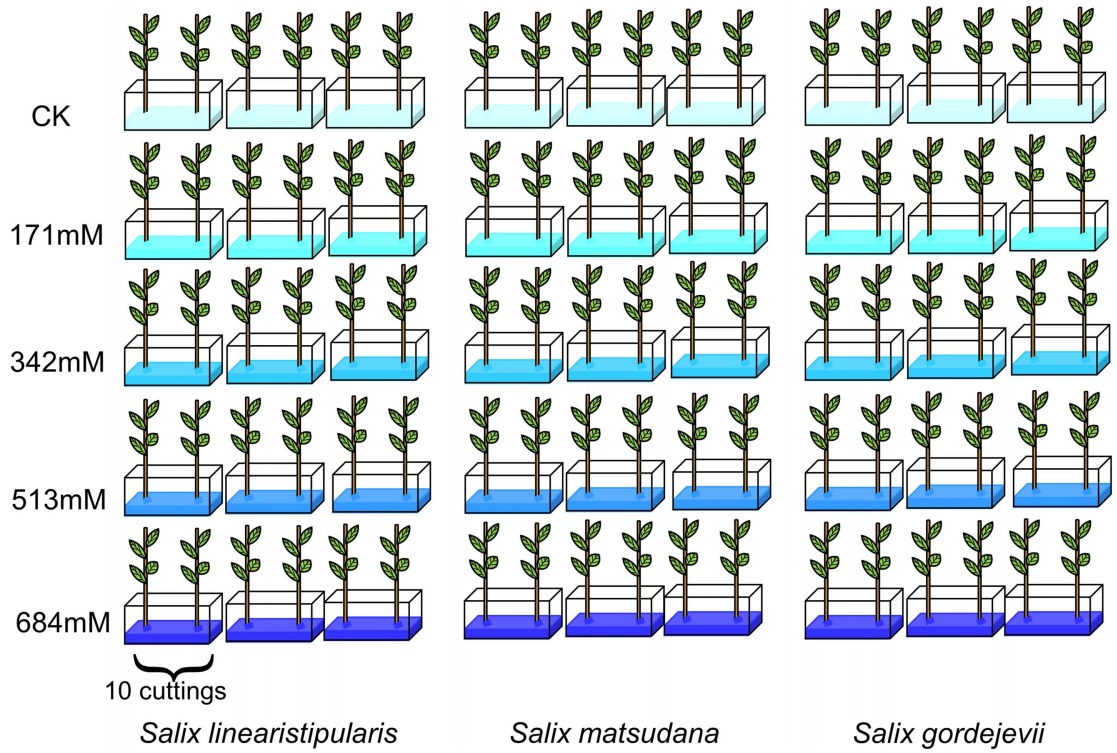


FIGURE 1
Design of three willows experimental treatment.

Results

Changes in the growth state of seedlings under salt stress

Figure 2 shows that salt stress had a direct impact on the growth state of plants. The leaves of the seedlings of the three species of willow all showed that with the aggravation of salt stress, the damage degree gradually increased, leaf tips and leaf margins gradually turned yellow, leaf margins became scorched and curled, leaves gradually lost their green color and even wilted and fell off, and the twigs became dry. The number of roots of the three species of willow gradually decreased with the aggravation of salt stress. Figures 2A–C also shows that the roots of *Salix linearistipularis*, *Salix gordejevii* and *Salix matsudana* significantly reduced at NaCl concentrations of 171, 513, and 684 mM, respectively, and they became obviously withered at NaCl concentrations of 171, 342, and 342 mM, respectively, and the leaves significantly reduced at NaCl concentrations of 171, 342, and 513 mM, respectively. The number and length of the roots of the three species of willow all decreased, and the sensitivity in descending order was *Salix linearistipularis*> *Salix gordejevii*> *Salix matsudana*.

Overall, the root and leaf tissues of *Salix linearistipularis* suffered the earliest and the most serious damage, followed by *Salix gordejevii* and *Salix matsudana*. There were differences in the growth changes among different species of willow. In comparison, *Salix matsudana* maintained a better apparent morphology under salt stress, followed by *Salix gordejevii* and *Salix linearistipularis*.

Changes in Na^+, K^+, and Ca^{2+} contents in roots and leaves under salt stress

Figure 3 shows that under normal circumstances (CK group), the K^+ content was the highest in the roots and leaves of the three species of willow, followed by Na^+ and Ca^{2+}. The Na^+ content in the roots and leaves of *Salix linearistipularis* was the lowest, and the K^+ and Ca^{2+} contents in the roots and leaves of *Salix matsudana* were the highest. With the aggravation of salt stress and prolonged stress time, the Na^+ contents in the roots and leaves of the three species of willow showed a cumulatively increasing trend. Salt stress significantly increased the Na^+ contents in the roots and leaves, and the Na^+ contents in the roots were always higher than those in the leaves, but the differences gradually decreased with the increase in stress degree and the prolongation of stress time (Figures 3D–F). Under different salt concentrations and times, the increase in Na^+

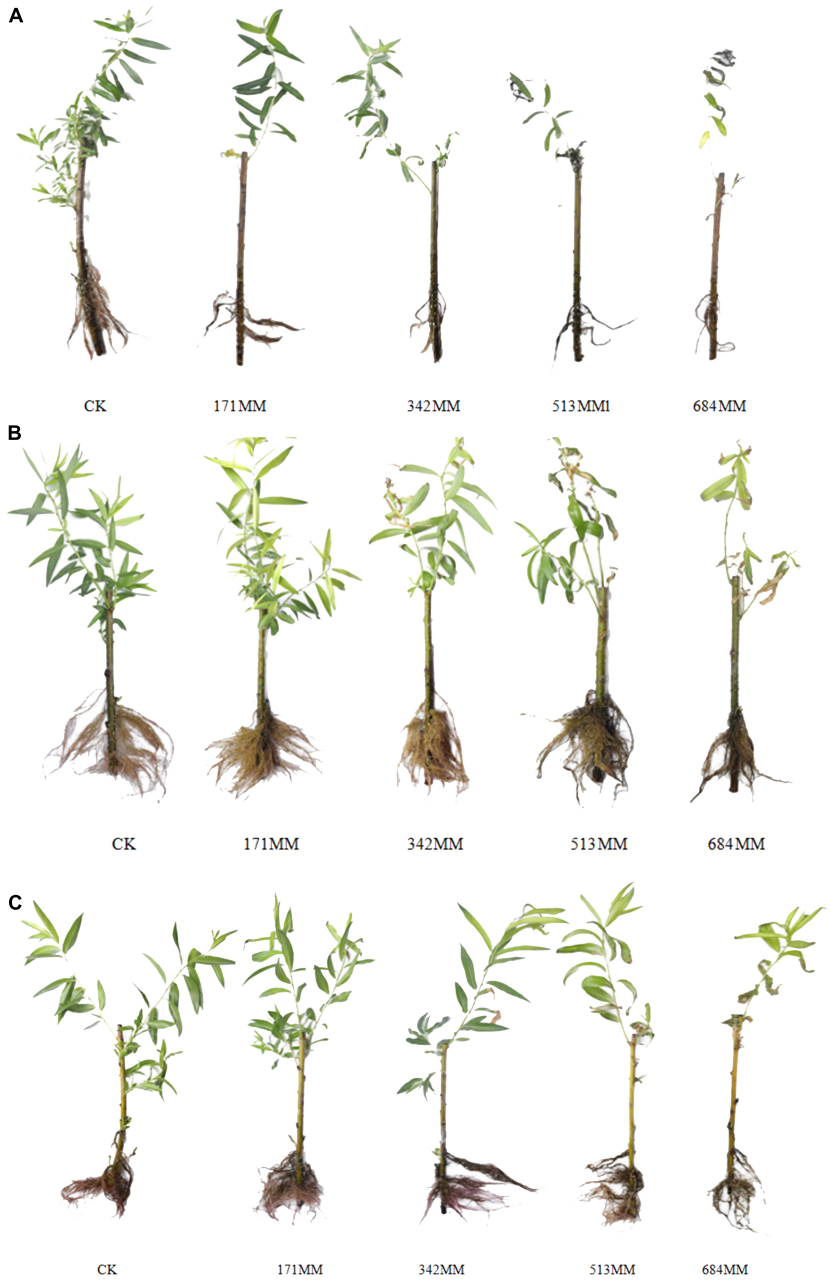


FIGURE 2
Phenotypic response of three willow seedlings to salt stress. **(A)** *Salix linearistipularis*; **(B)** *Salix matsudana*; **(C)** *Salix gordejevii*.

content in the roots and leaves was ranked in descending order: *Salix matsudana*, *Salix gordejevii,* and *Salix linearistipularis*. Under the same salt stress, the Na^+ contents and changes in the roots and leaves of *Salix linearistipularis* were lower than those of *Salix gordejevii* and *Salix matsudana*.

It can be seen from the **Figure 3** that the K^+ contents in the roots and leaves of the three willow species decreased with the aggravation of stress and prolonged stress time, and the K^+ content in the roots was lower than that in the leaves. Among the three tree species, the K^+ contents in the roots and leaves of *Salix matsudana* were higher than those of *Salix gordejevii* and *Salix linearistipularis*. With the increase in salt concentration and the prolongation of stress time, the K^+ contents in the roots of *Salix matsudana* and *Salix gordejevii* decreased more slowly than those of *Salix linearistipularis*.

With the aggravation of salt stress and the prolongation of stress time, the Ca^{2+} contents in the roots and leaves

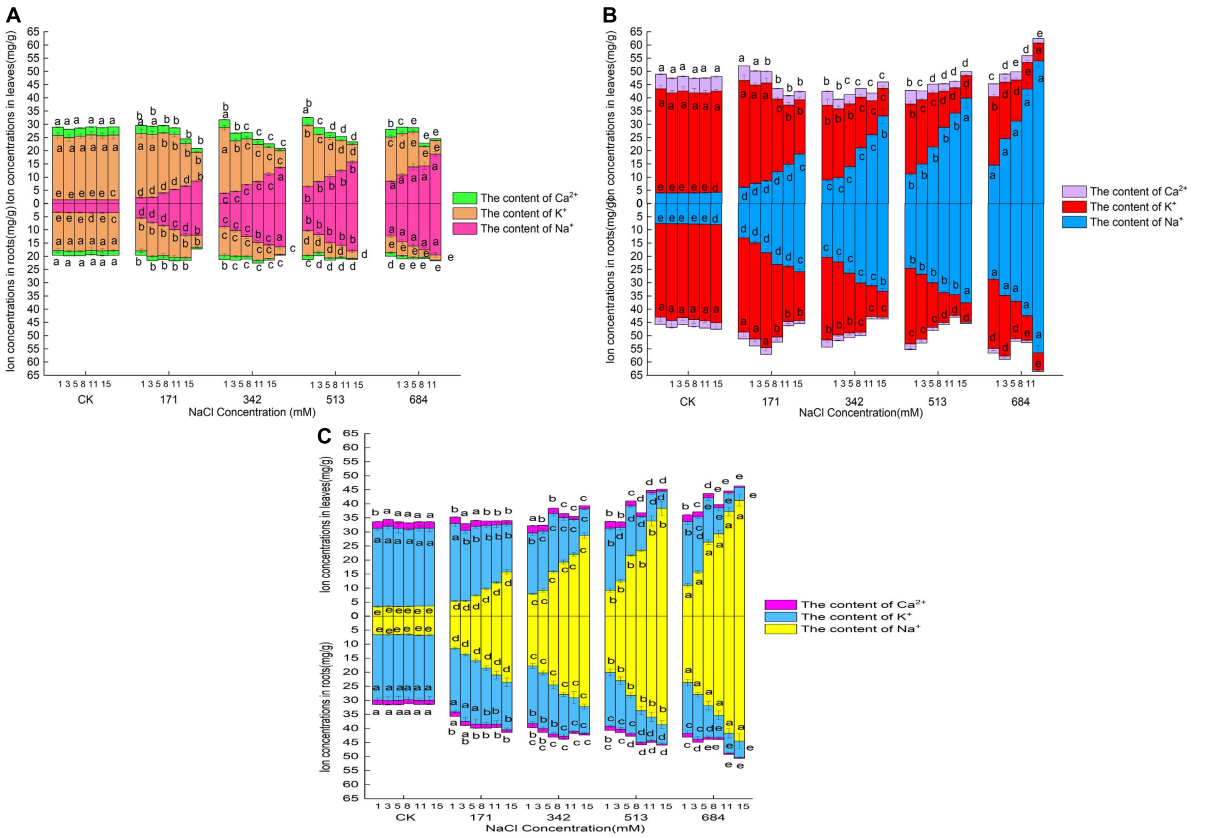


FIGURE 3
Effects of salt stress on Na^+, Ca^{2+}, and K^+ contents in roots and leaves of three willows. **(A)** *Salix linearistipularis*; **(B)** *Salix matsudana*; **(C)** *Salix gordejevii*.

of the three species of willow showed a decreasing trend (Figure 3). Among the three tree species, under normal growth conditions, the Ca^{2+} contents in the leaves and roots of *Salix matsudana* were higher than those of *Salix gordejevii* and *Salix linearistipularis*. After salt stress, *Salix gordejevii* maintained the strongest Ca^{2+} content, and the content in the leaves showed a gentler decreasing trend. With the aggravation of salt stress and prolonged time, the Na^+ content in roots and leaves continued to increase, while the K^+ and Ca^{2+} contents continued to decrease. The long-term stress at low salt concentrations and the short-term stress at high salt concentrations both could make salinity in roots and leaves reach high levels.

In the first 3, 8, and 8 days, with the increase of salt stress, *Salix linearistipularis*, *Salix matsudana* and *Salix gordejevii* showed a trend of increasing first and then decreasing (Figures 4A–C). The higher the concentration was, the more significant they differed from CK. Compared with CK, the ratio of K^+ in the root/leaf of *Salix linearistipularis* with different salt concentrations in the first 5 days showed a gradually decreasing trend, and the difference was significant (Figure 4D). When the NaCl was 171 mM, compared with CK, the root/leaf K^+ of *Salix matsudana* was no significant difference with CK except that 171 mM was significantly increased on the fifth day (Figure 4E). At the concentration of 342 mM, the *Salix gordejevii* showed a significant increase compared with CK with the prolongation of time (Figure 4F). From the 3rd day, the Ca^{2+} in the root/leaf of *Salix linearistipularis* under 513 mM NaCl showed a significant decreasing trend with the prolongation of time compared with CK (Figure 4G). Compared with CK, the Ca^{2+} in the root/leaf of *Salix matsudana* showed a trend of increasing at first and then decreasing with time at different salt concentrations (Figure 4H). At 171 mM salt concentration, the Ca^{2+} in the root/leaf of *Salix gordejevii* showed an upward trend with time, and there was no significant difference until the 8th day (Figure 4I).

Selective absorption and transport of ions in the roots and leaves of three tree species under salt stress

In the early stage of salt stress (1–3 days), the $SA_{K,\ Na}$ of the roots of *Salix linearistipularis* only had a temporary rise at a salt concentration of 513 mM on the first day, and the

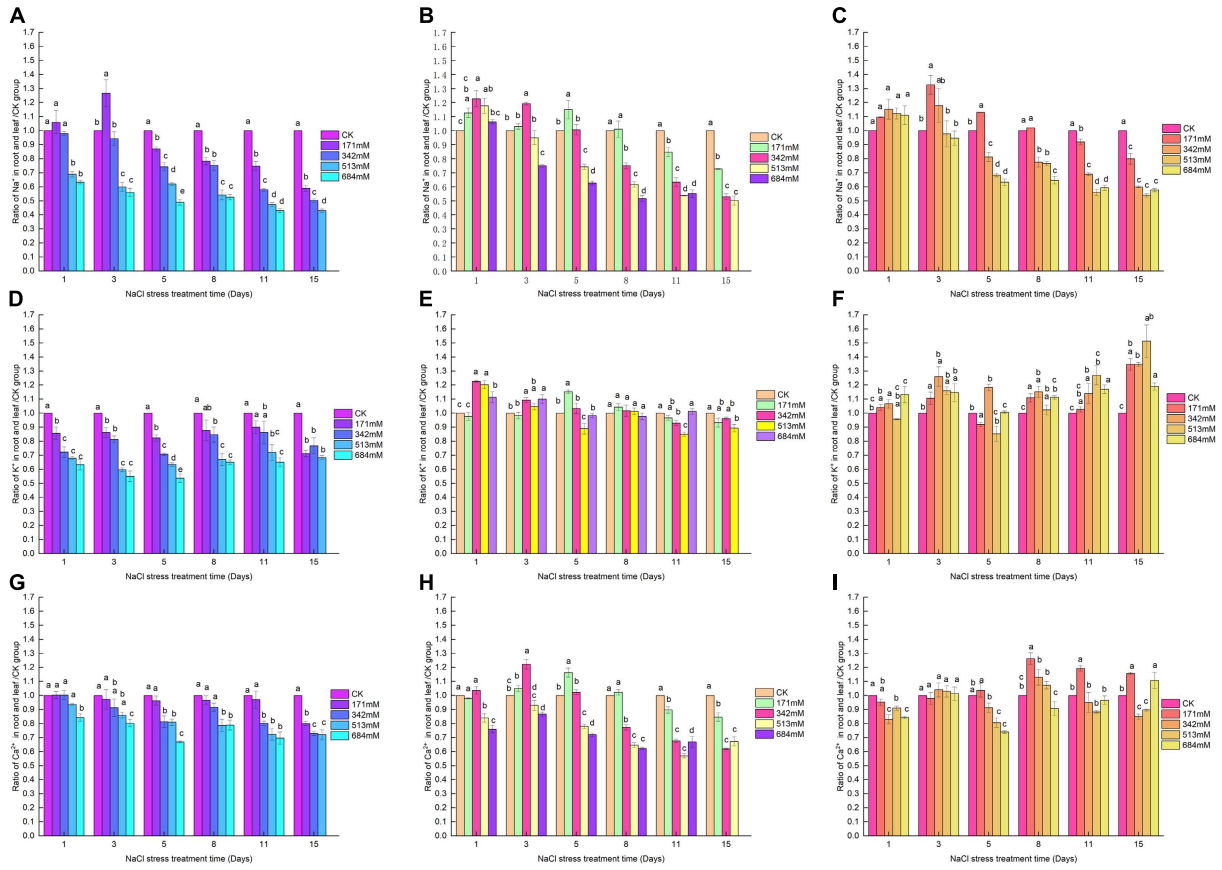


FIGURE 4
Ratios of Na^+, Ca^{2+}, K^+ to CK in roots/leaves of three willows under salt stress. Ratio of Na^+ to CK in roots/leaves of three willows. **(A)** *Salix linearistipularis*; **(B)** *Salix matsudana*; **(C)** *Salix gordejevii*. Ratio of K^+ to CK in roots/leaves of three willows. **(D)** *Salix linearistipularis*; **(E)** *Salix matsudana*; **(F)** *Salix gordejevii*. Ratio of Ca^{2+} to CK in roots/leaves of three willows. **(G)** *Salix linearistipularis*; **(H)** *Salix matsudana*; **(I)** *Salix gordejevii*. Different small letters indicate significant differences between treatments at 0.05 level among treatment.

roots of *Salix matsudana* and *Salix gordejevii* had increased $SA_{K,\ Na}$ with increasing salt concentration (Figures 5A–C). During this period, the $ST_{K,\ Na}$ of the leaves of the three species of willow increased slightly at low salt concentrations (171 mM or 342 mM) and then decreased. Then, from the 5th day, the $SA_{K,\ Na}$ of the roots and leaves of the three species of willow showed an overall balance or gradual decrease with increasing salt concentration and prolonged stress time. The higher the salt concentration and the longer the time was, the more significant the difference was. For *Salix matsudana* and *Salix gordejevii*, the $SA_{K,\ Na}$ of their roots were higher than those of their leaves at the beginning of salt stress, but with the increase in salt concentration and prolonged stress time, the $SA_{K,\ Na}$ of their roots were finally lower than those of their leaves. During the change, *Salix matsudana* maintained a longer time than *Salix gordejevii*, and the $SA_{K,\ Na}$ of roots were higher than those of leaves. For *Salix linearistipularis*, the $SA_{K,\ Na}$ of roots were lower than those of leaves. Under the same NaCl treatment level, *Salix linearistipularis* had higher $SA_{K,\ Na}$ of leaves than *Salix matsudana* and *Salix gordejevii*, and with the increase in salinity, the $SA_{K,\ Na}$ of leaves of *Salix linearistipularis* decreased slowly and were inferior to those of *Salix matsudana* and *Salix gordejevii*. Although the $SA_{K,\ Na}$ of the roots of the three tree species decreased in a similar trend with increasing salinity, *Salix linearistipularis* had an obliviously lower decline than *Salix matsudana* and *Salix gordejevii*. In general, under salt stress, *Salix linearistipularis* had the highest $SA_{K,\ Na}$ of leaves but the lowest $SA_{K,\ Na}$ of roots.

Under normal growth conditions, the three tree species had basically the same $SA_{Ca,\ Na}$ (Figures 6A–C). On the first day of salt stress, the $SA_{Ca,\ Na}$ of the leaves of *Salix matsudana* increased with the increasing amounts of salt treatment. *Salix gordejevii* showed different degrees of increase after 1–5 days of treatment, and its increasing trend was affected by both stress concentration and stress time, with an increase in a short time (1 day) and a tendency of selective increase at low concentrations with the extension of time (3–5 days). The $SA_{Ca,\ Na}$ of *Salix linearistipularis* showed a transient increase at a salt

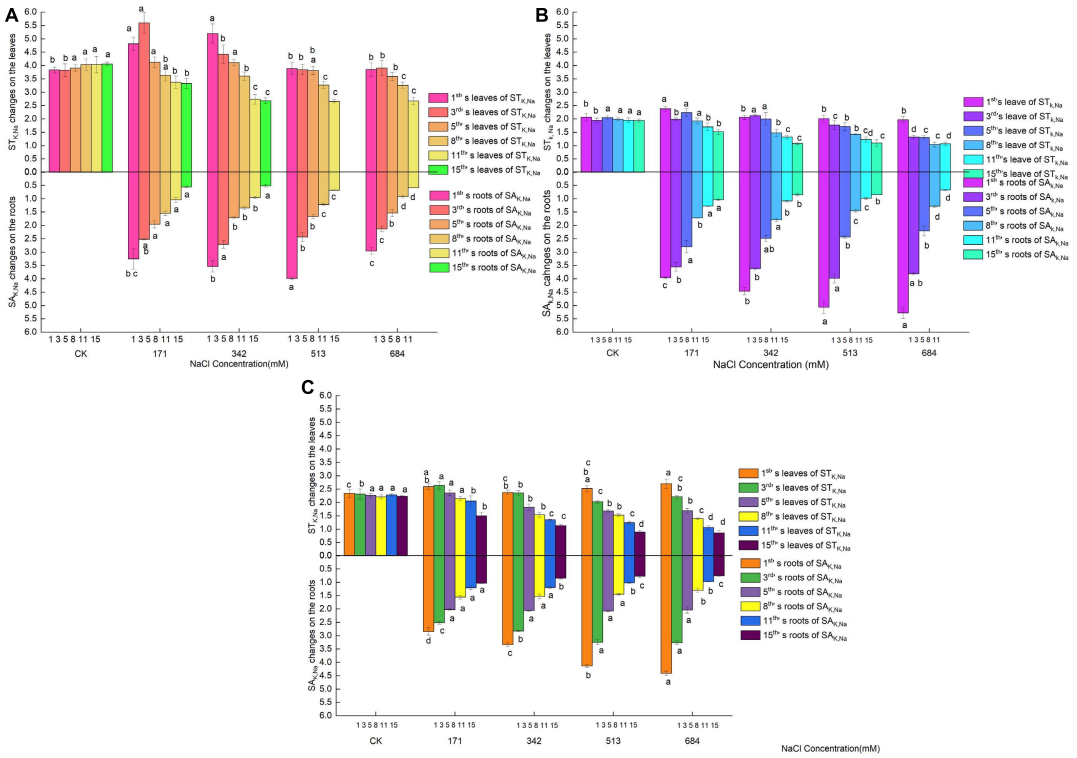


FIGURE 5
Changes of K^+ absorption and transport in roots and leaves of three willow species. **(A)** *Salix linearistipularis*; **(B)** *Salix matsudana*; **(C)** *Salix gordejevii*.

concentration of 171 mM on the 3rd day and then continued to decrease. Then, the $SA_{Ca,\ Na}$ of the leaves of the three species of willow decreased gradually with increasing salt concentration and over time. Large disparities existed among the three in the $SA_{Ca,\ Na}$ of roots. With the increase in the salt concentration, the increased $SA_{Ca,\ Na}$ of *Salix gordejevii* lasted for 8 days, followed by *Salix linearistipularis* (3 days) and *Salix matsudana* (1 day). Under the same treatment level, *Salix linearistipularis* presented the highest $SA_{Ca,\ Na}$ of roots, followed by *Salix matsudana* and *Salix gordejevii*. All three species had much higher $SA_{Ca,\ Na}$ in the leaves than in the roots. In general, under salt stress, *Salix matsudana* and *Salix gordejevii* maintained higher $SA_{Ca,\ Na}$ of leaves among the three species, but the $SA_{Ca,\ Na}$ of their roots were at a lower level. *Salix linearistipularis* had the highest $SA_{Ca,\ Na}$ of roots and the lowest $SA_{Ca,\ Na}$ of leaves.

Changes in Na^+/K^+ and Na^+/Ca^{2+} contents in the roots and leaves of the three tree species under salt stress

With the aggravation of salt stress and the passage of time, the Na^+/K^+ and Na^+/Ca^{2+} contents in roots and leaves increased significantly (Figure 7). Long-term salt stress at low salt concentrations and short-term salt stress at high salt concentrations could both make salinity in roots and leaves reach relatively high levels. At different salinity levels, the Na^+/K^+ and Na^+/Ca^{2+} contents in the roots were generally higher than those in the leaves, indicating that plants can reduce the damage of salt stress to aboveground tissues by regulating ion transport. No significant difference existed among *Salix linearistipularis*, *Salix matsudana,* and *Salix gordejevii* in Na^+/K^+ contents in roots, but *Salix linearistipularis* had apparently lower Na^+/K^+ contents in roots than *Salix matsudana* and *Salix gordejevii*, which indicates a strong effect on the inhibition of Na^+ or selective absorption of K^+ by its leaves (Figures 7A–C).

On the first day of salt stress, the growth rate of Na^+/Ca^{2+} in different concentrations of *Salix gordejevii* root was higher than that of the other two willows compared with CK (Figures 8A–C). Among them, the growth rate of Na^+/Ca^{2+} in the root system of *Salix matsudana* is the lowest. In the first 3 days, the Na^+/Ca^{2+} of willow root leaves showed an increasing trend compared with CK, but the difference was not significant. With the increased salt stress, the growth rate of Na^+/Ca^{2+} contents in the leaves and roots of *Salix gordejevii* were higher than those of *Salix linearistipularis* and *Salix matsudana*. This indicates that with the increased stress, the relative absorption of Na^+ by

Salix gordejevii increases greatly, while its selective absorption of Ca^{2+} becomes relatively weakened.

Correlation of Na^+, Na^+/K^+, and Na^+/Ca^{2+} contents in the roots and leaves of three tree species under salt stress

Taking the Na^+, Na^+/K^+, and Na^+/Ca^{2+} contents in leaves as dependent variables and Na^+, Na^+/K^+, and Na^+/Ca^{2+} contents in roots as independent variables for curve estimation, we built correlation equations. **Figure 9A** shows that with the aggravation of salt stress, the Na^+ contents in roots gradually increased, and the Na^+ transported from roots to leaves also increased. *Salix linearistipularis* had the highest degree of Na^+ correlation between roots and leaves (Eq. 3; $R^2 = 0.9762$). *Salix gordejevii* ranked second (Eq. 4) ($R^2 = 0.976$). *Salix matsudana* presented the lowest degree of correlation (Eq. 5) ($R^2 = 0.9594$). The three tree species presented higher root-leaf Na^+/K^+ correlations than root-leaf Na^+ correlations (**Figure 9B**). *Salix matsudana* presented the highest degree of correlation (Eq. 6) ($R^2 = 0.9908$). *Salix linearistipularis* ranked second (Eq. 7) ($R^2 = 0.9884$). *Salix gordejevii* presented the lowest degree of correlation (Eq. 8) ($R^2 = 0.9865$). Among the three tree species (**Figure 9C**), *Salix linearistipularis* presented the highest root-leaf Na^+/Ca^{2+} correlation (Eq. 9) ($R^2 = 0.9974$), followed by *Salix matsudana* (Eq. 10) ($R^2 = 0.9952$) and *Salix gordejevii* (Eq. 11) ($R^2 = 0.9871$).

$$y = 0.0008x^3 + 0.0249x^2 + 0.1499x^1 + 0.5734 \quad (3)$$

$$y = -0.0008x^3 + 0.0821x^2 - 1.2345x^1 + 8.5981 \quad (4)$$

$$y = -0.0011x^3 + 0.1129x^2 - 2.1363x^1 + 14.867 \quad (5)$$

$$y = 0.0191x^2 + 0.8135x^1 - 0.1936 \quad (6)$$

$$y = 0.01x^2 + 0.2853x^1 - 0.0388 \quad (7)$$

$$y = 0.1022x^2 + 0.4004x^1 - 0.024 \quad (8)$$

$$y = 0.0008x^2 + 0.3141x^1 - 0.2362 \quad (9)$$

$$y = 0.0005x^2 + 0.268x^1 - 0.2427 \quad (10)$$

$$y = 0.002x^2 + 0.414x^1 - 0.0977 \quad (11)$$

In this study, the root-leaf Na^+ accumulative concentration was used to fit the correlation equation, and the threshold of Na^+ absorption and rejection by the roots of *Salix matsudana* and *Salix gordejevii* was obtained as the fitting inflection point. The research results showed that when the Na^+ content in the roots of *Salix matsudana* reached 34.21 mg/g and the Na^+ content in leaves reached 29.88 mg/g, and when the Na^+ content in the roots of *Salix gordejevii* reached 34.21 mg/g and the Na^+ content in leaves reached 30.42 mg/g, the two willow species had the maximum root rejection capacity.

Discussion

Effects of salt stress on the phenotypes of three willow species

Under salt stress, plants adjust their own physiological and biochemical reactions, change their morphological structure and the selectivity of the protoplasmic membrane to absorb or reject ions, and increase the water content in their bodies to improve their saline-alkaline resistance (Guo et al., 2020; Zhang G .C. et al., 2020; Fahad et al., 2021a,c,f; Shah et al., 2021). Roots are the first organs of plants to contact, sense and respond to the salt environment (Tan et al., 2020). Under salt stress, the number and volume of roots of Zea mays L. both decrease (Wang et al., 2020). The results of this study also verified this conclusion: The time when roots change reflects the sensitivity of plants to salt stress. The yellowing and abscission of plant leaves is the most direct manifestation of the state of salt stress (Jimenez-Casas and Zwiazek, 2014). The higher the NaCl concentration is, the more serious the damage to plant leaves is. The degree of damage in descending order is *Salix linearistipularis* > *Salix gordejevii* > *Salix matsudana*. The change of leaf phenotype in this paper is not only related to the excessive accumulation of Na^+ in plant leaves, but also the low content of K^+ and Ca^{2+}, which is related to the toxicity to plants. Moreover, salt stress is actually a physiological drought phenomenon. Plants reduce water consumption by weakening the binding ability between pigment and pigment protein, degrading chlorophyll, reducing photosynthesis, and closing stomata to reduce water consumption, thereby maintaining their own stability.

Changes in Na^+, K^+, and Ca^{2+} contents in roots and leaves of three species under salt stress

Under salt stress, Na^+ is the main harmful ion that limits plant growth and causes salt damage (Li et al., 2019). The mechanism of ion accumulation and transport in plants under salt stress has always been a hot research topic. The localization of ions, the interception at roots, and the inhibition of transport

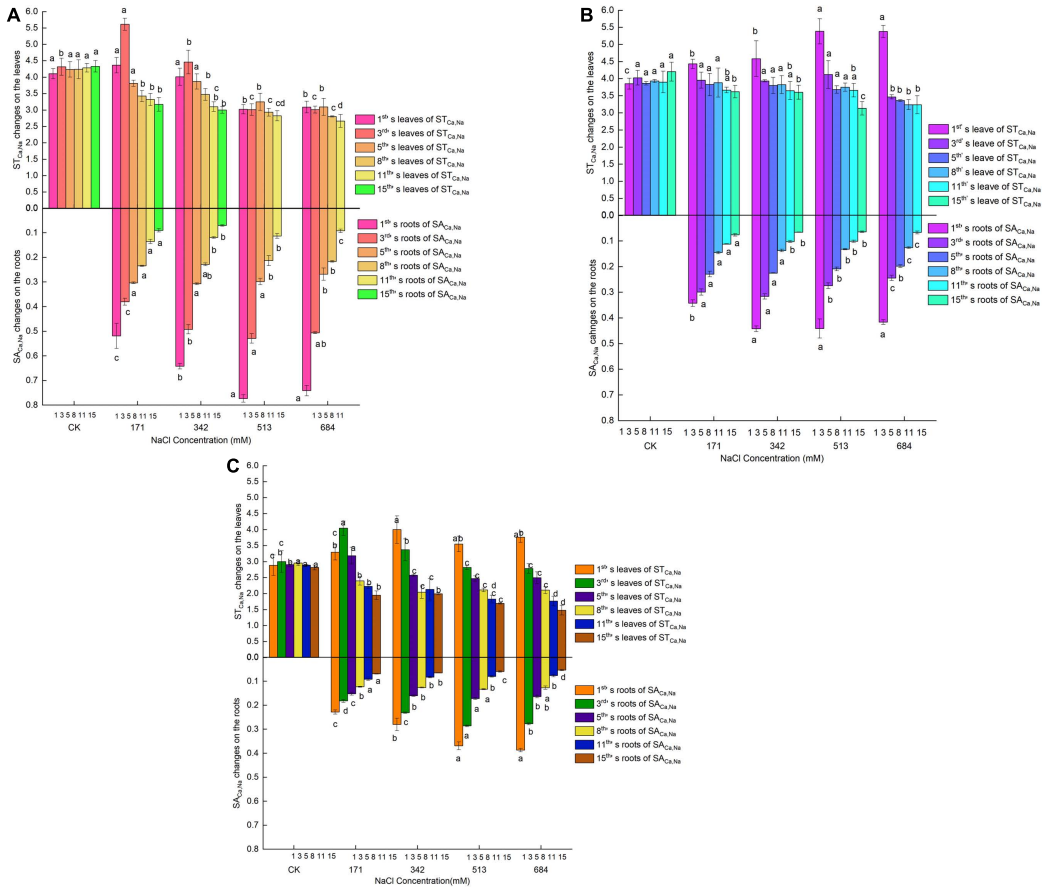


FIGURE 6
Changes of Ca^{2+} absorption and transport in roots and leaves of three willow species. **(A)** *Salix linearistipularis*; **(B)** *Salix matsudana*; **(C)** *Salix gordejevii*.

to shoots are the main ways in which plants respond to salt stress (Storey et al., 2003). In this experiment, compared with the control, salt stress increased the Na^+ contents in the roots and leaves of the seedlings, and the Na^+ contents in the roots were higher than those in the leaves. This result shows that the three plants all have a certain Na^+ interception ability. But there are some differences in interception ability. *Salix linearistipularis* has a stronger interception ability than *Salix matsudana* and *Salix gordejevii*. In this study, with the aggravation of salt stress and prolonged time, the Na^+ contents in root and leaf tissues increased significantly, and the corresponding K^+ contents continued to decrease, which was mainly affected by the accumulation of Na^+. In addition, Na^+ presents an apparent competitive inhibitory effect on the absorption and active sites of K^+, which caused plants under salt stress to suffer from damage both from Na^+ and insufficient K^+ (Shabala and Cuin, 2008). Therefore, K^+ content in roots and leaves of plants decreased with the aggravation of salt stress (Li et al., 2022).

The imbalance of Ca^{2+} is the primary response to NaCl stress. In this study, with the aggravation of salt stress and prolonged time, the Ca^{2+} of the three willows was continuously replaced by Na^+, with the contents of Ca^{2+} decreasing continuously. However, there were differences among tree species, and the Ca^{2+} stabilization ability of *Salix gordejevii* was higher than that of *Salix matsudana* and *Salix linearistipularis*. This is related to the difference in the selective absorption capacity of Ca^{2+} among different tree species after salt stress. The uptake of ions by plants in response to salt stress is affected by the plant species, stress intensity and time.

Responses of selective absorption and transport of irons to salt stress

The ion selective transport coefficient represents the selective ability of plants to ion upward transport. The greater the selective transport coefficient of nutrient ions under salt stress is, the stronger the ability of plants to promote the upward transport of nutrient ions and inhibit the upward transport of salt ions is. The more salt ions that are trapped in the root, the

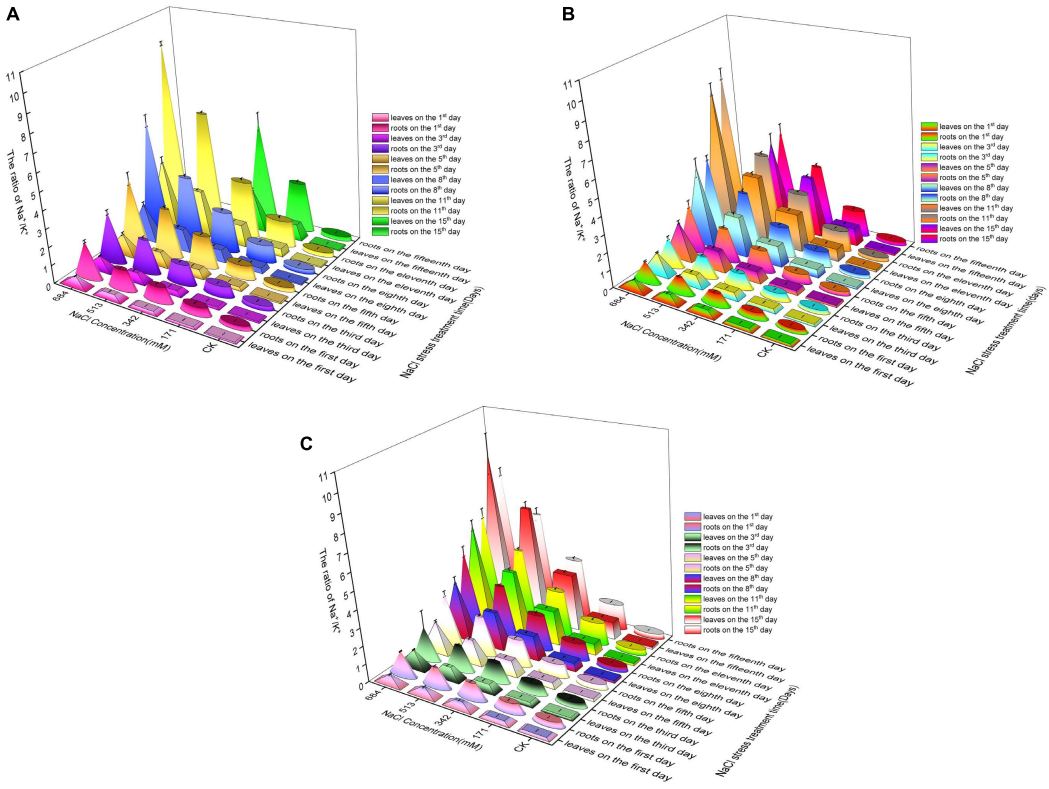


FIGURE 7
Effects of salt stress on Na^+/K^+ in roots and leaves of three willow species. Changes of Na^+/K^+ in roots and leaves of three willow species. **(A)** *Salix linearistipularis*; **(B)** *Salix matsudana*; **(C)** *Salix gordejevii*.

stronger its salt tolerance is Teakle et al. (2007). Liu et al. (2014) found that the $SA_{K,\ Na}$ and $SA_{Ca,\ Na}$ of the roots of Elaeagnus angustifolia were much higher than those of other tissues. After salt stress, the $SA_{K,\ Na}$ and $SA_{Ca,\ Na}$ of leaves increased, showing a higher ability of Elaeagnus angustifolia to selectively transport K^+ and Ca^{2+} from roots to leaves. Wu et al. (2017) found that the $SA_{K,\ Na}$ and $SA_{Ca,\ Na}$ of the leaves and roots of blueberry experienced a process of decrease-increase-decrease.

In this study, the selective absorption capacity of K^+ of the three willow species was affected by the variety, location and time. In the early stage of salt stress, the selective absorption capacity of K^+ is enhanced to reject Na^+ to maintain ion balance. This effect is stressful and has limited ability. With the increase in stress concentration and prolonged time, the accumulation of Na^+ in plants will cause ion imbalance until the selective absorption capacity of K^+ is lost. The $SA_{K,\ Na}$ significantly vary according to different varieties and parts. *Salix linearistipularis* presents higher $SA_{K,\ Na}$ of leaves than those of *Salix matsudana* and *Salix gordejevii*, but the $SA_{K,\ Na}$ of its roots are at the lowest level, which may be related to the different salt tolerance mechanisms of different willows.

The three willows had a selective absorption capacity of Ca^{2+} similar to that of K^+. Although *Salix gordejevii* has outstanding performance in the $SA_{Ca,\ Na}$ enhancement of roots and leaves, it is still lower than that of *Salix linearistipularis* and *Salix matsudana*. *Salix linearistipularis* presented the highest $SA_{Ca,\ Na}$ of roots and the lowest $SA_{Ca,\ Na}$ of leaves. Under high salt stress, the selective transport capacity of ions of the three willow trees decreased, possibly due to the accumulation of Na^+ causing smaller stomatal opening of plant leaves, decreased transpiration, increased cell membrane permeability and ion toxicity.

Effects of salt stress on the Na^+/K^+ and Na^+/Ca^{2+} ratios of roots and leaves

Na^+ has a strong competitive effect on the absorption of K^+. The strategy of most salt-tolerant plants is to prevent excessive Na^+ from entering cells or accelerate Na^+ excretion while increasing the absorption of K^+ and transporting it upward to reduce salt damage (Wakeel et al., 2011). Ca^{2+} participates in plant stress resistance signal transduction and regulates the response of plants to stress changes (Orhan Şenol et al., 2009; Cao et al., 2020). The ratios of Na^+/K^+ and Na^+/Ca^{2+} are often used to represent the degree of damage to ion balance caused by salt stress (Poustini and Siosemardeh, 2004; Manaa et al., 2013; Yang and Guo, 2018).

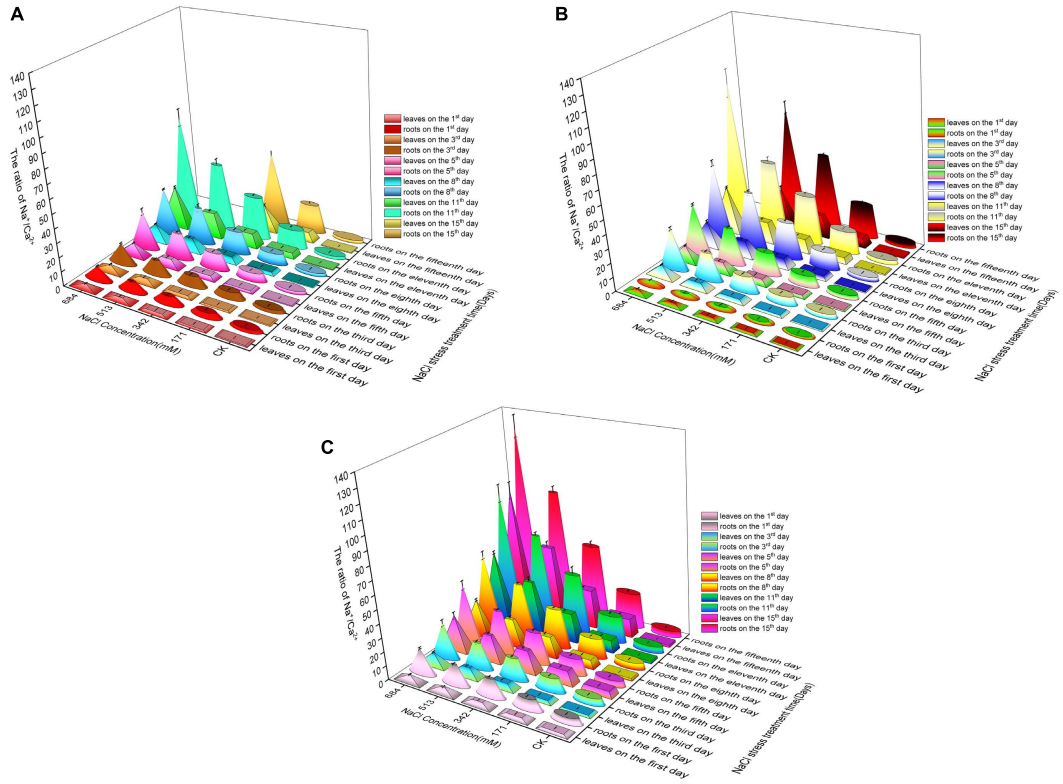


FIGURE 8
Effects of salt stress on Na^+/Ca^{2+} in roots and leaves of three willow species. **(A)** *Salix linearistipularis*; **(B)** *Salix matsudana*; **(C)** *Salix gordejevii*.

In this study, the Na^+/K^+ and Na^+/Ca^{2+} contents in the roots and leaves of the three tree species increased significantly with increasing NaCl stress concentration and stress duration, which is consistent with the ion metabolism characteristics of *Hordeum vulgare* and wheat (Mahlooji et al., 2018; Guo et al., 2021). The reason is that the influx of Na^+ will directly interfere with and inhibit the absorption and transport of K^+ and Ca^{2+} by the cytoplasmic membrane, resulting in ion imbalance, and the ratio of Na^+/K^+ and Na^+/Ca^{2+} of each organ will rise. This study also found that long-term stress at low salt concentrations and short-term stress at high salt concentrations could both lead to higher levels of salinity in roots and leaves. At different salt levels, the ratio of roots Na^+/K^+ and Na^+/Ca^{2+} was generally higher than that of leaves. This shows that all three willow trees can reduce the damage of salt stress to aboveground tissues by regulating the selection and transport of ions.

Analysis of root-leaf ion ratio correlation and threshold under salt stress

The root system is the first organ to face salt stress. The nutrient ions of the aerial part come from transport by roots (Fahad and Bano, 2012). In this study, Lowess (William, 1979) was used to fit the correlation equations of Na^+, Na^+/K^+, and Na^+/Ca^{2+} contents in roots and leaves. Overall, the three species of willow had the highest correlation of Na^+/Ca^{2+} contents in roots and leaves, followed by Na^+/K^+ and then Na^+. It may be that the influx of Na^+ affects the many ions that plants already have. Ions also interact with each other. Studies have confirmed that the presence of Ca^{2+} can also inhibit the efflux of K^+ (Guo et al., 2015), which leads to a high Na^+/Ca^{2+} correlation and a low Na^+ correlation.

The salt adaptation mechanism of plants mainly includes salt avoidance and salt tolerance. The former mainly avoids the accumulation of large amounts of salt ions by means of salt rejection, salt dilution or salt excretion. The latter can tolerate higher concentrations of salt ions in their bodies. The determination of the salt tolerance threshold of plants mainly focused on *Suaeda salsa*, *Plantago coronopus* (L.) and seagrass. They used the salt concentration at the beginning of a decline in the survival and growth rate of plants as a threshold (Koyro, 2006; Koch et al., 2007; He et al., 2017). Plant roots are directly exposed to Na^+, and the Na^+ content in roots accumulates with increasing salt concentration and the passage of time. Once the accumulation of Na^+ contents in roots exceeds the threshold value and the rejection capacity of the roots is broken

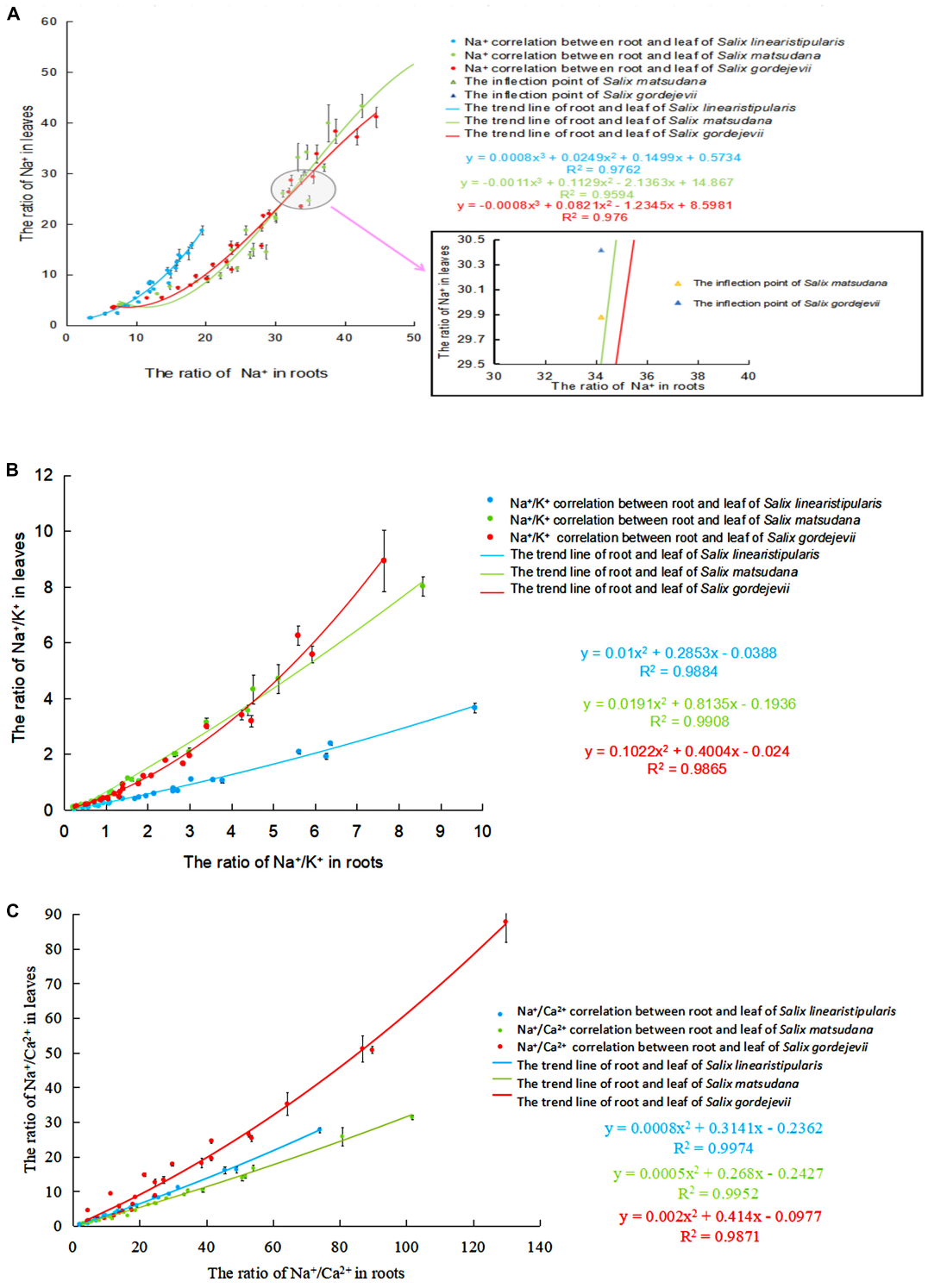


FIGURE 9
Correlation of Na^+, Na^+/K^+, and Na^+/Ca^{2+} in roots and leaves of three willows under salt stress. **(A)** Na^+ correlation; **(B)** Na^+/K^+ correlation; **(C)** Na^+/Ca^{2+} correlation.

through. Then a large amount of Na^+ enters the leaves, and the selective ion absorption capacity becomes weak, which easily leads to the death of the plant. *Salix linearistipularis* has a different mechanism in response to salt stress. It is a salt-rejecting tree species, and the Na^+ content range is very narrow for its roots and leaves. The Na^+ contents in leaves increased with the content increase in roots (the second derivation of the equation). It manifests itself as the selectivity of leaf leaves for Na^+ absorption does not diminish with the increase of root Na^+. Therefore, it cannot be fitted to its threshold with leaf and root Na^+ content.

Conclusion

Based on the above research and analysis, there are differences among three willows in ion absorption and distribution to different degrees under salt stress. The number of roots decreased with increased salt stress, followed by wilted, yellowed, curled, and dropped leaves. The selective absorption of Ca^{2+} and $K^+$by the three willow species was affected by variety, location and time, and the selective absorption was stressful and had limited regulation ability. During the stress process, the Na^+/K^+ and Na^+/Ca^{2+} in root and leaf organs were significantly increased. The Na^+/Ca^{2+} had the highest correlation.

When the Na^+ contents in the roots of *Salix matsudana* and *Salix gordejevii* reached 34.21 mg/g, the interception of Na^+ in their roots reached the maximum. The range of Na^+ contents in the roots and leaves of *Salix linearistipularis* is very narrow, so it is unable to fit thresholds with Na^+ contents in roots and leaves. In general, *Salix matsudana* and *Salix gordejevii* are salt-tolerant, and they grow stably under long-term high salt and short-term low salt environment, respectively. However, *Salix linearistipularis* is more suitable for planting as an indicative plant because of its sensitivity to salt stress.

Currently, some studies have shown that there is a strong correlation between the ion flow rate and various physiological indicators. In the future, we will use non-invasive micro-testing (NMT) technology to further explore the dynamic transport process of ion flux in willow cells and the mechanism of salt tolerance.

Data availability statement

The original contributions presented in the study are included in the article/**Supplementary material**, further inquiries can be directed to the corresponding authors.

Author contributions

XR performed conceptualization. XR and BL performed writing-original draft. XW performed investigation. XH, CM, and BL performed data curation. HL and BL performed resources. CM and BL performed methodology. BL, YW, ZH, and JL performed formal analysis. BL performed funding acquisition, writing-review, and editing. All authors commented on previous versions of the manuscript, read and approved the final manuscript, and contributed to the study conception and design.

Funding

This work was supported by Natural Science foundation of Hebei Province (grant nos. 22326806D and 17226320D-4). The former funded the publication of the paper and the latter funded the implementation of the experiment.

Supplementary material

The Supplementary Material for this article can be found online at: https://www.frontiersin.org/articles/10.3389/fpls.2022.969896/full#supplementary-material

References

Aghaleh, M., Niknam, V., Ebrahimzadeh, H., and Razavi, K. (2011). Effect of salt stress on physiological and antioxidative responses in two species of *Salicornia* (*S. persica* and *S. europaea*). *Acta Physiol. Plant.* 33, 1261–1270. doi: 10.1007/s11738-010-0656-x

Altaf, M. A., Shahid, R., Ren, M. X., Altaf, M. M., Khan, L. U., Shahid, S., et al. (2021). Melatonin alleviates salt damage in tomato seedling: a root architecture system, photosynthetic capacity, ion homeostasis, and antioxidant enzymes analysis. *Sci. Hortic.* 285:110145. doi: 10.1016/j.scienta.2021.110145

Ayars, J. E., Christen, E. W., and Hornbuckle, J. W. (2006). Controlled drainage for improved water management in arid regions irrigated agriculture. *Agric. Water Manag.* 86, 128–139. doi: 10.1016/j.agwat.2006.07.004

Banakar, M. H., Amiri, H., Ardakani, M. R. S., and Ranjbar, G. H. (2022). Susceptibility and tolerance of fenugreek (Trigonella foenum-graceum L.) to salt stress: physiological and biochemical inspections. *Environ. Exp. Bot.* 194:104748. doi: 10.1016/j.envexpbot.2021.104748

Bian, A. N., and Lu, L. M. (2022). Mechanism of physiological difference in response to substrate salinity and salt spray of Barringtoniaracemosa seedlings. *Plant Physiol. J.* 58, 415–424. Available online at: https://kns.cnki.net/kcms/detail/detail.aspx?FileName=ZWSL202202019&DbName=DKFX2022

Butcher, K., Wick, A. F., Desutter, T., Chatterjee, A., and Harmon, J. (2016). Soil salinity: a threat to global food security. *Agron. J.* 108, 2189–2200. doi: 10.2134/agronj2016.06.0368

Cao, Y., Zhang, M., Liang, X. Y., Li, F. R., Shi, Y. L., Yang, X. H., et al. (2020). Natural variation of an EF-hand Ca^{2+} -binding-protein coding gene confers saline-alkaline tolerance in maize. *Nat. Commun.* 11:186. doi: 10.1038/s41467-019-14027-y

Djanaguiraman, M., Sheeba, J. A., Shanker, A. K., Devi, D. D., and Bangarusamy, U. (2006). Rice can acclimate to lethal level of salinity by pretreatment with sublethal level of salinity through osmotic adjustment. *Plant Soil* 284, 363–373. doi: 10.1007/s11104-006-0043-y

Fahad, S., and Bano, A. (2012). Effect of salicylic acid on physiological and biochemical characterization of maize grown in saline area. *Pak. J. Bot.* 44, 1433–1438.

Fahad, S., Hasanuzzaman, M., Alam, M., Ullah, H., Saeed, M., Ali, K. I, et al. (eds) (2020). *Environment, Climate, Plant and Vegetation Growth*. New York, NY: Springer Nature, doi: 10.1007/978-3-030-49732-3

Fahad, S., Nie, L., Chen, Y., Wu, C., Xiong, D., Saud, S., et al. (2015b). Crop plant hormones and environmental stress. *Sust. Agric. Rev.* 15, 371–400.

Fahad, S., Hussain, S., Matloob, A., Khan, F. A., Khaliq, A., Saud, S., et al. (2015a). Phytohormones and plant responses to salinity stress: a review. *Plant Growth Regul.* 75, 391–404. doi: 10.1007/s10725-014-0013-y

Fahad, S., Sonmez, O., Saud, S., Wang, D., Wu, C., Adnan, M., et al. (eds) (2021b). *Climate Change and Plants: Biodiversity, Growth and Interactions, Footprints of Climate Variability on Plant Diversity*. Boca Raton, FL: CRC Press.

Fahad, S., Sönmez, O., Saud, S., Wang, D., Wu, C., Adnan, M., et al. (eds) (2021e). *Engineering Tolerance in Crop Plants Against Abiotic Stress, Footprints of Climate Variability on Plant Diversity*. Boca Raton, FL: CRC Press.

Fahad, S., Sönmez, O., Saud, S., Wang, D., Wu, C., Adnan, M., et al. (eds) (2021a). *Plant Growth Regulators for Climate-Smart Agriculture Footprints of Climate Variability on Plant Diversity*. Boca Raton, FL: CRC Press.

Fahad, S., Sonmez, O., Saud, S., Wang, D., Wu, C., Adnan, M., et al. (eds) (2021c). *Developing Climate Resilient Crops: Improving Global Food Security and Safety, Footprints of Climate Variability on Plant Diversity*. Boca Raton, FL: CRC Press.

Fahad, S., Saud, S., Yajun, C., Chao, W., and Depeng, W. (eds) (2021f). *Abiotic Stress in Plants*. London: IntechOpen, doi: 10.5772/intechopen.91549

Feng, G. X., Zhang, Z. Y., Wan, C. Y., Lu, P. R., and Bakour, A. (2017). Effects of saline water irrigation on soil salinity and yield of summer maize (*Zea* mays L) in subsurface drainage system. *Agric. Water Manag.* 193, 205–213. doi: 10.1016/j.agwat.2017.07.026

Feng, S., Sun, H. W., Ma, H. P., Zhang, X., Ma, S. R., Qiao, K., et al. (2020). Sexual Differences in Physiological and Transcriptional Responses to Salinity Stress of Salix linearistipularis. *Front. Plant Sci.* 11:517962. doi: 10.3389/fpls.2020.517962

Gao, Z. Q., Zhang, J. Y., Zhang, J., Zhang, W. X., Zheng, L. L., Borjigin, T., et al. (2022). Nitric oxide alleviates salt-induced stress damage by regulating the ascorbate–glutathione cycle and Na^+/K^+ homeostasis in Nitraria tangutorum Bobr. *Plant Physiol. Biochem.* 173, 46–58. doi: 10.1016/j.plaphy.2022.01.017

Gerona, M. E. B., Deocampo, M. P., Egdane, J. A., Ismail, A. M., and Dionisio-Sese, M. L. (2019). Physiological responses of contrasting rice genotypes to salt stress at reproductive stage. *Rice Sci.* 26, 207–219. doi: 10.1016/j.rsci.2019.05.001

Guo, H., Huang, Z., Li, M., and Hou, Z. N. (2020). Growth, ionic homeostasis, and physiological responses of cotton under different salt and alkali stresses. *Sci. Rep.* 10:21844. doi: 10.1038/s41598-020-79045-z

Guo, R., Yang, Z. Z., Li, F., Yan, C. G., Zhong, X. L., Liu, Q., et al. (2015). Comparative metabolic responses and adaptive strategies of wheat (*Triticum aestivum*) to salt and alkali stress. *BMC Plant Biol.* 15:170. doi: 10.1186/s12870-015-0546-x

Guo, W. W., Han, X. F., Zhang, Y. M., Shi, C. H., Zhang, H. S., Lin, Q., et al. (2021). Effects of Salt Stress on Absorption And Distribution of Osmotic Ions in Wheat Seedlings. *Bangladesh J. Bot.* 50, 1209–1214. doi: 10.3329/bjb.v50i4.57091

Hasan, M. M., Alabdallah, N. M., Alharbi, B. M., Waseem, M., Yao, G., Liu, X. D., et al. (2021). GABA: a key player in drought stress resistance in plants. *Int. J. Mol. Sci.* 22:10136. doi: 10.3390/ijms221810136

He, Q., Silliman, B. R., and Cui, B. S. (2017). Incorporating thresholds into understanding salinity tolerance: a study using salt-tolerant plants in salt marshes. *Ecol. Evol.* 7, 6326–6333. doi: 10.1002/ece3.3209

Hou, L. F., Li, X., He, X. L., Zuo, Y. L., Zhang, D. D., and Zhao, L. L. (2021). Effect of dark septate endophytes on plant performance of Artemisia ordosica and associated soil microbial functional group abundance under salt stress. *Appl. Soil Ecol.* 165:103998. doi: 10.1016/j.apsoil.2021.103998

Jimenez-Casas, M., and Zwiazek, J. J. (2014). Adventitious sprouting of Pinus leiophylla in response to salt stress. *Ann. For. Sci.* 71, 811–819. doi: 10.1007/s13595-014-0379-z

Karunasinghe, T. G., Al-Mahmooli, I. H., Al-Sadi, A. M., and Velazhahan, R. (2020). The effect of salt-tolerant antagonistic bacteria from tomato rhizosphere on plant growth promotion and damping-off disease suppression under salt-stress conditions. *Acta Agric. Scand. Sec. B Soil Plant Sci.* 70, 69–75. doi: 10.1080/09064710.2019.1668956

Kim, B. M., Lee, H. J., Song, Y. H., and Kim, H. J. (2020). Effect of salt stress on the growth, mineral contents, and metabolite profiles of spinach. *J. Sci. Food Agric.* 101, 3787–3794. doi: 10.1002/jsfa.11011

Koch, M. S., Schopmeyer, S. A., Kyhn-Hansen, C., Madden, C. J., and Peters, J. S. (2007). Tropical seagrass species tolerance to hypersalinity stress. *Aquat. Bot.* 86, 14–24. doi: 10.1016/j.aquabot.2006.08.003

Koyro, H. W. (2006). Effect of salinity on growth, photosynthesis, water relations and solute composition of the potential cash crop halophyte *Plantago coronopus* (L.). *Environ. Exp. Bot.* 56, 136–146. doi: 10.1016/j.envexpbot.2005.02.001

Kurunc, A., Aslan, G. E., Karaca, C., Tezcan, A., Turgut, K., Karhan, M., et al. (2020). Effects of salt source and irrigation water salinity on growth, yield and quality parameters of *Stevia rebaudiana* Bertoni. *Sci. Hortic.* 270:109458. doi: 10.1016/j.scienta.2020.109458

Li, L. X., Zhu, T. T., Liu, J., Zhao, C., Li, L. Y., and Chen, M. (2019). An orthogonal test of the effect of NO_3^-, PO_4^{3-}, K, and Ca^{2+} on the growth and ion absorption of *Elaeagnus angustifolia* L. seedlings under salt stress. *Acta Physiol. Plant* 41:179. doi: 10.1007/s11738-019-2969-8

Li, N., Cao, B., Chen, Z. J., and Xu, K. (2022). Root morphology ion absorption and antioxidative defense system of two Chinese cabbage cultivars (*Brassica rapa* L.) reveal the different adaptation mechanisms to salt and alkali stress. *Protoplasma* 259, 385–398. doi: 10.1007/s00709-021-01675-5

Li, X. Y., Liu, D. M., Wang, J., and Jian, S. G. (2021). Morphological, biochemical and physiological responses of a tropical coastal plant *Guettarda speciosa* to salt stress. *Glob. Ecol. Conserv.* 32:e01887. doi: 10.1016/j.gecco.2021.e01887

Li, Y. L., Su, X. H., Zhang, B. Y., Huang, Q. J., Zhang, X. H., and Huang, R. F. (2009). Expression of jasmonic ethylene responsive factor gene in transgenic poplar tree leads to increased salt tolerance. *Tree Physiol.* 29, 273–279. doi: 10.1093/treephys/tpn025

Litalien, A., and Zeeb, B. A. (2020). Curing the earth: a review of anthropogenic soil salinization and plant-based strategies for sustainable mitigation. *Sci. Total Environ.* 698:134235. doi: 10.1016/j.scitotenv.2019.134235

Liu, T., Cui, H. J., Wu, S. J., Zhu, J. Y., and Zhou, Z. Q. (2013). Response of photosynthetic and fluorescence characteristics of Japanese yew seedlings to different light conditions. *J. Beijing For. Univ.* 35, 65–73. doi: 10.13332/j.1000-1522.2013.03.018

Liu, Y., Wang, L., Li, X., and Luo, M. (2022). Detailed sphingolipid profile responded to salt stress in cotton root and the GhIPCS1 is involved in the regulation of plant salt tolerance. *Plant Sci.* 316:111174. doi: 10.1016/j.plantsci.2021.111174

Liu, Z. X., Zhang, H. X., Yang, X. Y., Liu, T., and Di, W. B. (2014). Growth, and cationic absorption, transportation and allocation of Elaeagnus angustifolia seedlings under NaCl stress. *Acta Ecol. Sin.* 34, 326–336.

Ma, S. G., Zhou, X. P., Jahan, M. S., Guo, S. R., Tian, M. M., Zhou, R. R., et al. (2022). Putrescine regulates stomatal opening of cucumber leaves under salt stress via the H_2O_2-mediated signaling pathway. *Plant Physiol. Biochem.* 170, 87–97. doi: 10.1016/j.plaphy.2021.11.028

Maggio, A., Raimondi, G., Martino, A., and Pascale, S. D. (2007). Salt stress response in tomato beyond the salinity tolerance threshold. *Environ. Exp. Bot.* 59, 276–282. doi: 10.1016/j.envexpbot.2006.02.002

Mahlooji, M., Seyed, S. R., Razmjoo, J., Sabzalian, M. R., and Sedghi, M. (2018). Effect of salt stress on photosynthesis and physiological parameters of three contrasting barley genotypes. *Photosynthetica* 56, 549–556. doi: 10.1007/s11099-017-0699-y

Manaa, A., Faurobert, M., Valot, B., Bouchet, J. P., Grasselly, D., Causse, M., et al. (2013). Effect of salinity and calcium on tomato fruit proteome. *OMICS* 17, 338–352. doi: 10.1089/omi.2012.0108

Markus-Michalczyk, H., Hanelt, D., Ludewig, K., Müller, D., Schröter, B., and Jensen, K. (2014). Salt intrusion in tidal wetlands: european willow species tolerate oligohaline conditions. *Estuar. Coast. Shelf Sci.* 136, 35–42. doi: 10.1016/j.ecss.2013.11.008

Meng, N., Huang, J. H., Jia, R., Rui, M., and Wei, S. H. (2020). Effect of Chloride Channel Blockerson lon Absorption, Transport and Content of Glycine max Seedlings under NaCI Induced Stress. *Acta Agric. Boreali Occidentalis Sin.* 29, 1814–1821. doi: 10.7606/ji.ssn.1004-1389.2020.12.006

Ni, L. J., Wang, Z. Q., Liu, X. D., Wu, S. T., Hua, J. F., Liu, L., et al. (2022). Genome-wide study of the GRAS gene family in *Hibiscus hamabo* Sieb. et Zucc and analysis of HhGRAS14-induced drought and salt stress tolerance in *Arabidopsis*. *Plant Sci.* 319:111260. doi: 10.1016/j.plantsci.2022.111260

Orhan Şenol, F. S., Gülpinar, A. R., Kartal, M., Şekeroglu, N., Deveci, M., Kan, Y., et al. (2009). Acetylcholinesterase inhibitory and antioxidant properties

of Cyclotrichium niveum, Thymus praecox subsp. caucasicus var. caucasicus, *Echinacea purpurea* and *E. pallida*. *Food Chem. Toxicol.* 47, 1304–1310. doi: 10.1016/j.fct.2009.03.004

Poustini, K., and Siosemardeh, A. (2004). Ion distribution in wheat cultivars in response to salinity stress. *Field Crops Res.* 85, 125–133. doi: 10.1016/S0378-4290(03)00157-6

Rabiei, Z., Hosseini, S. J., Pirdashti, H., and Hazrati, S. (2020). Physiological and biochemical traits in coriander affected by plant growth-promoting rhizobacteria under salt stress. *Heliyon* 6:e05321. doi: 10.1016/j.heliyon.2020.e05321

Regni, L., Del Pino, A. M., Mousavi, S., Palmerini, C. A., Baldoni, L., Mariotti, R., et al. (2019). Behavior of four olive cultivars during salt stress. *Front. Plant Sci.* 10:867. doi: 10.3389/fpls.2019.00867

Shabala, S., and Cuin, T. A. (2008). Potassium transport and plant salt tolerance. *Physiol. Plant.* 133, 651–669. doi: 10.1111/j.1399-3054.2007.01008.x

Shah, A. N., Tanveer, M., Abbas, A., Fahad, S., Baloch, M. S., Ahmad, M. I., et al. (2021). Targeting salt stress coping mechanisms for stress tolerance in *Brassica*: a research perspective. *Plant Physiol. Biochem.* 158, 53–64. doi: 10.1016/j.plaphy.2020.11.044

Shao, H. B., Chu, L. Y., Lu, H. Y., Qi, W. C., Chen, X., Liu, J., et al. (2019). Towards sustainable agriculture for the salt - affected soil. *Land Degrad. Dev.* 30, 574–579. doi: 10.1002/ldr.3218

Sheikh, A. T., Mugera, A., Pandit, R., Burton, M., and Davies, S. (2022). What determines the time to gypsum adoption to remediate irrigated salt-affected agricultural lands? Evidence from Punjab, Pakistan. *Soil Tillage Res.* 217:105266. doi: 10.1016/j.still.2021.105266

Shu, S., Tang, Y. Y., Zhou, X. P., Jahan, M. S., Sun, J., Wang, Y., et al. (2020). Physiological mechanism of transglutaminase-mediated improvement in salt tolerance of cucumber seedlings. *Plant Physiol. Biochem.* 156, 333–344. doi: 10.1016/j.plaphy.2020.09.010

Storey, R., Schachtman, D. P., and Thomas, M. R. (2003). Root structure and cellular chloride, sodium and potassium distribution in salinized grapevines. *Plant Cell Environ.* 26, 789–800. doi: 10.1046/j.1365-3040.2003.01005.x

Sui, D. Z. (2006). *Effect of Salt on Growth of Willow Clones Seedings*. Ph.D thesis. Nanjin: Nanjing Forestry University. .

Tan, J. L., Alon, B. G., Shtein, I., Bustan, A., Dag, A., and Erel, R. (2020). Root structural plasticity enhances salt tolerance in mature olives. *Environ. Exp. Bot.* 179:104224. doi: 10.1016/j.envexpbot.2020.104224

Teakle, N. L., Flowers, T. J., Real, D., and Colmer, T. D. (2007). Lotus tenuis tolerates the interactive effects of salinity and waterlogging by 'excluding' na^{+} and cl from the xylem. *J. Exp. Bot.* 8, 2169–2180. doi: 10.1093/jxb/erm102

Tian, S. C., and Li, Y. X. (2018). Effects of the Soils with Different Salt Contents on the Seedling Growth of Salix psammophila'Yanliu-11. *J. Northwest For. Univ.* 33, 120–125.

Wakeel, A., Farooq, M., Qadir, M., and Schubert, S. (2011). Potassium Substitution by Sodium in Plants. *Crit. Rev. Plant Sci.* 30, 401–413. doi: 10.1080/07352689.2011.587728

Wang, H., Liang, L. Y., Liu, S., An, T. T., Fang, Y., Xu, B. C., et al. (2020). Maize genotypes with deep root systems tolerate salt stress better than those with shallow root systems during early growth. *J. Agron. Crop Sci.* 206, 711–721. doi: 10.1111/jac.12437

Wang, X., Wang, W., Huang, J., Peng, S., and Xiong, D. (2018). Diffusional conductance to CO_2 is the key limitation to photosynthesis in salt-stressed leaves of rice (*Oryza sativa*). *Physiol. Plant.* 163, 45–58. doi: 10.1111/ppl.12653

Warmiński, K., Stolarski, M. J., Gil, Ł, and Krzyżaniak, M. (2021). Willow bark and wood as a source of bioactive compounds and bioenergy feedstock. *Ind. Crops Prod.* 171:113976. doi: 10.1016/j.indcrop.2021.113976

William, S. C. (1979). Robust Locally Weighted Regression and Smoothing Scatterplots. *J. Am. Stat. Assoc.* 74, 829–836. doi: 10.1080/01621459.1979.10481038

Wu, F. Z., Zhu, X. W., Hu, Y. F., Wang, H. X., and Chen, Y. M. (2017). Effects of NaCl Stress on Growth lon Uptake, Transportation and Distribution of Two Blueberry (*Vaccinium corymbosum*) Cultivars Seedlings. *Sci. Silvae Sin.* 53, 40–49.

Wu, J. Q., Liu, W. K., Jahan, M. S., Shu, S. J., Sun, J., and Guo, S. R. (2022). Characterization of polyamine oxidase genes in cucumber and roles of CsPAO3 in response to salt stress. *Environ. Exp. Bot.* 194:104696. doi: 10.1016/j.envexpbot.2021.104696

Xia, S. P., Guo, S. W., Xu, Y. Y., and Li, P. F. (2018). The Regulation of Accumulation and Secretion of Several Major Inorganic Cations by Chinese Iris under NaCI Stress. *J. Plant Nutr.* 41, 67–79. doi: 10.1080/01904167.2017.1381726

Yang, S. (2010). *Study on Selection and Evaluation Criteria of Salinitytolerance Tree Species in Coastal Region*. Ph.D thesis. Beijing: Chinese Academy of Forestry.

Yang, X. Y., Zhang, W. H., Wang, Q. Y., and Liu, Y. L. (2003). Salt tolerance of wild soybeans in Jiangsu and its relation with ionic distribution and selective transportation. *Chin. J. Appl. Ecol.* 12, 2237–2240.

Yang, Y., and Guo, Y. (2018). Elucidating the molecular mechanisms mediating plant salt-stress responses. *New Phytol.* 217, 523–539. doi: 10.1111/nph.14920

Zhang, G. C., Dai, L. X., Ding, H., Ci, D. W., Ning, T. Y., Yang, J. S., et al. (2020). Response and adaptation to the accumulation and distribution of photosynthetic product in peanut under salt stress. *J. Integr. Agric.* 19, 690–699. doi: 10.1016/S2095-3119(19)62608-0

Zhang, H. M., Zhu, J. H., Gong, Z. Z., and Zhu, J. K. (2022). Abiotic stress responses in plants. *Nat. Rev. Genet.* 23, 104–119. doi: 10.1038/s41576-021-00413-0

Zhang, J., Shi, S. Z., Jiang, Y., Zhong, F., Liu, G. Y., Yu, C. M., et al. (2021). Genome-wide investigation of the AP2/ERF superfamily and their expression under salt stress in Chinese willow (*Salix matsudana*). *PeerJ* 9:e11076. doi: 10.7717/peerj.11076

Zhang, K. H., Tang, J. R., Wang, Y., Kang, H. Y., and Zeng, J. (2020). The tolerance to saline–alkaline stress was dependent on the roots in wheat. *Physiol. Mol. Biol. Plants* 26, 947–954. doi: 10.1007/s12298-020-00799-x

Zhang, M. X., Dong, Z., Li, H. L., Wang, Q., Liang, Y., and Han, X. F. (2018). Improvement Effects of Different Ulmus Pumila Strains on Coastal Saline Alkali Soil and Distribution and Absorption of Salt Ions. *J. Soil Water Conserv.* 32, 340–345.

Zhao, Y. G., Wang, S. J., Li, Y., Zhuo, Y. Q., and Liu, J. (2019). Effects of straw layer and flue gas desulfurization gypsum treatments on soil salinity and sodicity in relation to sunflower yield. *Geoderma* 352, 13–21. doi: 10.1016/j.geoderma.2019.06.004

Zhu, H. L., Li, D., He, Y. Y., and Feng, X. D. (2019). Effect of water stress on the photo response characteristics of Jujube Pears. *J. Yan'an Univ.* 38, 72–75. doi: 10.13876/J.cnki.ydnse.2019.04.072

Zhu, Y. F., Jia, X. M., Wu, Y. X., Hu, Y., Cheng, L., Zhao, T., et al. (2020). Quantitative proteomic analysis of *Malus halliana* exposed to salt-alkali mixed stress reveals alterations in energy metabolism and stress regulation. *Plant Growth Regul.* 90, 205–222. doi: 10.1007/s10725-019-00563-6

Zhu, Y. X., Yin, J. L., Liang, Y. F., Liu, J. Q., Jia, J. H., Huo, H., et al. (2019). Transcriptomic dynamics provide an insight into the mechanism for silicon-mediated alleviation of salt stress in cucumber plants. *Ecotoxicol. Environ. Saf.* 174, 245–254. doi: 10.1016/j.ecoenv.2019.02.075

Zobolo, A. M., and Khumalo, G. P. (2017). Growth and nutrient content of *Ansellia africana* treated with Hoagland' s solution. *S. Af. J. Bot.* 100:376. doi: 10.1016/j.sajb.2017.01.202

frontiers | Frontiers in Plant Science

TYPE Original Research
PUBLISHED 18 August 2022
DOI 10.3389/fpls.2022.984233

Check for updates

OPEN ACCESS

EDITED BY
Mehtab Muhammad Aslam,
The Chinese University of Hong Kong,
Hong Kong SAR, China

REVIEWED BY
Antt Htet Wai,
Yangon University of Education
(YUOE), Myanmar
Umashankar Chandrasekaran,
Shanghai Center for Plant Stress
Biology, Shanghai Institute
for Biological Sciences (CAS), China

*CORRESPONDENCE
Xiaoping Niu
xpniu0613@126.com

SPECIALTY SECTION
This article was submitted to
Plant Abiotic Stress,
a section of the journal
Frontiers in Plant Science

RECEIVED 01 July 2022
ACCEPTED 01 August 2022
PUBLISHED 18 August 2022

CITATION
Chen M, She Z, Aslam M, Liu T,
Wang Z, Qi J and Niu X (2022)
Genomic insights of the *WRKY* genes
in kenaf (*Hibiscus cannabinus* L.) reveal
that *HcWRKY44* improves the plant's
tolerance to the salinity stress.
Front. Plant Sci. 13:984233.
doi: 10.3389/fpls.2022.984233

COPYRIGHT
© 2022 Chen, She, Aslam, Liu, Wang,
Qi and Niu. This is an open-access
article distributed under the terms of
the Creative Commons Attribution
License (CC BY). The use, distribution
or reproduction in other forums is
permitted, provided the original
author(s) and the copyright owner(s)
are credited and that the original
publication in this journal is cited, in
accordance with accepted academic
practice. No use, distribution or
reproduction is permitted which does
not comply with these terms.

Genomic insights of the *WRKY* genes in kenaf (*Hibiscus cannabinus* L.) reveal that *HcWRKY44* improves the plant's tolerance to the salinity stress

Meixia Chen[1], Zeyuan She[2], Mohammad Aslam[3], Ting Liu[1,3], Zerong Wang[1,3], Jianmin Qi[3] and Xiaoping Niu[3]*

[1]Industry and University Research Cooperation Demonstration Base in Fujian Province, College of Life Sciences, Ningde Normal University, Ningde, China, [2]State Key Laboratory for Conservation and Utilization of Subtropical Agro-Bioresources, College of Agriculture, Guangxi University, Nanning, China, [3]College of Life Science, Fujian Provincial Key Laboratory of Haixia Applied Plant Systems Biology, Fujian Agriculture and Forestry University, Fuzhou, China

The WRKY transcription factors (TFs) are among the most diverse TF families of plants. They are implicated in various processes related to plant growth and stress response. Kenaf (*Hibiscus cannabinus* L.), an important fiber crop, has many applications, including the phytoremediation of saline-alkaline soil. However, the roles of WRKY TFs in kenaf are rarely studied. In the present study, 46 kenaf WRKY genes were genome-widely identified and characterized by gene structure, phylogeny and expression pattern analysis. Furthermore, the *HcWRKY44* gene was functionally characterized in *Arabidopsis* under salinity and drought stresses. HcWRKY44 is a nuclear-localized protein that is positively induced by salinity and drought, with roots showing maximum accumulation of its transcripts. Under NaCl and abscisic acid (ABA) stress conditions, plants overexpressing *HcWRKY44* had higher germination rates, better root growth and increased survival than control plants; however, it did not improve the ability to withstand drought stress. Moreover, ABA signaling genes (*ABI1*, *ABI2*, and *ABI5*), ABA-responsive genes (*ABF4*, *RD29B*, *COR15A*, *COR47*, and *RD22*), stress-related genes (*STZ*, *P5CS*, and *KIN1*), and ionic homeostasis-related genes (*SOS1*, *AHA1*, *AHA2*, and *HKT1*) were positively induced in *HcWRKY44* transgenic plants under NaCl treatment. These results suggest that *HcWRKY44* improved plant's tolerance to salt stress but not osmotic stress through an ABA-mediated pathway. In summary, this study provides provided comprehensive information about *HcWRKY* genes and revealed that *HcWRKY44* is involved in salinity tolerance and ABA signaling.

KEYWORDS

kenaf (*Hibiscus cannabinus* L.), WRKY, salinity, drought, ABA

Introduction

Abiotic stresses, such as drought, salinity, and temperature extremes, are major environmental factors affecting plant growth and development (Zhu, 2016). To overcome these adverse conditions, plants have developed multiple defense strategies to adapt directly and/or indirectly. Conceptually, the adaptive responses could be classified into osmotic adjustment and basic defenses, including ion detoxification and growth regulation (Dang et al., 2013; Ding et al., 2014). During the stress responses, phytohormone abscisic acid (ABA) is essential in regulating osmotic responses and stress-responsive gene expression (Cutler et al., 2010; Ding et al., 2014; Zhu, 2016). From the perception of the ABA signal to the activation of the relevant protein kinases, phosphatases and transcription factors, the ABA signaling pathway has been thoroughly explored (Fujii and Zhu, 2009; Fujii et al., 2009; Cutler et al., 2010;Jiang et al., 2012; Luo et al., 2013; Ding et al., 2014). Many transcription factors have been reported to respond against osmotic stresses in both ABA-independent and ABA-dependent manner (Rushton et al., 2012; Ding et al., 2014; Zhu, 2016).

WRKY genes play a crucial role in responding to osmotic stress by indirectly and/or directly binding to the promoters of ABA-regulated genes such ABFs, ABI4, ABI5, and DREBs (Jiang et al., 2012; Bakshi and Oelmuller, 2014; Wani et al., 2021). In *Arabidopsis*, *AtWRKY63* and *AtWRKY57* are involved in regulating the ABA signaling pathway and enhancing plant tolerance to drought (Ren et al., 2010; Jiang et al., 2012). Similarly, *OsWRKY24*, *OsWRKY45*, *OsWRKY72*, and *OsWRKY77* also improved salinity tolerance in rice through ABA signaling (Xie et al., 2005). In wheat, overexpression of *TaWRKY2* and *TaWRKY19* enhanced tolerance to salinity stress by directly binding to the regulatory elements of well-known ABA signaling genes *DREB2A*, *RD29A*, *RD29B*, and *COR6.6* (Niu et al., 2012). Consistently, overexpression of *GsWRKY20* and *HcWRKY50* also improved drought tolerance by regulating ABA-mediated stomatal aperture (Luo et al., 2013; Niu et al., 2022).

Kenaf (*Hibiscus cannabinus* L.) is a diploid (2n = 36) herbaceous fiber crop belonging to the Malvaceae family. Kenaf was domesticated in Africa and is grown in the Asia-Pacific region as the third natural fiber species after cotton and jute (Chen P. et al., 2020; Zhang et al., 2020; Sim and Nyam, 2021). Kenaf can produce enormous amounts of fiber biomass with up to 100–150 t per hectare and grows quickly, reaching heights of 4–6 m over a 4-month growth period (**Supplementary Figure 1**) (Chen P. et al., 2020; Sim and Nyam, 2021). Kenaf has been widely applied in papermaking, building materials, biocomposites, animal feed, and recycled plastics due to its colossal fiber yield and biodegradable nature (Niu et al., 2015; Sim and Nyam, 2021). More importantly, kenaf performs well and has a high tolerance for drought, salinity, and barrenness (Danalatos and Archontoulis, 2010; Ramesh, 2016; Sim and Nyam, 2021). Therefore, kenaf could be used in phytoremediation of saline-alkali soil and/or as an osmotic-stress tolerant crop. However, its tolerance mechanism is still unclear, and how WRKY genes in kenaf regulate the tolerance remains obscure.

In this study, we performed a genome-wide identification of kenaf WRKY transcription factors and analyzed the gene structure, evolutionary relationship, and expression pattern of *HcWRKYs*. The results showed that the drought and salinity stress could positively induce *HcWRKY44*. Besides, *HcWRKY44* overexpression plants improved the tolerance to salinity stress but not drought stress. We further revealed that *HcWRKY44* increased plant tolerance to salinity stress through modulating the ABA signaling pathways.

Materials and methods

Identification and characterization of *WRKY* genes in *Hibiscus cannabinus*

The *HcWRKY* gene sequences were retrieved from the kenaf genome database[1] (Zhang et al., 2020). The sequence data of a kenaf relative species, *Gossypium hirsutum*, and other species were acquired from the Phytozome v13 database. The HMM model of the WRKY domain (PF03106) was used as the query to search the kenaf genome database. The resulting candidate WRKY genes were further confirmed by the CDD program to verify the C_XH_X domain and WRKYGQK domain. The properties of HcWRKY proteins, such as amino acid length, molecular weight (MW), and isoelectric point (pI), were predicted using ExPASy-Compute pI/Mw tool as described previously (She et al., 2022).

Phylogenetic analysis, chromosome localization, and syntenic analysis

Multiple sequence alignment of *Arabidopsis thaliana*, *G. hirsutum*, and *Hibiscus cannabinus* WRKY proteins were conducted by MUSCLE, using the default setting parameters. The maximum number was 20, and minimum/maximum width was 6/50, and the results were visualized by Jalview software. The phylogenetic tree was generated by the MEGA 7.0 program using the ML method based on the JTT substitution model. The loci of *HcWRKY* genes were retrieved from the kenaf annotation GFF3 files and gene locations on the chromosomes were visualized by TBtools (Chen C. et al., 2020). MCScanX software was used for collinearity analysis and generating collinearity blocks with the threshold value of 1×10^{-5} (Wang et al., 2012). The collinearity block

1 http://ngdc.cncb.ac.cn/gwh/Assembly/1033/show

mapping within the kenaf, *Arabidopsis*, and cotton genome were visualized by CIRCOS software. *Ka* and *Ks* values of paralogous genes were estimated by the K-estmator program, and *Ks* value was used for estimating time of segmental duplication events according to the method descripted by Chen et al. (2014).

Plant materials and growth conditions

Kenaf (*H. cannabinus* L.) cultivar Fuhong 992 was used in this study. The seeds were washed three times in running water and then cultured under controlled conditions at 28°C for 16 h in light and 26°C for 8 h in the dark with a relative humidity of 65–75%. For stress treatments, 2 weeks old healthy seedlings were cultivated in a solution containing 200 mM NaCl for salt stress and 15%(w/v) PEG6000 for osmotic stress treatment, according to the previously described method (Niu et al., 2015). Afterward, healthy seedlings were selected, and leaves were harvested from each treatment for further analysis (Niu et al., 2016).

Arabidopsis thaliana ecotype (Col-0) was cultured in a walk-in growth chamber at 22°C under a 16 h light/8 h dark cycle. For the differential expression analysis of the ABA-related or stress-responsive marker genes, the WT and transgenic lines (2-week-old) were treated with 15% (w/v) PEG6000, 200 mM NaCl, and 100 mM ABA, respectively. After the treatment, samples were harvested and used for further analysis.

RNA extraction, qRT-PCR, and gene expression analysis

Total RNA was isolated from independently collected samples using the Ultrapure RNA kit (CW0597, Beijing, China). The cDNA was synthesized according to the instruction manual of the Reverse Transcription Kit (Pimerscript^{TM} RT DRR037S TaKaRa, Japan), then used as PCR templates and/or qRT-PCR analysis. For sequencing, the amplified products were purified and ligated into the pMD18-T vector and then transformed into *Escherichia coli* DH5α cells. The qRT-PCR analysis was conducted using the qPCR SuperMix TransStart Top Green (TransGen, AQ132-11) on the Bio-Rad CFX-96 detection system with the following amplification programs of 94°C for 30 s, and 40 cycles of 94°C for 5 s, 60°C for 15 s, and a melting curve cycle from 65°C to 95°C. For normalization of *HcWRKYs*, *HcTUBα* (Niu et al., 2015) in kenaf and *AtACT2* in *Arabidopsis* were used. The primers used in qRT-PCR are listed in **Supplementary Table 1**. Each reaction was performed in three independent biological and three technical replicates.

Vector construction, subcellular localization, and transgenic transformation

The full-length CDS of *HcWRKY44* without terminator code was amplified from kenaf cDNA, and the PCR products were inserted into the pENTR$^{TM/D}$-topo vector. After sequencing, the positive clones were selected and recombined into the destination vector pGWB605. Finally, the positive plasmids were transformed into *Agrobacterium tumefaciens* GV3101 strain, which was used for *Arabidopsis* transformation. The 4-week-old plants of *A. thaliana* ecotype (Col-0) were transformed by the vacuum infiltration method using the 35S:*HcWRKY44-GFP* and 35S:GFP constructs. The T_1 transgenic seedlings were sprayed with 20 mg/L herbicide, and the positive T_1 lines were selected. The T_2 plants were further selected and separated, and the homozygous lines of T_3 generations were used for the subsequent experimental analysis. For subcellular localization analysis, the 35S:HcWRKY44-GFP constructs and the control 35S:GFP vector were introduced into the epidermal leaves of *Nicotiana benthamiana* and incubated in the dark for 36–48 h. GFP fluorescence signals were checked using an Olympus confocal microscope (Olympus FV500, Olympus, Japan) under a 488 nm exciting wavelength.

Stress treatments and physiological indexes measurement

For the stress treatments, the seeds of the *HcWRKY44*-transgenic lines and wild-type plants were surfaced-sterilized and then germinated on 1/2 MS agar medium with 200 and 300 mM mannitol to mimic the drought stress and with 150 and 200 mM NaCl for the salinity stress. The physiological indexes, such as germination rate, cotyledon greening, root length and survival rate assays, were measured and the corresponding phenotypes were photographed according to the methods described by Niu et al. (2022). For the relative electrolyte leakage measurement, the methods were referred to the reference described by Zhang et al. (2019). All assays were performed in three independent replicates.

Results

Identification and sequence characteristic of *HcWRKY* genes

A HMMER-BLASTP-InterProScan module method was used to identify the sequences containing the PF03106 domain and acquire the *WRKY* gene sequences in the kenaf genome. A total of 46 WRKY genes were identified in the kenaf

10.3389/fpls.2022.984233

TABLE 1 Protein information of *WRKY* genes in *Hibiscus cannabinus* L.

Gene name	Sequence ID	Chr	Length (aa)	MW (Da)	pI	Start	End
HcWRKY1	Hca.09G0003050-mRNA-1	Chr01	279	30,300.4	5.45	3073671	3074868
HcWRKY2	Hca.09G0009010-mRNA-1	Chr01	168	19,681.7	9.96	9047060	9048758
HcWRKY3	Hca.09G0011890-mRNA-1	Chr01	87	10,187.2	8.65	12928402	12929857
HcWRKY4	Hca.15G0005800-mRNA-1	Chr02	75	8,508.8	8.98	4689666	4689896
HcWRKY5	Hca.02G0001850-mRNA-1	Chr03	271	31,279.2	10.14	1267661	1269284
HcWRKY6	Hca.02G0005160-mRNA-1	Chr03	568	65,096.4	10.58	3421780	3424316
HcWRKY7	Hca.02G0024890-mRNA-1	Chr03	753	82,146.0	6.75	43156687	43163885
HcWRKY8	Hca.02G0034140-mRNA-1	Chr03	321	36,211.3	9.95	62393653	62396111
HcWRKY9	Hca.05G0017730-mRNA-1	Chr04	516	56,048.9	7.91	18360321	18363735
HcWRKY10	Hca.04G0001080-mRNA-1	Chr05	442	48,905.5	6.79	608483	610352
HcWRKY11	Hca.04G0008740-mRNA-1	Chr05	169	20,053.5	9.79	6956048	6958475
HcWRKY12	Hca.04G0026330-mRNA-1	Chr05	296	33,431.8	9.43	53398166	53399779
HcWRKY13	Hca.04G0028600-mRNA-1	Chr05	451	51,515.7	9.44	56198561	56200359
HcWRKY14	Hca.04G0029560-mRNA-1	Chr05	334	37,790.5	7.32	57223233	57225693
HcWRKY15	Hca.06G0008140-mRNA-1	Chr06	475	53,582.1	9.68	9983084	9986596
HcWRKY16	Hca.06G0019130-mRNA-1	Chr06	335	38,125.0	9.98	41779704	41781801
HcWRKY17	Hca.06G0030610-mRNA-1	Chr06	344	38,905.3	8.24	53411699	53413593
HcWRKY18	Hca.06G0041200-mRNA-1	Chr06	461	51,185.7	8.76	60729845	60731531
HcWRKY19	Hca.06G0041680-mRNA-1	Chr06	522	58,845.4	8.81	61029866	61032786
HcWRKY20	Hca.06G0043260-mRNA-1	Chr06	474	51,271.1	5.21	61929508	61931194
HcWRKY21	Hca.17G0006480-mRNA-1	Chr07	511	57,557.3	8.84	8797109	8799519
HcWRKY22	Hca.17G0018560-mRNA-1	Chr07	1142	132,719.9	9.36	38815933	38833317
HcWRKY23	Hca.17G0024970-mRNA-1	Chr07	294	33,882.0	10.72	44264516	44265589
HcWRKY24	Hca.17G0025330-mRNA-1	Chr07	403	42,950.4	5.22	44503418	44505152
HcWRKY25	Hca.08G0021600-mRNA-1	Chr08	305	33,119.2	7.79	21488822	21490559
HcWRKY26	Hca.08G0022540-mRNA-1	Chr08	199	23,528.0	10.28	22656914	22657706
HcWRKY27	Hca.07G0005140-mRNA-1	Chr09	228	26,557.6	9.47	9913278	9916495
HcWRKY28	Hca.07G0034360-mRNA-1	Chr09	298	33,275.3	8.55	53662401	53664551
HcWRKY29	Hca.07G0034910-mRNA-1	Chr09	443	47,988.0	4.70	54065803	54069060
HcWRKY30	Hca.07G0044750-mRNA-1	Chr09	100	11,957.9	9.85	60534662	60535445
HcWRKY31	Hca.07G0045110-mRNA-1	Chr09	521	58,456.4	10.28	60735546	60739983
HcWRKY32	Hca.18G0000330-mRNA-1	Chr11	296	32,318.3	10.14	1784500	1786194
HcWRKY33	Hca.18G0023790-mRNA-1	Chr11	163	20,311.3	10.03	40498640	40500411
HcWRKY34	Hca.01G0010340-mRNA-1	Chr12	304	35,221.0	10.15	10294517	10296388
HcWRKY35	Hca.01G0035190-mRNA-1	Chr12	277	31,706.4	6.39	63477812	63480069
HcWRKY36	Hca.01G0053260-mRNA-1	Chr12	497	55,961.4	9.21	77209926	77213030
HcWRKY37	Hca.10G0002810-mRNA-1	Chr13	337	37,923.1	9.85	2994415	2997891
HcWRKY38	Hca.10G0029300-mRNA-1	Chr13	350	39,007.0	8.69	57365445	57372383
HcWRKY39	Hca.10G0029380-mRNA-1	Chr13	487	52,380.6	7.62	57427418	57430001
HcWRKY40	Hca.14G0009150-mRNA-1	Chr15	245	27,933.4	11.49	10588296	10589385
HcWRKY41	Hca.14G0010950-mRNA-1	Chr15	518	57,214.5	10.10	11925152	11927979
HcWRKY42	Hca.16G0001160-mRNA-1	Chr16	923	107,621.3	10.60	883843	888625
HcWRKY43	Hca.03G0015230-mRNA-1	Chr17	329	36,992.9	5.08	19064622	19066261
HcWRKY44	Hca.03G0036480-mRNA-1	Chr17	356	40,158.6	7.44	64342190	64344301
HcWRKY45	Hca.03G0042970-mRNA-1	Chr17	306	34,240.4	9.51	69378612	69380101
HcWRKY46	Hca.03G0043540-mRNA-1	Chr17	421	45,242.9	7.17	69869256	69871431

genome with the complete WRKY domain (Table 1). Based on the gene distribution information on the chromosomes, the identified genes were named from *HcWRKY1* to *HcWRKY46*. The physicochemical analysis revealed that the amino acid length of HcWRKY ranged from 75 aa (HcWRKY4) to 1142 aa (HcWRKY22), and the corresponding protein MWs ranged

from 8508.8 to 132719.9 Da, and the predicted theoretical pIs of HcWRKYs ranged from 4.70 (HcWRKY29) to 11.49 (HcWRKY40) (Table 1).

To further confirm these *HcWRKY* genes, the typical conserved WRKYGQK domain was searched and visualized. According to the conserved 60 amino acids of the WRKY domain, the HcWRKY proteins were classified into three groups, and each group was divided into different subgroups. For example, the group I could be divided into I-N and I-C subgroups, which possessed two WRKY domains and $CX_4C_{22-23}HXH$ zinc finger structures. Group II was divided into five subgroups (II-a, II-b, II-c, II-d, and II-e), each containing 3, 6, 11, 5, and 8 members, with the structure of WRKYGQK and $CX_5C_{23}HXH$ in the II-a, II-b, II-d, and II-e subgroups except for II-c subgroup. On the other hand, group III had 7 members with the zinc finger structure of WRKYGQK and $CX_7C_{23}HXC$ at the C-terminal (Supplementary Figure 2). The WRKY proteins of kenaf generally had the same WRKYGQK domain as *Arabidopsis*, with the exception that the WRKYGQK domains of HcWRKY3 were changed into WRKYGKK and the QRKYGQK domains for HcWRKY35, as well as additional amino acid variations outside the WRKYGQK domains in *HcWRKY9/19/28/27/30/37* (Supplementary Figure 2). These results indicated that those mutated HcWRKY genes might gain a novel function during evolution.

Phylogenetic analysis, gene structure, and synteny analysis

The gene structure analysis revealed that natural mutation occurred in *HcWRKY* genes of kenaf, i.e., some WRKYGQK domains were changed into WRKYGKK, WRKYGEK and WRKYGQE. To further investigate the divergence of *HcWRKYs*, a comparative phylogenetic tree was constructed using the maximum-likelihood (ML) method between 46 *HcWRKYs* and 71 *AtWRKYs*. Expectedly, the phylogenetic tree classified the *WRKY* genes into groups I, II, and III and group II was also divided into five subgroups (II-a, II-b, II-c, II-d, and II-e) (Figure 1), indicating that these *HcWRKYs* may share the similar functions with that in *Arabidopsis* (Figure 1).

The *HcWRKYs* introns and exons investigation revealed a variable number of exons ranging from 1 to 18 (Figure 2). Group I *HcWRKY* genes had 1–5 introns, Group IIa had 4-6 introns, Group IIb, IIc, IId, IIe and III had 1-4 introns, with some exceptions for *HcWRKY22* (24 introns), *HcWRKY25* (5 introns), and *HcWRKY10* (0 introns) (Figure 2). On the other hand, gene motifs analysis showed the similar motifs shared in the each subgroups. For example, motif 1, 2, 3, and 5 jointly possessed in Group I, motif 2, 4, and 5 possessed in Group IIb and IIe (Figure 2). These findings indicate that exon and intron numbers vary between groups but are nearly constant within the same group.

The tandem and segment duplication events were also analyzed and identified using MCScanX software to understand the evolution of *HcWRKY* genes. The results showed 6 segmental duplication syntenic gene pairs (*HcWRKY1/HcWRKY40*, *HcWRKY5/HcWRKY17*, *HcWRKY8/HcWRKY16*, *HcWRKY18HcWRKY20*, *HcWRKY28/HcWRKY45*, *HcWRKY29/HcWRKY46*) (Figure 3A and Supplementary Table 2), and 11 tandem duplication gene pairs (*HcWRKY1/2/3*, *HcWRKY5/6*, *HcWRKY13/14*, *HcWRKY18/19/20*, *HcWRKY23/24*, *HcWRKY25/26*, *HcWRKY28/29*, *HcWRKY30/31*, *HcWRKY38/39*, *HcWRKY40/41*, *HcWRKY45/46*) in kenaf. In addition, the evolutionary dates of duplicated *HcWRKY* genes were also estimated using *Ks* as the proxy for time (Supplementary Table 2), the results showed that kenaf duplication events for kenaf 6 of 17 pairs occurred within the past 12.385–165.717 million years (Supplementary Table 2). These results suggested that during their evolution, both segmental and tandem duplications contributed to the gene expansion of *HcWRKYs*. In addition, the syntenic blocks were comparatively analyzed among *H. cannabinus*, *A. thaliana*, and *G. hirsutum* and 16 orthologous syntenic gene pairs were identified between *H. cannabinus* and *A. thaliana* (Figure 3B and Supplementary Table 3). Interestingly, one *HcWRKY* gene could match two or more *HcWRKY* genes, i.e., *HcWRKY39* could align with *AtWRKY3/4*, and *HcWRKY5* could match with *AtWRKY23/68* (Figure 3B and Supplementary Table 3). For *H. cannabinus* and its most relative *G. hirsutum*, 64 syntenic orthologous gene pairs were found, and a similar phenomenon of one *HcWRKY* syntenic with two or three *GhWRKYs* was also observed (Figure 3B and Supplementary Table 4).

Expression pattern analysis of *HcWRKYs* in different tissues and treatments

The expression pattern of genes is often associated with their specific gene function. Therefore, we examined the expression level of 20 *HcWRKYs* using qRT-PCR analysis to explore the *HcWRKYs* functions. The results for the various tissues revealed that the 20 *HcWRKYs* express differently in the roots, stems, leaves, and phloem. They were primarily expressed in the roots, except for *HcWRKY2*, *HcWRKY14* and *HcWRKY25*, which were expressed strongly in the phloem (Supplementary Figure 3). These findings suggested that the majority of *HcWRKYs* are crucial for root growth.

To verify *HcWRKYs* role in environmental response, the expression levels of the 20 *HcWRKYs* were further examined under salinity and drought stresses. The results showed that the expression level of 20 *HcWRKYs* significantly changed against the salinity and drought stimuli (Figure 4

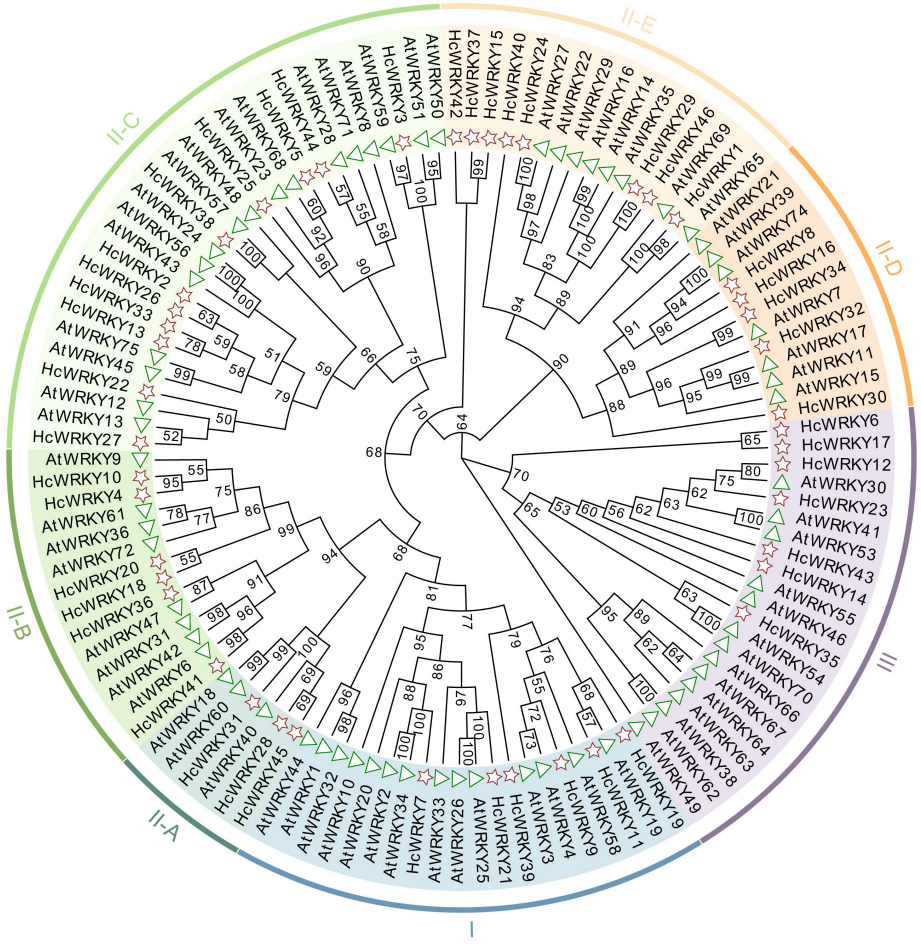


FIGURE 1
Phylogenetic tree analysis revealed the relationship of *WRKY* genes between kenaf and *Arabidopsis*. The unrooted phylogenetic tree was generated by the MEGA7.0 software using the neighbor-joining method, with bootstrap value was 1000 replicates. The different color arcs represent different groups and/or subgroups of *WRKY* genes. *AtWRKY* genes were represented by triangle, and *HcWRKY* genes were pentagon.

and Supplementary Figure 4). For the salinity stress, *HcWRKYs* positively responded after 12 h and *HcWRKY7*, *HcWRKY11*, *HcWRKY15*, *HcWRKY16*, *HcWRKY22*, *HcWRKY26*, *HcWRKY27*, and *HcWRKY38* showed increased expression levels after salinity stress. While *HcWRKY24* and *HcWRKY25* showed decreased expression in response to salinity stress. Compared to control conditions, the expressions of *HcWRKY13*, *HcWRKY15*, *HcWRKY25*, *HcWRKY33*, and *HcWRKY44* were lower at 6 h then it increased at 12 h and subsequently decreased at 24 h (Figure 4).

For the drought stress, most of *HcWRKYs* showed a negative expression pattern (Supplementary Figure 4). Despite having decreased expression compared to the control conditions (0 h), after drought stimuli, *HcWRKY11*, *HcWRKY13*, *HcWRKY14*, *HcWRKY15*, *HcWRKY22*, *HcWRKY25*, *HcWRKY26*, *HcWRKY27*, *HcWRKY30*, *HcWRKY31*, *HcWRKY33*, and *HcWRKY39* transcripts demonstrated an increased expression pattern from 6 to 24 h. *HcWRKY7*, *HcWRKY13*, *HcWRKY31* and *HcWRKY39* expression decreased from 0 to 12 h. While *HcWRKY16*, *HcWRKY24* and *HcWRKY44* showed increased expression levels from 0 to 24 h under drought stress (Supplementary Figure 4). Altogether, these findings indicate that the *HcWRKY* genes respond to the salinity and drought treatments and display differential expression patterns in response to these stress (Figure 4 and Supplementary Figure 4).

HcWRKY proteins localize in cell nuclei

Three representative HcWRKY proteins (HcWRKY39, HcWRKY44, and HcWRKY43) out of each group were randomly chosen for subcellular localization studies to explore the functional properties of HcWRKY proteins. The HcWRKY-GFP vectors (Figure 5A) and control 35S-GFP were injected into the epidermal cells of *N. benthamiana* leaves. The results showed that the GFP signals of *HcWRKY39/44/43*-GFP

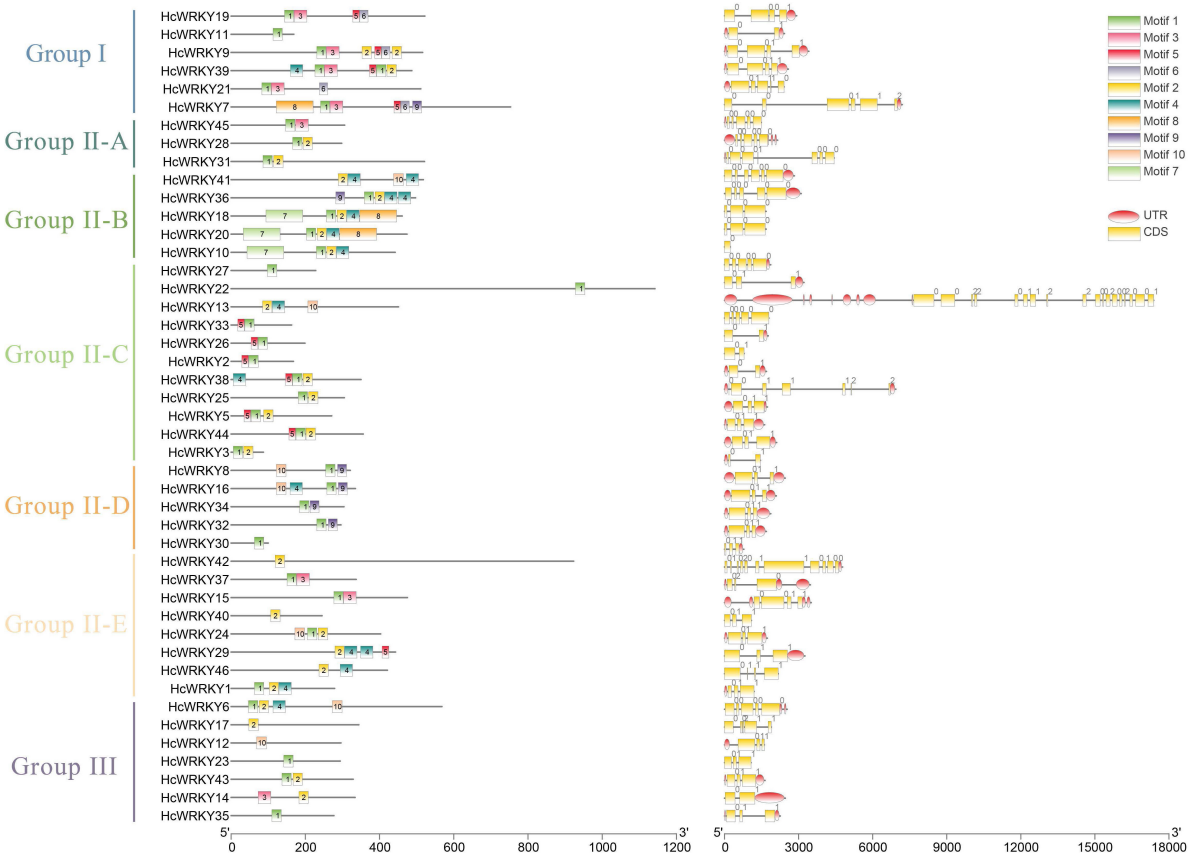


FIGURE 2
Conserved motifs and gene structures of the HcWRKY proteins. The left line shows the 10 conserved motifs of WRKY proteins were identified by the MEME program in kenaf, indicated by different colors and numbers. Motif 1 and motif 2 are essential components of the WRKY domain. The right line shows the exon-intron structure organization of the corresponding *HcWRKY* genes performed by the online tool GSDS. The red oval represents the UTR, the yellow rectangle represents the CDS, and the gray lines represent the introns.

were exclusively localized in the nuclei of epidermal cells of *N. benthamiana* (Figure 5B). In contrast, the control GFP protein was found in both the nucleus and cell membrane (Figure 5B). These results were coincided with previous studies that WRKY proteins functioned in the nuclear as transcription factors.

HcWRKY44 overexpression plants enhanced the salinity but not drought tolerance

The expression patterns of *HcWRKYs* revealed that the *HcWRKY44* strongly induces by salinity and drought stresses (Figure 4 and Supplementary Figures 3, 4). This led us to study the roles of *HcWRKY44* in response to osmotic stresses. Three independent transgenic lines of *HcWRKY44*, OE44-2#, OE44-3#, and OE44-4# (Supplementary Figure 5) were selected to investigate their performance against the salinity and drought stresses. The salinity and drought stresses were mimicked by using NaCl and mannitol irrigation, respectively. For the salinity stress, the results of germination rates showed no obvious difference between the *HcWRKY44* overexpression lines and control plants on the 1/2 MS media. After salinity treatment, OE44-2#, OE44-3#, and OE44-4# lines significantly reduced the germination rate compared to the control, and transgenic lines showed no seed coat breakage (Figures 6A,B). However, transgenic lines showed a faster root growth rate than control plants, and they possessed longer root lengths and more lateral root numbers (Figures 6C,D). To further investigate the tolerance performance of *HcWRKY44* in response to the salinity stress, the seedlings of 2-week-old transgenic lines were treated with different concentrations of NaCl solution. After treatment for 7 days, the leaves of transgenic and control plants turned yellow, wilted and showed no obvious difference. However, after being re-watered for 7 days, leaves of OE44-2#, OE44-3#, and OE44-4# transgenic lines returned green and thrived, while that of the control lines were yellow or even dry and wilted (Figure 6E). Eventually, the overexpression lines of *HcWRKY44* showed a higher survival rate than those of the control plants

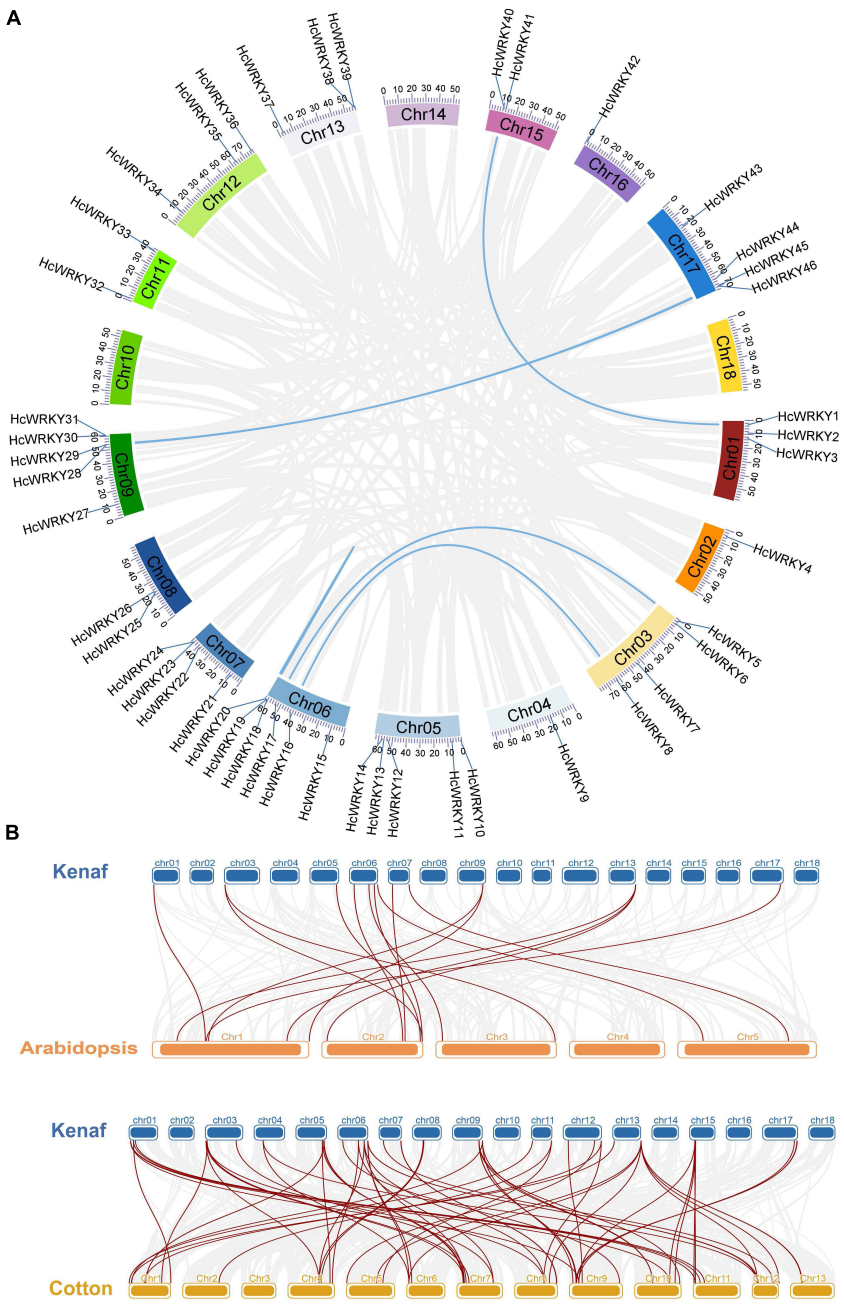


FIGURE 3
Collinearity analysis for all *HcWRKYs*. **(A)** *HcWRKY* genes mapped onto the corresponding chromosomes position of kenaf, as shown in different colors, were used for their collinearity analysis. **(B)** Synteny analysis among the *Arabidopsis*, kenaf and cotton.

(Figure 6F). Meanwhile, the relative electrolyte leakage was also checked to determine the plasma membrane permeability and lipid peroxidation under the salinity treatment. The results showed that the electrolyte leakage of all lines increased with the increased salinity concentrantions, and the OE44-2#, OE44-3#, and OE44-4# transgenic lines exhibited a significantly lower electrolyte leakage than the control lines under the salinity treatment (Figure 6G).

For the drought stress, similar indexes were investigated. The results showed no significant difference in germination rate between the transgenic lines and control plants under mannitol treatments. However, there was a slight difference under 300 mM mannitol treatment (Supplementary Figures 5B,C). The root length of *HcWRKY44* transgenic and control lines was also investigated under different mannitol concentrations and no significant difference was observed between the

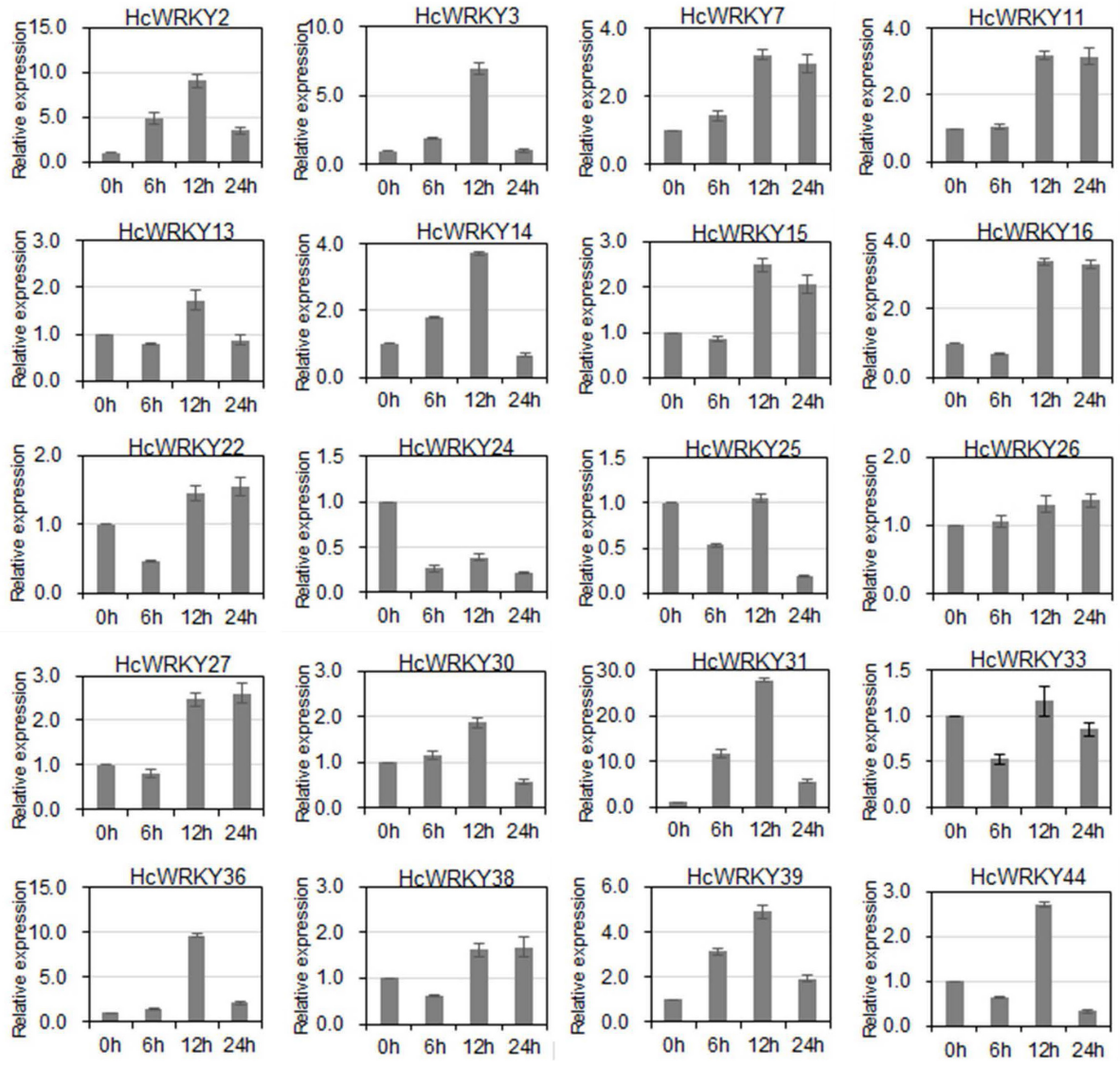


FIGURE 4
Expression profiles of 20 *HcWRKY* genes under NaCl stress. Twenty *HcWRKY* genes were cloned and selected for expression analysis under salinity stress, mimicked by 200 mM NaCl solution irrigation. After treatment, leaves were harvested and used for mRNA transcripts analysis by qRT-PCR. The *18S rRNA* and *TUBα* gene was used as the standard control to normalize the qRT-PCR results. Each assay was replicated three times.

overexpression lines and control plants (**Supplementary Figures 5D,E**). The performances of *HcWRKY44* transgenic lines indicated that overexpression of *HcWRKY44* enhance tolerance to the salinity stress but not to drought stress.

HcWRKY44 regulated plant's salinity tolerance through the abscisic acid pathway

To investigate the roles of *HcWRKY44* in ABA-mediated pathways, the germination rates and root lengths of *HcWRKY44* transgenic lines and control plants were comparatively analyzed with and/or without ABA. On the control medium, both *HcWRKY44* transgenic lines and control plants showed a similar growth tendency, with comparable germination rates, leaf greening and root lengths (**Figure 7**). On the contrary, when seedlings were grown on the ABA supplemented media, the *HcWRKY44* transgenic lines (OE44-2#, OE44-3#, and OE44-4#) showed better performance than that of the control plants in germination rates and root lengths. The germination of *HcWRKY44* transgenic lines (OE44-2#, OE44-3#, and OE44-4#) was much faster than the control lines in the presence of ABA

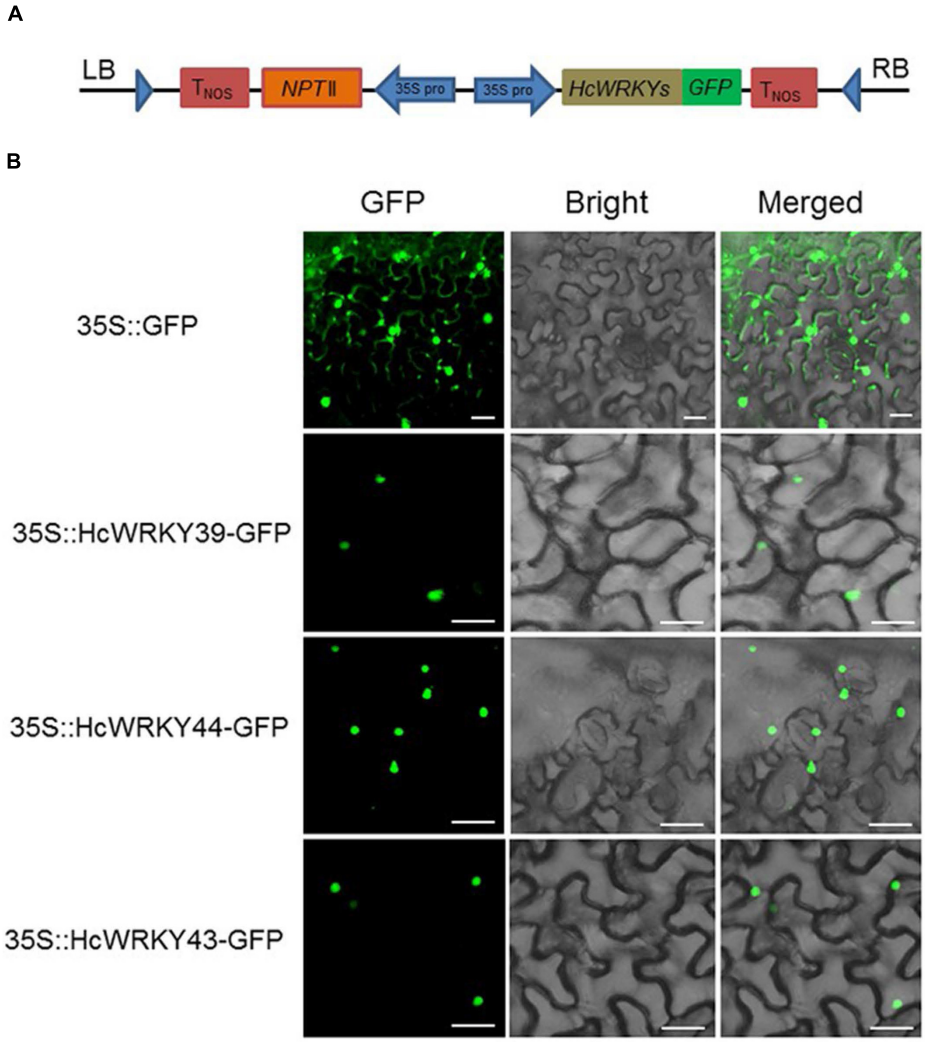


FIGURE 5
Subcellular localization of three HcWRKY proteins from each group. **(A)** A schematic representation of 35S:HcWRKYs-GFP fusion construct and 35S:GFP construct. The coding sequences of *HcWRKY39/44/43* genes were fused with GFP expression vector. **(B)** Subcellular localization analysis was performed using the transient transformation in leaves of *N. benthamiana*, and GFP signals were checked by a confocal laser scanning microscope.

(Figures 7A–C). The transgenic lines showed more open and green leaves than control lines when treated with different ABA concentrations (0.5 and 0.8 μM ABA) for 7 days (Figures 7B,C). Moreover, the root lengths of *HcWRKY44* transgenic lines showed significantly improved growth than control plants (Figures 7D,E). On 10 and 20 μM ABA ABA concentrations, the root growth of control plants was significantly inhibited, but *HcWRKY44* transgenic lines were slightly affected and had a significantly longer root length than control plants (Figures 7D,E). These results indicated that *HcWRKY44* transgenic lines were resistant to ABA treatment.

To further investigate the involvement of *HcWRKY44* in ABA pathways, we comparably analyzed the expression profiles of ABA signaling related genes under salinity stress in the *HcWRKY44* transgenic lines and control plants. After NaCl treatment for 7 days, the ABA-responsive genes, such as *ABA insensitive 1* and *2* (*ABI1*, *ABI2*, and *ABI5*), *ABA-responsive element binding factor 4* (*ABF4*), *COR15A* and *COR47*, were significantly up-regulated in these transgenic lines (OE44-2#, OE44-3#, and OE44-4#) (Figures 8A–F). Moreover, the stress-related marker genes, *DREB2A*, *RD29B*, *STZ*, *P5CS*, and *KIN1*, were also positively regulated in the transgenic lines (Figures 8G,H,J–L), while the *RD22* gene was down-regulated (Figure 8I). These results further confirmed that *HcWRKY44* improved the plant's salinity tolerance through the ABA-mediated signaling pathways.

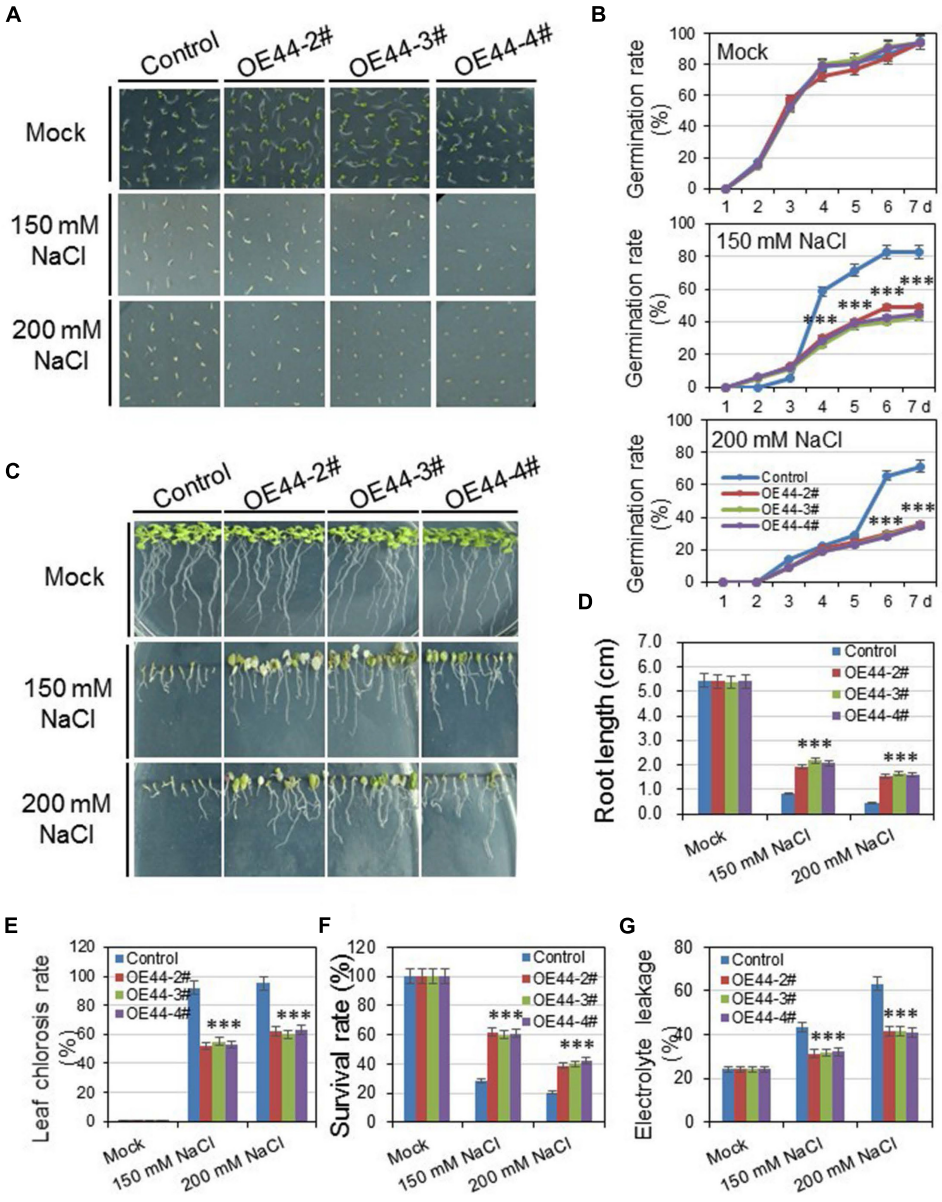


FIGURE 6
Overexpression of *HcWRKY44* in *Arabidopsis* enhanced tolerance to salinity stress. **(A,B)** The seed germination rate was comparably analyzed between the *HcWRKY44* transgenic lines and control lines on the 150 mM and 200 mM NaCl plates. The images were photographed at 7 d after germination. **(C–F)** The root length, leaf chlorosis rate, survival rate and electrolyte leakage were comparably analyzed between *HcWRKY44* transgenic and control lines after treated with 150 and 200 mM NaCl. All the values represent the means of three independent biological replicates; error bars indicate the SD. $^{*}P < 0.05$ and $^{***}P < 0.01$ represented the significant differences by Student's *t*-test, respectively.

To determine *HcWRKY44* improved the tolerance to salt stress but not osmotic stress, the transcript levels of Na^+/H^+ antiporter gene (*SOS1*), Na^+/K^+ homeostasis regulated genes (*AHA1* and *AHA2*), and high affinity K^+ transporter gene (*HKT1*) were further compared under salt treatment. The results showed that the mRNA transcripts of *SOS1* (Figure 8M), *AHA1* (Figure 8N), *AHA2* (Figure 8O), and *HKT1* (Figure 8P) were significantly enriched in the *HcWRKY44* transgenic lines than that in the control lines (Figures 8M–P). These results confirmed that *HcWRKY44* improved the plant's tolerance to salt stress but not osmotic stress.

Discussion

The WRKY transcription factors are characterized by a highly conserved WRKYGQK heptapeptide domain and are implicated in various aspects of plant growth, development and

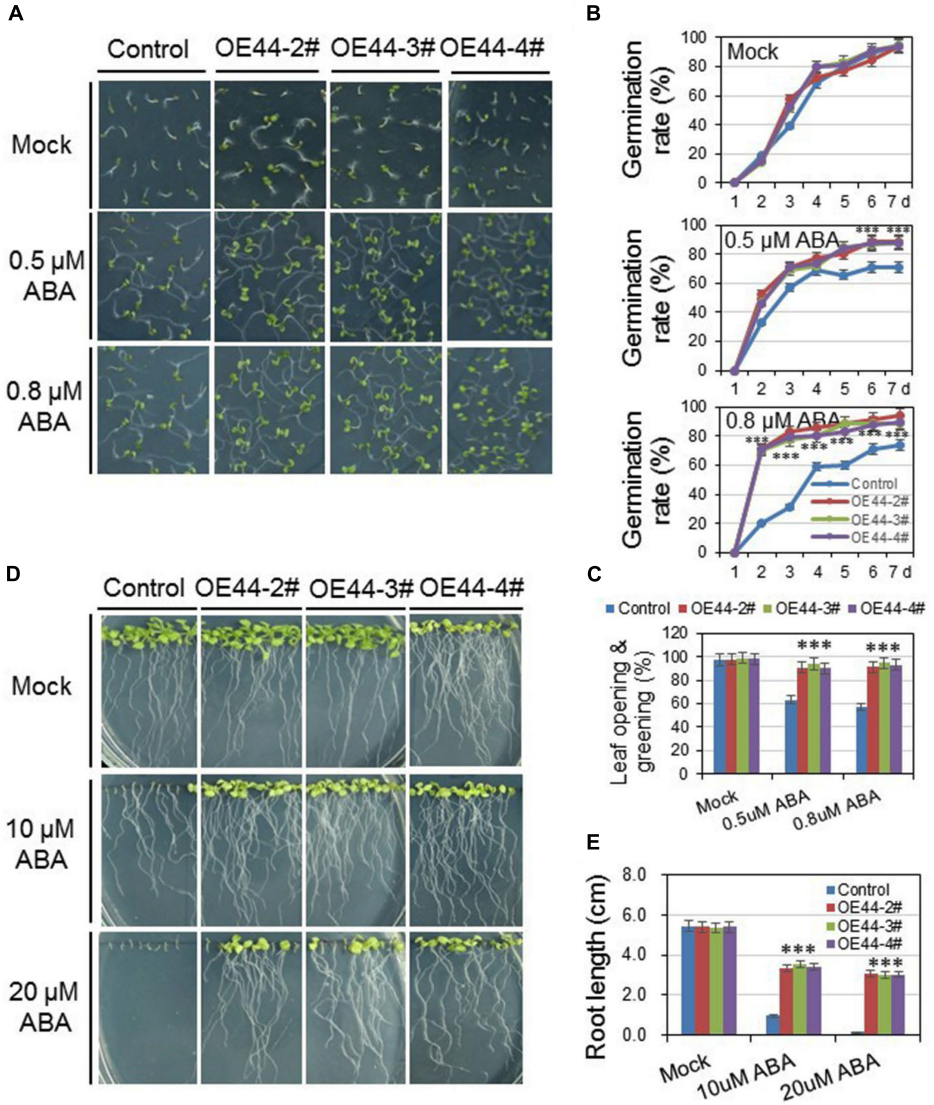


FIGURE 7
Overexpression of *HcWRKY44* in *Arabidopsis* was insensitivity to ABA. **(A–C)** The seed germination rate and leaf opening and greening rate of *HcWRKY44* transgenic lines and control lines were analyzed on 1/2 MS with or without ABA supplement. **(D,E)** Five-day-old seedlings grown on blank media were transferred onto new plates supplemented with 0, 10, and 20 μM ABA to investigate the ABA sensitivity between *HcWRKY44* transgenic lines and control lines. All values are means (±SD) from three independent experiments. ***$P < 0.01$ represented the significant differences by Student's *t*-test.

stress responses (Rushton et al., 2010; Bakshi and Oelmuller, 2014; Wani et al., 2021). Here we identified 46 *HcWRKY* genes in the genome of kenaf. Compared to kenaf, its relative species cotton possesses 116 WRKY members. The difference in WRKY members might be due to kenaf's poor genome assembly, which resulted in the lack of the entire WRKY domain in many HcWRKYs. The other possibility could be that kenaf did not experience whole genome duplication events unlike cotton. In general, the WRKY proteins of kenaf shared the typical WRKYGQK domain, and could be classified into three groups according to the types of WRKY domains and their zinc-finger domains. Gene structure analysis revealed natural mutations in *HcWRKY* genes, for instance, some WRKYGQK domains were altered to WRKYGKK, WRKYGEK and WRKYGQE (**Supplementary Figure 2**). This result coincided with the structural characteristics of *WRKY* genes of *Arabidopsis*, rice and wheat (Rushton et al., 2010; Jiang et al., 2012; Niu et al., 2012; Huang et al., 2021). The variations in *WRKY* gene architecture align with its functional diversity (Bakshi and Oelmuller, 2014; Zhu, 2016; Wani et al., 2021), and/or the acquisition of a novel function during the evolutionary progress. Moreover, gene duplication events,

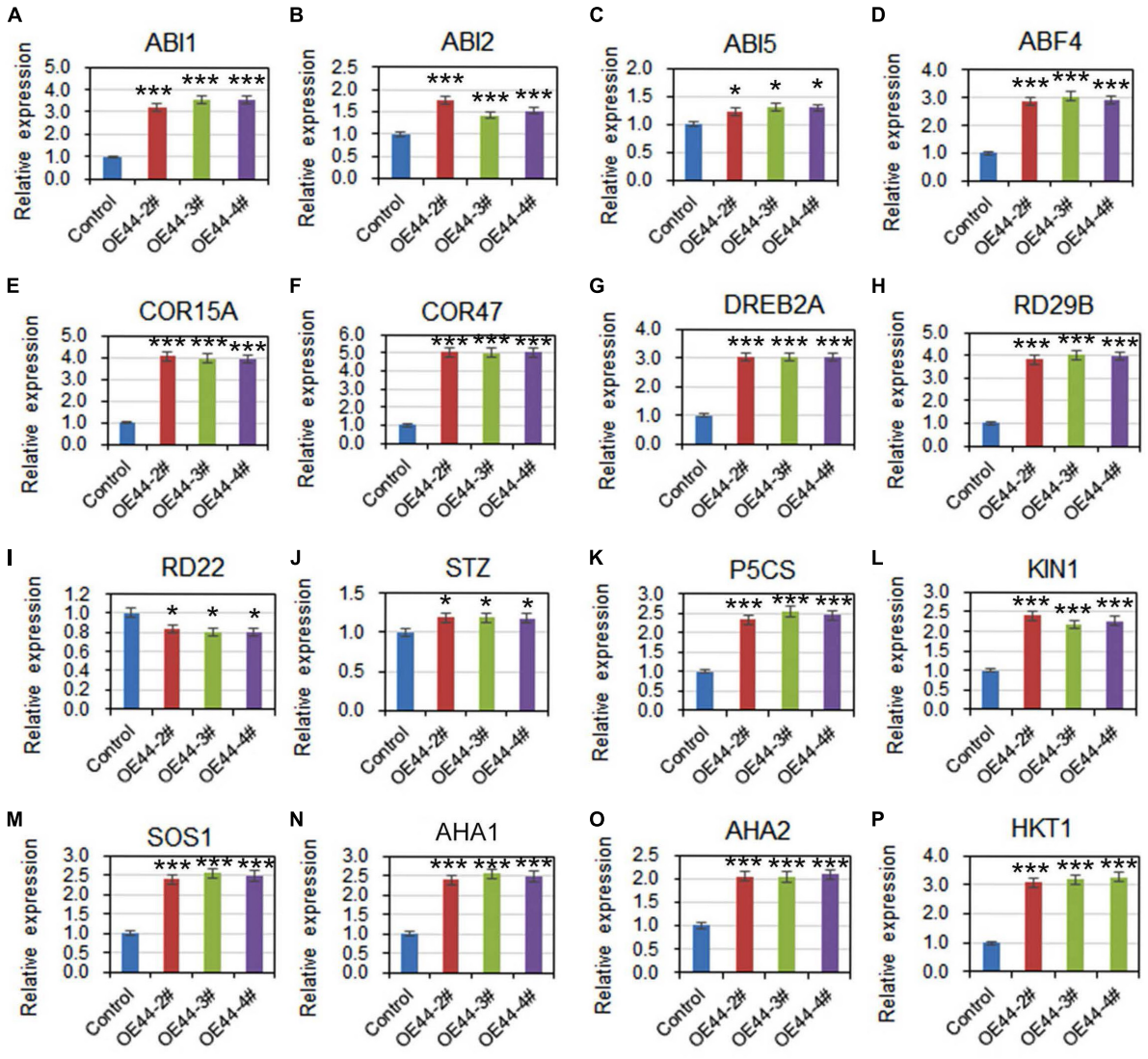


FIGURE 8
HcWRKY44 regulated the expression of ABA- and stress-related regulators. **(A–F)** ABA-mediated genes including *ABI1*, *ABI2*, *ABI5*, *ABF4*, *COR15A*, and *COR47* were selected to analyze their expression in *HcWRKY44* transgenic lines and control lines under salinity stress for 7 days. **(G–L)** Stress-responsive genes *DREB2A*, *KIN1*, *RD29B*, *STZ*, and *P5CS* were selected for evaluation of their expression level in the OE44-2#, OE44-3#, and OE44-4# lines and control lines. **(M–P)** Ionic homeotasis-related genes *SOS1*, *AHA1*, *AHA2*, and *HKT1* were selected for evaluation of their expression level in the *HcWRKY44* transgenic lines and control lines. Each value was the mean ± SD of three independent replicates. $*P < 0.05$ and $***P < 0.01$ represent significant differences between different samples by Student's *t*-test.

including tandem duplication, segmental duplication and whole-genome duplication, are significant factors influencing gene evolution (Qiao et al., 2018; She et al., 2022). This study found 17 (6 segmental and 11 tandem) duplication gene pairs in *HcWRKY* genes, and the evolutionary dates of these duplicated *HcWRKY* genes were also estimated using *Ks* as the proxy for time, the results showed that kenaf duplication events for kenaf 6 of 17 pairs occurred within the past 12.385-165.717 million years (**Supplementary Table 2**). This period is consistent with the speciation time of *H. cannabinus* that occurred 14–31 million years ago (MYA) (Zhang et al., 2020). Furthermore, several orthologous genes (64 gene pairs) were discovered between cotton and kenaf, indicating that the *WRKY* genes may have similar functions in different physiological processes.

In cotton, *GhWRKY1* and *GhWRKY6* mediated drought and salt tolerance by activating the ABA signaling pathway (Ullah et al., 2018; Hu et al., 2021). Phosphorylation of *GhWRKY16* by *MPK3-1* positively regulated fiber initiation and elongation (Wang et al., 2021). Interestingly, one *HcWRKY* gene could correspond with two or more *GhWRKY* genes, suggesting that these genes play a role in salinity and drought stress response as well as in fiber development. To investigate the

functional roles of *HcWRKY* genes, the expression profiles of *HcWRKY* genes were performed across different tissues and stress conditions. Due to the lack of full-length sequence information and the poor genome assembly of kenaf, only 20 *HcWRKY* genes' expression levels were availably obtained. The expression pattern suggested that most of the *HcWRKY* genes get enriched in root and are strongly induced by the salinity and drought stimuli (**Figure 4** and **Supplementary Figure 4**). In contrast, the phloem of kenaf showed strong expression of *HcWRKY2*, *HcWRKY14*, and *HcWRKY25* (**Supplementary Figure 3**). These findings suggested possible functions for *HcWRKYs* in response to salinity, drought conditions, and phloem fiber formation.

Expression pattern analysis revealed that *HcWRKY* genes were differencially regulated in response to salt and drought stress. Only *HcWRKY7*, *HcWRKY16*, and *HcWRKY44* positively responded to salt and drought. Among these three genes, *HcWRKY44* belongs to group II-c. Group II-c members are reported to be involved in abiotic stress response (Xie et al., 2005; Niu et al., 2012). Therefore, *HcWRKY44* was selected as a candidate for further functional characterization. We transformed *HcWRKY44* into *Arabidopsis* instead of kenaf because *Arabidopsis* plants have frequently been used in transgenic studies for gene function investigation for crops that are challenging for gene transformation (Niu et al., 2012, 2022; Luo et al., 2013; She et al., 2022). In transgenic lines, overexpression of *HcWRKY44* increased salinity stress tolerance, as evidenced by longer roots, more lateral roots and a greater survival rate (**Figure 6**). However, *HcWRKY44* overexpression lines did not respond to drought stress, and no noticeable difference was observed between the transgenic plants and control lines (**Supplementary Figure 5**).

Previous investigations have revealed that salinity stress is closely associated with ABA-mediated signaling pathways (Zou et al., 2004; Cutler et al., 2010; Bakshi and Oelmuller, 2014; Zhu, 2016). *ABI1*, *ABI2*, *ABF4*, *COR15A*, and *COR47* were up-regulated in *HcWRKY44* overexpression lines compared to control plants (**Figures 8A–F**). The upregulation of ABA-mediated genes is consistent with the ABA insensitive phenotype of *HcWRKY44* transgenic lines in seed germination and seedling growth (**Figure 7**). It is worth nothing that the seed germination is regulated by a delicate balance between phytohormones GA and ABA (Cutler et al., 2010), the ABA signaling is regulated in the *HcWRKY44* transgenic lines, which could be affected the seed germination. These results align with the previous studies that fine-regulation of ABA signal pathways could improve plant tolerance to salinity and drought stresses (Shen et al., 2006; Shang et al., 2010; Liu et al., 2012). Moreover, the stress-related marker genes were also positively regulated in these transgenic lines. For example, *DREB2A*, *RD29B*, *STZ*, *P5CS*, and *KIN1*, were positively regulated compared to control plants (**Figures 8G,H,J–L**). This result is consistent with previous studies that *DREB2A* overexpression could induce its target genes expression, including *RD29A* and *RD29B*, endowing plants with higher resistances to osmotic stress and finally improving plant's tolerance to abiotic stresses (Sakuma et al., 2006; Jia et al., 2012; Gao et al., 2020). On the other hand, *STZ*, *P5CS*, and *KIN1* were upregulated in *HcWRKY44* transgenic plants under salinity stress. This is consistent with earlier findings that overexpression of the *STZ* gene can improve the resistance to abiotic stress (Mittler et al., 2006; Zhou et al., 2008). *P5CS* encodes delta-1-pyrroline-5-carboxylate synthetase, controlling proline biosynthesis and positively regulating the response of plants to salt stress (Szekely et al., 2008; Funck et al., 2020). ABA and osmotic stressors potentially activate *KIN1* by binding to the dehydration-responsive element (DRE) motif in its promoter and increasing the plant's tolerance to stress (Knight et al., 2004; Chu et al., 2018).

In addition, Na^+ extrusion and K^+ maintenance are critical for plants adapting to the salt stress (Zhu, 2003; Zhang et al., 2019). In our study, the ironic homeostasis-regulated genes *SOS1*, *AHA1*, *AHA2*, and *HKT1* were significantly upregulated in the *HcWRKY44* transgenic lines under salt treatment (**Figures 8M–P**), indicating that overexpression of *HcWRKY44* gene could protect plant cells against Na^+ excess through upregulation of ironic transporter genes. This result is in lines with the previous studies that salt tolerance in plants is closely related to the ability of Na^+ extrusion and K^+ maintenance (Shi et al., 2000; Rus et al., 2004; Sun et al., 2009; Zhang et al., 2019). These results confirmed that *HcWRKY44* improved the plant's tolerance to salt stress but not osmotic stress by regulating the ironic homeostasis-related genes.

Conclusion

The present study identified and characterized 46 WRKY transcription factor genes in the kenaf genome. Gene structure and phylogenetic analysis revealed that tandem and segment duplication might have facilitated the natural variation of *HcWRKY* genes. Expression pattern analysis revealed that *HcWRKY2/14/25* play essential roles in the phloem of kenaf. Other *HcWRKY* members *HcWRKY7/16/44* were enriched in roots and positively responded to the drought and salinity stresses. Furthermore, the *HcWRKY44* gene was functionally characterized in *Arabidopsis*, and the results demonstrated overexpression of *HcWRKY44* improves salinity tolerance via regulating ABA and stress-related genes. In summary, this present study provides comprehensive information about *HcWRKY* genes and reveals that *HcWRKY44* is involved in salinity tolerance via the ABA signaling pathway.

Data availability statement

The original contributions presented in this study are included in the article/**Supplementary material**, further inquiries can be directed to the corresponding author.

Author contributions

MC and XN designed the research and wrote the manuscript. MC and ZS performed phylogenetic analysis and conducted the evolution analysis. MC, TL, ZW, and JQ performed the experiment and analyzed data. MA and XN revised the manuscript. All authors have read and approved the manuscript.

Funding

This work was supported by National Natural Science Foundation of China (31800262 and 31501347), the Ningde Normal University Project (2020FZ04), China Postdoctoral Science Foundation (2018M632564), Natural Science Foundation of Guangxi (2022GXNSFAA035601), and Weng Hongwu Academic Innovation Research Fund of Peking University.

Conflict of interest

The authors declare that the research was conducted in the absence of any commercial or financial relationships that could be construed as a potential conflict of interest.

Publisher's note

All claims expressed in this article are solely those of the authors and do not necessarily represent those of their affiliated organizations, or those of the publisher, the editors and the reviewers. Any product that may be evaluated in this article, or claim that may be made by its manufacturer, is not guaranteed or endorsed by the publisher.

Supplementary material

The Supplementary Material for this article can be found online at: https://www.frontiersin.org/articles/10.3389/fpls.2022.984233/full#supplementary-material

References

Bakshi, M., and Oelmuller, R. (2014). WRKY transcription factors: Jack of many trades in plants. *Plant Signal. Behav.* 9:e27700. doi: 10.4161/psb.27700

Chen, C., Chen, H., Zhang, Y., Thomas, H. R., Frank, M. H., He, Y., et al. (2020). TBtools: An Integrative Toolkit Developed for Interactive Analyses of Big Biological Data. *Mol. Plant* 13, 1194–1202. doi: 10.1016/j.molp.2020.06.009

Chen, P., Chen, T., Li, Z., Jia, R., Luo, D., Tang, M., et al. (2020). Transcriptome analysis revealed key genes and pathways related to cadmium-stress tolerance in Kenaf (*Hibiscus cannabinus* L.). *Ind. Crops Prod.* 158:112970.

Chen, Y., Hao, X., and Cao, J. (2014). Small auxin up-regulated RNA (SAUR) gene family in maize: Identification, evolution, and its phylogenetic comparison with Arabidopsis, rice and sorghum. *J. Integr. Plant Biol.* 56, 133–150. doi: 10.1111/jipb.12127

Chu, M. X., Li, J. J., Zhang, J. Y., Shen, S. F., Li, C. N., Gao, Y. J., et al. (2018). AtCaM4 interacts with a Sec14-like protein, PATL1, to regulate freezing tolerance in Arabidopsis in a CBF-independent manner. *J. Exp. Bot.* 69, 5241–5253. doi: 10.1093/jxb/ery278

Cutler, S. R., Rodriguez, P. L., Finkelstein, R. R., and Abrams, S. R. (2010). Abscisic acid: Emergence of a core signaling network. *Annu. Rev. Plant Biol.* 61, 651–679.

Danalatos, N. G., and Archontoulis, S. V. (2010). Growth and biomass productivity of kenaf (*Hibiscus cannabinus*, L.) under different agricultural inputs and management practices in central Greece. *Ind. Crops Prod.* 32, 231–240.

Dang, F. F., Wang, Y. N., Yu, L., Eulgem, T., Lai, Y., Liu, Z. Q., et al. (2013). CaWRKY40, a WRKY protein of pepper, plays an important role in the regulation of tolerance to heat stress and resistance to Ralstonia solanacearum infection. *Plant Cell Environ.* 36, 757–774. doi: 10.1111/pce.12011

Ding, Z. J., Yan, J. Y., Xu, X. Y., Yu, D. Q., Li, G. X., Zhang, S. Q., et al. (2014). Transcription factor WRKY46 regulates osmotic stress responses and stomatal movement independently in Arabidopsis. *Plant J.* 79, 13–27. doi: 10.1111/tpj.12538

Fujii, H., Chinnusamy, V., Rodrigues, A., Rubio, S., Antoni, R., Park, S. Y., et al. (2009). *In vitro* reconstitution of an abscisic acid signalling pathway. *Nature* 462, 660–664.

Fujii, H., and Zhu, J. K. (2009). Arabidopsis mutant deficient in 3 abscisic acid-activated protein kinases reveals critical roles in growth, reproduction, and stress. *Proc. Natl. Acad. Sci. U.S.A.* 106, 8380–8385. doi: 10.1073/pnas.0903144106

Funck, D., Baumgarten, L., Stift, M., Von Wiren, N., and Schonemann, L. (2020). Differential Contribution of P5CS Isoforms to Stress Tolerance in Arabidopsis. *Front. Plant Sci.* 11:565134. doi: 10.3389/fpls.2020.565134

Gao, Y. F., Liu, J. K., Yang, F. M., Zhang, G. Y., Wang, D., Zhang, L., et al. (2020). The WRKY transcription factor WRKY8 promotes resistance to pathogen infection and mediates drought and salt stress tolerance in Solanum lycopersicum. *Physiol. Plant.* 168, 98–117. doi: 10.1111/ppl.12978

Hu, Q., Ao, C. W., Wang, X. R., Wu, Y. F., and Du, X. Z. (2021). GhWRKY1-like, a WRKY transcription factor, mediates drought tolerance in Arabidopsis via modulating ABA biosynthesis. *BMC Plant Biol.* 21:458. doi: 10.1186/s12870-021-03238-5

Huang, S., Hu, L., Zhang, S., Zhang, M., Jiang, W., Wu, T., et al. (2021). Rice OsWRKY50 Mediates ABA-Dependent Seed Germination and Seedling Growth, and ABA-Independent Salt Stress Tolerance. *Int. J. Mol. Sci.* 22:8625. doi: 10.3390/ijms22168625

Jia, H. Y., Zhang, S. J., Ruan, M. Y., Wang, Y. L., and Wang, C. Y. (2012). Analysis and application of RD29 genes in abiotic stress response. *Acta Physiol. Plant.* 34, 1239–1250.

Jiang, Y., Liang, G., and Yu, D. (2012). Activated expression of WRKY57 confers drought tolerance in Arabidopsis. *Mol. Plant* 5, 1375–1388.

Knight, H., Veale, E. L., Warren, G. J., and Knight, M. R. (2004). The sfr6 mutation in Arabidopsis suppresses low-temperature induction of genes dependent on the CRT/DRE sequence motif. *Plant Cell* 16:2541. doi: 10.1105/tpc.11.5.875

Liu, Z. Q., Yan, L., Wu, Z., Mei, C., Lu, K., Yu, Y. T., et al. (2012). Cooperation of three WRKY-domain transcription factors WRKY18, WRKY40, and WRKY60 in repressing two ABA-responsive genes ABI4 and ABI5 in Arabidopsis. *J. Exp. Bot.* 63, 6371–6392. doi: 10.1093/jxb/ers293

Luo, X., Bai, X., Sun, X., Zhu, D., Liu, B., Ji, W., et al. (2013). Expression of wild soybean *WRKY20* in Arabidopsis enhances drought tolerance and regulates ABA signalling. *J. Exp. Bot.* 64, 2155–2169. doi: 10.1093/jxb/ert073

Mittler, R., Kim, Y., Song, L., Coutu, J., Coutu, A., Ciftci-Yilmaz, S., et al. (2006). Gain- and loss-of-function mutations in Zat10 enhance the tolerance of plants to abiotic stress. *FEBS Lett.* 580, 6537–6542. doi: 10.1016/j.febslet.2006.11.002

Niu, C. F., Wei, W., Zhou, Q. Y., Tian, A. G., Hao, Y. J., Zhang, W. K., et al. (2012). Wheat WRKY genes *TaWRKY2* and *TaWRKY19* regulate abiotic stress tolerance in transgenic Arabidopsis plants. *Plant Cell Environ.* 35, 1156–1170. doi: 10.1111/j.1365-3040.2012.02480.x

Niu, X., Chen, M., She, Z., Aslam, M., Qi, J., and Qin, Y. (2022). Ectopic Expression of Kenaf (*Hibiscus cannabinus* L.) *HcWRKY50* Improves Plants' Tolerance to Drought Stress and Regulates ABA Signaling in Arabidopsis. *Agronomy* 12:1176.

Niu, X., Chen, M., Tao, A., and Qi, J. (2016). Salinity and Drought Treatment Assays in Kenaf (*Hibiscus cannabinus* L.). *Bio-Protocol* 6:e1918.

Niu, X., Qi, J., Chen, M., Zhang, G., Tao, A., Fang, P., et al. (2015). Reference genes selection for transcript normalization in kenaf (*Hibiscus cannabinus* L.) under salinity and drought stress. *PeerJ* 3:e1347. doi: 10.7717/peerj.1347

Qiao, X., Yin, H., Li, L. T., Wang, R. Z., Wu, J. Y., Wu, J., et al. (2018). Different Modes of Gene Duplication Show Divergent Evolutionary Patterns and Contribute Differently to the Expansion of Gene Families Involved in Important Fruit Traits in Pear (*Pyrus bretschneideri*). *Front. Plant Sci.* 9:161. doi: 10.3389/fpls.2018.00161

Ramesh, M. (2016). Kenaf (*Hibiscus cannabinus* L.) fibre based bio-materials: A review on processing and properties. *Prog. Mater. Sci.* 78-79, 1–92.

Ren, X., Chen, Z., Liu, Y., Zhang, H., Zhang, M., Liu, Q., et al. (2010). ABO3, a WRKY transcription factor, mediates plant responses to abscisic acid and drought tolerance in Arabidopsis. *Plant J.* 63, 417–429. doi: 10.1111/j.1365-313X.2010.04248.x

Rus, A., Lee, B., Munoz-Mayor, A., Sharkhuu, A., Miura, K., Zhu, J. K., et al. (2004). AtHKT1 facilitates Na^+ homeostasis and K^+ nutrition in planta. *Plant Physiol.* 136, 2500–2511. doi: 10.1104/pp.104.042234

Rushton, D. L., Tripathi, P., Rabara, R. C., Lin, J., Ringler, P., Boken, A. K., et al. (2012). WRKY transcription factors: key components in abscisic acid signalling. *Plant Biotechnol. J.* 10, 2–11.

Rushton, P. J., Somssich, I. E., Ringler, P., and Shen, Q. J. (2010). WRKY transcription factors. *Trends Plant Sci.* 15, 247–258.

Sakuma, Y., Maruyama, K., Osakabe, Y., Qin, F., Seki, M., Shinozaki, K., et al. (2006). Functional analysis of an Arabidopsis transcription factor, DREB2A, involved in drought-responsive gene expression. *Plant Cell* 18, 1292–1309. doi: 10.1105/tpc.105.035881

Shang, Y., Yan, L., Liu, Z. Q., Cao, Z., Mei, C., Xin, Q., et al. (2010). The Mg-chelatase H subunit of Arabidopsis antagonizes a group of WRKY transcription repressors to relieve ABA-responsive genes of inhibition. *Plant Cell* 22, 1909–1935. doi: 10.1105/tpc.110.073874

She, Z., Huang, X., Aslam, M., Wang, L., Yan, M., Qin, R., et al. (2022). Expression characterization and cross-species complementation uncover the functional conservation of YABBY genes for leaf abaxial polarity and carpel polarity establishment in *Saccharum spontaneum*. *BMC Plant Biol.* 22:124. doi: 10.1186/s12870-022-03501-3

Shen, Y. Y., Wang, X. F., Wu, F. Q., Du, S. Y., Cao, Z., Shang, Y., et al. (2006). The Mg-chelatase H subunit is an abscisic acid receptor. *Nature* 443, 823–826.

Shi, H., Ishitani, M., Kim, C., and Zhu, J. K. (2000). The Arabidopsis thaliana salt tolerance gene SOS1 encodes a putative Na+/H+ antiporter. *Proc. Natl. Acad. Sci. U.S.A.* 97, 6896–6901.

Sim, Y. Y., and Nyam, K. L. (2021). *Hibiscus cannabinus* L. (*kenaf*) studies: Nutritional composition, phytochemistry, pharmacology, and potential applications. *Food Chem.* 344:128582. doi: 10.1016/j.foodchem.2020.128582

Sun, J., Chen, S., Dai, S., Wang, R., Li, N., Shen, X., et al. (2009). NaCl-induced alternations of cellular and tissue ion fluxes in roots of salt-resistant and salt-sensitive poplar species. *Plant Physiol.* 149, 1141–1153. doi: 10.1104/pp.108.129494

Szekely, G., Abraham, E., Cselo, A., Rigo, G., Zsigmond, L., Csiszar, J., et al. (2008). Duplicated *P5CS* genes of Arabidopsis play distinct roles in stress regulation and developmental control of proline biosynthesis. *Plant J.* 53, 11–28. doi: 10.1111/j.1365-313X.2007.03318.x

Ullah, A., Sun, H., Hakim, Yang, X. Y., and Zhang, X. L. (2018). A novel cotton WRKY gene, *GhWRKY6*-like, improves salt tolerance by activating the ABA signaling pathway and scavenging of reactive oxygen species. *Physiol. Plant.* 162, 439–454. doi: 10.1111/ppl.12651

Wang, N. N., Li, Y., Chen, Y. H., Lu, R., Zhou, L., Wang, Y., et al. (2021). Phosphorylation of WRKY16 by MPK3-1 is essential for its transcriptional activity during fiber initiation and elongation in cotton (*Gossypium hirsutum*). *Plant Cell* 33, 2736–2752. doi: 10.1093/plcell/koab153

Wang, Y., Tang, H., Debarry, J. D., Tan, X., Li, J., Wang, X., et al. (2012). MCScanX: A toolkit for detection and evolutionary analysis of gene synteny and collinearity. *Nucl. Acids Res.* 40:e49. doi: 10.1093/nar/gkr1293

Wani, S. H., Anand, S., Singh, B., Bohra, A., and Joshi, R. (2021). WRKY transcription factors and plant defense responses: latest discoveries and future prospects. *Plant Cell Rep.* 40, 1071–1085. doi: 10.1007/s00299-021-02691-8

Xie, Z., Zhang, Z. L., Zou, X., Huang, J., Ruas, P., Thompson, D., et al. (2005). Annotations and functional analyses of the rice WRKY gene superfamily reveal positive and negative regulators of abscisic acid signaling in aleurone cells. *Plant Physiol.* 137, 176–189. doi: 10.1104/pp.104.054312

Zhang, H., Deng, C., Yao, J., Zhang, Y., Zhang, Y., Deng, S., et al. (2019). *Populus euphratica* JRL mediates ABA response, ionic and ROS homeostasis in *Arabidopsis* under salt stress. *Int. J. Mol. Sci.* 20:815. doi: 10.3390/ijms20040815

Zhang, L., Xu, Y., Zhang, X., Ma, X., Zhang, L., Liao, Z., et al. (2020). The genome of kenaf (*Hibiscus cannabinus* L.) provides insights into bast fibre and leaf shape biogenesis. *Plant Biotechnol. J.* 18, 1796–1809. doi: 10.1111/pbi.13341

Zhou, Q. Y., Tian, A. G., Zou, H. F., Xie, Z. M., Lei, G., Huang, J., et al. (2008). Soybean WRKY-type transcription factor genes, *GmWRKY13*, *GmWRKY21*, and *GmWRKY54*, confer differential tolerance to abiotic stresses in transgenic Arabidopsis plants. *Plant Biotechnol. J.* 6, 486–503. doi: 10.1111/j.1467-7652.2008.00336.x

Zhu, J. K. (2003). Regulation of ion homeostasis under salt stress. *Curr. Opin. Plant Biol.* 6, 441–445.

Zhu, J. K. (2016). Abiotic Stress Signaling and Responses in Plants. *Cell* 167, 313–324.

Zou, X., Seemann, J. R., Neuman, D., and Shen, Q. J. (2004). A WRKY gene from creosote bush encodes an activator of the abscisic acid signaling pathway. *J. Biol. Chem.* 279, 55770–55779. doi: 10.1074/jbc.M408536200

frontiers | Frontiers in Plant Science

TYPE Original Research
PUBLISHED 06 September 2022
DOI 10.3389/fpls.2022.983600

Check for updates

OPEN ACCESS

EDITED BY
Muhammad Waseem,
Hainan University, China

REVIEWED BY
Muhammad Imran,
Tsinghua University, China
Iftikhar Ali,
State Key Laboratory of Molecular Developmental Biology, Institute of Genetics and Developmental Biology (CAS), China

*CORRESPONDENCE
Dazhuang Huang
huangdazhuang@126.com

SPECIALTY SECTION
This article was submitted to Plant Abiotic Stress, a section of the journal Frontiers in Plant Science

RECEIVED 01 July 2022
ACCEPTED 18 August 2022
PUBLISHED 06 September 2022

CITATION
Zhang J, Huang D, Zhao X, Zhang M, Wang Q, Hou X, Di D, Su B, Wang S and Sun P (2022) Drought-responsive WRKY transcription factor genes *IgWRKY50* and *IgWRKY32* from *Iris germanica* enhance drought resistance in transgenic *Arabidopsis*. *Front. Plant Sci.* 13:983600. doi: 10.3389/fpls.2022.983600

COPYRIGHT
© 2022 Zhang, Huang, Zhao, Zhang, Wang, Hou, Di, Su, Wang and Sun. This is an open-access article distributed under the terms of the Creative Commons Attribution License (CC BY). The use, distribution or reproduction in other forums is permitted, provided the original author(s) and the copyright owner(s) are credited and that the original publication in this journal is cited, in accordance with accepted academic practice. No use, distribution or reproduction is permitted which does not comply with these terms.

Drought-responsive WRKY transcription factor genes *IgWRKY50* and *IgWRKY32* from *Iris germanica* enhance drought resistance in transgenic *Arabidopsis*

Jingwei Zhang[1,2], Dazhuang Huang[1]*, Xiaojie Zhao[1], Man Zhang[3], Qian Wang[1], Xueyan Hou[1], Dongliu Di[1], Beibei Su[1], Shaokun Wang[1] and Pai Sun[1]

[1]College of Landscape Architecture and Tourism, Hebei Agricultural University, Baoding, China, [2]College of Landscape and Ecological Engineering, Hebei University of Engineering, Handan, China, [3]State Key Laboratory of North China Crop Improvement and Regulation, Hebei Agricultural University, Baoding, China

Drought greatly affects the growth and development of garden plants and affects their ornamental value. WRKY transcription factors make up one of the largest transcription factor families in plants and they play an important role in the plant response to drought stress. However, the function of the WRKY gene in response to drought stress in *Iris germanica*, which is commonly used in landscaping, has not been studied. In this study, we isolated two WRKY transcription factor genes from *Iris germanica*, *IgWRKY50* and *IgWRKY32*, which belong to Group II and Group III of the WRKY family, respectively. *IgWRKY50* and *IgWRKY32* could be induced by PEG-6000, high temperature and ABA in *Iris germanica*. *IgWRKY50* and *IgWRKY32* could quickly respond to drought and they peaked at 3 h after PEG-6000 treatment (19.93- and 23.32-fold). The fusion proteins IgWRKY50-GFP and IgWRKY32-GFP were located in the nucleus of mesophyll protoplasts of *Arabidopsis*. The overexpression of the *IgWRKY50* and *IgWRKY32* genes improved the osmotic tolerance of transgenic *Arabidopsis*, mainly exhibited by the transgenic plants having a higher germination rate and a longer total root length on 1/2 MS medium containing mannitol. Under PEG-6000 stress, the transgenic plants had higher stomatal closure than the wild type (WT). Under natural drought stress, the water loss rate of the isolated leaves of transgenic *Arabidopsis* was lower than that of WT, the contents of proline (Pro) and soluble protein (SP) and the activities of superoxide dismutase (SOD), peroxidase (POD) and catalase (CAT) in the transgenic plants were higher, but the content of malondialdehyde (MDA) was lower. Furthermore, the expression of several stress-related genes (*RD29A, DREB2A, PP2CA,* and *ABA2*) was significantly increased in *IgWRKY50*- and *IgWRKY32*- overexpressing transgenic *Arabidposis* plants after drought

treatment. These results suggest that *IgWRKY50* and *IgWRKY32*, as two positive regulators, enhance the drought resistance of transgenic *Arabidopsis* by mediating the ABA signal transduction pathway. *IgWRKY50* and *IgWRKY32* can be used as candidate genes for molecular breeding of drought resistance in *Iris*.

KEYWORDS

Iris germanica*, drought tolerance, WRKY transcription factor, stress response mechanisms, *Arabidopsis

Introduction

The intensification of the El Niño phenomenon has made the global drought area continue to expand. Drought seriously affects the growth, development and geographical distribution of plants (Anjum et al., 2011). Among the many abiotic stresses, drought damage to plants occupies first place (Shao et al., 2009). Due to the improvement of living standards, people pay more and more attention to ecological environment, and landscape construction has also made substantial developments. However, with the continuous expansion of urban construction, water consumption and maintenance costs of garden green lands have also increased. Water shortage has become one of the important factors restricting ecological construction (Fereres et al., 2003). For garden plants, drought significantly reduces their ornamental value and directly or indirectly affects economic development. Therefore, it is of great significance to thoroughly study the drought resistance mechanism of garden plants and fundamentally solve the contradiction between garden development and water shortages for the construction of energy-saving gardens.

The drought resistance of plants is determined to some extent by the genetic information they carry (Mwadzingeni et al., 2016). When plants are subjected to drought stress, the damage caused by stress is reduced through a series of genetic regulations (Huang et al., 2012). During the process of gene regulation, transcription factors play an important role in responding to stress signals and in controlling gene expression (Singh et al., 2002). Several TF families, such as bZIP, WRKY, NAC, and MYB, are widely involved in the regulation of plant drought stress resistance (Liu et al., 2012; Okay et al., 2014; Rahman et al., 2016; Zhao et al., 2018).

As one of the largest transcription factor families in plants, WRKYs are characterized by the highly conserved WRKY domains that can control gene transcription by specifically binding to the upstream W-box sequence of target genes, and plays an important role in gene regulation (Eulgem et al., 2000). The WRKY domain is a polypeptide sequence composed of 60 highly conserved amino acid residues, which comprises a short-conserved sequence WRKYGQK at the N-terminal and a zinc finger motif at the C-terminal (Eulgem et al., 2000). Although WRKYGQK sequences are highly conserved in plants, some studies have shown that WRKY transcription factors have experienced certain changes during evolution, such as the amino acid mutation of WRKY to WXKY, WSKY, WRRY, WKRY, WKKY, WVKY, or GRKY (Dong et al., 2003; Qiu et al., 2004). In addition to the 7-peptide conserved sequence and zinc finger structure, most WRKY transcription factors also have glutamate-rich regions, proline-rich regions, leucine zipper structures, and serine/threonine-rich regions (Zhang and Wang, 2005). The existence of these structures allows WRKY transcription factors to play multiple roles in gene regulation. According to the number of WRKY domains and the type of the zinc finger structure, WRKY family members are generally divided into three groups. Group I contains two WRKY domains and a C_2H_2 ($CX_{4-5}CX_{22-23}HXH$) zinc finger. Group II a-e and Group III contain one WRKY domain and a C_2H_2 motif or a C_2HC ($CX_7CX_{23}HXC$) motif, respectively (Rushton et al., 2010; Yousfi et al., 2016). By analyzing the WRKY family of rice, it was found that the number of Group III gradually increased during the process of evolution, and it was speculated that Group III might be more active in evolution than Group I and Group II (Wu et al., 2005).

WRKY transcription factors are indispensable response factors for plants to resist biotic and abiotic stresses (Jiang et al., 2017). Overexpression of the WRKY transcription factor genes in plants can improve the resistance of plants to adversity. *GsWRKY20* in wild soybean was overexpressed in *Arabidopsis*, and the transgenic lines showed stronger tolerance to drought stress (Luo et al., 2013). The *OsWRKY45* cloned from rice was overexpressed in *Arabidopsis*, which enhanced the disease resistance and drought tolerance of *Arabidopsis*, indicating that *OsWRKY45* is involved in biotic and abiotic stress response signal transduction (Qiu and Yu, 2009). The *ZmWRKY58* gene isolated from maize was overexpressed in rice, which enhanced the tolerance of the transgenic rice to drought and salt stress (Cai et al., 2014). At present, research on the function of WRKY transcription factors is related to high- (Cheng et al., 2021) and low-temperature resistance (Romero et al., 2019), high-salt resistance (Li et al., 2013), drought resistance (He et al., 2016), heavy metal resistance (Wu et al., 2022) and pest resistance (Xiong et al., 2019). However, these studies mainly focused on model plants such as *Arabidopsis* (Dong et al., 2003), rice (Yu et al., 2010), and tobacco (Maeo et al., 2001), as well as crops

such as maize (Wang et al., 2018), barley (Mangelsen et al., 2008), and cotton (Dou et al., 2014). There are few studies on the regulatory mechanism of WRKY transcription factors in garden plants under stress.

Iris germanica is a perennial herbaceous flower with good ornamental characteristics, and it is drought-resistant, water-saving and barren-resistant. It is the species with the highest ornamental value among irises and is widely used in landscaping (Zhang and Chen, 2013). The drought resistance of *Iris germanica* is obviously higher than that of other plants of the same genus (Han et al., 2006). *Iris germanica* is not only an important greening material for energy-saving garden construction but also a genetic treasure trove for drought-resistant breeding of *Iris* and other garden plants. It is of great value to deeply study the drought resistance of *Iris germanica*.

At present, the research of *Iris germanica* mainly focuses on the determination of physiological and biochemical indicators under abiotic stress (Bo et al., 2017; Zhao et al., 2021), hybrid breeding (Azimi and Alavijeh, 2021), phenotype analysis (Fan et al., 2022), and exploration of flowering mechanism (Fan et al., 2020). There are few studies on stress-resistant genes, and they are limited to the detection of gene expression (Wang et al., 2021), and the function of gene has not been verified. The mechanism of WRKY gene under abiotic stress in *Iris germanica* has not been studied. In our previous work, we completed the transcriptome sequencing of "Little Dream," a high drought-resistant cultivar of *Iris germanica*, and identified 20 differentially expressed genes belonging to the WRKY transcription factor family (Zhang et al., 2021). To further verify the role of WRKY transcription factors in stress resistance regulation, two WRKY transcription factor family genes, *IgWRKY50* and *IgWRKY32*, belonging to WRKY transcription factor family Group II and Group III, respectively, were isolated from "Little Dream." The drought resistance function of the *IgWRKY50* and *IgWRKY32* genes was verified in transgenic *Arabidopsis*. The results showed that the overexpression of these two genes improved the drought resistance of transgenic *Arabidopsis*. This result fills the gap in the study of abiotic stress resistance of the *Iris germanica* WRKY gene, provides a key clue for understanding the role of the WRKY gene in the drought response of *Iris germanica*, and provides excellent candidate genes for drought resistance breeding of *Iris* and other garden plants.

Materials and methods

Stress treatment of *Iris germanica*

The 1-year-old *Iris germanica* cultivar "Little Dream" was used as the experimental material. Seedlings at the vegetative growth stage that exhibited strong and similar growth were selected and cultured in 1/2 Hongland solution for 7 days. Plant culture was carried out in an artificial climate chamber with a temperature of 25°C, a photoperiod of 16 h/8 h and a light intensity of 180 μmol $m^{-2}s^{-1}$. Then, the plants were treated with 1/2 Hoagland solution containing 200 $g{\cdot}L^{-1}$ PEG 6000, 150 mM NaCl and 100 μM ABA for 24 h in the same chamber. Low- and high-temperature treatments were conducted in 4 and 42°C chambers for 24 h, respectively. All abiotic stresses were initiated on March 15, 2021. The seedlings cultivated in regular 1/2 Hongland solution were used as a control. For the multiple stress experiments, samples were taken at 0, 1, 3, 6, 12, and 24 h after PEG 6000, NaCl, ABA, low- and high-temperature treatments. The samples were collected from the middle and upper parts of one to two mature leaves next to the center leaf. For different organ expression pattern analyses, the leaves, fibrous roots, tubers, flag petals, and fall petals of the control seedlings were collected at 0 h. All samples were wrapped in tin foil, immediately frozen in liquid nitrogen and stored at –80°C until RNA extraction. The 1/2 Hongland solution used in the experiment was refreshed every day. Leaves of intact plants were always selected as material for the next experiments. Each treatment was repeated three times. The specific gene primers are listed in **Supplementary Table 1A**.

Gene isolation and bioinformatics analysis of *IgWRKY50* and *IgWRKY32*

Two groups of specific primers (**Supplementary Table 1B**) were designed with Primer Premier 5.0 software (Premier, Canada), and the complete coding sequences of the *IgWRKY50* and *IgWRKY32* genes were amplified twice. The PCR products were connected to the pEASYT3 cloning vector (TransGen Biotech, Beijing, China) and then sequenced by the company (Sangon Biotech, Shanghai, China). The open reading frames of *IgWRKY50* and *IgWRKY32* were found by NCBI ORF Finder.[1] The protein functional domains of *IgWRKY50* and *IgWRKY32* were predicted by SMART software (Letunic and Bork, 2018; Letunic et al., 2021).[2] The phylogenetic tree of amino acid sequences of other species with homology to *IgWRKY50* and *IgWRKY32* genes was constructed by MEGA 6 software using the neighbor-joining (NJ) method with 1,000 bootstrap replicates (Tamura et al., 2013). The accession numbers of the WRKYs are listed in **Supplementary Table 2**. The tertiary structure prediction of *IgWRKY50* and *IgWRKY32* proteins was completed by SWISS-MODEL software (Biasini et al., 2014), and the three-dimensional structure model of proteins was constructed by the I-TASSER website[3] and Chimera 1.11.2 software[4] (Pettersen et al., 2004).

1 https://www.ncbi.nlm.nih.gov/orffinder
2 http://smart.embl-heidelberg.de/
3 https://zhanglab.ccmb.med.umich.edu/I-TASSER/
4 https://www.rbvi.ucsf.edu/chimera

Subcellular localization analysis of *IgWRKY50* and *IgWRKY32*

The expression vector PBI221-GFP (YRGene, Changsha, China) was used for an investigation of subcellular localization. The coding regions of *IgWRKY50* and *IgWRKY32* were fused to the PBI221-GFP vector containing the CaMV35S promoter. The specific primers are listed in **Supplementary Table 3A**. *Arabidopsis* protoplasts were isolated from 3-week-old leaves of *Arabidopsis* (Columbia-0). The recombinant plasmids PBI221-IgWRKY50-GFP and PBI221-IgWRKY32-GFP and the nuclear localization plasmid pHBT-NLS-mCherry were transferred into *Arabidopsis* protoplasts by the PEG-mediated method (Sheen, 2001) and incubated at 22°C for 16 h in the dark. The empty vector was used as a control. The GFP fluorescence signals were observed by a laser confocal microscope (Olympus FV10-ASW, Tokyo, Japan).

Plant transformation and generation of overexpressing *Arabidopsis* plants

The complete coding sequences of *IgWRKY50* and *IgWRKY32* were ligated into the binary vector PBI121 (YRGene, Changsha, China) containing Xbal and Smal restriction sites under the control of the *Cauliflower mosaic virus* 35S (CaMV35S) promoter using specific primers (**Supplementary Table 3B**). The recombinant plasmid was introduced into *Agrobacterium tumefaciens* strain *GV3101* (AngYuBio, Shanghai, China) by the freeze–thaw method. A transgenic *Arabidopsis* strain was obtained by transforming wild-type (WT) *Arabidopsis* (Columbia-0) by the floral dip method (Clough and Bent, 2010). T1 plants were screened on 1/2 MS medium containing 0.1% kanamycin. T1 seedlings were confirmed by PCR and selfed through two more generations to generate T3 transgenic progeny. T3 seedlings confirmed by sequencing (Sangon Biotech, Shanghai, China). Twenty-five *IgWRKY50* overexpression lines and forty-four *IgWRKY32* overexpression lines were obtained. Three lines with higher expression levels were selected from the *IgWRKY50* and *IgWRKY32* transgenic lines by RT–qPCR for further analysis. The method used to clean the *Arabidopsis* seeds was described by Feng et al. (2015).

Determination of water loss rate

WT and transgenic *Arabidopsis* plants growing normally for 21 days in substrate ($V_{nutrientsoil}$: $V_{vermiculite}$ = 1:1) were used to calculate the water loss rate of the isolated leaves. WT and transgenic *Arabidopsis* lines with basically the same growth were selected. Five rosette leaves of a similar size were taken from each line, and the leaves were placed face up in a petri dish at room temperature. Losses in fresh weight were monitored at 0.5, 1, 2, 4, 6, 8, and 12 h. Water loss is expressed as the percentage of initial fresh weight. Three replicates were performed. All types of *Arabidopsis* were cultured in an artificial climate room. The culture conditions were a constant temperature at 22°C, photoperiod of 16 h/8 h, light intensity of 150 μmol $m^{-2}s^{-1}$ and relative humidity of 70%.

Measurement of antioxidant enzymes, malondialdehyde, proline and soluble protein

WT and transgenic *Arabidopsis thaliana* plants with normal growth for 21 days were adequately irrigated before inducing a drought, which lasted for 14 days. The physiological parameters of the leaves were measured at 14 d after treatment. All types of *Arabidopsis* grown under normal water conditions were used as controls. The activities of superoxide dismutase (SOD), catalase (CAT), and peroxidase (POD) were determined by the corresponding kits (Nanjing Jiancheng Bioengineering Institute, China). The MDA content was measured using a thiobarbituric acid (TBA) reaction (Zhang et al., 2021). The accumulation of Pro in the leaves was measured using the acid ninhydrin method (Fu et al., 2016). The SP content was determined by Coomassie Brilliant Blue G-250 staining (Fu et al., 2016).

Stress tolerance assay in overexpressing *Arabidopsis* plants

To determine the seed germination rate of various types of *Arabidopsis*, sterilized seeds of WT and transgenic *Arabidopsis* were spread on 1/2 MS medium containing 0, 100, 150, and 200 mM mannitol and cultured in an *Arabidopsis* artificial climate chamber for 7 days. The seed germination rate was recorded every day. Thirty-six seeds were taken from each strain, and each experiment was repeated 3 times. The seeds were vernalized at 4°C for 3 days in advance. Seeds were considered to be germinated when radicles emerged from the seed coats.

To compare the total root growth of various types of *Arabidopsis*, the sterilized seeds of WT and transgenic *Arabidopsis* strains were cultured in 1/2 MS medium for 3 days and then transferred to 1/2 MS medium containing 0 mM and 150 mM mannitol for 7 days. Then, the total root lengths of various types of *Arabidopsis* were measured and recorded by photographs. Thirty seeds were taken from each strain, and each experiment was repeated 3 times.

To observe the phenotypic changes of various types of *Arabidopsis thaliana* under natural drought, the sterilized seeds of the WT and transgenic lines were sown on 1/2 MS medium and transplanted to the substrate ($V_{nutrientsoil}$:$V_{vermiculite}$ = 1:1) after 10 days. Eighteen plants were selected from each line. The phenotype was photographed after normal culture in

an *Arabidopsis* artificial climate culture room for 3 weeks. After that, the irrigation was stopped, and the phenotype was photographed again after 21 days of drought.

To observe the stomatal opening and closing of various types of *Arabidopsis thaliana*, the rosette leaves of WT and transgenic *Arabidopsis* lines grown for 21 days were used as materials. The leaves were floated in stomata buffer containing 50 μM CaCl, 10 mM KCl, and 10 mM Mes-Tris, pH = 6.15, under the light of 80 μmol m^{-2} s^{-1} for 2 h until the stomata were fully opened (Akter et al., 2012). After that, the leaves were transferred into stomatal buffer containing 8% PEG-6000, and stomatal opening and closing were observed every 15 min. When the stomatal opening and closing changed, the lower epidermis of the leaves was torn off to make temporary mounts, and the stomatal images were collected with an optical microscope (Olympus FV10-ASW, Tokyo, Japan). Fifteen stomatal apertures were measured for each sample. The length and width of the stomata were determined by ImageJ software,[5] which was used to calculate the stomatal aspect ratio.

5 http://rsbweb.nih.gov/ij

Expression profile of stress-related genes

To elucidate the possible molecular mechanisms of *IgWRKY50* and *IgWRKY32*, the expression levels of *RD29A, DREB2A, PP2CA,* and *ABA2* were assessed in transgenic and WT plants after 14 days of continuous drought by RT–qPCR. The specific primers are listed in **Supplementary Table 3C**.

RNA extraction and qRT–PCR analysis

Total RNA was isolated using TRIzol reagent (Life Technologies, Inc., Grand Island, NY, United States) following the manufacturer's protocol. A 1 μg RNA sample was reverse transcribed using a HiFiScript cDNA Synthesis Kit (CWBIO, Beijing, China). Gene-specific primers were designed using Primer Premier 5.0 (Premier, Canada) software. RT–qPCR was performed with Fast Super EvaGreen qPCR Master Mix (US Everbright Inc., Jiangsu, China) on an ABI Prism 7500 system (Applied Biosystems, Waltham, MA, United States). The PCR volume was 20 μL, which included 10 μL of 2 × Fast Super Eva

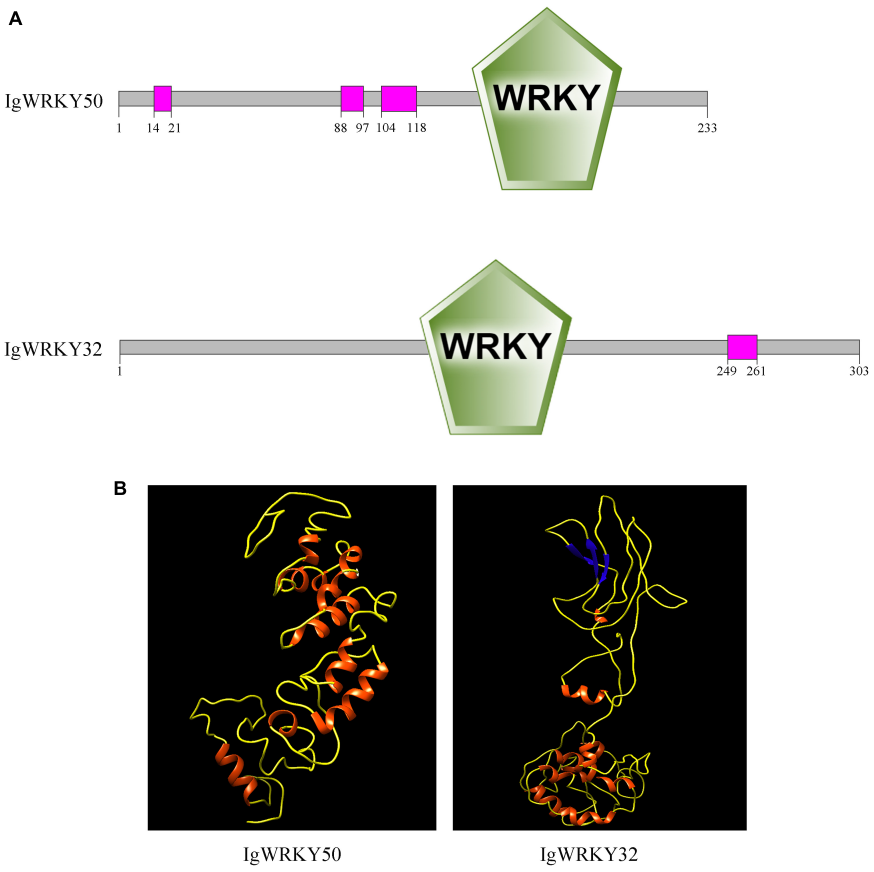


FIGURE 1
Protein domain organization **(A)** and three-dimensional structures **(B)** of *IgWRKY50* and *IgWRKY32*.

Green Master Mix, 0.5 μL of the forward primer, 0.5 μL of the reverse primer, 0.2 μL of 10 × ROX, 2 μL of the cDNA template, and 6.8 μL of denucleated acid water. The reaction conditions were 2 min at 95°C for denaturation followed by 45 cycles of 5 s at 95°C, 5 s at 60°C, and 50 s at 72°C. The RT–qPCR analysis consisted of three biological and three technical replications. The relative expression levels of the genes were calculated using the $2^{-\Delta\Delta Ct}$ method.

Statistical analysis

The data were analyzed using Microsoft Office Excel 2010 software and IBM SPSS 21.0 (IBM Corp., NY, United States), and Duncan's multitest and Student's *t*-test were used to evaluate the significance of the differences. GraphPad Prism 7.0 was used to generate the charts.

Results

Sequence analysis of *IgWRKY50* and I*gWRKY32*

In this study, *IgWRKY50* (GenBank Accession No. ON571660) and *IgWRKY32* (GenBank Accession No. ON571661) were cloned and isolated from *Iris germanica* "Little Dream." The complete coding sequence of *IgWRKY50* was 702 bp, encoding 233 amino acids. The unique WRKYGKK

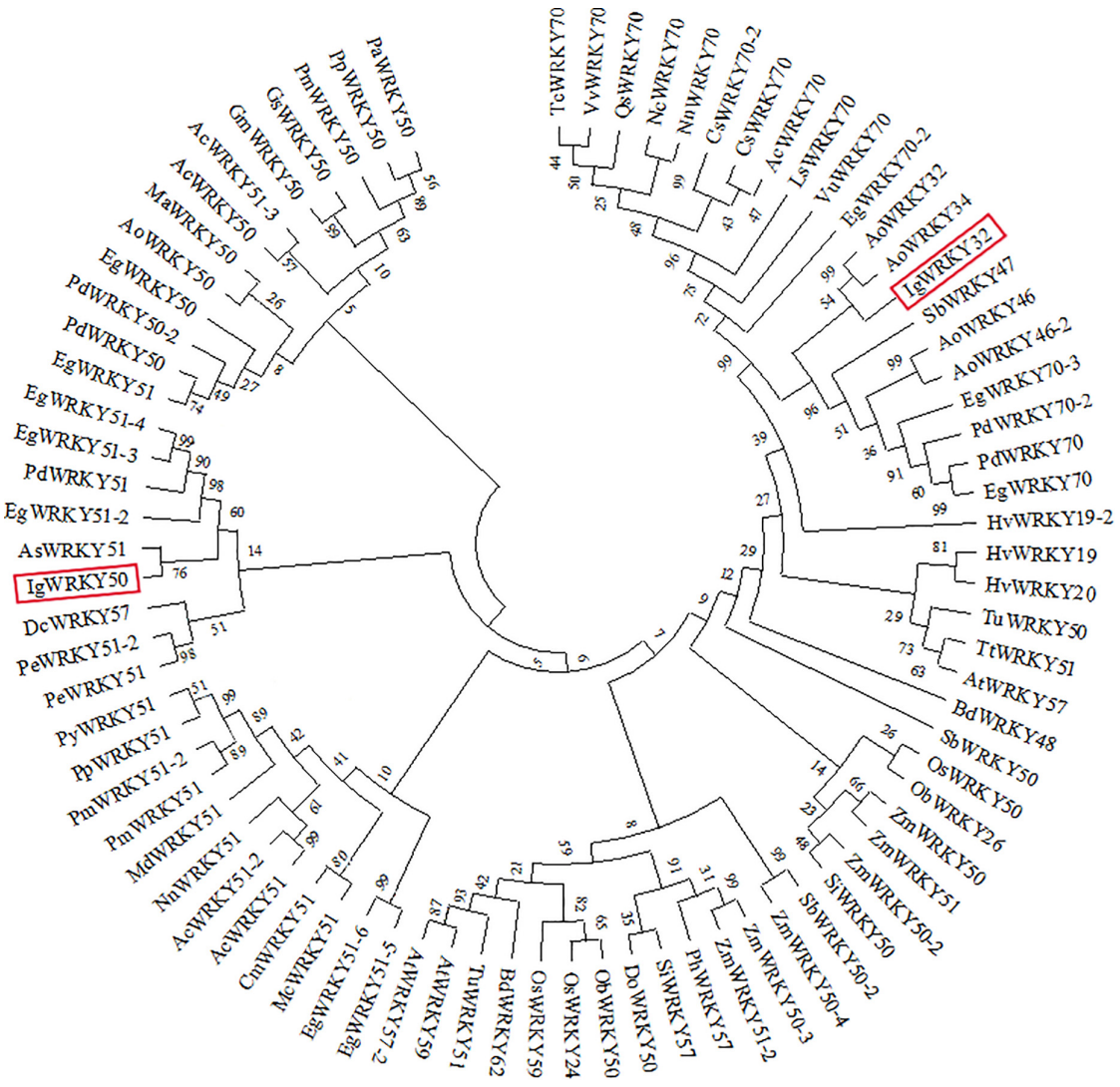


FIGURE 2
Phylogenetic relationship of *IgWRKY50* and *IgWRKY32* with their orthologous in other plant species. The phylogenetic tree was based on comparisons of amino acid sequences and produced by MEGA 6.0 software.

10.3389/fpls.2022.983600

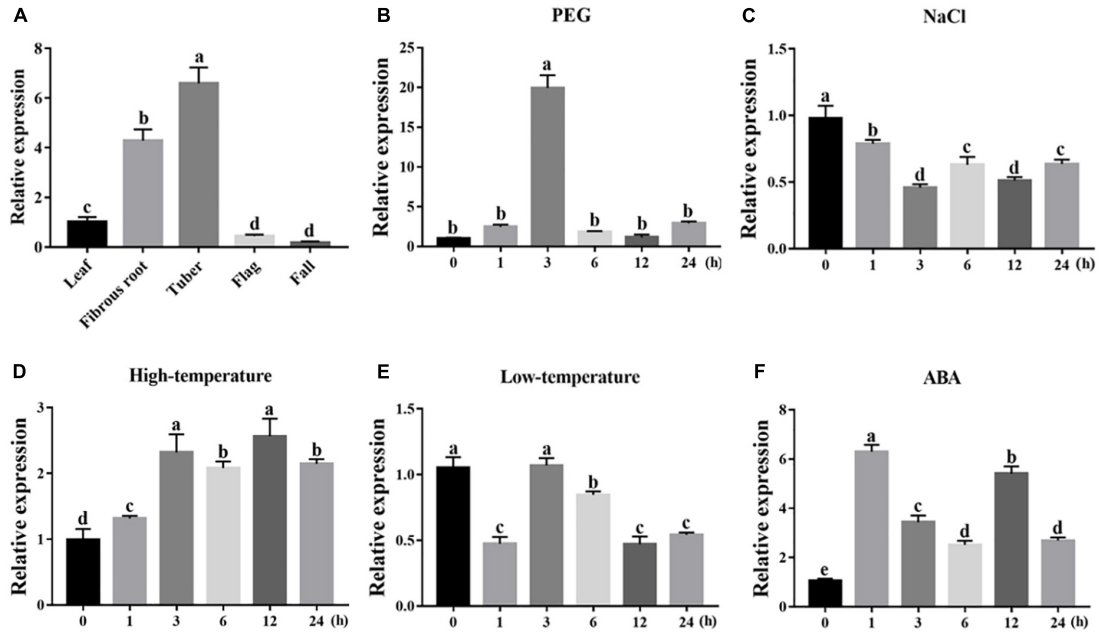


FIGURE 3
Transcription profiles of *IgWRKY50*. **(A)** Organ expression assay of *IgWRKY50* in different *Iris germanica* organs (leaf, fibrous, tuber, flag, fall). Transcription profiles of *IgWRKY50* under 200 g·L^{-1} PEG6000 **(B)**; 150 mM NaCl **(C)**; 42°C **(D)**; 4°C **(E)**; 100 μM ABA **(F)** treatments in *Iris germanica* leaves. The transcriptional level at time point 0 h (for the multiple stress experiments) and the leaf (for the organ expression assay) was defined as 1.0.

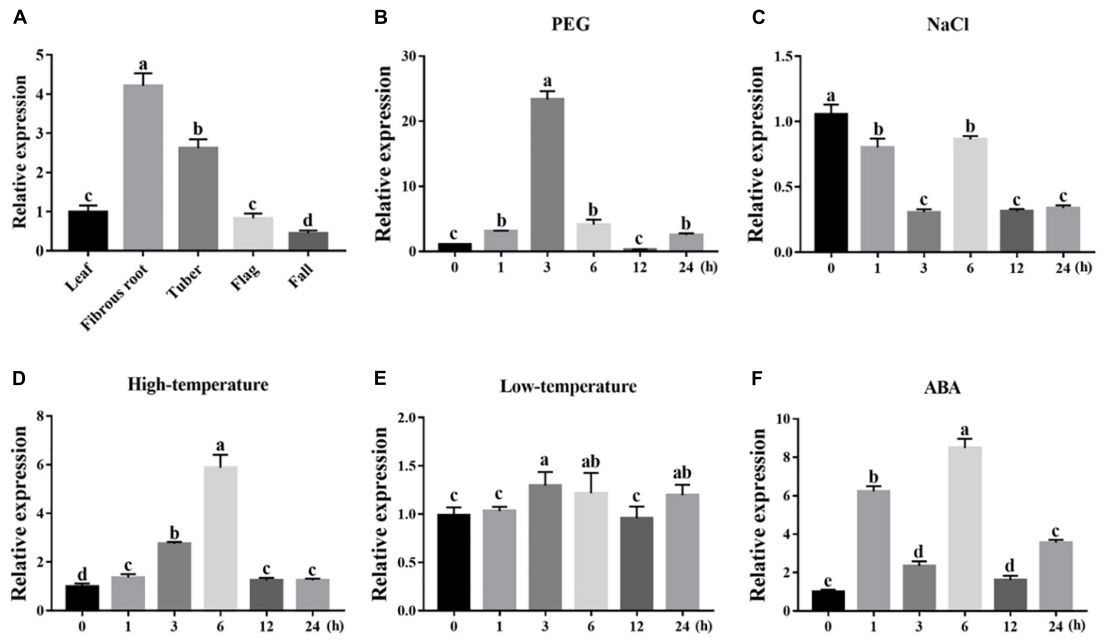


FIGURE 4
Transcription profiles of *IgWRKY32*. **(A)** Organ expression assay of *IgWRKY32* in different *Iris germanica* organs (leaf, fibrous, tuber, flag, fall). Transcription profiles of IgWRKY32 under 200 g·L^{-1} PEG6000 **(B)**; 150 mM NaCl **(C)**; 42°C **(D)**; 4°C **(E)**; 100 μM ABA **(F)** treatments in *Iris germanica* leaves. The transcriptional level at time point 0 h (for the multiple stress experiments) and the leaf (for the organ expression assay) was defined as 1.0. The vertical ordinates represent fold changes and the horizontal ordinates represent treatment times. Error bar represent standard deviations (*SD*). The data represent means ± *SD* of three biological replications. Different letters in bar graphs indicate significant differences at $p < 0.05$. ABA-abscisic acid.

sequence of the WRKY transcription factor family was found at amino acid sequence 146, and the zinc finger structure was the C2H2 type. The complete coding sequence of *IgWRKY32* was 912 bp, encoding 303 amino acids. The unique WRKYGQK sequence of the WRKY transcription factor family was found at amino acid sequence 129, and the zinc finger structure was the C2HC type (**Supplementary Figures 1A,B**). Using SMART software to analyze the gene structure, it was found that the proteins encoded by *IgWRKY50* and *IgWRKY32* had typical domains of the WRKY family. *IgWRKY50* was included in three low-complexity regions located at amino acids 14–21, 88–97, and 104–118. *IgWRKY32* was included in one low-complexity region located at amino acids 249–261 (**Figure 1A**).

The amino acid sequences of *IgWRKY50* and *IgWRKY32* were compared by BLAST, and it was found that the homology between the *IgWRKY50* and *MaWRKY50* proteins of *Musa acuminata* subsp. *malaccensis* was the highest, at 82.56%. *IgWRKY32* had the highest homology with the *AoWRKY32* protein of *Asparagus officinalis*, which was 76.62%, so the two genes were named *IgWRKY50* and *IgWRKY32*, respectively (**Supplementary Tables 4A,B**). *IgWRKY50* and *IgWRKY32* had similar tertiary structures, and both belonged to DNA-binding proteins, which were mainly composed of uncoiled structures and α-helices (**Figure 1B**). The crystal structures of *IgWRKY50* and *IgWRKY32* were highly similar to the conserved domains of the rice stress-responsive transcription factor *OsWRKY45*, and similar amino acids accounted for 43.55 and 46.88% of the total amino acid residues, respectively. Phylogenetic trees of 81 WRKY transcription factor family genes with high similarity to the *IgWRKY50* and *IgWRKY32* genes in 39 species were constructed by MEGA 6.0 software (**Supplementary Table 2**). The results showed that *IgWRKY50* was closely related to *AsWRKY51* of *Apostasia shenzhenica*, and *IgWRKY32* belonged to the same branch as *AoWRKY32* and *AoWRKY34* of *Asparagus officinalis* (**Figure 2**). It was speculated that *Iris germanica*, *Apostasia shenzhenica* and *Asparagus officinalis* belonged to Liliidae, so they had high homology.

Transcription profiles of *IgWRKY50* and *IgWRKY32* under abiotic stress

To dissect their potential functions, the expression of *IgWRKY50* and I*gWRKY32* was investigated in different tissues and under various stress conditions by RT–qPCR. The results showed that *IgWRKY50* and *IgWRKY32* were expressed in all organs, *IgWRKY50* had the highest expression in tubers, and *IgWRKY32* had the highest expression in

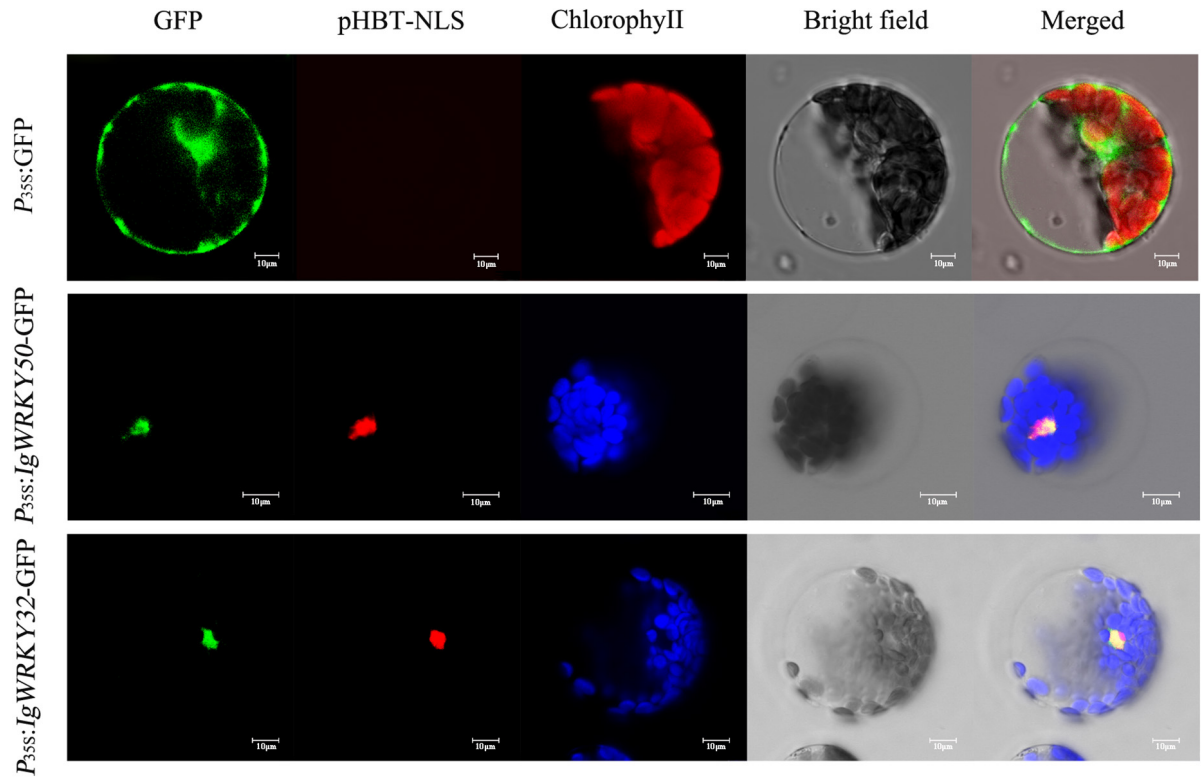


FIGURE 5
Subcellular localization of the *IgWRKY50* and *IgWRKY32*. P_{35S}:IgWRKY50-GFP, P_{35S}:IgWRKY32-GFP, and P_{35S}: GFP control vectors were transiently expressed in *Arabidopsis* leaf protoplasts. Scale bar = 10 μm.

10.3389/fpls.2022.983600

fibrous roots, indicating that *IgWRKY50* and *IgWRKY32* had important functions in tubers and fibrous roots of *Iris germanica*, respectively (Figures 3A, 4A). Transcription of *IgWRKY50* and *IgWRKY32* was induced by PEG-6000, high temperature and ABA treatments, while it was not affected by NaCl and low temperature. The transcriptional levels of

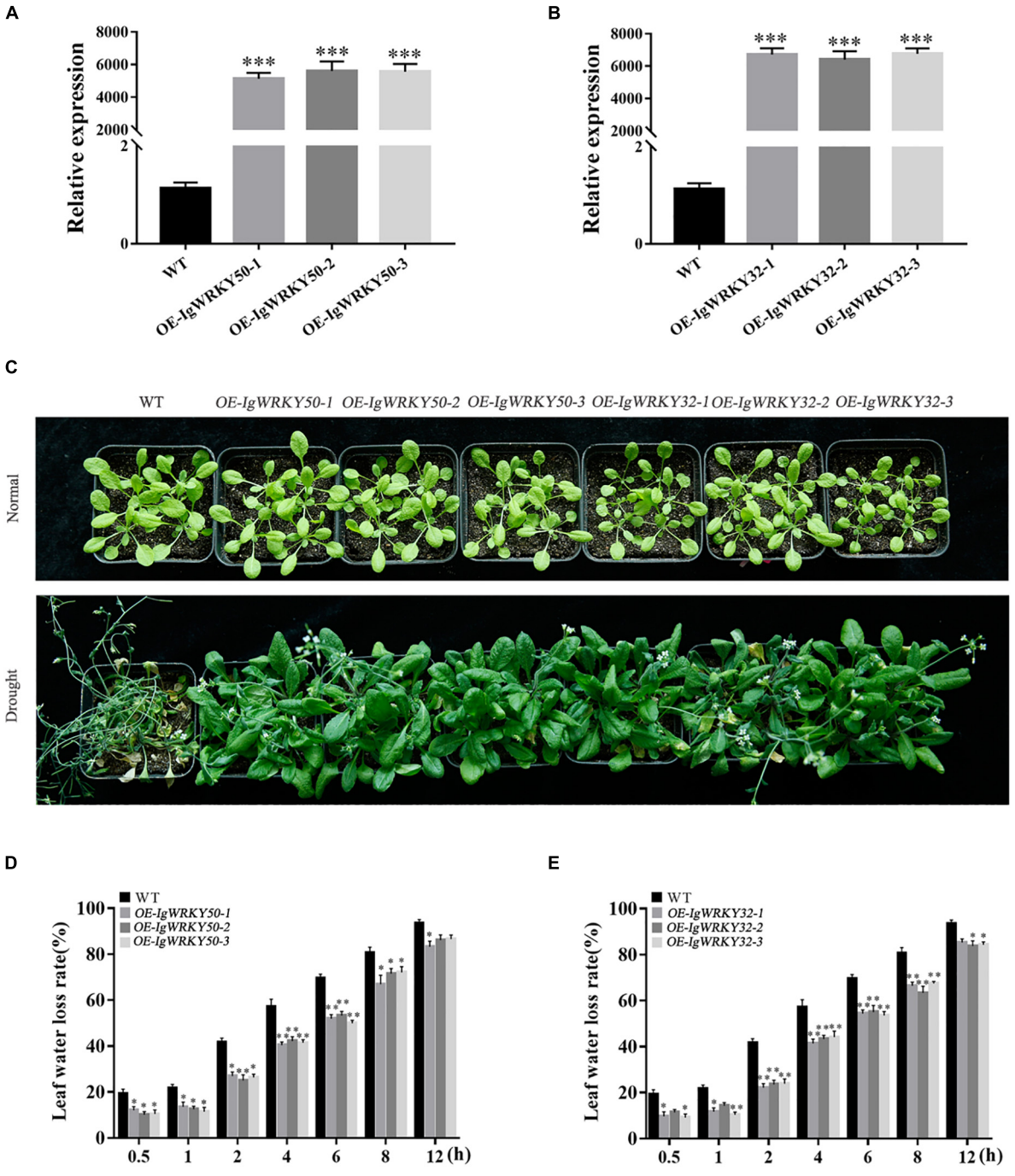


FIGURE 6
Phenotype analysis and tolerance assay of transgenic *Arabidopsis* and WT under drought treatment. Gene validation of *IgWRKY50* **(A)** and *IgWRKY32* **(B)** in transgenic *Arabidopsis* lines by qRT-PCR. Phenotype analysis of WT and the transgenic *Arabidopsis* under drought treatment **(C)**. The water loss rate of WT and *IgWRKY50* transgenic plants under drought condition **(D)**. The water loss rate of WT and *IgWRKY32* transgenic plants under drought condition **(E)**. Data are means ± *SD* of three independent experiments, and asterisks (*or**or***) represent the significant differences at $p < 0.05$ or $p < 0.01$ or $p < 0.001$, respectively (Student's *t*-test).

10.3389/fpls.2022.983600

IgWRKY50 and *IgWRKY32* peaked at 3 h after PEG-6000 treatment and were 19.93- and 23.32-fold higher than those of the control, respectively. Under high-temperature treatment, the transcriptional level of *IgWRKY50* was upregulated continuously and it reached its peak at 12 h (2.56-fold). The transcriptional level of *IgWRKY32* increased at first, reached its peak at 6 h (5.88-fold), and then it decreased rapidly to a level similar to that of the control. Under ABA treatment, the transcriptional levels of *IgWRKY50* and *IgWRKY32* peaked at 1 h (6.30-fold) and 6 h (8.49-fold), respectively (**Figures 3B–F**, **4B–F**).

IgWRKY50 and *IgWRKY32* were localized in the nucleus

The complete coding regions of *IgWRKY50* and *IgWRKY32* were cloned into the PBI221-GFP vector under the control of the CaMV 35S promoter. The protoplasts of *Arabidopsis* leaves were transformed and transferred into the nuclear targeting plasmid pHBT-NLS-mCherry. The empty vector was used as a control. The GFP signals of 35S:IgWRKY50-GFP and 35S:IgWRKY32-GFP were exclusively observed in the nucleus and they overlapped with the red fluorescence emitted by the

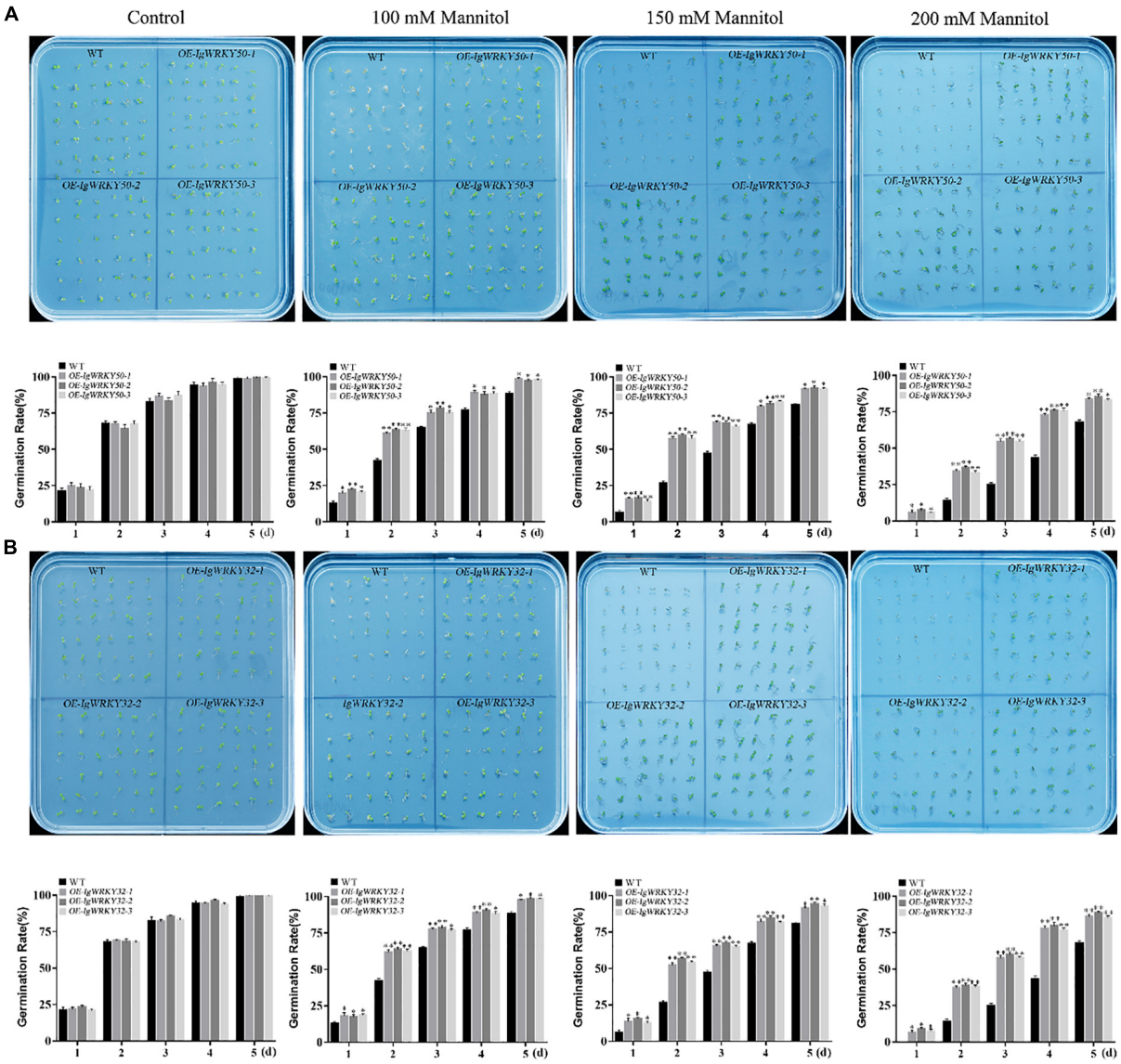


FIGURE 7
Germination of WT and transgenic *Arabidopsis* lines under mock drought stress. Seed germinations of WT and *IgWRKY50* transgenic *Arabidopsis* lines on ½ MS medium with 0 Mm, 100 mM, 150 mM, 200 mM Mannitol **(A)**. Seed germinations of WT and *IgWRKY32* transgenic *Arabidopsis* lines on ½ MS medium with 0 mM, 100 mM, 150 mM, 200 mM Mannitol **(B)**. Data are means ± *SD* of three independent experiments, and asterisks (*or**) represent the significant differences at $p < 0.05$ or $p < 0.01$, respectively (Student's *t*-test).

Maker-localized NLS protein in the nucleus, whereas the GFP signal of the control was discovered in the cytoplasm and nucleus (Figure 5). Therefore, *IgWRKY50* and *IgWRKY32* likely function as transcription factors in the nucleus.

Overexpression of *IgWRKY50* and *IgWRKY32* enhanced drought tolerance in transgenic plants

IgWRKY50 and *IgWRKY32* under the control of CaMV35S were transformed into *Arabidopsis*. Three highly expressed lines (OE-*IgWRKY50*-1, OE-*IgWRKY50*-2, OE-*IgWRKY50*-3, and OE-*IgWRKY32*-1, OE-*IgWRKY32*-2, OE-*IgWRKY32*-3) were selected from T3 homozygous lines with *IgWRKY50* and *IgWRKY32* to study their characteristics. The qRT-PCR analysis showed that *IgWRKY50* and *IgWRKY32* were detected in transgenic *Arabidopsis* plants, but not in WT (Figures 6A,B). The water loss rates of WT, *IgWRKY50*-overexpressing and *IgWRKY32*-overexpressing *Arabidopsis* lines were evaluated within a specified time interval. The results showed that the leaf water loss rate of the *IgWRKY50*- and *IgWRKY32*-overexpressing lines was lower than that of the WT, but there was no significant difference between the *IgWRKY50*- and *IgWRKY32*-overexpressing lines (Figures 6D,E). The 3-week-old WT and transgenic *Arabidopsis* seedlings were exposed to drought conditions for 21 days, and it was found that all types of *Arabidopsis* grown for 3 weeks under normal conditions grew robustly and had basically the same growth. After drought treatment, all of the leaves of the WT were seriously curled and withered and yellowed, while a few leaves of the *IgWRKY50*- and *IgWRKY32*-overexpressing lines showed curling and yellowing at the tip. Compared with the other transgenic lines, OE-*IgWRKY50*-1 and OE-*IgWRKY32*-2 had a relatively higher degree of leaf wilting, but their overall growth was good, and the yellowing and dryness degree of the leaves was significantly lower than that of the WT (Figure 6C).

To assess the osmotic stress tolerance of the transgenic *Arabidopsis* plants, WT and *IgWRKY50*- and *IgWRKY32*-overexpressing *Arabidopsis* seeds were sown on 1/2 MS medium containing mannitol (0, 100, 150, and 300 mM), and the seed germination rate was monitored for 5 days. There was no significant difference in seed germination between the transgenic lines and WT on the same medium without mannitol. On the medium containing 100 mM mannitol, the *IgWRKY50* and *IgWRKY32* transgenic seed germination rates were 97.62 and 98.08%, respectively, and the seed germination rate of WT was 88.28%. On the medium containing 150 mM mannitol, the seed germination rate of WT was 80.49%, while that of *IgWRKY50* and *IgWRKY32* was more than 90%. On the medium containing 200 mM mannitol, the transgenic seed germination rates of *IgWRKY50* and *IgWRKY32* were 83.81

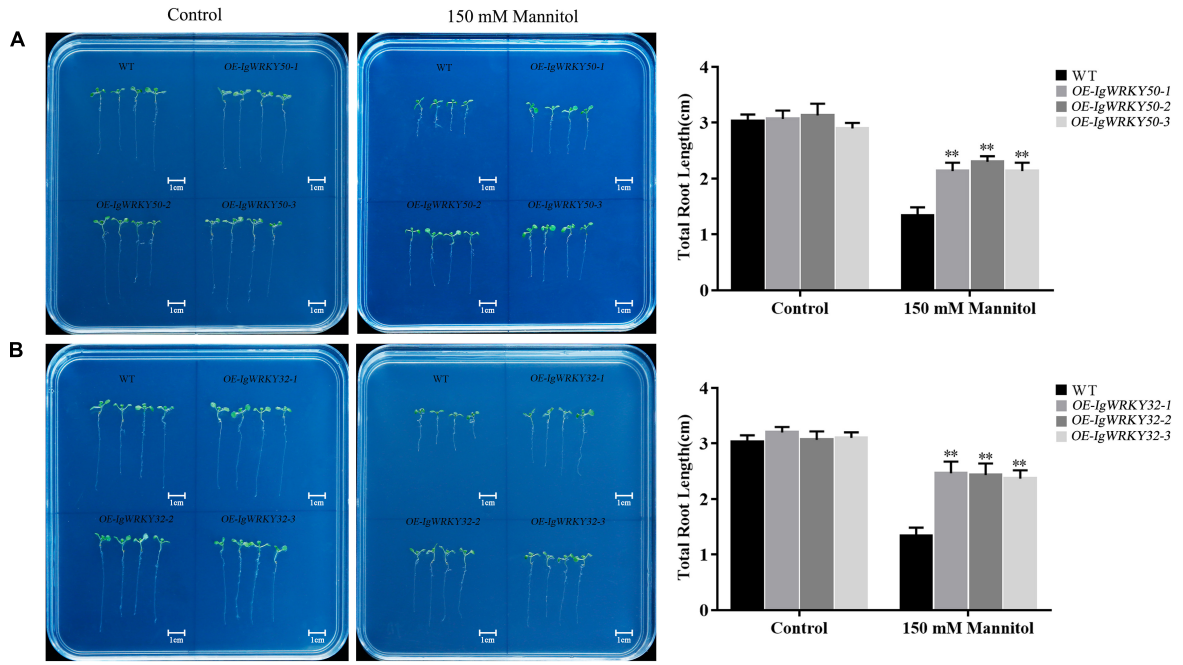


FIGURE 8
Root elongation of WT and transgenic *Arabidopsis* lines under mock drought stress. Root elongation of WT and *IgWRKY50* transgenic *Arabidopsis* lines on 1/2 MS medium with 0 and 150 mM Mannitol **(A)**. Root elongation of WT and *IgWRKY32* transgenic *Arabidopsis* lines on 1/2 MS medium with 0 and 150 mM Mannitol **(B)**. Scale bar = 1 cm. Data are means ± *SD* of three independent experiments, and asterisks (**) represent the significant differences at $p < 0.01$ (Student's *t*-test).

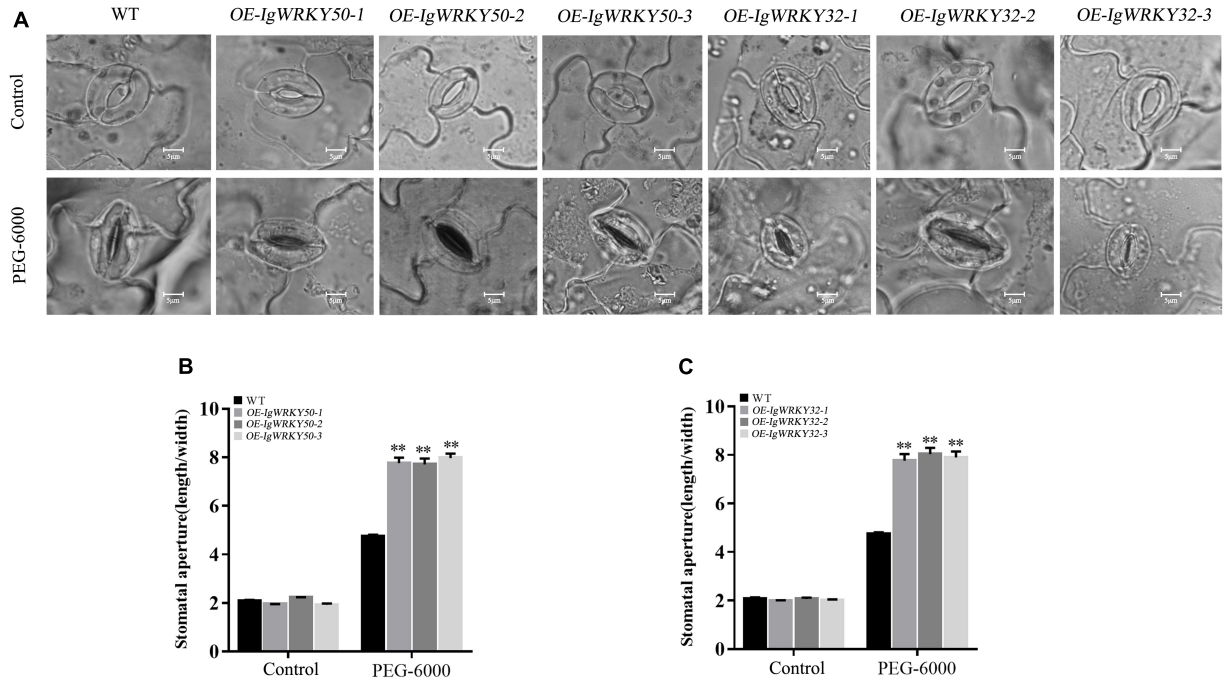


FIGURE 9
Stomatal opening and closing of WT and transgenic *Arabidopsis* leaves at seeding stage under 8% PEG-6000 stress. Stomatal closure of leaves of WT and transgenic lines **(A)**. Measurements of stomatal apertures (width/length) of *IgWRKY50* transgenic lines and WT plants **(B)**. Measurements of stomatal apertures (width/length) of *IgWRKY32* transgenic lines and WT plants **(C)**. Scale bar = 5 μm. Data are means ± *SD* of three independent experiments, and asterisks (**) represent the significant differences at $p < 0.01$ (Student's *t*-test).

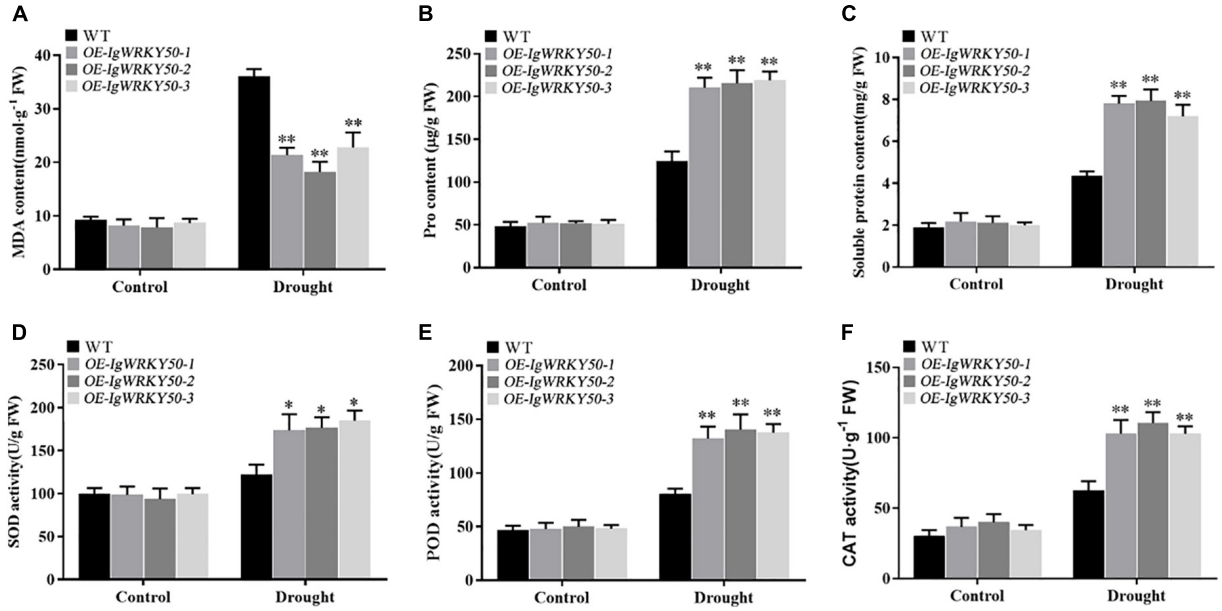


FIGURE 10
Changes of physiological indexes in WT and *IgWRKY50* transgenic lines under drought stress. **(A–F)** Are the changes of MDA content, Pro content, Soluble Protein content, SOD activity, POD activity, and CAT activity of WT and *IgWRKY50* transgenic lines under drought stress in sequence. Data are means ± *SD* of three independent experiments, and asterisks (*or**) represent the significant differences at $p < 0.05$ or $p < 0.01$, respectively (Student's *t*-test).

and 86.56%, respectively, and the seed germination rate of WT was only 67.90% (**Figure 7**). The results indicated that the overexpression of *IgWRKY50* and *IgWRKY32* genes improved the osmotic stress tolerance of transgenic *Arabidopsis* seeds during germination.

The transgenic lines and WT seeds were cultured on 1/2 MS medium at 22°C for 3 days and then transferred to 1/2 MS medium containing 0 and 150 mM mannitol for 7 days. On the medium without mannitol, the total roots of the transgenic lines and WT seedlings grew normally, and their lengths were basically the same. On the medium containing 150 mM mannitol, the growth of the total roots of the WT and transgenic lines was inhibited, and the inhibition degree of the WT was more obvious than that of the transgenic lines. The length of the total roots of the *IgWRKY32* strains was slightly longer than that of the *IgWRKY50* strains, but there was no significant difference (**Figure 8**). These results further confirmed that the overexpression of *IgWRKY50* and *IgWRKY32* genes enhanced the drought tolerance of the transgenic *Arabidopsis* plants.

In addition, we also observed stomatal opening and closing in leaves of transgenic lines and WT under osmotic stress. There was no significant difference in the degree of stomatal opening of each type of *Arabidopsis* before PEG-6000 treatment, while the degree of stomatal closure of the transgenic lines after treatment was more compact than that of the WT (**Figure 9A**). The ratio of the stomatal length to width also showed that the stomatal closure degree of the transgenic lines was stronger than that of the WT, but there was no significant difference among the transgenic lines (**Figures 9B,C**). Based on this result, it was speculated that the transgenic *Arabidopsis* could quickly close the stomata and reduce its transpiration rate to retain water, thereby obtaining a strong ability to resist drought stress in arid environments.

Overexpression of *IgWRKY50* and *IgWRKY32* changes the physiological and biochemical levels of the transgenic plants

To further confirm the role of *IgWRKY50* and *IgWRKY32* genes in the process of stress resistance of *Arabidopsis*, the physiological parameters of the WT and transgenic plants under drought stress for 14 days and normal water conditions were analyzed. Under normal conditions, the SOD, POD, and CAT activities and the MDA, Pro, SP contents were not significantly different between the WT and *IgWRKY50* and *IgWRKY32* transgenic lines. Under drought conditions, compared with the WT, the transgenic lines of *IgWRKY50* and *IgWRKY32* had a lower MDA content, a higher Pro and SP content, and higher SOD, POD, and CAT activity, but there was no significant difference between the *IgWRKY50* and *IgWRKY32* transgenic lines (**Figures 10**, **11**). These results suggest that *IgWRKY50* and *IgWRKY32* transgenic plants may improve drought resistance by accumulating osmotic substances and regulating the reactive oxygen species (ROS) system.

IgWRKY50 and *IgWRKY32* changed the transcripts of the stress-responsive genes

To explore the possible molecular mechanisms of *IgWRKY50* and *IgWRKY32* in stress responses, the relative expression levels of the stress-responsive genes were determined in transgenic and WT plants under drought conditions. The results showed that overexpression of *IgWRKY50* and *IgWRKY32* could promote the transcription of *RD29A, DREB2A, PP2CA,* and *ABA2*, especially the transcription of *PP2CA,* which reached a very high level in all transgenic lines. These results suggested that *IgWRKY50* and *IgWRKY32* may play a role in the drought stress response by regulating stress-related genes (**Figure 12**).

Discussion

The WRKY transcription factor family, as one of the largest transcription factor families in plants, could widely participate in the defense regulatory network and play an important regulatory role in the response of plants to abiotic stresses (Chen et al., 2012). In the past few years, the functions of WRKY transcription factors have been extensively explored in many plants, such as soybean (Wu et al., 2017; Shi et al., 2018), cotton (Yu et al., 2012; Wang et al., 2019), maize (Cai et al., 2014; Hu et al., 2021), and wheat (Okay et al., 2014; Ye et al., 2021). However, there are few studies of garden plants, and the role of the *Iris germanica* WRKY transcription factor in mediating abiotic stress responses has not been investigated.

In this study, two new WRKY genes, *IgWRKY50* and *IgWRKY32*, were isolated from the *Iris germanica* cultivar "Little Dream," and they belong to the WRKY transcription factor family Group II and Group III, respectively. Phylogenetic analysis showed that *IgWRKY50* and *IgWRKY32* had high homology with *Apostasia shenzhenica* and *Asparagus officinalis*, which belong to Liliidae. The IgWRKY50-GFP and IgWRKY32-GFP fusion proteins were exclusively localized to the nucleus of *Arabidopsis* protoplasts in a transient expression assay. This result was in agreement with their putative role as a transcription factor and similar to previous reports on some other WRKY TFs (Guo et al., 2011; Zhu et al., 2019). Most of the WRKY genes belonging to Group II and Group III could respond to drought stress signals. For example, the overexpression of wheat *TaWRKY1* and *TaWRKY33* genes (members of Group II and Group III) improved the drought

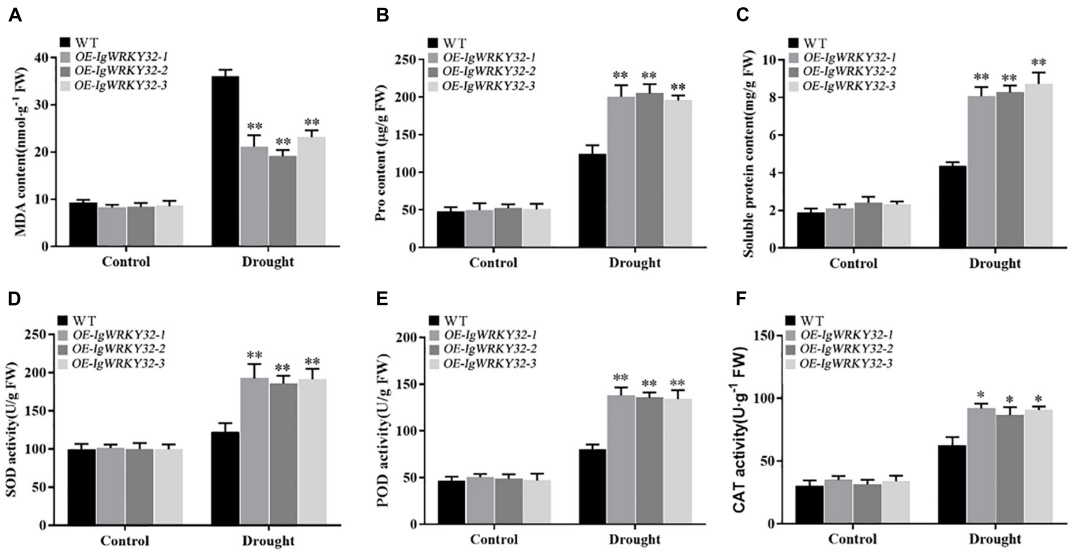


FIGURE 11
Changes of physiological indexes in WT and *IgWRKY32* transgenic lines under drought stress. **(A–F)** Are the changes of MDA content, Pro content, Soluble Protein content, SOD activity, POD activity, and CAT activity of WT and *IgWRKY32* transgenic lines under drought stress in sequence. Data are means ± *SD* of three independent experiments, and asterisks (*or**) represent the significant differences at $p < 0.05$ or $p < 0.01$, respectively (Student's *t*-test).

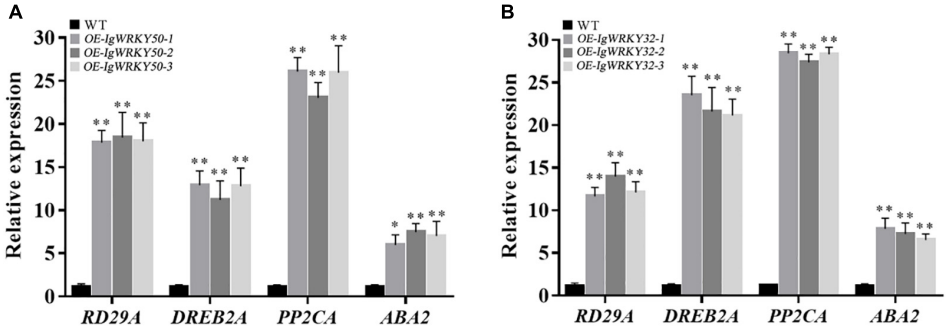


FIGURE 12
Expression levels of stress-responsive genes under regulation of *IgWRKY50* **(A)** and *IgWRKY32* **(B)**. The vertical ordinates are fold changes, and the horizontal coordinates are gene names. Data are means ± *SD* of three independent experiments, and asterisks (*or**) represent the significant differences at $p < 0.05$ or $p < 0.01$, respectively (Student's *t*-test).

resistance of *Arabidopsis* (He et al., 2016). *WRKY50* and *WRKY32* genes have been proven to be involved in plant hormone regulation and signal transduction pathways in *Arabidopsis* (Huang, 2018) and tobacco (Guo et al., 2018) under abiotic stress. At the same time, the significant expression patterns of *IgWRKY50* and *IgWRKY32* under PEG-6000, ABA and high-temperature stress also suggested that the two genes may play an important role in regulating the response of *Iris germanica* to abiotic stress.

WRKY gene overexpression could improve the tolerance of plants to multiple or single abiotic stresses (Jiang et al., 2012; Chu et al., 2015; Zhou et al., 2015). In our study, *IgWRKY50* and *IgWRKY32* were overexpressed in *Arabidopsis*, and the transgenic plants obtained a higher germination rate and a longer taproot length under osmotic stress. Transgenic *Arabidopsis* showed obvious drought resistance compared with WT under continuous natural drought. The water loss rate of the detached leaves has been widely used to reflect drought tolerance in plants (Li et al., 2020). The water loss rates of *IgWRKY50*- and *IgWRKY32*-overexpressing *Arabidopsis* plant isolated leaves were significantly lower than those of WT. This was consistent with the result that the stomatal closure of transgenic plants was higher than that of WT under PEG-6000 simulated drought stress. This result indicated that the overexpression of *IgWRKY50* and *IgWRKY32* improved the drought resistance of the transgenic plants to a certain extent.

Plants usually regulate their metabolism through a series of physiological and biochemical activities to reduce the damage caused by stress (Anjum et al., 2011). Drought stress often causes excessive accumulation of ROS and results in oxidative damage to cell components (Verslues et al., 2006). SOD, POD, and CAT are important antioxidant enzymes and they play an important role in scavenging active oxygen free radicals in plants (Wu et al., 2013). Many studies have shown that ROS scavenging ability was associated with plant tolerance to abiotic stress (Fang et al., 2015; Swain et al., 2017; Wang et al., 2017). Malondialdehyde (MDA) is one of the most important products of membrane lipid peroxidation (Grotto et al., 2009). Proline (Pro) and soluble proteins (SPs) play osmoregulatory roles in plant cytoplasm (Hanif et al., 2021). MDA, Pro, and SPs are the main indicators to determine plant stress resistance (Grotto et al., 2009; Jiao et al., 2012). Previous studies have shown that overexpression of *CKWRKY33* (isolated from *Caragana korshinskii*) in *Arabidopsis* could increase the activity of antioxidant enzymes and the content of osmotic regulators, reduce the accumulation of ROS and MDA, and thus improve the resistance of transgenic plants (Li et al., 2021). In this study, the SOD, POD and CAT activities and the proline and soluble protein contents of transgenic plants were significantly higher than those of the WT, while the MDA content was significantly lower than that of the WT under drought conditions, indicating that the *IgWRKY50* and *IgWRKY32* genes improve the drought resistance of plants by increasing the activities of antioxidant enzymes and accumulating more osmotic substances.

The ABA pathway plays a key role in regulating plant growth and development and in responding to abiotic stresses (Tuteja, 2007; Skubacz et al., 2016). When plants are in an adverse environment, they often respond to abiotic stress through ABA-dependent or ABA-independent pathways (Shinozaki and Yamaguchi-Shinozaki, 2007; Zhang et al., 2012). *PP2CA* (Ma et al., 2009; Nakashima et al., 2014), *ABA2* (Leoveanu, 2015; Nègre et al., 2019), *DREB2A* (Sakuma et al., 2006; Soma et al., 2021), and *RD29A* (Narusaka et al., 2003) are well known ABA responsive genes. The expression of *PP2CA* and *ABA2* (ABA-dependent) and *DREB2A* and *RD29A* (ABA-independent) genes were enhanced in I*gWRKY50*- and *IgWRKY32*-overexpressing transgenic *Arabidopsis thaliana* plants. It suggested that *IgWRKY50* and *IgWRKY32* may be involved in the regulation of drought stress through ABA-dependent and ABA-independent pathways. The similar findings were also found in the functions of *TaWRKY46* and *TaWRKY93* transcription factors. The former regulated *ABF3*, *RD29B*, *DREB2A*, *CBF2*, and *CBF3*, the latter acted on *ABF3*, *ABI1*, *ABI2*, *DREB2A*, *RD19A*, and *RD21* (Qin et al., 2015; Li et al., 2020). This may be because a single WRKT TF can participate in regulating several seemingly disparate processes (Rushton et al., 2010). The result of high expression of *PP2CA*, *ABA2*, *DREB2A*, and *RD29A* genes in transgenic *Arabidopsis thaliana* after drought stress is in accordance with previous findings that plants respond to abiotic stresses by enhancing the expression of stress-related genes (Sakuma et al., 2006; Bihmidine et al., 2013; He et al., 2016; Mao et al., 2016). It is speculated that the massive transcription

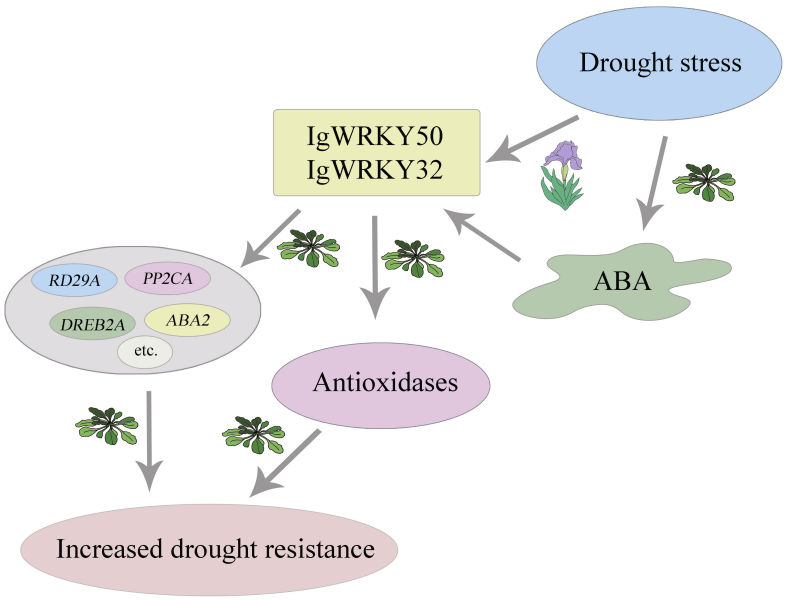


FIGURE 13
IgWRKY50 and *IgWRKY32* of *Iris germanica* improve plant drought resistance by mediating ABA signaling pathway. Simulating drought stress with 200 g·L^{-1} PEG 6000 induced the expression of *IgWRKY50* and *IgWRKY32* in *Iris germanica*. *IgWRKY50* and *IgWRKY32* improved the drought resistance of transgenic *Arabidopsis* by up-regulating the expression of related genes in ABA-dependent and −independent pathways, increasing the activity of antioxidant enzymes, and reducing oxidative damage.

of these genes involved in ABA signal transduction, thus the drought resistance of the transgenic lines is enhanced.

Based on the results of this study, we propose a diagram showing the role of *IgWRKY50* and *IgWRKY32* in the drought stress response regulation mechanism (**Figure 13**). Although *IgWRKY50* and *IgWRKY32* can improve the drought resistance of *transgenic Arabidopsis*, how *IgWRKY50* and *IgWRKY32* promote the expression of drought-responsive genes, how their products affect the network mechanism of drought resistance-related genes in *Arabidopsis* and how *IgWRKY50* and *IgWRKY32* function in *Iris germanica* plants still needs further verification.

Conclusion

Two *Iris germanica* WRKY genes, *IgWRKY50* and *IgWRKY32*, were isolated and identified for the first time, and their characteristics were investigated in this study. The proteins of the two genes were located in the nucleus. The expression of *IgWRKY50* and *IgWRKY32* was induced by PEG-6000, high temperature and ABA stresses. Further research revealed that overexpression of *IgWRKY50* and *IgWRKY32* could improve the drought resistance of transgenic *Arabidopsis*, and the transgenic plants could accumulate more osmotic regulatory substances, reduced MDA content, and enhanced the activities of SOD, POD, and CAT under natural drought treatment. At the same time, *IgWRKY50* and *IgWRKY32* also activated the expression of stress response genes such as *RD29A, DREB2A, PP2CA,* and *ABA2*. The results of this study indicated that *IgWRKY50* and *IgWRKY32*, as positive regulators of drought stress, have potential applications in molecular breeding for drought resistance in *Iris*.

Data availability statement

The datasets presented in this study can be found in online repositories. The names of the repository/repositories and accession number(s) can be found in the article/**Supplementary material**.

Author contributions

DH and JZ conceived and designed this study. JZ, MZ, QW, XH, DD, BS, SW, and PS performed the research and collected data. JZ analyzed the data and wrote the manuscript. JZ and XZ revised the manuscript. All authors read and approved the final manuscript, contributed to the article, and approved the submitted version.

Acknowledgments

This work was financially supported by the "14th Five-Year Plan" Breeding Innovation Team Building Modern Seed Industry Science and Technology Innovation Special Flower Modern Seed Industry Science and Technology Innovation Team Project of Hebei Province, China (21326317D).

Conflict of interest

The authors declare that the research was conducted in the absence of any commercial or financial relationships that could be construed as a potential conflict of interest.

Publisher's note

All claims expressed in this article are solely those of the authors and do not necessarily represent those of their affiliated organizations, or those of the publisher, the editors and the reviewers. Any product that may be evaluated in this article, or claim that may be made by its manufacturer, is not guaranteed or endorsed by the publisher.

Supplementary material

The Supplementary Material for this article can be found online at: https://www.frontiersin.org/articles/10.3389/fpls.2022.983600/full#supplementary-material

References

Akter, N., Sobahan, M. A., Uraji, M., Ye, W., Hossain, M. A., Mori, I. C., et al. (2012). Effects of depletion of glutathione on abscisic acid-and methyl jasmonate-induced stomatal closure in *Arabidopsis thaliana*. *Biosci. Biotech. Biochem.* 76, 2032–2037. doi: 10.1271/bbb.120384

Anjum, S. A., Xie, X. Y., Wang, L. C., Saleem, M. F., Man, C., and Lei, W. (2011). Morphological, physiological and biochemical responses of plants to drought stress. *Afr. J. Agric. Res.* 6, 2026–2032. doi: 10.5897/AJAR10.027

Azimi, M. H., and Alavijeh, M. K. (2021). Hybridization and assessment of new genotypes of *Iris germanica*. *Acta Horticulturae* 1315, 681–684. doi: 10.17660/ACTAHORTIC.2021.1315.101

Biasini, M., Bienert, S., Waterhouse, A., Arnold, K., Studer, G., Schmidt, T., et al. (2014). SWISS-MODEL: modelling protein tertiary and quaternary structure using evolutionary information. *Nucleic Acids Res.* 42, W252–W258. doi: 10.1093/nar/gku340

Bihmidine, S., Lin, J., Stone, J. M., Awada, T., Specht, J. E., and Clemente, T. E. (2013). Activity of the *Arabidopsis* RD29A and RD29B promoter elements in soybean under water stress. *Planta* 237, 55–64. doi: 10.1007/s00425-012-1740-9

Bo, W., Fu, B., Qin, G., Xing, G., and Wang, Y. (2017). Evaluation of drought resistance in *Iris germanica* L. based on subordination function and principal component analysis. *Emir. J. Food Agric.* 29, 770–778. doi: 10.9755/ejfa.2017.v29.i10.1260

Cai, R., Zhao, Y., Wang, Y., Lin, Y., Peng, X., Li, Q., et al. (2014). Overexpression of a maize WRKY58 gene enhances drought and salt tolerance in transgenic rice. *Plant Cell Tiss. Org.* 119, 565–577. doi: 10.1007/s11240-014-0556-7

Chen, L., Song, Y., Li, S., Zhang, L., Zou, C., and Yu, D. (2012). The role of WRKY transcription factors in plant abiotic stresses. *BBA Gene Regul. Mech.* 1819, 120–128. doi: 10.1016/j.bbagrm.2011.09.002

Cheng, Z., Luan, Y., Meng, J., Sun, J., Tao, J., and Zhao, D. (2021). WRKY transcription factor response to high-temperature stress. *Plants* 10:2211. doi: 10.3390/plants10102211

Chu, X., Wang, C., Chen, X., Lu, W., Li, H., Wang, X., et al. (2015). The cotton WRKY gene GhWRKY41 positively regulates salt and drought stress tolerance in transgenic *Nicotiana benthamiana*. *PLoS One* 10:e0143022. doi: 10.1371/journal.pone.0143022

Clough, S. J., and Bent, A. F. (2010). Floral dip: a simplified method for *Agrobacterium*-mediated transformation of *Arabidopsis thaliana*. *Plant J.* 16, 735–743. doi: 10.1046/j.1365-313x.1998.00343.x

Dong, J., Chen, C., and Chen, Z. (2003). Expression profiles of the *Arabidopsis* WRKY gene superfamily during plant defense response. *Plant Mol. Biol.* 51, 21–37. doi: 10.1023/A:1020780022549

Dou, L., Zhang, X., Pang, C., Song, M., Wei, H., Fan, S., et al. (2014). Genome-wide analysis of the WRKY gene family in cotton. *Mol. Genet. Genomics* 289, 1103–1121. doi: 10.1007/s00438-014-0872-y

Eulgem, T., Rushton, P. J., Robatzek, S., and Somssich, I. E. (2000). The WRKY superfamily of plant transcription factors. *Trends Plant Sci.* 5, 199–206. doi: 10.1016/S1360-1385(00)01600-9

Fan, Z., Gao, Y., Liu, R., Wang, S., Guo, Y., and Zhang, Q. (2022). Variations and heritability of phenotypic characters in the reblooming bearded *Iris* (*Iris germanica* L.). *Sci. Hortic.* 295:110844. doi: 10.1016/J.SCIENTA.2021.110844

Fan, Z., Gao, Y., Ren, Y., Guan, C., Liu, R., and Zhang, Q. (2020). To bloom once or more times: the reblooming mechanisms of *Iris germanica* revealed by transcriptome profiling. *BMC Genom.* 21:553. doi: 10.1186/s12864-020-06951-x

Fang, Y., Liao, K., Du, H., Xu, Y., Song, H., Li, X., et al. (2015). A stress-responsive NAC transcription factor SNAC3 confers heat and drought tolerance through modulation of reactive oxygen species in rice. *J. Exp. Bot.* 66, 6803–6817. doi: 10.1093/jxb/erv386

Feng, Z. J., Cui, X. Y., Cui, X. Y., Chen, M., Yang, G. X., Ma, Y. Z., et al. (2015). The soybean GmDi19-5 interacts with GmLEA3.1 and increases sensitivity of transgenic plants to abiotic stresses. *Front. Plant Sci.* 6:179. doi: 10.3389/fpls.2015.00179

Fereres, E., Goldhamer, D. A., and Parsons, L. R. (2003). Irrigation water management of horticultural crops. *HortScience* 38, 1036–1042. doi: 10.1007/s00122-003-1334-9

Fu, L., Ding, Z., Han, B., Hu, W., Li, Y., and Zhang, J. (2016). Physiological investigation and transcriptome analysis of polyethylene glycol (PEG)-induced dehydration stress in cassava. *Int. J. Mol. Sci.* 17:283. doi: 10.3390/ijms17030283

Grotto, D., Maria, L. S., Valentini, J., Paniz, C., Schmitt, G., Garcia, S. C., et al. (2009). Importance of the lipid peroxidation biomarkers and methodological aspects for malondialdehyde quantification. *Quim. Nova* 32, 169–174. doi: 10.1590/S0100-40422009000100032

Guo, D., Yang-Ying, Q. U., Zhi-Yong, N. I., and Chen, Q. J. (2018). Effects of PEG-6000 and NaCl Stress on seed germination and seedling growth of the tobacco with GbWRKY32 gene. *Xinjiang Agric. Sci.* 55, 1417–1427. doi: 10.6048/j.issn.1001-4330.2018.08.006

Guo, R., Yu, F., Gao, Z., An, H., Cao, X., and Guo, X. (2011). GhWRKY3, a novel cotton (*Gossypium hirsutum* L.) WRKY gene, is involved in diverse stress responses. *Mol. Biol. Rep.* 38, 49–58. doi: 10.1007/s11033-010-0076-4

Han, Y., Sun, G., and Huang, S. (2006). Effects of drought stress on physiological parameters of five ornamental groundcover *Iris* species. *Northern Horticult.* 6, 96–98. doi: 10.3969/j.issn.1001-0009.2006.06.052

Hanif, S., Saleem, M. F., Sarwar, M., Irshad, M., Shakoor, A., Wahid, M. A., et al. (2021). Biochemically triggered heat and drought stress tolerance in rice by proline application. *J. Plant Growth Regul.* 40, 305–312. doi: 10.1007/s00344-020-10095-3

He, G. H., Xu, J. Y., Wang, Y. X., Liu, J. M., Li, P. S., Chen, M., et al. (2016). Drought-responsive wrky transcription factor genes Tawrky1 and Tawrky33 from wheat confer drought and/or heat resistance in *Arabidopsis*. *BMC Plant Biol.* 16:116. doi: 10.1186/s12870-016-0806-4

Hu, W., Ren, Q., Chen, Y., Xu, G., and Qian, Y. (2021). Genome-wide identification and analysis of WRKY gene family in maize provide insights into regulatory network in response to abiotic stresses. *BMC Plant Biol.* 21:427. doi: 10.1186/s12870-021-03206-z

Huang, G. T., Ma, S. L., Bai, L. P., Zhang, L., Ma, H., Jia, P., et al. (2012). Signal transduction during cold, salt, and drought stresses in plants. *Mol. Biol. Rep.* 39, 969–987. doi: 10.1007/s11033-011-0823-1

Huang, R. (2018). Functional analysis of transcription factor genes PheWRKY11-2 and PheWRKY50-1 in Moso Bamboo. *Chinese Acad. Forest.* [Epub ahead of print].

Jiang, J., Ma, S., Ye, N., Jiang, M., Cao, J., and Zhang, J. (2017). WRKY transcription factors in plant responses to stresses. *J. Integr. Plant Biol.* 59, 86–101. doi: 10.1111/jipb.12513

Jiang, Y. J., Gang, L. G., and Yu, D. Q. (2012). Activated expression of WRKY57 confers drought tolerance in *Arabidopsis*. *Mol. Plant* 5, 1375–1388. doi: 10.1093/mp/sss080

Jiao, Z., Li, Y., Li, J., Xu, X., Li, H., Lu, D., et al. (2012). Effects of exogenous chitosan on physiological characteristics of potato seedlings under drought stress and rehydration. *Potato Res.* 55, 293–301. doi: 10.1007/s11540-012-9223-8

Leoveanu, C. (2015). *The Investigation of Novel Functions of Abscisic Acid 2 Through Protein-Protein Interactions*. Toronto, ON: University of Toronto.

Letunic, I., and Bork, P. (2018). 20 years of the SMART protein domain annotation resource. *Nucleic Acids Res.* 46, D493–D496. doi: 10.1093/nar/gkx922

Letunic, I., Khedkar, S., and Bork, P. (2021). SMART: recent updates, new developments and status in 2020. *Nucleic Acids Res.* 49, D458–D460. doi: 10.1093/nar/gkaa937

Li, H., Gao, Y., Xu, H., Dai, Y., Deng, D., and Chen, J. (2013). ZmWRKY33, a WRKY maize transcription factor conferring enhanced salt stress tolerances in *Arabidopsis*. *Plant Growth Regul.* 70, 207–216. doi: 10.1007/s10725-013-9792-9

Li, X., Tang, Y., Zhou, C., Zhang, L., and Lv, J. (2020). A wheat wrky transcription factor TaWRKY46 enhances tolerance to osmotic stress in transgenic *Arabidopsis* plants. *Int. J. Mol. Sci.* 21:1321. doi: 10.3390/ijms21041321

Li, Z., Liang, F. P., Zhang, T. B., Fu, N., Pei, X. W., and Long, Y. (2021). Enhanced tolerance to drought stress resulting from *Caragana korshinskii* CkWRKY33 in transgenic *Arabidopsis thaliana*. *BMC Genom. Data* 22:11. doi: 10.1186/s12863-021-00965-4

Liu, C., Wu, Y., and Wang, X. (2012). bZIP transcription factor OsbZIP52/RISBZ5: a potential negative regulator of cold and drought stress response in rice. *Planta* 235, 1157–1169. doi: 10.1007/s00425-011-1564-z

Luo, X., Bai, X., Sun, X., Zhu, D., Liu, B., Ji, W., et al. (2013). Expression of wild soybean WRKY20 in *Arabidopsis* enhances drought tolerance and regulates ABA signalling. *J. Exp. Bot.* 64, 2155–2169. doi: 10.1093/jxb/ert073

Ma, Y., Szostkiewicz, I., Korte, A., Moes, D., Yang, Y., Christmann, A., et al. (2009). Regulators of PP2C phosphatase activity function as abscisic acid sensors. *Science* 324, 1064–1068. doi: 10.1126/science.1172408

Maeo, K., Hayashi, S., Kojima-Suzuki, H., Morikami, A., and Nakamura, K. (2001). Role of conserved residues of the WRKY domain in the DNA-binding of tobacco WRKY family proteins. *Biosci. Biotech. Biochem.* 65, 2428–2436. doi: 10.1271/bbb.65.2428

Mangelsen, E., Kilian, J., Berendzen, K. W., Kolukisaoglu, ÜH., Harter, K., Jansson, C., et al. (2008). Phylogenetic and comparative gene expression analysis of barley (*Hordeum vulgare*) WRKY transcription factor family reveals putatively retained functions between monocots and dicots. *BMC Genomics* 9:194. doi: 10.1186/1471-2164-9-194

Mao, H., Yu, L., Han, R., Li, Z., and Liu, H. (2016). ZmNAC55, a maize stress-responsive NAC transcription factor, confers drought resistance in transgenic *Arabidopsis*. *Plant Physiol. Biochem.* 105, 55–66. doi: 10.1016/j.plaphy.2016.04.018

Mwadzingeni, L., Shimelis, H., Dube, E., Laing, M. D., and Tsilo, T. J. (2016). Breeding wheat for drought tolerance: progress and technologies. *J. Integr. Agric.* 15, 935–943. doi: 10.1016/S2095-3119(15)61102-9

Nakashima, K., Yamaguchi-Shinozaki, K., and Shinozaki, K. (2014). The transcriptional regulatory network in the drought response and its crosstalk in abiotic stress responses including drought, cold, and heat. *Front. Plant Sci.* 5:170. doi: 10.3389/fpls.2014.00170

Narusaka, Y., Nakashima, K., Shinwari, Z. K., Sakuma, Y., Furihata, T., Abe, H., et al. (2003). Interaction between two cis-acting elements, ABRE and DRE, in ABA-dependent expression of *Arabidopsis* RD29A gene in response to dehydration and high-salinity stresses. *Plant J.* 34, 137–148. doi: 10.1046/j.1365-313X.2003.01708.x

Nègre, D., Aite, M., Belcour, A., Frioux, C., Brillet-Guéguen, L., Liu, X., et al. (2019). Genome–scale metabolic networks shed light on the carotenoid biosynthesis pathway in the brown algae *Saccharina japonica* and *Cladosiphon okamuranus*. *Antioxidants* 8:564. doi: 10.3390/antiox8110564

Okay, S., Derelli, E., and Unver, T. (2014). Transcriptome-wide identification of bread wheat WRKY transcription factors in response to drought stress. *Mol. Genet. Genomics* 289, 765–781. doi: 10.1007/s00438-014-0849-x

Pettersen, E. F., Goddard, T. D., Huang, C. C., Couch, G. S., Greenblatt, D. M., Meng, E. C., et al. (2004). UCSF Chimera–a visualization system for exploratory research and analysis. *J. Comput. Chem.* 25, 1605–1612. doi: 10.1002/jcc.20084

Qin, Y., Tian, Y., and Liu, X. (2015). A wheat salinity-induced WRKY transcription factor TaWRKY93 confers multiple abiotic stress tolerance in *Arabidopsis thaliana*. *Biochem. Biophys. Res. Commun.* 464, 428–433. doi: 10.1016/j.bbrc.2015.06.128

Qiu, Y., Jing, S., Fu, J., Li, L., and Yu, D. (2004). Cloning and analysis of expression profile of 13 WRKY genes in rice. *Chinese Sci. Bull.* 49, 2159–2168. doi: 10.1360/csb2004-49-18-1860

Qiu, Y., and Yu, D. (2009). Over-expression of the stress-induced OsWRKY45 enhances disease resistance and drought tolerance in *Arabidopsis*. *Environ. Exp. Bot.* 65, 35–47. doi: 10.1016/j.envexpbot.2008.07.002

Rahman, H., Ramanathan, V., Nallathambi, J., Duraialagaraja, S., and Muthurajan, R. (2016). Over-expression of a NAC 67 transcription factor from finger millet (*Eleusine coracana* L.) confers tolerance against salinity and drought stress in rice. *BMC Biotechnol.* 16:35. doi: 10.1186/s12896-016-0261-1

Romero, I., Alegria-Carrasco, E., de Pradena, A. G., Vazquez-Hernandez, M., Escribano, M. I., Merodio, C., et al. (2019). WRKY transcription factors in the response of table grapes (cv. Autumn Royal) to high CO2 levels and low temperature. *Postharvest Biol. Technol.* 150, 42–51. doi: 10.1016/j.postharvbio.2018.12.011

Rushton, P. J., Somssich, I. E., Ringler, P., and Shen, Q. J. (2010). WRKY transcription factors. *Trends Plant Sci.* 15, 247–258. doi: 10.1016/j.tplants.2010.02.006

Sakuma, Y., Maruyama, K., Osakabe, Y., Qin, F., Seki, M., Shinozaki, K., et al. (2006). Functional analysis of an *Arabidopsis* transcription factor, DREB2A, involved in drought-responsive gene expression. *Plant Cell* 18, 1292–1309. doi: 10.1105/tpc.105.035881

Shao, H. B., Chu, L. Y., Jaleel, C. A., Manivannan, P., Panneerselvam, R., and Shao, M. A. (2009). Understanding water deficit stress-induced changes in the basic metabolism of higher plants–biotechnologically and sustainably improving agriculture and the ecoenvironment in arid regions of the globe. *Crit. Rev. Biotechnol.* 29, 131–151. doi: 10.1080/07388550902869792

Sheen, J. (2001). Signal transduction in maize and *Arabidopsis mesophyll* protoplasts. *Plant Physiol.* 127, 1466–1475. doi: 10.1104/pp.010820

Shi, W. Y., Du, Y. T., Ma, J., Min, D. H., Jin, L. G., Chen, J., et al. (2018). The WRKY transcription factor GmWRKY12 confers drought and salt tolerance in soybean. *Int. J. Mol. Sci.* 19:4087. doi: 10.3390/ijms19124087

Shinozaki, K., and Yamaguchi-Shinozaki, K. (2007). Gene networks involved in drought stress response and tolerance. *J. Exp. Bot.* 58, 221–227. doi: 10.1093/jxb/erl164

Singh, K. B., Foley, R. C., and Oñate-Sánchez, L. (2002). Transcription factors in plant defense and stress responses. *Curr. Opin. Plant Biol.* 5, 430–436. doi: 10.1016/S1369-5266(02)00289-3

Skubacz, A., Daszkowska-Golec, A., and Szarejko, I. (2016). The role and regulation of ABI5 (ABA-Insensitive 5) in plant development, abiotic stress responses and phytohormone crosstalk. *Front. Plant Sci.* 7:1884. doi: 10.3389/fpls.2016.01884

Soma, F., Takahashi, F., Yamaguchi-Shinozaki, K., and Shinozaki, K. (2021). Cellular phosphorylation signaling and gene expression in drought stress responses: ABA-dependent and ABA-independent regulatory systems. *Plants* 10:756. doi: 10.3390/plants10040756

Swain, D. M., Sahoo, R. K., Srivastava, V. K., Tripathy, B. C., Tuteja, R., and Tuteja, N. (2017). Function of heterotrimeric G-protein γ subunit RGG1 in providing salinity stress tolerance in rice by elevating detoxification of ROS. *Planta* 245, 367–383. doi: 10.1007/s00425-016-2614-3

Tamura, K., Stecher, G., Peterson, D., Filipski, A., and Kumar, S. (2013). MEGA6: molecular evolutionary genetics analysis version 6.0. *Mol. Biol. Evol.* 30, 2725–2729. doi: 10.1093/molbev/mst197

Tuteja, N. (2007). Abscisic acid and abiotic stress signaling. *Plant Signal Behav.* 2, 135–138. doi: 10.4161/psb.2.3.4156

Verslues, P. E., Agarwal, M., Katiyar-Agarwal, S., Zhu, J., and Zhu, J. K. (2006). Methods and concepts in quantifying resistance to drought, salt and freezing, abiotic stresses that affect plant water status. *Plant J. Cell Mol. Biol.* 45, 523–539. doi: 10.1111/j.1365-313X.2005.02593.x

Wang, C., Lu, G., Hao, Y., Guo, H., Guo, Y., Zhao, J., et al. (2017). ABP9, a maize bZIP transcription factor, enhances tolerance to salt and drought in transgenic cotton. *Planta* 246, 453–469. doi: 10.1007/s00425-017-2704-x

Wang, C. T., Ru, J. N., Liu, Y. W., Yang, J. F., Li, M., Xu, Z. S., et al. (2018). The maize WRKY transcription factor ZmWRKY40 confers drought resistance in transgenic *Arabidopsis*. *Int. J. Mol. Sci.* 19:2580. doi: 10.3390/ijms19092580

Wang, N. N., Xu, S. W., Sun, Y. L., Liu, D., Zhou, L., Li, Y., et al. (2019). The cotton WRKY transcription factor (GhWRKY33) reduces transgenic *Arabidopsis* resistance to drought stress. *Sci. Rep.* 9, 1–13. doi: 10.1038/s41598-018-37035-2

Wang, Y., Zhang, Y., Liu, Q., Zhang, T., Chong, X., and Yuan, H. (2021). Genome-wide identification and expression analysis of BBX transcription factors in *Iris germanica* L. *Int. J. Mol. Sci.* 22, 8793. doi: 10.3390/IJMS22168793

Wu, B., Zhang, S. W., Gao, D., and Pan, C. M. (2013). Effect of drought stress and re-watering on active oxygen scavenging system of fructus evodiae cutting seedling. *J. Guangzhou Univ. Traditional Chinese Med.* 30, 78–82. doi: 10.13359/j.cnki.gzxbtcm.2013.01.001

Wu, J., Chen, J., Wang, L., and Wang, S. (2017). Genome-wide investigation of WRKY transcription factors involved in terminal drought stress response in common bean. *Front. Plant Sci.* 8:380. doi: 10.3389/fpls.2017.00380

Wu, K. L., Guo, Z. J., Wang, H. H., and Li, J. (2005). The WRKY family of transcription factors in rice and *Arabidopsis* and their origins. *DNA research* 12, 9–26. doi: 10.1038/modpathol.3880104

Wu, X., Chen, Q., Chen, L., Tian, F., Chen, X., Han, C., et al. (2022). A WRKY transcription factor, PyWRKY75, enhanced cadmium accumulation and tolerance in poplar. *Ecotox. Environ. Saf.* 239:113630. doi: 10.1016/j.ecoenv.2022.113630

Xiong, X., Sun, S., Li, Y., Zhang, X., Sun, J., and Xue, F. (2019). The cotton WRKY transcription factor GhWRKY70 negatively regulates the defense response against *Verticillium dahliae*. *Crop J.* 7, 393–402. doi: 10.1016/j.cj.2018.10.005

Ye, H., Qiao, L., Guo, H., Guo, L., Ren, F., Bai, J., et al. (2021). Genome-wide identification of wheat WRKY gene family reveals that TaWRKY75-A is referred to drought and salt resistances. *Front. Plant Sci.* 12:812. doi: 10.3389/fpls.2021.663118

Yousfi, F. E., Makhloufi, E., Marande, W., Ghorbel, A. W., Bouzayen, M., and Berges, H. (2016). Comparative analysis of WRKY genes potentially involved in salt stress responses in *Triticum turgidum* L. ssp. durum. *Front. Plant Sci.* 7:2034. doi: 10.3389/fpls.2016.02034

Yu, F., Huaxia, Y., Lu, W., Wu, C., Cao, X., and Guo, X. (2012). GhWRKY15, a member of the wrky transcription factor family identified from cotton (*Gossypium hirsutum* L.), is involved in disease resistance and plant development. *BMC Plant Biol.* 12:144. doi: 10.1186/1471-2229-12-144

Yu, S., Ai, C. R., Jing, S. J., and Yu, D. Q. (2010). Research progress on functional analysis of rice WRKY genes. *Rice Sci.* 17, 60–72. doi: 10.1016/S1672-6308(08)60105-5

Zhang, C., and Chen, W. (2013). Physiological-ecological responses of *Iris germanica* L. to Cd stress and its accumulation of Cd. *Acta Ecol. Sin.* 33, 2165–2172. doi: 10.5846/stxb201112251969

Zhang, J., Huang, D., Zhao, X., and Zhang, M. (2021). Evaluation of drought resistance and transcriptome analysis for the identification of drought-responsive genes in *Iris germanica*. *Sci. Rep.* 11, 1–21. doi: 10.1038/s41598-021-95633-z

Zhang, L., Zhao, G., Jia, J., Liu, X., and Kong, X. (2012). Molecular characterization of 60 isolated wheat MYB genes and analysis of their expression during abiotic stress. *J. Exp. Bot.* 63, 203–214. doi: 10.1093/jxb/err264

Zhang, Y., and Wang, L. (2005). The WRKY transcription factor superfamily: its origin in eukaryotes and expansion in plants. *BMC Evol. Biol.* 5:1. doi: 10.1186/1471-2148-5-1

Zhao, Y., Cheng, X., Liu, X., Wu, H., Bi, H., and Xu, H. (2018). The wheat MYB transcription factor TaMYB31 is involved in drought stress responses in *Arabidopsis*. *Front. Plant Sci.* 9:1426. doi: 10.3389/fpls.2018.01426

Zhao, Z., Li, T., Cheng, Y., Wang, F., and Zhao, X. (2021). Morphological and metabolic responses of four *Iris germanica* cultivars under salinity stress. *Sci. Hortic.* 28:109960. doi: 10.1016/J.SCIENTA.2021.109960

Zhou, L., Wang, N. N., Gong, S. Y., Lu, R., Li, Y., and Li, X. B. (2015). Overexpression of a cotton (*Gossypium hirsutum*) wrky gene, Ghwrky34, in *Arabidopsis* enhances salt-tolerance of the transgenic plants. *Plant Physiol. Biochem.* 96, 311–320. doi: 10.1016/j.plaphy.2015.08.016

Zhu, D., Hou, L., Xiao, P., Guo, Y., Deyholos, M. K., and Liu, X. (2019). VvWRKY30, a grape WRKY transcription factor, plays a positive regulatory role under salinity stress. *Plant Sci.* 280, 132–142. doi: 10.1016/j.plantsci.2018.03.018

frontiers | Frontiers in Plant Science

TYPE Original Research
PUBLISHED 08 September 2022
DOI 10.3389/fpls.2022.989946

Check for updates

OPEN ACCESS

EDITED BY
PingWu Liu,
Hainan University,
China

REVIEWED BY
Atique ur Rehman,
Bahauddin Zakariya University,
Pakistan
Amjad Iqbal,
Abdul Wali Khan University Mardan,
Pakistan

*CORRESPONDENCE
Haiyan Lan
lanhaiyan@xju.edu.cn

†These authors have contributed equally to this work and share first authorship

SPECIALTY SECTION
This article was submitted to Plant Abiotic Stress, a section of the journal Frontiers in Plant Science

RECEIVED 09 July 2022
ACCEPTED 18 August 2022
PUBLISHED 08 September 2022

CITATION
Zhang Y, Mutailifu A and Lan H (2022) Structure, development, and the salt response of salt bladders in *Chenopodium album* L.. *Front. Plant Sci.* 13:989946. doi: 10.3389/fpls.2022.989946

COPYRIGHT
© 2022 Zhang, Mutailifu and Lan. This is an open-access article distributed under the terms of the Creative Commons Attribution License (CC BY). The use, distribution or reproduction in other forums is permitted, provided the original author(s) and the copyright owner(s) are credited and that the original publication in this journal is cited, in accordance with accepted academic practice. No use, distribution or reproduction is permitted which does not comply with these terms.

Structure, development, and the salt response of salt bladders in *Chenopodium album* L.

Yigong Zhang†, Ayibaiheremu Mutailifu† and Haiyan Lan*

Xinjiang Key Laboratory of Biological Resources and Genetic Engineering, College of Life Science and Technology, Xinjiang University, Urumqi, China

Salt bladders are specialized epidermal structures that halophytes use to store and excrete excess salt. However, the cell wall composition during salt bladder development is unclear, and the functions of salt bladders in a few wild plants remain unexplored. Therefore, the present study examined salt bladder development, cell wall composition, and their roles under salt stress by employing bladder-brushed and unbrushed *Chenopodium album* plants. We found that the bladder cell of *C. album* was connected to the epidermal cells through a rectangular stalk cell and developed from the shoot tip and the young leaves. The polysaccharides of salt bladder cell wall showed dynamic distribution at different stages of development. Moreover, salt bladders affected Na^+ and K^+ accumulation, increased reactive oxygen species scavenging, and improved the osmoregulation and photosynthetic efficiency in leaves, subsequently enhancing the salt tolerance of plants. The findings strengthen our knowledge of the physiological mechanisms of the accessory structures in desert plants, which can be used as a reference for further research at the molecular level.

KEYWORDS

***Chenopodium album*, halophyte, salt bladder, polysaccharides, NaCl**

Introduction

Soil salinization is a major issue that inhibits plant growth and development, limiting agricultural production worldwide (Zhao et al., 2020). Most crops are sensitive to salt stress. Nevertheless, few plants, called halophytes, are salt-resistant or salt-tolerant and can live in saline environments for a long time. These plants have evolved unique salt tolerance mechanisms to cope with specific environmental stress (Flowers and Colmer, 2008). Approximately 50% of halophytes cope with salt stress through specialized epidermal structures called the epidermal bladder cells or the salt bladders, which are often the modified form of trichomes and accumulate and excrete excess salt *via* rupture (Ding et al., 2010; Shabala and Mackay, 2011). Thus, salt bladders play an important role in stress tolerance *via* salt secretion, water storage, and osmotic regulation (Shabala et al., 2014).

Salt bladder cells have a huge central vacuole as the primary salt storage site and a dense cytoplasm that contains a nucleus, mitochondria, chloroplasts, and other organelles; typically, the bladder cell remains connected to the leaf epidermal cells through stalk cells

(Smaoui et al., 2011; Guo et al., 2020). Salt bladder cells, composed of stalk and bladder cells, originate from the plant epidermis. During bladder complex formation, the "destined" epidermal cell develops a dense protoplasm and protrudes perpendicular to form the initial cell of the salt bladder; subsequently, the protuberant cell divides into two cells, producing a stalk cell and a bladder cell (Shabala et al., 2014). As the bladder cell matures, it continuously absorb salt, swells, or breaks, releasing ions into the environment (Yuan et al., 2016). However, there are some exceptions, such as *Mesembryanthemum crystallinum*, which has no stalk cells; here, the salt bladder cells are directly connected to the epidermal cells (Barkla et al., 2012, 2016).

Salt stress drastically reduces the intracellular turgor pressure of plants, causing dehydration and shrinkage. However, halophytes accumulate sodium (Na^+) and potassium (K^+) ions and provide sufficient turgor pressure for cell morphological maintenance and volume expansion; these ions get secreted through a break by an external force (Shabala, 2013). Salt bladder formation has been associated with endopolyploidy. It has been proposed that increased ploidy helps mitigate stress damage, and the increase in cell size under salinity contributes to tolerance by expanding the store size for Na^+ sequestration in *M. crystallinum* (Barkla et al., 2018). Moreover, salt bladders continuously absorb salts under salt stress, increasing intracellular turgor pressure. The changes in turgor pressure influence the reorientation of microtubules and actin cytoskeleton. Studies have also shown that the transcriptional level of V-ATPase in salt bladders significantly increased under salt stress. The V-ATPase helps in vacuolar Na^+ uptake and turgor pressure generation, promoting the rapid expansion of bladders cells (Barkla et al., 2016).

In addition, salt bladders confer ion sequestration in the vacuole and protect plants from ionic poisoning. The bladder cells accommodate salts at a concentration 60 times higher than the mesophyll cells (Wu et al., 2018). In quinoa (*Chenopodium quinoa* Willd.), under salt stress, the salt bladders accumulated 50% K^+ and 40% Na^+ and chloride (Cl^-), leading to robust salt tolerance; however, when the salt bladders were removed, a large amount of Na^+ and Cl^- remained in the leaves, resulting in a salt-sensitive phenotype (Kiani-Pouya et al., 2019). In *Atriplex canescens*, brushing the salt bladders reduced the growth and photosynthetic indexes under salt stress; these brushed plants could not excrete salt, and a large amount of Na^+ got accumulated in the mesophyll tissue, causing ionic toxicity and osmotic stress (Guo et al., 2019, 2020). Meanwhile, the bladderless mutant of *M. crystallinum* demonstrated reduced salt tolerance and productivity, with significantly lower Na^+ and Cl^- content in the aerial parts than in the wild type (Agarie et al., 2007). Research has also shown that the salt bladders can accumulate osmotic regulators and metabolites and maintain intracellular ion balance and osmotic stability, thereby improving plant salt tolerance and maintaining normal growth and development (Barkla et al., 2016; Böhm et al., 2018). However, the changes in the cell wall composition during salt bladder development have not been analyzed. Moreover, the functions of the salt bladders have not been thoroughly investigated in some wild plant species.

Chenopodium album L. is an annual wild herb that grows in saline-alkali regions and has excellent drought and saline-alkali resistance (Yao et al., 2010b). Its seeds can achieve a high germination rate under 300 mM NaCl stress, and the plants can tolerate 300 mM NaCl treatment (Yao et al., 2010a). The leaves of *C. album* have a high density of salt bladders, which gradually break down and fall off with development. However, the physiological mechanisms *via* which salt bladders regulate the impact of Na^+ in *C. album* remain unexplained. Therefore, the present study examined the biogenesis of salt bladders in *C. album* and analyzed their cell wall composition. Furthermore, we investigated the role of salt bladders in stress response by employing brushed (to remove salt bladder) and unbrushed *C. album* plants. The findings of this research will extend our understanding of the biogenesis and functions of salt bladders in desert plants.

Materials and methods

Plant growth conditions and NaCl treatment

Chenopodium album seeds were obtained from Urumqi County in Xinjiang, China. These seeds were rinsed repeatedly with purified water and allowed to germinate in Petri dishes at 25°C in the dark for 7 days. Seedlings with uniform growth were transplanted into plastic pots (15 cm × 10 cm, five plants/pot) filled with a mixture of *nutrient soil, vermiculite, and perlite (2:1:1)* and maintained in a greenhouse at 25°C (day/night), 16 h/8 h photoperiod (light/dark; 800 μmol m^{-2} s^{-1} flux density), and 45% relative humidity. Plants were allowed to grow for 4 weeks and then treated with Hoagland solution containing salts as follows, maintaining 10 pots per treatment: (1) Control (Hoagland solution, 0 mM NaCl); (2) low salt stress (Hoagland solution with 100 mM NaCl); (3) high salt stress (Hoagland solution with 300 mM NaCl). After 7 days, the seedlings were collected to determine the physiological parameters.

Analysis of epidermal cell development

The true leaf, young leaves, and mature leaves at the early stages of *C. album* growth were collected to analyze the epidermal cell development. The collected tissue was first fixed in 50% FAA (formalin-acetic acid-alcohol) solution at 4°C for 24 h and dehydrated at different concentrations of ethanol and xylene. The tissue was then embedded in paraffin for about 3 h at 60°C, and the paraffin blocks were sliced into 5–7 μm sections with a microtome (Leica RM2126, Leica, Germany). The tissue sections on the slides were deparaffinized and stained with 1% safranin overnight and then with 0.5% fast green for 3 s. The stained

sections were sealed and observed under a microscope (SMZ25, Nikon, Japan).

Analysis of cell wall composition of salt bladders

Immunocytochemistry was performed to determine the composition of the bladder cell wall. The tissue section on the slide was incubated in blocking solution (1% bovine serum albumin in phosphate buffer saline; pH 7.2; PBS-BSA) at 37°C for 1 h and then with diluted (1:10 in BSA) CCRC-M1 (recognizes fucose (Fuc)-containing epitope), CCRC-M7 (arabinogalactan epitope), and CCRC-M38 (de-esterified homogalacturonan) primary monoclonal antibodies (Carbosource Services, Georgia, United States) for 1 h. After incubation, the slides were washed five times with PBS-BSA and allowed to react with horseradish peroxidase (HRP)-labeled secondary antibody (goat anti-mouse IgG) diluted in PBS-BSA (1:500) at 37°C for 1 h. In control, the primary antibodies were replaced with PBS. Finally, all sections were stained with diaminobenzidine (DAB; ZSGB-BIO, ZLI-9018) for 3 min and dehydrated twice in absolute ethanol and xylene for 5 min. The sections were observed under a Nikon ECLIPSE Ti-E microscope, and the digital images were captured with a Nikon DS-Fi1 digital camera; the extended focal range images were analyzed and visualized with the NIS-Elements D imaging software (version 4.0).

Determination of Na^+ and K^+ concentrations in leaves under salt stress

The leaves were used to analyze the Na^+ and K^+ concentrations after removing salt bladders from both sides of the leaf with a soft nylon brush, as described previously (Pan et al., 2016); the unbrushed leaves were used as the control. The Na^+ and K^+ ions were extracted from the oven-dried brushed and unbrushed tissues (young leaf and mature leaf) with 1% nitric acid under 120°C for 2 h and analyzed by inductively coupled plasma mass spectrometry (iCAP™ RQ ICP-MS, Thermo Fisher, United States), as described earlier (Cheng et al., 2004).

Physiological analysis of leaves under salt stress

Seedlings were grown for 4 weeks under controlled conditions. One day before the commencement of salt stress, the salt bladders were gently brushed off from the leaf surface using a nylon brush. All salt bladders on the stem and petioles were also removed. Plants were then irrigated daily with 100 or 300 mM NaCl for 2 weeks. As new leaves emerged, salt bladders were regularly removed from the leaf surface and the petioles until the end of the experiment. Proline and betaine content, malondialdehyde (MDA) and hydrogen peroxide (H_2O_2) levels, and catalase (CAT), superoxide dismutase (SOD), and peroxidase (POD) activities in the leaves were measured following the microplate technique using the corresponding detection kits (G0111W, G0122W, G0109W, G0112W, G0105W, G0101W, and G0107W, respectively; Suzhou Geruisi, China). Three biological replicates and three technical replicates were used for each assay.

Assessment of photosynthesis under salt stress

Chlorophyll content

Leaves were collected from each treatment, and the pigments were extracted by incubating the samples in 96% ethanol in darkness. The extracts were centrifuged, and the absorbance of the supernatant was recorded at 649 nm and 665 nm with a UV–visible spectrophotometer (Biomate 3S, Thermo Fisher Scientific, Waltham, MA, United States). The total chlorophyll content and the chlorophyll a and b concentrations were calculated using the following formulas (Ritchie, 2006):

$$\text{Chl a} = 13.95 \times \text{OD}_{665} - 6.88 \times \text{OD}_{649}$$

$$\text{Chl b} = 24.96 \times \text{OD}_{649} - 7.32 \times \text{OD}_{665}$$

$$\text{Chlorophyll content}\left(\text{mg} / \text{g}\right) = \text{Chl a} + \text{Chl b}$$

Photosynthesis-related parameters

The photosynthetic parameters, including the net photosynthesis rate (Pn), stomatal conductance (Gs), intercellular CO_2 concentration (Ci), and transpiration rate (Tr), were measured for the fully developed leaves of the 4-week-old seedlings under salt stress using a LiCor 6400XT gas exchange system (Lincoln, NE, United States). During the measurement, the leaf temperature was set at 25°C, the photosynthetic photon flux density (PPFD) at 780 $\mu mol\, m^{-2}\ s^{-1}$, CO_2 concentration at 400 $\mu mol\, mol^{-1}$, CO_2 mixer at 500 $\mu mol\, s^{-1}$, and relative humidity at 40%.

Statistical analysis

Statistical analysis was performed using the Statistical Package for Social Science software (SPSS Inc., Chicago, IL; version 18.0). Data were compared using one-way ANOVA, and the differences between the treatment means were considered statistically significant at $p < 0.05$, $p < 0.01$, or $p < 0.001$ following Tukey's test.

Results

Structure and development of salt bladders in *Chenopodium album*

The salt bladders in *C. album* were mainly found in the shoot tip and the young leaves (Figures 1A,B). Analysis of the leaf sections showed that salt bladders had one bladder cell and one stalk cell (Figure 1C). The bladder cell was huge, with a large vacuole that squeezed the nucleus to the edge of the cell (Figure 1D). The bladder cell was connected to the epidermal cells through a rectangular stalk cell with a nucleus at the center (Figures 1C,D).

The analysis of the salt bladder development showed that the epidermal cells on the shoot tips and young leaves generated the salt bladders. Initially, a few epidermal cells developed a dense protoplasm (presented in a darker color) that continuously enlarged (Figure 2A) and formed vertical protrusions (Figures 2B,C). These cells continued to stretch and divide to form two daughter cells (Figures 2D,E); one cell near the epidermis became the stalk cell, while the other one far from the epidermis continued to expand and developed into the bladder cell (Figure 2F). These salt bladders swelled during development and ruptured at leaf maturity due to increased internal lysate content or an external force.

Localization of cell wall polysaccharides

The sections of tissues from shoot tip to young leaf were probed with antibodies that recognize a diverse array of polysaccharide and glycoprotein epitopes. In this study, *in situ* immunohistochemical analysis detected no polysaccharide or glycoprotein in the control, indicating the specific action of the primary antibodies (Figures 3A,E). Meanwhile, the fucosylated epitope detected by CCRC-M1 was higher in the bladder cell wall than in the epidermal cell wall (Figure 3B), and the intensity was low in the salt bladders at young leaf (Figure 3F). These results indicated that the content of xyloglucan in cell walls gradually decreased with the development of salt bladder cells. Meanwhile, the arabinogalactan protein (AGP), recognized by the CCRC-M7 antibody, was evenly distributed in the cell wall of salt bladders at all stages of stem tip and young leaf development, and the content was higher than that of the epidermal cell wall (Figures 3C,G). The galacturonan (HG) epitope of pectin, recognized by CCRC-M38, remained a constant throughout salt bladder development; moreover, no difference was detected between the salt bladder cells and the epidermal cells (Figures 3D,H).

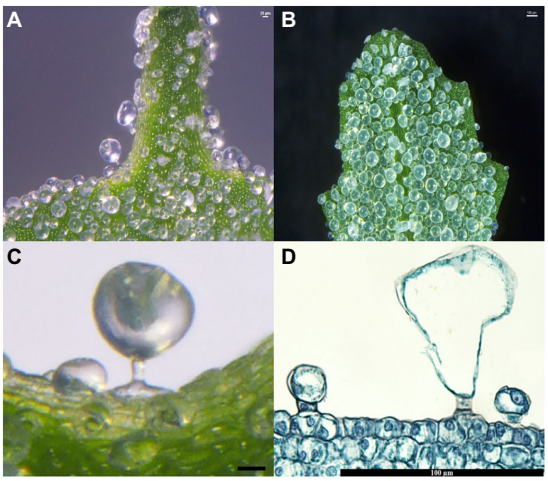


FIGURE 1
Salt bladders from *Chenopodium album*. **(A)** Salt bladders are appressed to the shoot tip surface; **(B)** Salt bladders are appressed to the young leaf surface; **(C,D)** Magnification of a single salt bladders.

Effects of salt stress on Na^+ and K^+ accumulation in *Chenopodium album* leaves

Further, to investigate the effect of salt stress on the Na^+/K^+ homeostasis of *C. album* leaves, the concentrations of Na^+ and K^+ in the young and mature leaves were measured under 100 mM or 300 mM NaCl stress. The analysis detected a significant increase in Na^+ content in young and mature leaves of both groups under NaCl stress (Figures 4A,B). The Na^+ content in the young and mature leaves of *C. album* with no salt bladders was substantially higher than that of the unbrushed group under control and NaCl stress. The Na^+ content in the mature leaves of the unbrushed and brushed groups under 300 mM NaCl treatment was 10.51- and 14.76-fold higher than that under control (Figures 4A,B). On the other hand, K^+ content under salt stress was the same as under control but significantly different between the brushed and unbrushed groups under each treatment (Figures 4C,D). This observation suggests an important role of K^+ in regulating cation-anion balance in the leaves.

Physiological indicators of *Chenopodium album* under salt stress

Osmotic regulators under salt stress

The brushed group accumulated significant amounts of osmotic regulators under salt stress compared with the unbrushed group. Under 300 mM NaCl stress, the unbrushed and the brushed groups showed an increase in proline content (2.02- and 3.63-fold, respectively) compared with the control. The proline content in the brushed group was significantly higher than that in the unbrushed group under salt stress; moreover, the proline content increased with the increase in salt concentration in both groups (Figure 5A). Meanwhile, the betaine content decreased in the unbrushed group and raised in the brushed group under salt stress; however, the brushed group had significantly higher betaine content than the unbrushed group. Under 300 mM NaCl stress,

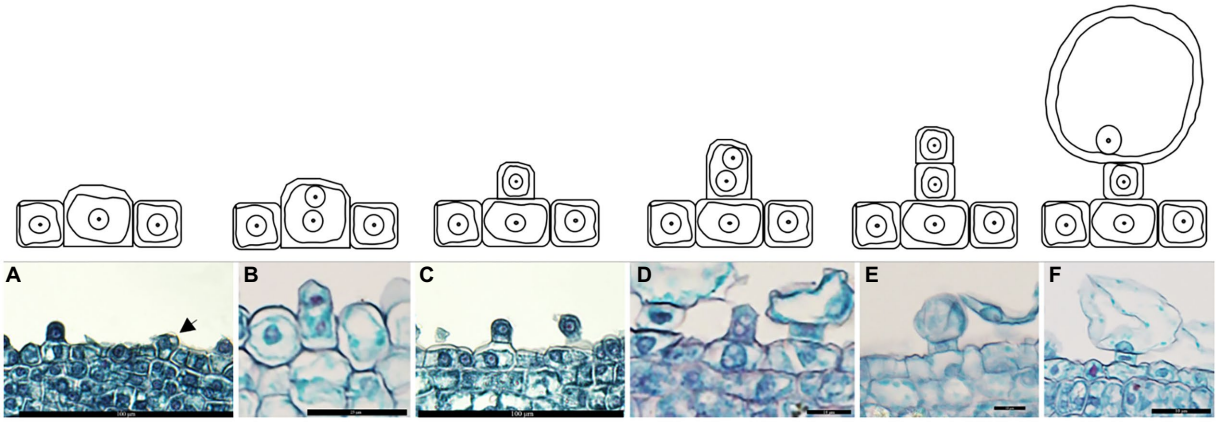


FIGURE 2
Development of salt bladder in *Chenopodium album*. **(A)** Expanded epidermal cells; **(B)** Dividing epidermal cells; **(C)** Initial bladder cell; **(D)** Dividing initial bladder cell; **(E)** Daughter cell; **(F)** Stalk cell and bladder cell.

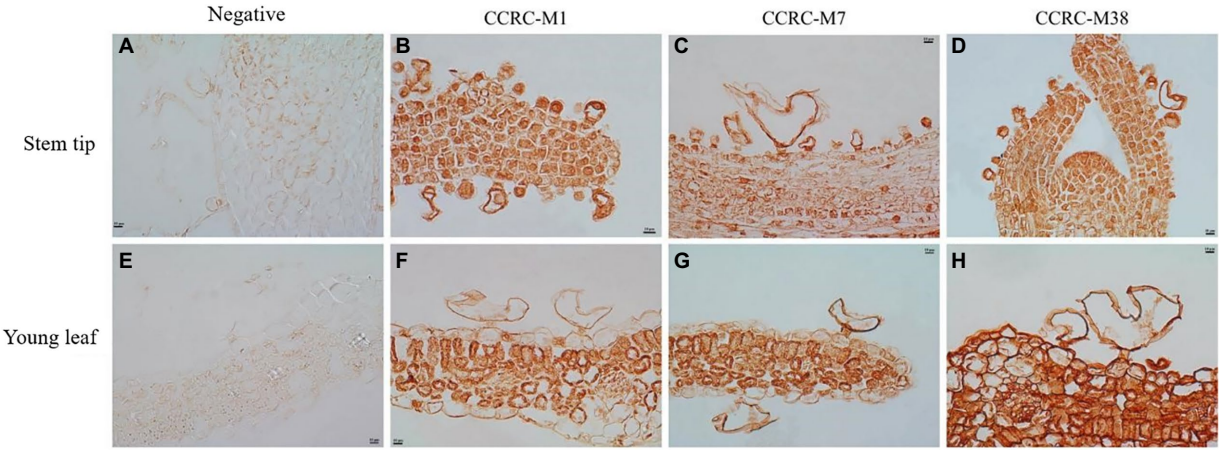


FIGURE 3
Fucose, arabinogalactan epitope, and de-esterified homogalacturonan in *Chenopodium album* stem tip and young leaf. **(A–D)** Stem tip; **(E–H)** Young leaf.

the betaine content in the brushed group was 1.99 times that of the unbrushed group (Figure 5B).

H_2O_2 and MDA content under salt stress

Furthermore, we detected a decline in H_2O_2 content in the brushed group and the unbrushed group under high salt stress compared with the control (Figure 6A). Meanwhile, the MDA content increased in the brushed group under salt stress compared with the control, and it was significantly higher than in the unbrushed group under the control and salt stress (Figure 6B).

Reactive oxygen species scavenging capacity under salt stress

The CAT activity of *C. album* plants in the brushed group was higher at 100 mM NaCl stress and lower at 300 mM NaCl stress than in control. In the unbrushed group, the CAT activity gradually lowered under stress. The CAT activity was significantly higher in the brushed group than in the unbrushed group under salt stress (Figure 7A). On the contrary, under control conditions, the activities of SOD and POD in the brushed group were higher than those in the unbrushed group. However, the activities in the brushed group were lower than those in the unbrushed group under high salt stress (Figures 7B,C).

External NaCl improves the photosynthetic efficiency of *Chenopodium album*

Chlorophyll content under salt stress

Salt stress can reduce the chlorophyll content of leaves, thereby affecting photosynthetic efficiency. The present study also found

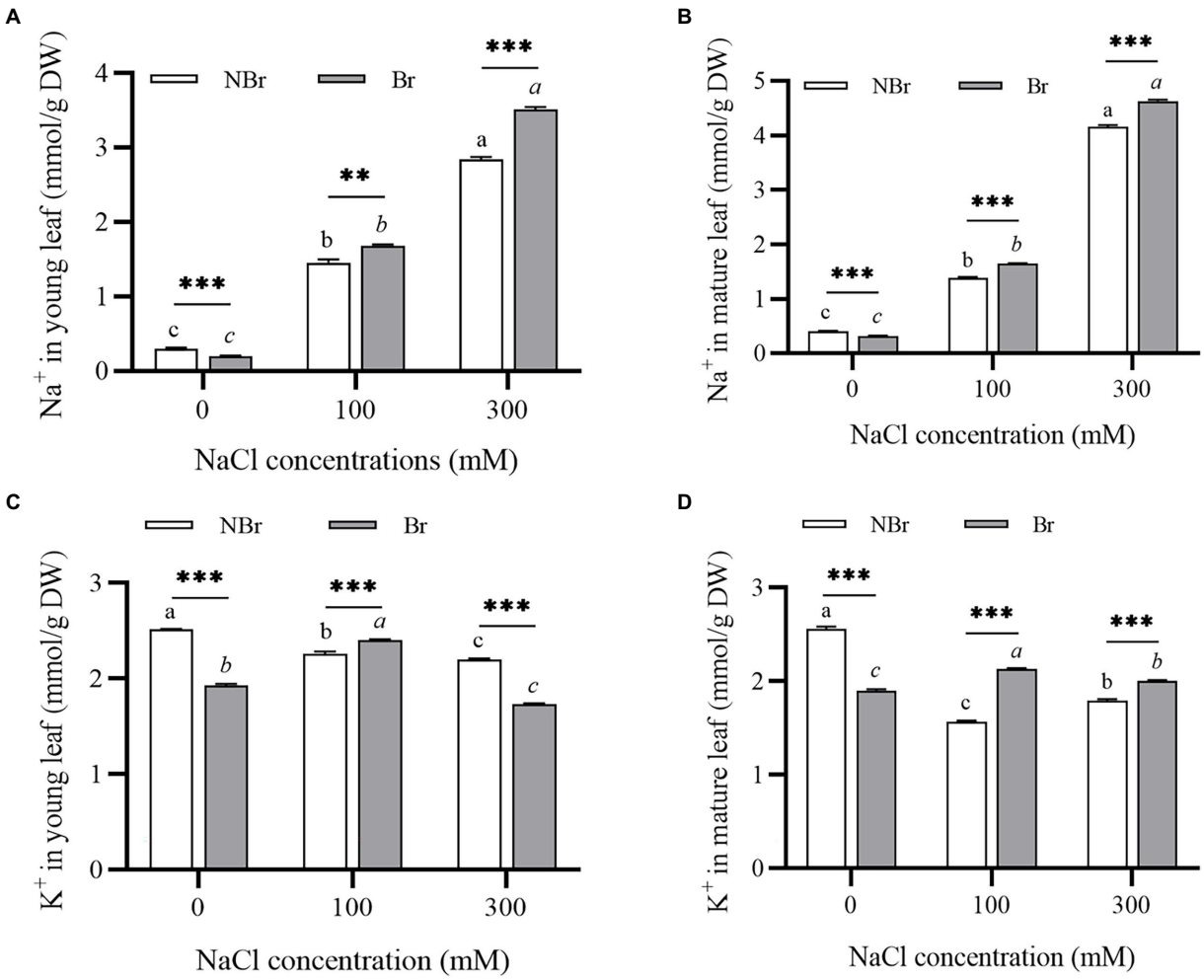


FIGURE 4
Ion contents in the leaves of *Chenopodium album* seedlings under different NaCl treatments. (**A**) Na^+ content in young leaf; (**B**) Na^+ content in mature leaf; (**C**) K^+ content in young leaf; (**D**) K^+ content in mature leaf. Different lowercase letters indicate significant differences among the treatments in the unbrushed group, and different italic lowercase letters indicate significant differences among the treatments in the brushed group. Asterisk indicates a significant difference between the brushed and unbrushed groups. $^{**}p<0.01$ and $^{***}p<0.001$ (Tukey's test).

a decrease in the chlorophyll a, b, and total chlorophyll content with increase in salt concentration (Figures 8A,B). Moreover, the total chlorophyll content in the brushed group was significantly lower than in the unbrushed group under control or salt stress (Figure 8C).

Photosynthetic characteristics of *Chenopodium album* under salt stress

Likewise, we found a decrease in photosynthetic efficiency in terms of various gas exchange parameters under salt stress. However, the decrease was evident in the unbrushed group only under high salt stress (300 mM NaCl). Meanwhile, the net photosynthesis rate (Pn), stomatal conductance (Gs), intercellular CO_2 concentration (Ci), and transpiration rate (Tr) were significantly lower in the brushed group than those of the unbrushed group under both control and salt stress (Figure 9).

Discussion

Salt bladders are a type of specialized epidermal hairs of halophytes. These epidermal hairs' cell structure and developmental process have been proposed in *Chenopodiaceae* (Shabala et al., 2014). Yet, the changes in the cell wall composition of salt bladders during development remain unexplored. In this experiment, we analyzed the shoot tips and young leaves of *C. album* and summarized the development of salt bladders. The results showed that the salt bladders had one bladder cell and one stalk cell in *C. album*, different from the salt bladders of other *Chenopodiaceae* species, with one or two stalk cells (Schirmer and Breckle, 1982). However, consistent with the other *Chenopodiaceae* plants, the salt bladders of *C. album* originate from the epidermal cells on the leaf surface. A few epidermal cells undergo expansion and then divide and expand, forming the

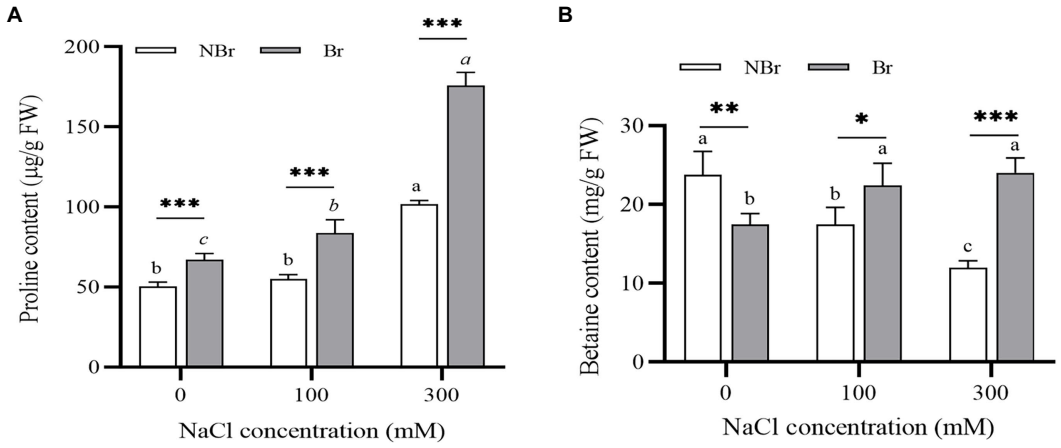


FIGURE 5
Free proline **(A)** and betaine **(B)** concentrations in the leaves of *Chenopodium album* seedlings under different NaCl treatments. Different lowercase letters indicate significant differences among the treatments in the unbrushed group, and different italic lowercase letters indicate significant differences among the treatments in the brushed group. Asterisk indicates a significant difference between the brushed and unbrushed groups. *p<0.05, **p<0.01, and ***p<0.001 (Tukey's test).

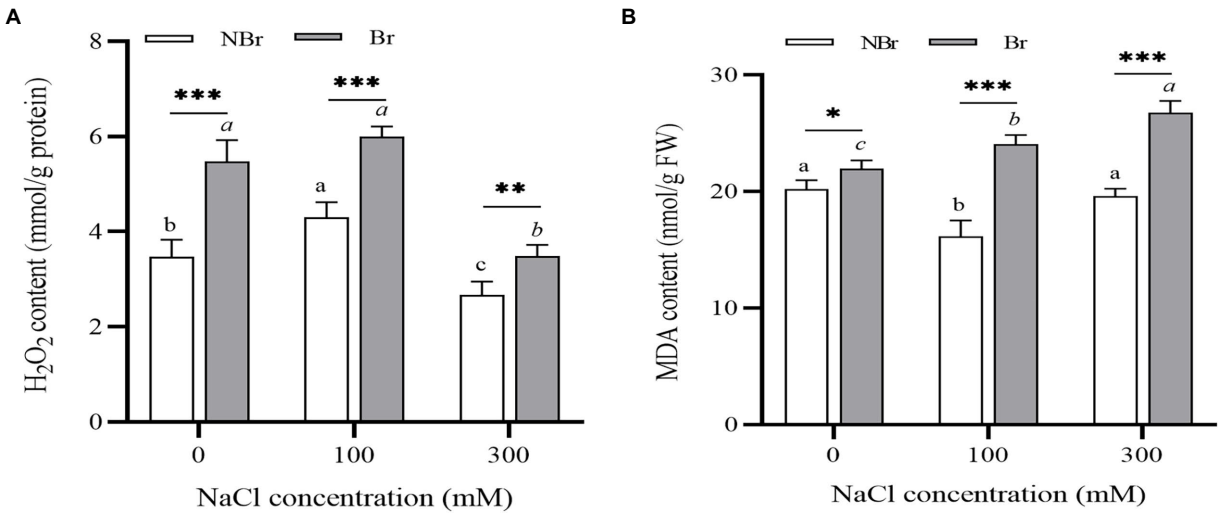


FIGURE 6
H_2O_2 **(A)** and MDA **(B)** concentrations in the leaves of *Chenopodium album* seedlings under different NaCl treatments. Different lowercase letters indicate significant differences among the treatments in the unbrushed group, and different italic lowercase letters indicate significant differences among the treatments in the brushed group. Asterisk indicates a significant difference between the brushed and unbrushed groups. *p<0.05, **p<0.01, and ***p<0.001 (Tukey's test).

bladder. We observed that only a fraction of the numerous epidermal cells on the leaf surface developed into salt bladders. Those epidermal cells forming salt bladders were usually larger than the normal cells (Figures 1, 2). Researchers have proven that the fate of an epidermal cell depends on the movement of transcription inhibitors from the differentiating cells into the neighboring cells, which possibly change the cell size (Shabala, 2013).

Under normal conditions, the plant cell wall maintains the cell structural integrity and coordinates cell division and expansion. The cell wall mainly comprises numerous polysaccharides and fewer proteins, enzymes, and fatty acids, and these components present dynamic distribution across the various stages of cell development (Samaj et al., 1999; Stenvik et al., 2006). In 1982, Schirmer and Breckle proposed that the development of the salt bladder may be closely related to the cell wall components or structures (Schirmer and Breckle, 1982); however, there was no evidence to clarify the relationship. The present study found that the content of hemicellulose xyloglucan in the cell wall of bladders at the

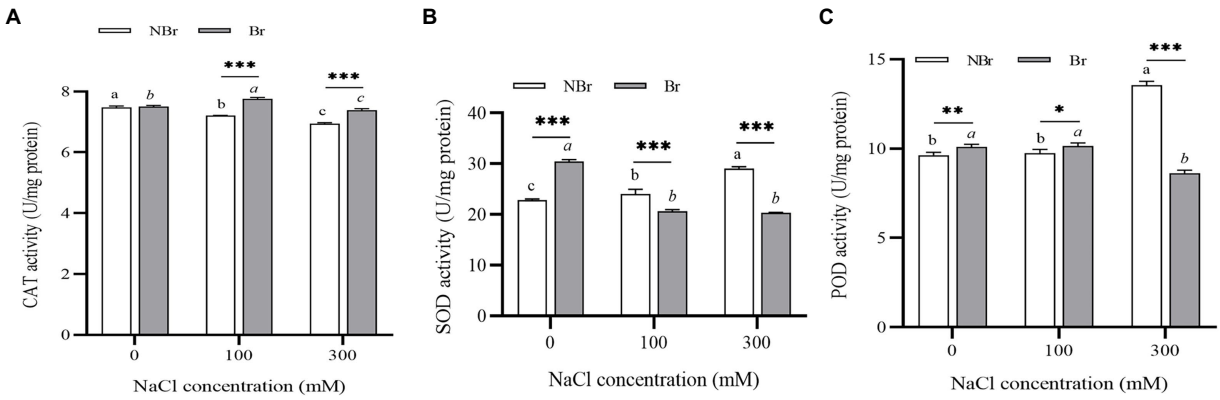


FIGURE 7
Catalase (CAT) **(A)**, superoxide dismutase (SOD) **(B)**, and peroxidase (POD) **(C)** activities in the leaves of *Chenopodium album* seedlings under different NaCl treatments. Different lowercase letters indicate significant differences among the treatments in the unbrushed group, and different italic lowercase letters indicate significant differences among the treatments in the brushed group. Asterisk indicates a significant difference between the brushed and unbrushed groups. *p<0.05, **p<0.01, and ***p<0.001 (Tukey's test).

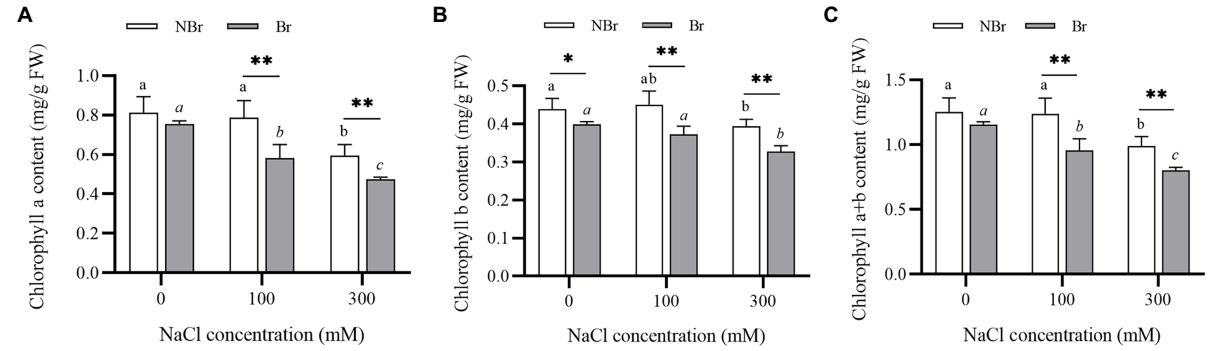


FIGURE 8
Chlorophyll a content (**A**), chlorophyll b content (**B**), and chlorophyll a+b content (**D**) in the leaves of *Chenopodium album* seedlings under different NaCl treatments. Different lowercase letters indicate significant differences among the treatments in the unbrushed group, and different italic lowercase letters indicate significant differences among the treatments in the brushed group. Asterisk indicates a significant difference between the brushed and unbrushed groups. *p<0.05 and **p<0.01 (Tukey's test).

early stage was significantly higher than that of the leaf epidermal cells (Figures 3B,F). We speculated that the high hemicellulose content might not only maintain the cell structure integrity and improve the cell wall flexibility but also contribute to the expansion and rupture of salt bladders. The detailed analysis showed that the cell wall had a higher content of pectin, which remained constant throughout the development of the salt bladders (Figures 3D,H). These ubiquitous cell wall pectin components are generally involved in developmental processes, such as cellular adhesion and stem elongation (Micheli, 2001). In *Gossypium* and *Galium aparine*, the arabinogalactan protein (AGP), a hydroxyproline-rich of glycoprotein, has been closely associated with cell division and expansion, tissue shedding, and growth signaling (Bowling et al., 2008, 2011). Moreover, a massive accumulation of AGP promoted the decomposition of xyloglucan, resulting in tissue shedding (Bowling et al., 2011). Labeling the AGP epitope in the cell wall in this study showed that AGP was abundantly distributed in the cell wall, and the content was higher in the bladder cell than that in the epidermal cells during the whole developmental process (Figures 3C,G). These findings suggest the role of AGP in the development and expansion of salt bladders in *C. album*.

In plants, salt stress hinders water absorption, leading to Na^+ accumulation and disrupting ion homeostasis; these changes result in metabolic disorders and growth retardation (Xu et al., 2016). Meanwhile, halophytes use the specialized salt-secreting structures called salt bladders to absorb excess Na^+ and excrete it through rupture (Shabala et al., 2014). Being a true halophyte, quinoa plants benefit from having Na^+ in the growth media; they chelate Na^+ mainly through salt

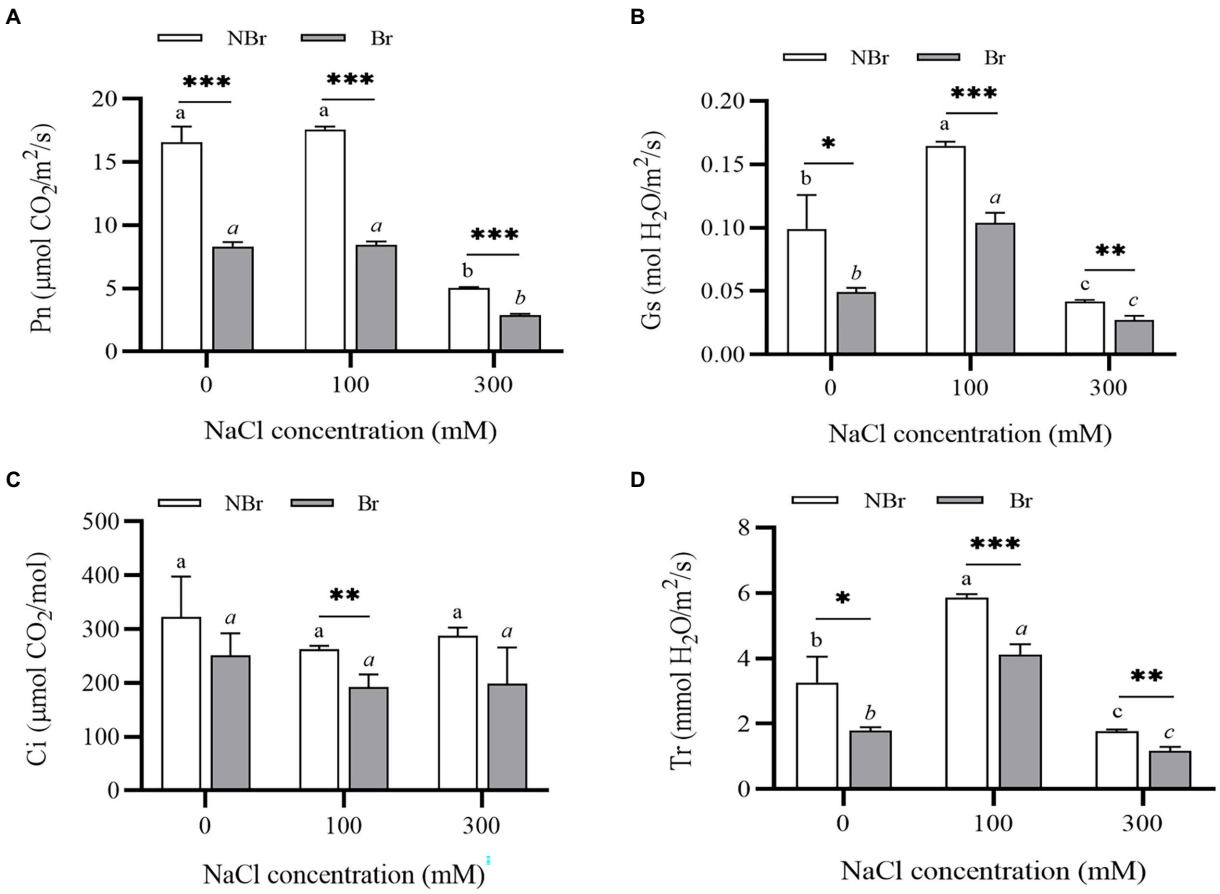


FIGURE 9
Net photosynthesis rate **(A)**, stomatal conductance **(B)**, intercellular CO_2 concentration (C_i) **(C)**, and transpiration rate (T) **(D)** of *Chenopodium album* seedlings under different NaCl treatments. Different lowercase letters indicate significant differences among the treatments in the unbrushed group, and different italic lowercase letters indicate significant differences among the treatments in the brushed group. Asterisk indicates a significant difference between the brushed and unbrushed groups. *p<0.05, **p<0.01, and ***p<0.001 (Tukey's test).

bladders, which also accumulate 50% of K^+ and 40% of Cl^- under salt stress (Kiani-Pouya et al., 2019). The present study confirmed that salt bladders absorbed a lot of Na^+ and K^+. However, when the salt bladders were removed, numerous Na^+ were detected in the mesophyll cells under salt stress (Figures 4A,B). In addition, the K^+ content in the leaves of the brushed group decreased under salt stress, and the content was significantly lower than that of the unbrushed group (Figure 4C). Therefore, we speculate that salt stress destroyed the structure of cell membranes and caused intracellular ion leakage; however, K^+ played a key role in maintaining intracellular ion balance and osmotic pressure stability. Thus, retaining K^+ and maintaining Na^+/K^+ homeostasis is important for salt tolerance (Shabala and Cuin, 2008; Hariadi et al., 2010). These results are consistent with the reports in *Chenopodium quinoa* Willd. (Kiani-Pouya et al., 2017) and *Atriplex canescens* (Guo et al., 2019) and confirm that salt bladders increase the leaf K^+ retention capacity and improve salt tolerance.

Under abiotic stress, plants accumulate osmotic regulators that maintain cell osmotic pressure, protect cell and protein integrity, and prevent cells from oxidative damage by scavenging reactive oxygen species (Szabados and Savouré, 2010; Uzilday et al., 2015). These changes reduce the adverse effects of abiotic stress on plants. In this experiment, the leaf proline and betaine content increased significantly in the brushed group under salt stress (Figure 5). Thus, the plants without salt bladders were more susceptible to ionic damage and had to deal with stress by accumulating proline. Under high NaCl treatment, CAT activity was higher in the brushed plants than in the unbrushed ones (Figure 7A), while the SOD and POD activities were significantly downregulated in the brushed plants (Figures 7B,C). These observations suggest that the plants without salt bladder (brushing) significantly increased reactive oxygen species scavenging through CAT activity; however, they did not get damaged by SOD and POD activities under NaCl treatment.

In addition, we found significantly low leaf chlorophyll content in the brushed plants (Figure 8). The Pn, Gs, Ci, and

Tr were substantially lower in the brushed group than in the unbrushed group under control and stress conditions (Figure 9). This observation is consistent with quinoa (Böhm et al., 2018) and indicates that the salt bladder of *C. album* contained many chloroplasts. Therefore, brushing reduced photosynthesis even under normal conditions. Moreover, the brushed plants had significantly low chlorophyll content and photosynthetic efficiency and were more sensitive to salt stress.

Conclusion

The present study found salt bladders on the young leaves of the desert plant *C. album* that ruptured and fell off with the development of leaves. Analysis of the salt bladder cell wall revealed variations in xyloglucan and AGP content during development. Salt bladders played a crucial role in salt tolerance by protecting young leaves and improving photosynthetic efficiency. However, the mechanisms *via* which the salt bladders initiate development, regulate volume, rupture, and shedding, and modulate the associated genes remain unexplored. Thus, the findings provide an important reference for further research on salt bladders in engineering salt-tolerant plants.

Data availability statement

The original contributions presented in the study are included in the article/supplementary material, further inquiries can be directed to the corresponding author.

Author contributions

YZ and HL designed the experiment and methodology. AM carried out experimental work. YZ wrote the manuscript. All authors contributed to experimental design and data analysis, commented on the manuscript, and gave final approval for publication.

Funding

This work was supported by the Science and Technology Training Project for Excellent Young Scholars of Xinjiang (no. 2019Q014) and National Natural Science Foundation of China (no. 31900270).

Conflict of interest

The authors declare that the research was conducted in the absence of any commercial or financial relationships that could be construed as a potential conflict of interest.

Publisher's note

All claims expressed in this article are solely those of the authors and do not necessarily represent those of their affiliated organizations, or those of the publisher, the editors and the reviewers. Any product that may be evaluated in this article, or claim that may be made by its manufacturer, is not guaranteed or endorsed by the publisher.

References

Agarie, S., Shimoda, T., Shimizu, Y., Baumann, K., Sunagawa, H., Kondo, A., et al. (2007). Salt tolerance, salt accumulation, and ionic homeostasis in an epidermal bladder-cell-less mutant of the common ice plant Mesembryanthemum crystallinum. *J. Exp. Bot.* 58, 1957–1967. doi: 10.1093/jxb/erm057

Barkla, B., Rhodes, T., Tran, K.-N., Wijesinghege, C., Larkin, J., and Dassanayake, M. (2018). Making epidermal bladder cells bigger: developmental- and salinity-induced Endopolyploidy in a model halophyte. *Plant Physiol.* 177, 615–632. doi: 10.1104/pp.18.00033

Barkla, B. J., Vera-Estrella, R., and Pantoja, O. (2012). Protein profiling of epidermal bladder cells from the halophyte *Mesembryanthemum crystallinum*. *Proteomics* 12, 2862–2865. doi: 10.1002/pmic.201200152

Barkla, B. J., Vera-Estrella, R., and Raymond, C. (2016). Single-cell-type quantitative proteomic and ionomic analysis of epidermal bladder cells from the halophyte model plant *Mesembryanthemum crystallinum* to identify salt-responsive proteins. *BMC Plant Biol.* 16:110. doi: 10.1186/s12870-016-0797-1

Böhm, J., Messerer, M., Müller, H. M., Scholz-Starke, J., Gradogna, A., Scherzer, S., et al. (2018). Understanding the molecular basis of salt sequestration in epidermal bladder cells of *Chenopodium quinoa*. *Curr. Biol.* 28, 3075–3085.e7. doi: 10.1016/j.cub.2018.08.004

Bowling, A. J., Maxwell, H. B., and Vaughn, K. C. (2008). Unusual trichome structure and composition in mericarps of catchweed bedstraw (*Galium aparine*). *Protoplasma* 233:275. doi: 10.1007/s00709-008-0008-5

Bowling, A. J., Vaughn, K. C., and Turley, R. B. (2011). Polysaccharide and glycoprotein distribution in the epidermis of cotton ovules during early fiber initiation and growth. *Protoplasma* 248, 579–590. doi: 10.1007/s00709-010-0212-y

Cheng, Z., Zheng, Y., Mortlock, R., and Van Geen, A. (2004). Rapid multi-element analysis of groundwater by high-resolution inductively coupled plasma mass spectrometry. *Anal. Bioanal. Chem.* 379, 512–518. doi: 10.1007/s00216-004-2618-x

Ding, F., Yang, J., Yuan, F., and Wang, B. (2010). Progress in mechanism of salt excretion in recretohalopytes. *Front. Biol.* 5, 164–170. doi: 10.1007/s11515-010-0032-7

Flowers, T. J., and Colmer, T. D. (2008). Salinity tolerance in halophytes. *New Phytol.* 179, 945–963. doi: 10.1111/j.1469-8137.2008.02531.x

Guo, H., Cui, Y., Pan, Y., Wang, S., and Bao, A. (2020). Sodium chloride facilitates the secretohalophyte *Atriplex canescens* adaptation to drought stress. *Plant Physiol. Biochem.* 150, 99–108. doi: 10.1016/j.plaphy.2020.02.018

Guo, H., Zhang, L., Cui, Y., Wang, S., and Bao, A. (2019). Identification of candidate genes related to salt tolerance of the secretohalophyte *Atriplex canescens* by transcriptomic analysis. *BMC Plant Biol.* 19:213. doi: 10.1186/s12870-019-1827-6

Hariadi, Y., Marandon, K., Tian, Y., Jacobsen, S.-E., and Shabala, S. (2010). Ionic and osmotic relations in quinoa (*Chenopodium quinoa* Willd.) plants grown at various salinity levels. *J. Exp. Bot.* 62, 185–193. doi: 10.1093/jxb/erq257

Kiani-Pouya, A., Rasouli, F., Bazihizina, N., Zhang, H., Hedrich, R., and Shabala, S. (2019). A large-scale screening of quinoa accessions reveals an important role of epidermal bladder cells and stomatal patterning in salinity tolerance. *Environ. Exp. Bot.* 168:103885. doi: 10.1016/j.envexpbot.2019.103885

Kiani-Pouya, A., Roessner, U., Jayasinghe, N. S., Lutz, A., Rupasinghe, T., Bazihizina, N., et al. (2017). Epidermal bladder cells confer salinity stress tolerance in the halophyte quinoa and *Atriplex* species. *Plant Cell Environ.* 40, 1900–1915. doi: 10.1111/pce.12995

Micheli, F. (2001). Pectin methylesterases: cell wall enzymes with important roles in plant physiology. *Trends Plant Sci.* 6, 414–419. doi: 10.1016/S1360-1385(01)02045-3

Pan, Y., Guo, H., Wang, S., Zhao, B., Ma, Q., Yin, H., et al. (2016). The photosynthesis, Na+/K+ homeostasis and osmotic adjustment of *Atriplex canescens* in response to salinity. *Front. Plant Sci.* 7:848. doi: 10.3389/fpls.2016.00848

Ritchie, R. J. (2006). Consistent sets of spectrophotometric chlorophyll equations for acetone, methanol and ethanol solvents. *Photosynth. Res.* 89, 27–41. doi: 10.1007/s11120-006-9065-9

Samaj, J., Ensikat, H., Baluska, F., Knox, P., Barthlott, W., and Volkmann, D. (1999). Immunogold localization of plant surface arabinogalactan-proteins using glycerol liquid substitution and scanning electron microscopy. *J. Microsc.* 193, 150–157. doi: 10.1046/j.1365-2818.1999.00441.x

Schirmer, U., and Breckle, S.-W. (1982). "The role of bladders for salt removal in some Chenopodiaceae (mainly *Atriplex* species)". In *Contributions to the ecology of halophytes. Tasks for vegetation science, vol 2*. eds. D. N. Sen and K. S. Rajpurohit (Dordrecht: Springer).

Shabala, S. (2013). Learning from halophytes: physiological basis and strategies to improve abiotic stress tolerance in crops. *Ann. Bot.* 112, 1209–1221. doi: 10.1093/aob/mct205

Shabala, S., Bose, J., and Hedrich, R. (2014). Salt bladders: do they matter? *Trends Plant Sci.* 19, 687–691. doi: 10.1016/j.tplants.2014.09.001

Shabala, S., and Cuin, T. A. (2008). Potassium transport and plant salt tolerance. *Physiol. Plant.* 133, 651–669. doi: 10.1111/j.1399-3054.2007.01008.x

Shabala, S., and Mackay, A. (2011). Ion transport in halophytes. *Adv. Bot. Res.* 57, 151–199. doi: 10.1016/B978-0-12-387692-8.00005-9

Smaoui, A., Barhoumi, Z., Rabhi, M., and Abdelly, C. (2011). Localization of potential ion transport pathways in vesicular trichome cells of *Atriplex halimus* L. *Protoplasma* 248, 363–372. doi: 10.1007/s00709-010-0179-8

Stenvik, G. E., Butenko, M. A., Urbanowicz, B. R., Rose, J. K. C., and Aalen, R. B. (2006). Overexpression of INFLORESCENCE DEFICIENT IN ABSCISSION activates cell separation in vestigial Abscission zones in Arabidopsis. *Plant Cell* 18, 1467–1476. doi: 10.1105/tpc.106.042036

Szabados, L., and Savouré, A. (2010). Proline: a multifunctional amino acid. *Trends Plant Sci.* 15, 89–97. doi: 10.1016/j.tplants.2009.11.009

Uzilday, B., Ozgur, R., Sekmen, A. H., Yildiztugay, E., and Turkan, I. (2015). Changes in the alternative electron sinks and antioxidant defence in chloroplasts of the extreme halophyte Eutrema parvulum (*Thellungiella parvula*) under salinity. *Ann. Bot.* 115, 449–463. doi: 10.1093/aob/mcu184

Wu, H., Zhang, X., Giraldo, J., and Shabala, S. (2018). It is not all about sodium: revealing tissue specificity and signalling roles of potassium in plant responses to salt stress. *Plant Soil* 431, 1–17. doi: 10.1007/s11104-018-3770-y

Xu, C., Tang, X., Shao, H., and Wang, H. (2016). Salinity tolerance mechanism of economic halophytes from physiological to molecular hierarchy for improving food quality. *Curr. Genet.* 17, 207–214. doi: 10.2174/1389202917666160202215548

Yao, S., Chen, S., Xu, D., and Lan, H. (2010a). Plant growth and responses of antioxidants of *Chenopodium album* to long-term NaCl and KCl stress. *Plant Growth Regul.* 60, 115–125. doi: 10.1007/s10725-009-9426-4

Yao, S., Lan, H., and Zhang, F. (2010b). Variation of seed heteromorphism in *Chenopodium album* and the effect of salinity stress on the descendants. *Ann. Bot.* 105, 1015–1025. doi: 10.1093/aob/mcq060

Yuan, F., Leng, B., and Wang, B. (2016). Progress in studying salt secretion from the salt glands in Recretohalophytes: how do plants secrete salt? *Front. Plant Sci.* 7:977. doi: 10.3389/fpls.2016.00977

Zhao, C., Zhang, H., Song, C., Zhu, J.-K., and Shabala, S. (2020). Mechanisms of plant responses and adaptation to soil salinity. *Innovation* 1:100017. doi: 10.1016/j.xinn.2020.100017

frontiers | Frontiers in Plant Science

TYPE Original Research
PUBLISHED 08 September 2022
DOI 10.3389/fpls.2022.983725

Check for updates

OPEN ACCESS

EDITED BY
Mehtab Muhammad Aslam,
The Chinese University of Hong Kong,
China

REVIEWED BY
Giampiero Cai,
University of Siena,
Italy
Mohammad Shah Jahan,
Sher-e-Bangla Agricultural University,
Bangladesh

*CORRESPONDENCE
Jwakyung Sung
jksung73@chungbuk.ac.kr
Choong Hwan Lee
chlee123@konkuk.ac.kr

†These authors have contributed equally to this work

SPECIALTY SECTION
This article was submitted to Plant Abiotic Stress, a section of the journal Frontiers in Plant Science

RECEIVED 01 July 2022
ACCEPTED 17 August 2022
PUBLISHED 08 September 2022

CITATION
Kim YX, Son SY, Lee S, Lee Y, Sung J and Lee CH (2022) Effects of limited water supply on metabolite composition in tomato fruits (*Solanum lycopersicum* L.) in two soils with different nutrient conditions. *Front. Plant Sci.* 13:983725. doi: 10.3389/fpls.2022.983725

COPYRIGHT
© 2022 Kim, Son, Lee, Lee, Sung and Lee. This is an open-access article distributed under the terms of the Creative Commons Attribution License (CC BY). The use, distribution or reproduction in other forums is permitted, provided the original author(s) and the copyright owner(s) are credited and that the original publication in this journal is cited, in accordance with accepted academic practice. No use, distribution or reproduction is permitted which does not comply with these terms.

Effects of limited water supply on metabolite composition in tomato fruits (*Solanum lycopersicum* L.) in two soils with different nutrient conditions

Yangmin X. Kim[1†], Su Young Son[2†], Seulbi Lee[1], Yejin Lee[1], Jwakyung Sung[3*] and Choong Hwan Lee[2,4*]

[1]National Institute of Agricultural Sciences, Rural Development Administration, Wanju, South Korea, [2]Department of Bioscience and Biotechnology, Konkuk University, Seoul, South Korea, [3]Department of Crop Science, College of Agriculture, Life and Environment Sciences, Chungbuk National University, Cheongju, South Korea, [4]Research Institute for Bioactive-Metabolome Network, Konkuk University, Seoul, South Korea

Effect of water supply to metabolites in tomato fruit was compared in two soils with different nutrient conditions, i.e., either limited or excess. Two types of soil nutrient condition, type A: nutrient-limited and type B: nutrient-excess, were prepared as follows; type A is a low nutrient-containing soil without a replenishment of starved nitrogen and phosphorous, type B is a high nutrient-containing soil exceeding the recommended fertilization. Soil water was adjusted either at −30kPa (sufficient) or −80kPa (limited). For harvested tomato fruits, we examined primary and secondary metabolites using non-targeted mass spectrometry based metabolomics. The fruit production and leaf SPAD were greatly dependent on soil nutrient levels, by contrast, the level of lycopene remained unchanged by different levels of water and nutrient supply. The perturbation of metabolites by water supply was clear in the nutrient-excess soil. In particular, limited water supply strongly decreased primary metabolites including sugars and amino acids. We demonstrated that water stress differently shifted primary metabolites of tomato fruits in two soils with different nutrient conditions *via* non-targeted mass spectrometry-based metabolomics. In conclusion, we suggest that the limited water supply in soils with surplus nutrient is not a recommendable way for tomato 'cv. Super Dotaerang' production if fruit nutritional quality such as sugars and amino acids is in the consideration, although there was no disadvantage in fruit yield.

KEYWORDS

lycopene, metabolite profiling, mineral nutrient, tomato fruit quality, water

Introduction

Water stress is a major problem where water is scarce (Hasan et al., 2021) and proper irrigation is essential in the greenhouse. Limited soil moisture reduces plant growth due to limited water uptake, which leads to the decrease in leaf elongation and stomatal conductance that results in the reduction in photosynthesis (Bista et al., 2018). Limited soil moisture also affects plant growth by reducing soil nutrient supply (Végh, 1991). Nutrient uptake during the water stress may decrease by reducing nutrient supply through mineralization, by hindering nutrient transport in the soil, and by affecting the kinetics of nutrient uptake by roots (Bista et al., 2018). The nutrient uptake by roots occurs *via* mass flow along water using the apoplastic pathway and *via* membrane-bound transporters in the transcellular pathway (Bassirirad, 2000; Kim et al., 2018). Therefore, the stress response by limited soil moisture can interact with soil nutrient conditions as nutrients transport is related to the water transport (Roy et al., 2020).

Tomato fruit quality has been demonstrated to be modified by nutrient and water supply using metabolomics approach (Kwon et al., 2019; Gil et al., 2020; Kim et al., 2020). Gil et al. (2020) reported that tomato fruit quality was shifted by the amount of N supply, and lowering the N supply resulted in low amino acid levels, and it could be by the decrease in amino acid biosynthesis due to the N shortage (Causin, 1996). The Mg^{2+} surplus in the soil worsened fruit quality including sugars, organic acids and amino acids, and the metabolites in the leaves and roots were simultaneously compared, and they suggested that metabolites were allocated to the root (sink) and it resulted in unfavorable fruit quality (Kwon et al., 2019). Tomato fruits increased lycopene by reducing N supply after fruit setting in combination of sufficient water supply condition, when tomato was grown in the Mg^{2+} excess soil (Kim et al., 2020). On the other hand, deficit irrigation has been used as a strategy to enhance the crop quality and it increased the tomato fruit soluble solid, hexoses, citric acid, and potassium concentration (Mitchell et al., 1991). Nutrient excess such as Na^{+}, Mg^{2+}, and Ca^{2+} occurs in the greenhouse environment due to extensive application of fertilizers where rainfall does not reach to the soil surface. The nutrient excess causes harmful impact on plants by osmotic stress, in which reactive oxygen species is generated and it results in the oxidative stress to plant cells (Du et al., 2015). The nutrient excess in the soil hinders root water uptake by negative water potential in the soil and by changes in root anatomy and hydraulic properties (Adams et al., 2019).

In this study, we handled two types of soil nutrient condition, type A: nutrient-limited condition and type B: nutrient-excess condition. Considering the interaction between nutrient and water transport, we have expected the different tomato quality by deficit irrigation in the farm lands with different nutrient status. In that context, we tested whether imposing a moderate water stress to tomato compared to the sufficient water supply (control) would differently shift the primary and secondary metabolites in tomato fruits in two different soil nutrient conditions (type A and B). The purpose of this paper was to investigate how the limited irrigation in the soils containing different levels of nutrients affects the fruit nutrition of tomato growing in the glasshouse. In this study, we selected two extreme soil nutrient cases, nutrient excess and limited. Primary and secondary metabolites of tomato fruits were investigated using a non-targeted metabolomics. The metabolomics is a comprehensive approach to evaluate different metabolomes under a specific set of conditions (Son et al., 2016), and we have applied it for various crops in response to varying environmental factors including light and mineral nutrient supply (Kwon et al., 2019; Gil et al., 2020; Kim et al., 2020, 2021; Suh et al., 2020).

Materials and methods

Plant materials and nutrient and water supply

Two-month-old tomato seedlings (*Solanum lycopersicum* L., 'Super Dotaerang'; Koregon Co., Ltd., Anseong, Korea) were transplanted into plastic pots (4.5 kg of soil) in March, 2019 and were grown for 18 weeks in the glasshouse in the National Institute of Agricultural Sciences, Rural Development Administration, Korea. The daily temperatures in the glasshouse was between 15–35°C and the heating and ventilating systems prevented extreme temperature conditions. There was no regulation in relative humidity of the glasshouse and the natural light penetrating the glasshouse was used for plant growth.

Two soils with different nutrient conditions were employed (Table 1) in order to set up the nutrient-limited soil condition and nutrient-excess soil condition during the plant growth. To produce the nutrient-limited soil condition during the plant growth, we did not supply nitrogen and phosphorous fertilizer to the low nutrient soil, while potassium chloride as a potassium fertilizer was supplied in accordance with the fertilizer recommendations for tomato cultivation in greenhouse soil (NIAS, 2017; Supplementary Table S1). To produce nutrient-excess soil condition during the plant growth, potassium fertilizer was applied to the high nutrient soil in accordance with the recommendations for tomato cultivation in greenhouse soil with high electrical conductivity, EC (NIAS, 2017). Three split applications of fertilizer were conducted by topdressing (Supplementary Table S1).

Variations in water supply was from the 12th week from the transplanting that was after fruit setting; water was supplied either at −30 kPa for the sufficient supply or −80 kPa of soil water potential for the limited supply by reading tensiometers (Soilmoisture Equipment Corp., Santa Babara, United States). The gypsum block in tensiometer sensing the water potential was at the depth of 0.07–0.13 m below the soil surface. The water potential that hinders the plant growth is −100 kPa and permanent wilting point is −1,500 kPa. There were 4 soil × water supply conditions. Ripened fruits from 16 plants were harvested (four

TABLE 1 Chemical properties of soils before transplanting tomato plants.

Soil	pH (1:5)	EC (1:5; dS m^{-1})	NO_3-N (mg kg^{-1})	OM (g kg^{-1})	Av. P_2O_5 (mg kg^{-1})	Ex. Cations (cmol$_c$ kg^{-1})		
						K	Ca	Mg
Low nutrient soil	6.3	0.8	75	15	172	0.09	2.9	0.6
High nutrient soil	5.9	8.6	871	32	791	1.69	13.3	5.0
Recommended*	6.0–6.5	<2.0	70–200	20–30	400–500	0.7–0.8	5.0–6.0	1.5–2.0

Mean values of three replicates. *Recommended is the proper value for tomato cultivation in Korean plastic house.

plants for each soil × water supply condition). Two to seven ripened tomato fruits from each plant were harvested from 28 June to 24 July, 2019.

Measurement of leaf SPAD values

On the final day of harvesting, the SPAD values of the tomato leaves near the harvested fruits were measured using a chlorophyll meter (SPAD-502Plus, Konica Minolta Sensing, Osaka, Japan). SPAD values were measured as an indicator of the plant performance rather than an accurate value of chlorophyll content (Kim et al., 2020).

Sample preparation and extraction

Sample preparation and extraction steps were adopted for our previous research (Kim et al., 2021). Cultivated tomato fruits under varied nutrient and water conditions were washed with distilled water and wiped before being stored at a deep freezer (−80°C). Frozen fruits samples were freeze-dried for 3 days at −98°C in lyophilizer (Operon, Gimpo, Korea) and grinded to powder using a mortar and pestle. Powdered samples (100 mg) were extracted with 80% methanol. To extract samples, all samples were homogenized with Retsch MM400 Mixer Mill (Retsch GmbH Co., Haan, Germany) and sonicated for 10 min. After then, extracted samples were centrifuged for 10 min at 12,000 rpm and 4°C (Gyrozen 1730R, Gyrozen Inc., Daejeon, Korea). The supernatants were filtered by polytetrafluoro-ethylene (Chromdisc, Daegu, Korea) and then filtered samples were completely dried using a speed vacuum concentrator for overnight. The final concentration of each analyzed samples was 20,000 ppm (20 mg/ml).

GC-TOF-MS and UHPLC-LTQ-Orbitrap-MS analysis

For GC-TOF-MS analysis, the samples adjusted for concentration (100 µl) were dried again using a speed vacuum. The dried samples were derivatized with the following protocol. First step, 50 µl of methoxyamine hydrochloride (20 mg/ml in pyridine) was added to the dried samples and placed on the thermomixer for 90 min at 30°C. Then, 50 µl of N-methyl-N-trimethylsilyl trifluoroacetamide (MSTFA) was incubated for 30 min at 30°C. One microliter of each sample was injected at split mode (ratio 1: 20). The GC-TOF-MS instrument, analytical protocol, and parameter setting for analysis were adopted for our previous research (Kim et al., 2021).

For secondary metabolites, the re-dissolved samples were analyzed using UHPLC-LTQ-Orbitrap-MS equipped with Vanquish binary pump H system (Thermo Fisher Scientific, Waltham, MA, United States) coupled with an auto-sampler and column compartment. The analytical methods and operation parameters were followed by our previous study (Kim et al., 2021). All samples were run in a randomized manner to reduce bias and systematic errors.

Lycopene analysis

The lycopene analysis including extraction method, analytical method and parameters, and operation setting was followed by our previous study (Kim et al., 2021; Mun et al., 2021). For lycopene extraction, powdered samples (200 mg) was extracted with 3 ml of solvent mixture (Chloroform: DCM = 2:1 (v/v)) coupled with orbital shaker (Biofree, Seoul, Korea) for 20 min and then 1 M sodium chloride solution (1 ml) added. The extracted samples were centrifuged at 5,000 rpm for 10 min at 4°C and the supernatants were completely concentrated using nitrogen gas. The concentrated samples were re-dissolved with methanol and tert-Butyl methyl ether solvent mixture (3:2, v/v). The level of lycopene was analyzed by liquid chromatography diode array detection system. Lycopene was identified with retention time and absorbance, which were compared to commercial standard compound of lycopene analyzed under identical states.

Data processing and multivariate statistical analysis

MS data processing and multivariate statistical analysis were proceeded as described in our previous research (Kim et al., 2021; Mun et al., 2021). The raw data derived from GC-TOF-MS and UHPLC-LTQ-Orbitrap-MS were converted to netCDF (*.cdf) by chromaTOF (version 4.44, LECO Corp., St. Joseph, MI, United States) and Xcalibur (Version 2.00, ThermoFisher

Scientific, Waltham, MA, United States) software, respectively. Then, the *.cdf files were performed with the Metalign software (RIKILT-Institute of Food Safety, Wageningen, The Netherlands) to determine peak mass value (m/z), retention time (min), baseline correction, and peak area normalization. After alignment, multivariate analysis was performed using final version of alignment data by SIMCA-P+ software (version 12.0, Umetrics, Umea, Sweden). Multivariate analysis such as principal component analysis (PCA) and partial least squares-discriminant analysis (PLS-DA) was proceeded to determine significantly distinguished metabolites between tomato cultivated under varied nutrient and water conditions. The significance of PLS-DA model was determined by analysis of variance testing of cross-validated predictive residuals (CV-ANOVA) came from SIMCA-P+ software. Distinguished metabolites were determined according to variable importance in the projection (VIP) value from PLS-DA model. Metabolites derived from GC-TOF-MS and UHPLC-LTQ-Orbitrap-MS analysis were tentatively identified by comparing mass spectrum, mass fragment pattern, retention time with available database including Wiley 9, the Human Metabolome Database (HMDB)[1], the National Institute of Standards and Technology (NIST) database (Version 2.0, 2001, FairCom, Gaitherburg, MD, United States), in house database, previous research datasets, and standard compounds analyzed with identical condition. Significant differences were evaluated by Student's *t*-test using PASW Statistics 18 software (SPSS Inc., Chicago, IL, United States).

Statistical analysis

Significant differences in the production and lycopene content of ripened fruit and leaf SPAD values were evaluated by a one-way analysis of variance (ANOVA) followed by Tukey's test ($p < 0.05$).

Results

Tomato production, lycopene contents of tomato fruits, and leaf SPAD

The fruit yield, lycopene content in fruits and leaf SPAD values were measured to compare the effects of water supply in the nutrient-limited and nutrient-excess soils (Table 2). The fruit production was significantly reduced in the nutrient-limited soil compared to nutrient-excess, when water supply was sufficient. The level of lycopene, a major functional metabolite of tomato fruit, on a dry-weight basis did not differ from both different conditions of water and nutrient of soils. The leaf SPAD values were significantly lower in tomato plants grown in the nutrient-limited soil than in nutrient-excess soil.

1 http://www.hmdb.ca/ accessed on 17 of February 2022

Non-targeted metabolite profiling of tomato fruits cultivated under different water supply in two soil nutrient conditions

To determine global metabolites including primary and secondary metabolites in tomato fruits cultivated under different water supply in two different soil nutrient conditions, metabolites profiling approach was performed by GC-TOF-MS and UHPLC-LTQ-Orbitrap-MS/MS. Subsequently, multivariate analysis including unsupervised PCA, as well as the supervised PLS-DA were performed to determine the distinguished metabolites. The PLS-DA score plots based on GC-TOF-MS and UHPLC-LTQ-Orbitrap-MS/MS showed distinct pattern between nutrient-limited and nutrient-excess soil by PLS1 (21.6% and 13.6%, respectively) and water supply (limited and sufficient) was divided by PLS2 (6.6% and 8.7%, respectively) (Figures 1A,B). The statistical model value of PLS-DA was determined by R^2X (0.281 and 0.223), R^2Y (0.608 and 0.603) and Q2 (0.319 and 0.288), which indicated the model prediction accuracy, fitness, and validation. Moreover, the PCA score plot showed a similar pattern to the PLS-DA (Supplementary Figures S1A,B). Distinguished metabolites among the four groups were identified and selected based on variable importance in projection (VIP) value (>0.7) from the PLS-DA model and Student's *t*-test was applied to determine statistical significance ($p < 0.05$).

A total of 47 discriminant metabolites were identified, of which 28 and 19 metabolites were determined by GC-TOF-MS and UHPLC-LTQ-Orbitrap-MS/MS, respectively (Supplementary Tables S2, S3). A total of 28 primary metabolites were determined by GC-TOF-MS analysis and categorized into the following metabolite classes including 8 amino acids *viz.*, isoleucine, valine, threonine, glycine, aspartic acid, pyroglutamic acid, phenylalanine, and glutamic acid, 3 organic acids *viz.*, malic acid, citric acid, and oxoglutaric acid, 8 sugars and sugar alcohols *viz.*, arabinose, xylose, fucose, fructose, glucose, glucuronic acid, myo-Inositol, and maltose, 3 others *viz.*, monopalmitin, urea, and quinic acid. Moreover, 19 secondary metabolite were tentatively identified by UHPLC-LTQ-Orbitrap-MS/MS and divided into sub-classes such as 5 polyamines *viz.*, feruloylagmatine, tris(dihydrocaffeoyl)spermine, feruloyl octopamine, feruloyl tyramine, and coumaroyl tyramine, 6 phenylpropanoids *viz.*, caffeoylquinicacid, tricaffeoylquinic acid, quercetin rutinoside pentoside, quercetin rutinoside, kaempferol rutinoside pentoside, and quercetin–glucose–rhamnose–apiose–ferulic acid, 1 alkaloids (esculeoside A), and 3 lipids *viz.*, 9,12,13-TriHODE, 9,10,13-TriHOME, and lysoPA (18:2).

The relative changes in metabolite levels by limited water supply were compared to sufficient water supply conditions in each nutrient condition and they were presented as a heatmap (Figures 1C,D). According to the heatmap analysis, the limited water condition in nutrient-excess soil (NE-WL) led to reduction in amino acids except for pyroglutamic acid, organic acids such as malic acid and oxoglutaric acid, and sugars and sugar alcohols

TABLE 2 Tomato fruit production per plant, lycopene contents of tomato fruits on a dry-weight basis, and leaf SPAD cultivated under varied nutrient and water conditions.

Soil nutrient	Water	Abbreviated name	Ripened tomato fruit production (g plant^{-1})	Ripened tomato fruit lycopene content (ppm)	Tomato leaf SPAD
Limited	Sufficient	NL-WS	189 ± 32b	889 ± 185a	22.3 ± 4.7b
	Limited	NL-WL	215 ± 14b	943 ± 453a	24.4 ± 4.5b
Excess	Sufficient	NE-WS	364 ± 100a	1,069 ± 212a	48.9 ± 10.4a
	Limited	NE-WL	237 ± 35a,b	960 ± 666a	49.9 ± 6.0a

Mean values ± SD of three biological replicates.

Different alphabetical letters in a column indicate significant differences, as determined by ANOVA followed by Tukey's tests ($p < 0.05$). NL, nutrient limited; WS, water sufficient; WL, water limited; NE, nutrient excess.

except for fructose, myo-Inositol, and maltose. Notably, amino acids (valine, threonine, and phenylalaine) and sugars and sugar alcohols (arabinose, xylose, and glucuronic acid) were significantly decreased compared to the sufficient water condition in nutrient-excess soil (NE-WS). In case of secondary metabolites from nutrient-excess soil condition, all secondary metabolites did not show statistical differences between NE-WL and NE-WS. Polyamines and lipids except for 9, 12, 13-TriHODE decreased in NE-WL compared to NE-WS. Conversely, phenylpropanoids (except for tricaffeoylquinic acid, kaempferol rutinoside pentoside and quercetin–glucose–rhamnose–apiose–ferulic acid) and esculeoside A increased in NE-WL. On the other hand, identified and selected metabolite from the limited water condition in nutrient-limited soil (NL-WL) and the sufficient water in nutrient-limited soil (NL-WS) showed no significant difference, but there were metabolites that showed a different pattern from nutrient-excess soil groups. Isoleucine, sugars and sugar alcohols (fucose, glucuronic acid, myo-Inositol, and maltose), others (monopalmitin, urea, and quinic acid), tris (dihydrocaffeoyl)spermine, and phenylpropanoids (kaempferol rutinoside pentoside and quercetin–glucose–rhamnose–apiose–ferulic acid) showed opposite characteristic pattern from the nutrient-excess soil groups.

Metabolic pathway anaylsis in two soil nutrient conditions

We performed a metabolic pathway analysis to understand the overall pattern of distinguished metabolites and the correlation between metabolites and water/nutrient conditions (Figure 2). The relative changes in metabolite levels by limited water (WL) compared to sufficient water (WS) condition for each nutrient condition (NL or NE) were presented in the pathway map. According to pathway map, amino acids-related metabolism was down-regulated in NL-WL and NE-WL compared to control conditions (NL-WS and NE-WS) except for pyroglutamic acid and isoleucine. Most of polyamines, organic acids, and sugar and sugar alcohols were also down-regulated in NL-WL and NE-WL compared to control conditions (NL-WS and NE-WS), respectively. Especially, myo-inositol and maltose were down-regulated only in NE-WL compared to control (NE-WS). In contrast, most of phenylpropanoids-related metabolism and glycoalkaloids (esculeoside A) were highly accumulated in NL-WL and NE-WL compared to control conditions (NL-WS and NE-WS) except for tricaffeoylquinic acid, kaempferol rutinoside pentoside, and quercetin–glucose–rhamnose–apiose–ferulic acid. Intriguingly, glucuronic acid, monopalmitin, urea, quinic acid, and tris(dihydrocaffeoyl)spermine were accumulated in NL-WL compared to control (NL-WS) but they were little accumulated or reduced in NE-WL compared to control (NE-WS).

Discussion

In this study, tomato fruit yield was not significantly affected by the water conditions, limited or sufficient. Our result is similar that the tomato fruit yield grown in Mg^{2+} surplus soil was not changed by water limitation by regulating the soil water potential at the same level using cv. Super Dotaerang (Kim et al., 2020). In the current study, tomato fruit yield was decreased in the nutrient-limited soil compared to the nutrient-excess soil. The leaf SPAD value did not vary by the regulation in water supply in the two soil nutrient conditions, but leaf SPAD values in nutrient-limited soil were lower than those in nutrient-excess soil. The low SPAD value in the nutrient-limited soil is comparable to the result that the tomato leaf SPAD grown in Mg^{2+} surplus soil was significantly lowered by lowering N supply (Kim et al., 2020). The shoot sizes in nutrient-limited soil were smaller than those in nutrient-excess soil (Supplementary Figure S2), and it suggests that the overall growth of tomato plants was significantly different in two different soils. The content of lycopene, a major functional metabolite of tomato fruit did not vary not only by the regulation in water supply but also by soil nutrient conditions, contrasting to the big differences in the tomato shoot traits (i.e., leaf SPAD and shoot size) in two soil nutrient conditions. In the literature, the tomato lycopene content is known to be affected by irrigation and fertilization (Mitchell et al., 1991; Stefanelli et al., 2010; Wang and Xing, 2017; Kim et al., 2020; see below for further discussion on lycopene). Overall, we can underline that the water limitation in

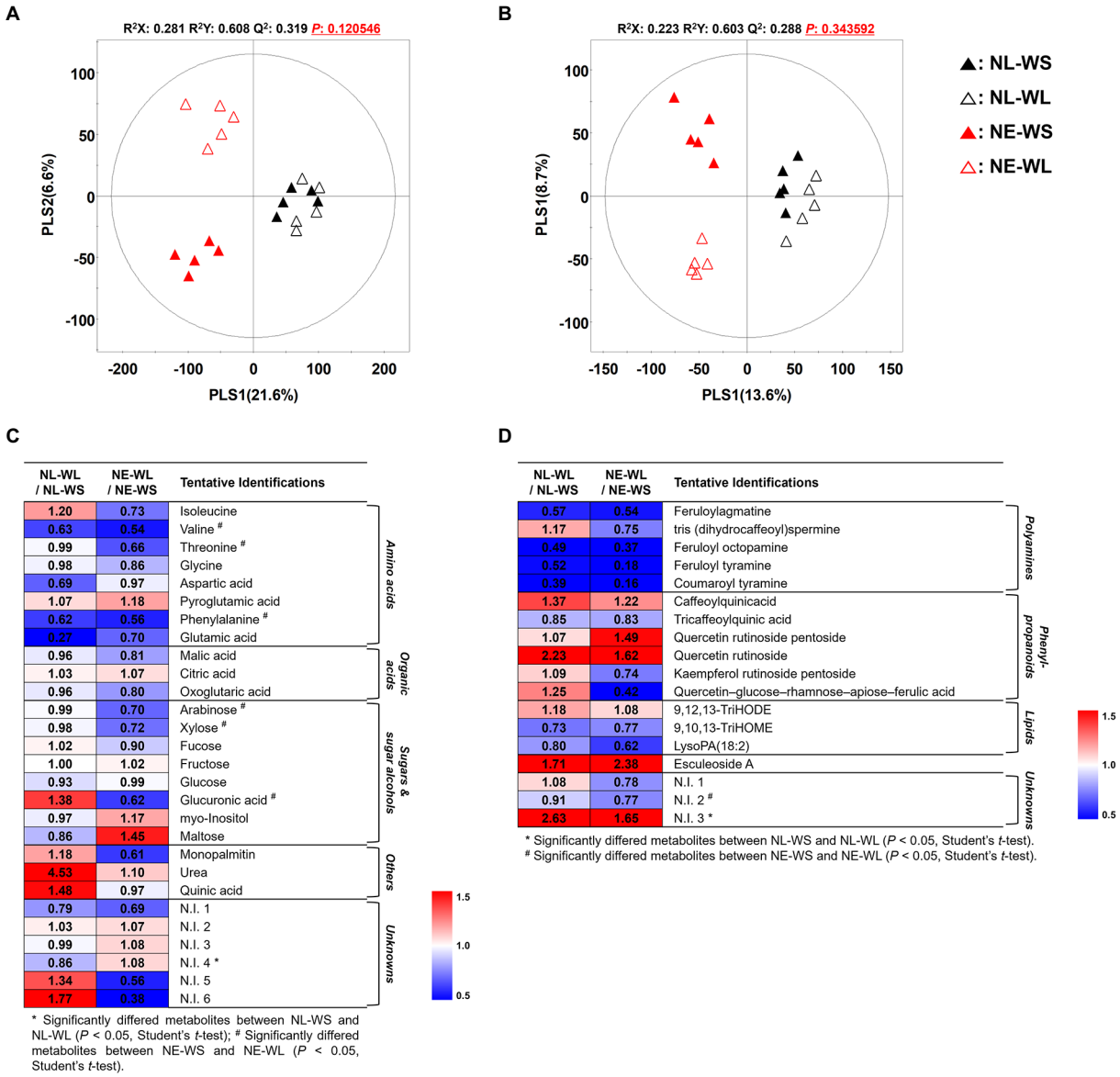


FIGURE 1
PLS-DA score plots from GC-TOF-MS **(A)** and UHPLC-LTQ-Orbitrap-MS **(B)** analysis of tomato cultivated under varied nutrient and water conditions. Symbol, NL-WS (▲); NL-WL (△); NE-WS (▲); NE-WL (△). Heatmap of the relative changes of metabolites by the water limitation for each soil nutrient condition for the distinguished metabolites derived from GC-TOF-MS **(C)** and UHPLC-LTQ-Orbitrap-MS **(D)** datasets (VIP>0.7). The colored squares (blue to red) indicate fold changes normalized by water sufficient condition for each soil nutrient condition.

the current study was not a level to affect the fruit yield and leaf SPAD.

In our study, primary and secondary metabolites did not change substantially by water stress in the nutrient-limited soil, although there was a tendency that the water stress, low water potential (−80 kPa), accumulated phenylpropanoids and reduced polyamines, but there was no significant changes in metabolites. Indeed, water limitation is likely to induce a stress response, since phenylpropanoid is known to be upregulated as a response of plants against stress (Kim et al., 2019). In the nutrient-excess soil of our study, the water stress significantly decreased the primary metabolites including amino acids and sugars and there was a tendency of increase in phenylpropanoids and decrease in polyamines. The decrease in sugars in response to water stress in the nutrient-excess soil was in line with tomato fruits (cv. Super Dotaerang) grown in Mg^{2+} excess soil (Kim et al., 2020). As Kim et al. (2020) suggested, limited water was not recommended to improve tomato fruit (cv. Super Dotaerang) quality in nutrient-excess soil. In the current study, as a focus on improving the quality of tomato fruits (cv. Super Dotaerang) in terms of sugars, amino acids, and polyamines, limited water was not appropriate especially in nutrient-excess soil.

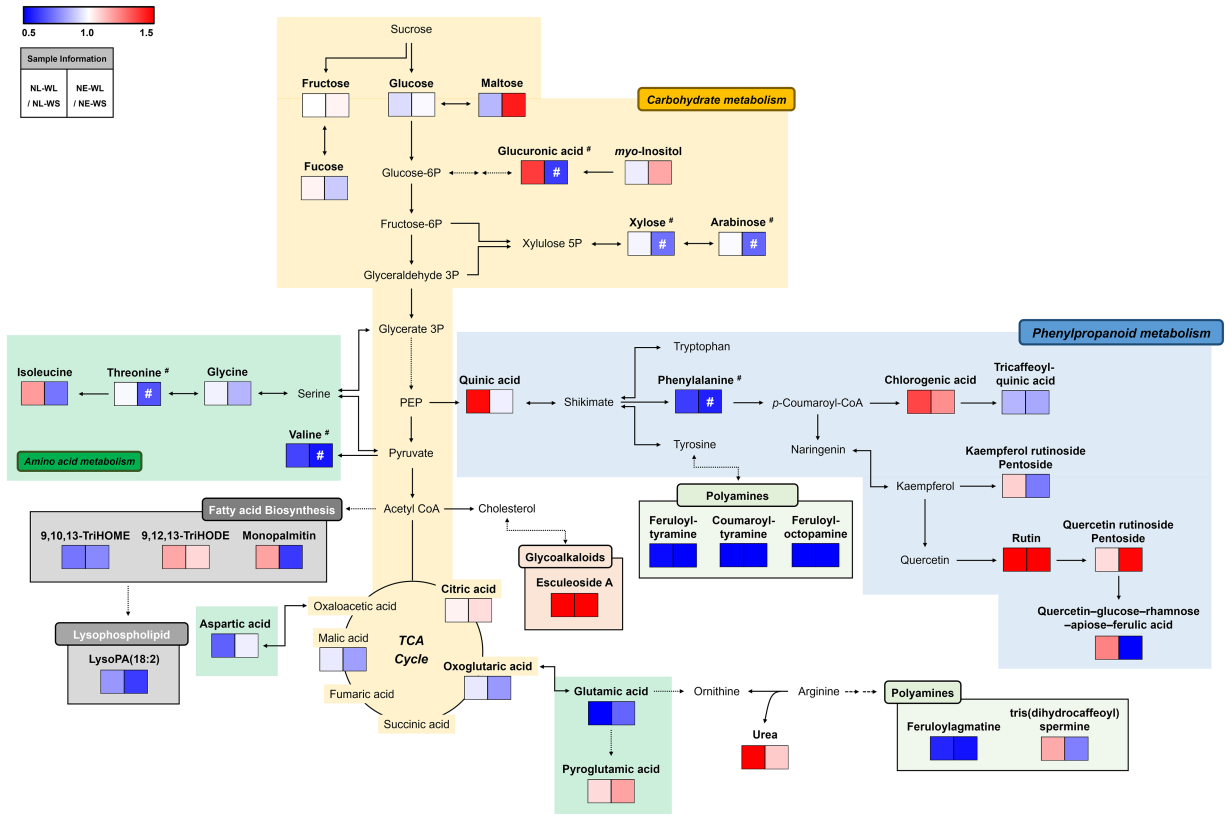


FIGURE 2
Schematic diagram of the metabolic pathway analysis and the relative changes in metabolites by water limitation in two different soils. The metabolic pathway was modified from the KEGG pathway database (https://www.genome.jp/kegg/pathway.html; URL accessed on 17 February 2022). The colored squares (blue to red) indicate fold changed normalized by water sufficient condition for each soil nutrient condition. #Significantly differed metabolites between NE-WS and NE-WL (p<0.05, Student's t-test).

In this study, we tested only one cultivar, Super Dotaerang that is widely cultivated in the plastic house of South Korea and we left a room for other tomato cultivars that may show different responses. The cultivar dependent differences in chemical composition of tomato fruits from four landraces have been demonstrated in response to biostimulant (Rouphael et al., 2021). Effects of abiotic stress on tomato primary and secondary metabolites are known to be variable depending on cultivars (Quinet et al., 2019). For example, water stress increased sugars and organic acids of tomato in many cultivars, however, sugars and organic acids were not affected or decreased in some cultivars (Quinet et al., 2019). The effect of water stress for 141 accessions of diverse small fruit tomato was investigated, and 55 accessions out them exhibited increased metabolite contents in the fresh weight basis and maintained the yield (Albert et al., 2016b). Albert et al. (2016a) investigated 119 recombinant inbred lines derived from a cross between a cherry tomato and a large fruit tomato in response to water deficit (decrease by 60% compared to the control), and they observed more reduction in plant height and fruit production and greater increase in soluble solid contents in larger fruits. Therefore, they suggested that large fruit tomatoes could improve tomato flavor with small yield loss by a slight water deficit. In response to moderate salt stress, Meza et al. (2020) compared three tomato varieties and their fruits had different amino acid content. Flores et al. (2016) investigated the metabolites in tomato fruits in response to saline stress and they compared between a dwarf tomato cultivar and a commercial cultivar. In their study, two cultivars similarly increased carotenoids by saline stress, however, there were slight differences, i.e., the dwarf cultivar had lower capacity to accumulate primary metabolites including sugars and organic acids than the commercial cultivar; the dwarf tomato did not accumulate phenolic compounds and vitamin C differently from the commercial one. Therefore, it is deserved to endeavor to further explore the combined effects of nutrient and water supply condition on different tomato varieties. At least, current knowledge suggests that exploring different tomato varieties and cultivars in order to employ abiotic stresses as a cultivation technology is promising. To improve fruit quality with enhanced nutrients and functional metabolites, many studies have applied minimal irrigation to horticultural plants (Stefanelli et al., 2010). Deficit irrigation

has been shown to improve the tomato fruit quality by increasing concentrations of hexoses, citric acid, and lycopene (Mitchell et al., 1991; Stefanelli et al., 2010; Wang and Xing, 2017). Beside of tomato, it was demonstrated that fruit quality increased under low irrigation conditions also in the cucumber (Zhang et al., 2011). In the future, we need to precisely define the cultivars and soil nutrient condition, when minimal irrigation would improve the crop quality, for practical application.

In terms of the interaction between nutrient and water, the limited water condition might have caused greater decrease in amino acids in tomato fruits in the nutrient-excess soil than in the nutrient-limited soil in our study. By a meta-analysis, water stress was demonstrated to decrease the concentration of nitrogen in plant tissue (He and Dijkstra, 2014). Decreases in nutrient concentration of plant tissues by drought was partly related to the decreases in the concentration of the root nutrient-uptake proteins (Bista et al., 2018). Nutrient availability to plant root is likely to be decreased by the shortage of available soil water, and nutrient uptake kinetics by the root could have been changed. We postulate that the nutrient uptake was substantially reduced by low soil moisture in the nutrient-excess soil. The cation contents such as Ca and Mg in the shoot of tomato plants grown in the nutrient-excess soil was also lower by limited water than that by sufficient water in the current study (data not shown). The combined effect of nutrient and water supply on tomato fruit quality was tested by Wang and Xing (2017). They applied three NPK fertilizer levels × three irrigation levels in a greenhouse and the highest nutrient × lowest water supply resulted in highest lycopene and organic acid content. Kim et al. (2020) investigated the effect of lowering either N or K supply in the combination of limiting water on quality of tomato fruit cultivated in Mg^{2+} excess soil. They showed the tomato fruit lycopene content was significantly lower in lowest N supply in the limiting water condition than in the sufficient water, while in other combinations the effect of limiting water supply was not significant.

Conclusion

In summary, we examined the effects of moderate water stress on the quality of tomato fruits in two soils with different fertility, i.e., nutrient-limited and nutrient-excess. Non-targeted mass spectrometry-based metabolomics successfully demonstrated that water stress differently shifted metabolites of tomato fruits grown in two soils with different nutrient conditions. The limited water condition led to the significant reduction in the concentration of sugars and amino acids in only nutrient-excess soil. Therefore, we carefully suggest that the limited water supply is not recommended as a practical use to improve tomato (cv. Super Dotaerang) fruit quality including sugars and amino acids in soils with excess nutrients.

Data availability statement

The original contributions presented in the study are included in the article/Supplementary material, further inquiries can be directed to the corresponding author.

Author contributions

SL and JS: conceptualization. SL, YL, SS, and JS: validation. SL, YK, and SS: investigation. SL, YL, and JS: resources. YK and SS: writing—original draft preparation. YK, SS, YL, and JS: writing—review and editing. CL: supervision. SL, YL, and YK: project administration. SL and YL: funding acquisition. All authors contributed to the article and approved the submitted version.

Funding

This research was funded by the "Cooperative Research Program for Agriculture Science & Technology Development (project no. PJ012523 and PJ014977)" and by 2022 RDA Fellowship Program of Rural Development Administration, Republic of Korea.

Acknowledgments

We are grateful to the staff of the Plant Nutrition Lab. of the National Institute of Agricultural Sciences for the technical support in tomato cultivation and soil chemical properties measurement.

Conflict of interest

The authors declare that the research was conducted in the absence of any commercial or financial relationships that could be construed as a potential conflict of interest.

Publisher's note

All claims expressed in this article are solely those of the authors and do not necessarily represent those of their affiliated organizations, or those of the publisher, the editors and the reviewers. Any product that may be evaluated in this article, or claim that may be made by its manufacturer, is not guaranteed or endorsed by the publisher.

Supplementary material

The Supplementary material for this article can be found online at: https://www.frontiersin.org/articles/10.3389/fpls.2022.983725/full#supplementary-material

References

Adams, S. N., Ac-Pangan, W. O., and Rossi, L. (2019). Effects of soil salinity on citrus rootstock 'US-942' physiology and anatomy. *HortScience* 54, 787–792. doi: 10.21273/HORTSCI13868-19

Albert, E., Gricourt, J., Bertin, N., Bonnefoi, J., Pateyron, S., Tamby, J. P., et al. (2016a). Genotype by watering regime interaction in cultivated tomato: lessons from linkage mapping and gene expression. *Theor. Appl. Genet.* 129, 395–418. doi: 10.1007/s00122-015-2635-5

Albert, E., Segura, V., Gricourt, J., Bonnefoi, J., Derivot, L., and Causse, M. (2016b). Association mapping reveals the genetic architecture of tomato response to water deficit: focus on major fruit quality traits. *J. Exp. Bot.* 67, 6413–6430. doi: 10.1093/jxb/erw411

Bassirirad, H. (2000). Kinetics of nutrient uptake by roots: responses to global change. *New Phytol.* 147, 155–169. doi: 10.1046/j.1469-8137.2000.00682.x

Bista, D. R., Heckathorn, S. A., Jayawardena, D. M., Mishra, S., and Boldt, J. K. (2018). Effects of drought on nutrient uptake and the levels of nutrient-uptake proteins in roots of drought-sensitive and-tolerant grasses. *Plan. Theory* 7:28. doi: 10.3390/plants7020028

Causin, H. F. (1996). The central role of amino acids on nitrogen utilization and plant growth. *J. Plant Physiol.* 149, 358–362. doi: 10.1016/S0176-1617(96)80134-9

Du, S. T., Liu, Y., Zhang, P., Liu, H. J., Zhang, X. Q., and Zhang, R. R. (2015). Atmospheric application of trace amounts of nitric oxide enhances tolerance to salt stress and improves nutritional quality in spinach (*Spinacia oleracea* L.). *Food Chem.* 173, 905–911. doi: 10.1016/j.foodchem.2014.10.115

Flores, P., Hernández, V., Hellín, P., Fenoll, J., Cava, J., Mestre, T., et al. (2016). Metabolite profile of the tomato dwarf cultivar micro-tom and comparative response to saline and nutritional stresses with regard to a commercial cultivar. *J. Sci. Food Agric.* 96, 1562–1570. doi: 10.1002/jsfa.7256

Gil, H. J., Kim, Y. X., Sung, J., Jung, E. S., Singh, D., Lee, Y., et al. (2020). Metabolomic insights of the tomato fruits (*Solanum lycopersicum* L.) cultivated under different supplemental LED lighting and mineral nutrient conditions. *Hortic. Environ. Biotechnol.* 61, 415–427. doi: 10.1007/s13580-019-00215-8

Hasan, M. M., Skalicky, M., Jahan, M. S., Hossain, M. N., Anwar, Z., Nie, Z. F., et al. (2021). Spermine: its emerging role in regulating drought stress responses in plants. *Cell* 10:261. doi: 10.3390/cells10020261

He, M., and Dijkstra, F. A. (2014). Drought effect on plant nitrogen and phosphorous: a meta-analysis. *New Phytol.* 204, 924–931. doi: 10.1111/nph.12952

Kim, N. S., Kwon, S. J., Cuong, D. M., Jeon, J., Park, J. S., and Park, S. U. (2019). Accumulation of phenylpropanoids in tartary buckwheat (*Fagopyrum tataricum*) under salt stress. *Agronomy* 9:739. doi: 10.3390/agronomy9110739

Kim, Y. X., Kwon, M. C., Lee, S., Jung, E. S., Lee, C. H., and Sung, J. (2020). Effects of nutrient and water supply during fruit development on metabolite composition in tomato fruits (*Solanum lycopersicum* L.) grown in magnesium excess soils. *Front. Plant Sci.* 11:562399. doi: 10.3389/fpls.2020.562399

Kim, Y. X., Ranathunge, K., Lee, S., Lee, Y., Lee, D., and Sung, J. (2018). Composite transport model and water and solute transport across plant roots: an update. *Front. Plant Sci.* 9:193. doi: 10.3389/fpls.2018.00193

Kim, Y. X., Son, S., Lee, S., Jung, E., Lee, Y., Sung, J., et al. (2021). Combined effects of nutrients x water x light on metabolite composition in tomato fruits (*Solanum lycopersicum* L.). *Plan. Theory* 10:1437. doi: 10.3390/plants10071437

Kwon, M. C., Kim, Y. X., Lee, S., Jung, E. S., Singh, D., Sung, J., et al. (2019). Comparative metabolomics unravel the effect of magnesium oversupply on tomato fruit quality and associated plant metabolism. *Metabolites* 9:231. doi: 10.3390/metabo9100231

Meza, S. L., Egea, I., Massaretto, I. L., Morales, B., Purgatto, E., Egea-Fernández, J. M., et al. (2020). Traditional tomato varieties improve fruit quality without affecting fruit yield under moderate salt stress. *Front. Plant Sci.* 11:587754. doi: 10.3389/fpls.2020.587754

Mitchell, J. P., Shennan, C., Grattan, S. R., and May, D. M. (1991). Tomato fruit yields and quality under water deficit and salinity. *J. Am. Soc. Hort. Sci.* 116, 215–221. doi: 10.21273/JASHS.116.2.215

Mun, H. I., Kwon, M. C., Lee, N.-R., Son, S. Y., Song, D. H., and Lee, C. H. (2021). Comparing metabolites and functional properties of various tomatoes using mass spectrometry-based metabolomics approach. *Front. Nutr.* 8:659646. doi: 10.3389/fnut.2021.659646

NIAS (2017) *Fertilizer recommendation for crop production. 3rd Edn. NIAS*. Jeonju, Korea, Rural Development Administration 66–67.

Quinet, M., Angosto, T., Yuste-Lisbona, F. J., Blanchard-Gros, R., Bigot, S., Martinez, J. P., et al. (2019). Tomato fruit development and metabolism. *Front. Plant Sci.* 10:1554. doi: 10.3389/fpls.2019.01554

Rouphael, Y., Corrado, G., Colla, G., De Pascale, S., Dell'Aversana, E., D'Amelia, L. I., et al. (2021). Biostimulation as a means for optimizing fruit phytochemical content and functional quality of tomato landraces of the san Marzano area. *Foods* 10:926. doi: 10.3390/foods10050926

Roy, R., Wang, J., Mostofa, M. G., Fornara, D., Sikdar, A., Sarker, T., et al. (2020). Fine-tuning of soil water and nutrient fertilizer levels for the ecological restoration of coal-mined spoils using *Elaeagnus angustifolia*. *J. Environ. Manag.* 270:110855. doi: 10.1016/j.jenvman.2020.110855

Son, S. Y., Kim, N. K., Lee, S., Singh, D., Kim, G. R., Lee, J. S., et al. (2016). Metabolite fingerprinting, pathway analyses, and bioactivity correlations for plant species belonging to the *Cornaceae*, *Fabaceae*, and *Rosaceae* families. *Plant Cell Rep.* 35, 1917–1931. doi: 10.1007/s00299-016-2006-y

Stefanelli, D., Goodwin, I., and Jones, R. (2010). Minimal nitrogen and water use in horticulture: effects on quality and content of selected nutrients. *Food Res. Int.* 43, 1833–1843. doi: 10.1016/j.foodres.2010.04.022

Suh, D. H., Kim, Y. X., Jung, E. S., Lee, S., Park, J., Lee, C. H., et al. (2020). Characterization of metabolic changes under low mineral supply (N, K, or mg) and supplemental LED lighting (red, blue, or red–blue combination) in *Perilla frutescens* using a metabolomics approach. *Molecules* 25:4714. doi: 10.3390/molecules25204714

Végh, K. R. (1991). "Effect of soil water and nutrient supply on root characteristics and nutrient uptake of plants," in *Developments in agricultural and managed forest ecology*, *Vol. 24*. eds. B. L. McMichael and H. Persson (Amsterdam, The Netherlands: Elsevier), 143–148.

Wang, X., and Xing, Y. (2017). Evaluation of the effects of irrigation and fertilization on tomato fruit yield and quality: a principal component analysis. *Sci. Rep.* 7, 1–13. doi: 10.1038/s41598-017-00373-8

Zhang, H.-X., Chi, D.-C., Wang, Q., Fang, J., and Fang, X.-Y. (2011). Yield and quality response of cucumber to irrigation and nitrogen fertilization under subsurface drip irrigation in solar greenhouse. *Agric. Sci. China* 10, 921–930. doi: 10.1016/S1671-2927(11)60077-1

frontiers | Frontiers in Plant Science

TYPE Original Research
PUBLISHED 21 September 2022
DOI 10.3389/fpls.2022.995810

Check for updates

OPEN ACCESS

EDITED BY
PingWu Liu,
Hainan University, China

REVIEWED BY
Lisa David,
North Carolina State University, United States
Sayed Mohammad Mohsin,
Sher-e-Bangla Agricultural University, Bangladesh

*CORRESPONDENCE
Suqin Zhang
zsqin2002@163.com
Guangdong Geng
gdgeng213@163.com

†These authors have contributed equally to this work

SPECIALTY SECTION
This article was submitted to Plant Abiotic Stress, a section of the journal Frontiers in Plant Science

RECEIVED 16 July 2022
ACCEPTED 26 August 2022
PUBLISHED 21 September 2022

CITATION
Guo H, Xiong X, Wang Y, Tian H, Zhang S and Geng G (2022) Integrative proteomic and physiological analyses of the molecular response to dessication-stress in *Auricularia fibrillifera*.
Front. Plant Sci. 13:995810.
doi: 10.3389/fpls.2022.995810

COPYRIGHT
© 2022 Guo, Xiong, Wang, Tian, Zhang and Geng. This is an open-access article distributed under the terms of the Creative Commons Attribution License (CC BY). The use, distribution or reproduction in other forums is permitted, provided the original author(s) and the copyright owner(s) are credited and that the original publication in this journal is cited, in accordance with accepted academic practice. No use, distribution or reproduction is permitted which does not comply with these terms.

Integrative proteomic and physiological analyses of the molecular response to dessication-stress in *Auricularia fibrillifera*

Hao Guo†, Xingwei Xiong†, Yiqin Wang, Huaizhi Tian, Suqin Zhang* and Guangdong Geng*

College of Agriculture, Guizhou University, Guiyang, Guizhou, China

Drought stress is one of the main factors influencing the growth and development of an organism. *Auricularia fibrillifera* has strong dessication resistance. In *A. fibrillifera* under dessication-stress, the melanin content of fruiting bodies elevated significantly by >10-fold compared with the control. Folate content also increased sharply but decreased significantly after rehydration, and amino acid and biotin levels increased by 40.11 and 22.14%, respectively. In proteomic analysis, 1,572 and 21 differentially abundant proteins (DAPs) were identified under dessication-stress and rehydration, respectively. A large number of DAPs were annotated in "amino acid metabolism," "carbohydrate metabolism," and "translation" pathways, and the DAPs related to osmotic regulation and antioxidant enzymes were significantly increased in abundance. Transcriptome-proteome association analysis showed that most DAPs (30) were annotated in the "biosynthesis of antibiotics" pathway. DAPs and corresponding differentially expressed genes were all up-regulated in the "biotin biosynthesis" pathway and associated with "folate biosynthesis" and "phenylalanine, tyrosine, and tryptophan biosynthesis." In the analysis of protein–protein interactions, the DAPs annotated in the "phenylalanine, tyrosine, and tryptophan biosynthesis" pathway had the strongest interactions with other DAPs. These enriched pathways could enhance amino acid, folate, biotin, and melanin levels during desiccation stress, which is consistent with the physiological data (amino acid, folate, biotin, and melanin contents). In addition, many DAPs related to the cytoskeleton were significantly increased in abundance under dessication-stress. Physiological and transcriptome data were in agreement with proteomic results. This work provides valuable insight into the dessication-tolerant mechanisms of *A. fibrillifera*.

KEYWORDS

***Auricularia fibrillifera*, proteome, dessication stress, melanin, antibiotics, folate, biotin, cytoskeleton**

Introduction

Auricularia fibrillifera is a common traditional Chinese food and medicine, which is the third most important cultivated mushroom worldwide (Yuan et al., 2019). It has a pleasant taste and many health-associated characteristics such as antioxidant, anticoagulant, antitumor, immunomodulatory, and cholesterol-lowering properties (Sekara et al., 2015). It is expected that the duration and severity of droughts will increase, resulting in adverse effects on agriculture and causing significant declines in crop production on a global scale (Lesk et al., 2016). Thus, it is important to improve drought tolerance in organisms for global food security and necessary to clarify the physiological and molecular mechanisms of dessication tolerance.

Some mechanisms of drought response are similar between *A. fibrillifera* and plant species (Wang et al., 2016, 2022; Zandalinas et al., 2018; Mahmood et al., 2019). The physiological effects induced by drought stress include altered cell wall elasticity, increased oxidative stress (Caruso et al., 2009), toxic metabolite generation, and extensive cellular damage in plants (Ahuja et al., 2010; Zandalinas et al., 2018). Plants have also evolved various drought tolerance mechanisms to adapt to drought stress. The drought resistance of plants is quite complex (Wang et al., 2015). Osmotic adjustment, hormonal regulation, antioxidant systems, and signal transduction play vital roles in drought tolerance (Zandalinas et al., 2018; Mahmood et al., 2019). Amino acids have crucial roles in osmotic adjustment. Melanins exist in fungi, plants, and microorganisms, and have the functions of free-radical scavenging, antioxidant activity, and radiation protection (Burmasova et al., 2019; Cordero and Casadevall, 2020; Cao et al., 2021). Biotin and biotinylation might be involved in energy management to cope with drought and flooding in the early stage of soybean-root tip (Wang et al., 2016). Foliar application of folate was found to be not only suitable for drought stress alleviation in *Coriandrum sativum* L. but also beneficial for improvement in growth and yield under water-deficit circumstances (Khan et al., 2022).

A loss of more than 10% of plant fresh weight can lead to water stress, which can induce the synthesis of some specific ones (including S-like RNase homolog, actin depolymerizing factor, rubisco activase, and translational initiation factor EF-Tu), maintain others, and decrease the levels of some plant proteins (such as isoflavone reductase-like protein and chloroplast Rieske Fe-S protein) (Hsiao, 1973; Salekdeh et al., 2002). Investigating the proteome profiles under drought stress can provide detailed information regarding the specific protein changes associated with drought responses (Koh et al., 2015). Under drought stress response/tolerance, numerous proteins related to metabolism, photosynthesis, stress, and defense were identified by a comparative proteome analysis in *Brassica napus* seedlings (Koh et al., 2015). Proteomic studies on post-drought recovery have clarified the mechanisms of plants in response to drought stress (Khan and Komatsu, 2016). Four novel drought-responsive proteins were identified during drought stress and recovery in rice leaves by proteomic analysis (Salekdeh et al., 2002). Aldehyde dehydrogenase and peroxidase are known to decrease aldehydes and toxic reactive oxygen species from soybean roots and help in the recovery from drought stress (Khan and Komatsu, 2016). Under drought stress, the abundance of most protein changes may be associated with gene transcription. There was a positive correlation between protein expression and gene transcription in *B. napus*, although different patterns between proteins and transcripts were detected at various time points (Koh et al., 2015). These reports provide valuable information for investigating the molecular mechanisms of dessication tolerance in *A. fibrillifera*.

For general organisms (the majority of terrestrial plants and mushrooms), the vegetative bodies will dry up or even die under severe drought stress. *Selaginella lepidophylla* is a desiccation-tolerant plant capable of surviving complete vegetative tissue dehydration and reviving under water conditions (Pampurova and Van Dijck, 2014). A candidate basic helix-loop-helix (bHLH) transcription factor was observed to be highly expressed at 4% relative water content in *S. lepidophylla* (*SlbHLH*), and its overexpression significantly increased integrated water-use efficiency and green cotyledon emergence rates under water-deficit stress in *Arabidopsis* (Ariyarathne and Wone, 2022). The fruit bodies of *Auricularia* dries out and enters dormancy under dessication conditions. The dormancy may be broken once watered. Hence, the dessication tolerance and rehydration capability of *A. fibrillifera* make it a suitable model to elucidate its adaptive mechanism against dessication-stress (Ma et al., 2014). Currently, there are limited reports on the molecular mechanisms of dessication tolerance in *A. fibrillifera*. In this study, protein markers and pathways were investigated under dessication-stress in *A. fibrillifera* by data-independent acquisition (DIA) proteomic profiling to explore the dessication-tolerant mechanism of *A. fibrillifera* and provide novel information for dessication-tolerant breeding for *A. fibrillifera*.

Materials and methods

Materials and treatments

A dessication-tolerant *A. fibrillifera* cultivar "CSLZ" was used for this study. The strain was maintained in a culture medium to generate fruiting bodies (Wang et al., 2022). Upon reaching full mycelial colonization, polyethylene bags were removed, and the substrate was cultured at 25 ± 1°C under a 15:9 h-light/dark cycle. The substrate-containing bags were routinely sprayed with 15 mL water/bag 8 times daily. When the diameters of the fruit bodies reached 2-3 cm, dessication-stress treatment was initiated, and the fruit bodies on the substrate naturally dehydrated. The regularly watered fruit bodies on the substrate served as a parallel control. When the water loss rate of fruit bodies achieved 60% (desiccation-stress, DS) compared

to the CK1 parallel control, uniformly sized fruit bodies were harvested as the first samples. The fruit bodies were rewatered. The next sampling process was conducted when the water loss rate of fruit bodies was 50% [after rehydration (RE) for 1 h] compared to the CK2 parallel control. Each sample pool included 15 individual fruit bodies, and the experiment was performed in triplicate. All the specimens were immediately frozen in liquid nitrogen and kept at -80°C for further analysis.

Physiological analysis

The amino acid (Cas No.: BC1575, Solarbio, Beijing, China), biotin (Cas No.: BC4804, Solarbio), and folate (Cas No.: BC4834, Solarbio) contents were determined according to the kit instructions. In brief, the α-amino group of amino acids can react with hydrated ninhydrin to produce a blue-violet compound with an absorption peak at 570 nm, which was detected with a microplate reader (Thermo-Fisher-Scientific, San Jose, CA, United States). Both biotin and folate have ultraviolet absorption at 210 nm, and their contents were determined by high performance liquid chromatography (HPLC) (Shimadzu, Kyoto, Japan) and ultraviolet detector (Shimadzu). Melanin was extracted using a method by Wang et al. (2022). Shortly, 1.0 g fruit body was ground in 50 mL of 1 M NaOH. The samples were treated in an ultrasonic cleaner (300 W) for 2 h at 60°C. The supernatant (pH adjusted to 1.5) was immersed in a boiling water bath for 10 h, and then centrifuged at 9,156 × *g* for 15 min. After air-drying the precipitation, the melanin content was calculated.

Protein extraction

Total proteins of fruit bodies were isolated according to the phenol method (Isaacson et al., 2006) with slight modifications: briefly, 0.5 g fruit bodies were ground into a fine powder in a lysis buffer containing 877 mM sucrose, 100 mM EDTA, 20 mM Tris-HCL (pH = 8.0), 1 mM dithiothreitol (DTT), 2% (v:v) β-mercaptoethanol, 1% (v:v) Triton X-100, and 0.1 × Cocktail (Roche, Switzerland). Subsequently, 2 × volume of tris-saturated phenol (pH = 7.5) was added and centrifuged at 25,000 × *g* for 15 min at 4°C. After collecting the supernatant, 5 × volume of precooled precipitate solution, containing 0.1 M ammonium acetate in methanol and 10 mM DTT, was added to the protein mixture. Every sample was maintained for 2 h at -20°C. Then, the samples were centrifuged at 25,000 *g* for 15 min at 4°C, and the supernatant was removed. The pellets were further washed with 1 mL of precooled acetone [precooled acetone:sample = 5:1 (v/v)] with centrifugation at 25,000 × *g* for 15 min at 4°C. After air-drying the pellets, 200 μL of L3 lysis buffer containing 7 M urea, 2 M thiourea, 20 mM Tris, 10 mM DTT, and 1 × Cock-tail (Roche) were added, ground (60 Hz, 2 min), and centrifuged at 25,000 × *g* for 15 min at 4°C. DTT (10 mM) was added to the supernatant and it was kept in a water bath at 56°C for 1 h. Subsequently, iodoacetamide (55 mM) was added and kept in the dark for 45 min and, after adding 1 mL cold acetone, all samples were maintained 2 h at -20°C. All samples were centrifuged at 25,000 × *g* for 15 min at 4°C. After removing the supernatants, the pellets were air-dried and dissolved in 200 μL L3 lysis buffer. Trypsin [protein:trypsin = 40:1 (w/w)] was added for enzymolysis, and then desalinated, vacuum-dried and redissoluted. Nanodrop ND-1000 (Thermo-Fisher-Scientific) was used to measure protein concentrations.

Liquid chromatography-tandem mass spectrometry analysis

As an internal standard for quantification, 2 mL of mixed extract solution (100 μg/mL) were used. After HPLC (Shimadzu) fractionation, the eluents were combined into 10 fractions for LC-tandem mass spectrometry (MS/MS). The freeze-dried peptides were dissolved in Solvent A (2% acetonitrile and 0.1% formic acid), and the peptide specimens were separated using an UltiMate 3000 UHPLC (Thermo-Fisher-Scientific). The analytical conditions were as follows: LC column, C18 (150 μm × 35 cm, 1.8 μm, 100 Å); gradient program, 5% B (98% acetonitrile and 0.1% formic acid) for 5.0 min, 5%–25% B for 115 min, 25%–35% B for 40 min, 35%–80% B for 10 min, 80% B for 5 min, and 5% B for 5 min; and flow rate, 300 nL/min. The peptide specimens were ionized by a nanoESI, and then put into a Q-Exactive HF tandem mass spectrometer (Thermo-Fisher-Scientific) for data-dependent acquisition mode detection (Tsou et al., 2015). The spectra of first-grade MS (MS1) were acquired in the scan range of 350–1,500 m/z with spray voltage of 1.6 kV, resolution of 120,000, automatic gain control (AGC) target of $3E^6$, and maximum injection time (MIT) of 50 ms. The spectra of second-grade MS (MS2) were obtained using the following parameters: resolution of 30,000, MIT of 100 ms, dynamic exclusion duration of 30 s, and AGC target of $1E^5$. Moreover, the mode of MS2 spectra was high-energy collisional dissociation (HCD), and the collision energy was 28%. For DIA analysis, the same nano-LC system and gradient were used as those employed for data-dependent acquisition analysis. The following were the DIA MS parameters: scan range of 400–1,250 m/z, resolution of 120,000, and MIT of 50 ms. The DIA isolation window was set to 17 m/z with loop count of 50, automatic MIT, resolution of 30,000, stepped collision energy of 22.5%, 25.0%, and 27.5%, and AGC target of $1E^6$.

Spectronaut was employed to efficiently deconvolute, precisely identify, and quantitatively analyze the data (Bernhardt et al., 2014).

Identification of differentially abundant protein and bioinformatics analysis

The peak areas of an ion pair were extracted using Spectronaut (Bruderer et al., 2015). The error correction and normalization steps were performed using the Msstats software package (Choi et al., 2014). The DAPs fit these two criteria, fold-change ≥ 2 and Q-value ≤ 0.05. The consistency and probability of DAPs were scored and compared with the Swissprot library, and the threshold was set as $1E^{-5}$ for protein description. The subcellular localization, protein-protein interaction (PPI) and Kyoto Encyclopedia of Genes and Genomes (KEGG) enrichment analyses were performed with these DAPs. A hypergeometric test was used to detect significantly enriched pathways ($p < 0.05$).

Proteome-transcriptome-associated analysis

We carried out proteome-transcriptome-associated analysis to gain a deeper understanding of the biological functions by combining results of two separate-omics techniques. The samples were analyzed at both mRNA and protein levels. The transcriptome data were retrieved from our previous study (NCBI SRA database under accession no. PRJNA695780) (Wang et al., 2022). Differentially expressed genes (DEGs) were chosen by DESeq software according to the following criteria: fold-change ≥ 2 and Q-value ≤ 0.001. Correlation analyses were performed between DAPs and DEGs of two omics, and the associated DAPs/DEGs were used for expression correlation analysis and metabolic pathway map integration analysis.

Construction of protein-protein interaction network

STRING v11.5 (string-db.org) was applied to analyze the PPIs of DAPs identified in this study and their PPI network was constructed. The minimum required interaction score parameter was set at a high confidence level (0.70).

Quantitative real-time polymerase chain reaction assays

Total RNA was isolated from fruiting bodies using an RNApre Pure Plant Plus Kit (Polyphenolics & Polysaccharides-rich) (Tiangen, Beijing, China). Using FastKing gDNA Dispelling RT SuperMix Kit (Tiangen), the extracted RNA was reverse-transcribed by following the manufacturer's kit. Specific primers of 16 selected DAPs were designed using Primer 5 (**Supplementary Table 1**). The *18S* gene was used for reference (Zhao et al., 2019). The qRT-PCR amplification was conducted on an ABI StepOne Real-Time polymerase chain reaction (PCR) System (Applied Biosystems, CA, United States). The relative expression levels of target genes were determined using the $2^{-\Delta\Delta Ct}$ method with 3 technical and biological replications (Livak and Schmittgen, 2001).

Statistical analysis

Statistical tests were conducted with SPSS v19.0 (IBM Corp., NY, United States). The differences between means were compared with ANOVA followed by Duncan's multiple range test. Pearson's correlation analysis of binary variables was carried out. Level of statistical significance was set at $p < 0.05$.

Results

Physiological responses to dessication-stress and rehydration

The phenotype of fruiting bodies changed significantly under dessication-stress. In response to dessication, the fruiting bodies shrank and became hard but after rehydration, they began to expand and appeared softened (**Figure 1A**). Levels of amino acids and biotin in fruiting bodies increased significantly by 40.11 and 22.14%, respectively, under dessication-stress compared with those of the controls (**Figures 1B,C**). The melanin content increased significantly by > 10-fold compared to the control (**Figure 1D**). The folate peak was not detected in the control, which might be owing to its extremely low level; but levels increased rapidly under dessication-stress. After rehydration, the decrease in folate was the greatest (21.79%) compared with amino acids, biotin, and melanin (**Figure 1E**).

Differentially abundant proteins under dessication-stress

The proteomic analysis of fruiting bodies was performed during dessication-stress and rehydration stages, and stable results were obtained among the replicates of each treatment (**Supplementary Figure 1**). A total of 1,572 DAPs (1,005 more-abundant and 567 less-abundant) were observed under dessication-stress, and 10 more-abundant and 11 less-abundant DAPs were found after rehydration (**Figure 2A** and **Supplementary Table 2**). Fifteen DAPs appeared under both dessication-stress and rehydration (**Figure 2B**). The number of DAPs under dessication-stress was 74.86-fold of that after rehydration. Subcellular localization showed that under dessication-stress the DAPs were mainly located in

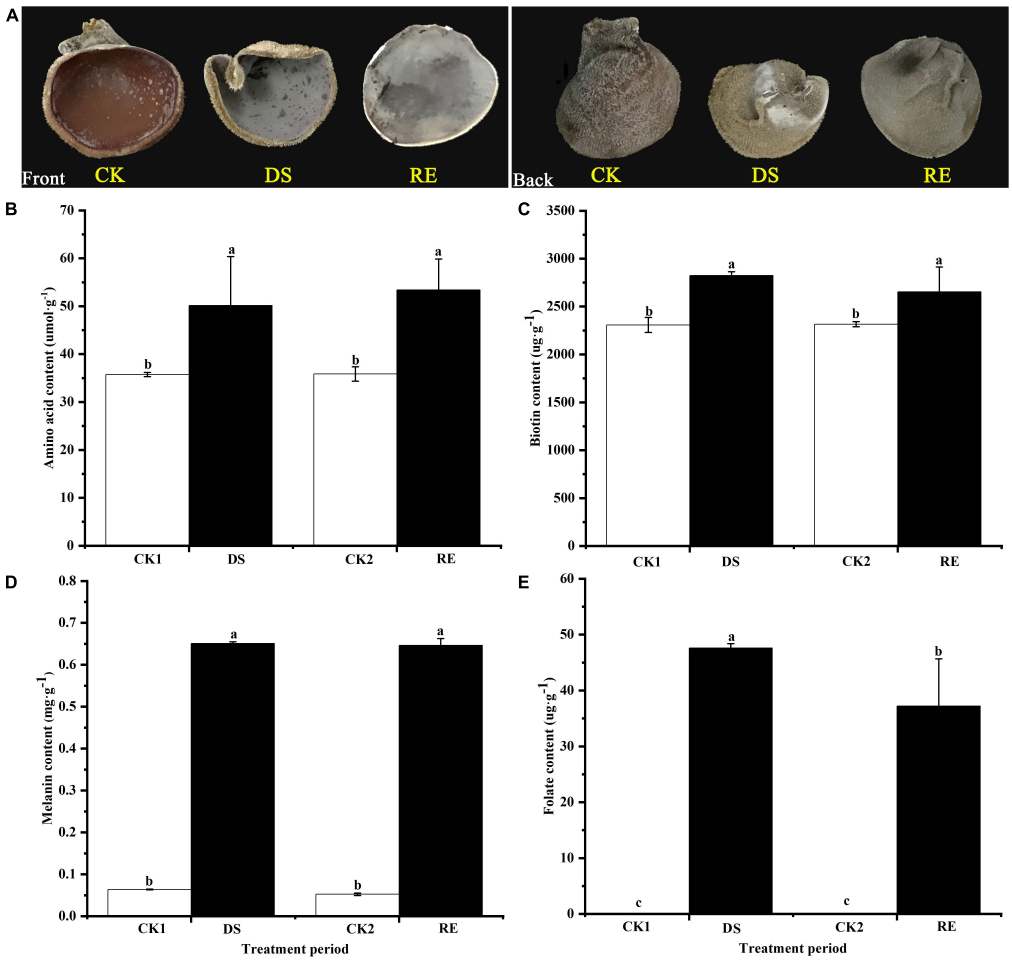


FIGURE 1
Phenotype and physiological responses to dessication-stress and rehydration in *Auricularia fibrillifera*. **(A)** Phenotypes of fruiting bodies. The front is on the left and the back is on the right. **(B)** Amino acid, **(C)** biotin, **(D)** melanin, and **(E)** folate content. CK1, CK2, DS, and RE represent the parallel control of desiccation-stress, parallel control of rehydration, desiccation-stress, and rehydration process, respectively. Bars indicate mean ± SD (n = 3). Values with different letters are significantly different at $p < 0.05$.

mitochondria, followed by the cytoplasm and extracellular locations (Figure 2C).

To verify the reliability of proteome data, we selected 16 DAPs for qRT-PCR assays (Supplementary Table 3). The correlation coefficient of the fold-change values between proteome and qRT-PCR was statistically significant (r = 0.84, p = 3.80E^{-7}; Figure 2D). The more- or less-abundant of the proteins, as revealed by proteomics analysis, was corroborated by qRT-PCR.

Kyoto encyclopedia of genes and genomes enrichment analysis under dessication-stress

In plants, different proteins coordinate with each other to activate cellular responses, and pathway analysis is helpful in further understanding biological function. Under dessication-stress, there were 874 DAPs annotated to different pathways, among these most DAPs were enriched in "metabolism" pathways, such as "carbohydrate metabolism" (202) and "amino acid metabolism" (133) (Figure 3A and Supplementary Table 4). Many DAPs were also annotated in "translation" (154) and "transport and catabolism" (127) pathways. After rehydration, the DAP number decreased rapidly, and only six DAPs were enriched in KEGG pathways (Figure 3B). Some DAPs were not annotated to any KEGG pathway, while some DAPs were in more than one KEGG pathway at desiccation and rehydration stages. "Glyoxylate and dicarboxylate metabolism," "folate biosynthesis," "fructose and mannose metabolism," "biosynthesis of antibiotics," "biosynthesis of amino acids," "phenylalanine, tyrosine and tryptophan biosynthesis," "biotin metabolism," and other pathways were significantly enriched during the desiccation stress (Figure 3C). The highest number

10.3389/fpls.2022.995810

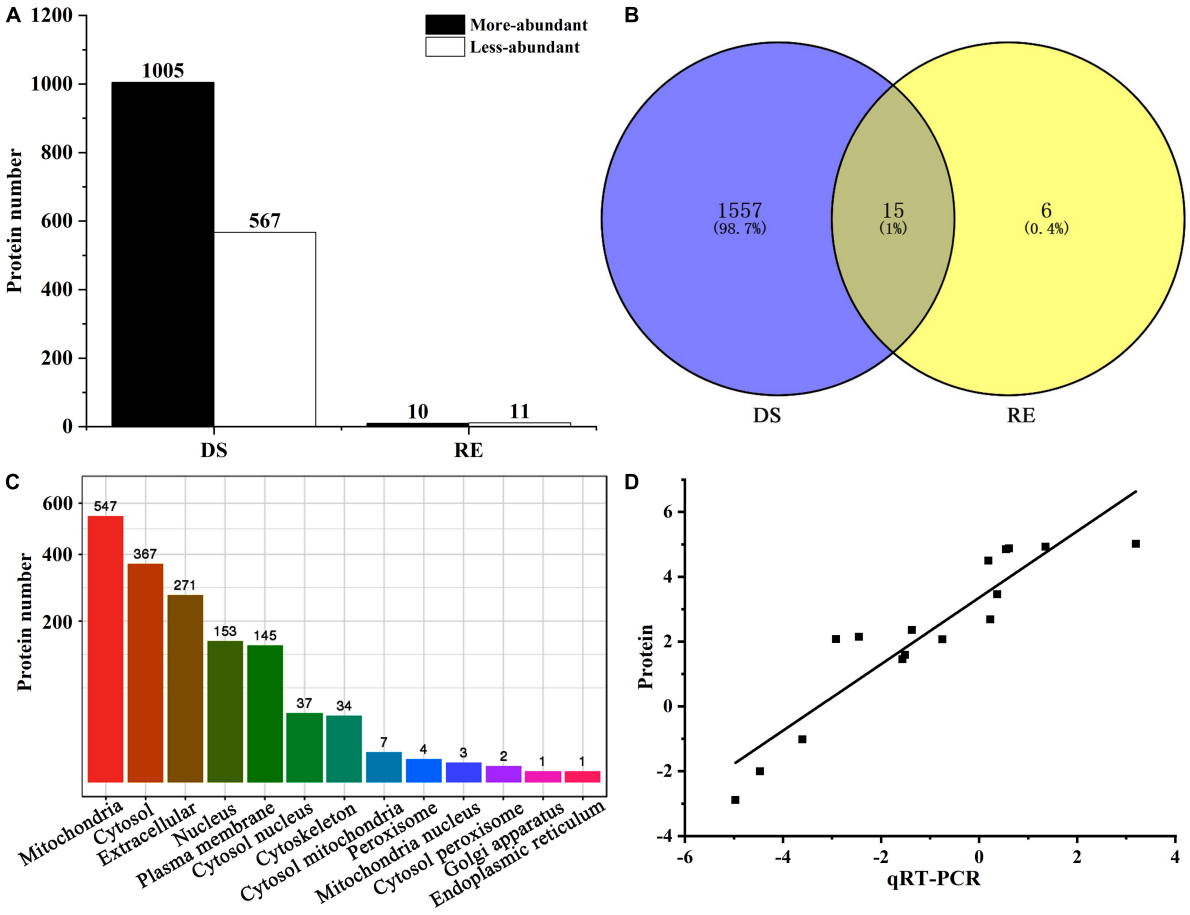


FIGURE 2
Number **(A)**, Venn diagram **(B)**, subcellular localization **(C)**, and correlation coefficient of differentially abundant proteins between proteome and qRT-PCR **(D)**. DS and RE represent dessication-stress and rehydration, respectively.

of DAPs occurred in the "biosynthesis of antibiotics" pathway (Figure 3C). There was no significantly enriched pathway after rehydration.

Proteome-transcriptome-associated analysis

The joint proteome and transcriptome analysis was useful in finding the regulation of gene expression (Maier et al., 2009). A total of 391 DAPs were associated with dessication-stress (Supplementary Tables 5, 6). The expression of corresponding DAPs and DEGs were focused mainly on two patterns: (1) both were up-regulated and (2) the DAPs were increased in abundance but the DEGs were down-regulated (Figure 4). The main associated pathways were "starch and sucrose metabolism," "biosynthesis of antibiotics" and "biosynthesis of amino acids." Interestingly, in the "biotin metabolism" pathway, all DAPs were associated, and both DAPs and DEGs were up-regulated. In the "folate biosynthesis," "phenylalanine, tyrosine, and tryptophan biosynthesis" pathways, the associated DAPs were mainly increased in abundance, whereas the corresponding DEGs were expressed in the opposite direction (Figure 4). After rehydration, there were eight associated DAPs (Supplementary Tables 5, 6). Unfortunately, some proteins were not annotated in the KEGG pathway database.

Protein-protein interaction analysis

Protein-protein interaction is essential for almost every process in cells and may be related to the specific function performed by proteins after binding into complexes through PPI. We selected 133 DAPs related to the dessication-stress response (e.g., stress response, sugar metabolism, and signal transduction) for PPI analysis. A total of 45 nodal DAPs were identified, which were divided into three clusters (Figure 5). Cluster 1 (blue bubbles) included 16 DAPs, which were mainly involved in stress response. CTA1 (catalase A), HOG1 (mitogen-activated protein kinase involved in osmoregulation), and

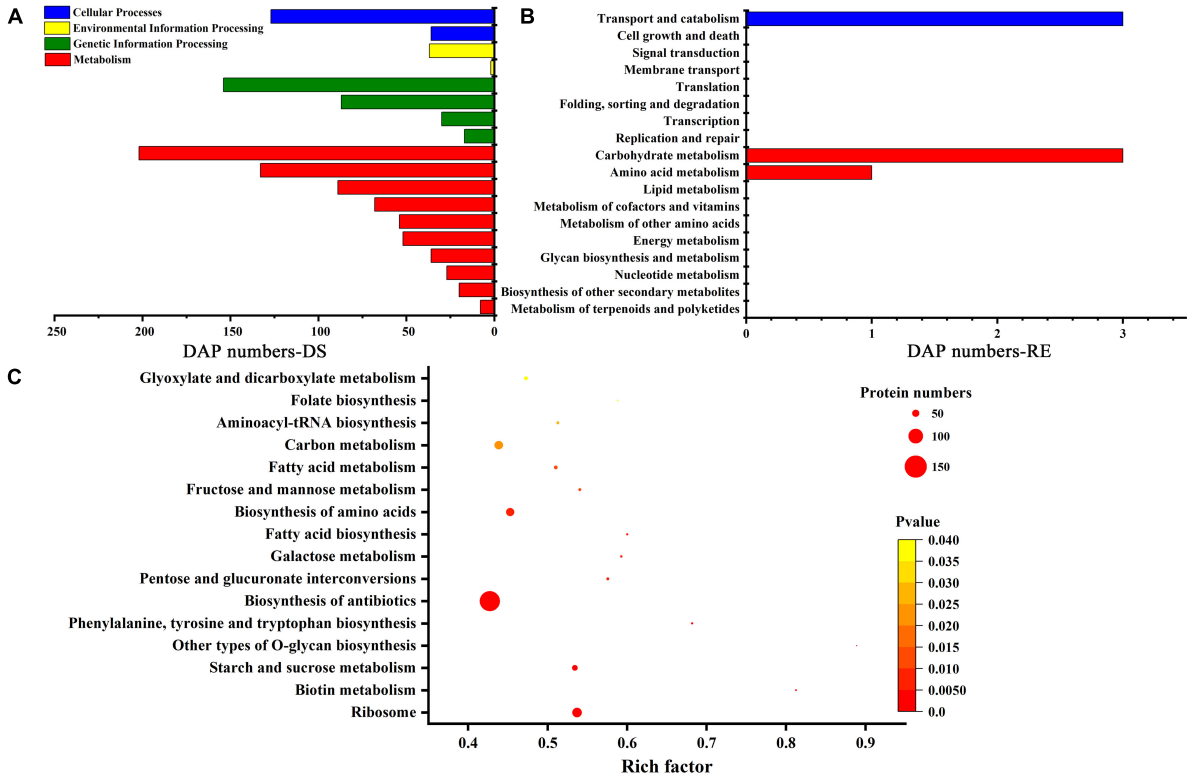


FIGURE 3
Kyoto Encyclopedia of Genes and Genomes (KEGG) pathways. **(A)** KEGG pathways under dessication-stress. **(B)** KEGG pathways after rehydration. **(C)** Significantly enriched pathways under dessication-stress. DS, RE, and DAP represent dessication-stress, rehydration, and differentially abundant protein, respectively.

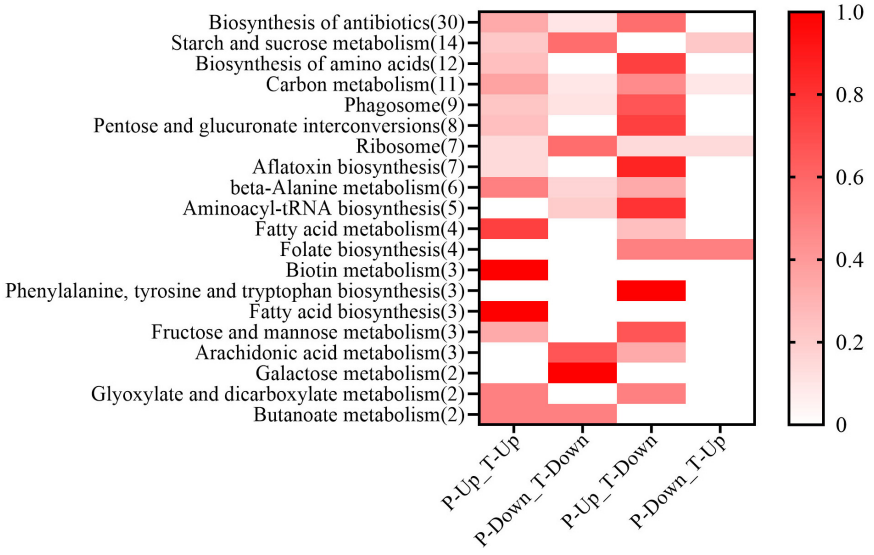


FIGURE 4
Proteome–transcriptome-associated Kyoto Encyclopedia of Genes and Genomes (KEGG) analysis. In the horizontal axis, T, P, Up, and Down show differentially expressed genes from the transcriptome, differentially abundant proteins from the proteome, up-regulation, and down-regulation, respectively. On the Y axis, the number of differentially abundant proteins in each pathway is shown in parentheses. The color of the heat map represents the proportion of proteins in the pathway.

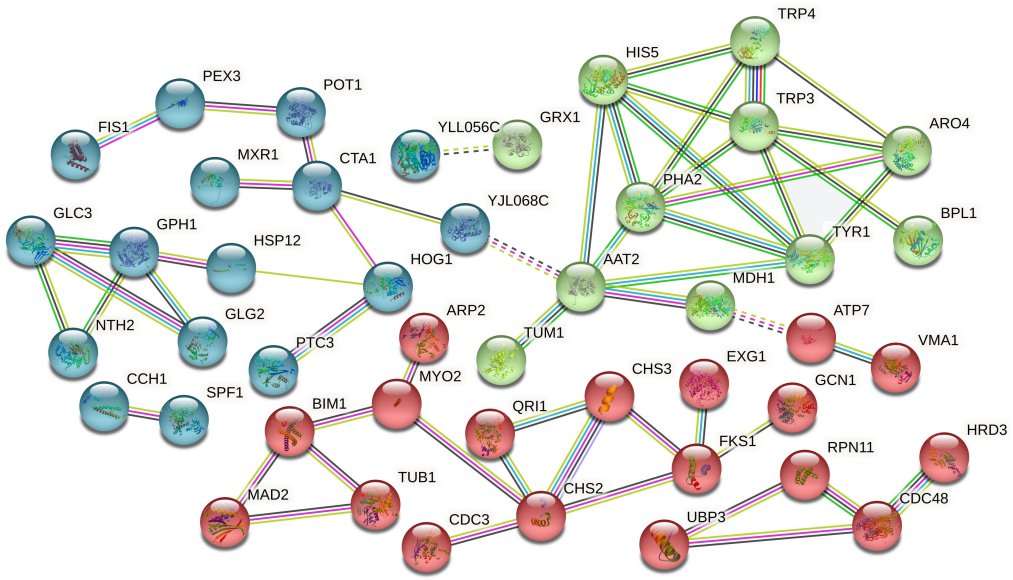


FIGURE 5
Protein-protein interaction analysis of dessication-responsive differentially abundant proteins. Different line colors represent the types of evidence used in predicting the associations: gene fusion (red), neighborhood (green), co-occurrence across genomes (blue), co-expression (black), experimental (purple), association in curated databases (light blue), or co-mentioned in PubMed abstracts (yellow).

PH1 (glycogen phosphorylase required for the mobilization of glycogen) were increased in abundance, which was conducive to the removal of excess reactive oxygen species, osmotic adjustment, and energy supply under dessication-stress.

Cluster 2 (green bubbles) included 11 more-abundant DAPs, most of which were related to amino acid metabolism. PHA2 (putative prephenate dehydratase) and TRP3 (multifunctional tryptophan biosynthesis protein) were important hub proteins in this cluster. The most nodal proteins were in the "phenylalanine, tyrosine, and tryptophan biosynthesis" and "tyrosine metabolism" pathways, and might participate in melanin synthesis.

Eighteen DAPs were found in cluster 3 (red bubbles), which were mainly involved in the synthesis and elasticity of the cell wall, such as chitin synthase II (CHS2), chitin synthase III (CHS3), and β-1,3-glucan synthase component (FKS1). These three kinds of proteins were less-abundant under dessication-stress and might contribute to dessication tolerance and the shrinkage of fruiting bodies.

Important proteins associated with the response to dessication-stress

Melanin synthesis

Melanins are derived from tyrosine, and referred to as "fungal armor" due to the ability of the polymer to protect microorganisms against a broad range of toxic insults (Gómez and Nosanchuk, 2003; Glagoleva et al., 2020). Sixteen (12 more-abundant and four less-abundant) DAPs were identified in the "tyrosine metabolism" pathway (Table 1). The fold-change values of more-abundant proteins were higher than those that decreased. Tyrosine synthesis mainly exists in the "phenylalanine, tyrosine, and tryptophan biosynthesis" pathway. Fifteen DAPs were identified in this pathway, they were all increased in abundance. Among them, two proteins that directly promote tyrosine synthesis were histidinol-phosphate aminotransferase (Unigene7245_All, $Log_2FC = 2.60$) and aspartate aminotransferase (CL2639.Contig2_All, $Log_2FC = 2.78$) (Table 1). They provided a reactive substrate for melanin synthesis.

Vitamin synthesis

Tetrahydrofolic acid (THF) and its derivatives are known as folate or B9 vitamins (Basset et al., 2005). Biotin is also known as vitamin H or B7 (Lazar et al., 2017). The pathways of "folate biosynthesis" and "biotin metabolism" were remarkably enriched under dessication-stress (Figure 3C). In the "folate biosynthesis" pathway, 10 DAPs were identified, including six more-abundant and four less-abundant. Folylpolyglutamate synthase (CL112.Contig1_All) and probable dihydrofolate synthetase (CL8178.Contig1_All) were increased in abundance to promote folate synthesis and were consistent with the folate content (Figure 1D). Thirteen more-abundant DAPs were identified in the "biotin metabolism" pathway (Table 2). Among them, the fold-change value of CL4671.Contig1_All was the highest (4.51) (Table 2). This was consistent with the biotin content (Figure 1B).

10.3389/fpls.2022.995810

TABLE 1 Differentially abundant proteins in the "tyrosine metabolism" and "phenylalanine, tyrosine, and tryptophan biosynthesis" pathways.

Pathway	Protein ID	log_2FC	Swissprot description	Gene name
Tyrosine metabolism	CL2936.Contig5_All	3.7326	–	–
	CL2639.Contig2_All	2.7795	Aspartate aminotransferase	*aat2*
	Unigene7245_All	2.6020	Histidinol-phosphate aminotransferase	*HIS5*
	CL1387.Contig4_All	2.5615	Copper amine oxidase 1	*cao1*
	Unigene219_All	2.3641	Tyrosinase-like protein	*orsC*
	CL2879.Contig1_All	2.3046	–	–
	CL6592.Contig1_All	2.2886	Uncharacterized oxidoreductase	*SPAC26H5.09c*
	CL5670.Contig1_All	1.7234	Alcohol dehydrogenase	*adh-1*
	CL1960.Contig4_All	1.7060	–	–
	CL1605.Contig3_All	1.5051	Uncharacterized oxidoreductase	*SPAC26H5.09c*
	CL1960.Contig3_All	1.3695	–	–
	CL6346.Contig2_All	1.3095	Dehydrogenase	*FUM7*
	Unigene76_All	−1.1781	UPF0303 protein	*YBR137W*
	CL1387.Contig2_All	−1.1973	Copper amine oxidase 1	*YBR137W*
	CL4484.Contig2_All	−1.4209	UPF0303 protein	*YBR137W*
	CL8627.Contig1_All	−1.6618	Tyrosinase-like protein	*orsC*
Phyenylalanine, tyrosine and tryptophan biosynthesis	CL4340.Contig1_All	3.2800	Multifunctional tryptophan biosynthesis protein	*TRPC*
	CL7709.Contig1_All	2.8417	Tryptophan synthase	*TRP-1*
	CL2639.Contig2_All	2.7795	Aspartate aminotransferase	*aat2*
	Unigene7245_All	2.6020	Histidinol-phosphate aminotransferase	*HIS5*
	CL2975.Contig3_All	2.4172	Probable prephenate dehydrogenase	*tyr1*
	CL8380.Contig2_All	2.2679	Putative prephenate dehydratase	*pha2*
	CL753.Contig4_All	2.1225	Phospho-2-dehydro-3-deoxyheptonate aldolase	*aro-8*
	Unigene3893_All	1.9892	–	–
	CL7603.Contig2_All	1.9430	Phospho-2-dehydro-3-deoxyheptonate aldolase	*aro4*
	CL2975.Contig2_All	1.8930	Probable prephenate dehydrogenase	*tyr1*
	CL3419.Contig1_All	1.7061	Probable anthranilate synthase component 1	*trp3*
	CL5368.Contig1_All	1.6306	Pentafunctional AROM polypeptide	*LACBIDRAFT_233717*
	CL702.Contig1_All	1.6001	–	–
	Unigene3701_All	1.0130	Chorismate synthase	*SPCC1223.14*
	CL1983.Contig2_All	1.0079	Anthranilate phosphoribosyltransferase	*trp4*

Antibiotic synthesis

The associated number of DAPs/DEGs in the "biosynthesis of antibiotics" pathway was the greatest under dessication-stress by proteome–transcriptome-associated analysis. There were 135 DAPs enriched in this pathway, of which 117 DAPs were increased in abundance, and the fold-change value of more-abundant DAPs was much higher than that of the less-abundant value. The top 12 DAPs with $|\log_2FC| \geq 3$ were increased in abundance (**Table 3**). Two DAPs (CL711.Contig2_All and CL6373.Contig2_All) were involved in isopenicillin-N synthase and glutamate-5-semi aldehyde dehydrogenase, respectively, and could enhance the synthesis of penicillin, cephalosporins, or carbapenem (**Figure 6**). Other 132 DAPs could promote intermediate synthesis of penicillin, carbapenem, or cephalosporin. For example, fumarase (CL6387.Contig1_All) could catalyze the conversion of fumarate to malate (Nunes-Nesi et al., 2007), then malate is oxidized to oxoloacetate by NAD^+-dependent malate dehydrogenase (Nunes-Nesi, 2005). Oxoloacetate facilitates the synthesis of cysteine, and L-cysteine is the precursor for penicillin and cephalosporin synthesis in the "penicillin and cephalosporin biosynthesis" pathway.

Cytoskeleton

The fruiting bodies of *A. fibrillifera* shrank and became hard under dessication-stress, whereas they recovered rapidly after rehydration (**Figure 1A**). Long-lived cytoskeleton structure may be an epigenetic regulator of cellular function and fate (Fletcher and Mullins, 2010). A total of 28 (27 more-abundant and one less-abundant) DAPs were associated with cytoskeleton under dessication and rehydration conditions, and the fold-change of more-abundant proteins was much higher than that of less-abundant proteins (**Figure 7**). These DAPs usually had high fold-change, among which the $|\log_2FC|$ value of 16 proteins was ≥ 2.

TABLE 2 Differentially abundant proteins in "folate biosynthesis" and "biotin metabolism" pathways.

Pathway	Protein ID	log_2FC	Swissprot description	Gene name
Folate biosynthesis	CL3176.Contig2_All	3.6059	Short chain dehydrogenase	*yanD*
	CL112.Contig1_All	2.8412	Folylpolyglutamate synthase	*MET7*
	CL7813.Contig2_All	2.0205	–	–
	CL4756.Contig1_All	1.7722	Uracil-regulated protein 1	*urg1*
	CL7253.Contig3_All	1.2942	–	–
	CL8178.Contig1_All	1.0659	Probable dihydrofolate synthetase	*fol3*
	Unigene10797_All	−1.3183	–	–
	CL5565.Contig2_All	−1.7700	Uncharacterized protein	*SPAC57A10.07*
	CL1254.Contig1_All	−1.9403	Repressible alkaline phosphatase	*PHO8*
	CL1254.Contig2_All	−2.1234	Repressible alkaline phosphatase	*PHO8*
Biotin metabolism	CL4671.Contig1_All	4.5140	Uncharacterized oxidoreductase	*SPBC30D10.05c*
	CL1463.Contig1_All	3.9789	Uncharacterized oxidoreductase	*SPAC4H3.08*
	CL3919.Contig4_All	2.9139	Uncharacterized oxidoreductase	*SPBC30D10.05c*
	Unigene347_All	2.7646	Uncharacterized oxidoreductase	*SPCC663.06c*
	CL8130.Contig2_All	2.6830	Biotin–protein ligase	*bpl1*
	CL1463.Contig2_All	2.6794	Uncharacterized oxidoreductase	*SPAC4H3.08*
	CL2219.Contig1_All	2.4481	Short chain dehydrogenase	*citE*
	CL5550.Contig1_All	1.9873	Probable NADP-dependent mannitol dehydrogenase	*YALI0B16192g*
	CL3784.Contig3_All	1.6988	Versicolorin reductase	*stcU*
	CL5385.Contig4_All	1.6626	Uncharacterized oxidoreductase	*SPAC4H3.08*
	CL4968.Contig1_All	1.5692	Trihydroxynaphthalene reductase	*THR1*
	CL3093.Contig2_All	1.4250	Uncharacterized oxidoreductase	*SPAC4H3.08*
	CL8130.Contig3_All	1.4111	Biotin–protein ligase	*bpl1*

CL4846.Contig5_All (Log_2FC = 3.87) and CL8973.Contig5_All (Log_2FC = 3.55) had the highest fold differences, which play roles in microtubule-related proteins and tubulin alpha chain, respectively (**Figure 7**). The functions of other significantly more-abundant DAPs were mainly concentrated in actin, tubulin, fimbrin, and cofilin. Fimbrin and cofilin bind to actin to function. The number of DAPs decreased rapidly after rehydration. The DAP (Unigene22219_All) with the highest fold-change (Log_2FC = 2.02) was also related to actin (**Figure 7**).

Discussion

Proteomics technology is a tool for the comprehensive identification of plant proteins related to drought resistance (Gupta et al., 2020; Qiu et al., 2021). Proteome research has been successfully applied in drought-resistant crops, such as cucumber (Du et al., 2019), corn (Liu et al., 2019), and cassava (Zhao et al., 2015). The strategies of plants to deal with drought stress usually include osmotic regulation, antioxidant capacity, and dehydration tolerance (Zhang, 2007). Similar results were obtained in this experiment. In PPI cluster 1, the DAPs with stronger interactions were concentrated mainly in the above functions. In addition, the DAPs with high fold-change, such as CL4047.Contig1_All (Log_2FC = 5.02), CL1516.Contig1_All (Log_2FC = 4.93), CL7279.Contig1_All (Log_2FC = 4.57), and Unigene10667_All (Log_2FC = 4.50) were mainly related to antioxidant mechanisms and heat shock proteins in response to dessication-stress. Meanwhile, the excellent dessication tolerance of *A. fibrillifera* might be caused by secondary metabolites (melanin, antibiotics, and vitamins).

Melanin response to dessication-stress

Melanin protects dark-pigmented fungi from environmental stresses (Brunskole et al., 2009; Li et al., 2019). Plants highly pigmented are more resistant to biotic and abiotic stresses (Carletti et al., 2014). Melanin has a variety of functions, structures, and forms, which can resist a variety of abiotic factors (Cordero and Casadevall, 2020). Melanin compounds are endowed with excellent photoprotective properties and antioxidative activity (Liberti et al., 2020). Melanin has both free radical scavenging and antioxidant activities. The melanin of *Aureobasidium melanogenum* XJ5-1 in the Taklimakan Desert plays a vital role in the adaptation of yeasts to drought stress (Jiang et al., 2018). Here, the

TABLE 3 Highly differentially abundant proteins in the "biosynthesis of antibiotic" pathway.

Protein ID	log_2FC	Swissprot description
CL4671.Contig1_All	4.5140	Uncharacterized oxidoreductase
CL1006.Contig5_All	4.3139	AB hydrolase superfamily protein
CL1463.Contig1_All	3.9789	Uncharacterized oxidoreductase
CL5160.Contig2_All	3.7181	3-ketoacyl-CoA thiolase
CL3888.Contig1_All	3.5051	Uncharacterized protein
CL1870.Contig3_All	3.4639	Phosphoglucomutase
Unigene388_All	3.4583	Branched-chain-amino-acid aminotransferase
Unigene385_All	3.4537	3-ketoacyl-CoA thiolase
CL1155.Contig1_All	3.4053	Probable aldose 1-epimerase
CL4340.Contig1_All	3.2800	Multifunctional tryptophan biosynthesis protein
CL6387.Contig1_All	3.1756	Fumarate hydratase
Unigene17153_All	3.0785	Uncharacterized oxidoreductase

"phenylalanine, tyrosine and tryptophan biosynthesis" pathway was significantly enriched. TRP3 in this pathway played a central role and had the strongest interaction with other proteins in the PPI analysis. Physiological data showed that the level of melanin increased more than 10-fold under dessication-stress. Tyrosine is the precursor of melanin formation (Gómez and Nosanchuk, 2003; Micillo et al., 2016). In the "tyrosine metabolism" pathway, the melanin-related protein Unigene219_All (Log_2FC = 2.36) was significantly increased in abundance too. Under dessication-stress, the DAPs involved in melanin synthesis were significantly increased in abundance, and the melanin content was significantly increased. Proteome data were consistent with the above melanin content. Therefore, specific melanin should contribute to high desiccation tolerance because of its antioxidant and free-radical-scavenging activities in *A. fibrillifera*.

Vitamin response to dessication-stress

Folate plays a crucial role in overcoming drought-stress during plant development. The foliar application of folate was found to be suitable for drought stress alleviation in *Coriandrum sativum* L. (Khan et al., 2022). In addition, folates are necessary for the biosynthesis of lignin (Hanson and Gregory, 2011). In this experiment, "folate biosynthesis" and "biotin metabolism" pathways were significantly enriched under dessication-stress. The "folate biosynthesis" pathway was enriched by both transcriptomic and proteomic analysis. The DAP CL112.Contig1_All in this pathway played a role in folylpolyglutamate synthase. This enzyme was very important for maintaining folate homeostasis (Strobbe and Van Der Straeten, 2017). The folate content increased significantly under dessication-stress, whereas it decreased significantly after rehydration. Therefore, folate was the most sensitive to both drought stress and rehydration, and may have a close relation to drought tolerance in *A. fibrillifera*.

Biotin not only plays a key role in immune regulation in animals but also in the response of plants to various abiotic stresses. Biotin enhances the resistance of *Arabidopsis* to carbonate stress (Wang et al., 2020). Biotin synthetases and biotin attachment domain containing protein were identified in the root tip of soybean, indicating that biotin and biotinylation were involved in glucose metabolism under drought stress (Wang et al., 2016). In this work, the DAPs and their associated DEGs were up-regulated in the "biotin metabolic" pathway. The significant abundance increase of biotin-related DAPs might supply energy sources to *A. fibrillifera* under dessication-stress.

Antibiotics involved in dessication tolerance

Antibiotics are a group of secondary metabolites generated by microorganisms or higher organisms in life processes (Mohr, 2016). "Biosynthesis of antibiotics" pathways were significantly enriched in six wheat genotypes under drought stress (Rasool et al., 2022). The enhancement of pyrimidine nucleoside antibiotics can alleviate abiotic stress in *Nicotiana tabacum* (Song et al., 2022). Penicillins and cephalosporins are the most important classes of β-lactam antibiotics. In this experiment, antibiotic-related DAPs were highly increased in abundance, including fumarate hydratase (FH) (CL6387.Contig1_All), isopenicillin-N synthase (IPNS) (CL711.Contig2_All), and glutamate-5-semialdehyde dehydrogenase (CL6373.Contig2_All), which are beneficial to the synthesis of β-lactam antibiotics. FH facilitates the synthesis of cysteine, which is the precursor for penicillin and cephalosporin synthesis. IPNS can catalyze the specific reaction of L-δ-(α-aminoadipoyl)-L-cysteinyl-D-valine with dioxygen giving isopenicillin-N, a precursor of cephalosporins and penicillins (Rabe et al., 2021). The significant abundance increase of these DAPs under dessication-stress is beneficial to the accumulation of penicillin and cephalosporin in *A. fibrillifera*. In the "carbapenem biosynthesis" pathway, glutamate-5-semialdehyde dehydrogenase-related DAP was significantly increased in abundance and might be beneficial to the synthesis of carbapenem. In transcriptome-proteome-association analysis, many DEGs/DAPs were enriched in the "biosynthesis of antibiotics" pathway, which could be beneficial to dessication tolerance in *A. fibrillifera*.

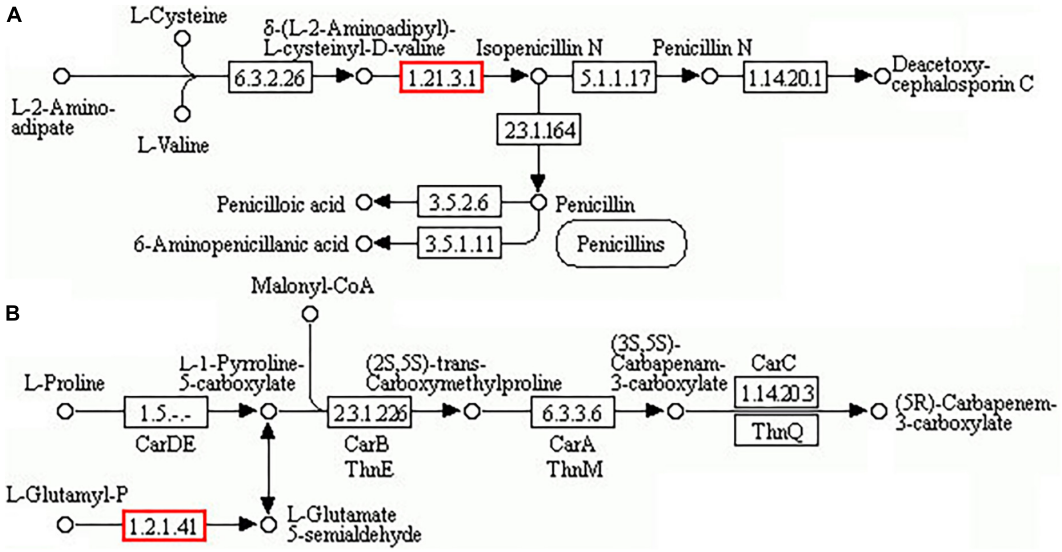


FIGURE 6
"Biosynthesis of antibiotics" pathway. **(A)** Biosynthesis of penicillin and cephalosporin. **(B)** Carbapenem biosynthesis.

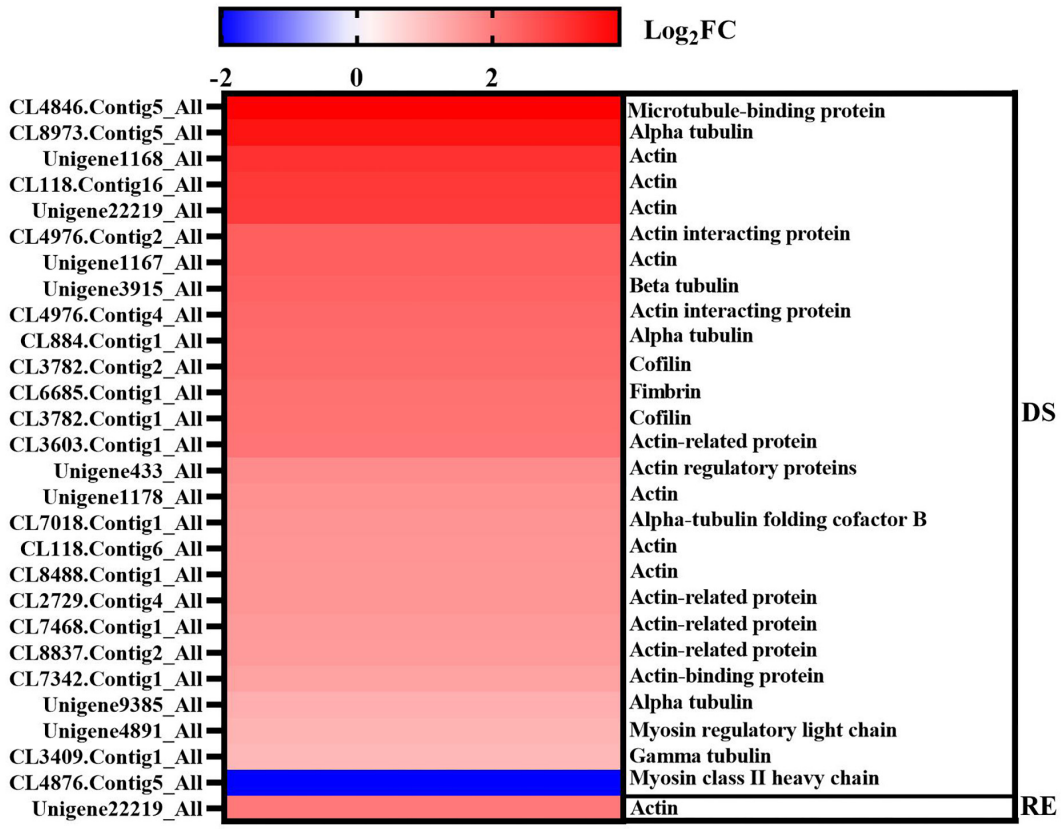


FIGURE 7
Differentially abundant proteins related to the cytoskeleton under dessication and rehydration. The left and right Y axes represent the protein ID and functional annotation, and DS and RE represent dessication-stress and rehydration, respectively.

Cytoskeleton response to dessication-stress

The cytoskeleton is the main mechanical structure of cells; it is a complex and dynamic biopolymer network composed of microtubules, actin, and intermediate filaments (Pegoraro et al., 2017). The plant cytoskeleton is associated with plant stress responses, such as drought, salt, and cold (Chun et al., 2021). A balance in the metabolism of cell wall component biosynthesis and cytoskeleton homeostasis can affect the response of cotton fibers to drought stress (Zheng et al., 2014). The microtubule cytoskeleton functions as a sensor for stress response signaling in plants and maintains mechanical stability by forming bundles (Ma and Liu, 2019). Furthermore, actin filaments may control drought-induced signal perception and are involved in regulating the accumulation of *HVA1* (a dehydrin-encoding gene) transcripts in barley leaves exposed to drought stress (Śniegowska-Świerk et al., 2016). In this experiment, the fruiting bodies of *A. fibrillifera* shrink under dessication-stress. A total of 28 DAPs were associated with the cytoskeleton under dessication-stress and rehydration conditions, and the fold-change of more-abundant proteins was much higher than that of less-abundant proteins (**Figure 7**). The functions of significantly more-abundant DAPs were mainly concentrated in actin, tubulin, fimbrin, and cofilin. Fimbrin and cofilin bind to actin to function. The number of DAPs decreased rapidly after rehydration. The DAP (Unigene22219_All) with the highest fold-change was also related to actin. After rehydration, the fruiting bodies could quickly absorb water and return to the control level, which might be related to the rapid assembly or disassembly of actin. Therefore, the DAPs related to the cytoskeleton might be helpful in adaptation to dessication tolerance and the shape changes of fruiting bodies.

Conclusion

The levels of melanin, amino acids, folate, and biotin in fruiting bodies increased significantly under dessication-stress compared with those of the controls. Folate showed a sensitive response to both dessication-stress and rehydration. In total, 1,572 DAPs were identified under dessication-stress. The number of DAPs decreased rapidly after rehydration. Under dessication-stress, many DAPs were annotated in "amino acid metabolism," "carbohydrate metabolism," "folate biosynthesis," "biotin metabolism," "biosynthesis of antibiotics," and "transport and catabolism" pathways. Proteome–transcriptome association analysis revealed that "biosynthesis of antibiotics," "folate biosynthesis," "biotin metabolism," "phenylalanine, tyrosine, and tryptophan biosynthesis" pathways were significantly enriched in response to dessication-stress. The DAPs in these pathways were beneficial to the synthesis of antibiotics, folate, biotin, and melanin, and played important roles in enhancing the dessication tolerance of *A. fibrillifera*. The findings of transcriptome and physiological analyses were in good agreement with the proteomic data. Some molecular pathways and mechanisms of dessication response are similar between *A. fibrillifera* and plant species. This work may shed light on the mechanism of dessication tolerance and provide a novel framework for the breeding and cultivation of *Auricularia* and crops.

Data availability statement

The data presented in this study are deposited in the ProteomeXchange repository, accession number PXD033449.

Author contributions

SZ and GG designed the experiments. HG, XX, YW, and HT were performed material preparation, data collection, and analysis. HG, XX, YW, HT, SZ, and GG wrote the manuscript. All authors have read and approved the final manuscript.

Funding

This study was financially supported by the Science and Technology Program of Guizhou Province [(2022)050].

Acknowledgments

We thank International Science Editing (http//www.internationalscienceediting.com) for editing this manuscript.

Conflict of interest

The authors declare that the research was conducted in the absence of any commercial or financial relationships that could be construed as a potential conflict of interest.

Publisher's note

All claims expressed in this article are solely those of the authors and do not necessarily represent those of their affiliated organizations, or those of the publisher, the editors and the reviewers. Any product that may be evaluated in this article, or claim that may be made by its manufacturer, is not guaranteed or endorsed by the publisher.

Supplementary material

The Supplementary Material for this article can be found online at: https://www.frontiersin.org/articles/10.3389/fpls.2022.995810/full#supplementary-material

SUPPLEMENTARY FIGURE 1
Heatmap of sample correlation analysis. Both X and Y axes represent samples. The color denotes the correlation coefficient. CK1, CK2, DS, and RE represent the parallel control of desiccation-stress, parallel control of rehydration, desiccation-stress, and rehydration process, respectively. "−1," "−2," and "−3" indicate three biological replicates.

References

Ahuja, I., de-Vos, R. C., Bones, A. M., and Hall, R. D. (2010). Plant molecular stress responses face climate change. *Trends Plant Sci.* 15, 664–674.

Ariyarathne, M. A., and Wone, B. W. M. (2022). Overexpression of the *Selaginella lepidophylla* bHLH transcription factor enhances water-use efficiency, growth, and development in *Arabidopsis*. *Plant Sci.* 315:111129. doi: 10.1016/j.plantsci.2021.111129

Basset, G. J. C., Quinlivan, E. P., Gregory, J. F., and Hanson, A. D. (2005). Folate synthesis and metabolism in plants and prospects for biofortification. *Crop Sci.* 45, 449–453. doi: 10.2135/cropsci2005.0449

Bernhardt, O., Selevsek, N., Gillet, L., Rinner, O., and Reiter, L. (2014). "Spectronaut: A fast and efficient algorithm for MRM-like processing of data independent acquisition (SWATH-MS) data," in *Proceedings of the 60th American Society for Mass Spectrometry Conference*, Vancouver.

Bruderer, R., Bernhardt, O. M., Gandhi, T., Miladinović, S. M., Cheng, L. Y., Messner, S., et al. (2015). Extending the limits of quantitative proteome profiling with data-independent acquisition and application to acetaminophen-treated three-dimensional liver microtissues. *Mol. Cell. Proteomics* 14, 1400–1410. doi: 10.1074/mcp.m114.044305

Brunskole, M., Zorko, K., Kerbler, V., Martens, S., Stojan, J., Gobec, S., et al. (2009). Trihydroxynaphthalene reductase of *Curvularia lunata*—a target for flavonoid action? *Chem. Biol. Interact.* 178, 259–267. doi: 10.1016/j.cbi.2008.10.023

Burmasova, M. A., Utebaeva, A. A., Sysoeva, E. V., and Sysoeva, M. A. (2019). Melanins of *Inonotus obliquus*: Bifidogenic and antioxidant properties. *Biomolecules* 9:248. doi: 10.3390/biom9060248

Cao, W., Zhou, X., McCallum, N. C., Hu, Z., Ni, Q. Z., Kapoor, U., et al. (2021). Unraveling the structure and function of melanin through synthesis. *J. Am. Chem. Soc.* 143, 2622–2637. doi: 10.1021/jacs.0c12322

Carletti, G., Nervo, G., and Cattivelli, L. (2014). Flavonoids and melanins: A common strategy across two kingdoms. *Int. J. Biol. Sci.* 10, 1159–1170. doi: 10.7150/ijbs.9672

Caruso, G., Cavaliere, C., Foglia, P., Gubbiotti, R., Samperi, R., and Laganà, A. (2009). Analysis of drought responsive proteins in wheat (*Triticum durum*) by 2D-PAGE and MALDI-TOF mass spectrometry. *Plant Sci.* 177, 570–576. doi: 10.1016/j.plantsci.2009.08.007

Choi, M., Chang, C. Y., Clough, T., Broudy, D., Killeen, T., MacLean, B., et al. (2014). MSstats: An R package for statistical analysis of quantitative mass spectrometry-based proteomic experiments. *Bioinformatics* 30, 2524–2526. doi: 10.1093/bioinformatics/btu305

Chun, H. J., Baek, D., Jin, B. J., Cho, H. M., Park, M. S., Lee, S. H., et al. (2021). Microtubule dynamics plays a vital role in plant adaptation and tolerance to salt stress. *Int. J. Mol. Sci.* 22:5957. doi: 10.3390/ijms22115957

Cordero, R. J. B., and Casadevall, A. (2020). Melanin. *Curr. Biol.* 30, R142–R143. doi: 10.1016/j.cub.2019.12.042

Du, C., Chai, L., Wang, Z., and Fan, H. (2019). Response of proteome and morphological structure to short-term drought and subsequent recovery in *Cucumis sativus* leaves. *Physiol. Plant.* 167, 676–689. doi: 10.1111/ppl.12926

Fletcher, D. A., and Mullins, R. D. (2010). Cell mechanics and the cytoskeleton. *Nature* 463, 485–492. doi: 10.1038/nature08908

Glagoleva, A. Y., Shoeva, O. Y., and Khlestkina, E. K. (2020). Melanin pigment in plants: Current knowledge and future perspectives. *Front. Plant Sci.* 11:770. doi: 10.3389/fpls.2020.00770

Gómez, B. L., and Nosanchuk, J. D. (2003). Melanin and fungi. *Curr. Opin. Infect. Dis.* 16, 91–96. doi: 10.1097/01.aco.0000065076.06965.04

Gupta, S., Mishra, S. K., Misra, S., Pandey, V., Agrawal, L., Nautiyal, C. S., et al. (2020). Revealing the complexity of protein abundance in chickpea root under drought-stress using a comparative proteomics approach. *Plant Physiol. Biochem.* 151, 88–102. doi: 10.1016/j.plaphy.2020.03.005

Hanson, A. D., and Gregory, J. F. (2011). Folate biosynthesis, turnover, and transport in plants. *Annu. Rev. Plant Biol.* 62, 105–125. doi: 10.1146/annurev-arplant-042110-103819

Hsiao, T. C. (1973). Plant responses to water stress. *Annu. Rev. Plant Physiol.* 24, 519–570. doi: 10.1146/annurev.pp.24.060173.002511

Isaacson, T., Damasceno, C. M. B., Saravanan, R. S., He, Y. H., Catalá, C., Saladié, M., et al. (2006). Sample extraction techniques for enhanced proteomic analysis of plant tissues. *Nat. Protoc.* 1, 769–774. doi: 10.1038/nprot.2006.102

Jiang, H., Liu, G. L., Chi, Z., Hu, Z., and Chi, Z. M. (2018). Genetics of trehalose biosynthesis in desert-derived *Aureobasidium melanogenum* and role of trehalose in the adaptation of the yeast to extreme environments. *Curr. Genet.* 64, 479–491. doi: 10.1007/s00294-017-0762-z

Khan, M. N., and Komatsu, S. (2016). Proteomic analysis of soybean root including hypocotyl during recovery from drought stress. *J. Proteom.* 144, 39–50. doi: 10.1016/j.jprot.2016.06.006

Khan, M. T., Ahmed, S., and Shah, A. A. (2022). Regulatory role of folic acid in biomass production and physiological activities of *Coriandrum sativum* L. under irrigation regimes. *Int. J. Phytoremediation* 24, 1025–1038. doi: 10.1080/15226514.2021.1993785

Koh, J., Chen, G., Yoo, M. J., Zhu, N., Dufresne, D., Erickson, J. E., et al. (2015). Comparative proteomic analysis of *Brassica napus* in response to drought stress. *J. Proteome Res.* 14, 3068–3081. doi: 10.1021/pr501323d

Lazar, N., Fay, A., Nandakumar, M., Boyle, K. E., Xavier, J., Rhee, K., et al. (2017). Control of biotin biosynthesis in mycobacteria by a pyruvate carboxylase dependent metabolic signal. *Mol. Microbiol.* 106, 1018–1031. doi: 10.1111/mmi.13865

Lesk, C., Rowhani, P., and Ramankutty, N. (2016). Influence of extreme weather disasters on global crop production. *Nature* 529, 84–87. doi: 10.1038/nature16467

Li, J. J., Zhou, L., Yin, C. M., Zhang, D. D., Klosterman, S. J., Wang, B. L., et al. (2019). The *Verticillium dahliae* Sho1-MAPK pathway regulates melanin biosynthesis and is required for cotton infection. *Environ. Microbiol.* 21, 4852–4874. doi: 10.1111/1462-2920.14846

Liberti, D., Alfieri, M. L., Monti, D. M., Panzella, L., and Napolitano, A. (2020). A melanin-related phenolic polymer with potent photoprotective and antioxidant activities for dermo-cosmetic applications. *Antioxidants* 9:270. doi: 10.3390/antiox9040270

Liu, S., Zenda, T., Dong, A., Yang, Y., Liu, X., Wang, Y., et al. (2019). Comparative proteomic and morpho-physiological analyses of maize wild-type vp16 and mutant vp16 germinating seed responses to peg-induced drought stress. *Int. J. Mol. Sci.* 20, 1–24. doi: 10.3390/ijms20225586

Livak, K. J., and Schmittgen, T. D. (2001). Analysis of relative gene expression data using real-time quantitative PCR and the $2^{\Delta}\Delta^{CT}$ method. *Methods* 25, 402–408. doi: 10.1006/meth.2001.1262

Ma, H., and Liu, M. (2019). The microtubule cytoskeleton acts as a sensor for stress response signaling in plants. *Mol. Biol. Rep.* 46, 5603–5608. doi: 10.1007/s11033-019-04872-x

Ma, H., Xu, X., and Feng, L. (2014). Responses of antioxidant defenses and membrane damage to drought stress in fruit bodies of *Auricularia auricula-judae*. *World J. Microbiol. Biotechnol.* 30, 119–124. doi: 10.1007/s11274-013-1416-z

Mahmood, T., Khalid, S., Abdullah, M., Ahmed, Z., Shah, M. K. N., Ghafoor, A., et al. (2019). Insights into drought stress signaling in plants and the molecular genetic basis of cotton drought tolerance. *Cells* 9:105. doi: 10.3390/cells9010105

Maier, T., Güell, M., and Serrano, L. (2009). Correlation of mRNA and protein in complex biological samples. *FEBS Lett.* 583, 3966–3973. doi: 10.1016/j.febslet.2009.10.036

Micillo, R., Panzella, L., Koike, K., Monfrecola, G., Napolitano, A., and d'Ischia, M. (2016). "Fifty shades" of black and red or how carboxyl groups fine tune

eumelanin and pheomelanin properties. *Int. J. Mol. Sci.* 17, 1–13. doi: 10.3390/ijms17050746

Mohr, K. I. (2016). History of antibiotics research. *Curr. Top. Microbiol. Immunol.* 398, 237–272. doi: 10.1007/82_2016_499

Nunes-Nesi, A. (2005). Enhanced photosynthetic performance and growth as a consequence of decreasing mitochondrial malate dehydrogenase activity in transgenic tomato plants. *Plant Physiol.* 137, 611–622. doi: 10.1104/pp.104.055566

Nunes-Nesi, A., Carrari, F., Gibon, Y., Sulpice, R., Lytovchenko, A., Fisahn, J., et al. (2007). Deficiency of mitochondrial fumarase activity in tomato plants impairs photosynthesis via an effect on stomatal function. *Plant J.* 50, 1093–1106. doi: 10.1111/j.1365-313x.2007.03115.x

Pampurova, S., and Van Dijck, P. (2014). The desiccation tolerant secrets of *Selaginella lepidophylla*: What we have learned so far? *Plant Physiol. Biochem.* 80, 285–290. doi: 10.1016/j.plaphy.2014.04.015

Pegoraro, A. F., Janmey, P., and Weitz, D. A. (2017). Mechanical properties of the cytoskeleton and cells. *Cold Spring Harb. Perspect. Biol.* 9:a022038. doi: 10.1101/cshperspect.a022038

Qiu, C., Sun, J. H., Shen, J. Z., Zhang, S. N., Ding, Y. Q., Gai, Z. S., et al. (2021). Fulvic acid enhances drought resistance in tea plants by regulating the starch and sucrose metabolism and certain secondary metabolism. *J. Proteom.* 247:104337. doi: 10.1016/j.jprot.2021.104337

Rabe, P., Kamps, J. J. A. G., Sutherlin, K. D., Linyard, J. D. S., Aller, P., Pham, C. C., et al. (2021). X-ray free-electron laser studies reveal correlated motion during isopenicillin *N* synthase catalysis. *Sci. Adv.* 7:eabh0250. doi: 10.1126/sciadv.abh0250

Rasool, F., Khan, M. R., Schneider, M., Uzair, M., Aqeel, M., Ajmal, W., et al. (2022). Transcriptome unveiled the gene expression patterns of root architecture in drought-tolerant and sensitive wheat genotypes. *Plant Physiol. Biochem.* 178, 20–30. doi: 10.1016/j.plaphy.2022.02.025

Salekdeh, G. H., Siopongco, J., Wade, L. J., Ghareyazie, B., and Bennett, J. (2002). Proteomic analysis of rice leaves during drought stress and recovery. *Proteomics* 2, 1131–1145.

Sekara, A., Kalisz, A., Grabowska, A., and Siwulski, M. (2015). Auricularia spp. - mushrooms as novel food and therapeutic agents - a review. *Sydowia* 67, 1–10. doi: 10.12905/0380.sydowia67-2015-001

Śniegowska-Świerk, K., Dubas, E., and Rapacz, M. (2016). Actin microfilaments are involved in the regulation of *HVA1* transcript accumulation in drought-treated barley leaves. *J. Plant Physiol.* 193, 22–25. doi: 10.1016/j.jplph.2016.02.006

Song, Z., Wang, P., Chen, X., Peng, Y., Cai, B., Song, J., et al. (2022). Melatonin alleviates cadmium toxicity and abiotic stress by promoting glandular trichome development and antioxidant capacity in *Nicotiana tabacum*. *Ecotoxicol. Environ. Saf.* 236:113437. doi: 10.1016/j.ecoenv.2022.113437

Strobbe, S., and Van Der Straeten, D. (2017). Folate biofortification in food crops. *Curr. Opin. Biotechnol.* 44, 202–211. doi: 10.1016/j.copbio.2016.12.003

Tsou, C. C., Avtonomov, D., Larsen, B., Tucholska, M., Choi, H., Gingras, A. C., et al. (2015). DIA-Umpire: Comprehensive computational framework for data-independent acquisition proteomics. *Nat. Methods* 12, 258–264. doi: 10.1038/nmeth.3255

Wang, N., Zhao, J., He, X., Sun, H., Zhang, G., and Wu, F. (2015). Comparative proteomic analysis of drought tolerance in the two contrasting Tibetan wild genotypes and cultivated genotype. *BMC Genomics* 16:432. doi: 10.1186/s12864-015-1657-3

Wang, X., Oh, M., Sakata, K., and Komatsu, S. (2016). Gel-free/label-free proteomic analysis of root tip of soybean over time under flooding and drought stresses. *J. Proteomics* 130, 42–55. doi: 10.1016/j.jprot.2015.09.007

Wang, Y., Wang, M., Ye, X., Liu, H., Takano, T., Tsugama, D., et al. (2020). Biotin plays an important role in *Arabidopsis thaliana* seedlings under carbonate stress. *Plant Sci.* 300:110639. doi: 10.1016/j.plantsci.2020.110639

Wang, Y., Yang, Z., Shi, L., Yang, R., Guo, H., Zhang, S., et al. (2022). Transcriptome analysis of *Auricularia fibrillifera* fruit-body responses to drought stress and rehydration. *BMC Genomics* 23:58. doi: 10.1186/s12864-021-08284-9

Yuan, Y., Wu, F., Si, J., Zhao, Y. F., and Dai, Y. C. (2019). Whole genome sequence of *Auricularia heimuer* (Basidiomycota, Fungi), the third most important cultivated mushroom worldwide. *Genomics* 111, 50–58. doi: 10.1016/j.ygeno.2017.12.013

Zandalinas, S. I., Mittler, R., Balfagón, D., Arbona, V., and Gómez-Cadenas, A. (2018). Plant adaptations to the combination of drought and high temperatures. *Physiol. Plant* 162, 2–12. doi: 10.1111/ppl.12540

Zhang, Q. (2007). Strategies for developing green super rice. *Proc. Natl. Acad. Sci. U.S.A.* 104, 16402–16409. doi: 10.1073/pnas.0708013104

Zhao, P., Liu, P., Shao, J., Li, C., Wang, B., Guo, X., et al. (2015). Analysis of different strategies adapted by two cassava cultivars in response to drought stress: Ensuring survival or continuing growth. *J. Exp. Bot.* 66, 1477–1488. doi: 10.1093/jxb/eru507

Zhao, Y., Wang, L., Zhang, D., Li, R., Cheng, T., Zhang, Y., et al. (2019). Comparative transcriptome analysis reveals relationship of three major domesticated varieties of *Auricularia auricula*-judae. *Sci. Rep.* 9:78. doi: 10.1038/s41598-018-36984-y

Zheng, M., Meng, Y., Yang, C., Zhou, Z., Wang, Y., and Chen, B. (2014). Protein expression changes during cotton fiber elongation in response to drought stress and recovery. *Proteomics* 14, 1776–1795. doi: 10.1002/pmic.201300123

frontiers | Frontiers in Plant Science

TYPE Review
PUBLISHED 06 October 2022
DOI 10.3389/fpls.2022.1015317

Check for updates

OPEN ACCESS

EDITED BY
Muhammad Waseem,
Hainan University, China

REVIEWED BY
Shah Fahad,
The University of Haripur, Pakistan
Md. Rafiqul Islam,
Bangabandhu Sheikh Mujibur Rahman Agricultural University, Bangladesh

*CORRESPONDENCE
Qingquan Han
han_qing_quan@126.com
Sheng Zhang
shengzhang@scu.edu.cn

SPECIALTY SECTION
This article was submitted to Plant Abiotic Stress, a section of the journal Frontiers in Plant Science

RECEIVED 09 August 2022
ACCEPTED 20 September 2022
PUBLISHED 06 October 2022

CITATION
Yang L, Xia L, Zeng Y, Han Q and Zhang S (2022) Grafting enhances plants drought resistance: Current understanding, mechanisms, and future perspectives.
Front. Plant Sci. 13:1015317.
doi: 10.3389/fpls.2022.1015317

COPYRIGHT
© 2022 Yang, Xia, Zeng, Han and Zhang. This is an open-access article distributed under the terms of the Creative Commons Attribution License (CC BY). The use, distribution or reproduction in other forums is permitted, provided the original author(s) and the copyright owner(s) are credited and that the original publication in this journal is cited, in accordance with accepted academic practice. No use, distribution or reproduction is permitted which does not comply with these terms.

Grafting enhances plants drought resistance: Current understanding, mechanisms, and future perspectives

Le Yang[1], Linchao Xia[1], Yi Zeng[1], Qingquan Han[1,2]* and Sheng Zhang[1]*

[1]Key Laboratory of Bio-Resource and Eco-Environment of Ministry of Education, College of Life Sciences, Sichuan University, Chengdu, China, [2]The Engineering Research Institute of Agriculture and Forestry, Ludong University, Yantai, China

Drought, one of the most severe and complex abiotic stresses, is increasingly occurring due to global climate change and adversely affects plant growth and yield. Grafting is a proven and effective tool to enhance plant drought resistance ability by regulating their physiological and molecular processes. In this review, we have summarized the current understanding, mechanisms, and perspectives of the drought stress resistance of grafted plants. Plants resist drought through adaptive changes in their root, stem, and leaf morphology and structure, stomatal closure modulation to reduce transpiration, activating osmoregulation, enhancing antioxidant systems, and regulating phytohormones and gene expression changes. Additionally, the mRNAs, miRNAs and peptides crossing the grafted healing sites also confer drought resistance. However, the interaction between phytohormones, establishment of the scion-rootstock communication through genetic materials to enhance drought resistance is becoming a hot research topic. Therefore, our review provides not only physiological evidences for selecting drought-resistant rootstocks or scions, but also a clear understanding of the potential molecular effects to enhance drought resistance using grafted plants.

KEYWORDS

scion, rootstock, drought tolerance, phytohormones, miRNA

Introduction

Water is essential for the growth and development of plants, and it accounts for 70%-90% of the plant's fresh weight. With global climate change, arid and semi-arid areas are accounting for ~40% of global land area and will cross over 50% by the end of the 21st century (Huang et al., 2015). This will cause a severe water shortage for plants in this area,

resulting in a series of morphological, physiological, and molecular changes in them (Ahmed et al., 2009; Liu et al., 2014; Kumar et al., 2017). For example, drought reduces the plant cell's water potential, transpiration rate, turgor pressure, and photosynthetic rate, while increasing their reactive oxygen species (ROS) accumulation, which causes poor plant growth, early flowering, and ultimately plant yield losses (Alan et al., 2007; Kumar et al., 2017; Chaimala et al., 2020; Gupta et al., 2020; Zia et al., 2021). According to the past decade's data, drought caused global crop yield losses of ~$30 billion (Gupta et al., 2020). With the rapid growth of global population and moderate increase in global arable land, water demand for crop growth could double by 2050, whereas the available freshwater is predicted to drop by 50% due to climate change (Gupta et al., 2020). Under such conditions, as plants are stationary, it is crucial to cultivate plants that can adapt to the arid environment and maintain their normal yield and growth. Additionally, using artificial methods (*e.g.*, drought hardening, directive breeding, and exogenous application of plant growth regulators) can also improve plant drought resistance (Farooq et al., 2009; Tesfahun and Yildiz, 2018). Interestingly, grafting has shown promise in improving plant drought resistance through the use of drought-resistant plant materials.

Grafting is a type of asexual propagation method that connects the budding stem segment of one plant (scion) to that of another plant containing roots (rootstock), to allow them to grow together. It is widely used in commercial fruit and vegetable cultivation, landscaping, and for verifying molecular movement in plants (Fullana-Pericàs et al., 2018; Li et al., 2020). Moreover, it can promote the growth and development of the grafted plants, maintain the excellent properties of the parents, change their branch structure, increase plant yield, positively influence fruit flavor, improve nutritional value, and enhance abiotic stress resistance (Sánchez-Rodríguez et al., 2014; Melnyk and Meyerowitz, 2015; Thomas and Frank, 2019; Ellenberger et al., 2021). Unfortunately, grafting cannot be applied to all plants, as it is determined by grafting compatibility (Habibi et al., 2022). Grafting compatibility means the successful connection between the vascular and non-vascular systems at the grafted junction. Generally, the survival rate of intra-generic grafting is high, while that of inter-genera is low. Recently, studies on the physiological and molecular mechanisms of grafting junction have gradually become a new hotspot, like the key responsive genes in grafted healing sites (Melnyk et al., 2018; Notaguchi et al., 2020; Kurotani and Notaguchi, 2021; Thomas et al., 2021; Chambaud et al., 2022) and genetic information exchange between rootstocks and scions (Thomas and Frank, 2019; Yang et al., 2019; Cerruti et al., 2021; Okamoto et al., 2022).

Since drought greatly influences plant growth and development, it is essential to learn how to mitigate the negative effects through grafting (Zia et al., 2021). Grafting improves plant drought resistance (Ellialtioglu et al., 2019; Lopez-Serrano et al., 2019; Chen et al., 2020), which is primarily determined by the rootstock, despite the scion also affecting the grafted plant (Han et al., 2013; Han et al., 2019; Chen et al., 2020; Lopez-Hinojosa et al., 2021). Despite there being multiple studies and reviews on grafting and drought resistance, few have summarized how the molecular response of grafted plants is linked to their physiology and phenotype under drought stress. Therefore, this paper mainly summarizes the research to date on molecular mechanisms and physiological and morphological changes in grafted plants, while also listing the drought responsive genes and mobile molecules that generate drought resistance in grafted plants (Tables 1, 2).

Rootstock changes

The root is an important organ for water and nutrient uptake from the soil to support plant growth and development. Drought usually reduces root biomass, damages root system architecture (RSA) and decreases root hydraulic conductivity (Yang et al., 2021; Zia et al., 2021). As shown in Figure 1, drought-resistant grafted plants usually mitigate these effects by appropriately adjusting their roots.

Morphological changes of rootstock

Increased root biomass and root-shoot ratio confer great advantages to grafted plants under drought stress (Li et al., 2020). The grafted grapevine and pepper plants display enhanced drought resistance by maintaining high root biomass and water absorption and storage ability (Lopez-Serrano et al., 2019; Prinsi et al., 2021). The accumulation of carbohydrates and nitrogen which need transporter proteins to move to drought-resistant roots, on the one hand, is from detached leaves, and on the other hand, is from photosynthesis (Yildirim et al., 2018; Han et al., 2019). The bidirectional sugar transporter (SWEET14) and nitrate transporter 1/peptide transporter (NRT1/PTR), were two significantly accumulating proteins in drought-resistant grapevine rootstock 110R, which promoted the carbohydrates and nitrogen accumulation in roots (Chen et al., 2012; Yildirim et al., 2018; Ji et al., 2022). Although we believe that during drought stress, transporter proteins will accumulate in the grafted plants, the underlying regulated pathways need further investigation.

Besides accumulating greater root biomass, drought-resistant rootstocks display higher root plasticity and root vigor than drought-sensitive ones (Han et al., 2019; Silva et al., 2021). Maintaining the rapid growth and large roots under water stress is important for drought-resistant improvement (Li et al., 2020). By using the accumulated assimilate, the root system architecture (RSA) (*e.g.*, root length, root diameter, root area, and root volume) of drought-resistant grapevine rootstocks changes to better absorb the water and nutrients in deep soil,

TABLE 1 Grafting influences the expression of drought responsive genes.

Category	Gene name	Effects	Scion/Rootstock	Reference
Substance transport	*SWEET 14*	Up-regulated, transporting sugars, promoting the accumulation of carbohydrates in roots, and providing energy for root elongation and growth	(*Vitrus. vinifera*/(*V. rupestris* × *V. berlandieri*)	Yildirim et al., 2018
	NRT1/PTR	Up-regulated, transporting proteins, promoting nitrogen accumulated in roots and providing energy for root elongation and growth		
Osmoregulation	*P5SC*	Up-regulated, regulating proline biosynthesis and alleviating osmotic stress	(*P. persica*/(*P. dulcis* × *P. persica*)	Jimenez et al., 2013
	SIP1	Up-regulated, regulating raffinose biosynthesis and alleviating osmotic stress		
	LEA5, *ERD10C*	Up-regulated, preventing cell dehydration	*Nicotiana tabacum*/*N. tabacum*	Liu et al., 2014
	BFRUCT3, *SPSIF*, *SUS3 and 4*	Up-regulated, regulating glucose and sucrose biosynthesis, stabilizing cellular membranes and maintaining cell turgor	*Citrus sinensis* (L.) Osbeck/*C. limonia* Osbeck	Goncalves et al., 2019
Water reservation	*TIP1*, *TIP2* and *PIP*	Down-regulated in severe drought conditions, preventing water escaping from roots into soil and maintaining water in roots	*V. vinifera*/(*V. rupestris* × *V. berlandieri)*	Yildirim et al., 2018
ABA biosynthesis	*NCED1*	Up-regulated, involving in ABA biosynthesis and increasing ABA content	*C. sinensis*/*C. limonia*	Allario et al., 2013
	ABCG22		*Cucumis sativus*/*Luffa cylindrica*	Liu et al., 2016
ABA-dependent signaling pathway	*YTP1*	Up-regulated, induced *RD22* and *ABF*, involving in ABA-dependent signaling pathway	Overexpression *MhYTP1 Malus domestica*/*M. domestica*	Guo et al., 2019
	RD22	Up-regulated, participating in ABA signal transduction process		
	AREB		*N. tabacum*/*N. tabacum*	Liu et al., 2014
	PYR/PYL		*Lycopersicum esculentum '112'*/*L. esculentum '606'*	Zhang et al., 2019b
	SnRK2			
	AREB/ABF			
	PP2C		*V. vinifera*/(*V. vinifera* ×*V. berlandieri*) × *V. berlandieri*	Prinsi et al., 2021
ABA-independent signaling pathway	*DREB2A*	Up-regulated, stimulating drought responsive genes	*C. sinensis* (L.) Osbeck/*C. limonia* Osbeck	Goncalves et al., 2019
Antioxidative system	*NRX*	Up-regulated, protecting the ROS scavenging capacity of CAT	*C. sativus*/*Cucurbita moschata*	Davoudi et al., 2022
	CAT	Up-regulated, clearing the ROS		
	SOD, *APX*		*C. sinensis* (L.) Osbeck/*C. limonia* Osbeck	Goncalves et al., 2019
	CHY1	Up-regulated, involving in carotenoid biosynthesis		
Photosynthesis	*RbcL* and *RbcS*	Up-regulated, maintaining Rubisco expression and activity and improving photosynthetic performance	*Chrysanthemum morifolium*/*Artemisia annua*	Chen et al., 2018
	Cab	Up-regulated, encoding chlorophyll a binding protein and maintaining chlorophyll and photon absorption		
	psaB	Up-regulated, involving in enhancing PS I activity		
Casparian band	*COMT*	Up-regulated, contributing to suberin and lignin biosynthesis	(*V. vinifera*/(*V. rupestris* × *V. berlandieri*)	Yildirim et al., 2018
	eceriferum 3	Up-regulated, regulating wax biosynthetic processes		
	KCS	Up-regulated, connected with the suberization		

Genes that have similar function are gathered together in the first row named 'category'. The names and functions of each differentially expressed genes in the grafted plants, the grafted combinations that were found those genes and the cited references are listed in the other rows of table.

with the root hydraulic conductivity being greater than drought-sensitive ones (Alsina et al., 2011; Sucu et al., 2017; Yildirim et al., 2018). Similar results were obtained in tomatoes (Suchoff et al., 2018). These root architecture changes depend on signal molecules and multiple genes. Glutamate is a common signaling molecule in RSA under drought stress (Qiu et al., 2019). Decreased glutamate in drought-resistant citrus rootstocks during severe drought stress inhibited the growth of lateral roots, which allocated more resources towards the primary root elongation to expand their reach of the available water supply (Sousa et al., 2022). Additionally, the up-regulation of genes encoding cell wall modification enzymes and pathogenesis-related (PR) proteins in the rootstock can also alter cell wall structure to easily modify the RSA to enhance the water uptake capacity (Sels et al., 2008; Yildirim et al., 2018). The miR160 moving from scion to rootstock in the grafted apple and tobacco plants improved root development by extending the root length (Shen et al., 2022).

TABLE 2 The exchanging molecules between scions and rootstocks to improve drought resistance.

Category	Mobile molecules	Effects	Scion/Rootstock	Reference
Antioxidants	HSP70	Alleviating lipid peroxidation and protecting cell membrane integrity	*Cucumis sativus/Cucurbita moschata*	Davoudi et al., 2022
	HSP81			
	Prx	Improving peroxidase activity		
	DnaJ	Maintaining the stability of intracellular protein components and is related to protein domain specific binding		
	DnaJ-like B8	Maintaining the stability of intracellular protein components and is related to protein folding		
Photosynthesis	*psbB*	Binding chlorophyll and helping catalyze the primary light-induced photochemical processes of PSII		
	psbD	Assembling stable PSII complexes		
	LhcI	Promoting light energy collection and energy transfer to photosynthetic reaction centers		
	psaA	Encoding P700 chlorophyll A1 apolipoprotein and involving in PSI response process		
	psaB	Encoding P700 chlorophyll A2 apolipoprotein and involving in PSI response process		
ABA biosynthesis and response	STK	Maintaining the integrity of cell membrane and is related to protein phosphorylation		
	DRM	Improving drought resistance and is related to ABA response progress	*Pyrus bretchneideri/P. betulaefolia*	Hao et al., 2020
	NDUFB7	Related to ABA signaling, stomatal aperture and improving drought resistance	*Nicotiana benthamiana/Arabidopsis thaliana*	Notaguchi et al., 2015
	CLE25	Inducing *NCED3* expression and ABA accumlation	cle25 #10 *A. thaliana*/wild-type *A. thaliana*	Takahashi et al., 2018
Root regulation	miR160	Regulating RSA adjustment	Mdm-miR160e OE *Malus domestica*/GL-3 *M. domestica*	Shen et al., 2022

The category is composed of the molecules that has the same functions. The molecules in table are mainly miRNAs. Only the CLE25 is a kind of peptides and the miR160 is a kind of miRNAs. The last two rows demonstrate which the grafted combinations and references the molecules are from.

Root water preservation and nutrient uptake

Root biomass accumulation and RSA regulation are the two primary water storage methods in roots. Besides these, genes related to suberization and wax biosynthesis, like *caffeic acid 3-O-methyltransferase* (*COMT*), *eceriferum 3* and *3-ketoacyl-CoA synthase* (*KCS*), were up-regulated to build and thicken the Casparian strip (Vincent et al., 2005; Lee et al., 2009; Li et al., 2015; Yildirim et al., 2018). The Casparian strip helped prevent the water backflow from the root to the soil (Yildirim et al., 2018). Aquaporins, are water channels encoded by *plasma membrane intrinsic proteins* (*PIPs*) and *tonoplast intrinsic proteins* (*TIPs*) genes, and their expression pattern varied with the extent of drought stress and plant species (Gautam and Pandey, 2021; Shivaraj et al., 2021). The *PIP* genes were differentially expressed in the grafted plants of two plum rootstocks (R20 and R40), but it was difficult to explain their drought-induced expression patterns and their effects (Opazo et al., 2020). However, during severe drought-stressed conditions, *TIP1*, *TIP2*, and *PIP2* were down-regulated in the grapevine rootstocks, which reduced aquaporins and prevented water loss from roots (Afzal et al., 2016; Yildirim et al., 2018). The *PIP1;2* was considered a candidate gene for improving the plant water conductivity in grafted hickory plants (Kumar et al., 2018). Additionally, aquaporins were reported to be transported from pumpkin rootstocks to cucumber scions during drought (Davoudi et al., 2022). Therefore, aquaporins and their related genes need further exploration in grafted plants under drought stress. Furthermore, the root's water and nutrient uptake ability was improved in the grafted poplars, which may be related to the high relative abundance of rhizosphere fungi (Liu et al., 2019).

The plant nutrient uptake and utilization depend on the root's nutrient absorption capacity or the strength of signals arising from the scions (Savvas et al., 2010). Obviously, grafting with vigorous drought-resistant rootstocks can enhance the nutrient uptake ability to improve plant yield when compared to self-rooted plants (Savvas et al., 2010; Zhang et al., 2020). For example, compared with the scions grafted with drought-sensitive tomato rootstocks 'S', the concentrations of vital macronutrients like N, P, K, Ca, and Mg were higher in the leaves of scions grafted with drought-resistant 'T' under drought-stressed conditions, thereby indicating that drought-resistant rootstocks enhanced the uptake and translocation of

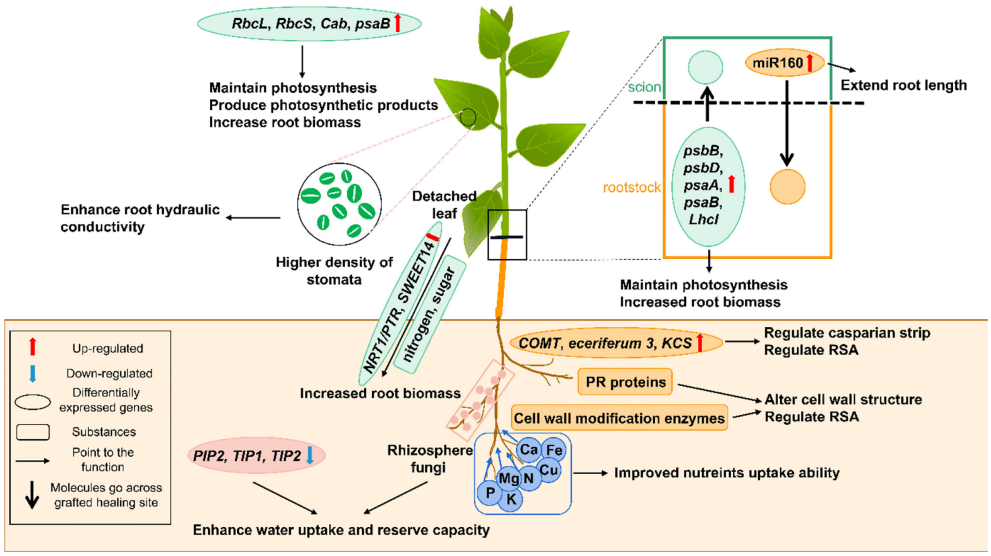


FIGURE 1
A schematic model shows the physiological and molecular mechanisms that enhancing drought resistance by root and shoot regulation in grafted plants. The green part represents for the scion, and the brown part represents for the rootstock. The black box shows the figure notes. *Cab, chlorophyll a/b binding protein; COMT, caffeic acid 3-O-methyltransferase; KCS, 3-ketoacyl-CoA synthase; Lhcl, photosystem I light-harvesting chlorophyll a/b-binding protein; NRT1/PTR, nitrate transporter 1/peptide transporter; PIP, plasma membrane intrinsic proteins; psaA, photosystem I P700 chlorophyll a apoprotein A1; psaB, photosystem I P700 chlorophyll a apoprotein A2; psbB, photosystem II CP47 reaction center protein; psbD, photosystem II protein D2; RbcS, ribulose-1,5-bisphosphate carboxylase/oxygenase small subunit; RbcL, Ribulose-1,5-diphosphate carboxylase/oxygenase large subunit; SWEET14, bidirectional sugar transporter; TIP1* and *2, tonoplast intrinsic proteins 1* and *2.*

nutrients toward the shoots (Zhang et al., 2020). Similarly, plants grafted with drought-tolerant tomato rootstocks (Zarina) showed higher macronutrient (N, P and K) and micronutrient (Fe and Cu) concentrations under water stressed conditions (Sánchez-Rodríguez et al., 2013; Sánchez-Rodríguez et al., 2014). Water stress may also inhibit the nitrogen metabolism enzymes, thereby limiting the plant's nitrogen assimilation ability (Sánchez-Rodríguez et al., 2013). When drought-tolerant tomato variety was used as rootstocks, the grafted plants showed an improved N uptake and NO^{3-} assimilation, which promoted their growth (Sánchez-Rodríguez et al., 2013).

Scion changes

Scions maintain their own growth and development through photosynthetic products. The drought stress-induced adverse effects on scions included leaf wilting, reduction of leaf area and numbers, reduced leaf and stem biomass, and weakened photosynthesis, all of which decreased the photosynthetic products and water contents, and water use efficiency of scions (Shao et al., 2008). Grafting onto drought-resistant rootstocks can be a good strategy to alleviate these problems (Shehata et al., 2022).

Morphological changes of the scion

Morphological observations post water deficit conditions showed a lower proportion of yellow and dry leaves in the scions grafted onto drought-resistant grapevine rootstocks (Sucu et al., 2017). The leaf area size directly affects plant photosynthetic intensity (Yang et al., 2021). Under the drought treatment, the drought-resistant apple rootstocks had a greater leaf area, which improved photosynthesis, thereby positively affecting the whole plant productivity (Valverdi and Kalcsits, 2021). Shoot growth is sensitive to water stress and may stop even with minor water reduction (Sabir and Kucukbasmaci, 2019). Naturally, the drought-resistant grapevine rootstocks were found to maintain the shoot growth of scions under water deficit conditions. (Sabir and Kucukbasmaci, 2019). Fresh and dry weights of the leaf and shoot are considered important indexes to screen and identify drought-tolerant genotypes (Bikdeloo et al., 2021). When scions are grafted onto drought-tolerant grapevine rootstocks, their leaf dry weight were higher than the grafted plants containing sensitive rootstocks (Gullo et al., 2018). Plants grafted onto high vigor watermelon rootstocks exhibited a relatively lower reduction in growth and shoot biomass (Ali et al., 2019; Bikdeloo et al., 2021).

The micro-morphological changes of leaves and stems also promoted the water absorption of scions. Drought-resistant rootstocks increased the diameter and density of the xylem vessels and decreased the numbers of emboli at the grafted site to increase the hydraulic conductance capacity and ultimately altered the drought resistance of the scion (Bauerle et al., 2011). When two plum scions (An and Np) were grafted onto the same rootstocks, the grafted combination with An scion had higher root hydraulic conductivity, probably due to the higher stomatal density of scions, thereby causing great internal pressure in the transpiration stream (Opazo et al., 2020). Using scions and rootstocks of xeric origin can not only improve the drought tolerance of grafted plants, but also shape their phenology, including delaying bud-break and reducing stem secondary growth of trees (Camisón et al., 2021).

Photosynthesis

Scions that are grafted with drought-resistant tomato rootstocks demonstrated a lower photosynthetic rate reduction (Alves et al., 2021). The maintenance of a high CO_2 assimilation rate in drought-resistant grafted plants provides the basis for good plant growth and productivity under long-term drought situations. This causes drought-resistant grafted plants to accumulate greater biomass accumulation than their drought-sensitive counterparts, despite this accumulation being lesser than during normal conditions. Photosynthesis is adversely affected by stomatal and non-stomatal factors. The stomatal movement and development will be discussed later. The non-stomatal factors are the main photosynthesis inhibitory factors and they include chloroplast rupturing, inhibition of chlorophyll synthesis, a decrease of photosystem II reaction center activity, and inhibition of ribulose-1,5-diphosphate carboxylase/oxygenase (Rubisco) activity (Flexas and Medrano, 2002; Flexas et al., 2004; Twalla et al., 2021). As shown in Figure 1, these problems are alleviated by grafting onto high vigor rootstocks. The chlorophyll content is a useful index for evaluating plant drought resistance. The chlorophyll content of leaves was the highest in the scions grafted with the strongest drought-resistant rootstocks among three different rootstocks during drought stress treatment, which also indicated higher photosystem II activity (Dong et al., 2021). The *Rubisco large subunit* (*RbcL*), *Rubisco small subunit* (*RbcS*), *chlorophyll a/b binding protein* (*Cab*) and *photosystem I p700 chlorophyll a apoprotein A2* (*psaB*) genes were up-regulated in chrysanthemum scions of the drought-resistant grafted plants and it helped maintain the photosynthetic performance (Chen et al., 2018; Wilson and Hayer-Hartl, 2018). The movement of a series of mobile mRNAs from the pumpkin roots to the scions, also called scion-rootstock communication, can also improve the photosynthetic performance during drought conditions (Davoudi et al., 2022). Specifically, multiple genes, including *photosystem II CP47 reaction center protein* (*psbB*), *photosystem I p700 chlorophyll a apoprotein A2* (*psaB*), *photosystem II protein D2* (*psbD*), *photosystem I p700 chlorophyll a apoprotein A1* (*psaA*) and *photosystem I light-harvesting chlorophyll a/b-binding protein* (*LhcI*), functional in different photosynthesis-related processes, were induced to maintain the photosynthetic activity of the grafted plants (Davoudi et al., 2022). Among them, *psaB* is the common gene that was not only detected in chrysanthemum scions, but also identified in the molecule movement from pumpkin rootstocks to cucumber scions. Therefore, we believe that some photosynthesis-related genes are being activated in the roots and their transcripts are being moved to scions.

Crop yield and quality

For trees, improving drought resistance through grafting is the most important aspect, as it allows better growth under drought stressed conditions. However, for grafted vegetables and fruits, it is not only important to improve their drought resistance, but also to retain adequate yield and high vegetable/fruit quality in the process (Fullana-Pericàs et al., 2020). Many studies have suggested that the drought-induced negative effects on the yield and quality of fruits and vegetables can be mitigated by grafting with drought-resistant rootstocks (Supplementary Table 1) (Ellenberger et al., 2021).

To improve plant yield during drought stress, there are two pivotal indices we must consider: water use efficiency and photosynthesis. Drought always negatively affects the plants due to the lack of both water and photosynthetic products, which directly reduces plant biomass production (Proietti et al., 2008; Rouphael et al., 2008). Therefore, it is imperative to select rootstocks capable of raising the water and nutritional status of scions. (López-Marín et al., 2017). Previous studies found that some drought-resistant pepper, watermelon, and tomato rootstocks could alleviate the negative effects on roots and improve their water use efficiency to increase yields under limited irrigation conditions (Poudyal et al., 2017; Al-Harbi et al., 2018; Yavuz et al., 2020). Thus, the less the reduction of photosynthetic ability, the higher the yield in grafted vegetables (López-Marín et al., 2017; Gisbert-Mullor et al., 2020).

The fruit quality includes nutritional value, taste, shape, uniformity, and odor (Khadivi-Khub and Anjam, 2016; Ellenberger et al., 2021). Drought causes yield reduction, but its effects on fruit quality are still undetermined. Nevertheless, grafting has been widely recommended as a useful tool to help plants acclimatize to drought conditions. Many studies have found that grafting altered the composition of secondary metabolites to improve the fruit's nutrients and flavor (Čolić et al., 2021; Ellenberger et al., 2021; Seymen et al., 2021; El-Mogy et al., 2022). By using drought-tolerant 'Zarina' as the rootstock, the grafted tomato plants showed a moderate accumulation of

antioxidant compounds, sugars, organic acids, and minerals, which ultimately improved the quality of fruits under moderate water stressed conditions (Sánchez-Rodríguez et al., 2012). Similarly, under water stress, 'Durinta' cultivars that were grafted with 'Beaufort' rootstocks had accumulated vitamin C and total soluble solids, which could improve tomato quality (Abdulaziz et al., 2017).

Due to the different genotypes of scions and rootstocks, connecting the two may cause genetic limitations. For example, in some grafted combinations, when drought-resistant plants and drought-sensitive plants were used as rootstocks and scions, respectively, the grafted plants had better drought resistance than the contrary combinations where drought-resistant plants and drought-sensitive plants were respectively used as scions and rootstocks. However, sometimes despite the drought-resistant soybean being used as the scion or the rootstock, the grafted plants could maintain photosynthesis (Li et al., 2019; Spiral et al., 2022). This genetic limitation is more obvious when we consider fruit quality. The scion variety theoretically determines the fruit composition in grafted plants. Due to the genetic limitation in grafted plants, varied rootstocks can drastically influence and alter the agronomic traits as well, whereas the role of the scion will be weakened (Zhang et al., 2016). Sometimes when drought-resistant rootstock was grafted with high-yielding scion, this combination did not always have high yield and fruit quality, thus indicating that the effect of grafting partly depended on the grafted combination (Sánchez-Rodríguez et al., 2012). Ignoring the scion-rootstock interaction or randomly choosing only vigorous rootstock and high-yielding scion is not a good strategy to improve yield and fruit quality (Karunakaran and Ilango, 2019). Therefore, besides the drought-resistant rootstock, considering the scion-rootstock interaction, and choosing the best combination for better drought acclimatization and the consequent increase in yield and fruit quality is a commonly used strategy (Khadivi-Khub and Anjam, 2016; Al-Harbi et al., 2018). Various grafted combinations must be thoroughly evaluated through studies in the field for the final identification of the most suitable combination (Karunakaran and Ilango, 2019).

Phytohormones

Abscisic acid (ABA) is the most important phytohormone for intensifying plant drought resistance *via* various morpho-physiological and molecular processes. Other phytohormones, like jasmonic acid (JA), salicylic acid (SA), ethylene (ET), auxins (IAA), gibberellins (GAs), cytokinins (CKs), and brassinosteroids (BRs), are also important for water deficit conditions (Ullah et al., 2018). These phytohormones usually cross-talk with each other to promote the plant's survival during drought stress. In grafted plants, as shown in Figure 2, roots can primarily sense soil water deficit and activate the appropriate signaling molecules to resist drought stress (Acharya and Assmann, 2009; Gaion et al., 2018; Zhang et al., 2019a).

ABA

Stomata are vital organs that exchange gas and water with the external environment to ensure maximum CO_2 absorption for photosynthesis and efficient control of optimal transpiration during plant life. To cope with drought stress, plants mainly use stomatal movement to control transpiration and the stomatal density changes for a long-term drought period (Marguerit et al., 2012). ABA is considered a key regulator in stomatal closure and is important in drought stress resistance. Extensive studies on the synergetic role of drought and ABA have already been conducted (Muhammad Aslam et al., 2022). They have shown that ABA triggered diverse physiological and molecular responses, like stomatal closure, cuticular wax deposition, root system modulation, activation of transcriptional and post-transcriptional gene expression, and metabolic changes in regular plants (Muhammad Aslam et al., 2022). In grafted plants, the mechanisms of ABA-mediated stomatal movement under drought stress have also been reported in detail. Under short-term drought, ABA was synthesized in roots and then transported into the guard cells to trigger stomatal closure and reduced transpiration *via* the branch signal cascade (Wilkinson and Davies, 2002; Allario et al., 2013; Sarwat and Tuteja, 2017). Under long-term drought, decreased stomatal density was found in the newly developed leaves of the grafted plants, thereby demonstrating that the high ABA content in new leaves decreased the leaf stomatal density and enabled the grafted plants to maintain long-term drought resistance (Tanaka et al., 2013; Liu et al., 2016). Despite their usual function, studies have also shown that the accumulated ABA in the grafted cucumber/luffa combination might also improve the activity of antioxidative enzymes (Liu et al., 2016). Since the ABA-dependent signaling pathway is one of the stress signal transduction-related pathways, ABA can be the signal that triggers the expression of drought-resistant genes in grafted plants. This will be discussed in the following parts (Gong et al., 2015; Du et al., 2018; Silva et al., 2018). Therefore, ABA has multiple functions in grafted plants and its significant accumulation of ABA is a helpful feature for selecting drought-resistant grafted combinations.

Other phytohormones

SA is a common defensive hormone that also participates in drought resistance (Santana-Vieira et al., 2016). Studies revealed that foliar SA accumulation was detected in grafted citrus plants, which could positively regulate stomatal closure (Santana-Vieira et al., 2016). Furthermore, exogenous SA application before

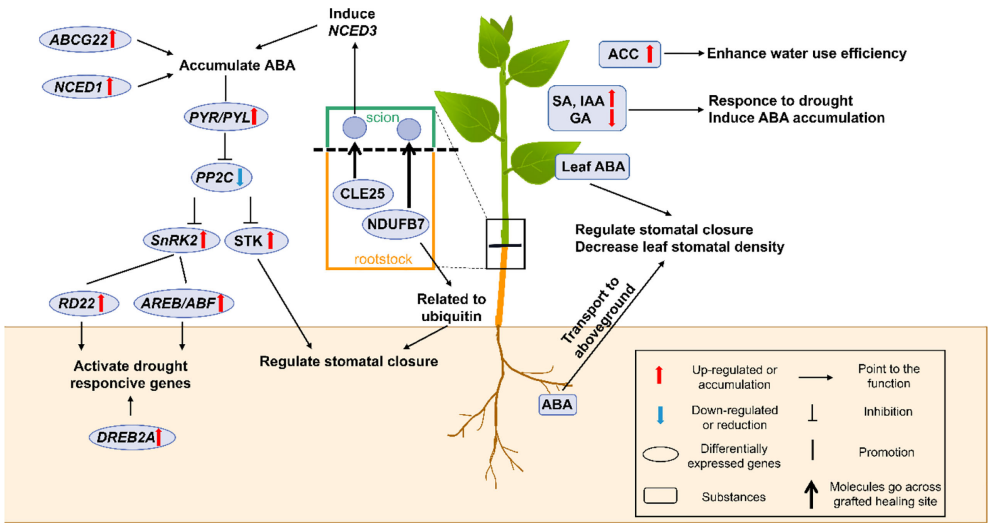


FIGURE 2
A schematic model shows the physiological and molecular mechanisms that enhancing drought resistance by the accumulation of phytohormones (especially ABA) in grafted plants. In grafted plants, the green part represents for the scion, and the brown part represents for the rootstock. The box shows the figure notes. ABA, abscisic acid; *ABCG22, ATP-binding cassette subfamily G transporter 22*; ACC, ethylene 1-amynocyclopropane-1-carboxylic; *AREB/ABF, ABA-responsive element binding protein/ABA-responsive element binding factor*; CLE25, clavata3/embryo-surrounding region-related 25; *DREB2A, dehydration-responsive element-binding protein 2 A*; GA, gibberellin; IAA, Indole-3-acetic acid; *NCED1* and *3, 9-cis-epoxycarotenoid dioxygenase 1* and *3*; NDUFB7, NADH-ubiquinone oxidoreductase B18 subunit; PP2C, protein phosphatase 2C; *PYR/PYL, pyrabactin resistance1/pyr1-like*; *RD22, responsive to dehydration 22*; SA, salicylic acid; *SnRK2*, sucrose non-fermenting-1-related protein kinase 2; *STK, serine/threonine-protein kinase-transforming protein*.

drought treatment triggered the ABA synthesis during water deficiency (Bandurska and Stroinski, 2005; Santana-Vieira et al., 2016). IAA is synthesized in the root tip or shoot apex and has been thoroughly studied to date (Ullah et al., 2018). It was reported that IAA could regulate drought resistance by adjusting root architecture and promoting the ABA-responsive genes' expression in citrus rootstocks (Shi et al., 2014). The transgenic *gretchen hagen 3* (*GH3*) RNAi plants (*GH3* silencing) used as rootstock caused IAA accumulation, which further induced RSA enlargement to absorb water and maintain water use efficiency (Jiang et al., 2022). GA plays a vital role throughout the plant life cycle (Ullah et al., 2018). Studies have revealed that a low GA level is useful for improving plant drought resistance (Ullah et al., 2018). Similarly, the high ABA content triggered by the low GA content in the grafted tomato plants could finally enhance their drought resistance (Gaion et al., 2018). However, the role of other phytohormones, like JA, CKs, and BRs during drought treatment, is poorly studied in grafted plants. In summary, the changes in the SA, IAA, and GA contents are commonly accompanied by ABA synthesis and they interact synergistically and antagonistically to regulate each other in the grafted plants (Santana-Vieira et al., 2016; Gaion et al., 2018; Sousa et al., 2022).

Additionally, in the grafted tomato plants, the root-derived precursor of ethylene 1-aminocyclopropane-1-carboxylic (ACC) could increase the fruit yield and agronomic water use efficiency (Cantero-Navarro et al., 2016). Applying exogenous melatonin onto the rootstocks improved their drought resistance by regulating the key metabolic pathways, like the phenylpropanoid pathway, chlorophyll and carotenoid biosynthesis, carbon fixation, and sugar metabolism (Lunn et al., 2014; Sharma et al., 2020). However, how the accumulation of melatonin and ACC can enhance drought resistance in grafted plants still needs further investigation.

Signaling pathway

ABA-dependent pathway

As shown in Figure 2, the ABA-dependent signaling pathway is crucial in regulating stomatal movement and activating drought-responsive gene expression in plants (Ullah et al., 2018). This includes the accumulation and signal transduction pathways. Roots are the main sites of ABA biosynthesis, followed by leaves. 9-cis-epoxycarotenoid dioxygenase (NCED) is the key rate-limiting enzyme in ABA biosynthesis (Seo and Koshiba, 2002; Ksouri et al., 2016; Ali et al., 2020). In autotetraploid clones of citrus rootstock (Rangpur lime), *NCED1* was found highly up-regulated, and it improved ABA accumulation that ultimately enhanced drought resistance (Allario et al., 2013). Additionally, an ABA

transporter gene, *ATP-binding cassette subfamily G transporter 22* (*ABCG22*) was also indirectly up-regulated in the cucumber/luffa grafted combination, thereby suggesting an ABA accumulation (Liu et al., 2016). There are molecules crossing grafted healing sites to build the scion-rootstock communication. Grafting experiments have demonstrated that clavata3/embryo-surrounding region-related 25 (CLE25) was transported from the roots to leaves, where it induced *NCED3* expression and ABA accumulation to promote stomatal closure under drought stress (Takahashi et al., 2018).

Besides the ABA accumulation, the leaf transcriptome showed that drought resistance in scions induced by rootstocks was related to transcriptional activation of ABA-dependent signaling pathway genes (Goncalves et al., 2019). ABA sensing and signaling are mediated by three classes of proteins: *PYR/PYL*, *PP2C*, and *SnRK2*. Being a hormonal signal, ABA first binds to the pyrabactin resistance1/pyr1-like (PYR/PYL) receptor, followed by constant binding with protein phosphatase 2C (PP2C) to form a ternary complex, which triggers the release of the transcription factor *sucrose non-fermenting-1-related protein kinase 2* (*SnRK2*) (Zhang et al., 2019b). This is the main ABA signal transduction pathway. The up-regulated *PYR/PYL*, and *SnRK2* along with down-regulated *PP2C* were detected in the grafted tomato plants during drought stress, thereby indicating that the ABA signal transduction pathway was activated in the grafted tomato (Zhang et al., 2019b). *SnRK2* plays important role in ABA-responsive stomatal closure and ABA-dependent gene expression. *ABA-responsive element binding protein/ABA-responsive element binding factor* (*AREB/ABF*) is activated through multi-site phosphorylation of the conserved domains by *SnRK2* in the grafted tobacco plants, and it directly acts on numerous drought-responsive genes (Liu et al., 2014; Ullah et al., 2018; Soma et al., 2021). Furthermore, the activated SnRK2 induces stomatal closure through downstream regulation of ion channels and transcription factors (Soma et al., 2021). For example, the serine/threonine-protein kinase (STK) transported from the pumpkin rootstocks to cucumber scions participated in ABA-dependent stomatal movement by phosphorylating the ion channels (Staples, 2003; Ali et al., 2020). Moreover, molecules like the NADH-ubiquinone oxidoreductase B18 subunit (NDUFB7), transported from *Arabidopsis* rootstock to the tobacco scion, were related to ubiquitin, which was an important drought stress response occurring through regulating ABA signals and stomatal aperture (Notaguchi et al., 2015; Yang et al., 2017; Pan et al., 2020; Yu et al., 2020). Thus, we can speculate that ubiquitination and phosphorylation exist in the ABA-dependent signaling pathway and play important roles in grafted plants (Soma et al., 2021).

Gene overexpression in scions can also affect the ABA-dependent signaling pathway and enhance their drought resistance. *YTH domain-containing RNA binding proteins* (*YTPs*) are important in conferring drought resistance to plants (Li et al., 2014; Wang et al., 2017). The overexpression of *YTP1* in transgenic apple scions promotes the expression of the *ABF3* and *stress response monitor gene responsive to dehydration 22* (*RD22*) genes, which were involved in the ABA-dependent pathway to stimulate stomatal aperture reduction and improve water use efficiency under long-term drought-stressed conditions (Guo et al., 2019). Researchers also pointed out that grafted plants with *YTP1* transgenic apple being used as the scions exhibited better drought resistance (Guo et al., 2019).

ABA-independent pathway

Besides the ABA-dependent signaling pathway, there are ABA-independent pathways that activate the plant drought defense system (Figure 2). According to microarray analysis in *Arabidopsis*, there were several pathways that independently were abiotic stress-responsive and one such important pathway is the dehydration-responsive element-binding protein (DREB) regulon (Agarwal et al., 2006). The transcription factor *DREB2* is involved in the ABA-independent pathway and uses the DRE *cis*-acting element to activate the drought responsive genes (Agarwal et al., 2006). In the grafted citrus and tomato plants, the upregulated *DREB2A*, a key drought response regulator, was detected, thus indicating that the ABA-independent pathway was activated to resist drought stress (Gaion et al., 2018; Goncalves et al., 2019).

Osmotic adjustment

Drought causes water deficiency and osmotic stress in plant cells, leading to ion imbalance and adversely affecting cellular functions (Zia et al., 2021). Under low water potential, the osmoregulation of grafted plants depends on the accumulation of different osmotically active compounds, which can improve their water retention ability and water use efficiency (Figure 3) (Ozturk et al., 2021). Due to the higher osmoregulatory capacity, grafted plants with drought-resistant grapevine rootstocks showed greater drought tolerance than those with drought-sensitive grapevine rootstocks (Lucini et al., 2020). Thus, choosing the right rootstocks is pivotal for grafted plants.

Proline is one of the most important osmoprotectants that can stabilize membrane and protein conformation by forming protective films with water molecules on their surface (Ozturk et al., 2021). In many grafted plants, proline was found accumulating in plant tissues to improve drought resistance (Liang et al., 2013; Penella et al., 2014; Ozturk et al., 2021). The proline accumulation in plant tissues under drought conditions can be obtained from the activation of proline biosynthesis, inactivation of proline degradation, protein hydrolysis, or

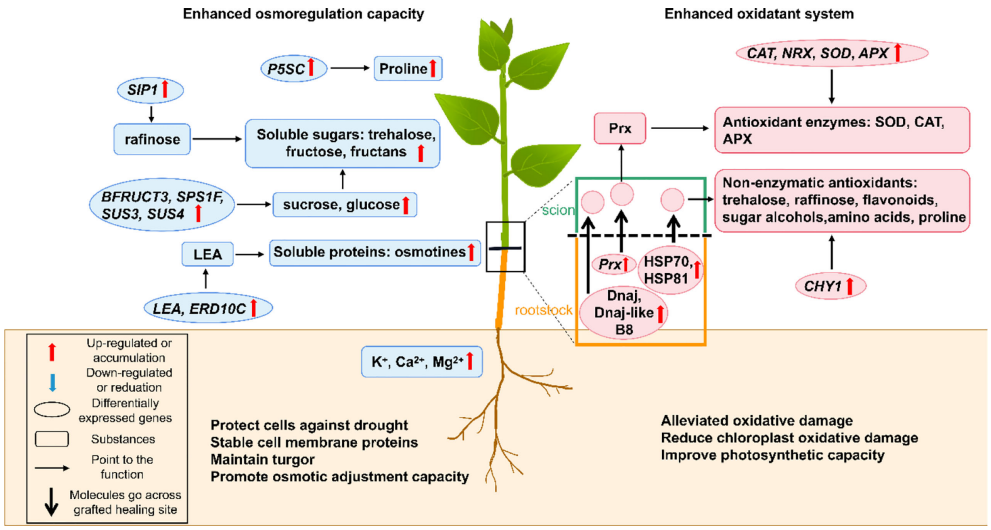


FIGURE 3
A schematic model shows the physiological and molecular mechanisms that enhancing drought resistance by osmoregulation and anti-oxidant system in grafted plants. The green part represents for the scion while the brown part represents for the rootstock. The box shows the figure notes. APX, ascorbate peroxidase; *BFRUCT3, β-fructosidase 3*; CAT, catalase; *CHY1, chloroplast β-carotene hydroxylase*; Dnaj, Chaperone protein DnaJ; Dnaj-like B8, DnaJ-like subfamily B member 8; ERD10C, early responsive to dehydration 10C; GA, gibberellin; HSP70, 70-kDa heat shock protein; HSP81, heat shock protein 81.4; *LEA, late embryogenesis abundant protein*; NRX, nucleoredoxin; *P5SC, Δ-1-pyrroline-carboxylate synthase*; *Prx, peroxiredoxin*; *SIP1, raffinose synthase*; SOD, superoxide dismutase; *SPS1F, sucrose phosphate synthase 1F*; *SUS3 and 4, sucrose synthase 3* and *4*.

oxidative inhibition of protein synthesis (Szabados and Savoure, 2010; Ozturk et al., 2021). In higher plants, the glutamate and the ornithine pathways of proline biosynthesis are known, with the former being the primary pathway in response to osmotic stress (Ozturk et al., 2021). *Δ-1-pyrroline-carboxylate synthase* (*P5SC*) encoded a key enzyme involved in proline anabolism that converts L-glutamate to glutamate γ-semialdehyde and was found to be up-regulated in the grafted plum plants. Thus, the glutamate pathway of proline biosynthesis was proven to be activated in grafted plants under water-deficit conditions (Jimenez et al., 2013). Additionally, when suffering from repeated-drought stress, the grafted plants continuously accumulated osmoregulatory substances by changing epigenetic modifications. For example, during the repeated-drought conditions, turnip rootstock altered the epigenetic modification of the *Δ1-pyrroline-5-carboxylate synthetase 1-2* (*P5CS1-2*) gene and improved its expression, which led to proline accumulation, when compared with the none-grafted rapeseed (Luo et al., 2020). However, under recurring drought stressed conditions, how the rootstock signal mediates the histone H3K4me3 modification of the P5CS1-2 locus in the scion to regulate proline biosynthesis, is still not understood clearly.

The higher contents of soluble sugars and soluble proteins were found in the grafted poplar, tomato, and citrus plants under drought stress, which generated a stronger osmotic adjustment effect (Han et al., 2018; Zhang et al., 2020; Dong et al., 2021). Soluble proteins, *e.g.*, late embryogenesis abundant (LEA) proteins and osmotins, are common osmoprotectants that stabilize cell membrane proteins and promote osmoregulation capacity (Ozturk et al., 2021). Many genes involved in soluble protein biosynthesis were found up-regulated in drought-resistant grafted plants. The *LEA5* and *early responsive to dehydration 10C* (*ERD10C*) genes encoding dehydrins in the grafted tobacco plants and genes encoding osmotins in drought-resistant rootstocks were up-regulated during drought treatment (Kovacs et al., 2008; Witte et al., 2010; Liu et al., 2014; Yildirim et al., 2018; Yang et al., 2021). Soluble sugars, *e.g.*, sucrose, trehalose, fructose, and fructan, can significantly reduce the cell osmotic potential, stabilize cellular membrane and protein conformation, or promote the osmotic adjustment and turgor maintenance as osmotic agents (Goncalves et al., 2019; Ozturk et al., 2021). Soluble sugars biosynthesis genes were also up-regulated in drought-resistant grafted plants under drought conditions. The *raffinose synthase* (*SIP1*) gene was found up-regulated in the grafted peach plants (Jimenez et al., 2013). Furthermore, the genes encoding starch branching enzymes increased the starch content in the cucumber/pumpkin grafted combination (Davoudi et al., 2022). The carbohydrate metabolism-related genes *β-fructosidase 3* (*BFRUCT3*), *sucrose phosphate synthase 1F* (*SPS1F*), *sucrose synthase 3* and *4* (*SUS3* and *SUS4*) were upregulated in grafted drought-resistant rootstocks (Goncalves et al., 2019).

The concentrations of inorganic ions also affect osmotic regulation, as they are closely related to ion pumps (Yang et al.,

2021). For example, the K^+ pump can change the cell osmotic potential by regulating the inorganic ion concentration both inside and outside the cells (Yang et al., 2021). Thus, the accumulated inorganic ions (K^+, Ca^{2+}, and Mg^{2+}) in grafted plants protect cell membrane integrity and enhance osmoregulatory capacity (Zhang et al., 2020). Additionally, the osmotic substances, like glycine betaine, sugar alcohols, and polyamines, are also drought-inducible. However, this phenomenon is poorly reported in grafted plants (Ozturk et al., 2021).

Antioxidative regulation

Drought leads to excessive ROS accumulation in plant chloroplast, mitochondria, and peroxisomes, thereby resulting in membrane peroxidation, enzyme inactivation, protein degradation, and even cell death (Dubey et al., 2021; Qamer et al., 2021). The grafted plants could improve drought resistance by activating the antioxidative defense system to scavenge the excess stress-induced ROS being generated (Figure 3) (Sanchez-Rodriguez et al., 2012).

Antioxidative enzymes

Oxidative damage is first alleviated by antioxidant enzymes including superoxide dismutase (SOD), catalase (CAT), ascorbate peroxidase (APX), and peroxidase (POD). It is a passive mechanism primarily mediated by ROS overproduction (Sucu et al., 2017; Dubey et al., 2021). Besides ROS, ABA and free polyamines could also activate the antioxidant enzymes in grafted plants during drought stress (Liu et al., 2016; Sanchez-Rodriguez et al., 2016). SOD is a metalloenzyme that catalyzes superoxide anion (O^{2-}) molecules into oxygen (O_2) and hydrogen peroxide (H_2O_2) (Laxa et al., 2019). CAT, APX, and POD can convert H_2O_2 into water (H_2O) and O_2 (Laxa et al., 2019). High activity and content of these enzymes alleviate oxidative stress by reducing ROS production in the scions of grafted plants with drought-resistant poplar, citrus, apple, cucumber, and tobacco rootstocks (Liu et al., 2012; Liu et al., 2014; Melnikova et al., 2017; Chen et al., 2020; Balfagon et al., 2021; Shehata et al., 2022). Furthermore, the high antioxidant enzymatic activity of these grafted plants can reduce chlorophyll decomposition, alleviate chloroplast membrane damage, and improve photosynthesis (Sanchez-Rodriguez et al., 2012; Zhang et al., 2019a). Several up-regulated genes related to antioxidative enzyme biosynthesis were detected in grafted plants having drought-resistant rootstocks. The *SOD* and *APX* genes were up-regulated in citrus grafted plants (Goncalves et al., 2019). The *nucleoredoxin* (*NRX*) encodes a protein that protects the CAT enzyme from abiotic stress-induced damage (Kneeshaw et al., 2017). The up-regulated *NRX* and *CAT* genes could strengthen the antioxidant system in the grafted cucumber/pumpkin combination (Davoudi et al., 2022). Additionally, the mobile mRNA, encoding peroxiredoxin (Prx) (an antioxidant cysteine-dependent peroxidase) was also identified in the grafted plants (Davoudi et al., 2022). We believe that drought stress-induced antioxidant system activation is a trait transmissible from the rootstock to the scion, which depends on scion-rootstock communication (Balfagon et al., 2021). Additionally, previous studies showed that drought-resistant plants induced greater activation of the ascorbate-dependent scavenging system. Contrastingly, the drought-sensitive plants only activated the glutathione-dependent scavenging system, with only moderate induction or even down-regulation of the ascorbate-dependent system (Laxa et al., 2019). When they used as rootstocks grafted onto the same scions, this different antioxidative activated mechanisms existed between two grafted combinations or not can be explored further in depth.

Non-enzymatic antioxidants

Drought resistance can also be improved by non-enzymatic antioxidants. Flavonoids, the common non-enzymatic antioxidants, could enhance antioxidative capacity (Lopez-Hinojosa et al., 2021). Studies have shown that most flavonoid biosynthesis-related genes were up-regulated in grafted plants (Lopez-Hinojosa et al., 2021). Furthermore, it has been reported that trehalose and raffinose in the citrus rootstock, and sugar alcohols (*e.g.*, sorbitol) and amino acids (*e.g.*, tyrosine, aspartic acid, methionine, ornithine, and tryptophan) in drought-resistant rootstocks could support the antioxidant system and scavenge ROS to protect the membrane integrity (Jimenez et al., 2013; Keunen et al., 2013; Lunn et al., 2014; Santana-Vieira et al., 2016; Sousa et al., 2022). It also indicated that the proline accumulation in the plants grafted with drought-resistant rootstocks could stabilize the membrane and proteins under water-deficient conditions (Jimenez et al., 2013; Schneider et al., 2018; Ozturk et al., 2021). Some photosynthesis-related molecules may play antioxidant roles in grafted plants. Decreased tetrapyrrole, the chlorophyll intermediates in grafted grapevine plants, could scavenge the excess ROS (Lucini et al., 2020). Carotenoid is also another well-known non-enzymatic antioxidant (Laxa et al., 2019). Upregulation of the *chloroplast β-carotene hydroxylase* (*CHY1*), encoding a carotenoid biosynthesis enzyme, indicated that the accumulated carotenoid could enhance osmoregulation in grafted citrus plants (Goncalves et al., 2019). DnaJ-like subfamily B member 8 (DnaJ-like B8) and Chaperone protein DnaJ (DnaJ), which was transported from the pumpkin rootstock to cucumber scion, helped prevent protein misfolding and aggregation, thus contributing to stress tolerance, redox maintenance and photosynthetic balance (Wang et al., 2014; Amiya and Shapira, 2021; Davoudi et al., 2022). The 70-kDa heat shock protein (HSP70) and heat shock protein 81.4 (HSP81) were transported from the pumpkin to the

cucumber and they accumulated in the cucumber scions during drought stress to enhance membrane stability and detoxify the accumulating ROS (Ul Haq et al., 2019; Davoudi et al., 2022). Additionally, ascorbate (ASA), glutathione (GSH) and α-tocopherol are important plant non-enzymatic antioxidants, which need further exploration in grafted plants (Schneider et al., 2018; Hasanuzzaman et al., 2019).

Summary and outlook

The selection of suitable rootstocks or scions is crucial in generating the drought resistance of grafted plants. Besides enabling the grafted plants to regulate general morphological, physiological, and molecular processes and allow adaptive changes to improve drought resistance, the graft-responsive genes, especially through the exchange of genetic information between rootstocks and scions, are important in improving plant performance under drought stress. It also is vital in promoting water use efficiency, osmoregulation, anti-oxidant-mediated stress tolerance, etc. Furthermore, future research can focus more on the improvement of drought resistance of grafted trees, which is a potential research avenue that can be applied in arid and semi-arid areas. Moreover, with the increasing in-depth research, we believe that the scion-rootstock communication is a complex bidirectional feedback loop that is crucial for enhancing drought resistance *via* transport molecules. Therefore, studying the scion-rootstock communication holds the key to future understanding and improving plant drought resistance.

Author contributions

LY collected and analyzed the data, and written the manuscript. LX and YZ collected some data. QH and SZ designed the framework, given some advises and revised the manuscript. All authors read and approved the final manuscript.

Funding

This work was supported by the National Natural Science Foundation of China (32101478), the Second Tibetan Plateau Scientific Expedition and Research Program (2019QZKK0404) and China Postdoctoral Science Foundation (2021M702360).

Acknowledgments

The authors would like to express their gratitude to EditSprings (https://www.editsprings.cn) for the expert linguistic services provided.

Conflict of interest

The authors declare that the research was conducted in the absence of any commercial or financial relationships that could be construed as a potential conflict of interest.

Publisher's note

All claims expressed in this article are solely those of the authors and do not necessarily represent those of their affiliated organizations, or those of the publisher, the editors and the reviewers. Any product that may be evaluated in this article, or claim that may be made by its manufacturer, is not guaranteed or endorsed by the publisher.

Supplementary material

The Supplementary Material for this article can be found online at: https://www.frontiersin.org/articles/10.3389/fpls.2022.1015317/full#supplementary-material

References

Abdulaziz, A. H., Abdulrasoul, A. O., Thabet, A., Hesham, A. R., Khadejah, A., Saad, M., et al. (2017). Tomato grafting impacts on yield and fruit quality under water stress conditions. *J. Exp. Bio. Agric. Sci.* 5, 136–147. doi: 10.18006/2017.5(Spl-1-SAFSAW).S136.S147

Acharya, B. R., and Assmann, S. M. (2009). Hormone interactions in stomatal function. *Plant Mol. Biol.* 69, 451–462. doi: 10.1007/s11103-008-9427-0

Afzal, Z., Howton, T. C., Sun, Y., and Mukhtar, M. S. (2016). The roles of aquaporins in plant stress responses. *J. Dev. Biol.* 4, 9. doi: 10.3390/jdb4010009

Agarwal, P. K., Agarwal, P., Reddy, M. K., and Sopory, S. K. (2006). Role of DREB transcription factors in abiotic and biotic stress tolerance in plants. *Plant Cell Rep.* 25, 1263–1274. doi: 10.1007/s00299-006-0204-8

Ahmed, C. B., Rouina, B. B., Sensoy, S., Boukhris, M., and Abdallah, F. B. (2009). Changes in gas exchange, proline accumulation and antioxidative enzyme activities in three olive cultivars under contrasting water availability regimes. *Environ. Exp. Bot.* 67, 345–352. doi: 10.1016/j.envexpbot.2009.07.006

Alan, O., Ozdemir, N., and Gunen, Y. (2007). Effect of grafting on watermelon plant growth, yield and quality. *J. Agron.* 6, 362–365. doi: 10.3923/ja.2007.362.365

Al-Harbi, A. R., Al-Omran, A. M., Alqardaeai, T. A., Abdel-Rassak, H. S., Alharbi, K. R., Obadi, A., et al. (2018). Grafting affects tomato growth, productivity, and water use efficiency under different water regimes. *J. Agr. Sci. Tech.* 20, 1227–1241. Available at: http://jast.modares.ac.ir/article-23-20094-en.html

Ali, S., Hayat, K., Iqbal, A., and Xie, L. (2020). Implications of abscisic acid in the drought stress tolerance of plants. *Agronomy* 10. doi: 10.3390/agronomy10091323

Ali, P., Jabe, P., and Davoud, Z. (2019). Assessment of iranian rainfed and seedy watermelon landraces as potential rootstocks for enhancing drought tolerance. *Hortic. Sci. Technol.* 37, 354–364. doi: 10.7235/HORT.20190036

Allario, T., Brumos, J., Colmenero-Flores, J. M., Iglesias, D. J., Pina, J. A., Navarro, L., et al. (2013). Tetraploid rangpur lime rootstock increases drought tolerance *via* enhanced constitutive root abscisic acid production. *Plant Cell Environ.* 36, 856–868. doi: 10.1111/pce.12021

Alsina, M. M., Smart, D. R., Bauerle, T., de Herralde, F., Biel, C., Stockert, C., et al. (2011). Seasonal changes of whole root system conductance by a drought-tolerant grape root system. *J. Exp. Bot.* 62, 99–109. doi: 10.1093/jxb/erq247

Alves, F. M., Joshi, M., Djidonou, D., Joshi, V., Gomes, C. N. , and Leskovar, D. I. (2021). Physiological and biochemical responses of tomato plants grafted onto *Solanum pennellii* and *Solanum peruvianum* under water-deficit conditions. *Plants (Basel)* 10, 2236. doi: 10.3390/plants10112236

Amiya, R., and Shapira, M. (2021). ZnJ6 is a thylakoid membrane DnaJ-like chaperone with oxidizing activity in *Chlamydomonas reinhardtii*. *Int. J. Mol. Sci.* 22, 1136. doi: 10.3390/ijms22031136

Balfagon, D., Teran, F., de Oliveira, T. D. R., Santa-Catarina, C., and Gomez-Cadenas, A. (2021). Citrus rootstocks modify scion antioxidant system under drought and heat stress combination. *Plant Cell Rep.* 41, 593–602. doi: 10.1007/s00299-021-02744-y

Bandurska, H., and Stroinski, A. (2005). The effect of salicylic acid on barley response to water deficit. *Acta Physiol. Plant* 27, 379–386. doi: 10.1007/s11738-005-0015-5

Bauerle, T. L., Centinari, M., and Bauerle, W. L. (2011). Shifts in xylem vessel diameter and embolisms in grafted apple trees of differing rootstock growth potential in response to drought. *Planta* 234, 1045–1054. doi: 10.1007/s00425-011-1460-6

Bikdeloo, M., Colla, G., Rouphael, Y., Hassandokht, M. R., Soltani, F., Salehi, R., et al. (2021). Morphological and physio-biochemical responses of watermelon grafted onto rootstocks of wild watermelon [*Citrullus colocynthis* (L.) schrad] and commercial interspecific cucurbita hybrid to drought stress. *Horticulturae* 7, 359. doi: 10.3390/horticulturae7100359

Camisón, Á., Martín, M.Á., Flors, V., Sánchez-Bel, P., Pinto, G., Vivas, M., et al. (2021). Exploring the use of scions and rootstocks from xeric areas to improve drought tolerance in *Castanea sativa* miller. *Environ. Exp. Bot.* 187, 104467. doi: 10.1016/j.envexpbot.2021.104467

Cantero-Navarro, E., Romero-Aranda, R., Fernandez-Munoz, R., Martinez-Andujar, C., Perez-Alfocea, F., and Albacete, A. (2016). Improving agronomic water use efficiency in tomato by rootstock-mediated hormonal regulation of leaf biomass. *Plant Sci.* 251, 90–100. doi: 10.1016/j.plantsci.2016.03.001

Cerruti, E., Gisbert, C., Drost, H. G., Valentino, D., Portis, E., Barchi, L., et al. (2021). Grafting vigour is associated with DNA de-methylation in eggplant. *Hortic. Res.* 8, 241. doi: 10.1038/s41438-021-00660-6

Chaimala, A., Jogloy, S., Vorasoot, N., Toomsan, B., Jongrungklang, N., Kesmala, T., et al. (2020). Responses of total biomass, shoot dry weight, yield and yield components of Jerusalem artichoke (*Helianthus tuberosus* l.) varieties under different terminal drought duration. *Agriculture* 10. doi: 10.3390/agriculture10060198

Chambaud, C., Cookson, S. J., Ollat, N., Bayer, E., and Brocard, L. (2022). A correlative light electron microscopy approach reveals plasmodesmata ultrastructure at the graft interface. *Plant Physiol.* 188, 44–55. doi: 10.1093/plphys/kiab485

Chen, C. Z., Lv, X. F., Li, J. Y., Yi, H. Y., and Gong, J. M. (2012). Arabidopsis NRT1.5 is another essential component in the regulation of nitrate reallocation and stress tolerance. *Plant Physiol.* 159, 1582–1590. doi: 10.1104/pp.112.199257

Chen, Y., Sun, X., Zheng, C., Zhang, S., and Yang, J. (2018). Grafting onto *Artemisia annua* improves drought tolerance in *Chrysanthemum* by enhancing photosynthetic capacity. *Hortic. Plant J.* 4, 117–125. doi: 10.1016/j.hpj.2018.03.008

Chen, S., Yi, L., Korpelainen, H., Yu, F., and Liu, M. (2020). Roots play a key role in drought-tolerance of poplars as suggested by reciprocal grafting between male and female clones. *Plant Physiol. Bioch.* 153, 81–91. doi: 10.1016/j.plaphy.2020.05.014

Čolić, S. D., Bakić, I. V., Dabić Zagorac, D.Č., Natić, M. M., Smailagić, A. T., Pergal, M. V., et al. (2021). Chemical fingerprint and kernel quality assessment in different grafting combinations of almond under stress condition. *Sci. Hortic-Amsterdam* 275, 10975. doi: 10.1016/j.scienta.2020.109705

Davoudi, M., Song, M., Zhang, M., Chen, J., and Lou, Q. (2022). Long-distance control of pumpkin rootstock over cucumber scion under drought stress as revealed by transcriptome sequencing and mobile mRNAs identifications. *Hortic. Res.* 9, uhab033. doi: 10.1093/hr/uhab033

Dong, T., Xi, L., Xiong, B., Qiu, X., Huang, S., Xu, W., et al. (2021). Drought resistance in harumi tangor seedlings grafted onto different rootstocks. *Funct. Plant Biol.* 48, 529–541. doi: 10.1071/FP20242

Dubey, A., Kumar, A., Malla, M. A., Chowdhary, K., Singh, G., Ravikanth, G., et al. (2021). Approaches for the amelioration of adverse effects of drought stress on crop plants. *Front. Biosci. (Landmark Ed)* 26, 928–947. doi: 10.52586/4998

Du, H., Huang, F., Wu, N., Li, X., Hu, H., and Xiong, L. (2018). Integrative regulation of drought escape through ABA-dependent and -independent pathways in rice. *Mol. Plant* 11, 584–597. doi: 10.1016/j.molp.2018.01.004

Ellenberger, J., Bulut, A., Blömeke, P., and Röhlen-Schmittgen, S. (2021). Novel *S. pennellii* × *S. lycopersicum* hybrid rootstocks for tomato production with reduced water and nutrient supply. *Horticulturae* 7, 355. doi: 10.3390/horticulturae7100355

Ellialtioglu, S. S., Talhouni, M., Kiran, S., Ates, C., and Kusvuran, S. (2019). Antioxidative response of grafted and non-grafted eggplant seedlings under drought and salt stresses. *Agrochimica* 63, 123–137. doi: 10.12871/00021857201922

El-Mogy, M. M., Atia, M. A. M., Dhawi, F., Fouad, A. S., Bendary, E. S. A., Khojah, E., et al. (2022). Towards better grafting: SCoT and CDDP analyses for prediction of the tomato rootstocks performance under drought stress. *Agronomy* 12, 153. doi: 10.3390/agronomy12010153

Farooq, M., Wahid, A., Lee, D. J., Ito, O., and Siddique, K. H. M. (2009). Advances in drought resistance of rice. *Crit. Rev. Plant Sci.* 28, 199–217. doi: 10.1080/07352680902952173

Flexas, J., Bota, J., Loreto, F., Cornic, G., and Sharkey, T. D. (2004). Diffusive and metabolic limitations to photosynthesis under drought and salinity in C(3) plants. *Plant Biol. (Stuttg)* 6, 269–279. doi: 10.1055/s-2004-820867

Flexas, J., and Medrano, H. (2002). Drought-inhibition of photosynthesis in C3 plants: stomatal and non-stomatal limitations revisited. *Ann. Bot.* 89, 183–189. doi: 10.1093/aob/mcf027

Fullana-Pericàs, M., Conesa, M.À., Ribas-Carbó, M., and Galmés, J. (2020). The use of a tomato landrace as rootstock improves the response of commercial tomato under water deficit conditions. *Agronomy* 10, 748. doi: 10.3390/agronomy10050748

Fullana-Pericàs, M., Ponce, J., Conesa, M.À., Juan, A., Ribas-Carbó, M., and Galmés, J. (2018). Changes in yield, growth and photosynthesis in a drought-adapted Mediterranean tomato landrace (*Solanum lycopersicum* 'Ramellet') when grafted onto commercial rootstocks and *Solanum pimpinellifolium*. *Sci. Hort-Amsterdam* 233, 70–77. doi: 10.1016/j.scienta.2018.01.045

Gaion, L. A., Monteiro, C. C., Cruz, F. J. R., Rossatto, D. R., Lopez-Diaz, I., Carrera, E., et al. (2018). Constitutive gibberellin response in grafted tomato modulates root-to-shoot signaling under drought stress. *J. Plant Physiol.* 221, 11–21. doi: 10.1016/j.jplph.2017.12.003

Gautam, A., and Pandey, A. K. (2021). Aquaporins responses under challenging environmental conditions and abiotic stress tolerance in plants. *Botanical Rev.* 87, 467–495. doi: 10.1007/s12229-021-09249-z

Gisbert-Mullor, R., Pascual-Seva, N., Martínez-Gimeno, M. A., López-Serrano, L., Badal Marín, E., Pérez-Pérez, J. G., et al. (2020). Grafting onto an appropriate rootstock reduces the impact on yield and quality of controlled deficit irrigated pepper crops. *Agronomy* 10, 1529. doi: 10.3390/agronomy10101529

Goncalves, L. P., Boscariol Camargo, R. L., Takita, M. A., Machado, M. A., Dos Soares Filho, W. S., and Costa, M. G. C. (2019). Rootstock-induced molecular responses associated with drought tolerance in sweet orange as revealed by RNA-seq. *BMC Genomics* 20, 110. doi: 10.1186/s12864-019-5481-z

Gong, X., Liu, M., Zhang, L., Ruan, Y., Ding, R., Ji, Y., et al. (2015). Arabidopsis *AtSUC2* and *AtSUC4*, encoding sucrose transporters, are required for abiotic stress tolerance in an ABA-dependent pathway. *Physiol. Plant* 153, 119–136. doi: 10.1111/ppl.12225

Gullo, G., Dattola, A., Vonella, V., and Zappia, R. (2018). Evaluation of water relation parameters in vitis rootstocks with different drought tolerance and their effects on growth of a grafted cultivar. *J. Plant Physiol.* 226, 172–178. doi: 10.1016/j.jplph.2018.04.013

Guo, T., Wang, N., Xue, Y., Guan, Q., van Nocker, S., Liu, C., et al. (2019). Overexpression of the RNA binding protein MhYTP1 in transgenic apple enhances drought tolerance and WUE by improving ABA level under drought condition. *Plant Sci.* 280, 397–407. doi: 10.1016/j.plantsci.2018.11.018

Gupta, A., Rico-Medina, A., and Caño-Delgado, A. I. (2020). The physiology of plant responses to drought. *Science* 368, 266–269. doi: 10.1126/science.aaz7614

Habibi, F., Liu, T., Folta, K., and Sarkhosh, A. (2022). Physiological, biochemical, and molecular aspects of grafting in fruit trees. *Hortic. Res.* 9, uhac032. doi: 10.1093/hr/uhac032

Han, Q., Guo, Q., Korpelainen, H., Niinemets, U., and Li, C. (2019). Rootstock determines the drought resistance of poplar grafting combinations. *Tree Physiol.* 39, 1855–1866. doi: 10.1093/treephys/tpz102

Han, Q., Luo, J., Li, Z., Korpelainen, H., and Li, C. (2018). Improved drought resistance by intergeneric graftingin salicaceae plants under water deficits. *Environ. Exp. Bot.* 155, 217–225. doi: 10.1016/j.envexpbot.2018.07.003

Han, Y., Wang, Y., Jiang, H., Wang, M., Korpelainen, H., and Li, C. (2013). Reciprocal grafting separates the roles of the root and shoot in sex-related drought

responses in populus cathayana males and females. *Plant Cell Environ.* 36, 356–364. doi: 10.1111/j.1365-3040.2012.02578.x

Hao, L., Zhang, Y., Wang, S., Zhang, W., Wang, S., Xu, C., et al. (2020). A constitutive and drought-responsive mRNA undergoes long-distance transport in pear (*Pyrus betulaefolia*) phloem. *Plant Sci.* 293, 110419. doi: 10.1016/j.plantsci.2020.110419

Hasanuzzaman, M., Bhuyan, M., Anee, T. I., Parvin, K., Nahar, K., Mahmud, J. A., et al. (2019). Regulation of ascorbate-glutathione pathway in mitigating oxidative damage in plants under abiotic stress. *Antioxid. (Basel)* 8, 384. doi: 10.3390/antiox8090384

Huang, J., Yu, H., Guan, X., Wang, G., and Guo, R. (2015). Accelerated dryland expansion under climate change. *Nat. Clim. Change* 6, 166–171. doi: 10.1038/nclimate2837

Jiang, L., Shen, W., Liu, C., Tahir, M. M., Li, X., Zhou, S., et al. (2022). Engineering drought-tolerant apple by knocking down six *GH3* genes and potential application of transgenic apple as a rootstock. *Hortic. Res.* 9, uhac122. doi: 10.1093/hr/uhac122

Jimenez, S., Dridi, J., Gutierrez, D., Moret, D., Irigoyen, J. J., Moreno, M. A., et al. (2013). Physiological, biochemical and molecular responses in four prunus rootstocks submitted to drought stress. *Tree Physiol.* 33, 1061–1075. doi: 10.1093/treephys/tpt074

Ji, J., Yang, L., Fang, Z., Zhang, Y., Zhuang, M., Lv, H., et al. (2022). Plant SWEET family of sugar transporters: structure, evolution and biological functions. *Biomolecules* 12, 205. doi: 10.3390/biom12020205

Karunakaran, R., and Ilango, R. V. J. (2019). Grafting influence on productivity and drought tolerance of tea clones. *J. Agr. Sci-cambridag.* 157, 217–225. doi: 10.1017/s0021859619000480

Keunen, E., Peshev, D., Vangronsveld, J., Van Den Ende, W., and Cuypers, A. (2013). Plant sugars are crucial players in the oxidative challenge during abiotic stress: extending the traditional concept. *Plant Cell Environ.* 36, 1242–1255. doi: 10.1111/pce.12061

Khadivi-Khub, A., and Anjam, K. (2016). Prunus scoparia, a suitable rootstock for almond (*Prunus dulcis*) under drought condition based on vegetative and fruit characteristics. *Sci. Hort-Amsterdam* 210, 220–226. doi: 10.1016/j.scienta.2016.07.028

Kneeshaw, S., Keyani, R., Delorme-Hinoux, V., Imrie, L., Loake, G. J., Le Bihan, T., et al. (2017). Nucleoredoxin guards against oxidative stress by protecting antioxidant enzymes. *Proc. Natl. Acad. Sci. U. S. A.* 114, 8414–8419. doi: 10.1073/pnas.1703344114

Kovacs, D., Kalmar, E., Torok, Z., and Tompa, P. (2008). Chaperone activity of ERD10 and ERD14, two disordered stress-related plant proteins. *Plant Physiol.* 147, 381–390. doi: 10.1104/pp.108.118208

Ksouri, N., Jimenez, S., Wells, C. E., Contreras-Moreira, B., and Gogorcena, Y. (2016). Transcriptional responses in root and leaf of prunus persica under drought stress using RNA sequencing. *Front. Plant Sci.* 7, 1715. doi: 10.3389/fpls.2016.01715

Kumar, R. M. S., Ji, G., Guo, H., Zhao, L., and Zheng, B. (2018). Over-expression of a grafting-responsive gene from hickory increases abiotic stress tolerance in arabidopsis. *Plant Cell Rep.* 37, 541–552. doi: 10.1007/s00299-018-2250-4

Kumar, P., Rouphael, Y., Cardarelli, M., and Colla, G. (2017). Vegetable grafting as a tool to improve drought resistance and water use efficiency. *Front. Plant Sci.* 8, 1130. doi: 10.3389/fpls.2017.01130

Kurotani, K. I., and Notaguchi, M. (2021). Cell-to-cell connection in plant grafting-molecular insights into symplasmic reconstruction. *Plant Cell Physiol.* 62, 1362–1371. doi: 10.1093/pcp/pcab109

Laxa, M., Liebthal, M., Telman, W., Chibani, K., and Dietz, K. J. (2019). The role of the plant antioxidant system in drought tolerance. *Antioxid. (Basel)* 8, 94. doi: 10.3390/antiox8040094

Lee, S. B., Jung, S. J., Go, Y. S., Kim, H. U., Kim, J. K., Cho, H. J., et al. (2009). Two arabidopsis 3-ketoacyl CoA synthase genes, *KCS20* and *KCS2/DAISY*, are functionally redundant in cuticular wax and root suberin biosynthesis, but differentially controlled by osmotic stress. *Plant J.* 60, 462–475. doi: 10.1111/j.1365-313X.2009.03973.x

Liang, X., Zhang, L., Natarajan, S. K., and Becker, D. F. (2013). Proline mechanisms of stress survival. *Antioxid. Redox Sign.* 19, 998–1011. doi: 10.1089/ars.2012.5074

Li, S., Cao, Y., Wang, C., Sun, X., Wang, W., and Song, S. (2020). Contribution of different genotypic roots to drought resistance in soybean by a grafting experiment. *Plant Prod. Sci.* 24, 317–325. doi: 10.1080/1343943x.2020.1839350

Li, C., Liu, C., Ma, X., Wang, A., Duan, R., Nawrath, C., et al. (2015). Characterization and genetic mapping of eceriferum-ym (cer-ym), a cutin deficient barley mutant with impaired leaf water retention capacity. *Breed Sci.* 65, 327–332. doi: 10.1270/jsbbs.65.327

Liu, B. H., Cheng, L., Ma, F. W., Liang, D., and Zou, Y. J. (2012). Influence of rootstock on drought response in young 'Gale gala' apple (*Malus domestica* borkh.) trees. *J. Sci. Food Agric.* 92, 2421–2427. doi: 10.1002/jsfa.5647

Liu, S., Li, H., Lv, X., Ahammed, G. J., Xia, X., Zhou, J., et al. (2016). Grafting cucumber onto luffa improves drought tolerance by increasing ABA biosynthesis and sensitivity. *Sci. Rep.* 6, 20212. doi: 10.1038/srep20212

Liu, J., Li, J., Su, X., and Xia, Z. (2014). Grafting improves drought tolerance by regulating antioxidant enzyme activities and stress-responsive gene expression in tobacco. *Environ. Exp. Bot.* 107, 173–179. doi: 10.1016/j.envexpbot.2014.06.012

Liu, W., Wang, Y., Gong, X., Li, S., Smoak, J. M., and Duan, B. (2019). Changes in growth and soil microbial communities in reciprocal grafting clones between populus deltoides males and females exposed to water deficit conditions. *Ann. For. Sci.* 76, 118. doi: 10.1007/s13595-019-0897-9

Li, S. Y., Wang, W. B., Yao, X. D., Wang, C. L., Cao, Y. Q., Zhang, L. J., et al. (2019). Photosynthesis in reciprocal grafts of drought-tolerant and drought-sensitive cultivars of soybean under water stress. *Photosynthetica* 57, 942–949. doi: 10.32615/ps.2019.109

Li, D., Zhang, H., Hong, Y., Huang, L., Li, X., Zhang, Y., et al. (2014). Genome-wide identification, biochemical characterization, and expression analyses of the YTH domain-containing RNA-binding protein family in arabidopsis and rice. *Plant Mol. Bio. Rep.* 32, 1169–1186. doi: 10.1007/s11105-014-0724-2

Lopez-Hinojosa, M., de Maria, N., Guevara, M. A., Velez, M. D., Cabezas, J. A., Diaz, L. M., et al. (2021). Rootstock effects on scion gene expression in maritime pine. *Sci. Rep.* 11, 11582. doi: 10.1038/s41598-021-90672-y

López-Marín, J., Gálvez, A., del Amor, F. M., Albacete, A., Fernández, J. A., Egea-Gilabert, C., et al. (2017). Selecting vegetative/generative/dwarfing rootstocks for improving fruit yield and quality in water stressed sweet peppers. *Sci. Hortic-Amsterdam* 214, 9–17. doi: 10.1016/j.scienta.2016.11.012

Lopez-Serrano, L., Canet-Sanchis, G., Vuletin Selak, G., Penella, C., San Bautista, A., Lopez-Galarza, S., et al. (2019). Pepper rootstock and scion physiological responses under drought stress. *Front. Plant Sci.* 10, 38. doi: 10.3389/fpls.2019.00038

Lucini, L., Miras-Moreno, B., Busconi, M., Marocco, A., Gatti, M., and Poni, S. (2020). Molecular basis of rootstock-related tolerance to water deficit in *Vitis vinifera L.* cv. sangiovese: A physiological and metabolomic combined approach. *Plant Sci.* 299, 110600. doi: 10.1016/j.plantsci.2020.110600

Lunn, J. E., Delorge, I., Figueroa, C. M., Van Dijck, P., and Stitt, M. (2014). Trehalose metabolism in plants. *Plant J.* 79, 544–567. doi: 10.1111/tpj.12509

Luo, L., Zheng, Y., Gao, Z., Chen, Q., Kong, X., and Yang, Y. (2020). Grafting improves drought stress memory by increasing the *P5CS1* gene expression in brassica rapa. *Plant Soil* 452, 61–72. doi: 10.1007/s11104-020-04547-8

Marguerit, E., Brendel, O., Lebon, E., Van Leeuwen, C., and Ollat, N. (2012). Rootstock control of scion transpiration and its acclimation to water deficit are controlled by different genes. *New Phytol.* 194, 416–429. doi: 10.1111/j.1469-8137.2012.04059.x

Melnikova, N. V., Borkhert, E. V., Snezhkina, A. V., Kudryavtseva, A. V. , and Dmitriev, A. A. (2017). Sex-specific response to stress in populus. *Front. Plant Sci.* 81827. doi: 10.3389/fpls.2017.01827

Melnyk, C. W., Gabel, A., Hardcastle, T. J., Robinson, S., Miyashima, S., Grosse, I., et al. (2018). Transcriptome dynamics at arabidopsis graft junctions reveal an intertissue recognition mechanism that activates vascular regeneration. *Proc. Natl. Acad. Sci. U. S. A.* 115, E2447–E2456. doi: 10.1073/pnas.1718263115

Melnyk, C. W., and Meyerowitz, E. M. (2015). Plant grafting. *Curr. Biol.* 25, R183–R188. doi: 10.1016/j.cub.2015.01.029

Muhammad Aslam, M., Waseem, M., Jakada, B. H., Okal, E. J., Lei, Z., Saqib, H. S. A., et al. (2022). Mechanisms of abscisic acid-mediated drought stress responses in plants. *Int. J. Mol. Sci.* 23, 1084. doi: 10.3390/ijms23031084

Notaguchi, M., Higashiyama, T., and Suzuki, T. (2015). Identification of mRNAs that move over long distances using an RNA-seq analysis of Arabidopsis/*Nicotiana benthamiana* heterografts. *Plant Cell Physiol.* 56, 311–321. doi: 10.1093/pcp/pcu210

Notaguchi, M., Kurotani, K. I., Sato, Y., Tabata, R., Kawakatsu, Y., Okayasu, K., et al. (2020). Cell-cell adhesion in plant grafting is facilitated by β-1,4-glucanases. *Science* 369, 698–702. doi: 10.1126/science.abc3710

Okamoto, S., Kawasaki, A., Makino, Y., Ishida, T., and Sawa, S. (2022). Long-distance translocation of CLAVATA3/ESR-related 2 peptide and its positive effect on root sucrose status. *Plant Physiol.* 189, 2357–2367. doi: 10.1093/plphys/kiac227

Opazo, I., Toro, G., Salvatierra, A., Pastenes, C., and Pimentel, P. (2020). Rootstocks modulate the physiology and growth responses to water deficit and long-term recovery in grafted stone fruit trees. *Agr. Water Manage* 228, 105897. doi: 10.1016/j.agwat.2019.105897

Ozturk, M., Turkyilmaz Unal, B., Garcia-Caparros, P., Khursheed, A., Gul, A., and Hasanuzzaman, M. (2021). Osmoregulation and its actions during the drought stress in plants. *Physiol. Plant* 172, 1321–1335. doi: 10.1111/ppl.13297

Pan, W., Lin, B., Yang, X., Liu, L., Xia, R., Li, J., et al. (2020). The UBC27-AIRP3 ubiquitination complex modulates ABA signaling by promoting the degradation of

ABI1 in arabidopsis. *Proc. Natl. Acad. Sci. U. S. A.* 117, 27694–27702. doi: 10.1073/pnas.2007366117

Penella, C., Nebauer, S. G., Bautista, A. S., Lopez-Galarza, S., and Calatayud, A. (2014). Rootstock alleviates PEG-induced water stress in grafted pepper seedlings: physiological responses. *J. Plant Physiol.* 171, 842–851. doi: 10.1016/j.jplph.2014.01.013

Poudyal, D., Akash, M., Khatri, L., Shrestha, D. S., and Uptmoor, R. (2017). Solanum habrochaites introgression line grafted as rootstock in cultivated tomato maintains growth and improves yield under cold and drought stresses. *J. Crop Improvement* 31, 589–607. doi: 10.1080/15427528.2017.1319887

Prinsi, B., Simeoni, F., Galbiati, M., Meggio, F., Tonelli, C., Scienza, A., et al. (2021). Grapevine rootstocks differently affect physiological and molecular responses of the scion under water deficit condition. *Agronomy* 11, 289. doi: 10.3390/agronomy11020289

Proietti, S., Rouphael, Y., Colla, G., Cardarelli, M., De Agazio, M., Zacchini, M., et al. (2008). Fruit quality of mini-watermelon as affected by grafting and irrigation regimes. *J. Sci. Food Agric.* 88, 1107–1114. doi: 10.1002/jsfa.3207

Qamer, Z., Chaudhary, M. T., Du, X., Hinze, L., and Azhar, M. T. (2021). Review of oxidative stress and antioxidative defense mechanisms in *Gossypium hirsutum L.* in response to extreme abiotic conditions. *J. Cotton Res.* 4, 9. doi: 10.1186/s42397-021-00086-4

Qiu, X. M., Sun, Y. Y., Ye, X. Y., and Li, Z. G. (2019). Signaling role of glutamate in plants. *Front. Plant Sci.* 101743. doi: 10.3389/fpls.2019.01743

Rouphael, Y., Cardarelli, M., Colla, G., and Rea, E. (2008). Yield, mineral composition, water relations, and water use efficiency of grafted mini-watermelon plants under deficit irrigation. *Hortscience* 43, 730–736. doi: 10.21273/HORTSCI.43.3.730

Sabir, A., and Kucukbasmaci, A. (2019). Long-term impact of deficit irrigation on the physiology and growth of grapevine cv. 'Prima' grafted on various rootstocks. *Acta Sci. Pol-Hortoru.* 18, 57–70. doi: 10.24326/asphc.2019.4.6

Sánchez-Rodríguez, E., Leyva, R., Constán-Aguilar, C., Romero, L., and Ruiz, J. M. (2012). Grafting under water stress in tomato cherry: improving the fruit yield and quality. *Ann. Appl. Biol.* 161, 302–312. doi: 10.1111/j.1744-7348.2012.00574.x

Sánchez-Rodríguez, E., Leyva, R., Constán-Aguilar, C., Romero, L., and Ruiz, J. M. (2014). How does grafting affect the ionome of cherry tomato plants under water stress? *Soil Sci. Plant Nutr.* 60, 145–155. doi: 10.1080/00380768.2013.870873

Sánchez-Rodríguez, E., Romero, L., and Ruiz, J. M. (2013). Role of grafting in resistance to water stress in tomato plants: Ammonia production and assimilation. *J. Plant Growth Regul.* 32, 831–842. doi: 10.1007/s00344-013-9348-2

Sanchez-Rodriguez, E., Romero, L., and Ruiz, J. M. (2016). Accumulation of free polyamines enhances the antioxidant response in fruits of grafted tomato plants under water stress. *J. Plant Physiol.* 190, 72–78. doi: 10.1016/j.jplph.2015.10.010

Sanchez-Rodriguez, E., Rubio-Wilhelmi Mdel, M., Blasco, B., Leyva, R., Romero, L., and Ruiz, J. M. (2012). Antioxidant response resides in the shoot in reciprocal grafts of drought-tolerant and drought-sensitive cultivars in tomato under water stress. *Plant Sci.* 188, 89–96. doi: 10.1016/j.plantsci.2011.12.019

Santana-Vieira, D. D., Freschi, L., Almeida, L. A., Moraes, D. H., Neves, D. M., Santos, L. M., et al. (2016). Survival strategies of citrus rootstocks subjected to drought. *Sci. Rep.* 6, 38775. doi: 10.1038/srep38775

Sarwat, M., and Tuteja, N. (2017). Hormonal signaling to control stomatal movement during drought stress. *Plant Gene* 11, 143–153. doi: 10.1016/j.plgene.2017.07.007

Savvas, D., Colla, G., Rouphael, Y., and Schwarz, D. (2010). Amelioration of heavy metal and nutrient stress in fruit vegetables by grafting. *Sci. Hortic-Amsterdam* 127, 156–161. doi: 10.1016/j.scienta.2010.09.011

Schneider, J. R., Caverzan, A., and Chavarria, G. (2018). Water deficit stress, ROS involvement, and plant performance. *Arch. Agron. Soil Sci.* 65, 1160–1181. doi: 10.1080/03650340.2018.1556789

Sels, J., Mathys, J., De Coninck, B. M., Cammue, B. P., and De Bolle, M. F. (2008). Plant pathogenesis-related (PR) proteins: a focus on PR peptides. *Plant Physiol. Biochem.* 46, 941–950. doi: 10.1016/j.plaphy.2008.06.011

Seo, M., and Koshiba, T. (2002). Complex regulation of ABA biosynthesis in plants. *Trends Plant Sci.* 7, 41–48. doi: 10.1016/S1360-1385(01)02187-2

Seymen, M., Yavuz, D., Ercan, M., Akbulut, M., Çoklar, H., Kurtar, E. S., et al. (2021). Effect of wild watermelon rootstocks and water stress on chemical properties of watermelon fruit. *Hortic. Environ. Biote.* 62, 411–422. doi: 10.1007/s13580-020-00329-4

Shao, H. B., Chu, L. Y., Jaleel, C. A., and Zhao, C. X. (2008). Water-deficit stress-induced anatomical changes in higher plants. *C. R. Biol.* 331, 215–225. doi: 10.1016/j.crvi.2008.01.002

Sharma, A., Wang, J., Xu, D., Tao, S., Chong, S., Yan, D., et al. (2020). Melatonin regulates the functional components of photosynthesis, antioxidant system, gene expression, and metabolic pathways to induce drought resistance in grafted carya cathayensis plants. *Sci. Total Environ.* 713, 136675. doi: 10.1016/j.scitotenv.2020.136675

Shehata, S. A., Omar, H. S., Elfaidy, A. G. S., El-Sayed, S. S. F., Abuarab, M. E., and Abdeldaym, E. A. (2022). Grafting enhances drought tolerance by regulating stress-responsive gene expression and antioxidant enzyme activities in cucumbers. *BMC Plant Biol.* 22, 408. doi: 10.1186/s12870-022-03791-7

Shen, X., He, J., Ping, Y., Guo, J., Hou, N., Cao, F., et al. (2022). The positive feedback regulatory loop of miR160-auxin response factor 17-HYPONASTIC LEAVES 1 mediates drought tolerance in apple trees. *Plant Physiol.* 188, 1686–1708. doi: 10.1093/plphys/kiab565

Shi, H., Chen, L., Ye, T., Liu, X., Ding, K., and Chan, Z. (2014). Modulation of auxin content in arabidopsis confers improved drought stress resistance. *Plant Physiol. Biochem.* 82, 209–217. doi: 10.1016/j.plaphy.2014.06.008

Shivaraj, S. M., Sharma, Y., Chaudhary, J., Rajora, N., Sharma, S., Thakral, V., et al. (2021). Dynamic role of aquaporin transport system under drought stress in plants. *Environ. Exp. Bot.* 184, 104367. doi: 10.1016/j.envexpbot.2020.104367

Silva, S. F., Miranda, M. T., Costa, V. E., Machado, E. C., and Ribeiro, R. V. (2021). Sink strength of citrus rootstocks under water deficit. *Tree Physiol.* 41, 1372–1383. doi: 10.1093/treephys/tpab008

Silva, V. A., Prado, F. M., Antunes, W. C., Paiva, R. M. C., Ferrão, M. A. G., Andrade, A. C., et al. (2018). Reciprocal grafting between clones with contrasting drought tolerance suggests a key role of abscisic acid in coffee acclimation to drought stress. *Plant Growth Regul.* 85, 221–229. doi: 10.1007/s10725-018-0385-5

Soma, F., Takahashi, F., Yamaguchi-Shinozaki, K., and Shinozaki, K. (2021). Cellular phosphorylation signaling and gene expression in drought stress responses: ABA-dependent and ABA-independent regulatory systems. *Plants (Basel)* 10, 10756. doi: 10.3390/plants10040756

Sousa, A. R., d., O., d. A., E. M., Filho, M. A. C., Costa, M. G. C., Filho, W., et al. (2022). Metabolic responses to drought stress and rehydration in leaves and roots of three citrus scion/rootstock combinations. *Sci. Hortic-Amsterdam* 292. doi: 10.1016/j.scienta.2021.110490

Spiral, J., Ouazzani, S., Vial, N. H., Michaux, S., Barro, L., Darracq, O., et al. (2022). Reciprocal grafting reveals differential metabolic responses between robusta clones with contrasting tolerances to drought. *Agric. Res.* doi: 10.1007/s40003-022-00622-x

Staples, R. C. (2003). A novel gene for rust resistance. *Trends Plant Sci.* 8, 149–151. doi: 10.1016/s1360-1385(03)00030-x

Suchoff, D. H., Gunter, C. C., Schultheis, J. R., Kleinhenz, M. D., and Louws, F. J. (2018). Rootstock effect on grafted tomato transplant shoot and root responses to drying soils. *HortScience* 53, 1586–1592. doi: 10.21273/hortsci13215-18

Sucu, S., Yağcı, A., and Yıldırım, K. (2017). Changes in morphological, physiological traits and enzyme activity of grafted and ungrafted grapevine rootstocks under drought stress. *Erwerbs-Obstbau* 60, 127–136. doi: 10.1007/s10341-017-0345-7

Szabados, L., and Savoure, A. (2010). Proline: a multifunctional amino acid. *Trends Plant Sci.* 15, 89–97. doi: 10.1016/j.tplants.2009.11.009

Takahashi, F., Suzuki, T., Osakabe, Y., Betsuyaku, S., Kondo, Y., Dohmae, N., et al. (2018). A small peptide modulates stomatal control *via* abscisic acid in long-distance signalling. *Nature* 556, 235–238. doi: 10.1038/s41586-018-0009-2

Tanaka, Y., Nose, T., Jikumaru, Y., and Kamiya, Y. (2013). ABA inhibits entry into stomatal-lineage development in arabidopsis leaves. *Plant J.* 74, 448–457. doi: 10.1111/tpj.12136

Tesfahun, W., and Yildiz, F. (2018). A review on: Response of crops to paclobutrazol application. *Cogent Food Agric.* 4, 1525169. doi: 10.1080/23311932.2018.1525169

Thomas, H. R., and Frank, M. H. (2019). Connecting the pieces: uncovering the molecular basis for long-distance communication through plant grafting. *New Phytol.* 223, 582–589. doi: 10.1111/nph.15772

Thomas, H., Van den Broeck, L., Spurney, R., Sozzani, R., and Frank, M. (2021). Gene regulatory networks for compatible versus incompatible grafts identify a role for SlWOX4 during junction formation. *Plant Cell* 34, 535–556. doi: 10.1093/plcell/koab246

Twalla, J. T., Ding, B., Cao, G., Bao, S., Li, M., Chen, X., et al. (2021). Roles of stomata in gramineous crops growth and biomass production. *Cereal Res. Commun.* doi: 10.1007/s42976-021-00216-3

Ul Haq, S., Khan, A., Ali, M., Khattak, A. M., Gai, W. X., Zhang, H. X., et al. (2019). Heat shock proteins: Dynamic biomolecules to counter plant biotic and abiotic stresses. *Int. J. Mol. Sci.* 20, 5321. doi: 10.3390/ijms20215321

Ullah, A., Manghwar, H., Shaban, M., Khan, A. H., Akbar, A., Ali, U., et al. (2018). Phytohormones enhanced drought tolerance in plants: a coping strategy. *Environ. Sci. pollut. Res. Int.* 25, 33103–33118. doi: 10.1007/s11356-018-3364-5

Valverdi, N. A., and Kalcsits, L. (2021). Apple rootstock genotype affects scion responses to water limitations under field conditions. *Acta Physiol. Plant* 43, 97. doi: 10.1007/s11738-021-03266-6

Vincent, D., Lapierre, C., Pollet, B., Cornic, G., Negroni, L., and Zivy, M. (2005). Water deficits affect caffeate O-methyltransferase, lignification, and related enzymes in maize leaves. a proteomic investigation. *Plant Physiol.* 137, 949–960. doi: 10.1104/pp.104.050815

Wang, G., Cai, G., Kong, F., Deng, Y., Ma, N., and Meng, Q. (2014). Overexpression of tomato chloroplast-targeted DnaJ protein enhances tolerance to drought stress and resistance to pseudomonas solanacearum in transgenic tobacco. *Plant Physiol. Biochem.* 82, 95–104. doi: 10.1016/j.plaphy.2014.05.011

Wang, N., Guo, T., Wang, P., Sun, X., Shao, Y. , Jia, X., et al. (2017). *MhYTP1* and *MhYTP2* from apple confer tolerance to multiple abiotic stresses in arabidopsis thaliana. *Front. Plant Sci.* 81367. doi: 10.3389/fpls.2017.01367

Wilkinson, S., and Davies, W. J. (2002). ABA-based chemical signalling: the co-ordination of responses to stress in plants. *Plant Cell Environ.* 25, 195–210. doi: 10.1046/j.0016-8025.2001.00824.x

Wilson, R. H., and Hayer-Hartl, M. (2018). Complex chaperone dependence of rubisco biogenesis. *Biochemistry* 57, 3210–3216. doi: 10.1021/acs.biochem.8b00132

Witte, C. P., Keinath, N., Dubiella, U., Demouliere, R., Seal, A., and Romeis, T. (2010). Tobacco calcium-dependent protein kinases are differentially phosphorylated *in vivo* as part of a kinase cascade that regulates stress response. *J. Biol. Chem.* 285, 9740–9748. doi: 10.1074/jbc.M109.052126

Yang, X., Lu, M., Wang, Y., Wang, Y., Liu, Z., and Chen, S. (2021). Response mechanism of plants to drought stress. *Horticulturae* 7, 50. doi: 10.3390/horticulturae7030050

Yang, L., Perrera, V., Saplaoura, E., Apelt, F., Bahin, M., Kramdi, A., et al. (2019). m(5)C methylation guides systemic transport of messenger RNA over graft junctions in plants. *Curr. Biol.* 29, 2465–2476.e5. doi: 10.1016/j.cub.2019.06.042

Yang, W., Zhang, W., and Wang, X. (2017). Post-translational control of ABA signalling: the roles of protein phosphorylation and ubiquitination. *Plant Biotechnol. J.* 15, 4–14. doi: 10.1111/pbi.12652

Yavuz, D., Seymen, M., Süheri, S., Yavuz, N., Türkmen, Ö., and Kurtar, E. S. (2020). How do rootstocks of citron watermelon (*Citrullus lanatus* var. citroides) affect the yield and quality of watermelon under deficit irrigation? *Agr. Water Manage* 241, 106351. doi: 10.1016/j.agwat.2020.106351

Yildirim, K., Yagci, A., Sucu, S., and Tunc, S. (2018). Responses of grapevine rootstocks to drought through altered root system architecture and root transcriptomic regulations. *Plant Physiol. Biochem.* 127, 256–268. doi: 10.1016/j.plaphy.2018.03.034

Yu, S. G., Kim, J. H., Cho, N. H., Oh, T. R., and Kim, W. T. (2020). Arabidopsis RING E3 ubiquitin ligase JUL1 participates in ABA-mediated microtubule depolymerization, stomatal closure, and tolerance response to drought stress. *Plant J.* 103, 824–842. doi: 10.1111/tpj.14775

Zhang, Z., Cao, B., Gao, S., and Xu, K. (2019a). Grafting improves tomato drought tolerance through enhancing photosynthetic capacity and reducing ROS accumulation. *Protoplasma* 256, 1013–1024. doi: 10.1007/s00709-019-01357-3

Zhang, Z., Cao, B., Li, N., Chen, Z., and Xu, K. (2019b). Comparative transcriptome analysis of the regulation of ABA signaling genes in different rootstock grafted tomato seedlings under drought stress. *Environ. Exp. Bot.* 166, 103814. doi: 10.1016/j.envexpbot.2019.103814

Zhang, Z., Liu, Y., Cao, B., Chen, Z., and Xu, K. (2020). The effectiveness of grafting to improve drought tolerance in tomato. *Plant Growth Regul.* 91, 157–167. doi: 10.1007/s10725-020-00596-2

Zhang, L., Marguerit, E., Rossdeutsch, L., Ollat, N., and Gambetta, G. A. (2016). The influence of grapevine rootstocks on scion growth and drought resistance. *Theor. Exp. Plant Phys.* 28, 143–157. doi: 10.1007/s40626-016-0070-x

Zia, R., Nawaz, M. S., Siddique, M. J., Hakim, S., and Imran, A. (2021). Plant survival under drought stress: Implications, adaptive responses, and integrated rhizosphere management strategy for stress mitigation. *Microbiol. Res.* 242, 126626. doi: 10.1016/j.micres.2020.126626

Glossary

ABA	abscisic acid
ABCG22	ATP-binding cassette subfamily G transporter 22
ACC	ethylene 1-aminocyclopropane-1-carboxylic
AREB/ABF	*ABA-responsive element binding protein/ABA-responsive element binding factor*
ASA	Ascorbate
APX	ascorbate peroxidase
BFRUCT3	*β-fructosidase 3*
BRs	brassinosteroids
Cab	*Chlorophyll a/b binding protein*
CAT	Catalase
CHY1	*Chloroplast β-carotene hydroxylase*
CKs	Cytokinins
CLE25	Clavata3/embryo-surrounding region-related 25
COMT	*Caffeic acid 3-O-methyltransferase*
DEGs	Differentially expressed genes
Dnaj	*Chaperone protein DnaJ*
Dnaj-like B8	*DnaJ-like subfamily B member 8*
DREB2A	*Dehydration-responsive element-binding protein 2 A*
DRM	*Drought-responsive mobile gene*
ERD10C	*Early responsive to dehydration 10C*
ET	Ethylene
FADs	*Fatty acid desaturase enzymes*
GA	Gibberellin
GH3	*Gretchen hagen 3*
GNS1	*Glucan endo-1,3-β-glucosidase*
GPX	glutathione peroxidase
GSH	Glutathione
HMGB	*High mobility group B protein 2*
H_2O	water
H_2O_2	hydrogen peroxide
HSP81	*Heat shock protein 81.4*
HSP70	*70-kDa heat shock protein*
IAA	Indole-3-acetic acid
JA	jasmonic acid
KCS	*3-ketoacyl-CoA synthase*
LEA5	*Late embryogenesis abundant protein 5*
LhcI	*Photosystem I light-harvesting chlorophyll a/b-binding protein*
NCED	*9-cis-epoxycarotenoid dioxygenase*
NDUFB7	*NADH-ubiquinone oxidoreductase B18 subunit*
NRT1/PTR	*Nitrate transporter 1/peptide transporter*
NRX	*Nucleoredoxin*
O_2	oxygen
O^{2-}	superoxide anion
PIP	*Plasma membrane intrinsic proteins*
P5SC	*Δ-1-pyrroline-carboxylate synthase*
POD	Peroxidase
PP2C	*Protein phosphatase 2C*
PR	Pathogenesis-related
psaA	*Photosystem I P700 chlorophyll a apoprotein A1*
psaB	*Photosystem I P700 chlorophyll a apoprotein A2*
psbB	*Photosystem II CP47 reaction center protein*
psbD	*Photosystem II protein D2*
Prx	*Peroxiredoxin*
PYR/PYL	*Pyrabactin resistance1/pyr1-like*
RbcL	*Ribulose-1,5-diphosphate carboxylase/oxygenase large subunit*
RbcS	*Ribulose-1,5-bisphosphate carboxylase/oxygenase small subunit*
RD22	*Responsive to dehydration 22*
ROS	Reactive oxygen species
RSA	Root system architecture
Rubisco	Ribulose-1,5-diphosphate carboxylase/oxygenase
SA	Salicylic acid
SIP1	*Raffinose synthase*
SnRK2	*Sucrose non-fermenting-1-related protein kinase 2*
SPS1F	*Sucrose phosphate synthase 1F*
SOD	Superoxide dismutase
STK	Serine/threonine-protein kinase-transforming protein
SUS3 and 4	*Sucrose synthase 3 and 4*
SWEET14	*Bidirectional sugar transporter*
TIP	*Tonoplast intrinsic protein*
YTPs	*YTH domain-containing RNA binding proteins*

frontiers | Frontiers in Plant Science

TYPE Review
PUBLISHED 19 October 2022
DOI 10.3389/fpls.2022.1002302

Check for updates

OPEN ACCESS

EDITED BY
PingWu Liu,
Hainan University, China

REVIEWED BY
Ling Xu,
Zhejiang Sci-Tech University, China
Agnieszka Kiełbowicz-Matuk,
Institute of Plant Genetics (PAN), Poland
Wen-Cheng Liu,
Henan University, China
Quanle Xu,
Northwest A&F University, China

*CORRESPONDENCE
Mingzhe Sun
sunmingzhe@byau.edu.cn
Xiaoli Sun
csmbl2016@126.com

†These authors have contributed equally to this work

SPECIALTY SECTION
This article was submitted to Plant Abiotic Stress, a section of the journal Frontiers in Plant Science

RECEIVED 25 July 2022
ACCEPTED 29 September 2022
PUBLISHED 19 October 2022

CITATION
Cai X, Jia B, Sun M and Sun X (2022) Insights into the regulation of wild soybean tolerance to salt-alkaline stress. *Front. Plant Sci.* 13:1002302. doi: 10.3389/fpls.2022.1002302

COPYRIGHT
© 2022 Cai, Jia, Sun and Sun. This is an open-access article distributed under the terms of the Creative Commons Attribution License (CC BY). The use, distribution or reproduction in other forums is permitted, provided the original author(s) and the copyright owner(s) are credited and that the original publication in this journal is cited, in accordance with accepted academic practice. No use, distribution or reproduction is permitted which does not comply with these terms.

Insights into the regulation of wild soybean tolerance to salt-alkaline stress

Xiaoxi Cai†, Bowei Jia†, Mingzhe Sun* and Xiaoli Sun*

Crop Stress Molecular Biology Laboratory, College of Agriculture, Heilongjiang Bayi Agricultural University, Daqing, China

Soybean is an important grain and oil crop. In China, there is a great contradiction between soybean supply and demand. China has around 100 million ha of salt-alkaline soil, and at least 10 million could be potentially developed for cultivated land. Therefore, it is an effective way to improve soybean production by breeding salt-alkaline-tolerant soybean cultivars. Compared with wild soybean, cultivated soybean has lost a large number of important genes related to environmental adaptation during the long-term domestication and improvement process. Therefore, it is greatly important to identify the salt-alkaline tolerant genes in wild soybean, and investigate the molecular basis of wild soybean tolerance to salt-alkaline stress. In this review, we summarized the current research regarding the salt-alkaline stress response in wild soybean. The genes involved in the ion balance and ROS scavenging in wild soybean were summarized. Meanwhile, we also introduce key protein kinases and transcription factors that were reported to mediate the salt-alkaline stress response in wild soybean. The findings summarized here will facilitate the molecular breeding of salt-alkaline tolerant soybean cultivars.

KEYWORDS

wild soybean, salt stress, carbonate stress, ion balance, ROS scavenging, protein kinase, transcription factor

Introduction

Soybean is a world-widely grown crop, providing vegetable oils and proteins. Although soybean yield per acre has increased by approximately 40% during the past 20 years, current soybean production in China is still in severe shortage along with the population increase (USDA, 2021). On the other hand, roughly over 6% of the world's soil resources are affected by saline and alkaline (data from GSASmap- https://www.fao.org/global-soil-partnership/gsasmap/en/). It is an effective way to expand the total soybean production by planting salt-alkaline tolerant soybean cultivars in the salt-alkaline soils. Therefore, it is an urgent demand to breed soybean cultivars with salt-alkaline tolerance.

Cultivated soybean (*Glycine max* L. Merr.) is domesticated from wild soybean (*Glycine soja* Siebold & Zucc.). Only approximately 50% of genes in *G. soja* are selected during long-term domestication and improvement, and many important genes related to environmental adaptation are lost (Kofsky et al., 2018). The narrow genetic variation in cultivated soybean seriously restricts the improvement of salt-alkaline stress tolerance. *G. soja* retains a higher level of genetic diversity and better adaptation to harsh environments (Kofsky et al., 2018). An effective way to breed stress-tolerant cultivars is to retrieve the stress tolerant genes from wild soybean and reintroduce them into cultivated soybean.

During the past decades, an increasing number of studies have demonstrated that plant cells were severely damaged by the primary ionic toxicity and secondary oxidative damage under salt-alkaline stress (Das and Roychoudhury, 2014). Therefore, researchers have made many efforts to identify genes involved in ion balancing and ROS scavenging (Zhao et al., 2021). Furthermore, current studies in the model plant Arabidopsis have strongly suggested that protein kinases and transcription factors are of paramount importance in governing the signaling transduction of plant adaptation to salt-alkaline stress (Chen et al., 2021a; Pan et al., 2022).

This review summarized the current research progress regarding the salt-alkaline stress response in *G. soja*. In this review, we summarized the functionally characterized genes in *G. soja* that regulated the capacity to the ion toxicity and ROS damage caused by salt-alkaline stress. We also introduced the protein kinases and transcription factors in *G. soja* that modulated the salt-alkaline tolerance. The findings summarized here will give soybean breeders an overall impression concerning the functional characterization of crucial salt-alkaline tolerant genes in *G. soja*, and will facilitate to illustrate the regulatory mechanism and signaling transduction pathways, as well as the molecular breeding of salt-alkaline tolerant soybean cultivars.

Regulation of ion toxicity under salt-alkaline stress in wild soybean

Under salt stress, ionic toxicity caused by excess Na^+ and Cl^- is the direct and primary damage to plants. Excess Na^+ accumulation in plants further affects the uptake of other ions (such as K^+) and causes osmotic stress, leading to water deficit inside plant cells (Assaha et al., 2017). Hence, balancing cytoplasmic ion status is very important for plants to survive under salt-alkaline stress. In this review, we summarized the genes (Table 1) and regulatory mechanism (Figure 1) of ion balance in *G. soja* response to salt-alkaline stress.

Cation/H^+ exchangers

Cation/H^+ exchangers (CHXs), belonging to the cation/proton antiporter 2 (CPA2) family, are suggested to mediate K^+, Na^+, and H^+ flow (Isayenkov et al., 2020). In 2014, a salt-tolerant gene *Gs/GmCHX1*, the homolog of *AtCHX20*, was identified by whole-genome sequencing of a *G. soja* accession W05, and genotyping-by-sequencing and phenotypic analyses of a recombinant inbred line (RIL) population (Qi et al., 2014). In *G. soja* W05, *GsCHX1* (Glysoja01g005509) encodes a CHX protein with 811 amino acids in length. In *G. max* Williams 82 and C08 (one parent of the RIL population), a Ty1/Copia retrotransposon was inserted into the third exon of *GmCHX1* (Glyma03g32900), resulting in a truncated transcript encoding only 376 residues. In the same year, Guan et al. identified *GmSALT3* (salt tolerance-associated gene on chromosome 3) using the RIL population derived from the salt-tolerant variety Tiefeng 8 and the salt-sensitive variety 85-140 (Guan et al., 2014). In 2016, Do et al. isolated a salt tolerance-related QTL from a Brazilian soybean cultivar FT-Abyara, and named the causal gene as *GmNcl* (Do et al., 2016). Actually, both *GmSALT3*

TABLE 1 Genes involved in ion balance under salt-alkaline stress in wild soybean.

Gene name	Gene ID	ID for *G. max* Homolog	Gene description	Function description
GsCHX1/SALT3/Ncl	Glyso.01G005509	Glyma.03G171600	Cation/H^+ exchanger	It confers salt tolerance in soybean (Guan et al., 2014; Qi et al., 2014; Do et al., 2016; Liu et al., 2016; Lee et al., 2018; Qu et al., 2021).
GsCHX19.3	Glyso.17G039900	Glyma.17G043400	Cation/H^+ exchanger	Its overexpression in Arabidopsis confers salt and bicarbonate alkaline tolerance (Jia et al., 2017).
GmsSOS1	Glyso.08G084400	Glyma.08G092000	Na^+/H^+ antiporter	Its overexpression in Arabidopsis confers salt tolerance (Nie et al., 2015).
GsCLC-c2	Glyso.16G165500	Glyma.16G208400	Chloride channel	Its overexpression in Arabidopsis and soybean composite plants confers chloride/salt tolerance (Wei et al., 2019; Liu et al., 2021b).
GsSLAH3	Glyso.10G192900	Glyma.10G229300	Slow-type anion channel homolog	Its overexpression in Arabidopsis confers bicarbonate alkaline tolerance (Duan et al., 2017).
GsBOR2	Glyso.06G166900	Glyma.06G181900	Boron transporter	Its overexpression in Arabidopsis confers bicarbonate alkaline tolerance (Duan et al., 2018).

Gene ID and ID for *G. max* Homolog were retrieved from the plant genomic resource Phytozome with the *Glycine max* Wm82.a4.v1 and *Glycine soja* v1.1 versions respectively, according to the corresponding information given in the references.

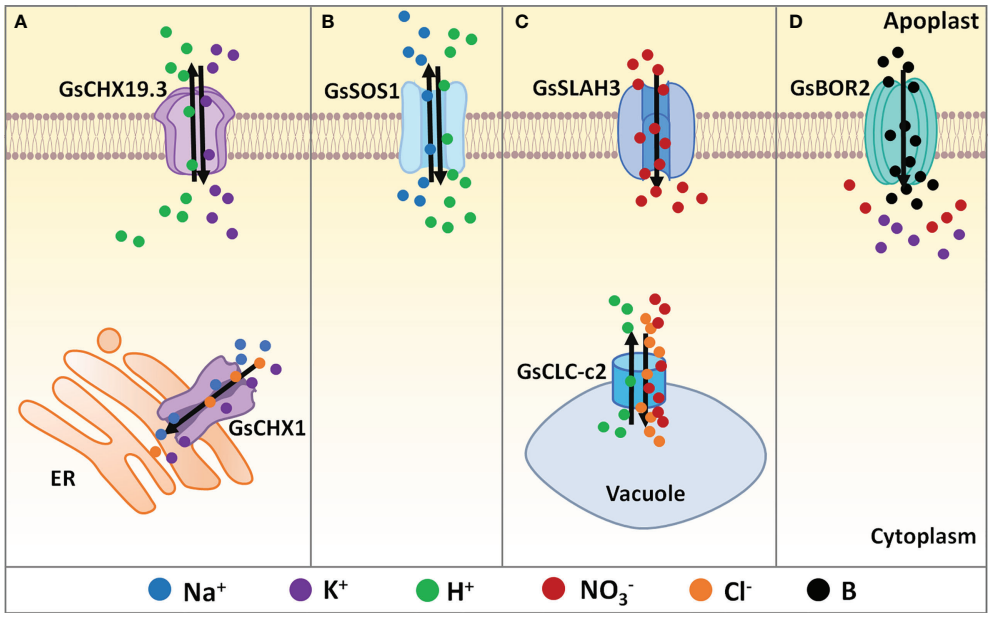


FIGURE 1
Regulation of ion balance under salt-alkaline stress in wild soybean. **(A)** Cation/H^+ exchangers, **(B)** Na^+/H^+ antiporters, **(C)** Anion channels, **(D)** Boron transporters identified in *G. soja* involving in ion balancing under salt-alkaline stress. ER, endoplasmic reticulum. Solid dots with different colors represent different types of ions. Black arrows mean the direction of ion flow across the membrane.

and *GmNcl* are the same gene as *GmCHX1*. Therefore, *GmCHX1/SALT3/Ncl* is a critical determinant of salt tolerance in soybean. *GmCHX1/SALT3/Ncl* contributed to salt tolerance at the seedling stage and conferred improved soybean yield in the field by maintaining a higher seed weight (Do et al., 2016; Liu et al., 2016). However, *GmCHX1/SALT3/Ncl* does not affect the seedling emergence rate or early vigor under salt stress (Liu et al., 2016). Therefore, identifying the key genes improving the seed germination vigor in saline soil is of great importance for salt-tolerant soybean breeding with *GmCHX1/SALT3/Ncl*.

In Guan et al. study, 9 haplotypes of *GmCHX1/SALT3/Ncl*, including 2 salt-tolerant haplotypes and 7 salt-sensitive haplotypes were identified by sequencing 31 soybean landraces and 22 wild soybeans (Guan et al., 2014). In another work, SNPs within the coding region and 2-kb promoter region of *Gs/GmCHX1* were highly conserved in the 12 salt-tolerant accessions but varied among the 11 salt-sensitive accessions (Qi et al., 2014). Recently, 40 different haplotypes were identified in 216 *G. max* and *G. soja* accessions from Korea, China, and Japan (Lee et al., 2018). In summary, the consequence of these SNPs in salt-sensitive accessions is either the dysfunction of Gs/GmCHX1 protein or the deficient levels of *Gs/GmCHX1* transcripts. However, it is still unknown whether there is a regulation of *Gs/GmCHX1* at the post-transcriptional level. Besides, the regulatory mechanism of Gs/GmCHX1 transporting activity also remains obscure.

As a CHX family protein, *GmCHX1/SALT3/Ncl* was found to affect Na^+, K^+, and Cl^- accumulation under salt stress (Figure 1A). Upon salt stress, Na^+ accumulation in stems and leaves in the salt-tolerant soybean accessions was significantly less than that in the salt-sensitive accessions (Guan et al., 2014; Do et al., 2016; Liu et al., 2016). The salt-tolerant soybean accumulated less K^+ in leaves and stems than the salt-sensitive line (Do et al., 2016). Interestingly, the salt-tolerant NIL line accumulated less Cl^- in the leaves and more Cl^- in the roots prior to any difference in Na^+ (Do et al., 2016; Liu et al., 2016). A recent study showed that *GmCHX1/SALT3/Ncl* expression contributed to net influx and accumulation of Na^+, K^+, and Cl^- in *Xenopus laevis* oocytes (Qu et al., 2021). In soybean shoots, *GmCHX1/SALT3/Ncl* mediated Na^+ exclusion by restricting the net xylem loading of Na^+, and contributed to Cl^- exclusion by re-translocating Cl^- back into roots *via* the phloem. GmCHX1/SALT3/Ncl protein is localized in the endoplasmic reticulum (ER) in plant cells (Guan et al., 2014; Qi et al., 2014). It is still unknown how the ER-localized GmCHX1/SALT3/Ncl affects the Na^+ and Cl^- exclusion across PM. One possible explanation is that the ER-localized GmCHX1/SALT3/Ncl influences ion gradients across the PM through currently unknown downstream effects. GmCHX1/SALT3/Ncl is also possible to mediate Na^+ and Cl^- exclusion *via* an ER-derived vesicle trafficking system.

Similarly, *GsCHX19.3* is a plasma membrane localized CHX isolated from bicarbonate stress tolerant *G. soja* G07256. Overexpression of *GsCHX19.3* in Arabidopsis resulted in higher K^+ content under normal growth conditions, and lower

Na^+ accumulation under $NaHCO_3$ treatment (Jia et al., 2017), indicating the role of *GsCHX19.3* in both K^+ uptake and Na^+ excretion (Figure 1A). In Jia et al. study, 34 *GsCHXs* were identified and phylogenetically clustered into five groups (Group I-V). Only five Group IVa members (*GsCHX18.1*, *GsCHX18.2*, *GsCHX19.2*, *GsCHX19.3*, and *GsCHX20*) exhibited enhanced expression at the transcript level under carbonate alkaline stress, indicating the involvement of *GsCHX18/19/20s* in salt-alkaline stress response. Therefore, further studies are needed to identify the key cis-elements and transcription factors that trigger the expression of *GsCHX18/19/20s* under salt-alkaline stress.

Na^+/H^+ antiporters

Na^+/H^+ antiporters (NHXs) belong to the cation/proton antiporter 1 (CPA1) family. They play critical roles in the exclusion of cytoplasmic Na^+ mediated by plasma membrane NHXs and compartmentalization of vacuole Na^+ driven by vacuole membrane NHXs (Jia et al., 2018). In Arabidopsis, the plasma membrane SOS1 (Salt Overlay Sensitive 1), also called AtNHX7, is the major transporter removing intracellular Na^+ in exchange for extracellular H^+. Upon salt stress, SOS3 senses the calcium signal induced by salt stress and interacts with the protein kinase SOS2, thereby activating its kinase activity and recruiting it to the plasma membrane. SOS2 then activates SOS1 Na^+/H^+ reverse transport activity to exclude cytoplasmic Na^+ (Zhu, 2002).

Until now, only one NHX gene *GmsSOS1* from *G. soja* has been functionally reported to modulate salt tolerance (Nie et al., 2015). The *GmsSOS1* gene was cloned from *G. max* and *G. soja* and encoded a plasma membrane NHX protein. Ectopic expression of *GmsSOS1* in the wild type Arabidopsis, as well as the *atsos1-1* mutant deleting 14bp (1330-1343bp) (Shi et al., 2000), improved the salt stress tolerance by decreasing Na^+ absorption in roots and transportation in shoots (Figure 1A). Considering the importance of NHXs in the regulation of cytoplasmic Na^+ concentration, more attention should be paid to identifying *G. soja* NHX genes and illustrating the main SOS signaling pathway that contributes to salt tolerance.

Anion channels

In addition to cation toxicity caused by Na^+, Cl^- is the major factor resulting in the anionic toxicity under salt stress. Excessive Cl^- in cells disturbs the NO_3^- uptake (Rosales et al., 2020). Therefore, under salt stress, plants must simultaneously cope with cation and anionic toxicity.

The chloride channels (CLCs) could simultaneously transport Cl^- and NO_3^- (Jentsch and Pusch, 2018). There are eight CLC genes in soybean, among which the tonoplast-localized CLC-c2 showed different expression patterns between the salt-sensitive *G. max* N23674 and salt-tolerant *G. soja* BB52 (Wei et al., 2019). Under salt stress, *GsCLC-c2* overexpression in soybean composite plants increased Cl^- and Na^+ content in roots and reduced Cl^- and Na^+ accumulation in stems and leaves. Furthermore, *GsCLC-c2* overexpression in soybean composite plants also resulted in higher content of NO_3^- in shoots, without significant changes in K^+ accumulation (Figure 1B). Consequently, *GsCLC-c2* contributes to salt stress tolerance by increasing NO_3^-/Cl^- and K^+/Na^+ ratios, especially in shoots (Wei et al., 2019; Liu et al., 2021b). In the *GsCLC-c2* RNAi composite plants, Cl^- content was significantly decreased in roots but increased in stems and leaves, while the NO_3^- content was decreased in roots, stems, and leaves, resulting in the increased Cl^-/NO_3^- ratios (Liu et al., 2021b). In addition, *GsCLC-c2* overexpression in the wild type and *atclc-c* mutant Arabidopsis also led to increased Cl^-/NO_3^- and K^+/Na^+ ratios in roots under salt stress. The K^+/Na^+ ratio in shoots of *GsCLC-c2* transgenic Arabidopsis was increased under salt stress, however, the Cl^-/NO_3^- ratio was not altered (Liu et al., 2021b). Researchers also suggested that GsCLC-c2 could transport both Cl^- and NO_3^- by using a two-electrode voltage clamp on *Xenopus laevis* oocytes (Wei et al., 2019). Therefore, *GsCLC-c2* plays a key positive role in regulating *G. soja* salt-alkaline tolerance by simultaneously transporting Cl^- and NO_3^-. More importantly, *CLC-c2* is the only gene with non-synonymous changes between *G. max* N23674 and *G. soja* BB52. It is important to investigate the sequence variations of the *CLC-c2* gene in wild and cultivated soybean populations and identify the salt-alkaline tolerant haplotypes.

Besides CLCs, slow anion channels (SLACs) and SLAC homologs (SLAHs) also play critical roles in anion transport (Barbier-Brygoo et al., 2011). Most characterized SLAC/SLAHs are NO_3^- conductive. An alkaline stress-induced SLAH gene *GsSLAH3*, the homologous gene to *AtSLAH3*, was identified in the bicarbonate ($NaHCO_3$) stress tolerant *G. soja* G07256 based on RNA-seq data. Transgenic Arabidopsis over-expressing *GsSLAH3* displayed higher tolerance to HCO_3^- stress ($NaHCO_3$ and $KHCO_3$) rather than high pH stress, by increasing NO_3^- accumulation in shoots (Duan et al., 2017). Consistently, under $NaHCO_3$ treatment, the NO_3^- concentrations in the T-DNA insertion Arabidopsis mutants *atslah3-1* and *atslah3-2* were relatively lower than WT (Zheng et al., 2015) (Figure 1B). It is possible that *GsSLAH3* specifically controls the response to carbonate salt-alkaline stress, not high pH stress, by mediating NO_3^- transport. However, direct evidence supporting the conductivity of GsSLAH3 to NO_3^- is still missing. Further studies should also analyze the sequence and expression differences of *SLAH* genes between *G. soja* and *G. max*.

Boron transporters

Boron (B) deficiency decreases NO_3^- uptake and increases K^+ leakage across the plasma membrane. Plant B transporters

(BORs) belong to the solute carrier (SLC4) family, which is homologous to the human bicarbonate transporter-related protein HsBTR1, and each BOR protein harbors a sodium-coupled bicarbonate transporter domain (Saouros et al., 2021). A recent study reported that a *G. soja* BOR gene *GsBOR2* could improve the tolerance to bicarbonate stress ($NaHCO_3$ and $KHCO_3$) rather than high pH stress (Duan et al., 2018). Functional complementation showed that *GsBOR2* restored the sensitivity of *Scbor1* mutant yeasts to H_3BO_3 treatment, suggesting the involvement of boron and BORs in salt-alkaline stress response (Duan et al., 2018) (Figure 1C). However, direct evidence is required to characterize whether BORs affect NO_3^- uptake and K^+ leakage under bicarbonate stress.

Till now, only these six *G. soja* genes encoding ion transporters have been functionally characterized to maintain ion balance and alleviate ion toxicity under salt-alkaline stress. Among them, GmCHX1 has been suggested to transport Na^+, K^+, and Cl^- (Qu et al., 2021), and GsCLC-c2 transported Cl^- and NO_3^- (Wei et al., 2019). Even though the regulation of *GsCHX19.3, GmsSOS1, GsSLAH3*, and *GsBOR2* on the cytoplasmic ion accumulation has been studied through functional complementation in yeast mutants and quantification analyses of ion contents in transgenic plants, direct biochemical evidence is still lacking to verify their transporting properties. Therefore, techniques monitoring ion fluctuation in real-time, for example, non-invasive micro-test technology and two photon-total internal refraction fluorescence microscopy, should be applied to directly verify the transporting capability of ion transporters in *G. soja*. Besides, there are still a few points that need further detailed investigation. Firstly, it is imperative to investigate whether these ion transporter genes could improve soybean yields in the salt-alkaline fields. Secondly, further studies are needed to reveal the regulatory mechanism of the activity of these ion transporters, for example, identifying the protein kinases that trigger their transporting activity and the transcription factors that promote their transcription.

ROS signaling and scavenging under salt-alkaline stress in wild soybean

Under salt-alkaline stress, ion imbalance promotes the generation and accumulation of reactive oxygen species (ROS) in plant cells. ROS play dual roles in plant response to salt-alkaline stress. At low concentrations, it can serve as a signaling molecule, which activates downstream signal transduction under salt-alkaline stress. However, ROS accumulation at high concentrations leads to oxidative damage or apoptotic death and damages plant cells (Liu et al., 2021c). Plants have developed enzymatic and nonenzymatic antioxidant defense systems to protect against oxidative damage. For now, a serial of genes involved in ROS signaling and scavenging have been transcriptionally and functionally characterized to regulate salt-alkaline stress tolerance in *G. soja* (Table 2; Figure 2).

ROS-activated signaling under salt-alkaline stress in wild soybean

Previous studies have demonstrated the positive role of ROS in salt-alkaline stress response by activating the downstream signaling. Exogenous H_2O_2 application could improve salt tolerance in rice and maize (Uchida et al., 2002; Azevedo Neto et al., 2005). ROS-production deficiency *Arabidopsis* mutants *atrbohd* and *atrbohf* are sensitive to salt stress (Ben Rejeb et al., 2015). Recently, it has been reported that H_2O_2 could sulfenylate TSB1 (tryptophan synthase β subunit 1) to increase ABA accumulation, thus increasing salt stress tolerance in Arabidopsis (Liu Y. L. et al., 2022). A recent study in *G. max* reported that a ROS-involving positive feed-forward loop acted as a signal amplifier in salt stress response (Li et al., 2019). Overexpression of a NAC transcription factor *GmSIN1* (SALT INDUCED NAC1) in soybean promoted root growth and salt tolerance and increased yield under salt stress. *GmSIN1* upregulated expression of *GmRbohB* (Respiratory burst oxidase homolog B) genes to generate ROS, and ROS further induced *GmSIN1* expression under salt stress (Li et al., 2019). Even though researchers have unraveled the ROS-mediated regulatory mechanism in plant response to salt stress, its role is rarely reported in *G. soja*. A previous study reported that a methionine sulfoxide reductase B (MSRB) gene in *G. soja GsMSRB5a* could regulate alkaline stress tolerance by modifying the expression of ROS signaling genes (Sun et al., 2016). Therefore, more studies are needed to clarify the positive regulatory mechanism mediated by ROS on salt-alkaline tolerance in *G. soja*.

Antioxidant enzymes

Enzymes that detoxify ROS include superoxide dismutases (SODs), catalases (CATs), peroxidases (PODs), glutathione peroxidases (GPXs), ascorbate peroxidases (APXs), monodehydroascorbate reductases (MDHARs), dehydroascorbate reductases (DHARs), and glutathione reductases (GRs). Among them, SODs serve as the front line of antioxidant defense by catalyzing O_2^- radicals into H_2O_2 and molecular oxygen (O_2). A recent study showed that *G. soja* W05 had a total of 13 SOD genes (*GsoSODs*), and the expression of three *GsoSODs* (*GsoSOD6.1, GsoSOD11.1*, and *GsoSOD20.1*) has been found to respond to salt stress *via* qRT-PCR analyses (Aleem et al., 2022). Under 250mM NaCl treatment, *GsoSOD11.1* showed continuously up-regulated expression (Figure 2A). The increase in *GsoSODs* expression will help to remove O_2^- radicals.

TABLE 2 Genes involved in ROS scavenging under salt-alkaline stress in wild soybean.

Gene name	Gene ID	ID for *G. max* Homolog	Gene description	Function description
GsoSOD6.1	Glyso.06G132100	Glyma.06G144500	Superoxide dismutase	Its expression responds to salt stress (Aleem et al., 2022).
GsoSOD11.1	Glyso.11G155700	Glyma.11G192700	Superoxide dismutase	Its expression responds to salt stress (Aleem et al., 2022).
GsoSOD20.1	Glyso.20G036200	Glyma.20G050800	Superoxide dismutase	Its expression responds to salt stress (Aleem et al., 2022).
GsoGPX1.1	Glyso.01G178300	Glyma.01G219400	Glutathione peroxidase	Its expression responds to salt stress (Aleem et al., 2022).
GsoGPX10.1	Glyso.10G022800	Glyma.10G024600	Glutathione peroxidase	Its expression responds to salt stress (Aleem et al., 2022).
GsoGPX17.1	Glyso.17G189500	Glyma.17G223900	Glutathione peroxidase	Its expression responds to salt stress (Aleem et al., 2022).
GsPRX9	Glyso.14G062700	Glyma.14G070800	Secretory peroxidase	Its overexpression in soybean composite plants confers salt tolerance (Jin et al., 2019).
GsSAMS2	Glyso.17G036200	Glyma.17G039100	S-Adenosyl-L-Methionine synthetase	Its overexpression in alfalfa confers salt tolerance (Hua et al., 2012).
GsGST	Glyso.01G081200	Glyma.01G106000	Tau class glutathione S-transferase	Its overexpression in tobacco confers salt tolerance (Ji et al., 2010).
GsGST13/ GSTU13	Glyso.03G056100	Glyma.03G073702	Tau class glutathione S-transferase	Its overexpression in alfalfa confers salt and bicarbonate alkaline tolerance (Wu et al., 2014; Jia et al., 2015).
GsGST14	Glyso.05G135100	Glyma.05G161600	Tau class glutathione S-transferase	Its overexpression in alfalfa confers salt and bicarbonate alkaline tolerance (Wang et al., 2012b; Lin et al., 2013).
GsGST19	Glyso.02G157600	Glyma.02G187200	Tau class glutathione S-transferase	Its overexpression in alfalfa confers salt and bicarbonate alkaline tolerance (Wang et al., 2012b).
GsGSTL1	Glyso.03G139400	Glyma.03G176300	Lambda class glutathione S-transferase	Its overexpression in tobacco BY-2 cells and Arabidopsis confers salt tolerance (Chan, 2014)
GsMIOX1a	Glyso.08G182700	Glyma.08G199300	Myo-inositol oxygenase	Its overexpression in Arabidopsis confers bicarbonate alkaline tolerance (Chen et al., 2015a).
GsMIPS2	Glyso.18G020300	Glyma.18G022100	L-myo-inositol-1-phosphate synthase	Its overexpression in Arabidopsis confers bicarbonate alkaline tolerance (Chen et al., 2015b).

Gene ID and ID for *G. max* Homolog were retrieved from the plant genomic resource Phytozome with the *Glycine max* Wm82.a4.v1 and *Glycine soja* v1.1 versions respectively, according to the corresponding information given in the references.

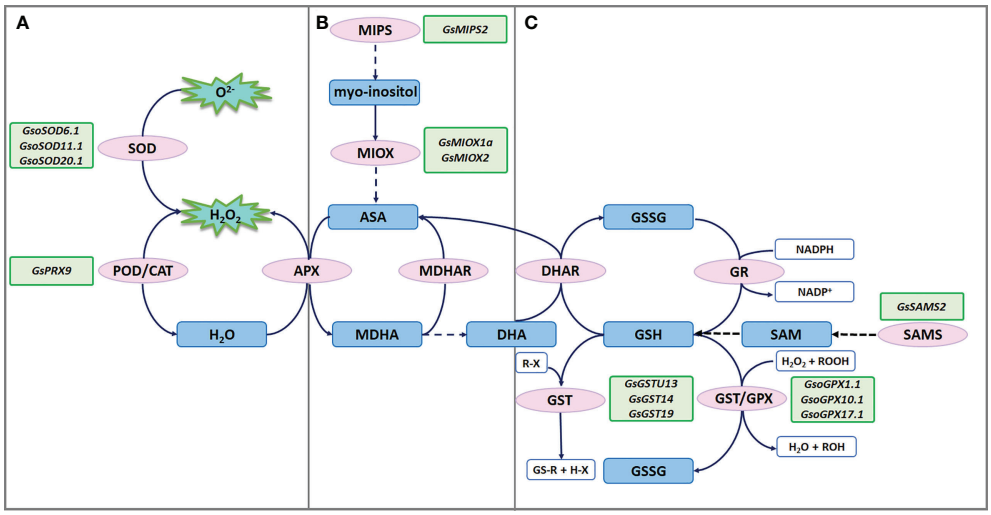


FIGURE 2
ROS scavenging under salt-alkaline stress in wild soybean. **(A)** SODs and PRXs in enzymatic antioxidant defense system. **(B)** MIPSs and MIOXs responsible for AsA biosynthesis. **(C)** GSTs, GPXs and SAMSs responsible for glutathione mediated nonenzymatic antioxidant defense system.

H_2O_2 is subsequently removed by CATs and PODs. In plants, PODs are divided into three classes: class I (Ascorbate peroxidase, APXs), class II (lignin peroxidases), and class III (secretory peroxidases, PRXs). Class III PRXs are bifunctional enzymes that could scavenge ROS and also produce ROS. A recent study suggested that overexpression of salt stress-induced *G. soja* PRX gene *GsPRX9* in soybean composite plants improved salt tolerance by increasing both POD and SOD activity, and glutathione levels (Jin et al., 2019) (Figure 2A). The coding sequence of *GsPRX9* is identical to that of *GmPRX9*. Interestingly, in *G. max*, *GmPRX9* expression showed a significantly higher increase in the salt-tolerant varieties than the salt-sensitive varieties after salt treatment. These findings imply that the expression level of *PRX9* is related to the salt tolerance of soybean. Therefore, it will be interesting to check the sequences of the *PRX9* promoter in the soybean natural population to identify the haplotype that confers higher expression levels of *PRX9* and higher salt tolerance.

Even though the expression response and genetic function of *CAT* and *APX* genes under salt-alkaline stress have not been reported in *G. soja*, and CATs and APXs indeed play crucial roles in ROS scavenging in wild soybean response to salt-alkaline stress. For example, compared with a cultivated soybean ZH13, the wild soybean BB52 grown in coastal saline land in the Yellow River Delta displayed higher CAT and APX activities under salt stress (Chen et al., 2013). Therefore, it is essential to identify *CATs* and *APXs* genes in *G. soja* that could improve the tolerance to salt-alkaline stress.

Ascorbic acid

Ascorbic acid (AsA) contributes to abiotic stress tolerance by scavenging ROS through the AsA-GSH cycle. Myo-inositol is one of the main precursors of AsA biosynthesis, while L-myo-inositol-1-phosphate synthases (MIPSs) are rate-limiting enzymes in myo-inositol biosynthesis (Donahue et al., 2010). There are three *MIPS* genes in soybean. According to the public RNA-seq data of the salt-alkaline tolerant *G. soja* 07256, *GsMIPS2* expression was dramatically increased by about 20 folds at 3 h treated with 50 mM $NaHCO_3$, which was further verified *via* qRT-PCR analyses. Transcript levels of *GsMIPS3* was decreased, while *GsMIPS1* expression was not changed by $NaHCO_3$ treatment. Consistently, *GsMIPS2* overexpression in Arabidopsis conferred increased tolerance to $NaHCO_3$ and NaCl stresses, and the T-DNA insertion Arabidopsis mutant *atmips2* displayed reduced tolerance (Chen et al., 2015b; Nisa, 2016) (Figure 2B).

Myo-inositol oxygenases (MIOXs) catalyze the conversion of myo-inositol into D-glucuronic acid (D-GlcUA), which is finally oxidized into AsA (Endres and Tenhaken, 2009). A previous study reported that there were 5 MIOX genes in wild soybean and *GsMIOX1a* expression displayed a noticeable increase at 6 h treated with 50 mM $NaHCO_3$ (Chen et al., 2015a). Interestingly, expression of *GsMIOX1a* was dramatically induced by $NaHCO_3$ treatment in *G. soja* accessions (G07256 and G50109), but not in *G. max* accessions (Suinong 28 and Hefeng 55). This difference indicates that *GsMIOX1a* might be a key factor for *G. soja* response to $NaHCO_3$ stress. Genetic evidence suggests that *GsMIOX1a* overexpression in Arabidopsis improved POD activity and increased the bicarbonate alkaline stress tolerance (Chen et al., 2015a) (Figure 2B). Taken together, it is absolute that AsA biosynthesis might contribute to soybean tolerance to salt-alkaline stress, possibly *via* the AsA-GSH cycle.

Glutathione

Glutathione is one important component of the nonenzymatic antioxidant system, having two forms reduced glutathione (GSH) and oxidized glutathione (GSSG). The glutathione peroxidases (GPXs) catalyze the oxidation of GSH to produce GSSG, reducing H_2O_2 or organic hydroperoxide to H_2O and alcohol, which will protect cells against ROS-mediated oxidative damage. A recent study showed that *G. soja* W05 has 13 GPX (*GsoGPXs*) genes, three of which were responsive to salt stress (Aleem et al., 2022). Under 250mM NaCl treatment, *GsoGPX10.1* showed continuously up-regulated expression (Figure 2C). Even though no genetic evidence supporting the function of *GsoGPXs* in regulating salt tolerance has been given, it is easy to speculate that the increase in *GsoGPXs* transcript levels will facilitate the removal of H_2O_2 or organic hydroperoxide.

S-Adenosyl-L-Methionine Synthetases (SAMSs) catalyze the synthesis of S-Adenosyl-L-Methionine (SAM), which generates glutathione (GSH) through sulfur transfer. Hence, the activity of SAMSs is closely related to the GSH content in plant cells (Hasanuzzaman et al., 2017). It has been reported that ectopic expression of a *G. soja* SAMS gene *GsSAMS2* driven by a stress-inducible promoter RD29A conferred salt tolerance in *Medicago sativa* (Hua et al., 2012) (Figure 2C). It will be an easy way to improve the GSH content by overexpressing *SAMS* genes, which can help plants to cope with ROS damage.

The glutathione S-transferases (GSTs) catalyze the conjugation of GSH to the electrophilic groups of a large variety of hydrophobic molecules to detoxify cells. Under abiotic stress, GSTs detoxify the lipid hydroperoxides generated in membrane peroxidation. GSTs could be grouped into six classes, and most GSTs in plants belong to the phi (GSTF) and tau (GSTU) classes. Several studies have revealed the regulatory function of GSTUs in *G. soja* response to salt-alkaline stress (Figure 2C). A previous study isolated a GSTU gene *GsGST* from the cDNA library of salt-treated *G. soja* 50109 seedlings, and overexpression of *GsGST* in *Nicotiana tabacum* significantly improved the salt and drought tolerance (Ji et al., 2010). Furthermore, three *G. soja* GSTUs *GsGST13* (also named

GsGSTU13), *GsGST14* and *GsGST19* were found to contribute to higher tolerance under both salt (NaCl), and bicarbonate ($NaHCO_3$) stresses (Wang et al., 2012a; Wang et al., 2012b; Jia et al., 2015). In another study, overexpression of *GsGSTU24* and *GsGSTU42* in soybean hairy root composite plants and transgenic Arabidopsis seedlings significantly enhanced antioxidant ability to detoxify ROS damage under submergence stress (Li et al., 2020). Experimental data are needed to determine whether *GsGSTU24* and *GsGSTU42* regulate salt-alkaline tolerance. In addition, a *lambda* class GST gene *GSTL1* was suggested to be induced by salt stress by over 7 folds in *G. soja* W05, compared to less than 4 folds in *G. max* C08 (Chan, 2014). *GSTL1* expression in tobacco BY-2 cells and Arabidopsis increased survival rates under salt stress by reducing ROS accumulation. In summary, *GST* genes are important candidates for improving salt-alkaline tolerance *via* transgene technology.

Flavonoids

Flavonoids are a group of secondary metabolites derived from the phenylpropanoid pathway, including flavonol, flavanol, flavone, isoflavone, flavanone, proanthocyanidins, and anthocyanin (Liu et al., 2021d). Current studies have demonstrated that flavonoids, as antioxidants, are closely associated with salt-alkaline stress tolerance in soybean. For example, the knockout of a flavone synthase (FNS) gene *GmFNSII* in soybean hairy roots reduced the salt tolerance. *GmMYB183* activated the expression of *GmCYP81E11* (Cytochrome P450 monooxygenase) and increased the accumulation of monohydroxy B-ring flavonoids, which negatively regulates soybean tolerance to salinity (Pi et al., 2019). Another MYB transcription factor *GmMYB173* directly activated the transcription of *GmCHS5* and contributed to salt tolerance by enhancing the accumulation of dihydroxy B-ring flavonoids (Pi et al., 2018). Recently, researchers have found that soybean HSFB2b, a class B heat shock factor, improved salt tolerance by promoting flavonoid biosynthesis (Bian et al., 2020). Four haplotypes of HSFB2b in its promoter region were identified among the population consisting of 38 wild soybean and 113 cultivated soybean accessions, and haplotypes II and III from salt-tolerant wild soybean display higher promoter activity under salt stress. The distribution frequency of haplotype III, which showed the highest promoter activity, in cultivated soybeans was very low. Therefore, it will be an effective way to introduce the haplotype III promoter of *GsHSFB2b* into cultivated soybean to breed salt-tolerant cultivars.

ROS balance is regulated by generation, removal, and transportation. Currently, most studies in *G. soja* focused on the regulation of ROS scavenging under salt-alkaline stress. Genes responsible for ROS generation in *G. soja* have not been reported until now. Furthermore, little is known about the positive role of ROS-activated signaling pathways in *G. soja*. Therefore, future studies regarding ROS-mediated regulation on salt-alkaline response should focus on two points. Firstly, respiratory burst oxidase homologues (Rboh) genes in *G. soja* should be systematically investigated to uncover the mechanism driving the reduction of ROS generation under salt-alkaline stress. Secondly, identification of target genes that are directly activated by ROS at low concentrations is urgently needed to understand the positive role of ROS by serving as signaling molecules under salt-alkaline stress.

Protein kinases involved in salt-alkaline stress response in wild soybean

Protein kinases (PKs) transfer phosphate groups from adenosine triphosphate (ATP) to serine, threonine, or tyrosine residues of substrate proteins, thereby directly affect substrates' function by modifying their activity, 3D structure, subcellular localization, or protein stability. The PK superfamily is one of the largest and most highly conserved families in plants. There are 2166 putative PK genes in soybean genome, representing 4.67% of all protein-coding genes (Liu et al., 2015). PKs could be classified into different families based on sequence similarity and domain structure within and outside the catalytic domains. In *G. soja*, several kinase genes from the RLKs (receptor like kinases), MAPKs (mitogen-activated protein kinases), and SnRKs (sucrose non-fermenting1-related protein kinases) families have been reported to play important roles in signal transduction under salt-alkaline stress (Table 3; Figure 3).

Receptor like kinases

RLKs consist of an extracellular domain to receive signal molecules, a transmembrane domain and a cytoplasmic kinase catalytic domain. RLKs could be further classified into different groups, for example, LRR-RLK (leucine-rich repeat RLK), LecRLK (Lectin RLK), RLCK (cytoplasmic RLK). In soybean, 1418 genes were identified as RLKs (Liu et al., 2015), including 467 LRR-RLKs (Zhou et al., 2016) and 185 LecRLKs (Liu et al., 2018). Until now, only a few *G. soja* RLKs were reported to involve in salt-alkaline stress (Figure 3A).

GsSRK encodes a LecRLK protein from *G. soja*, whose extracellular domain consists of an N-terminal signal peptide, a G-type lectin domain, an S-locus-glycop domain, and a PAN-AP domain (Sun et al., 2013b). *GsSRK* expression was greatly and rapidly induced by ABA, salt, and drought stresses. *GsSRK* overexpression in Arabidopsis enhanced salt stress tolerance and promoted seed yields under salt stress (Sun et al., 2013b). Furthermore, ectopic expression of the full-length (*GsSRK-f*) and

TABLE 3 The genes encoding protein kinases involved in regulating salt-alkaline stress response in wild soybean.

Gene name	Gene ID	ID for *G. max* Homolog	Gene description	Function description
GsSRK	Glyso.06G220200	Glyma.06G255900	Lectin receptor like kinase	Its overexpression in Arabidopsis and alfalfa confers salt tolerance (Sun et al., 2013b; Sun et al., 2018).
GsRLCK	Glyso.17G108900	Glyma.17G117800	Receptor like cytoplasmic kinase	Its overexpression in Arabidopsis confers salt and drought tolerance (Sun et al., 2013a).
GsCBRLK/CRCK1d	Glyso.18G058500	Glyma.18G064100	Receptor like cytoplasmic kinase	Its overexpression in soybean, alfalfa, rice and Arabidopsis confers salt and bicarbonate alkaline tolerance (Bai et al., 2013; Zhao et al., 2014; Ji et al., 2015; Cai et al., 2020).
GsCRCK1a	Glyso.02G185500	Glyma.02G224000	Receptor like cytoplasmic kinase	Its expression is induced by salt and bicarbonate alkaline stresses (Sun et al., 2016).
GsCRCK1b	Glyso.11G182100	Glyma.11G178300	Receptor like cytoplasmic kinase	Its expression is induced by salt and bicarbonate alkaline stresses (Feng et al., 2020).
GsCRCK1c	Glyso.14G151000	Glyma.14G190700	Receptor like cytoplasmic kinase	Its expression is induced by salt and bicarbonate alkaline stresses (Zhu et al., 2012a).
GsSnRK1.1	Glyso.13G037400	Glyma.13G060400	SnRK1 kinase	Its overexpression in soybean composite plants confers salt tolerance (Feng et al., 2020).
GsSnRK1.2	Glyso.18G205100	Glyma.18G262900	SnRK1 kinase	Its expression is induced by salt and bicarbonate alkaline stresses (Chen et al., 2021a).
GsAPK	Glyso.01G164500	Glyma.01G204200	SnRK2b kinase	Its overexpression in Arabidopsis confers salt tolerance (Yang et al., 2012).
GsMAPK4	Glyso.01G180800	Glyma.01G222000	MAPK kinase	Its overexpression in soybean confers salt tolerance (Qiu et al., 2019).

Gene ID and ID for *G. max* Homolog were retrieved from the plant genomic resource Phytozome with the *Glycine max* Wm82.a4.v1 and *Glycine soja* v1.1 versions respectively, according to the corresponding information given in the references.

truncated *GsSRK* deleting the G-type lectin domain (*GsSRK-t*) in alfalfa both increased salt tolerance by improving the capacity in ion homeostasis, ROS scavenging, and osmotic regulation. Interestingly, *GsSRK-t* transgenic lines were more tolerant to salt stress than *GsSRK-f* lines, showing more branches and higher fresh weight under salt stress. However, no difference in the physiological indices under salt stress was detected between *GsSRK-f* and *GsSRK-t* transgenic lines (Sun et al., 2018). Interestingly, overexpression of *GsSRK-t*, but not *GsSRK-f*, caused more branches and shorter shoots, indicating a potential role of the extracellular G-type lectin domain in regulating plant architecture. Therefore, *GsSRK* is an ideal target to improve yield under salt stress.

Current studies also demonstrated the important roles of *G. soja* RLCKs in regulating salt-alkaline stress tolerance. *GsRLCK* encodes a plasma membrane localized RLCK, containing a conserved catalytic domain and two transmembrane domains at the N-terminus (Sun et al., 2013a). The expression of *GsRLCK* was induced by ABA, salt, alkaline, and drought stresses. *GsRLCK* overexpression in Arabidopsis increased salt and drought tolerance by promoting the expression of salt responsive marker genes. Furthermore, a group of calcium/calmodulin-binding receptor-like cytoplasmic kinases (CRCKs) in *G. soja* (GsCRCK1a-d) were reported to function in salt-alkaline stress response. GsCRCK1s, without any extracellular or transmembrane domain, contained only intracellular catalytic domains whose amino acid sequences are highly conserved. The N-terminal sequences of GsCRCK1s were quite variable, named the variable domain. This domain has been demonstrated to fulfill a crucial role in mediating the protein-protein interaction and subcellular localization (Sun et al., 2016; Sun et al., 2019; Sun et al., 2021). It has been suggested that GsCRCK1d, also named GsCBRLK (*G. soja* calcium/calmodulin-binding receptor-like kinase), localized on plasma membrane in plant cells. The N-terminal variable domain was responsible for its plasma membrane localization (Yang et al., 2010; Sun et al., 2021). *GsCBRLK* was initially characterized to confer salt and carbonate alkaline tolerance by overexpressing in Arabidopsis (Yang et al., 2010; Sun et al., 2016). Further studies verified its positive regulation on soybean (Ji et al., 2015), alfalfa (Bai et al., 2013; Zhao et al., 2014), and rice (Cai et al., 2020) tolerance to both salt and carbonate alkaline stresses.

Current studies have identified the interacting partners of GsCBRLK and illustrated the functional mechanism and signal transduction mediated by GsCBRLK in salt-alkaline stress response (Yang et al., 2010; Sun et al., 2014; Sun et al., 2016; Sun et al., 2019; Sun et al., 2021). Upon salt-alkaline stress, cytoplasmic free Ca^{2+} ($[Ca^{2+}]$cyt) was rapidly accumulated in a short time, and this $[Ca^{2+}]$cyt oscillation was sensed by calmodulins (CaMs). The Ca^{2+}/CaM complex activated GsCBRLK kinase activity by directly interacting with CaM and the CaM binding domain within GsCBRLK (Yang et al., 2010). Recently, a group of BET1-like soluble NSF attachment protein receptor (SNARE) proteins (GsBET11a/b/c and GsBET12a/b)

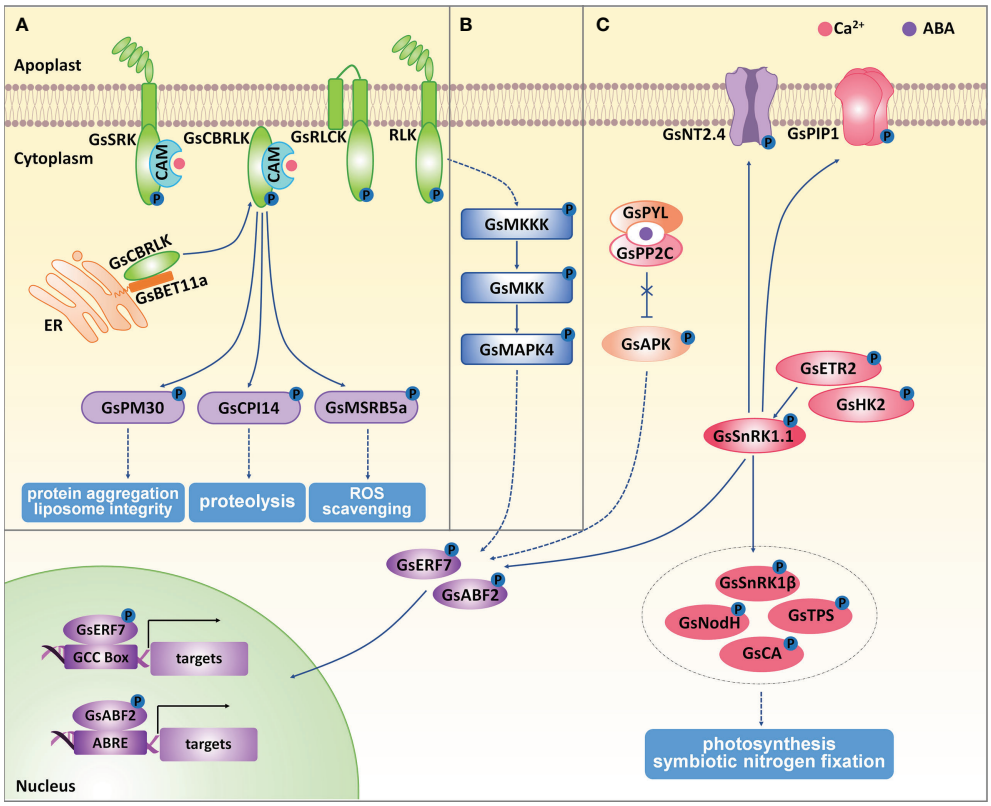


FIGURE 3
The regulation of protein kinases on wild soybean response to salt-alkaline stress. **(A)** Receptor like kinases, **(B)** MAPK kinases, **(C)** SnRK kinases mediated stress response in *G. soja* under salt-alkaline stress. ER, endoplasmic reticulum. Solid lines represent direct physical interaction, and dotted lines represent indirect interaction or results. Arrows represent positive effects, and lines ending with a short bar indicate negative effects.

were suggested to mediate the plasma membrane localization of GsCBRLK by directly interacting with the N-terminal variable domain of GsCBRLK, and contributed to salt stress tolerance (Sun et al., 2021). For now, three types of GsCBRLK interacting partners, including a cysteine proteinase inhibitor GsCPI14 (Sun et al., 2014), several group 3A late embryogenesis abundant (LEA) proteins (Sun et al., 2019), methionine sulfoxide reductase B (MSRB) subfamily proteins (Sun et al., 2016), have been identified as potential downstream substrates of GsCBRLK. Among them, *GsCPI14* was suggested to regulate the proteolysis process and confer the tolerance to carbonate alkaline stress. The group 3A LEA gene *GsPM30* was found to improve salt tolerance, possibly by preventing protein aggregation and maintaining liposome integrity. *GsMSRB5a* overexpression in Arabidopsis could increase the tolerance to carbonate alkaline stress by enhancing the ROS scavenging capacity. Even though no biochemical evidence has been given to show the direct phosphorylation of GsCBRLK on these proteins, there are two pieces of evidence supporting that GsCBRLK might work upstream of GsMSRBs. Firstly, *GsCBRLK* overexpression in Arabidopsis, soybean and alfalfa conferred tolerance to both salt and carbonate alkaline stresses, while *GsMSRB5a* only activated carbonate alkaline stress responses when overexpressed in Arabidopsis. Secondly, the total MSR enzyme activity was obviously increased in both *GsCBRLK* and *GsMSRB5a* transgenic lines. Therefore, future studies are needed to determine the phosphorylation of GsCBRLK on its substrates. Moreover, it will be helpful to identify the upstream regulators that directly interact with and activate GsCBRLK.

MAPK kinases

The MAPK kinase cascade has been well documented to play important roles in abiotic stress response in plants (Lin et al., 2021). A MAPK module generally comprises three kinases: a MAPKKK (MAPK kinase), a MKK (MAPK kinase), and a MAPK. In this module, MAPKKKs phosphorylate and activate MKKs, and MKKs then phosphorylate and activate MAPKs. In soybean, there are 38 MAPKs, 11 MKKs, and 150 MKKKs. According to the amino acid sequences, these 38 MAPKs could

be clustered into four groups (Group A-D) (Neupane et al., 2013). Even though a number of researches have strongly demonstrated the important roles of MAPK pathway in abiotic stress response in Arabidopsis and rice, only two MAPK kinases in *G. max*, *GMK1/GmMPK6* (Group D) (Im et al., 2012; Im et al., 2021) and *GmMMK1* (Group B) (Liao et al., 2021), have been functionally characterized to regulate salt tolerance. By association analysis of *GmMKK1* sequence variations and salt tolerance in the natural soybean population, researchers showed that the sequence variation in *GmMKK1* promoter was the main reason for the functional differences of *GmMKK1* in the natural population in terms of the germination rates under salt treatment. In *G. soja*, *GsMAPK4* (Group B) was the only MAPK kinase reported to participate in salt stress response. *GsMAPK4* expression was up-regulated under salt stress, and overexpression of *GsMAPK4* in *G. max* significantly improved the tolerance to salt stress (Qiu et al., 2019) (Figure 3B). However, the upstream MKKs and MKKKs of *GsMAPK4* are still unknown. Therefore, it is vital to identify the core MAPK components in soybean response to salt-alkaline stress.

SnRK kinases

In plants, SnRK family kinases are classified into SnRK1, SnRK2, and SnRK3 subfamilies (Wang et al., 2019b). In *G. soja*, there are four SnRK1 genes named *GsSnRK1.1-1.4* (Chen et al., 2021b). Among them, the expression of *GsSnRK1.1* and *GsSnRK1.2* were induced by both salt (NaCl) and bicarbonate alkaline ($NaHCO_3$) stresses, while *GsSnRK1.3* and *GsSnRK1.4* were not affected by either salt or bicarbonate alkaline stress. By using the *Agrobacterium rhizogenes*-mediated transformation of soybean hairy roots, *GsSnRK1* (identical to *GsSnRK1.1*) overexpression contributed to higher salt tolerance (Feng et al., 2020). Researchers have identified the putative substrates of GsSnRK1 by using the yeast two-hybrid assays (Song et al., 2019) and the quantitative phosphoproteomics technology (Li et al., 2022) (Figure 3C). Phosphorylation assays found that GsSnRK1 phosphorylated plasma membrane-localized GsNT2.4 (Nitrate transporter 2.4) and GsPIP1 (Plasma membrane intrinsic protein 1), which might be involved in the nitrate and water uptake under salt-stress. GsSnRK1β (SnRK1 beta subunit), GsNodH (Sulfotransferase NodH), GsTPS (Alpha, alpha-trehalose-phosphate synthase) and GsCA (Carbonic anhydrase) were also phosphorylated by GsSnRK1, suggesting the possible role of GsSnRK1 in the regulation of photosynthesis and symbiotic nitrogen fixation. Furthermore, two transcription factors GsERF7 (ethylene-responsive factor 7) and GsABF2 (ABRE-binding bZIP factor 2) were also demonstrated to be phosphorylation substrates of GsSnRK1 (Li et al., 2022). The phosphorylation of GsERF7 by GsSnRK1 could facilitate its translocation from the cytoplasm to the nucleus and enhance its transactivation activity. GsERF7 could bind the GCC cis-acting element and up-regulate the expression levels of abiotic stress-responsive and hormone synthetic genes. *GsERF7* overexpression, especially co-overexpression with GsSnRK1, could significantly improve soybean tolerance to salt and bicarbonate alkaline stresses (Feng et al., 2020). In addition, two phytohormone-related histidine kinases GsHK2 (Histidine Kinase 2-like) and GsETR2 (Ethylene receptor 2-like), whose C-terminal kinase domain interacted with GsSnRK1, were suggested to phosphorylate GsSnRK1.1 in plant cells (Song et al., 2019). In the future, more genetic and physiological experiments are needed to clearly show the regulatory function of these GsSnRK1 interacting partners in salt-alkaline stress response.

SnRK2 kinases have been well-demonstrated as core components of ABA-mediated stress signaling. An SnRK2b-type kinase from *G. soja*, GsAPK, was found to contribute to salt stress tolerance when ectopically expressed in Arabidopsis (Yang et al., 2012). GsAPK exhibited ABA-activated and Ca^{2+}-independent kinase activity (Figure 3C). The first abscisic acid-activated and Ca^{2+}-independent protein kinase (AAPK) was identified in the fava bean (Li and Assmann, 1996). AtSnRK2.6/OST1 (Open stomatal 1) is the homologous protein to fava bean AAPK, and also displayed ABA-activated and Ca^{2+}-independent kinase activity (Maszkowska et al., 2021). It is possible that the negative regulator PP2Cs was inhibited upon ABA treatment, thereby resulting in the successful activation of GsAPK. As expected, *GsAPK* overexpression Arabidopsis displayed higher ABA insensitivity, suggesting that *GsAPK* regulated salt tolerance *via* the ABA dependent signaling pathway. In Arabidopsis, SnRK2.2, SnRK2.3, and SnRK2.6 acted as redundant ABA-activated SnRK2s and functioned together in ABA-mediated stress response (Nakashima et al., 2009). There are 22 SnRK2 kinases in soybean (Zhao et al., 2017). Therefore, more work is needed for the functional characterization of soybean *SnRK2* genes in salt-alkaline stress.

In summary, current research has characterized the function of several protein kinase genes, including *GsSRK*, *GsRLCK*, *GsCRCK1d*, *GsSnRK1*, *GsAPK2*, and *GsMPK4*, in regulating salt-alkaline tolerance. Several studies have identified interacting partners of GsCRCK1d and GsSnRK1 to illustrate their regulatory role in salt-alkaline stress signal transduction. However, more work is needed to depict the regulatory network in which PKs occupy a core connecting role. Based on the current reports in *G. soja*, some interesting hypotheses are needed to verify. For example, it is an interesting work to determine whether these functionally characterized PKs could phosphorylate the ion transporters or antioxidant enzymes reported in *G. soja* to mediate the salt-alkaline stress responses. Besides, a multi-year filed trial is needed to evaluate the potential application of these *G. soja* PK genes in improving soybean yields on salt-alkaline fields.

Transcription factors regulating salt-alkaline stress response in wild soybean

Transcription factors (TFs) are key regulators of transcriptional changes and core components of signal transduction in plant response to abiotic stress. Researchers have identified a great deal of TFs in soybean genome, which belong to different families, such as APETALA2/ethylene-responsive factors (AP2/ERF), TIFY, WRKY, homeodomain leucine zipper (HD-Zip), basic helix-loop-helix (bHLH), Cys2/His2-type zinc finger (C2H2), NAC (no apical meristem (NAM), *Arabidopsis thaliana* transcription activation factor (ATAF1/2) and cup-shaped cotyledon (CUC2)). Up to now, genetic evidence has been reported to show the function of AP2/ERFs, TIFYs, WRKYs, and NACs in *G. soja* response to salt-alkaline stress (Table 4; Figure 4).

AP2/ERF transcription factors

The AP2/ERF family TFs are characterized by an AP2 DNA binding domain, consisting of 60 highly conserved amino acids. The AP2/ERF family in plants could be divided into five major subfamilies, AP2, ERF, RAV (Related to Abscisic acid insensitive 3/Viviparous 1), DREB (Dehydration-Responsive Element Binding), and Soloist (Xie et al., 2019). According to a recent study, the soybean genome contains 301 *AP2/ERF* genes, among which 153 were classified into the ERF subfamily (Wang H. et al., 2022a). In *G. soja*, only three ERF subfamily TFs (*GsERF7*, *GsERF71* and, *GsERF6*) have been suggested to participate in salt-alkaline stress response (Figure 4A). GsERF7, belonging to the ERF subfamily, was identified as a phosphorylation substrate of GsSnRK1 kinase, and the phosphorylation of GsERF7 on S36 was necessary for its nucleus localization and transactivation activity (Feng et al., 2020). Transformation of *GsERF7* in soybean hairy roots improved the dry weight of composite

TABLE 4 The genes encoding transcription factors involved in regulating salt-alkaline stress response in wild soybean.

Gene name	Gene ID	ID for *G. max* Homologs	Gene description	Function description
GsERF6	Glyso.05G057200	Glyma.05G063500	ERF subfamily	Its overexpression in Arabidopsis confers bicarbonate alkaline tolerance (Yu et al., 2016a).
GsERF71	Glyso.02G015000	Glyma.02G016100	ERF subfamily	Its overexpression in Arabidopsis confers bicarbonate alkaline tolerance (Yu et al., 2017).
GsERF7	Glyso.16G011200	Glyma.16G012600	ERF subfamily	Its overexpression in soybean transgenic hairy roots confers salt and bicarbonate alkaline tolerance (Feng et al., 2020).
GsDREB3b	Glyso.04G093800	Glyma.04G103900	DREB subfamily	Its overexpression in soybean transgenic hairy roots confers salt tolerance (Hou et al., 2022).
GsDREB1	Glyso.01G150800	Glyma.01G188600	DREB subfamily	(Hu et al., 2007)
GsDREB2	Glyso.06G038100	Glyma.06G042100	DREB subfamily	Overexpression of GsDREB2 deleting the negative regulatory domain in Arabidopsis confers salt tolerance (Cai et al., 2018).
GsTIFY10a	Glyso.15G161400	Glyma.15G179600	JAZ subfamily	Its overexpression in Arabidopsis and alfalfa confers bicarbonate alkaline tolerance (Zhu et al., 2011; Zhu et al., 2014).
GsTIFY10e/JAZ2	Glyso.01G164700	Glyma.01G204400	JAZ subfamily	Its overexpression in Arabidopsis and soybean confers bicarbonate alkaline tolerance (Zhu et al., 2012a; Zhao et al., 2020).
GsTIFY11b	Glyso.16G008900	Glyma.16G010000	JAZ subfamily	Its overexpression in Arabidopsis decreases bicarbonate alkaline tolerance (Zhu et al., 2012a).
GsWRKY15	Glyso.05G175600	Glyma.05G207100	group II WRKY	Its overexpression in alfalfa confers bicarbonate alkaline tolerance (Zhu et al., 2017).
GsWRKY20	Glyso.08G020100	Glyma.08G021900	group III WRKY	Its overexpression in alfalfa confers salt tolerance (Tang et al., 2014).
GsbZIP33	Glyso.03G179600	Glyma.03G219300	subfamily S bZIP	Its overexpression in Arabidopsis decreases salt tolerance (Cai et al., 2011a).
GsbZIP67	Glyso.08G248900	Glyma.08G282202	subfamily S bZIP	Its overexpression in alfalfa confers bicarbonate alkaline tolerance (Wu et al., 2018).
GsNAC20	Glyso.13G012100	Glyma.13G030900	NAC	Its overexpression in Arabidopsis decreases salt tolerance (Cai et al., 2011b).
GsNAC019	Glyso.13G233900	Glyma.13G279900	NAC	Its overexpression in Arabidopsis confers bicarbonate alkaline tolerance (Cao et al., 2017).
Gshdz4	Glyso.11G063700	Glyma.11G069400	HD-ZIP	Its overexpression in Arabidopsis confers bicarbonate alkaline tolerance (Cao et al., 2016).
GsHSFB2b	Glyso.11G023200	Glyma.11G025700	Class B HSF	It contributes to salt tolerance by promoting flavonoid biosynthesis (Bian et al., 2020).
GsMYB15	Glyso.12G163900	Glyma.12G199200	R2R3-MYB	Its overexpression in alfalfa confers salt tolerance (Shen et al., 2018).
GsZFP1	Glyso.10G251500	Glyma.10G295200	C2H2 zinc finger	Its overexpression in alfalfa confers salt tolerance (Tang et al., 2013).

Gene ID and ID for *G. max* Homolog were retrieved from the plant genomic resource Phytozome with the *Glycine max* Wm82.a4.v1 and *Glycine soja* v1.1 versions respectively, according to the corresponding information given in the references.

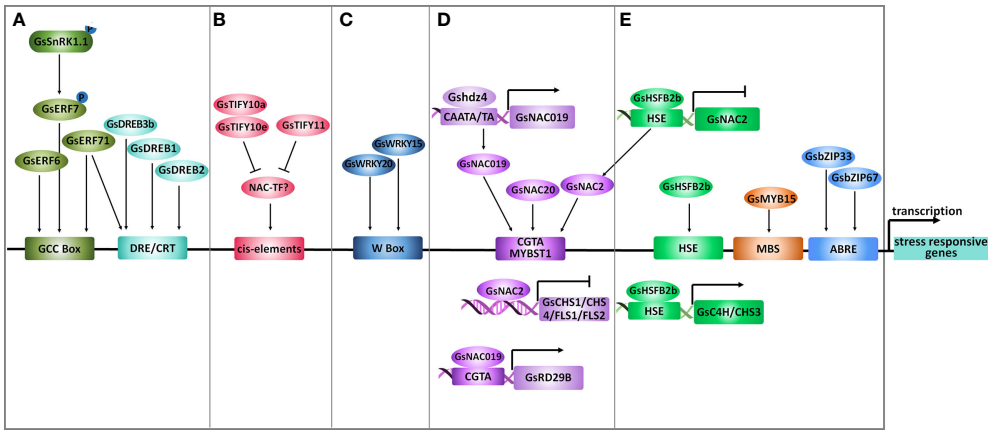


FIGURE 4
Transcriptional regulation under salt-alkaline stress in wild soybean. **(A)** AP2/ERFs, **(B)** TIFYs, **(C)** WRKYs, **(D)** NACs and **(E)** other transcription factors mediating the transcriptional response of *G. soja* to salt-alkaline stress. Arrows represent positive effects, and lines ending with a short bar indicate negative effects.

soybean plants under salt stress. At the same time co-transformation of *GsERF7* and *GsSnRK1* further promoted the tolerance of composite soybean to salt and bicarbonate alkaline stress. *GsERF71* and *GsERF6* also encode ERF subfamily TFs (Yu et al., 2016a; Yu et al., 2017). By overexpressing in Arabidopsis, *GsERF71* and *GsERF6* were demonstrated to specifically confer plant tolerance to bicarbonate ($NaHCO_3$ and $KHCO_3$) alkaline stress, but not to high pH stress caused by KOH. Both GsERF71 and GsERF6 showed nucleus localization and transactivation activity, and GsERF71 was suggested to bind the GCC box (core sequence AGCCGCC). Interestingly, under bicarbonate stress, *GsERF71* overexpression in Arabidopsis could up-regulate *AHA2* (Arabidopsis H^+-ATPase 2) expression to facilitate the neutralization of rhizosphere pH and increase the expression of auxin biosynthesis and transporting genes to promote auxin accumulation in roots (Yu et al., 2016a; Yu et al., 2017).

The dehydration-responsive element-binding (DREB) TFs are classified as a subfamily of the AP2/ERF family and have been well-documented to modulate multiple abiotic stress responses. There are 103 *DREB* genes in the soybean genome. Recently, a DREB transcription factor DREB3b was identified to contribute to salt stress tolerance of *G. soja* by combining RNA-sequencing and population genetics analysis (Hou et al., 2022) (Figure 4A). Among the 103 soybean *DREB* genes, 24 showed differential expression under salt stress, including 14 up-regulated and 10 down-regulated genes. Out of the 14 up-regulated *DREBs*, 9 displayed natural sequence variation detected by a panel of 424 accessions comprised of 85 wild soybeans, 153 landraces, and 186 cultivars. The natural variation in *DREB3a* and *DREB3b* is statistically related to differences in salt tolerance, and *DREB3b*, undergoes artificial selection during soybean domestication. Soybean plants carrying the *G. soja DREB3b* allele ($DREB3b^{39Del}$) are more salt tolerant than those containing the reference genome allele ($DREB3b^{Ref}$). Consistently, $DREB3b^{39Del}$ improved salt tolerance more than $DREB3b^{Ref}$ in transgenic soybean hairy roots. An InDel marker was developed to identify the $DREB3b^{39Del}$ allele, and could facilitate the molecular breeding of salt-tolerant soybean varieties in the future. In 2007, Hu et al. also found a Gypsy-like retrotransposon in the 5' upstream region of *GsDREB1* (GenBank Accession EF051460.1) of individuals among the saline population of wild soybean (Hu et al., 2007). Therefore, these two *DREB* genes are likely targets for molecular breeding to improve soybean salt-alkaline tolerance.

Cai et al. reported that *GsDREB2* deleting the negative regulatory domain (NRD, amino acid residues 140-204) confers salt tolerance in transgenic Arabidopsis, while the full-length *GsDREB2* could not (Cai et al., 2018). The NRD negatively controlled the transactivation ability and DRE element (core sequence A/GCCGAC) binding affinity of GsDREB2, thereby inhibited the function of *GsDREB2* in stress response (Figure 4A). Similarly, in Arabidopsis, deletion of the NRD (residues 136 and 165) within AtDREB2A could transform it to a constitutively active form (Sakuma et al., 2006), and the NRD is important for AtDREB2A protein degradation *via* the BPM-CUL3 E3 ligase (Morimoto et al., 2017). In this context, it will be a good choice for soybean breeding through gene manipulation of *DREB2s* by deleting the NRD domain to improve its regulatory effect on salt-alkaline stress tolerance.

TIFY transcription factors

The TIFY family TFs are characterized by a conserved TIFY motif (TIFF/YXG) and have been demonstrated to widely

participate in plant response to various abiotic stresses (Singh and Mukhopadhyay, 2021; Liu W. C. et al., 2022). The TIFY family was divided into *TIFY*, Jasmonate ZIM (JAZ), ZIM-like (ZML), and PEAPOD (PPD) subfamilies. A previous genome-wide analysis identified 34 *TIFY* genes in *G. soja* (Zhu et al., 2013), and a recent study reported 38 *TIFY* genes in *G. max* (Liu X. et al., 2022). In *G. soja*, *GsTIFY10s* (10a, 10b, 10c, 10d, 10e, and 10f) and *GsTIFY11s* (11a and 11b) shared the highest sequence identity and were clustered together in the JAZ subfamily. Notably, all *GsTIFY10/11s* were dramatically up-regulated at the early stage of $NaHCO_3$ treatment (Zhu et al., 2013) (Figure 4B). Among them, overexpression of *GsTIFY10* (identical to *GsTIFY10a*) and *GsJAZ2* (identical to *GsTIFY10e*) in Arabidopsis improved the tolerance to both salt (NaCl) and bicarbonate ($NaHCO_3$) alkaline stress (Zhu et al., 2011; Zhu et al., 2012b). The positive regulation of *GsTIFY10a* and *GsTIFY10e* on bicarbonate alkaline tolerance was further verified by overexpressing in alfalfa (Zhu et al., 2014) and soybean (Zhao et al., 2020), respectively. Recently, a study in *G. max* showed that *GmTIFY10s* expression displayed an apparent response to abiotic stresses, and overexpression of *GmTIFY10e* and *GmTIFY10g* in Arabidopsis and soybean improved salt tolerance (Liu Y. L. et al., 2022). In summary, the *GsTIFY10* genes are key positive regulators of soybean tolerance to salt-alkaline stress. Intriguingly, even though *GsTIFY11b* was highly homologous to *GsTIFY10s*, its overexpression in Arabidopsis resulted in an obvious decrease in salt tolerance (Zhu et al., 2012a). *GsTIFY10s* and *GsTIFY11s* may regulate different signaling pathways under salt-alkaline stress.

Further research is needed to illustrate the regulatory mechanism mediated by *GsTIFY10/11s*. The TIFY proteins generally localize in the nucleus and are considered to be transcriptional repressors even though without a DNA binding domain. Both GsTIFY10a and GsTIFY10e were localized to the nucleus, and neither showed transcriptional activity in yeasts. All *G. soja* TIFY10/11 proteins contain a TIFY domain and a Jas domain. The TIFY domain has been found to mediate homo- and hetero-dimerization of TIFYs and protein interaction with other TFs, such as MYCs. GsTIFY10a could form homodimers or heterodimers with GsTIFY10e. Therefore, screening the interacting TFs of GsTIFY10s is extremely important to understand the *GsTIFY10s*-mediated responsive mechanism under salt-alkaline stress. Besides, more experiments are needed to investigate the background molecular basis to reveal the opposite function between *GsTIFY10s* and *GsTIFY11s* in salt-alkaline stress.

WRKY transcription factors

The WRKY family TFs are characterized by a conserved DNA-binding domain that harbors the WRKYGQK heptapeptide followed by a C2H2 or C2HC zinc finger. WRKY TFs specifically recognize and bind to the W-Box (core sequence TTGAC) to regulate gene transcription. Several studies have focused on the genome-wide analysis of soybean WRKY genes and their response to abiotic stress (Song et al., 2016; Yu et al., 2016b). The soybean genome contains around 180 genes encoding WRKY transcription factors, which were classified into three groups (Group I-III). Until now, only one *WRKY* gene in *G. soja*, *GsWRKY20* (group III) has been reported to be involved in salt-alkaline stress response (Figure 4C). *GsWRKY20* conferred drought tolerance when overexpressing in Arabidopsis *via* an ABA-dependent signaling pathway and by increasing the thickness of the cuticle (Luo et al., 2013a; Tang et al., 2014). Overexpression of *GsWRKY20* and *GsWRKY15* in alfalfa also increased tolerance to salt stress and bicarbonate alkaline stress, respectively (Tang et al., 2014; Zhu et al., 2017). Notably, expression of *GsWRKY20* also resulted in earlier flowering (Luo et al., 2013b), which is an effective strategy for avoiding adverse environmental stress. These studies strongly suggested the multiple regulatory roles of *GsWRKY20* in stress response, which makes *GsWRKY20* a perfect target for soybean molecular breeding to improve the tolerance to diverse abiotic stress simultaneously. In addition, a *G. soja* group III WRKY transcription factor *GsWRKY57* was also suggested to contribute to drought tolerance (Wang et al., 2019a). Considering the high conservation between *GsWRKY20* and *GsWRKY57*, it is possible that *GsWRKY57* also acts as a positive regulator of salt tolerance.

NAC transcription factors

The plant-specific NAC family is one of the largest TF families, with 226 members in soybean (Hussain et al., 2017). A number of studies have shown that NACs play important roles in the salt-alkaline stress response in plants. Two *NAC* genes in *G. soja* have been suggested to be involved in salt-alkaline stress response. A recent study reported that a NAC family gene *NAC2* functioned downstream of a class B heat shock factor HSFB2b to negatively regulate salt tolerance (Bian et al., 2020). Overexpression of the *NAC2* gene in soybean hairy roots decreased salt tolerance. Under salt stress, *GsHSFB2b* could promote flavonoid biosynthesis by directly inhibiting *GsNAC2*, which repressed the expression of *GsCHS1/CHS4/FLS1/FLS2* (Figure 4D). In addition, *GsHSFB2b* can also directly bind to the promoter of *GsC4H* and *GsCHS3* and activate their expression to trigger the flavonoid biosynthesis pathway.

In addition, the Gshdz4-GsNAC019-GsRD29B module was reported to confer tolerance to bicarbonate ($NaHCO_3$ and $KHCO_3$) alkaline stress but not to high pH stress caused by KOH (Cao et al., 2016; Cao et al., 2017). Gshdz4 binds to the CAATA/TA motif in the *GsNAC019* promoter region and activates the expression of *GsNAC019*; thereby, *GsNAC019* could possibly bind to the CGTA core sequence in the

GsRD29B promoter (Figure 4D). However, further evidence is needed to confirm some details in this module. There is still no genetic data supporting the *GsRD29B* regulation on bicarbonate stress tolerance. Further experiments, for example, EMSA or ChiP-qPCR, are required to verify the binding affinity of Gshdz4 to the *GsNAC019* promoter, and the binding and regulation of GsNAC019 to *GsRD29B*.

It is widely accepted that transcription factors function downstream of protein kinases in the signal transduction network in response to salt-alkaline stress. Phosphorylation is critical for the subcellular localization, DNA binding, and transcriptional activity of transcription factors. Till now, fourteen *G. soja* TF genes have been functionally characterized to participate in salt-alkaline stress response. However, only GsERF7 has been suggested to be directedly targeted and phosphorylated by GsSnRK1. Therefore, identifying protein kinases that interact with and phosphorylate these reported transcription factors in *G. soja* will greatly facilitate to unravel the transcriptional regulation under salt-alkaline stress. Moreover, downstream genes that are directly targeted and transcriptionally regulated by these *G. soja* transcription factors also need to be identified to establish the transcriptionally regulatory network under salt-alkaline stress.

Conclusions and future prospects

Soybean is one of the most vital beans in the world, providing high-quality vegetable protein, edible oil, and industrial raw materials. Under the background of repeated COVID-19 and the increasing worldwide population, the demand for soybean is increasing day by day. Therefore, it is urgently demanded to improve the soybean production, especially in China. However, its yield is greatly restricted by adverse environmental stresses. Compared with cultivated soybean, *G. soja* retains much higher genetic diversity and displays much higher salt-alkaline stress tolerance. Therefore, *G. soja* is considered as genetic reservoir for breeding new salt-alkaline tolerant soybean cultivars with profitable agronomic traits (Kofsky et al., 2018).

Over the years, researchers have demonstrated that the regulation of ion balance and ROS scavenging is critical for wild soybean to survive on saline-alkaline soil. Genes involved in ion uptake, exclusion, and transport, as well as ROS signaling, and scavenging, have been functionally characterized in *G. soja*. Furthermore, regulatory components of signal transduction pathways, including protein kinases and transcription factors were also revealed. However, these *G. soja* genes were functionally characterized mainly by ectopically expressed in the model plant Arabidopsis or transiently expressed in soybean hairy roots. Considering the potential dysfunction of ectopic expression and functional redundancy of homologues genes, functional characterization of *G. soja* genes in future studies should directly be conducted in transgenic soybean plants.

Although current studies have depicted the roles of some protein kinases, transcription factors and functional genes (such as antioxidant enzymes and ion channels) in salt-alkaline stress, few studies focus on the genetic interplay and protein interaction of these regulators. Therefore, the molecular mechanism and signal pathways of soybean response to salt-alkaline stress are still vague. To facilitate the soybean breeding by multigene pyramiding breeding technology, further studies should be concentrated on characterizing the genetic interplay and protein interaction of these genes to construct the signal transduction pathways of soybean salt-alkaline stress response.

Phytohormones, especially ABA, play key roles in regulating plant tolerance to salt-alkaline stress. Current research has well-illustrated the core components of the hormone signal transduction pathway in plants and has demonstrated the regulation of hormone signaling genes on the tolerance to salt-alkaline stress (Fang et al., 2021; Wang N. et al., 2022b). In *G. soja*, several genes were characterized to modulate salt-alkaline tolerance *via* hormone-dependent signaling pathways. For instance, the expression of ABA-induced genes was up-regulated in *GsWRKY20* and *GsCBRLK* transgenic plants under salt-alkaline treatment (Yang et al., 2010; Tang et al., 2014). *GsTIFY10a* and *GsTIFY10e* mediated the sensitivity to MeJA treatment by suppressing the expression of JA responsive and biosynthesis genes (Zhu et al., 2011; Zhu et al., 2012a). Moreover, *GsERF71* enhanced alkaline stress tolerance by modifying auxin accumulation (Yu et al., 2017). The expression of auxin biosynthesis genes and IAA contents were downregulated by *GsERF71* under alkaline stress. However, how hormone signaling activates salt-alkaline stress response in *G. soja* is still lacking. Therefore, more genetic and biochemical experiments should be conducted to unravel the regulatory mechanism of hormone signaling in *G. soja* response to salt-alkaline stress.

In addition, taking advantage of high-throughput genomic sequencing of hundreds of soybean varieties, more and more attention has been paid to the identification of sequence variations in key genes that regulate salt-alkaline tolerance, for example, *GsCHX1* (Qi et al., 2014), *GsERD15B* (Jin et al., 2021), *GsDREB3b* (Hou et al., 2022) and *GsSALT18* (Guo et al., 2021). Currently, molecular markers of *GsCHX1* have been developed for breeding salt-tolerant soybean cultivars (Lee et al., 2018; Guan et al., 2021). Genes harboring sequence variations between *G. soja* and *G. max* are potential targets for molecular breeding of salt-alkaline tolerant soybean. Therefore, future work should concentrate on identifying salt-alkaline tolerant haplotypes in *G. soja* and re-introduce them into *G. max* to improve the salt-alkaline tolerance.

Author contributions

Conceptualization, XS and MS. Original draft preparation, XC and BJ. Manuscript review and editing, XS and MS. Funding acquisition, XS and MS. All authors contributed to the article and approved the submitted version.

Funding

This research was funded by Natural Science Foundation of Heilongjiang Province (grant number JQ2021C002), National Natural Science Foundation of China (grant number 32101672), Special Funds from the Central Finance to Support the Development of Local Universities (To XS, no grant number), and Postdoctoral Science Foundation of Heilongjiang Province (grant number LBH-Q21161).

Conflict of interest

The authors declare that the research was conducted in the absence of any commercial or financial relationships that could be construed as a potential conflict of interest.

Publisher's note

All claims expressed in this article are solely those of the authors and do not necessarily represent those of their affiliated organizations, or those of the publisher, the editors and the reviewers. Any product that may be evaluated in this article, or claim that may be made by its manufacturer, is not guaranteed or endorsed by the publisher.

References

Aleem, M., Aleem, S., Sharif, I., Wu, Z., Aleem, M., Tahir, A., et al. (2022). Characterization of *SOD* and *GPX* gene families in the soybeans in response to drought and salinity stresses. *Antioxid. (Basel)* 11 (3), 460. doi: 10.3390/antiox11030460

Assaha, D. V. M., Ueda, A., Saneoka, H., Al-Yahyai, R., and Yaish, M. W. (2017). The role of Na^+ and K^+ transporters in salt stress adaptation in glycophytes. *Front. Physiol.* 8, 509. doi: 10.3389/fphys.2017.00509

Azevedo Neto, A. D., Prisco, J. T., Enéas-Filho, J., Rolim Medeiros, J.-V., and Gomes-Filho, E. (2005). Hydrogen peroxide pre-treatment induces salt-stress acclimation in maize plants. *J. Plant Physiol.* 162 (10), 1114–1122. doi: 10.1016/j.jplph.2005.01.007

Bai, X., Liu, J., Tang, L. L., Cai, H., Chen, M., Ji, W., et al. (2013). Overexpression of *GsCBRLK* from *Glycine soja* enhances tolerance to salt stress in transgenic alfalfa (*Medicago sativa*). *Funct. Plant Biol.* 40 (10), 1048–1056. doi: 10.1071/fp12377

Barbier-Brygoo, H., De Angeli, A., Filleur, S., Frachisse, J.M., Gambale, F., Thomine, S., et al. (2011). Anion channels/transporters in plants: from molecular bases to regulatory networks. *Annu. Rev. Plant Biol.* 62 (1), 25–51. doi: 10.1146/annurev-arplant-042110-103741

Ben Rejeb, K., Lefebvre-De Vos, D., Le Disquet, I., Leprince, A.-S., Bordenave, M., Maldiney, R., et al. (2015). Hydrogen peroxide produced by NADPH oxidases increases proline accumulation during salt or mannitol stress in *Arabidopsis thaliana New Phytol.* 208 (4), 1138–1148. doi: 10.1111/nph.13550

Bian, X., Li, W., Niu, C., Wei, W., Hu, Y., Han, J., et al. (2020). A class b heat shock factor selected for during soybean domestication contributes to salt tolerance by promoting flavonoid biosynthesis. *New Phytol.* 225 (1), 268–283. doi: 10.1111/nph.16104

Cai, X., Shen, Y., Hu, B., Wang, Y., Chen, Y., Sun, M., et al. (2020). Overexpression of a *Glycine soja* receptor-like protein kinase gene *GsCBRLK* in rice increases salt-alkaline tolerance. *Plant Physiol. J.* 56, 2683–2694. doi: 10.13592/j.cnki.ppj.2020.0266

Cai, H., Sun, N., and Song, T. (2018). Modification of *GsDREB2* from *Glycine soja* increases plant tolerance to salt and osmotic stress. *Acta Pratac Sin.* 27, 168–176. doi: CYXB20180601&DbName=CJFQ2018

Cai, H., Zhu, Y., Bai, X., Ji, W., Li, Y., Wang, D., et al. (2011a). Isolation and tolerance analysis of *GsbZIP33* gene linked to response on stress in *Glycine soja*. *Mol. Plant Breed.* 9, 397–401. doi: FZZW201104002&DbName=CJFQ2011

Cai, H., Zhu, Y., Li, Y., Bai., X., Ji, W., Wang, D., et al. (2011b). Isolation and tolerance analysis of *GsNAC20* gene linked to response to stress in *Glycine soja*. *Acta Agron. Sin.* 37, 1351–1359. doi: 10.3724/SP.J.1006.2011.01351

Cao, L., Yu, Y., Ding, X., Zhu, D., Yang, F., Liu, B., et al. (2017). The *Glycine soja* NAC transcription factor *GsNAC019* mediates the regulation of plant alkaline tolerance and ABA sensitivity. *Plant Mol. Biol.* 95 (3), 253–268. doi: 10.1007/s11103-017-0643-3

Cao, L., Yu, Y., DuanMu, H., Chen, C., Duan, X., Zhu, P., et al. (2016). A novel *Glycine soja* homeodomain-leucine zipper (HD-zip) I gene, *Gshdz4*, positively regulates bicarbonate tolerance and responds to osmotic stress in *Arabidopsis*. *BMC Plant Biol.* 16 (1), 184. doi: 10.1186/s12870-016-0872-7

Chan, C. (2014). *Biochemical and functional study of a putative lambda class glutathione-s-transferase gene in the wild soybean* (The Chinese University of Hong Kong: Doctor of Philosophy).

Chen, X., Ding, Y., Yang, Y., Song, C., Wang, B., Yang, S., et al. (2021a). Protein kinases in plant responses to drought, salt, and cold stress. *J. Integr. Plant Biol.* 63 (1), 53–78. doi: 10.1111/jipb.13061

Chen, J., Li, Q., Zhang, P., Lu, H., Bian, Y., Jian, Y., et al. (2021b). Cloning and functional characterization of two *GsSnRK1* gene promoters from wild soybean. *Plant Biotechnol. Rep.* 15 (5), 627–639. doi: 10.1007/s11816-021-00700-6

Chen, C., Sun, X., Duanmu, H., Yu, Y., Liu, A., Xiao, J., et al. (2015a). Ectopic expression of a *Glycine soja* myo-inositol oxygenase gene (*GsMIOX1a*) in *Arabidopsis* enhances tolerance to alkaline stress. *PloS One* 10 (6), e0129998. doi: 10.1371/journal.pone.0129998

Chen, C., Sun, X., Liu, A., Duan Mu, H., Yu, Y., Xiao, J., et al. (2015b). Cloning and functional analysis of *Glycine soja* bicarbonate stress responsive gene *GsMIPS2*. *Acta Agron. Sin.* 41, 1343–1352. doi: 10.3724/SP.J.1006.2015.01343

Chen, P., Yan, K., Shao, H., and Zhao, S. (2013). Physiological mechanisms for high salt tolerance in wild soybean (*Glycine soja*) from yellow river delta, China: photosynthesis, osmotic regulation, ion flux and antioxidant capacity. *PloS One* 8 (12), e83227. doi: 10.1371/journal.pone.0083227

Das, K., and Roychoudhury, A. (2014). Reactive oxygen species (ROS) and response of antioxidants as ROS-scavengers during environmental stress in plants. *Front. Environ. Sci.* 2, 53. doi: 10.3389/fenvs.2014.00053

Do, T., Chen, H., Hien, V. T., Hamwieh, A., Yamada, T., Sato, T., et al. (2016). Ncl synchronously regulates NA^+, K^+, and Cl^- in soybean and greatly increases the grain yield in saline field conditions. *Sci. Rep.* 6, 19147. doi: 10.1038/srep19147

Donahue, J. L., Alford, S. R., Torabinejad, J., Kerwin, R. E., Nourbakhsh, A., Ray, W. K., et al. (2010). The *Arabidopsis thaliana* myo-inositol 1-phosphate synthase1 gene is required for myo-inositol synthesis and suppression of cell death. *Plant Cell* 22 (3), 888–903. doi: 10.1105/tpc.109.071779

Duan, X., Yu, Y., Duanmu, H., Chen, C., Sun, X., Cao, L., et al. (2017). GsSLAH3, a *Glycine soja* slow type anion channel homologue, positively modulates plant bicarbonate stress tolerance. *Physiol. Plant* 164 (2), 145–162. doi: 10.1111/ppl.12683

Duan, X., Yu, Y., Zhang, Y., Chen, C., Duanmu, H., Cao, L., et al. (2018). A potential efflux boron transporter gene *GsBOR2*, positively regulates *Aarabidopsis* bicarbonate tolerance. *Plant Sci.* 274, 284–292. doi: 10.1016/j.plantsci.2018.05.032

Endres, S., and Tenhaken, R. (2009). Myoinositol oxygenase controls the level of myoinositol in *Arabidopsis*, but does not increase ascorbic acid. *Plant Physiol.* 149 (2), 1042–1049. doi: 10.1104/pp.108.130948

Fang, S., Hou, X., and Liang, X. (2021). Response mechanisms of plants under saline-alkali stress. *Front. Plant Sci.* 12, 667458. doi: 10.3389/fpls.2021.667458

Feng, X., Feng, P., Yu, H., Yu, X., Sun, Q., Liu, S., et al. (2020). GsSnRK1 interplays with transcription factor GsERF7 from wild soybean to regulate soybean stress resistance. *Plant Cell Environ.* 43 (5), 1192–1211. doi: 10.1111/pce.13726

Guan, R., Qu, Y., Guo, Y., Yu, L., Liu, Y., Jiang, J., et al. (2014). Salinity tolerance in soybean is modulated by natural variation in *GmSALT3*. *Plant J.* 80 (6), 937–950. doi: 10.1111/tpj.12695

Guan, R., Yu, L., Liu, X., Li, M., Chang, R., Gilliham, M., et al. (2021). Selection of the salt tolerance gene *GmSALT3* during six decades of soybean breeding in China. *Front. Plant Sci.* 12, 794241. doi: 10.3389/fpls.2021.794241

Guo, X., Jiang, J., Liu, Y., Yu, L., Chang, R., Guan, R., et al. (2021). Identification of a novel salt tolerance-related locus in wild soybean (*Glycine soja* sieb. & zucc.). *Front. Plant Sci.* 12, 791175. doi: 10.3389/fpls.2021.791175

Hasanuzzaman, M., Nahar, K., Anee, T. I., and Fujita, M. (2017). Glutathione in plants: biosynthesis and physiological role in environmental stress tolerance. *Physiol. Mol. Biol. Pla.* 23 (2), 249–268. doi: 10.1007/s12298-017-0422-2

Hou, Z., Li, Y., Cheng, Y., Li, W., Li, T., Du, H., et al. (2022). Genome-wide analysis of *DREB* genes identifies a novel salt tolerance gene in wild soybean (*Glycine soja*). *Front. Plant Sci.* 13, 821647. doi: 10.3389/fpls.2022.821647

Hua, Y., Zhang, B., Cai, H., Li, Y., Bai, X., Ji, W., et al. (2012). Stress-inducible expression of *GsSAMS2* enhances salt tolerance in transgenic *Medicago sativa*. *Afr. J. Biotechnol.* 11 (17), 4030–4038. doi: 10.5897/AJB11.2583

Hu, Z., Jiang, G., Deng, X., and Wang, H. (2007). Moleculer adaptation through diversity of retrotransposons and transcriptional factors in populations of wild soybean (*Glycine soja*). *Chin. J. Plant Ecol.* 31, 952–959. doi: 10.17521/cjpe.2007.0121

Hussain, R. M., Ali, M., Feng, X., and Li, X. (2017). The essence of NAC gene family to the cultivation of drought-resistant soybean (*Glycine max* l. merr.) cultivars. *BMC Plant Biol.* 17 (1), 55. doi: 10.1186/s12870-017-1001-y

Im, J. H., Lee, H., Kim, J., Kim, H. B., Seyoung, K., Kim, B. M., et al. (2012). A salt stress-activated mitogen-activated protein kinase in soybean is regulated by phosphatidic acid in early stages of the stress response. *J. Plant Biol.* 55 (4), 303–309. doi: 10.1007/s12374-011-0036-8

Im, J. H., Son, S., Ko, J. H., Kim, K. H., An, C. S., and Han, K. H. (2021). Nuclear translocation of soybean MPK6, GmMPK6, is mediated by hydrogen peroxide in salt stress. *Plants (Basel)* 10 (12), 2611. doi: 10.3390/plants10122611

Isayenkov, S. V., Dabravolski, S. A., Pan, T., and Shabala, S. (2020). Phylogenetic diversity and physiological roles of plant monovalent Cation/H^+ antiporters. *Front. Plant Sci.* 11, 573564. doi: 10.3389/fpls.2020.573564

Jentsch, T. J., and Pusch, M. (2018). CLC chloride channels and transporters: structure, function, physiology, and disease. *Physiol. Rev.* 98 (3), 1493–1590. doi: 10.1152/physrev.00047.2017

Jia, B., Sun, M., DuanMu, H., Ding, X., Liu, B., Zhu, Y., et al. (2017). *GsCHX19.3*, a member of cation/H^+ exchanger superfamily from wild soybean contributes to high salinity and carbonate alkaline tolerance. *Sci. Rep.* 7 (1), 9423. doi: 10.1038/s41598-017-09772-3

Jia, B., Sun, M., Sun, X., Li, R., Wang, Z., Wu, J., et al. (2015). Overexpression of *GsGSTU13* and *SCMRP* in *Medicago sativa* confers increased salt-alkaline tolerance and methionine content. *Physiol. Plant* 156, 176–189. doi: 10.1111/ppl.12350

Jia, Q., Zheng, C., Sun, S., Amjad, H., Liang, K., and Lin, W. (2018). The role of plant cation/proton antiporter gene family in salt tolerance. *Biol. Plantarum* 62 (4), 617–629. doi: 10.1007/s10535-018-0801-8

Ji, W., Koh, J., Li, S., Zhu, N., Dufresne, C. P., Zhao, X., et al. (2015). Quantitative proteomics reveals an important role of *GsCBRLK* in salt stress response of soybean. *Plant Soil* 402 (1-2), 159–178. doi: 10.1007/s11104-015-2782-0

Jin, T., Sun, Y., Shan, Z., He, J., Wang, N., Gai, J., et al. (2021). Natural variation in the promoter of *GsERD15B* affects salt tolerance in soybean. *Plant Biotechnol. J.* 19 (6), 1155–1169. doi: 10.1111/pbi.13536

Jin, T., Sun, Y., Zhao, R., Shan, Z., Gai, J., and Li, Y. (2019). Overexpression of peroxidase gene *GsPRX9* confers salt tolerance in soybean. *Int. J. Mol. Sci.* 20, 3745. doi: 10.3390/ijms20153745

Ji, W., Zhu, Y., Li, Y., Yang, L., Zhao, X., Cai, H., et al. (2010). Over-expression of a glutathione s-transferase gene, *GsGST*, from wild soybean (*Glycine soja*) enhances drought and salt tolerance in transgenic tobacco. *Biotechnol. Lett.* 32 (8), 1173–1179. doi: 10.1007/s10529-010-0269-x

Kofsky, J., Zhang, H., and Song, B. H. (2018). The untapped genetic reservoir: the past, current, and future applications of the wild soybean (*Glycine soja*). *Front. Plant Sci.* 9, 949. doi: 10.3389/fpls.2018.00949

Lee, S., Kim, J. H., Sundaramoorthy, J., Park, G. T., Lee, J. D., Kim, J. H., et al. (2018). Identification of *GmSALT3* haplotypes and development of molecular markers based on their diversity associated with salt tolerance in soybean. *Mol. Breed.* 38 (7), 86. doi: 10.1007/s11032-018-0845-7

Liao, X., Shi, M., Zhang, W., Ye, Q., Li, Y., Feng, X., et al. (2021). Association analysis of *GmMAPKs* and functional characterization of *GmMMK1* to salt stress response in soybean. *Physiol. Plantarum* 173 (4), 2026–2040. doi: 10.1111/ppl.13549

Li, J., and Assmann, S.M. (1996). An abscisic acid-activated and calcium-independent protein kinase from guard cells of fava bean. *Plant Cell* 8 (12), 2359–2368. doi: 10.1105/tpc.8.12.2359

Lin, F., Bai, X., Fan, C., Zhao, C., Cai, H., Ji, W., et al. (2013). Investigation and analysis of the main agronomic traits of different transgenic soybean lines with *GsGST14* gene. *Soybean Sci.* 32, 56–58. doi: DDKX201301016&DbName=CJFQ2013

Lin, L., Wu, J., Jiang, M., and Wang, Y. (2021). Plant mitogen-activated protein kinase cascades in environmental stresses. *Int. J. Mol. Sci.* 22 (4), 1543. doi: 10.3390/ijms22041543

Li, Q., Sun, Q., Wang, D., Liu, Y., Zhang, P., Lu, H., et al. (2022). Quantitative phosphoproteomics reveals the role of wild soybean GsSnRK1 as a metabolic regulator under drought and alkali stresses. *J. Proteomics* 258, 104528. doi: 10.1016/j.jprot.2022.104528

Liu, J., Chen, N., Grant, J. N., Cheng, Z., Stewart, C. N., and Hewezi, T. (2015). Soybean kinome: functional classification and gene expression patterns. *J. Exp. Bot.* 66 (7), 1919–1934. doi: 10.1093/jxb/eru537

Liu, W., Feng, Y., Yu, S., Fan, Z., Li, X., Li, J., et al. (2021d). The flavonoid biosynthesis network in plants. *Int. J. Mol. Sci.* 22 (23), 12824. doi: 10.3390/ijms222312824

Liu, J., Fu, C., Li, G., Khan, M., and Wu, H. (2021c). ROS homeostasis and plant salt tolerance: plant nanobiotechnology updates. *Int. J. Mol. Sci.* 13 (6), 3552. doi: 10.3390/su13063552

Liu, P., Huang, Y., Shi, P., Yu, M., Xie, J., and Xie, L. (2018). Duplication and diversification of lectin receptor-like kinases (LecRLK) genes in soybean. *Sci. Rep.* 8 (1), 5861. doi: 10.1038/s41598-018-24266-6

Liu, X., Liu, F., Zhang, L., Cheng, C., Wei, P., and Yu, B. (2021b). *GsCLC-c2* from wild soybean confers chloride/salt tolerance to transgenic *Arabidopsis* and soybean composite plants by regulating anion homeostasis. *Physiol. Plant* 172 (4), 1867–1879. doi: 10.1111/ppl.13396

Liu, W., Song, R., Zheng, S., Li, T., Zhang, B., Gao, X., et al. (2022). Coordination of plant growth and abiotic stress responses by tryptophan synthase β; subunit 1 through modulation of tryptophan and ABA homeostasis in *Arabidopsis*. *Mol. Plant* 15 (6), 973–990. doi: 10.1016/j.molp.2022.04.009

Liu, Y., Yu, L., Qu, Y., Chen, J., Liu, X., Hong, H., et al. (2016). *GmSALT3*, which confers improved soybean salt tolerance in the field, increases leaf Cl^- exclusion prior to Na^+ exclusion but does not improve early vigor under salinity. *Front. Plant Sci.* 7, 1485. doi: 10.3389/fpls.2016.01485

Liu, X., Yu, F., Yang, G., Liu, X., and Peng, S. (2022). Identification of TIFY gene family in walnut and analysis of its expression under abiotic stresses. *BMC Genomics* 23 (1), 190. doi: 10.1186/s12864-022-08416-9

Liu, Y., Zheng, L., Jin, L., Liu, Y., Kong, Y., Wang, Y., et al. (2022). Genome-wide analysis of the soybean TIFY family and identification of *GmTIFY10e* and *GmTIFY10g* response to salt stress. *Front. Plant Sci.* 13, 845314. doi: 10.3389/fpls.2022.845314

Li, S., Wang, N., Ji, D., Zhang, W., Wang, Y., Yu, Y., et al. (2019). A GmSIN1/GmNCED3s/GmRbohBs feed-forward loop acts as a signal amplifier that regulates root growth in soybean exposed to salt stress. *Plant Cell* 31 (9), 2107–2130. doi: 10.1105/tpc.18.00662

Li, X., Wang, Y., Liu, F., Pi, B., Zhao, T., and Yu, B. (2020). Transcriptomic analysis of *Glycine soja* and *G. max* seedlings and functional characterization of *GsGSTU24* and *GsGSTU42* genes under submergence stress. *Environ. Exp. Bot.* 171, 103963. doi: 10.1016/j.envexpbot.2019.103963

Luo, X., Bai, X., Sun, X., Zhu, D., Liu, B., Ji, W., et al. (2013a). Expression of wild soybean WRKY20 in *Arabidopsis* enhances drought tolerance and regulates ABA signalling. *J. Exp. Bot.* 64 (8), 2155–2169. doi: 10.1093/jxb/ert073

Luo, X., Sun, X., Liu, B., Zhu, D., Bai, X., Cai, H., et al. (2013b). Ectopic expression of a WRKY homolog from *Glycine soja* alters flowering time in *Arabidopsis*. *PloS One* 8 (8), e73295. doi: 10.1371/journal.pone.0073295

Maszkowska, J., Szymanska, K.P., Kasztelan, A., Krzywinska, E., Sztatelman, O., and Dobrowolska, G. (2021). The multifaceted regulation of SnRK2 kinases. *Cells* 10 (9), 2180. doi: 10.3390/cells10092180

Morimoto, K., Ohama, N., Kidokoro, S., Mizoi, J., Takahashi, F., Todaka, D., et al. (2017). BPM-CUL3 E3 ligase modulates thermotolerance by facilitating negative regulatory domain-mediated degradation of DREB2A in *Arabidopsis*. *Proc. Natl. Acad. Sci. U.S.A.* 114 (40), E8528–E8536. doi: 10.1073/pnas.1704189114

Nakashima, K., Fujita, Y., Kanamori, N., Katagiri, T., Umezawa, T., Kidokoro, S., et al. (2009). Three *Arabidopsis* SnRK2 protein kinases, SRK2D/SnRK2.2, SRK2E/SnRK2.6/OST1 and SRK2I/SnRK2.3, involved in ABA signaling are essential for the control of seed development and dormancy. *Plant Cell Physiol.* 50 (7), 1345–1363. doi: 10.1093/pcp/pcp083

Neupane, A., Nepal, M.P., Piya, S., Subramanian, S., Rohila, J.S., Reese, R.N., et al. (2013). Identification, nomenclature, and evolutionary relationships of

mitogen-activated protein kinase (MAPK) genes in soybean. *Evol. Bioinform. Online* 9, 363–386. doi: 10.4137/EBO.S12526

Nie, W., Xu, L., and Yu, B. (2015). A putative soybean *GmsSOS1* confers enhanced salt tolerance to transgenic *Arabidopsis sos1-1* mutant. *Protoplasma* 252 (1), 127–134. doi: 10.1007/s00709-014-0663-7

Nisa (2016). *Functional analysis of GsMIPS2 and GsSNAP33 genes under salt and alkali stress conditions* (Northeast Agricultural University: Doctor of Philosophy).

Pan, L., Ma, J., LI, J., and Fu, C. (2022). Advances of salt stress-responsive transcription factors in plants. *Chin. J. Biotech.* 38 (1), 50–65. doi: 10.13345/j.cjb.210135

Pi, E., Xu, J., Li, H., Fan, W., Zhu, C., Zhang, T., et al. (2019). Enhanced salt tolerance of rhizobia-inoculated soybean correlates with decreased phosphorylation of the transcription factor GmMYB183 and altered flavonoid biosynthesis. *Mol. Cell Proteomics* 18 (11), 2225–2243. doi: 10.1074/mcp.RA119.001704

Pi, E., Zhu, C., Fan, W., Huang, Y., Qu, L., Li, Y., et al. (2018). Quantitative phosphoproteomic and metabolomic analyses reveal GmMYB173 optimizes flavonoid metabolism in soybean under salt stress. *Mol. Cell Proteomics* 17 (6), 1209–1224. doi: 10.1074/mcp.RA117.000417

Qi, X., Li, M. W., Xie, M., Liu, X., Ni, M., Shao, G., et al. (2014). Identification of a novel salt tolerance gene in wild soybean by whole-genome sequencing. *Nat. Commun.* 5, 4340. doi: 10.1038/ncomms5340

Qiu, Y., Feng, Z., Fu, M., Yuan, X., Luo, C., Yu, Y., et al. (2019). *GsMAPK4*, a positive regulator of soybean tolerance to salinity stress. *J. Integr. Agr.* 18 (2), 372–380. doi: 10.1016/s2095-3119(18)61957-4

Qu, Y., Guan, R., Bose, J., Henderson, S. W., Wege, S., Qiu, L., et al. (2021). Soybean CHX-type ion transport protein GmSALT3 confers leaf na^+ exclusion *via* a root derived mechanism, and cl^- exclusion *via* a shoot derived process. *Plant Cell Environ.* 44 (3), 856–869. doi: 10.1111/pce.13947

Rosales, M. A., Franco-Navarro, J. D., Peinado-Torrubia, P., Díaz-Rueda, P., Álvarez, R., and Colmenero-Flores, J. M. (2020). Chloride improves nitrate utilization and NUE in plants. *Front. Plant Sci.* 11, 442. doi: 10.3389/fpls.2020.00442

Sakuma, Y., Maruyama, K., Osakabe, Y., Qin, F., Seki, M., Shinozaki, K., et al. (2006). Functional analysis of an *Arabidopsis* transcription factor, DREB2A, involved in drought-responsive gene expression. *Plant Cell* 18 (5), 1292–1309. doi: 10.1105/tpc.105.035881

Saouros, S., Mohan, T.C., Cecchetti, C., Lehmann, S., Barrit, J.D., Scull, N.J., et al. (2021). Structural and functional insights into the mechanism of action of plant borate transporters. *Sci. Rep.* 11 (1), 12328. doi: 10.1038/s41598-021-91763-6

Shen, X., Wang, Y., Zhang, Y., Guo, W., Jiao, Y., and Zhou, X. (2018). Overexpression of the wild soybean R2R3-MYB transcription factor *GsMYB15* enhances resistance to salt stress and *Helicoverpa armigera* in transgenic *Arabidopsis*. *Int. J. Mol. Sci.* 19 (12), 3958. doi: 10.3390/ijms19123958

Shi, H., Ishitani, M., Kim, C., and Zhu, J. (2000). The *Arabidopsis thaliana* salt tolerance gene *SOS1* encodes a putative Na^+/H^+ antiporter. *P. Natl. Acad. Sci. U.S.A.* 97 (12), 6896–6901. doi: 10.1073/pnas.120170197

Singh, P., and Mukhopadhyay, K. (2021). Comprehensive molecular dissection of TIFY transcription factors reveal their dynamic responses to biotic and abiotic stress in wheat (*Triticum aestivum* l.). *Sci. Rep.* 11 (1), 9739. doi: 10.1038/s41598-021-87722-w

Song, H., Wang, P., Hou, L., Zhao, S., Zhao, C., Xia, H., et al. (2016). Global analysis of WRKY genes and their response to dehydration and salt stress in soybean. *Front. Plant Sci.* 7, 9. doi: 10.3389/fpls.2016.00009

Song, Y., Zhang, H., You, H., Liu, Y., Chen, C., Feng, X., et al. (2019). Identification of novel interactors and potential phosphorylation substrates of GsSnRK1 from wild soybean (*Glycine soja*). *Plant Cell Environ.* 42 (1), 145–157. doi: 10.1111/pce.13217

Sun, X., Cai, X., Yin, K., Gu, L., Shen, Y., Hu, B., et al. (2021). Wild soybean SNARE proteins BET1s mediate the subcellular localization of the cytoplasmic receptor-like kinases CRCK1s to modulate salt stress responses. *Plant J.* 105 (3), 771–785. doi: 10.1111/tpj.15072

Sun, M., Qian, X., Chen, C., Cheng, S., Jia, B., Zhu, Y., et al. (2018). Ectopic expression of *GsSRK* in *Medicago sativa* reveals its involvement in plant architecture and salt stress responses. *Front. Plant Sci.* 9, 226. doi: 10.3389/fpls.2018.00226

Sun, M., Shen, Y., Yin, K., Guo, Y., Cai, X., Yang, J., et al. (2019). A late embryogenesis abundant protein GsPM30 interacts with a receptor like cytoplasmic kinase GsCBRLK and regulates environmental stress responses. *Plant Sci.* 283, 70–82. doi: 10.1016/j.plantsci.2019.02.015

Sun, X., Sun, M., Jia, B., Qin, Z., Yang, K., Chen, C., et al. (2016). A *Glycine soja* methionine sulfoxide reductase B5a interacts with the Ca^{2+}/CAM-binding kinase GsCBRLK and activates ROS signaling under carbonate alkaline stress. *Plant J.* 86 (6), 514–529. doi: 10.1111/tpj.13187

Sun, X., Sun, M., Luo, X., Ding, X., Ji, W., Cai, H., et al. (2013a). A *Glycine soja* ABA-responsive receptor-like cytoplasmic kinase, *GsRLCK*, positively controls plant tolerance to salt and drought stresses. *Planta* 237 (6), 1527–1545. doi: 10.1007/s00425-013-1864-6

Sun, X., Yang, S., Sun, M., Wang, S., Ding, X., Zhu, D., et al. (2014). A novel *Glycine soja* cysteine proteinase inhibitor GsCPI14, interacting with the calcium/calmodulin-binding receptor-like kinase GsCBRLK, regulated plant tolerance to alkali stress. *Plant Mol. Biol.* 85 (1-2), 33–48. doi: 10.1007/s11103-013-0167-4

Sun, X., Yu, Q., Tang, L., Ji, W., Bai, X., Cai, H., et al. (2013b). GsSRK, a G-type lectin s-receptor-like serine/threonine protein kinase, is a positive regulator of plant tolerance to salt stress. *J. Plant Physiol.* 170 (5), 505–515. doi: 10.1016/j.jplph.2012.11.017

Tang, L., Cai, H., Ji, W., Luo, X., Wang, Z., Wu, J., et al. (2013). Overexpression of *GsZFP1* enhances salt and drought tolerance in transgenic alfalfa (*Medicago sativa* l.). *Plant Physiol. Biochem.* 71, 22–30. doi: 10.1016/j.plaphy.2013.06.024

Tang, L., Cai, H., Zhai, H., Luo, X., Wang, Z., Cui, L., et al. (2014). Overexpression of *Glycine soja* WRKY20 enhances both drought and salt tolerance in transgenic alfalfa (*Medicago sativa* l.). *Plant Cell Tiss Org. Cul.* 118 (1), 77–86. doi: 10.1007/s11240-014-0463-y

Uchida, A., Jagendorf, A.T., Hibino, T., Takabe, T., and Takabe, T. (2002). Effects of hydrogen peroxide and nitric oxide on both salt and heat stress tolerance in rice. *Plant Sci.* 163 (3), 515–523. doi: 10.1016/S0168-9452(02)00159-0

USDA (2021). "Soybeans: Acreage planted, harvested, yield, production, value, and loan rate, U.S 1980-2021," in *Oil crops yearbook* (Agriculture United States Department of Agriculture: Economic Research Service, USDA). Available at: https://www.ers.usda.gov/data-products/oil-crops-yearbook/.

Wang, Z., Cai, H., Bai, X., Ji, W., Li, Y., Wei, Z., et al. (2012a). Isolation of *GsGST19* from *Glycine soja* and analysis of saline-alkaline tolerance for transgenic *Medicago sativa*. *Acta Agron. Sin.* 38, 971–979. doi: 10.3724/SP.J.1006.2012.00971

Wang, H., Ni, D., Shen, J., Deng, S., Xuan, H., Wang, C., et al. (2022a). Genome-wide identification of the AP2/ERF gene family and functional analysis of *GmAP2/ERF144* for drought tolerance in soybean. *Front. Plant Sci.* 13, 848766. doi: 10.3389/fpls.2022.848766

Wang, N., Fan, X., Lin, Y., Li, Z., Wang, Y., Zhou, Y., et al. (2022b). Alkaline stress induces different physiological, hormonal and gene expression responses in diploid and autotetraploid rice. *Int. J. Mol. Sci.* 23 (10), 5561. doi: 10.3390/ijms23105561

Wang, Z., Song, F., Cai, H., Zhu, Y.M., Bai, X., Ji, W., et al. (2012b). Over-expressing *GsGST14* from *Glycine soja* enhances alkaline tolerance of transgenic *Medicago sativa*. *Biol. Plantarum* 56 (3), 516–520. doi: 10.1007/s10535-012-0075-5

Wang, Y., Yan, H., Qiu, Z., Hu, B., Zeng, B., Zhong, C., et al. (2019b). Comprehensive analysis of SnRK gene family and their responses to salt stress in eucalyptus grandis. *Int. J. Mol. Sci.* 20 (11), 2786. doi: 10.3390/ijms20112786

Wang, Y., Zhang, Y., Guo, W., Dai, W., Zhou, X., Jiao, Y., et al. (2019a). Cloning and function of *GsWRKY57* transcription factor gene response to drought stress. *Chin. J. Oil Crop Sci.* 41, 524–530.

Wei, P., Che, B., Shen, L., Cui, Y., Wu, S., Cheng, C., et al. (2019). Identification and functional characterization of the chloride channel gene, *GsCLC-c2* from wild soybean. *BMC Plant Biol.* 19 (1), 121. doi: 10.1186/s12870-019-1732-z

Wu, J., Cai, H., Bai, X., Ji, W., Wei, Z., Tang, L., et al. (2014). An analysis of salt tolerance of transgenic alfalfa with the *GsGST13/SCMRP* gene. *Acta Pratac Sin.* 23, 257–265.

Wu, S., Zhu, P., Jia, B., Yang, J., Shen, Y., Cai, X., et al. (2018). A *Glycine soja* group S2 bZIP transcription factor GsbZIP67 conferred bicarbonate alkaline tolerance in *Medicago sativa*. *BMC Plant Biol.* 18 (1), 234. doi: 10.1186/s12870-018-1466-3

Xie, Z., Nolan, T.M., Jiang, H., and Yin, Y. (2019). AP2/ERF transcription factor regulatory networks in hormone and abiotic stress responses in *Arabidopsis*. *Front. Plant Sci.* 10, 228. doi: 10.3389/fpls.2019.00228

Yang, L., Ji, W., Gao, P., Li, Y., Cai, H., Bai, X., et al. (2012). GsAPK, an ABA-activated and calcium-independent SnRK2-type kinase from *G. soja*, mediates the regulation of plant tolerance to salinity and ABA stress. *PloS One* 7 (3), e33838. doi: 10.1371/journal.pone.0033838

Yang, L., Ji, W., Zhu, Y. M., Gao, P., Li, Y., Cai, H., et al. (2010). GsCBRLK, a calcium/calmodulin-binding receptor-like kinase, is a positive regulator of plant tolerance to salt and ABA stress. *J. Exp. Bot.* 61 (9), 2519–2533. doi: 10.1093/jxb/erq084

Yu, Y., Duan, X., Ding, X., Chen, C., Zhu, D., Yin, K., et al. (2017). A novel AP2/ERF family transcription factor from *Glycine soja*, GsERF71, is a DNA binding protein that positively regulates alkaline stress tolerance in *Arabidopsis*. *Plant Mol. Biol.* 94 (4-5), 509–530. doi: 10.1007/s11103-017-0623-7

Yu, Y., Liu, A., Duan, X., Wang, S., Sun, X., Duanmu, H., et al. (2016a). GsERF6, an ethylene-responsive factor from *Glycine soja*, mediates the regulation of plant bicarbonate tolerance in *Arabidopsis*. *Planta* 244 (3), 681–698. doi: 10.1007/s00425-016-2532-4

Yu, Y., Wang, N., Hu, R., and Xiang, F. (2016b). Genome-wide identification of soybean WRKY transcription factors in response to salt stress. *Springerplus* 5 (1), 920. doi: 10.1186/s40064-016-2647-x

Zhao, W., Cheng, Y., Zhang, C., Shen, X., You, Q., Guo, W., et al. (2017). Genome-wide identification and characterization of the *GmSnRK2* family in soybean. *Int. J. Mol. Sci.* 18 (9), 1834. doi: 10.3390/ijms18091834

Zhao, C., Pan, X., Yu, Y., Zhu, Y., Kong, F., Sun, X., et al. (2020). Overexpression of a TIFY family gene, *GsJAZ2*, exhibits enhanced tolerance to alkaline stress in soybean. *Mol. Breed.* 40 (3), 33. doi: 10.1007/s11032-020-01113-z

Zhao, S., Zhang, Q., Liu, M., Zhou, H., Ma, C., and Wang, P. (2021). Regulation of plant responses to salt stress. *Int. J. Mol. Sci.* 22 (9), 4609. doi: 10.3390/ijms22094609

Zhao, Y., Zhu, Y. M., Xi, B., Wei, J., and Hua, C. (2014). Over-expressing *GsCBRLK/SCMRP* enhances alkaline tolerance and methionine content in transgenic *Medicago sativa*. *Acta Agron. Sin.* 40 (3), 431. doi: 10.3724/SP.J.1006.2014.00431

Zheng, X., He, K., Kleist, T., Chen, F., and Luan, S. (2015). Anion channel SLAH3 functions in nitrate-dependent alleviation of ammonium toxicity in *Arabidopsis*. *Plant Cell Environ.* 38 (3), 474–486. doi: 10.1111/pce.12389

Zhou, F., Guo, Y., and Qiu, L. (2016). Genome-wide identification and evolutionary analysis of leucine-rich repeat receptor-like protein kinase genes in soybean. *BMC Plant Biol.* 16, 58. doi: 10.1186/s12870-016-0744-1

Zhu, J. (2002). Salt and drought stress signal transduction in plants. *Annu. Rev. Plant Biol.* 53 (1), 247–273. doi: 10.1146/annurev.arplant.53.091401.143329

Zhu, D., Bai, X., Chen, C., Chen, Q., Cai, H., Li, Y., et al. (2011). GsTIFY10, a novel positive regulator of plant tolerance to bicarbonate stress and a repressor of jasmonate signaling. *Plant Mol. Biol.* 77 (3), 285–297. doi: 10.1007/s11103-011-9810-0

Zhu, D., Bai, X., Luo, X., Chen, Q., Cai, H., Ji, W., et al. (2013). Identification of wild soybean (*Glycine soja*) TIFY family genes and their expression profiling analysis under bicarbonate stress. *Plant Cell Rep.* 32 (2), 263–272. doi: 10.1007/s00299-012-1360-7

Zhu, D., Bai, X., Zhu, Y., Cai, H., Li, Y., Ji, W., et al. (2012a). Isolation and functional analysis of *GsTIFY11b* relevant to salt and alkaline stress from *Glycine soja*. *Hereditas* 34, 230–239. doi: 10.3724/SP.J.1005.2012.00230

Zhu, D., Cai, H., Luo, X., Bai, X., Deyholos, M. K., Chen, Q., et al. (2012b). Over-expression of a novel JAZ family gene from *Glycine soja*, increases salt and alkali stress tolerance. *Biochem. Biophys. Res. Commun.* 426 (2), 273–279. doi: 10.1016/j.bbrc.2012.08.086

Zhu, P., Chen, R., Yu, Y., Song, X., Li, H., Du, J., et al. (2017). Cloning of gene *GsWRKY15* related to alkaline stress and alkaline tolerance of transgenic plants. *Acta Agron. Sin.* 43, 1319–1327. doi: 10.3724/SP.J.1006.2017.01319

Zhu, D., Li, R., Liu, X., Sun, M., Wu, J., Zhang, N., et al. (2014). The positive regulatory roles of the TIFY10 proteins in plant responses to alkaline stress. *PloS One* 9 (11), e111984. doi: 10.1371/journal.pone.0111984

frontiers | Frontiers in Plant Science

TYPE Original Research
PUBLISHED 21 October 2022
DOI 10.3389/fpls.2022.1035750

Check for updates

OPEN ACCESS

EDITED BY
PingWu Liu,
Hainan University, China

REVIEWED BY
Weidong Wang,
Northwest A&F University, China
Pannaga Krishnamurthy,
National University of Singapore, Singapore

*CORRESPONDENCE
Genfa Zhang
gfzh@bnu.edu.cn
Jie Bing
bingjie@bnu.edu.cn

SPECIALTY SECTION
This article was submitted to Plant Abiotic Stress, a section of the journal Frontiers in Plant Science

RECEIVED 03 September 2022
ACCEPTED 29 September 2022
PUBLISHED 21 October 2022

CITATION
Wu Y, Liu H, Bing J and Zhang G (2022) Integrative transcriptomic and TMT-based proteomic analysis reveals the mechanism by which *AtENO2* affects seed germination under salt stress.
Front. Plant Sci. 13:1035750.
doi: 10.3389/fpls.2022.1035750

COPYRIGHT
© 2022 Wu, Liu, Bing and Zhang. This is an open-access article distributed under the terms of the Creative Commons Attribution License (CC BY). The use, distribution or reproduction in other forums is permitted, provided the original author(s) and the copyright owner(s) are credited and that the original publication in this journal is cited, in accordance with accepted academic practice. No use, distribution or reproduction is permitted which does not comply with these terms.

Integrative transcriptomic and TMT-based proteomic analysis reveals the mechanism by which *AtENO2* affects seed germination under salt stress

Yu Wu, Huimin Liu, Jie Bing* and Genfa Zhang*

Beijing Key Laboratory of Gene Resource and Molecular Development, College of Life Sciences, Beijing Normal University, Beijing, China

Seed germination is critical for plant survival and agricultural production and is affected by many cues, including internal factors and external environmental conditions. As a key enzyme in glycolysis, enolase 2 (ENO2) also plays a vital role in plant growth and abiotic stress responses. In our research, we found that the seed germination rate was lower in the *AtENO2* mutation (*eno2*$^{-}$) than in the wild type (WT) under salt stress in *Arabidopsis thaliana*, while there was no significant difference under normal conditions. However, the mechanisms by which *AtENO2* regulates seed germination under salt stress remain limited. In the current study, transcriptome and proteome analyses were used to compare *eno2*$^{-}$ and the WT under normal and salt stress conditions at the germination stage. There were 417 and 4442 differentially expressed genes (DEGs) identified by transcriptome, and 302 and 1929 differentially expressed proteins (DEPs) qualified by proteome under normal and salt stress conditions, respectively. The combined analysis found abundant DEGs and DEPs related to stresses and hydrogen peroxide removal were highly down-regulated in *eno2*$^{-}$. In addition, several DEGs and DEPs encoding phytohormone transduction pathways were identified, and the DEGs and DEPs related to ABA signaling were relatively greatly up-regulated in *eno2*$^{-}$. Moreover, we constructed an interactive network and further identified GAPA1 and GAPB that could interact with AtENO2, which may explain the function of AtENO2 under salt stress during seed germination. Together, our results reveal that under salt stress, *AtENO2* mainly affects the expression of genes and proteins related to the phytohormone signal transduction pathways, stress response factors, and reactive oxygen species (ROS), and then affects seed germination. Our study lays the foundation for further exploration of the molecular function of *AtENO2* under salt stress at the seed germination stage in *Arabidopsis thaliana*.

KEYWORDS

ENO2*, salt stress, seed germination, transcriptome, proteome, *Arabidopsis thaliana

Introduction

The transition of seeds of higher plants from dormancy to germination is one of the key stages at the beginning of a new life cycle, which is of great significance for plants to complete their entire life cycle (Wu et al., 2021). Physiologically, seed germination is defined as the transformation of seeds from a relatively quiescent state to a vigorous stage. Morphologically, it shows that the radicle and germ break through the seed coat and elongate outward to develop into a new individual (Koller et al., 1962). Whether the seed can germinate smoothly depends on its internal factors, such as whether it has a complete embryo, sufficient nutrients, and the hormone content is balanced, which affects the germination of seeds. Abscisic acid (ABA) and gibberellin (GA) play indispensable roles. ABA mainly inhibits germination (Sun et al., 2021). In ABA-deficient mutants, ABA synthesis is inhibited, and the germination rate of the mutants is higher than that of the wild type (WT). In ABA overexpressing transgenic materials, the phenotype is the opposite (Martinez-Andujar et al., 2011; Nonogaki et al., 2014). A major mechanism by which GA promotes seed germination is by promoting the degradation of the DELLA protein RGA-LIKE 2 (RGL2), a major repressor of germination in *Arabidopsis* seeds (Lee et al., 2022). Meanwhile, the germination process is also affected by external environmental factors. As one of the main abiotic stresses affecting plant growth and development, salt stress also affects the germination of seeds. At present, the physiological effect of salt stress on seed germination is very clear, but different scholars hold different views on its specific mechanisms. Some studies have believed that the decrease in the germination rate under salt stress is mainly due to the high osmotic pressure caused by high salt, which makes the metabolic activities of seeds unable to be carried out due to insufficient water absorption, which affects germination (Munns and Tester, 2008). Some researchers thought that the effect of high salt on seed germination was mainly due to ion toxicity (Zhu et al., 2017; Liu et al., 2021). Based on previous studies, other studies suggested that high salt stress mainly affected the activity of amylase, leading to the obstruction of the process of providing energy and nutrients for radicles (Zhu et al., 2021).

With the continuous development of the research field, an increasing number of gene functions related to seed germination under salt stress have been identified. The *ENO* genes are widely distributed and highly conserved in mammals and plants and encode the glycolytic enzyme ENO2, which catalyzes the dehydration of 2-phospho-D-glycerate (2-PGA) to phosphoenolpyruvate (PEP) (Wu et al., 2021). In *Arabidopsis*, ENO1, ENO2, and ENO3 are the main isozymes, and the expression of ENO2 is much higher than that of ENO1 and ENO3 (Andriotis et al., 2010). More and more studies have shown that ENO2 is a multifunctional enzyme that not only plays a role in glycolysis but also plays an essential role in the normal growth and development of plants and response to abiotic stresses (Lee et al., 2002a; Kang et al., 2013; Eremina et al., 2015; Yang et al., 2021a). Our laboratory obtained homozygous mutants (*eno2*$^-$) of *AtENO2* through continuous screening and identification. The absence of *AtENO2* causes defective growth and reproduction, such as stunted plants, a reduced germination rate of pollen, impaired floral organogenesis, and damaged male gametophytes (Eremina et al., 2015). In addition, the germination rate between *eno2*$^-$ and the WT was not significantly different on Murashige and Skoog (MS) medium, but under salt stress, the germination rate of the mutant was lower than that of the WT. However, the mechanisms of *AtENO2* affecting seed germination under salt stress are not clear thus far.

Recently, large-scale omics methods, such as genomics, metabolomics, transcriptomics, and proteomics, have made it possible to investigate the mechanisms of plant defenses against different abiotic stresses (Deshmukh et al., 2014; Calhoun et al., 2021; Zeng et al., 2021). Transcriptomics can comprehensively and quickly obtain almost all mRNA sequence information of a specific sample in a specific period and is widely used in basic research, clinical diagnosis, pharmaceutical studies, and other fields. Protein is the embodiment of biological function; therefore, the study of biological function is inseparable from proteomics. Several studies have been conducted to explore the salt stress response mechanisms in plant species, such as rice (*Oryza sativa*) (Zhao et al., 2021b), maize (*Zea mays*) (Wang et al., 2016), soybeans (*Glycine max*) (Arai et al., 2008), and other species. Numerous salt-responsive genes and proteins have been identified. To determine the exact mechanism by which *AtENO2* affects seed germination under salt stress in *Arabidopsis*, we considered the use of omics methods. To avoid the limitations of single omics, we employed a conjoint analysis. Transcriptomics and proteomics offer an effective approach for identifying genes, proteins, gene ontology (GO) terms, and associated pathways that are crucial for understanding the functions of *AtENO2* in seed germination under salt stress.

In our research, we aimed to identify DEGs and DEPs in *eno2*$^-$ under salt stress compared to the WT and to investigate the molecular mechanisms regulating seed germination under salinity. For this reason, we performed RNA-Seq and TMT with the WT and *eno2*$^-$ on MS medium with or without 100 mM NaCl. First, the germination phenotypes under normal and salt stress were counted, and the related physiological indices were detected. Finally, with the help of omics, we found 4249 DEGs and 1831 DEPs only under salt stress. Through joint analysis, the key genes, proteins, GO terms, and pathways were also identified in *eno2*$^-$ compared to WT. These results will provide more information for understanding the function of *ENO2* in seed germination in *Arabidopsis thaliana*.

Result

AtENO2 regulates seed germination in response to abiotic stress

We set different concentrations of NaCl to explore the optimal concentration affecting seed germination, and finally, we chose 100 mM with an obvious difference for subsequent experiments (Supplementary Figure S1). After statistical analysis of the 1/2 MS medium, we found that *eno2*$^-$ was faster than the WT and *ER* in the first three days of germination, but there was no significant difference in the later stage of germination. On medium with NaCl, the seed germination of *eno2*$^-$ was more sensitive than that of the WT and *ER*. To investigate whether *ENO2* mainly affected *Arabidopsis* germination through ion toxicity or osmotic stress, we also investigated the germination of each line under isotonic conditions and K^+ stress at the same concentration as Na^+. On medium with mannitol, the seed germination rate showed no obvious difference among the genotypes. However, the green cotyledon percentage of the mutant was lower than that of the WT and *ER*. Additionally, on the medium with KCl, both the seed germination and green cotyledon rate displayed no significant difference among the lines (Figure 1). The leaf size and chlorophyll content during germination also showed similar growth tendencies (Supplementary Figure S2). These results indicated that under salt stress, *ENO2* mainly affected the content of Na^+ or the cell signaling related to Na^+ during seed germination, and had a certain degree of osmotic stress effect.

Identification and classification of the DEGs between *eno2*$^-$ and WT under salt stress

Transcriptome sequencing was applied to reveal the effect of *ENO2* mutation on seed germination under normal and salt stress conditions. After analysis, we preliminarily determined the quality of RNA used for sequencing (Supplementary Figure S3, Table S1), and analyzed the base quality value (Q) and the Pearson correlation coefficient (R), etc (Supplementary Figures S4, S5, Tables S1, S2). All these data further indicated that our data met the sequencing requirements and could be used for further analysis.

To explore which genes would be affected by *ENO2* under salt stress, we analyzed the DEGs. A total of 417 DEGs were identified under normal conditions, of which 208 and 209 genes were upregulated and downregulated in *eno2*$^-$ plants, respectively (Figure 2A). Under salt stress, there were a total of 4442 significant DEGs, of which 2032 genes were significantly upregulated and 2410 genes were significantly downregulated (Figure 2B). To further identify the genes that were significantly expressed only under salt stress, the UpSet graph was drawn with the help of the Omicstudio cloud platform (https://www.omicstudio.cn/tool/43). A total of 193 genes were expressed jointly, 224 genes were expressed only under normal conditions, and 4249 genes were specifically expressed differently only under salt stress (Figure 2C). To further explore the functions of DEGs under salt stress, according to the previous analysis, we selected the 4249 genes that were significantly expressed only under salt stress for GO analysis. In addition, we used the OmicShare cloud platform to calculate the classification statistics (Figure 2D). The results showed that there were 54 GO terms, including 25 biological processes, 13 molecular functions, and 16 cellular components, with FDR<0.05 (Table S4). Of them, the top 3 terms were "cellular process" (2304 DEGs), "metabolic process" (2171 DEGs), and "response to stimulus" (1258 DEGs) in the biological process category. The GO terms with the highest DEG count number in the cellular component category were "cell" and "cell part" (both have 2654 DEGs), followed by "organelle" (2093 DEGs) and "membrane" (1519 DEGs). Molecular functions such as

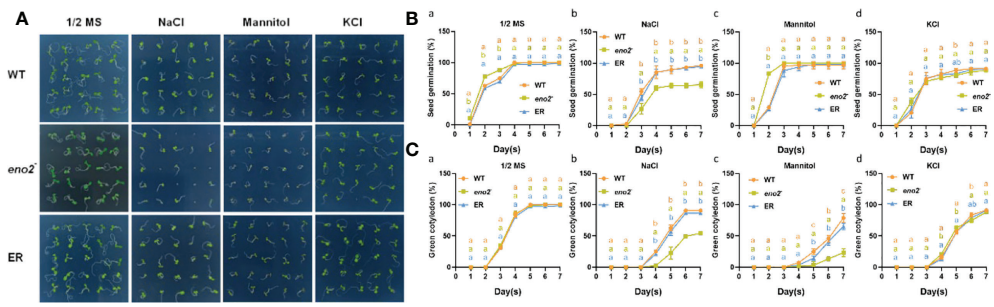


FIGURE 1
AtENO2 regulates seed germination under salt stress. Seed germination of the WT, *eno2*$^-$, and *ER* lines. Seeds were horizontally germinated on 1/2 MS medium with or without 100 mM NaCl, 200 mM mannitol, and 100 mM KCl for 7 days. Photographs were taken on the seventh day of germination **(A)**. The seed germination rate was measured at the indicated time point **B(a-d)**. The green cotyledon rate was measured every day for seven days **C(a-d)**. The orange, green, and blue dashed lines represent the WT, *eno2*$^-$, and *ER*, respectively. Values are expressed as the means ± SD (n=3 replicates). Different letters indicate significant differences by one-way ANOVA ($P < 0.05$) with SPSS.

"binding" (2200 DEGs), "catalytic activity" (1618 DEGs), and "transcription regulator activity" (322 DEGs) were significantly enriched.

Identification and classification of the DEPs between *eno2*⁻ and WT under salt stress

Although transcriptome data can provide abundant information at the transcriptional level, they only represent the intermediate state of gene expression and only represent the potential protein expression and functional significance. Proteins are the real functional embodiment of organisms. Therefore, to obtain the difference in protein expression levels in comparison groups, TMT quantitative proteomics was used in our study. The quality of the samples sent for sequencing was tested (Supplementary Figure S6; Table S5), and there was good repeatability in the data groups and great differences between groups (Supplementary Figures S7, S8), which could be used for further analysis.

To analyze proteins with different expression differences between different groups, the DEPs were further screened. We found that under normal growth conditions, when *eno2*⁻ was compared with the WT, a total of 302 proteins changed significantly, including 120 upregulated proteins and 182 downregulated proteins (Figure 3A). However, under salt stress, a total of 1929 proteins of *eno2*⁻ were significantly different from the WT, including 761 significantly upregulated proteins and 1168 significantly downregulated proteins

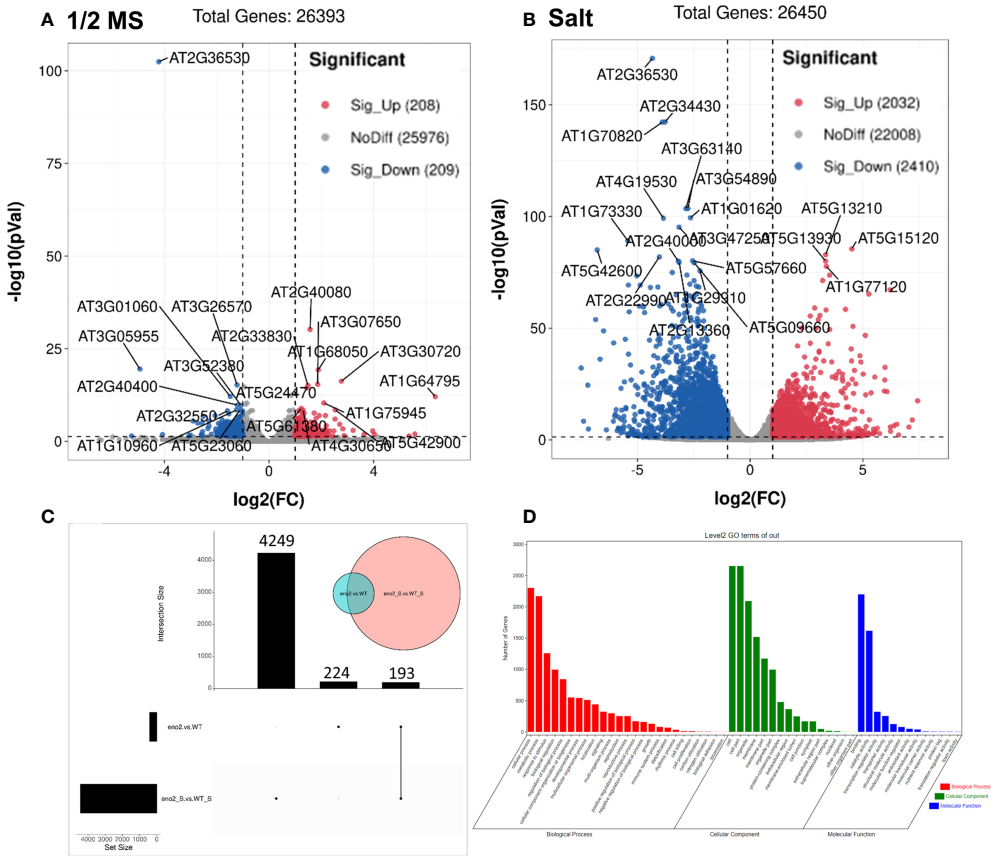


FIGURE 2
The analysis of DEGs in *eno2*⁻ compared to the WT under different conditions. Volcano plot of the distribution of DEGs under normal conditions **(A)** and salt stress **(B)**. The X-axis represents the change in gene expression in different samples. The Y-axis indicates the statistical significance of changes in gene expression levels. The dots represent different genes. The grey dots represent genes with no significant difference, the red dots represent genes with significant differences in upregulation, and the blue dots represent genes with significant differences in downregulation. Transcriptomics UpSet diagram **(C)**. Green circles indicate genes that are differentially expressed under normal conditions, and pink circles indicate genes that are differentially expressed under salt stress. The left bar chart shows the number of DEGs under normal conditions. The middle column chart represents the number of DEGs under salt stress. And the right one means the DEGs that are common under normal and salt stress conditions. GO of key DEGs of *eno2*⁻ compared to the WT under salt stress **(D)**. Red represents the classification of biological processes, green represents the classification of cellular components, and blue represents the classification of molecular functions.

(Figure 3B). To further identify the proteins that were significantly expressed only under salt stress, the UpSet graph was drawn with the Omicstudio cloud platform, from which 98 proteins were expressed jointly, 204 proteins were expressed only under normal conditions, and 1831 proteins were specifically expressed differently only under salt stress (Figure 3C). To fully understand the function, localization, and biological pathway of proteins in organisms, proteins were annotated through GO. We used the OmicShare cloud platform to perform GO annotation analysis on 1831 proteins that were significantly differentially expressed only under salt stress after the above analysis (Figure 3D). The results showed that there were 54 GO terms, including 26 biological processes, 12 molecular functions, and 16 cellular components, with FDR<0.05 (Table S6). The top 3 terms were "cellular process" (1205 DEPs), "metabolic process" (1146 DEPs), and "response to stimulus" (573 DEPs) in the terms of biological process, which were the same as RNA-Seq. The GO terms with the highest number of DEPs in the cellular component category were "cell" and "cell part" (both had 1605 DEPs). In addition, "binding" (1141 DEPs), "catalytic activity" (973 DEPs), and "transporter activity" (122 DEPs) were significantly enriched in molecular function.

Conjoint analysis of transcriptome and proteome data

Generally, biological phenomena are complex and variable, and internal regulation is complex; therefore, the conclusion of a

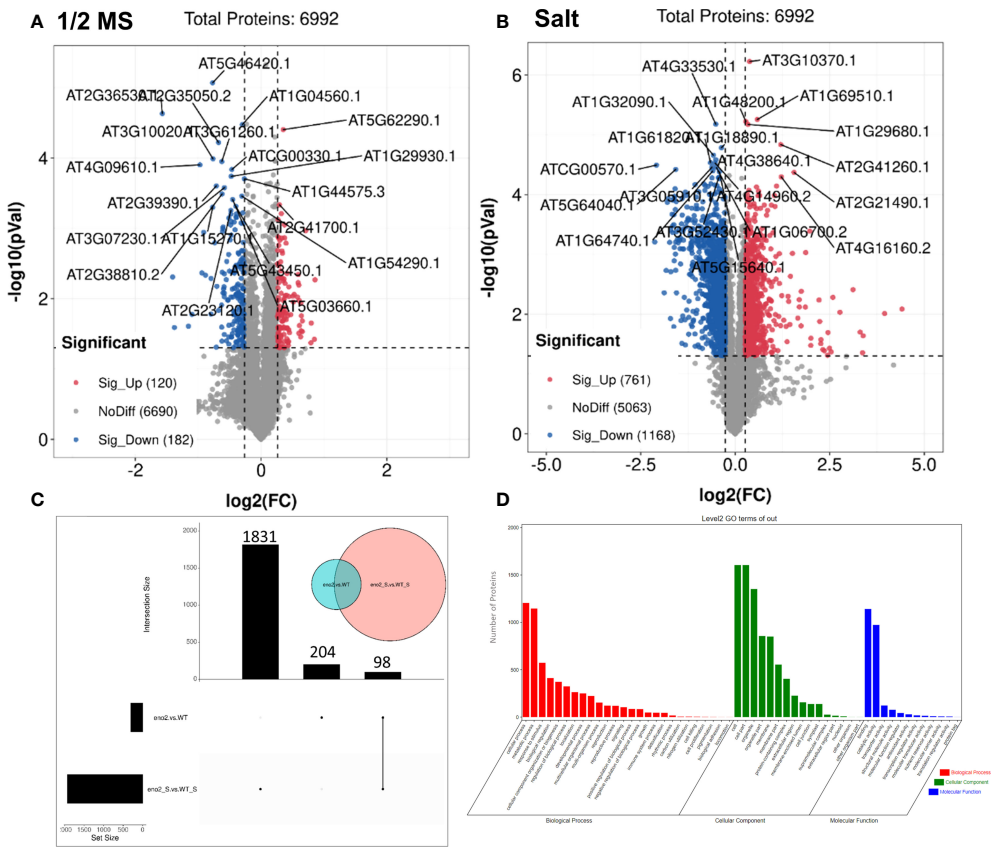


FIGURE 3
The analysis of differentially expressed proteins (DEPs) in *eno2*$^{-}$ compared to the WT under different conditions.Volcano plot of the distribution of DEPs under normal conditions **(A)** and salt stress **(B)**. The X-axis is the multiple of difference (logarithmic transformation based on 2), the Y-axis is the significance p-value of the difference (logarithmic transformation based on 10), the red dots are the upregulated significance differentially expressed proteins, the blue dots are downregulated significance differentially expressed proteins, and the grey dots are the proteins with no difference. Proteomics UpSet diagram **(C)**. Green circles indicate proteins that are differentially expressed under normal conditions, and pink circles indicate proteins that are differentially expressed under salt stress. The left bar chart shows the number of DEGs under normal conditions. The middle column chart represents the number of DEGs under salt stress. And the right one means the DEGs that are common under normal and salt stress conditions. GO of key DEPs of *eno2*$^{-}$ compared to the WT under salt stress **(D)**. Red represents the classification of biological processes, green represents the classification of cellular components, and blue represents the classification of molecular functions.

single omics study is often not comprehensive. Therefore, we conducted a joint analysis of transcriptome and proteomic sequencing, hoping to have a more systematic exploration of the sequencing data. We integrated quantitative and differential expression information of the transcriptome and proteome conducted quantitative correlation analysis and drew Venn diagrams. Under normal growth conditions, only 6 genes and proteins were associated (Figure 4A), while 628 were associated under salt stress (Figure 4B).

In addition, we mapped the GO annotation map of genes and proteins associated under normal and salt stress conditions, respectively. On the MS medium, in 2 biological processes, the DEPs and DEGs were mainly enriched in "response to lipid" (18 DEPs and 24 DEGs) and "water homeostasis" (3 DEPs and 4 DEGs). Among the 4 molecular functions, the DEPs and DEGs were enriched in "substrate-specific channel activity" (6 DEPs and 7 DEGs), "passive transmembrane transporter activity" (6 DEPs and 8 DEGs), "channel activity" (6 DEPs and 8 DEGs), and "phosphopyruvate hydratase activity" (2 DEPs and 1 DEGs). Only the "phosphopyruvate hydratase complex" (2 DEPs and 1 DEGs) was enriched in cell components (Figure 4C; Table S7). Under salt stress, response to stimulus (651 DEPs and 1344 DEGs), response to stress (394 DEPs and 799 DEGs), "response to abiotic stimulus" (293 DEPs and 566 DEGs), "response to hormone" (219 DEPs and 407 DEGs), and other GO terms were enriched in biological process. The top 3 terms were "oxidoreductase activity" (267 DEPs and 412 DEGs), "cofactor binding" (188 DEPs and 298 DEGs), and "transporter activity" (149 DEPs and 268 DEGs). In addition, "membrane" (930 DEPs and 1582 DEGs), "organelle part" (828 DEPs and 1018 DEGs), and "intracellular organelle part" (826 DEPs and 1016 DEGs) were significantly enriched in cell components (Figure 4D; Table S8). These associated GO terms preliminarily indicated that *ENO2* plays a role mainly by affecting the expression of stress-related genes and proteins.

To further elucidate the pathway changes associated with DEPs under salt stress after combined analysis, proteins were annotated through the Kyoto Encyclopedia of Genes and Genomes (KEGG) pathway database. The KEGG analysis revealed that 74 pathways were mapped, and 20 pathways were significantly enriched (p-value <0.05) (Figure 4E). KEGG pathway enrichment analysis further found that "Metabolic pathways", "Biosynthesis of secondary metabolites", "Carbon metabolism", "Photosynthesis", "Carbon fixation in photosynthetic organisms", and "Glycolysis/Gluconeogenesis" were significantly enriched. All these significantly enriched pathways were related to metabolism.

DEPs and DEGs associated with stress in the combined analysis

Seed germination can be affected by the external environment. Phenotypic analysis showed that under normal growth conditions, there was no significant difference between the WT and *eno2*$^{-}$ in germination; nevertheless, under a certain degree of salt stress, the germination rate and cotyledon- greening rate were significantly lower in *eno2*$^{-}$. Consequently, we intended to explore which proteins and genes related to tolerance were mainly affected by *ENO2* under salt stress. The previous part revealed the changes in protein and gene levels caused by *ENO2* under normal and salt stress conditions from transcriptome and proteomics, respectively. Meanwhile, the sequencing data were further analyzed by joint analysis, which could avoid the limitation of relying only on a single omics analysis. To further investigate the results of the joint analysis, we first selected the stress-related proteins and genes significantly enriched in the GO annotation (Figure 4D). There were 799 DEGs enriched in the stress GO term in the transcriptome data, and 394 DEPs enriched in the stress GO term in proteomics. A total of 127 were significantly enriched in both the transcriptome and proteome (Table S9), in which the protein expression is shown in the form of a heatmap (Figure 5A).

In the process of plant roots absorbing water from the soil and transporting water to various tissues of plants, aquaporin-mediated water transport across membranes plays a crucial role (Maurel et al., 2015). *PIP1B* (*PIP1;2*) is a vital member of the *Arabidopsis* aquaporin family. Under normal conditions, there was no significant difference in the expression of PIP1B between the WT and *eno2*$^{-}$, but it was significantly reduced under salt stress. Transcriptome and proteome data were maintained consistently, and the data reliability of the transcriptome was verified by qRT–PCR (Figure 5B). Peroxidases are important respiratory enzymes in plants. Their content is closely related to phenol metabolism and plant resistance (Gaudet et al., 2011). Generally, the higher its activity is, the stronger the stress resistance of the plant; in contrast, its resistance is reduced. L-ascorbate peroxidase T, chloroplastic (EC:1.11.1.11) (APXT) plays an important role in the scavenging process of reactive oxygen species. Under normal conditions, APXT in *eno2*$^{-}$ was lower than that in the WT. Under salt stress, APXT in the WT and *eno2*$^{-}$ was lower than that under normal conditions; in addition, APXT in mutants was significantly lower than that in the WT. In addition, under salt stress, the expression levels of cryptochrome-1 (CRY1), glyceraldehyde-3-phosphate dehydrogenase GAPA1, chloroplastic (EC:1.2.1.13) (GAPA1), glyceraldehyde-3-phosphate dehydrogenase GAPB, chloroplastic (EC:1.2.1.13) (GAPB), and other proteins in response to stress were significantly reduced in *eno2*$^{-}$. The results of transcriptome sequencing were consistent with the expression trends of proteome sequencing. Meanwhile, some data were selected for qRT–PCR verification to further prove the reliability of the data.

DEPs and DEGs associated with phytohormones in the combined analysis

Phytohormones play indispensable roles in the process of seed germination. Plant endogenous hormones are produced under the action of external environmental signals. Through signal transduction, they induce the activation of enzymes and proteins

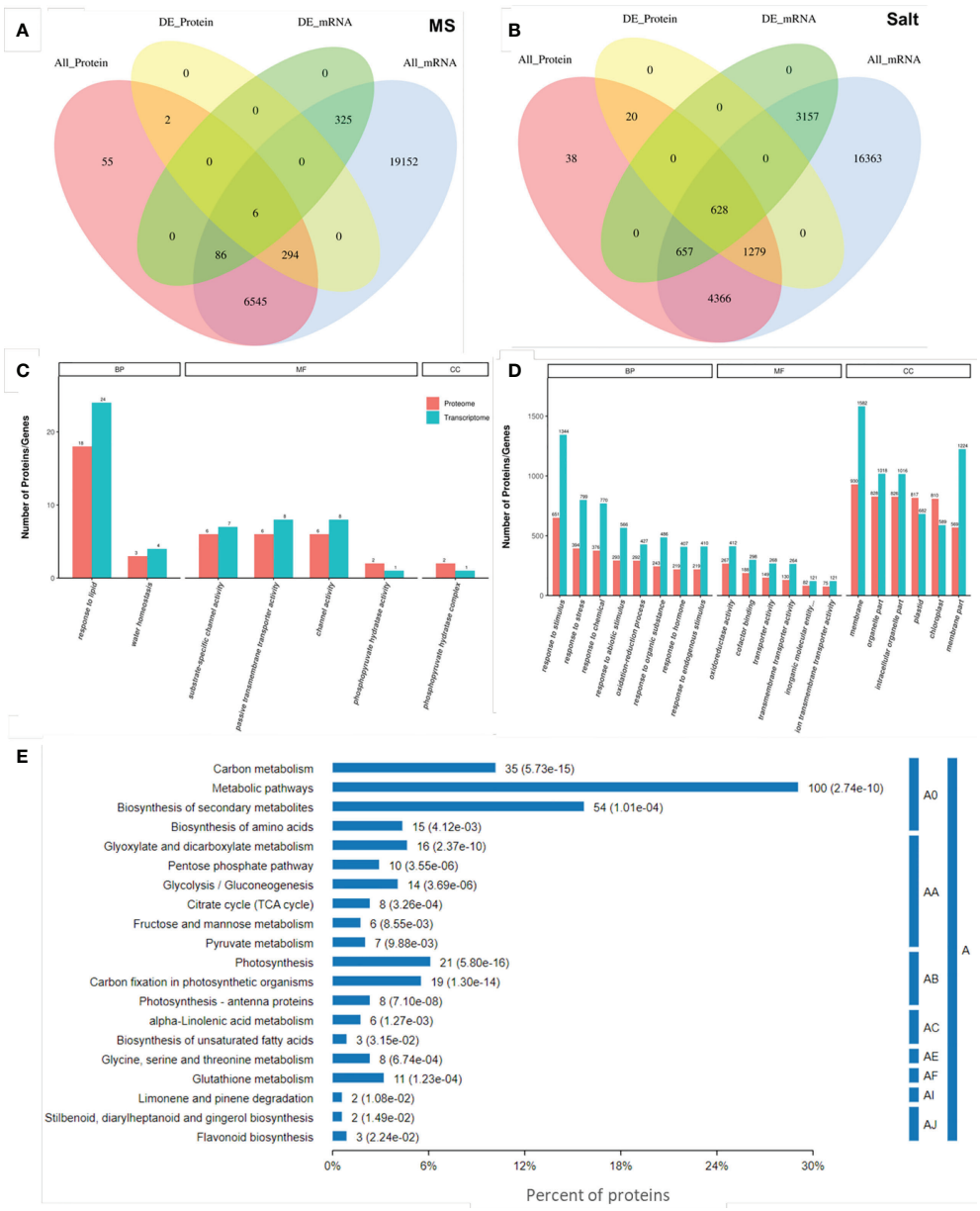


FIGURE 4
Combined analysis of transcriptome and proteome. Quantitative Venn diagrams of the transcriptome and proteome at the quantitative and differential expression levels under normal **(A)** and salt stress **(B)**. All_protein represents all quantifiable proteins in the proteome. All_Gene represents all quantifiable genes obtained from the transcriptome. DE_Protein indicates the differential proteins identified by the proteome, and DE_Gene is the differentially expressed gene that represents transcriptome identification. GO items are enriched under normal **(C)** and salt stress conditions **(D)**. Each column represents a GO second-level annotation item, red represents DEPs, and green represents DEGs. In the order of the number of DEPs contained from left to right, the higher the column is, the more active the GO second-level annotation item is in the tested samples. BP: Biological Process, MF: Molecular Function, and CC: Cellular Component. **(E)** KEGG pathway analysis of the DEPs in association under salt stress. A: Metabolism, A0: global and overview maps, AA: carbohydrate metabolism, AB: energy metabolism, AC: lipid metabolism, AE: amino acid metabolism, AF: metabolism of other amino acids, AI: metabolism of terpenoids and polyketides, and AJ: biosynthesis of other secondary metabolites.

and cause changes in cellular physiological metabolism. At present, GA, ABA, cytokinin (CK), and ethylene are the main endogenous hormones known to affect seed germination. To further investigate the results of the joint analysis, we selected phytohormone-related proteins and genes significantly enriched in the GO annotation (Figure 4D). There were 407 DEGs enriched in the "response to hormone" of transcriptome data, and 219 DEPs enriched in the phytohormone GO term in proteomics. A total of 41 were

significantly enriched in both the transcriptome and proteome (Table S10), in which the protein expression is shown in the form of a heatmap (Figure 6A). At the same time, some data were randomly selected for qRT–PCR verification (Figure 6B), which further demonstrated the reliability of sequencing data.

In previous studies, ABA-insensitive *Arabidopsis* mutants and the WT were used for experiments. Under suitable germination conditions, the mutants could germinate directly without going through dormancy, indicating that ABA inhibited seed germination (Kermode, 2005; Song et al., 2020). Under salt stress, the expression levels of proteins related to the ABA-signaling pathway in *eno2*, such as Aconitate hydratase 3, mitochondrial (EC:4.2.1.3) (ACO3), 3-ketoacyl-CoA thiolase 2, peroxisomal (EC:2.3.1.16) (PED1), and Basic-leucine zipper (BZIP) transcription factor family protein (HY5), were significantly upregulated, and the expression levels of genes were consistent with proteins. GA is a plant hormone closely related to seed germination and dormancy; however, its specific regulatory mechanism is not clear. Using GA alone did not improve seed germination. GA could help the radicle break

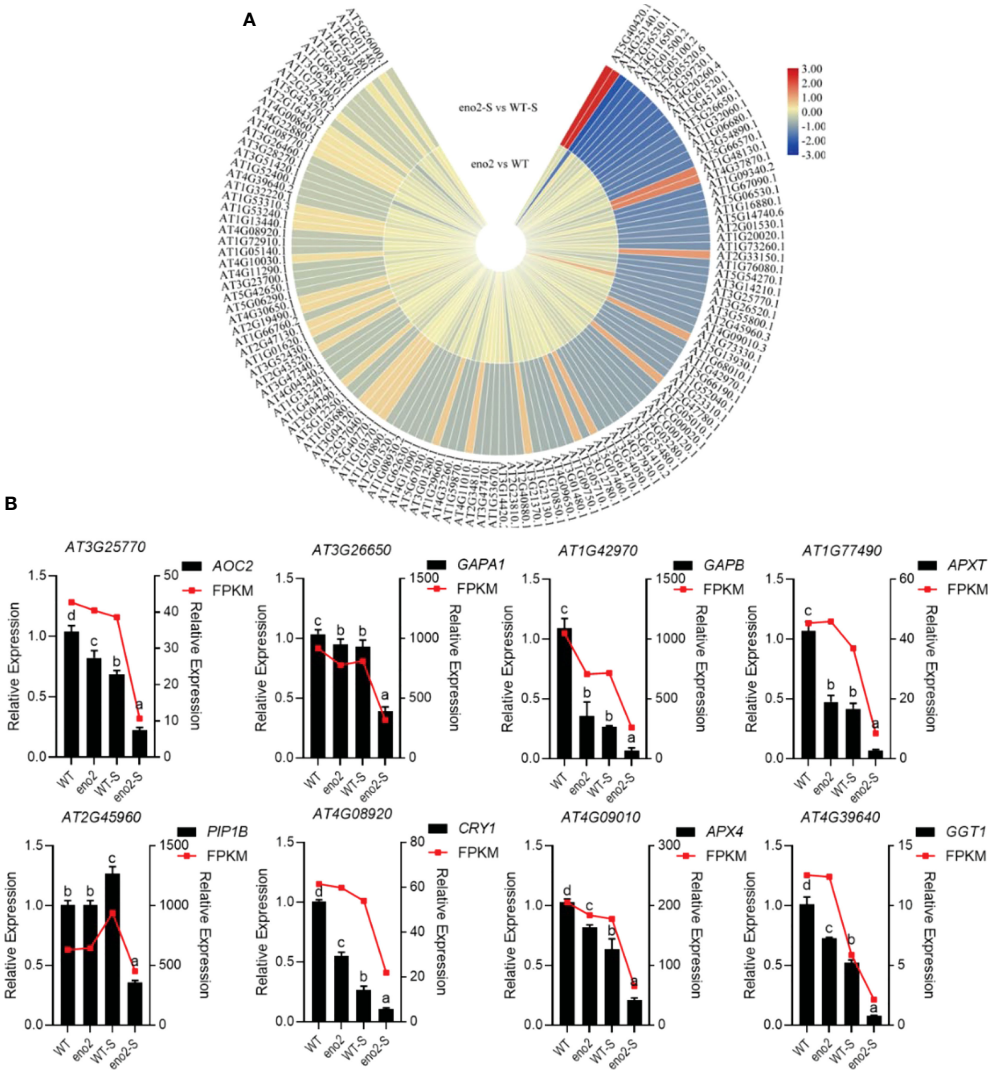


FIGURE 5
Heatmap of stress-related protein expression in the combined analysis and qRT–PCR validation of corresponding genes Expression of stress-related DEPs in the combined analysis **(A)**. The heatmap was drawn with log2FC by TBtools (Chen et al., 2020). The red to yellow colors represent significantly upregulated proteins, and the yellow to blue colors represent significantly downregulated proteins. qRT–PCR validation of DEGs that were related to stress **(B)**. The FPKM value was taken as the relative expression level of DEGs, which is shown as the red line, corresponding to the Y-axis on the right side. The qRT–PCR validation used the black bar chart, corresponding to the Y-axis on the left side, and *UBQ5* was used for each sample as an endogenous control. Three independent biologicals and three technical replicates were employed. Different letters indicate significant differences by one-way ANOVA ($P < 0.05$) with SPSS.

through the limitation of the seed coat and promote seed germination by enhancing the growth ability of the embryo and softening the seed coat and endosperm (Yamauchi et al., 2004). Under salt stress, GA-regulated protein 1 (GASA1), which is related to GA synthesis, was significantly lower in *eno2*$^{-}$. The content of auxin can also affect the seed germination process; usually, a low concentration (0.03~3 nmol/L) promotes seed germination (He et al., 2012), and a high concentration (0.3~1 μmol/L) inhibits germination (Liu et al., 2007). Under salt stress, the expression levels of genes and proteins related to the auxin-signaling pathway in *eno2*$^{-}$ were significantly lower than those in the WT. These changes in plant hormone content also explain the phenotype of seed germination in *eno2*$^{-}$.

Protein–protein interaction analysis and interaction protein validation

One of the important ways for proteins to perform their functions is to interact with other proteins and play biological regulatory roles through protein-mediated pathways or complex formation. Therefore, the study of protein–protein interactions is of

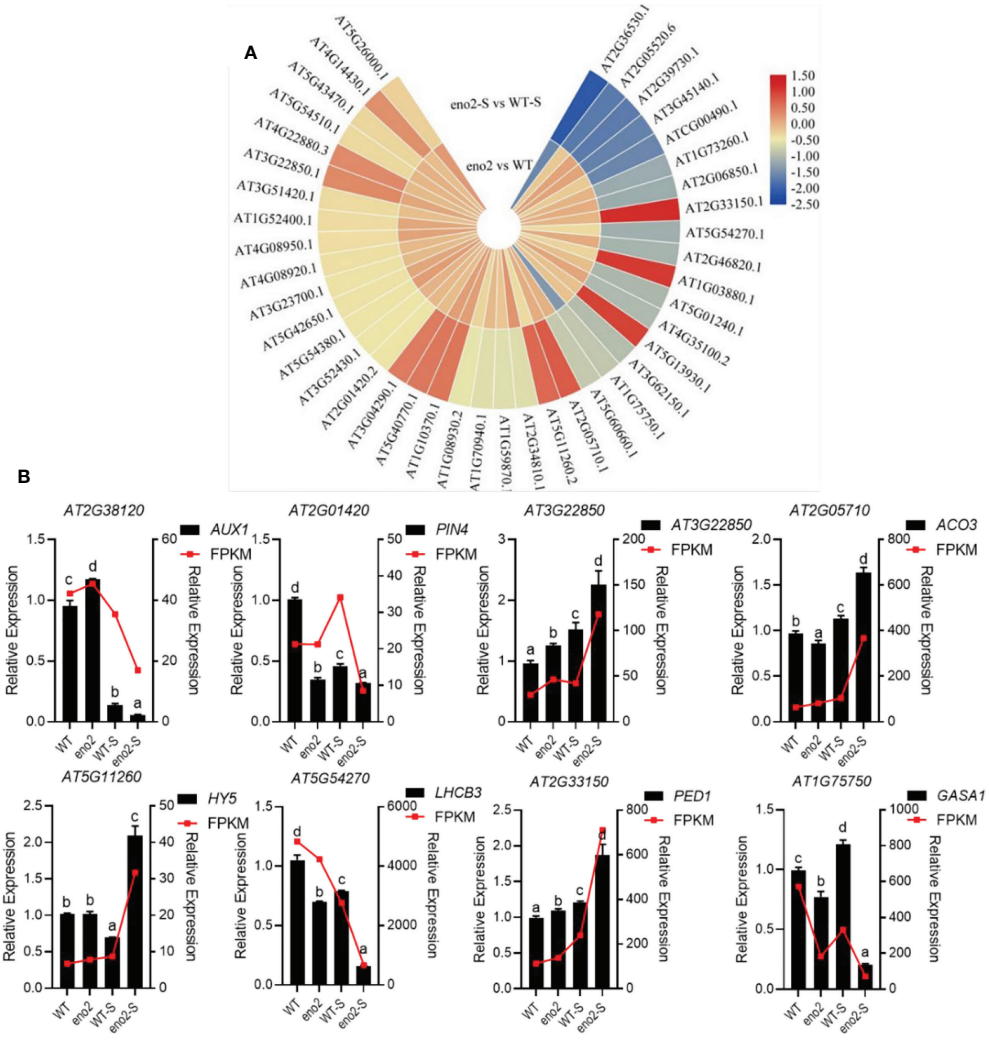


FIGURE 6
Heatmap of hormone-related protein expression in the combined analysis and qRT–PCR validation of corresponding genes. Expression of phytohormone-related DEPs in the combined analysis **(A)**. The heatmap was drawn with log2FC by TBtools (Chen et al., 2020). The red to yellow colors represent significantly upregulated proteins, and the yellow to blue colors represent significantly downregulated proteins. qRT–PCR validation of DEGs related to plant hormones **(B)**. The FPKM value was taken as the relative expression level of DEGs, which is shown as the red line, corresponding to the Y-axis on the right side. The qRT–PCR validation used the black bar chart, corresponding to the Y-axis on the left side, and *UBQ5* was used for each sample as an endogenous control. Three independent biologicals and three technical replicates were employed. Different letters indicate significant differences by one-way ANOVA ($P < 0.05$) with SPSS.

great significance. In this study, OmicsBean was used to analyze the DEPs under salt stress after a combined analysis. The proteins from five pathways of the KEGG pathway (Figure 4E) were mainly selected to construct the PPI network (Figure 7A). In addition, we found that 3 proteins (PGK1, GAPA1, and GAPB) interacted with ENO2 (Figure 7B). Previous studies in our laboratory have proven that ENO2 can interact with PGK1 by Y2H (yeast two-hybrid) (Zhang et al., 2018). To verify PPI result, we next performed split luciferase complementation assays. Luciferase activity was detected in *Nicotiana benthamiana* leaves cotransformed with ENO2-nLuc and cLuc-GAPA1/GAPB constructs, whereas the negative control did not have signals, which indicates that ENO2 associates with GAPA1/GAPB *in vivo* (Figures 7C, D).

Discussion

AtENO2 is a positive germination regulator under salt stress

In *Arabidopsis*, as a glycolytic metalloenzyme, AtENO2 catalyzes the dehydration of 2-phospho-D-glycerate (2-PGA) to phosphoenolpyruvate (PEP). Previous studies have shown that ENO2 is not only essential in glycolysis but also plays an indispensable role in the normal growth of *Arabidopsis* and response to abiotic stress. Twelve-day-old seedlings of *eno2*$^{-}$ had much shorter roots as well as smaller, pale green leaves, with shorter petioles than the WT. The mutations were characterized by severe dwarfism (Eremina et al., 2015). Our laboratory found that ENO2 can influence seed size and weight by adjusting the CK content and forming the ENO2-bZIP75 complex (Liu et al., 2020). *eno2*$^{-}$ impaired cold-responsive gene transcription, acquired freezing tolerance, and plant resistance to chilling under certain conditions (Lee et al., 2002a). Our laboratory also used deep sequencing of small RNAs to reveal the molecular regulatory network of *AtENO2* on the seed germination rate (Wu et al., 2021). However, the role of *AtENO2* in germination under salt stress is unclear. We found that *eno2*$^{-}$ was hypersensitive to NaCl and mannitol treatments during seed germination but less sensitive to KCl treatment compared to the WT (Figure 1), which revealed that *AtENO2* was involved in seed germination by affecting the content of Na+ and osmotic pressure. Together, these results clearly showed that *AtENO2* responded to multiple abiotic stresses and that *AtENO2* was a positive germination regulator under salt stress.

AtENO2 regulates a large array of stress-responsive genes and corresponding proteins

Integrative transcriptomic and TMT-based proteomic analysis revealed many DEGs and DEPs involved in the

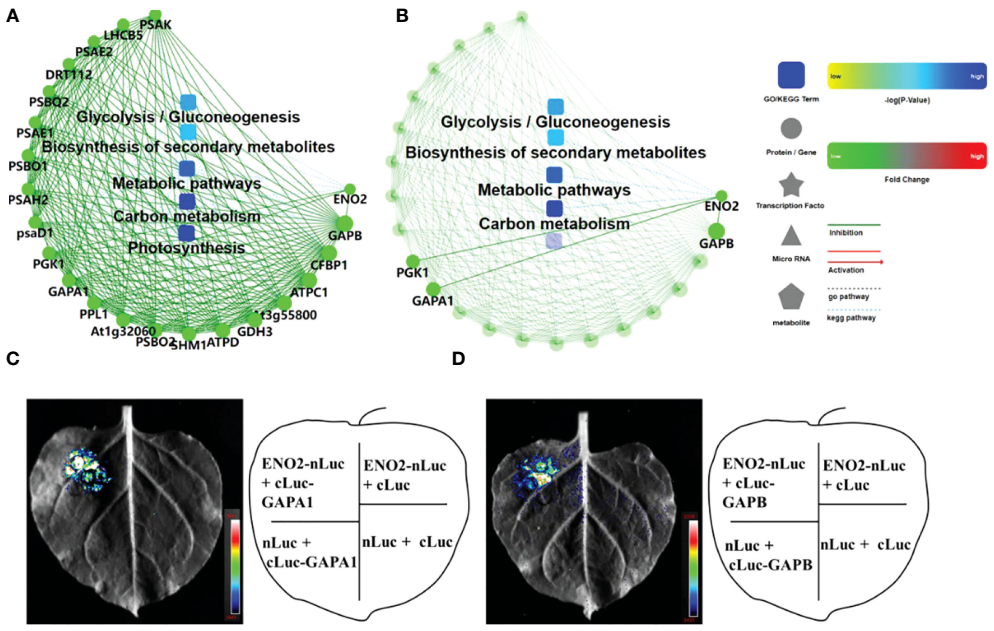


FIGURE 7
PPI network and interaction protein validation with LCA. **(A)** PPI of the proteins enriched in the top 5 KEGG pathways of Figure 5 **(E)**. **(B)** The proteins interacting with AtENO2 in **(A)**. Green represents downregulation, and red represents upregulation in *eno2*$^{-}$ compared to the WT. **(C)** Luciferase complementation assays (LCAs) revealed that ENO2 interacts with GAPA1. **(D)** LCA indicates that ENO2 interacts with GAPB. The pseudocolour represents the range of luminescence intensity in the image.

response to stimulus, and stresses were enriched in *eno2*$^-$ compared to the WT under salt stress (Figure 4D). The expression of a large number of stress-responsive genes and corresponding proteins was significantly lower in the mutant. Water transportation is a major physiological process of vegetative and reproductive growth in plants that can be tightly influenced under different conditions (Blum, 2009; Wang et al., 2021). Aquaporins (AQPs) play a central role in the symplastic pathway, which is efficient in transporting water across membranes (Maurel et al., 2008; Maurel et al., 2015). In addition to transporting water, AQPs also involve many physiological and developmental processes, including seed germination, reproductive growth, and stress responses in plants (Durbak et al., 2014; Beamer et al., 2021; Su et al., 2022). *PIP1B* (*PIP1;2*) is a vital member of the *Arabidopsis* aquaporin family. Essential for the water permeability of the plasma membrane and the morphology of the root system (Tournaire-Roux et al., 2003). Under normal conditions, there was no significant difference in the expression of PIP1B between the WT and *eno2*$^-$, but it was significantly reduced under salt stress. The trend of gene expression was the same as that of protein expression (Figure 5). We hypothesized that under salt stress, the expression of PIP1B in *eno2*$^-$ was significantly reduced, and the water transport capacity was also lower, thus affecting the seed germination process.

The activity of peroxidases is positively correlated with plant resistance (Gaudet et al., 2011); that is, the higher its activity is, the stronger the stress resistance of the plant. Hydrogen peroxide (H_2O_2) is one of the important representatives of ROS (Liu et al., 2018; Wu et al., 2020). Hormone signals and abiotic stress can induce the production and accumulation of H_2O_2 in plant cells. Under normal conditions, the production and removal process of H_2O_2 maintains a fine dynamic balance, which not only ensures the physiological function of H_2O_2 in plants but also minimizes the harmful effect on plants. If the balance of H_2O_2 production and scavenging is broken, excessive accumulation of H_2O_2 occurs, which can cause oxidative damage due to its high redox activity. To reduce the toxicity of H_2O_2, plants have formed complex and effective coping mechanisms, mainly including superoxide dismutase (SOD), catalase (CAT), ascorbate peroxidase (APX), and peroxidase (POD) enzymatic scavenging systems, as well as ascorbic acid, oxidized glutathione, and other nonenzymatic scavenging systems that can remove H_2O_2 (Akbar et al., 2020; Meng et al., 2022). APXT plays a key role in hydrogen peroxide removal. APX4 was originally thought to be an ascorbate peroxidase (Panchuk et al., 2002; Lu et al., 2007). Under normal growth conditions, the expression of APXT and APX4 in *eno2*$^-$ was lower than that in the WT, and the difference was more obvious under salt stress (Figure 5). All these results revealed that more H_2O_2 accumulated in the mutant, and the balance was broken, which affected the germination process of seeds under salt stress.

AtENO2 affects phytohormone-related genes and corresponding proteins

In addition to external stress-related factors, internal phytohormones also play an indispensable role in seed germination. As an important regulatory factor of plant growth, ABA can promote seed dormancy, inhibit seed germination, inhibit seedling root growth, promote leaf senescence, and participate in a variety of metabolic synthesis pathways and signal transduction pathways (Breeze, 2020; Varshney and Majee, 2021; Ali et al., 2022; Mphande et al., 2022). GA and ABA play opposite roles in seed germination. GA can break seed dormancy and promote seed germination (Liu and Hou, 2018; Abley et al., 2021). Seeds of GA-deficient mutants *ga1* and *ga2* showed an enhanced dormancy phenotype, while exogenous GA could promote seed germination (Lee et al., 2002b; Shu et al., 2013). In the absence of GA, DELLA proteins such as RGL2, a negative regulator, promote the expression of XERICO, a ring finger protein that encodes ABA synthesis, which in turn increases the expression of RGL2 and ABA-signaling proteins such as ABI5, thereby inhibiting seed germination. GA interrupts this pathway by promoting the degradation of DELLA, which promotes the germination process of seeds (Piskurewicz et al., 2008; Ariizumi et al., 2013; Park et al., 2013).

In our research, integrative transcriptomic and proteomic analyses revealed that a large number of DEGs and DEPs involved in the response to the hormones were enriched in *eno2*$^-$ compared to the WT under salt stress (Figure 4D). After *ENO2* deletion, the expression levels of many genes and proteins related to phytohormone synthesis were significantly changed. 3-Ketoacyl-CoA thiolase-2 (PED1/KAT2/PKT3) (EC 2.3.1.16) is an enzyme catalyzing the β-oxidation of fatty acids involved in ABA signaling. Previous research has proven that PED1 positively regulates ABA signaling in all major ABA responses, including ABA-induced inhibition of seed germination and postgermination growth arrest and ABA-induced stomatal closure and stomatal opening inhibition in *Arabidopsis thaliana* (Jiang et al., 2011). Our results showed that the content of PED1 was prominently upregulated in *eno2*$^-$ under salt stress, which indicated that the concentration of ABA also increased correspondingly. We noticed that the protein expression indices of HY5 and ACO3 related to ABA were also upregulated in *eno2*$^-$ compared to the WT under salt stress. In addition, we found a protein named GASA1, which may function in hormonal controlled steps of development such as seed germination, flowering, and seed maturation and was

downregulated notably in *eno2*$^-$ under salt stress. Interestingly, GASA1 was also downregulated by ABA (Raventos et al., 2000). Together, the change in these phytohormones corresponded with the lower seed germination rate in the *eno2*$^-$ mutant.

AtENO2 interacts with GAPA1/GAPB to regulate seed germination under salt stress

Interaction with other proteins is one of the important mechanisms of protein functions. Protein interaction experiments confirmed that AtENO2 could interact with GAPA1 and GAPB (Figure 7). Whether it was normal or under salt stress, the GAPA1/GAPB content in *eno2*$^-$ was markedly lower than that in the WT (Figure 5). GAPDH is a constitutively expressed enzyme that plays a vital role in carbon metabolism mainly by participating in glycolysis. There are four major GAPDHs in higher plants: GAPA/GAPB, GAPC, NP-GAPDH, and GAPCp. The expression of GAPDH is very abundant in organisms, and it is generally expressed constantly in the same tissues and is highly conserved; therefore, it is usually used as a housekeeping gene. However, an increasing number of studies have shown that GAPDH not only participates in glycolysis and the Calvin cycle but also plays an important role in protein transport and modification, cell apoptosis control, and response to abiotic stress (Sirover, 2018; Dar et al., 2021; Lim et al., 2021). *GAPC* can respond to a variety of stresses and can play an indispensable regulatory role in the process of plant resistance to stress (Zhang et al., 2019; Yang et al., 2021b). The main reason for this may be that as the main regulator of energy metabolism in cells, plants can maintain their growth under stress by adjusting the energy and metabolism in cells. GAPA and GAPB, which we focused on, are NADPH-specific phosphorylases that play a role in carbon dioxide fixation in chloroplast photosynthesis. Previous studies have shown that overexpressing GAPB in *Arabidopsis thaliana* can improve its salt resistance (Chang et al., 2015), which may be because GAPB can maintain the high circulation of ADP and NADP+ under salt stress, thus reducing the damage caused by excessive ROS production and maintaining the photosynthetic efficiency and growth of plants under high salt stress. Under salt stress, the contents of GAPB and GAPA1 in *eno2*$^-$ decreased significantly, indicating that their corresponding photosynthetic efficiency also decreased notably. Correspondingly, we detected chlorophyll content in seedlings of different lines growing for the seventh day, and the chlorophyll content in the mutant was prominently lower than that in the WT (Supplementary Figure S2). Therefore, we inferred that ENO2 could regulate seed germination by forming the ENO2-GAPA1 or ENO2-GAPB complex under salt stress in *Arabidopsis thaliana*. Of course, the role of GAPA1 or GAPB in seed germination still needs to be further studied.

Materials and methods

Plant materials and growth conditions

The ecotype Columbia (Col-0) of *Arabidopsis thaliana* was used as the WT, and the *AtENO2* T-DNA insertion mutants *los2-2* (also called *eno2*$^-$) (SALK_021737), *los2-3* (SALK_077784), and *los2-4* (SAIL_208_B09) were obtained from the Arabidopsis Biological Resource Center (ABRC) at Ohio State University. The details of these mutants were described previously (Eremina et al., 2015). Because *los2-3* and *los2-4* were embryonic lethal, we only used *eno2*$^-$ in our research. The *eno2*$^-$/35S:*AtENO2* lines (*ER*, the CDS of entire *AtLOS2* rescued to *eno2*$^-$) were preserved in our lab. Seeds were surface-sterilized for 5 min in 2% sodium hypochlorite (Lvtao Environ-mental Technology, Cangzhou, China) and rinsed three times with sterile water. The seeds were plated on 1/2 MS medium supplemented with 1.5% sucrose (w/v) (Coolaber, Beijing, China) and 0.8% agar (w/v) (Coolaber, Beijing, China). The plates were placed at 4°C for 3 days and moved to a long-day (16 h light/8 h dark) growth room at 21°C for subsequent research.

Seed germination assay

To explore the role of *AtENO2* in the stress response, the WT, *eno2*$^-$, and *ER* (the CDS of entire *AtLOS2* rescued to *eno2*$^-$) constructed, screened, and identified in our laboratory (Liu et al., 2020) were used as materials to calculate germination status. The seeds of the WT, *eno2*$^-$, and *ER* were germinated on 1/2 MS medium with or without 100 mM NaCl, isotonic mannitol, or 100 mM KCl (the same concentration as NaCl), and the germination rates were checked every day for 7 days. We regarded radicle breaks through seed coats as germination (Zhao et al., 2021a). The germination and cotyledon greening of each line were counted at a fixed time every day. The average seed germination rate was obtained from three experimental replicates, and approximately 30 seeds were observed for each genotype. The seed germination rate was obtained by counting the number of germinated seeds divided by the total number of seeds tested. On the seventh day, the overall situation of germination and leaves were photographed, and the width and length of leaves were measured for further statistical analysis. Meanwhile, we collected and immediately froze the seedlings on the seventh day in liquid nitrogen. The samples were stored at -80°C until RNA and protein extraction.

Chlorophyll content measurement

Chlorophyll was extracted from seedlings germinated for seven days using 95% ethanol (v/v) and the absorbance of the supernatant was measured using a SpectraMax Plus 384 (Molecular Devices,

USA). Chlorophyll content was estimated as described by the following equation (Wintermans and Demots, 1965).

Transcriptome profiling

Total RNA was extracted from the seedlings (WT and *eno2*$^-$) on the seventh day under normal and salt conditions (100 mM) using TRIzol® Reagent according to the instructions (Magen, Guangzhou, China). RNA samples were detected based on the A260/A280 absorbance ratio with a Nanodrop ND-2000 system (ThermoFisher Scientific, Waltham, USA), and the RIN of RNA was determined by an Agilent Bioanalyzer 4150 system (Agilent Technologies, California, USA). Only qualified samples were used for library construction. Paired-end libraries were prepared using an ABclonal mRNA-seq Lib Prep Kit (ABclonal, Wuhan, China) following the manufacturer's recommendations. mRNA was enriched by oligo (DT) beads and decomposed by fragmentation buffer. These short fragments were reverse-transcribed into cDNA using random primers, and the second-strand cDNA was subsequently synthesized using dNTPs, DNA polymerase I, RNase H, and buffer. The ligated products were selected by agarose gel electrophoresis, PCR amplified, and then sequenced on an Illumina Novaseq 6000/MGISEQ-T7 instrument.

The data generated from the Illumina/BGI platform were used for bioinformatics analysis. Clean data were obtained by removing unqualified reads with ambiguous nucleotides, and adapter sequences were filtered from raw data. Then, the clean data were separately aligned to the reference genome with orientation mode using HISAT2 software (http://daehwankimlab.github.io/hisat2/) to obtain mapped reads. The mapped reads were spliced with StringTie software (http://ccb.jhu.edu/software/stringtie/), and we used Gffcompare software (http://ccb.jhu.edu/software/stringtie/gffcompare.shtml) to compare them with the reference genome GTF/GFF file to detect the original unannotated transcription region and find new transcripts and new genes of the species. We used FeatureCounts (http://subread.sourceforge.net/) to count the read numbers that mapped to each gene. Then, the FPKM of each gene was calculated based on the length of the gene, and the read count was mapped to this gene. DESeq2 was used to screen the DEGs, and DEGs with $|\log2FC|>1$, and p value<0.05 were considered to be significant DEGs. The volcano plot and UpSet graph were drawn with the help of the Omicstudio cloud platform (https://www.omicstudio.cn/tool/43). The GO was plotted by the OmicShare cloud platform (https://www.omicshare.com/).

Protein extraction, protein digestion, and TMT labeling

Total proteins were extracted from seedlings (WT and *eno2*$^-$) on the seventh day under normal and salt conditions (100 mM) using SDT buffer (4% (w/v) SDS, 100 mM Tris/HCl, 1 mM DTT, pH 7.6), and the amount of protein was quantified with the BCA Protein Assay Kit (Bio–Rad, California, USA). Protein digestion by trypsin was performed according to the filter-aided sample preparation (FASP) procedure described by Jacek R Wiśniewski (Wisniewski et al., 2009). The digest peptides of every sample were desalted on C18 Cartridges (Empore™ SPE Cartridges C18 (standard density), bed I.D. 7 mm, volume 3 ml, Sigma), concentrated by vacuum centrifugation and reconstituted in 40 µl of 0.1% (v/v) formic acid. We took 100 µg of peptide from each sample and labeled it according to the instructions of the kit (ThermoFisher Scientific, Waltham, USA). The samples were labelled (WT-1)-126, (WT-2)-127 N, (WT-3)-127 C, (*eno2*–1)-128 N, (*eno2*–2)-128 C, (*eno2*–3)-129 N, (WT-S-1)-129 C, (WT-S-2)-130 N, (WT-S-3)-130 C, (*eno2*$^-$–S-1)-131 N, (*eno2*$^-$–S-2)-131 C, and (*eno2*–S-3)-132 N. Our project designed 4 groups, and each group contained 3 biological repeat samples, for a total of 12 samples.

High pH reversed-phase fractionation and liquid chromatography-tandem mass spectrometry analysis

The labeled peptides in each group were mixed in equal amounts, and the labeled peptides were fractionated by the High pH Reversed-Phase Peptide Fractionation Kit (ThermoFisher Scientific, Waltham, USA). The dried peptide mixture was reconstituted and acidified with 0.1% TFA solution and loaded onto an equilibrated, high-pH, reversed-phase fractionation spin column. The peptide segments were combined with hydrophobic resin in the aqueous phase and desalted by low-speed centrifugation and washing the column with water. A step gradient of acetonitrile concentration in a volatile high pH elution solution was then applied to the column to elute the binding peptide into 10 distinct parts by centrifugal collection. The collected fraction was desalted on C18 cartridges (Empore™ SPE Cartridges C18 (standard density), bed I.D. 7 mm, volume 3 ml) and then concentrated by vacuum centrifugation.

Each sample in the project was separated by an Easy nLC HPLC system at a nanolitre flow rate. Buffer Solution A was a 0.1% formic acid aqueous solution, and buffer Solution B was a 0.1% formic acid acetonitrile aqueous solution (acetonitrile was 84%). The chromatographic column was balanced with 95% Liquid A, and the samples were transferred from an automatic sampler to the loading column and separated by an analytical column at a flow rate of 300 NL/min. The chromatographic column was balanced with 95% Liquid A, and the samples were transferred from an automatic sampler to the loading column (Thermo Scientific Acclaim PepMap100, 100 µm*2 cm, nanoViper C18) and separated by an analytical column (Thermo Scientific Easy Column, 10 cm long, 75 µm inner diameter, 3 µm resin) at a flow rate of 300 NL/min. After

chromatographic separation, the samples were analyzed by a Q-exactive mass spectrometer (ThermoFisher Scientific, Waltham, USA). The detection method was positive ion, the scanning range of parent ion was 300-1800 m/z, the resolution of primary mass spectrometry was 70000 at 200 m/z, the target of automatic gain control (AGC) was 1e6, the maximum was 50 ms, and the dynamic exclusion time was 60.0 s. The mass charge ratios of peptides and peptide fragments were collected as follows: Twenty MS2 Scan were collected after each full scan. The MS2 activation type was HCD, and the isolation window was 2 m/z. The secondary mass spectrometry resolution was 17,500 at 200 m/z. The normalized collision energy was 30 eV, and the underfill was 0.1%.

Bioinformatics analysis of proteomic data

The MS raw data for each sample were searched using the MASCOT engine (Matrix Science, London, UK; Version 2.2) embedded into Proteome Discoverer 1.4 software for identification and quantitation analysis. The volcano plot and UpSet graph were drawn with the help of the Omicstudio cloud platform (https://www.omicstudio.cn/tool/43). The GO was plotted by the OmicShare cloud platform (https://www.omicshare.com/). KEGG and PPI analyses were performed using OmicsBean (http://www.omicsbean.cn/dashboard/).

RNA extraction and qRT–PCR assay

Total RNA was extracted from seedlings on the seventh day of germination using Eastep® Super (Promega, Madison, USA). Total RNA from each sample was converted into cDNA by using First-Strand cDNA Synthesis SuperMix (TransGen, Beijing, China). The specific forward primers and the universal reverse primer were designed by Primer 5.0 (Table S11). qRT–PCR was performed using TransStart® Top Green qPCR SuperMix (TransGen, Beijing, China) on an ABI7500 Real-time PCR system. The 20 μL reactions contained 2 μL reverse transcription cDNA products, 10 μL qPCR SuperMix, 2 μL primer mix, and supplemented with nuclease-free water to 20 μL. The qRT-PCR were performed as follows: 94°C for 30 s, followed by 40 cycles of 94°C for 5 s and 60°C for 30 s. Each reaction had three technical replicates, and the expression levels were calculated using the $2^{-\Delta\Delta Ct}$ method. *UBQ5* was used as the internal standard.

Luciferase complementation assay

The coding sequences of AtENO2 were cloned into pCAMBIA1300-nLuc, while the coding sequences of AtGAPA1 and AtGAPB were cloned into pCAMBIA1300-cLuc. The sequences of primers for these constructs are listed in Table S12. The pairs of Agrobacterium tumefaciens strain (GV3101) carrying ENO2-nLuc/cLuc-GAPA1, ENO2-nLuc/cLuc, nLuc/cLuc-GAPA1, ENO2-nLuc/cLuc-GAPB, nLuc/cLuc-GAPB, and nLuc/cLuc were cotransformed into four-week N. *benthamiana* leaves. After infiltration, plants were covered with plastic bags and placed at 21°C for 24 h in a dark room. Plants were then incubated at 21°C with 48 h light before the signals were detected with CCD (Chen et al., 2008).

Statistical analysis

The data are presented as the means ± SD and were compared using SPSS software with one-way ANOVA followed by Duncan's multiple range test at a significance level of $p < 0.05$. Different letters represent a significant difference.

Accession numbers

The sequence information in our study could be found in the National Center for Biotechnology Information (NCBI) under the following accession numbers: *ENO2* (*LOS2*) (At2g36530), *ENO1* (At1g74030), *ENO3* (At2g29560), *UBQ5* (At3g62250), *AUX1* (AT2G38120), *PIN4* (AT2G01420), *AT3G22850* (AT3G22850), *ACO3* (AT2G05710), *HY5* (AT5G11260), *LHCB3* (AT5G54270), *PED1* (AT2G33150), *GASA1* (AT1G75750), *AOC2* (AT3G25770), *GAPA1* (AT3G26650), *GAPB* (AT1G42970), *APXT* (AT1G77490), *PIP1B* (AT2G45960), *CRY1* (AT4G08920), *APX4* (AT4G09010), *GGT1* (AT4G39640), *PGK1* (At3g12780).

Conclusion

This is the first systematic report on the mechanism by which *AtENO2* (*AtLOS2*) affects seed germination under salt stress in *Arabidopsis thaliana* based on transcriptome and proteomic analysis. Phenotypic observation and statistics revealed that *AtENO2* acts as a positive regulator in the stress response at the germination stage. The combined analysis found many DEGs and DEPs in *eno2*$^{-}$ under salt stress compared to the WT. Genes and corresponding proteins related to stresses (PIP1B, GAPA1, GAPB, etc.) were highly downregulated in the mutant, and the DEGs and DEPs related to hydrogen peroxide removal (APXT, APX4, etc.) were also downregulated in *eno2*$^{-}$. In addition, several DEGs and DEPs encoding phytohormone transduction pathways, i.e., auxin

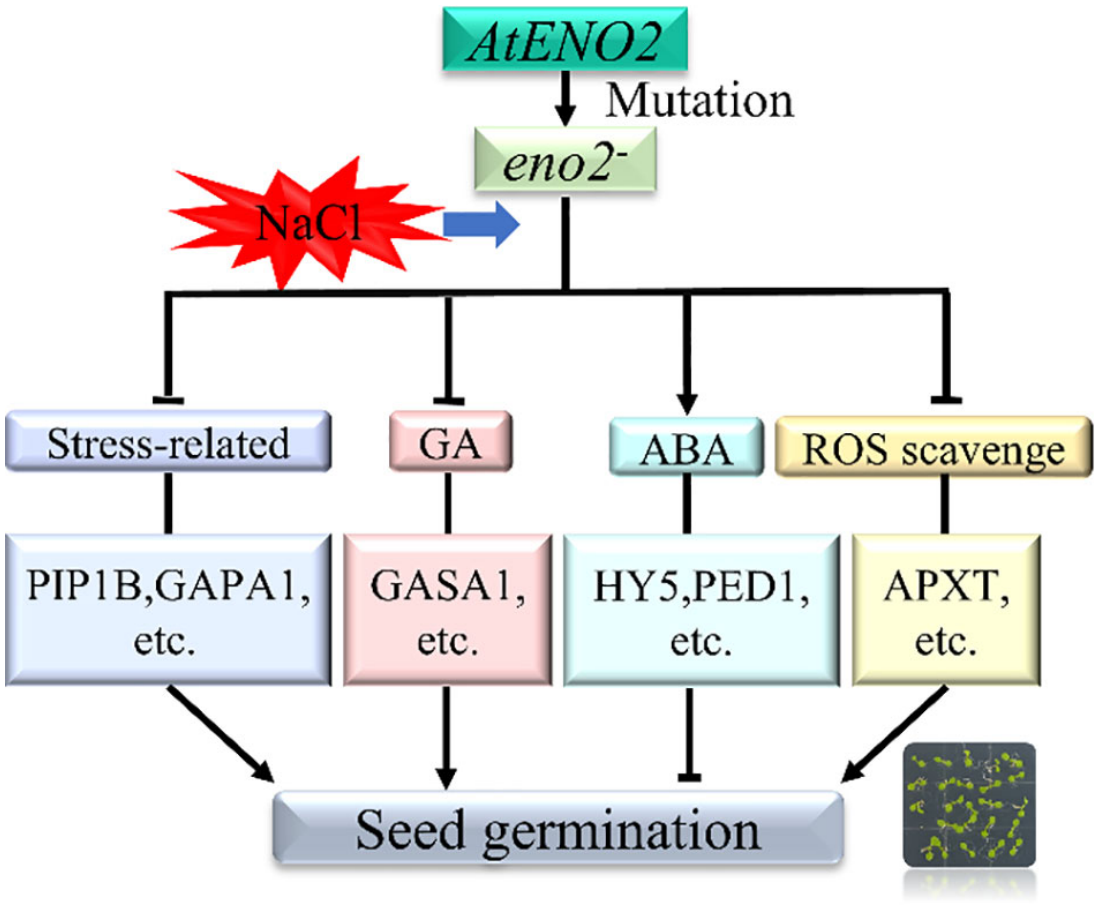


FIGURE 8
Mechanistic model of *AtENO2* affecting seed germination under salt stress Under salt stress, *AtENO2* gene mutation up-regulated genes and proteins related to the ABA signaling pathway. The mutant also down-regulated genes and proteins related to stress, GA, and ROS scavenging, ultimately affecting seed germination rate.

(PIN4, and AUX1) and GA (GASA1) were identified and may have a vital role in the contribution to salt tolerance in seed germination under *AtENO2* deficiency. The DEGs or DEPs related to ABA signalings, such as PED1, ACO3, and HY5, were relatively highly upregulated in *eno2*$^{-}$ under salt stress. These genes or proteins could participate in salt sensitivity and seed dormancy. Moreover, we constructed an interactive network with OmicsBean and further identified GAPA1 and GAPB that could interact with AtENO2 by LCA to explain the function of AtENO2 under salt stress during seed germination. Overall, all the results reveal that under salt stress, *AtENO2* mainly affects the expression of genes and proteins related to the phytohormone signal transduction pathways, stress response factors, and ROS, and then affects seed germination (Figure 8). Our research provides a better understanding of the molecular function of *AtENO2* in enhancing salt resistance in *Arabidopsis thaliana* at the seed germination stage.

Data availability statement

The RNA-Seq data presented in the study are deposited in the NCBI, PRJNA839519. The proteomics data have been deposited to ProteomeXchange Consortium via the iProX partner repository, PXD033483.

Author Contributions

GZ and YW designed this project. YW performed most of the experiments and analyzed the data. YW drew all the graphs, and YW wrote the paper. HL assisted in the experiment of seed germination. JB collected some references related to omics. GZ provided financial support. All authors contributed to the article and approved the submitted version.

Funding

This study was funded by the National Natural Science Foundation of China (31872672) and the Open fund from the Beijing Key Laboratory of Gene Resource and Molecular Development.

Acknowledgments

We would like to thank the experimental technology center for life sciences, Beijing Normal University. We are also grateful to Shanghai Applied Protein Technology for assisting in sequencing.

Conflict of interest

The authors declare that the research was conducted in the absence of any commercial or financial relationships that could be construed as a potential conflict of interest.

Publisher's note

All claims expressed in this article are solely those of the authors and do not necessarily represent those of their affiliated organizations, or those of the publisher, the editors and the reviewers. Any product that may be evaluated in this article, or claim that may be made by its manufacturer, is not guaranteed or endorsed by the publisher.

Supplementary material

The Supplementary Material for this article can be found online at: https://www.frontiersin.org/articles/10.3389/fpls.2022.1035750/full#supplementary-material

References

Abley, K., Formosa-Jordan, P., Tavares, H., Chan, E. Y. T., Afsharinafar, M., Leyser, O., et al. (2021). An ABA-GA bistable switch can account for natural variation in the variability of arabidopsis seed germination time. *Elife* 10. doi: 10.7554/eLife.59485.sa2

Akbar, S., Wei, Y., Yuan, Y., Khan, M. T., Qin, L. F., Powell, C. A., et al. (2020). Gene expression profiling of reactive oxygen species (ROS) and antioxidant defense system following sugarcane mosaic virus (SCMV) infection. *BMC Plant Biol.* 20. doi: 10.1186/s12870-020-02737-1

Ali, F., Qanmber, G., Li, F. G., and Wang, Z. (2022). Updated role of ABA in seed maturation, dormancy, and germination. *J. Adv. Res.* 35, 199–214. doi: 10.1016/j.jare.2021.03.011

Andriotis, V. M. E., Kruger, N. J., Pike, M. J., and Smith, A. M. (2010). Plastidial glycolysis in developing arabidopsis embryos. *New Phytol.* 185, 649–662. doi: 10.1111/j.1469-8137.2009.03113.x

Arai, Y., Hayashi, M., and Nishimura, M. (2008). Proteomic identification and characterization of a novel peroxisomal adenine nucleotide transporter supplying ATP for fatty acid beta-oxidation in soybean and arabidopsis. *Plant Cell* 20, 3227–3240. doi: 10.1105/tpc.108.062877

Ariizumi, T., Hauvermale, A. L., Nelson, S. K., Hanada, A., Yamaguchi, S., and Steber, C. M. (2013). Lifting DELLA repression of arabidopsis seed germination by nonproteolytic gibberellin signaling. *Plant Physiol.* 162, 2125–2139. doi: 10.1104/pp.113.219451

Beamer, Z. G., Routray, P., Choi, W. G., Spangler, M. K., Lokdarshi, A., and Roberts, D. M. (2021). Aquaporin family lactic acid channel NIP2;1 promotes plant survival under low oxygen stress in arabidopsis. *Plant Physiol.* 187, 2262–2278. doi: 10.1093/plphys/kiab196

Blum, A. (2009). Effective use of water (EUW) and not water-use efficiency (WUE) is the target of crop yield improvement under drought stress. *Field Crop Res.* 112, 119–123. doi: 10.1016/j.fcr.2009.03.009

Breeze, E. (2020). Make, modify, move: Multilayered regulation of ONAC054 during ABA-induced leaf senescence. *Plant Cell* 32, 532–533. doi: 10.1105/tpc.20.00003

Calhoun, S., Bell, T. A. S., Dahlin, L. R., Kunde, Y., LaButti, K., Louie, K. B., et al. (2021). A multi-omic characterization of temperature stress in a halotolerant scenedesmus strain for algal biotechnology. *Commun. Biol.* 4. doi: 10.1038/s42003-021-01859-y

Chang, L. L., Guo, A. P., Jin, X., Yang, Q., Wang, D., Sun, Y., et al. (2015). The beta subunit of glyceraldehyde 3-phosphate dehydrogenase is an important factor for maintaining photosynthesis and plant development under salt stress-based on an integrative analysis of the structural, physiological and proteomic changes in chloroplasts in thellungiella halophila. *Plant Sci.* 236, 223–238. doi: 10.1016/j.plantsci.2015.04.010

Chen, C. J., Chen, H., Zhang, Y., Thomas, H. R., Frank, M. H., He, Y. H., et al. (2020). TBtools: An integrative toolkit developed for interactive analyses of big biological data. *Mol. Plant* 13, 1194–1202. doi: 10.1016/j.molp.2020.06.009

Chen, H. M., Zou, Y., Shang, Y. L., Lin, H. Q., Wang, Y. J., Cai, R., et al. (2008). Firefly luciferase complementation imaging assay for protein-protein interactions in plants. *Plant Physiol.* 146, 368–376. doi: 10.1104/pp.107.111740

Dar, G. H., Mendes, C. C., Kuan, W. L., Speciale, A. A., Conceicao, M., Gorgens, A., et al. (2021). GAPDH controls extracellular vesicle biogenesis and enhances the therapeutic potential of EV mediated siRNA delivery to the brain. *Nat. Commun.* 12. doi: 10.1038/s41467-021-27056-3

Deshmukh, R., Sonah, H., Patil, G., Chen, W., Prince, S., Mutava, R., et al. (2014). Integrating omic approaches for abiotic stress tolerance in soybean. *Front. Plant Sci.* 5. doi: 10.3389/fpls.2014.00244

Durbak, A. R., Phillips, K. A., Pike, S., O'Neill, M., Mares, J., Gallavotti, A., et al. (2014). Transport of boron by the tassel-less1 aquaporin is critical for vegetative and reproductive development in maize. *Plant Cell* 26, 2978–2995. doi: 10.1105/tpc.114.125898

Eremina, M., Rozhon, W., Yang, S. Q., and Poppenberger, B. (2015). ENO2 activity is required for the development and reproductive success of plants, and is feedback-repressed by AtMBP-1. *Plant J.* 81, 895–906. doi: 10.1111/tpj.12775

Gaudet, P., Livstone, M. S., Lewis, S. E., and Thomas, P. D. (2011). Phylogenetic-based propagation of functional annotations within the gene ontology consortium. *Brief Bioinform.* 12, 449–462. doi: 10.1093/bib/bbr042

He, J. N., Duan, Y., Hua, D. P., Fan, G. J., Wang, L., Liu, Y., et al. (2012). DEXH box RNA helicase-mediated mitochondrial reactive oxygen species production in arabidopsis mediates crosstalk between abscisic acid and auxin signaling. *Plant Cell* 24, 1815–1833. doi: 10.1105/tpc.112.098707

Jiang, T., Zhang, X. F., Wang, X. F., and Zhang, D. P. (2011). Arabidopsis 3-Ketoacyl-CoA thiolase-2 (KAT2), an enzyme of fatty acid beta-oxidation, is

involved in ABA signal transduction. *Plant Cell Physiol.* 52, 528–538. doi: 10.1093/pcp/pcr008

Kang, M. Y., Abdelmageed, H., Lee, S., Reichert, A., Mysore, K. S., and Allen, R. D. (2013). AtMBP-1, an alternative translation product of LOS2, affects abscisic acid responses and is modulated by the E3 ubiquitin ligase AtSAP5. *Plant J.* 76, 481–493. doi: 10.1111/tpj.12312

Kermode, A. R. (2005). Role of abscisic acid in seed dormancy. *J. Plant Growth Regul.* 24, 319–344. doi: 10.1007/s00344-005-0110-2

Koller, D., Mayer, A. M., Poljakoffmayber, A., and Klein, S. (1962). Seed germination. *Annu. Rev. Plant Phys.* 13, 437. doi: 10.1146/annurev.pp.13.060162.002253

Lee, S. C., Cheng, H., King, K. E., Wang, W. F., He, Y. W. , Hussain, A., et al. (2002b). Gibberellin regulates arabidopsis seed germination *via* RGL2, a GAI/RGA-like gene whose expression is up-regulated following imbibition. *Gene Dev.* 16, 646–658. doi: 10.1101/gad.969002

Lee, H., Guo, Y., Ohta, M., Xiong, L. M., Stevenson, B. , and Zhu, J. K. (2002a). LOS2, a genetic locus required for cold-responsive gene transcription encodes a bi-functional enolase. *EMBO J.* 21, 2692–2702. doi: 10.1093/emboj/21.11.2692

Lee, B. D., Yim, Y., Canibano, E., Kim, S. H., Garcia-Leon, M., Rubio, V., et al. (2022). CONSTITUTIVE PHOTOMORPHOGENIC 1 promotes seed germination by destabilizing RGA-LIKE 2 in arabidopsis. *Plant Physiol* 189, 1662–1676. doi: 10.1093/plphys/kiac060

Lim, H., Hwang, H., Kim, T., Kim, S., Chung, H., Lee, D., et al. (2021). Transcriptomic analysis of rice plants overexpressing PsGAPDH in response to salinity stress. *Genes-Basel* 12. doi: 10.3390/genes12050641

Liu, Y. Y., Cao, Y. L., Zhang, Q. L., Li, X. H., and Wang, S. P. (2018). A cytosolic triosephosphate isomerase is a key component in XA3/XA26-mediated resistance. *Plant Physiol.* 178, 923–935. doi: 10.1104/pp.18.00348

Liu, W., Feng, J. P., Ma, W. Y., Zhou, Y., and Ma, Z. B. (2021). GhCLCg-1, a vacuolar chloride channel, contributes to salt tolerance by regulating ion accumulation in upland cotton. *Front. Plant Sci.* 12. doi: 10.3389/fpls.2021.765173

Liu, X., and Hou, X. L. (2018). Antagonistic regulation of ABA and GA in metabolism and signaling pathways. *Front. Plant Sci.* 9. doi: 10.3389/fpls.2018.00251

Liu, P. P., Montgomery, T. A., Fahlgren, N., Kasschau, K. D., Nonogaki, H., and Carrington, J. C. (2007). Repression of AUXIN RESPONSE FACTOR10 by microRNA160 is critical for seed germination and post-germination stages. *Plant J.* 52, 133–146. doi: 10.1111/j.1365-313X.2007.03218.x

Liu, Z., Zheng, L., Pu, L., Ma, X., Wang, X. , Wu, Y., et al. (2020). ENO2 affects the seed size and weight by adjusting cytokinin content and forming ENO2-bZIP75 complex in arabidopsis thaliana. *Front. Plant Sci.* 11, 574316. doi: 10.3389/fpls.2020.574316

Lu, Z. Q., Liu, D. L., and Liu, S. K. (2007). Two rice cytosolic ascorbate peroxidases differentially improve salt tolerance in transgenic arabidopsis. *Plant Cell Rep.* 26, 1909–1917. doi: 10.1007/s00299-007-0395-7

Martinez-Andujar, C., Ordiz, M. I., Huang, Z. L., Nonogaki, M., Beachy, R. N., and Nonogaki, H. (2011). Induction of 9-cis-epoxycarotenoid dioxygenase in arabidopsis thaliana seeds enhances seed dormancy. *P. Natl. Acad. Sci. U.S.A.* 108, 17225–17229. doi: 10.1073/pnas.1112151108

Maurel, C., Boursiac, Y., Luu, D. T., Santoni, V., Shahzad, Z., and Verdoucq, L. (2015). Aquaporins in plants. *Physiol. Rev.* 95, 1321–1358. doi: 10.1152/physrev.00008.2015

Maurel, C., Verdoucq, L., Luu, D. T., and Santoni, V. (2008). Plant aquaporins: Membrane channels with multiple integrated functions. *Annu. Rev. Plant Biol.* 59, 595–624. doi: 10.1146/annurev.arplant.59.032607.092734

Meng, X. Y., Chen, C., Song, T., Xu, J. W., Zhang, X. B., Wang, J., et al. (2022). Effect of nano-silica coating combined with pressurized ar treatment on postharvest quality and reactive oxygen species metabolism in sweet cherry fruit. *Food Chem.* 374. doi: 10.1016/j.foodchem.2021.131715

Mphande, W., Farrell, A. D., Grove, I. G., Vickers, L. H., and Kettlewell, P. S. (2022). Metabolic and film antitranspirants both reduce drought damage to wheat yield despite having contrasting effects on leaf ABA. *J. Agron. Crop Sci.* 208, 143–157. doi: 10.1111/jac.12567

Munns, R., and Tester, M. (2008). Mechanisms of salinity tolerance. *Annu. Rev. Plant Biol.* 59, 651–681. doi: 10.1146/annurev.arplant.59.032607.092911

Nonogaki, M., Sall, K., Nambara, E., and Nonogaki, H. (2014). Amplification of ABA biosynthesis and signaling through a positive feedback mechanism in seeds. *Plant J.* 78, 527–539. doi: 10.1111/tpj.12472

Panchuk, I. I., Volkov, R. A., and Schoffl, F. (2002). Heat stress- and heat shock transcription factor-dependent expression and activity of ascorbate peroxidase in arabidopsis. *Plant Physiol.* 129, 838–853. doi: 10.1104/pp.001362

Park, J., Nguyen, K. T., Park, E., Jeon, J. S., and Choi, G. (2013). DELLA proteins and their interacting RING finger proteins repress gibberellin responses by binding to the promoters of a subset of gibberellin-responsive genes in arabidopsis. *Plant Cell* 25, 927–943. doi: 10.1105/tpc.112.108951

Piskurewicz, U., Jikumaru, Y., Kinoshita, N., Nambara, E., Kamiya, Y., and Lopez-Molina, L. (2008). The gibberellic acid signaling repressor RGL2 inhibits arabidopsis seed germination by stimulating abscisic acid synthesis and ABI5 activity. *Plant Cell* 20, 2729–2745. doi: 10.1105/tpc.108.061515

Raventos, D., Meier, C., Mattsson, O., Jensen, A. B., and Mundy, J. (2000). Fusion genetic analysis of gibberellin signaling mutants. *Plant J.* 22, 427–438. doi: 10.1046/j.1365-313X.2000.00759.x

Shu, K., Zhang, H. W., Wang, S. F., Chen, M. L., Wu, Y. R., Tang, S. Y., et al. (2013). ABI4 regulates primary seed dormancy by regulating the biogenesis of abscisic acid and gibberellins in arabidopsis. *PloS Genet.* 9. doi: 10.1371/journal.pgen.1003577

Sirover, M. A. (2018). Pleiotropic effects of moonlighting glyceraldehyde-3-phosphate dehydrogenase (GAPDH) in cancer progression, invasiveness, and metastases. *Cancer Metast. Rev.* 37, 665–676. doi: 10.1007/s10555-018-9764-7

Song, Y., Zhu, J. J., and Yan, Q. L. (2020). Roles of abscisic acid and gibberellins in maintaining primary and secondary dormancy of Korean pine seeds. *J. Forestry. Res.* 31, 2423–2434. doi: 10.1007/s11676-019-01026-4

Su, Y. C., Liu, Z. H., Sun, J. H., Wu, C. L., Li, Y., Zhang, C. Q., et al. (2022). Genome-wide identification of maize aquaporin and functional analysis during seed germination and seedling establishment. *Front. Plant Sci.* 13. doi: 10.3389/fpls.2022.831916

Sun, L. L., Yuan, Z., Wang, D. X., Li, J. B., Shi, J., Hu, Y. Y., et al. (2021). Carbon starved anther modulates sugar and ABA metabolism to protect rice seed germination and seedling fitness. *Plant Physiol.* 187, 2405–2418. doi: 10.1093/plphys/kiab391

Tournaire-Roux, C., Sutka, M., Javot, H., Gout, E., Gerbeau, P., Luu, D. T., et al. (2003). Cytosolic pH regulates root water transport during anoxic stress through gating of aquaporins. *Nature* 425, 393–397. doi: 10.1038/nature01853

Varshney, V., and Majee, M. (2021). JA shakes hands with ABA to delay seed germination. *Trends Plant Sci.* 26, 764–766. doi: 10.1016/j.tplants.2021.05.002

Wang, G. F., Wang, G., Wang, J. J., Du, Y. L., Yao, D. S., Shuai, B. L., et al. (2016). Comprehensive proteomic analysis of developing protein bodies in maize (Zea mays) endosperm provides novel insights into its biogenesis. *J. Exp. Bot.* 67, 6323–6335. doi: 10.1093/jxb/erw396

Wang, X., Wu, Y., Liu, Z. J., Liu, T., Zheng, L. M., and Zhang, G. F. (2021). The pip1s quintuple mutants demonstrate the essential roles of PIP1s in the plant growth and development of arabidopsis. *Int. J. Mol. Sci.* 22. doi: 10.3390/ijms22041669

Wintermans, J. F., and Demots, A. (1965). Spectrophotometric characteristics of chlorophylls a and b and their pheophytins in ethanol. *Biochim. Biophys. Acta* 109, 448. doi: 10.1016/0926-6585(65)90170-6

Wisniewski, J. R., Zougman, A., Nagaraj, N., and Mann, M. (2009). Universal sample preparation method for proteome analysis. *Nat. Methods* 6, 359–U360. doi: 10.1038/nmeth.1322

Wu, F. H., Chi, Y., Jiang, Z. H., Xu, Y. Y., Xie, L., Huang, F. F., et al. (2020). Hydrogen peroxide sensor HPCA1 is an LRR receptor kinase in arabidopsis. *Nature* 578, 577. doi: 10.1038/s41586-020-2032-3

Wu, Y., Zheng, L. M., Bing, J., Liu, H. M., and Zhang, G. F. (2021). Deep sequencing of small RNA reveals the molecular regulatory network of AtENO2 regulating seed germination. *Int. J. Mol. Sci.* 22. doi: 10.3390/ijms22105088

Yamauchi, Y., Ogawa, M., Kuwahara, A., Hanada, A., Kamiya, Y., and Yamaguchi, S. (2004). Activation of gibberellin biosynthesis and response pathways by low temperature during imbibition of arabidopsis thaliana seeds. *Plant Cell* 16, 367–378. doi: 10.1105/tpc.018143

Yang, M., Duan, X. H., Wang, Z. Y., Yin, H., Zang, J. R. , Zhu, K., et al. (2021b). Overexpression of a voltage-dependent anion-selective channel (VDAC) protein-encoding gene, MsVDAC, from medicago sativa confers cold and drought tolerance to transgenic tobacco. *Genes-Basel* 12. doi: 10.3390/genes12111706

Yang, L. Y., Wang, Z. X., Zhang, A. Q., Bhawal, R., Li, C. L. , Zhang, S., et al. (2021a). Reduction of the canonical function of a glycolytic enzyme enolase triggers immune responses that further affect metabolism and growth in arabidopsis. *Plant Cell* 34, 1745–1767. doi: 10.1093/plcell/koab283

Zeng, T., Fang, B. H., Huang, F. L., Dai, L., Tang, Z., Tian, J. L., et al. (2021). Mass spectrometry-based metabolomics investigation on two different indica rice grains (Oryza sativa l.) under cadmium stress. *Food Chem.* 343. doi: 10.1016/j.foodchem.2020.128472

Zhang, Y. H., Chen, C., Shi, Z. H., Cheng, H. M., Bing, J., Ma, X. F., et al. (2018). Identification of salinity-related genes in ENO2 mutant (eno2(-)) of arabidopsis thaliana. *J. Integr. Agr.* 17, 94–110. doi: 10.1016/S2095-3119(17)61720-9

Zhang, L., Xu, Z. Y., Ji, H. K., Zhou, Y., and Yang, S. S. (2019). TaWRKY40 transcription factor positively regulate the expression of TaGAPC1 to enhance drought tolerance. *BMC Genomics* 20. doi: 10.1186/s12864-019-6178-z

Zhao, Q. Y., Lin, J. H., Wang, C., Yousaf, L., Xue, Y. , and Shen, Q. (2021b). Protein structural properties and proteomic analysis of rice during storage at different temperatures. *Food Chem.* 361. doi: 10.1016/j.foodchem.2021.130028

Zhao, P. X., Zhang, J., Chen, S. Y., Wu, J., Xia, J. Q. , Sun, L. Q., et al. (2021a). Arabidopsis MADS-box factor AGL16 is a negative regulator of plant response to salt stress by downregulating salt-responsive genes. *New Phytol.* 232, 2418–2439. doi: 10.1111/nph.17760

Zhu, H., Yang, X., Wang, X., Li, Q. Y., Guo, J. Y., Ma, T., et al. (2021). The sweetpotato beta-amylase gene IbBAM1.1 enhances drought and salt stress resistance by regulating ROS homeostasis and osmotic balance. *Plant Physiol. Bioch.* 168, 167–176. doi: 10.1016/j.plaphy.2021.09.034

Zhu, M., Zhou, M. X., Shabala, L., and Shabala, S. (2017). Physiological and molecular mechanisms mediating xylem na+ loading in barley in the context of salinity stress tolerance. *Plant Cell Environ.* 40, 1009–1020. doi: 10.1111/pce.12727

frontiers | Frontiers in Plant Science

TYPE Original Research
PUBLISHED 26 October 2022
DOI 10.3389/fpls.2022.1030140

Check for updates

OPEN ACCESS

EDITED BY
Muhammad Waseem,
Hainan University, China

REVIEWED BY
Varunseelan Murugaiyan,
International Rice Research Institute (IRRI), Philippines
Farhat Abbas,
South China Agricultural University, China

*CORRESPONDENCE
Hyun Seok Kim
cameroncrazies@snu.ac.kr
Ah reum Han
subalphine@nie.re.kr

SPECIALTY SECTION
This article was submitted to Plant Abiotic Stress, a section of the journal Frontiers in Plant Science

RECEIVED 28 August 2022
ACCEPTED 10 October 2022
PUBLISHED 26 October 2022

CITATION
Chandrasekaran U, Byeon S, Kim K, Kim SH, Park CO, Han AR, Lee Y-S and Kim HS (2022) Short-term severe drought influences root volatile biosynthesis in eastern white pine *(Pinus strobus L)*. *Front. Plant Sci.* 13:1030140. doi: 10.3389/fpls.2022.1030140

COPYRIGHT
© 2022 Chandrasekaran, Byeon, Kim, Kim, Park, Han, Lee and Kim. This is an open-access article distributed under the terms of the Creative Commons Attribution License (CC BY). The use, distribution or reproduction in other forums is permitted, provided the original author(s) and the copyright owner(s) are credited and that the original publication in this journal is cited, in accordance with accepted academic practice. No use, distribution or reproduction is permitted which does not comply with these terms.

Short-term severe drought influences root volatile biosynthesis in eastern white pine *(Pinus strobus L)*

Umashankar Chandrasekaran[1,2], Siyeon Byeon[1], Kunhyo Kim[1], Seo Hyun Kim[1], Chan Oh Park[1], Ah reum Han[3]*, Young-Sang Lee[3] and Hyun Seok Kim[1,2,4,5]*

[1]Department of Agriculture, Forestry and Bioresources, College of Agriculture and Life Sciences, Seoul National University, Seoul, South Korea, [2]Research Institute of Agriculture and Life Sciences, College of Agriculture and Life Sciences, Seoul National University, Seoul, South Korea, [3]Division of Basic Research, National Institute of Ecology, Seocheon-gun, South Korea, [4]Interdisciplinary Program in Agricultural and Forest Meteorology, College of Agriculture and Life Sciences, Seoul National University, Seoul, South Korea, [5]National Center for Agro Meteorology, Seoul, South Korea

Climate change-related drought stress is expected to shift carbon partitioning toward volatile organic compound (VOC) biosynthesis. The effect of drought stress on VOC synthesis remains unknown in several tree species. Therefore, we exposed eastern white pine (*Pinus strobus*) plants to severe drought for 32 days and performed physiological analysis (chlorophyll content, leaf water content, and root/shoot index), biochemical analysis (non-structural carbohydrates, proline, lipid peroxidation, and antioxidant assay), and total root VOC analysis. Drought stress decreased the relative water and soil moisture contents. Root proline accumulation and antioxidant activity increased significantly, whereas leaf chlorophyll synthesis and fresh weight decreased significantly in drought-treated plants. A non-significant increase in sugar accumulation (leaves and roots), proline accumulation (leaves), antioxidant activity (leaves), and lipid peroxidation (leaves and roots) was observed in drought-treated plants. Drought stress caused a non-significant decline in root/shoot ratio and starch accumulation (leaves and roots) and caused a significant increase in root abscisic acid content. Drought-treated plants showed an increase in overall monoterpene synthesis (16%) and decline in total sesquiterpene synthesis (3%). Our findings provide an overall assessment of the different responses of VOC synthesis to severe water deficit that may help unravel the molecular mechanisms underlying drought tolerance in *P. strobus*.

KEYWORDS

drought stress, starch, terpenoids α-pinene, limonene, limonene oxide, root

Abbreviations: ABA, abscisic acid; C, carbon; DAT, days after treatment; DPPH, 1,1-diphenyl-2-picrylhydrazyl; MDA, malondialdehyde; NSC, non-structural carbohydrate; ROS, reactive oxygen species; RWC, relative moisture content; SMC, soil moisture content; VOC, volatile organic compound.

Introduction

Global warming-mediated climate change is expected to increase the frequency of water shortage, heat stress, and increased soil salinity. Drought stress significantly decreases the growth and yield of most plants (Polle et al., 2019; dos Santos et al., 2022). It has been speculated that the expected environmental changes will strongly affect growth, reproduction, defense, and communication processes of plants (Zhang et al., 2020; Ullah et al., 2021). Drought is a multifaceted environmental restraint that can elicit tree responses from the molecular to the forest level (Li et al., 2021; Bradford et al., 2022). It affects soil nutrient availability for plants and the uptake capacities of plant roots, and consequently influences the nutrient status of trees (Bista et al., 2020; Tan et al., 2021). Drought stress causes elevated production of reactive oxygen species (ROS) in plants (Vijayaraghavareddy et al., 2022). To survive drought stress, trees respond at morphological (decreased leaf area and altered leaf structure), physiological (stomatal closure, activation of autotrophic respiration, and accumulation of osmolytes and stress-resistant proteins), and molecular (altered gene expression patterns) levels (Moran et al., 2017; Semerci et al., 2017; Haas et al., 2021).

Plants have developed various mechanisms to perceive, transduce, and respond to ROS signals to protect themselves from soil pathogens and from abiotic stress-derived damage, such as drought, salinity, and extreme temperatures. Tree root systems are key components of forest ecosystems which influence water and nutrient uptake and function as sensors for water-deficit conditions and send signals to shoots above ground (Quan and Ding, 2017; Yang et al., 2021). Roots play a crucial role in protecting plants against oxidative stress by mainly inducing the biosynthesis of volatile terpenoids, which is thought to quench ROS (Possell and Loreto, 2013; Kleiber et al., 2017). Further, plant roots can improve pest control *via* these chemical signals (Delory et al., 2016). Volatiles emitted by roots act as anti-microbial or anti-herbivore substances in contributing to belowground defence (Schenkel et al., 2015).

Tree roots synthesize volatile organic compounds (VOCs) *via* secondary metabolism, which mainly includes production of terpenoids and fatty acid derivatives, and they serve as an important regulator of plant resistance to attenuate stress (Kleiber et al., 2017; Gfeller et al., 2019). Terpenoids, mainly monoterpenes and sesquiterpenes, are thought to play important roles in abiotic (heat and oxidative stress) and biotic stress defense mechanisms (Kleiber et al., 2017; Bertamini et al., 2019). In addition, root terpenoids play a crucial role in the defense against herbivores and pathogens (Sharma et al., 2017; Lackus et al., 2018). Previous studies have analyzed the VOCs of *Pinus* species including *Pinus tabuliformis, Pinus bungeana, Cedrus deodara, Pinus thunbergii* (Ji and Ji, 2021), *Pinus densiflora* (Otaka et al., 2017), *Pinus halepensis* (Blanch et al., 2007), *Pinus mugo* (Celiński et al., 2015), *Pinus sylvestris* (Szmigielski et al., 2011), *Pinus massoniana* (Quan and Ding, 2017), with a majority of the studies focusing on needles rather than roots.

While few studies have focused on root terpenoids in tree species (Kleiber et al., 2017; Otaka et al., 2017; Quan and Ding, 2017; Chang et al., 2021), there is a complete lack of knowledge on the relationship between root terpenoids and water deficit conditions. More importantly, it is currently unknown whether terpenoid biosynthesis mitigates or alleviates drought stress in tree species *Pinus strobus*. Eastern west pine (P. strobus L), native to eastern North America, is an ecologically and economically important species of temperate white pine ecosystems. P. strobus was imported to Korea in the early 1970s and represents an essential tree species to preserve the Korean ecosystem. Pine trees are very important as they represent one of the dominant species of global forests as they provide food and cover for small animals and birds. Studies on several pine species have revealed the vulnerability of these species to abiotic stress, especially drought stress (Mitchell et al., 2013; Quan and Ding, 2017; Asbjornsen et al., 2021; Lee et al., 2021b). However, Korean pine species show seasonal variations in their drought response (Song et al., 2020; Lee et al., 2021a). A previous study on the response of P. strobus to drought only evaluated the woody growth response and threshold dynamics (Asbjornsen et al., 2021). Therefore, there is a need to conduct a drought response study in young P. strobus saplings to understand the early physiological and biochemical responses.

Soil water availability represents a major environmental constraint in Korean forests, and estimates suggest that the decline in total rainfall will be drastic in the near future (Kim et al., 2014; Nam et al., 2015) Under such conditions, it is likely that young Pinus plants will experience increasing water deficit stress in Korean natural communities. There is a considerable need to elucidate the response of *P. strobus* seedlings to drought to develop strategies for the preservation of tree growth and survival owing to this particular environmental threat at early stages. Therefore, we evaluated the short-term severe drought response in *P. strobus* saplings in relation to their root VOC biosynthesis in the present study.

The main aims of this study were to investigate the physiological characteristics (plant height, chlorophyll content, relative water content, fresh weight, root length, and root color diameter), biochemical changes (proline biosynthesis, non-structural carbohydrate (NSC) content, lipid peroxidation, radical scavenging activity, and abscisic acid (ABA) biosynthesis), and root volatile biosynthesis patterns in *P. strobus* after a severe drought stress period.

Materials and methods

Experimental design and treatment

The study was conducted at an experimental site on mountain Jiri (E 127°27′09″ N 35°16′50″, elevation 1,289 m above sea level) in Gurye, South Jeolla Province, Republic of Korea. The mean annual temperature in the area is 13.4°C, the maximum summer temperature is approximately 38°C, and the average annual precipitation is 1,345.7 mm, based on data collected between 1997–2018 (Korea Meteorological Administration, 2018). A frame of galvanized metal allowing sufficient air circulation was constructed over the study plots, and transparent Plexiglas roof allowing 91% light transmission was installed at a height of 3 m. Two pot (circular, 16 cm height × 16 cm top diameter × 12 cm bottom diameter) treatments were applied: control (100% natural precipitation) and drought (20% precipitation) (Supplementary Figure S1). The drought treatments were applied by excluding natural precipitation by opening only 20% (severe) of the Plexiglas roof area (Bhusal et al., 2021). The pots were placed exactly under the wider opening region for control and narrow region for inducing drought stress (Supplementary Figure S1). The seedlings for each group (5 + 5) were kept at two different spots under the same plexiglass roof. The soil consisted of a mixture of sandstone, sand, mudstone, and gravel, with a pH of 6.5. The treatment was performed up to 32 days using three-year old P. strobus saplings (10 replicates). Precipitation (mm) was measured using a HOBO S-RGF sensor (Onset Computer Corporation, Bourne, MA, USA) throughout the study period. The study was conducted at the end of the growing season (1 November 2021 to 2 December 2021).

Morphological traits

The height, root length (primary root), and root collar diameter (one spot with two different angles) of all plants were measured using a millimeter tape and Vernier caliper (Mitutoyo, Kawasaki, Japan), respectively. Leaf FW (five leaves per plant) was measured using a high precision balance (Sartorius-BCE64i, Göttingen, Germany). The measurements were recorded twice during the experiment: at the beginning and at the end of the drought stress period. The root/shoot (R/S) ratio was estimated as follows:

$$R/S\ ratio\ (g\ DW^{-1}) = DW\ of\ the\ roots/DW\ of\ the\ shoots$$

Soil moisture content

Soil from all the pots was collected using a stainless-steel metal cup (3 × 3 cm, SZ metals, Korea). Soil samples were collected at five-centimeter-depth after removing the litter layer, weighed, and dried in an oven at 80°C for 72 h before measuring the DW. Moisture content of the soil sample was expressed in percentage according to the formula:

$$Soil\ moisture\ content\ (SMC)(\%) = [(FW - DW)/DW] \times 100$$

Leaf relative water content

Relative water content (RWC) was measured using 10 fully expanded needles from the current year's lateral branch. To evaluate leaf RWC, the FW, DW, and turgid weights (TWs) of the leaves were measured after 32 days after treatment (DAT). Ten replicates for each treatment were used for measuring RWC and the percentage of RWC was calculated using the formula:

$$RWC(\%) = (FW - DW)/(TW - DW) \times 100$$

Chlorophyll analysis

Chlorophyll content was measured based on the Arnon method (Arnon, 1949). Fresh leaf sample (0.5 g) was ground in liquid nitrogen and added to 10 mL of pre-chilled 80% acetone and mixed well. The mixture was centrifuged at 12000 rpm for 10 min and the supernatant was collected. The supernatant was then diluted using 80% acetone and the absorbance was measured at 645 and 663 nm using acetone as blank in a UV-visible spectrophotometer (OPTIZEN 2120UV; Mecasys, Daejeon, Korea). Ten samples per treatment were used for chlorophyll analysis. Total chlorophyll content was calculated using the formula:

$$Total\ chlorophyll = 20.2\,(A_{645}) - 8.02\,(A_{663}) \times V/100 \times W$$

Where V = final volume of the extract; W = FW of the sample.

Biochemical analysis

For the NSC analysis, hot air oven-dried leaves (70°C) were used. NSC analysis was performed using a previously described protocol with modifications (Li et al., 2018). In total, 0.1 g DW^{-1} of powdered leaf and root samples were placed in 10 mL

centrifuge tubes, and 5 mL of 80% ethanol was added. The mixture was incubated at 80°C in a water bath shaker for 30 min, and then centrifuged at 3500 rpm for 10 min. The pellets were extracted two more times using 80% ethanol. Supernatants were retained, combined, and stored at 4°C to determine the total soluble sugar content. The ethanol-insoluble pellet was used for starch extraction. Ethanol was removed via evaporation. Starch in the residue was released in 2 mL distilled water for 15 min in a boiling water bath. The solution was cooled to room temperature (22°C) and 2 mL of 9.2 M perchloric acid was added. Starch was hydrolyzed for 15 min and 4 mL distilled water was added to the solution following centrifugation at 4000 rpm for 10 min. The pellets were extracted again using 2 mL of 4.6 M perchloric acid. Supernatants were retained, combined, and made up to 25 mL to determine starch content. The soluble sugar and starch concentrations were measured spectrophotometrically (OPTIZEN 2120UV, Korea) at 620 nm using the anthrone method, and the starch content was calculated by multiplying the glucose concentrations by a conversion factor of 0.9. Glucose was used as the standard. Ten replicates per treatment were used for NSC analysis.

Proline adjustment

Proline concentration in leaves and roots was determined using a previously described protocol (Forlani and Funck, 2020). A mixture of 0.3 g fresh leaf samples and root samples (freeze stored) and 5 mL sulfosalicylic acid was homogenized and then centrifuged at 3000 rpm for 20 min. The supernatant was mixed with 2 mL glacial acetic acid and 2 mL acid ninhydrin, and the resulting mixture was boiled at 100°C for 25 min in a water bath. After cooling, 4 mL of toluene was added and allowed to settle. The absorbance of the extracts at 520 nm was evaluated using a UV visible spectrophotometer. Ten samples per each treatment were used for proline estimation.

Lipid peroxidation activity

Lipid peroxidation was evaluated by estimating malondialdehyde (MDA) content. MDA was measured based on a method established (Zhang et al., 2021). A mixture of 0.5 g fresh plant material and 5 mL of 5% trichloroacetic acid was centrifuged at 12000 rpm for 25 min. The supernatant was mixed with 2 mL of 0.67% thiobarbituric acid solution and heated for 30 min at 100°C in a water bath. Sample absorbance at 450, 532, and 600 nm was measured using a blank containing all reagents. Ten replicates per each treatment were used for lipid peroxidation analysis. MDA content in the sample was calculated using the formula:

$$C\,(\mu mol\,g^{-1}) = 6.45(A_{532} - A_{600}) - 0.56A_{450}$$

DPPH antioxidant assay

The antioxidant activity of the extracts was evaluated using 1,1-diphenyl-2-picrylhydrazyl (DPPH) assays (Dao et al., 2012). Briefly, a 0.1 mM solution of DPPH in 90% methanol was prepared and then 1.5 mL of this solution was mixed with 1.5 mL of each sample (crude extract prepared with naturally dried leaf samples) at concentrations of 100, 50, 25, and 10 µg/mL in 90% ethanol. After 30 min incubation in the dark, the decrease in absorbance of the solution at 517 nm was measured spectrophotometrically. DPPH inhibitory activity was expressed as the percentage inhibition (I %) of DPPH in the aforementioned assay system calculated as:

$$I = (1 - B/A) \times 100$$

Where A and B are the activities of the DPPH without and with test material. The inhibitory concentration at 50% values were calculated from the mean values of data from three determinations. Butylated hydroxyanisole at various concentrations (1, 2.5, 5, and 10 µM) was used as a positive control. Ten replicates per treatment was used in DPPH assays.

GC/MS analysis conditions

For the VOC analysis the seedling roots for the treatments (control and drought) were harvested, immediately transferred to liquid nitrogen and stored a -80°C until analysis. VOC analysis was performed using a GC/MS-TSQ8000QQQ2014 instrument (Thermoscientific, USA), solid-phase microextraction (SPME, Supelco, PC-420D, USA), SPME fiber assemblies (Supelco, PDMS/DVB/CAR; Sigma–Aldrich, St. Louis, MO, USA), and headspace bottles with caps (22ml, Santa Clara, CA, USA). Freeze-stored seedling root samples were cut into pieces, and sample preparation and headspace solid phase microextraction (HS-SPME) procedure was performed as previously described (Xiang et al., 2014). The seedling roots (10 mg) were transferred to the headspace bottle, which was placed in a dry heat block adjusted to 60°C and then incubated for 20 min. Three measurements were made using at least three replicates for each sample of seedling roots. Reproducibility was indicated by the relative standard deviation. The operation conditions for GC/MS were as follows: VFWAXms (30 m × 0.25 mm (0.25 lm); temperature of 40°C (held for 5 min) and 250°C (held for 5 min) with an increase rate of 5°C min^{-1}; the carrier gas was helium (99.999%), which was allowed to flow for 25 min with an inlet temperature of 230°C. The characteristics of the MS system were as follows: ion source of 70 eV EI at a temperature of 200°C; transfer line temperature of 250°C; mass range of 45–450 amu with a collection time of 3–20 min. Four replicates per treatment was used for VOC analysis.

Identification and quantification of volatile compounds

Volatile substances from the leaf samples were identified by comparing the components of the mass spectra with the MS database (NIST version 2.0) in addition to comparing the sample spectra to those of authentic reference standard (1,2,3-trichloropropane) when required. A previously described peak normalization method was used to determine the relative content of each VOC (Yang et al., 2015). Quantitative analysis in the percentage of each VOC was calculated using the formula below:

$$Relative\ content\ =\ M/N * 100\ \%$$

where, M is the peak area of the individual aromatic compounds; N is the total peak area.

ABA content

Freeze stored root samples were prepared based on a previously established protocol (Liu et al., 2012). Briefly, five replicates of each frozen root sample (approximately 100 mg for each replicate) were ground to a fine power in liquid nitrogen using a mortar and pestle. Each sample was weighed into a 1.5 mL tube, mixed with 750 µL cold extraction buffer (methanol: water: acetic acid, 80:19:1, v/v/v) supplemented with internal standard (10 ng $^2H_6$ ABA), vigorously shaken on a shaking bed for 16 h at 4°C in dark, and then centrifuged at 13000 rpm for 15 min at 4°C. The supernatant was carefully transferred to a new 1.5 mL tube and the pellet was remixed with 400 µL extraction buffer, shaken for 4 h at 4°C, and centrifuged. The two supernatants were then combined and filtered using a syringe-facilitated 13 mm diameter nylon filter with a pore size of 0.22 µm (Hyundai Micro, Seoul, Korea). The filtrate was dried via evaporation under the flow of nitrogen gas for approximately 4 h at room temperature and then dissolved in 200 µL methanol. The dissolved mixture was used for LC/MS analysis. LC/MS, SPME and GC/MS analysis were performed at the National Instrumentation Center for Environmental Management (NICEM), Seoul National University, Republic of Korea.

Statistical analysis

All experiments were conducted twice and the results are reported as mean ± SE. Data were analyzed *via* two-factor analysis of variance (ANOVA) using the R program (v.3.5.1). The treatment mean values were compared *via* Tukey's (least significance difference) test; statistical significance was set at $P \leq 0.05$. Pearson correlation coefficient was carried out among the treatments and a heat map was generated with *corrplot* package using the R program (v.3.5.1).

Results

Plant growth, water relation, and chlorophyll content

Total precipitation recorded during the study period showed a higher percentage of rainfall received in control plots compared to a minimal amount in treatment plots (Figure 1A). The SMC in drought-treated pots (3.2 ± 0.09%) significantly decreased compared to that in control pots (12 ± 0.3%) (Figure 1B). RWC is regarded as a measure of the water status in plants, reflecting the metabolic activity in plants. RWC content in leaves of drought-treated plants (72% ± 0.05) significantly decreased compared to that in control plants (84 ± 0.09%) (Figure 1C).

No significant difference was observed in plant height, root length, and root collar diameter between control and drought plants (Figures 2A–C). In contrast, drought stress significantly decreased the leaf weight ($P< 0.05$) (Figure 2D). This decrease was evident based on pre and post-treatment values. The leaf weight in control plants increased by 2% after the treatment period whereas that in drought-treated plants increased only by 0.2%. Similar to leaf weight, but a non-significant decline in root/shoot ratio was observed (Figure 2E). The chlorophyll content significantly decreased in the leaves of drought-treated plants compared to that in control plants (Figure 2F).

Non-structural carbohydrate changes

NSCs represent major substrates in plant metabolism and have been implicated in mediating drought-induced tree mortality (Signori-Müller et al., 2021). A non-significant increase in soluble sugar content was observed in both leaves and roots in drought-treated plants (Figures 3A, B). In contrast, a non-significant decrease in starch content was observed in both leaves and roots in drought-treated plants compared to that in the control plants 32 DAT (Figures 3C, D). The decrease in starch content was 1.5% higher in roots than that in leaves.

Proline content

Free proline functions as an important osmoprotectant during abiotic stress. A non-significant increase in free proline level was observed in leaves of drought-treated plants compared to that in leaves of control plants (Figure 3E). A significant accumulation of free proline was observed in roots of drought-treated plants compared to that in control plants 32 DAT ($P< 0.05$; Figure 3F). This accumulation was 5-fold higher than that in the control plants.

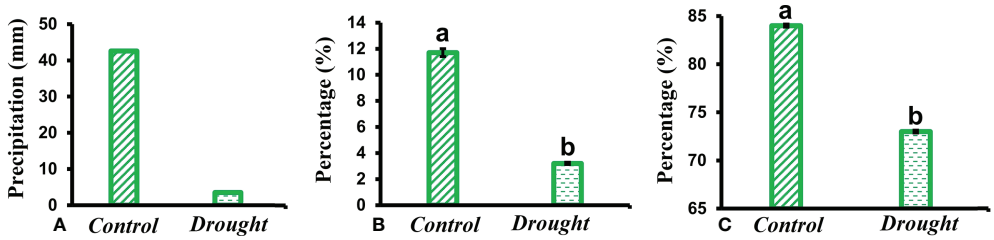


FIGURE 1
Meteorological data. **(A)** total rainfall received in control and drought plots throughout the study period **(B)** soil moisture content (SMC) measured in soil obtained from control and drought treated pots kept within the Plexiglas roof **(C)** relative water content (RWC) measured in leaves of control and drought stressed plants 32 DAT. Means denoted with different letters indicate significance at $p<0.05$.

Lipid peroxidation

MDA content is an indicator of membrane lipid peroxidation, which reflects the extent of damage at adverse conditions. A non-significant increase in MDA content was observed in both the leaves and roots of drought-treated plants at 32 days (Figures 3G, H). Therefore, the oxidative damage caused to roots was greater (1-fold increase) than that in leaves during drought treatment.

Antioxidant changes

Since the majority of natural antioxidants possess reactive hydrogen atoms, which serve as reductants, the DPPH assay is a good measure of the standard antioxidant profile. High antioxidant activity was observed in roots compared to that in leaves at 32 DAT (Figures 3I, J). A non-significant increase in antioxidant activity was observed in drought-treated leaves compared to that in control leaves (Figure 3I). In contrast, a

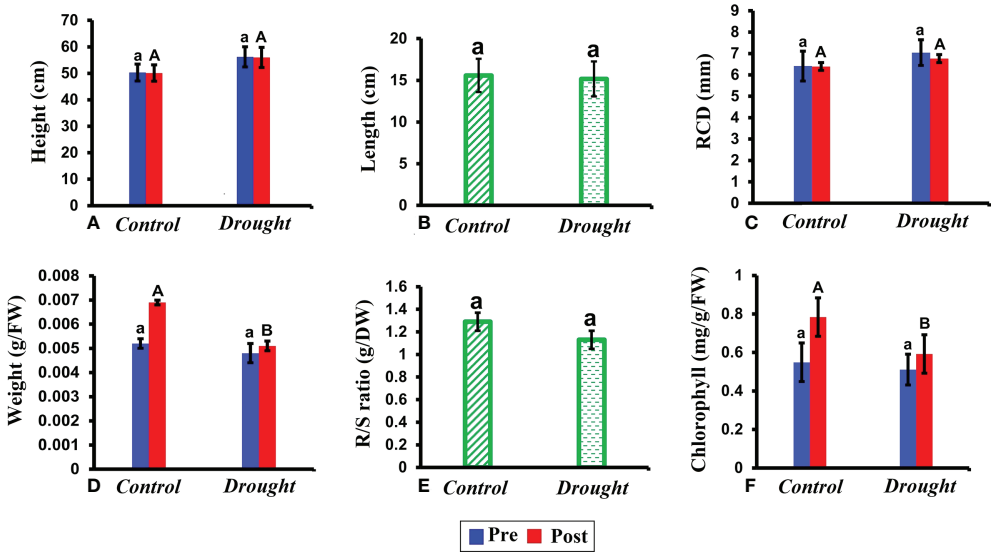


FIGURE 2
Morphological and physiological responses of *P.strobus* seedlings under drought. **(A)** plant height measured before and after the treatment period 32 DAT **(B)** root length measured in control and drought plants **(C)** root collar diameter (RCD) recorded 32 DAT **(D)** fresh leaf weight recorded before and after 32 DAT **(E)** root/shoot ratio measured after the treatment period **(F)** total chlorophyll content measured in leaves of control and drought plants before and after the treatment period. Results represent that short term severe drought has not caused drastic morphologically changes, rather caused physiological changes in the leaf fresh weight, chlorophyll pigment content and R/S ratio index. Means denoted with different letters indicate significance at $p<0.05$.

significant increase (2-fold) in antioxidant activity was observed in drought-treated roots compared to that in the control.

Effect of drought stress on root ABA and VOC composition

The phytohormone ABA is a key signal in drought response. ABA concentrations in drought-treated plant roots showed a significant increase (1.2-fold) compared to that in control plant roots (Figure 3K). Analysis of the spectrum for each VOC and subsequent data verification allowed identification of several types of VOCs in the control and severe drought-treated plants. Few of the commonly occurring VOCs after drought stress included several monoterpenes and sesquiterpenes (Figures 4, 5). In total, 11 types of monoterpenes (including α-pinene, β-pinene, D-limonene, and α-phellandrene) and 7 types of sesquiterpenes (including cadinene, α and β-caryophyllene, copaene, and caryophyllene oxide) were predominantly detected in our study (Figures 4, 5). The relative contents of monoterpenes like α-pinene and 3-carene were significantly higher in drought-treated plants than in control plants (Figure 4A). The relative content of other monoterpenes including β-pinene, camphene, linalool, limonene, α-phellandrene, sabinene, α-terpene, and β-terpene showed a non-significant increase, with myrcene being the only monoterpene showing a non-significant decline in content compared to that in control plants (Figure 4A). Overall, the total monoterpene content was relatively higher in drought-treated plants (94%) than in control plants (78%) (Figure 4B). In contrast, the relative content of total sesquiterpenes reduced to 2% in drought-treated plants compared to 5% in control plants (Figure 5B). A major sesquiterpene, α-caryophyllene content showed a significant decline in drought-treated plants (Figure 5A). Farnescene was the only sesquiterpene showing a significant increase in content in drought-treated plants compared to that in control plants at 32 DAT (Figure 5A). The contents of other sesquiterpenes, including β-caryophyllene, caryophyllene oxide, cadinene, copaene, and cubene, showed a non-significant decrease in drought-treated plants (Figure 5A). A strong negative correlation (cadinene), weak positive correlation (copaene, cubenene, farnescene) and a strong positive correlation (α-caryophyllene, β-caryophyllene) was observed between ABA and sesquiterpenes profiles (Figure 6). On the other hand, a strong positive correlation (β-pinene, camphene, α-terpinene, γ-terpinene) and a weak negative correlation (α-pinene, myrcene, linalool, limonene, α-phellandrene, sabinene), was found between ABA and monoterpene profiles (Figure 6). A list of all the other volatiles including alcohols, terpenes, esters, ketones and aldehydes

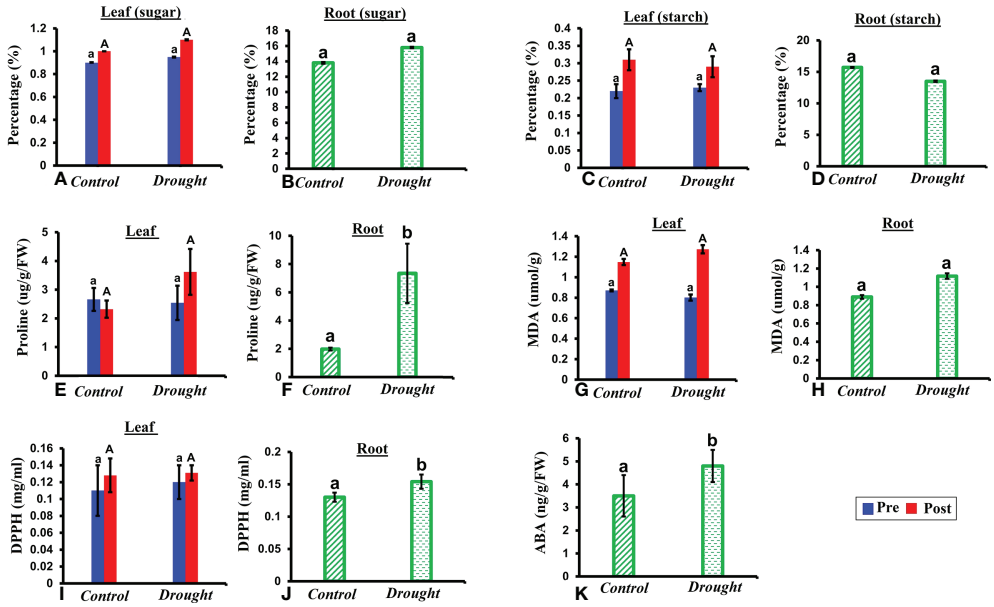


FIGURE 3
Biochemical responses of *P.strobus* seedlings to drought. **(A, B)** total soluble sugar content in leaves and root of control and stressed plants **(C, D)** total starch content in leaves and roots 32 DAT **(E, F)** proline content in leaves and root samples of control and drought plants **(G, H)** lipid peroxidase activity-MDA content in leaves and root samples of control and drought plants **(I, J)** antioxidant assay measured *via* DPPH content in root and leaf samples 32 DAT **(K)** ABA content in roots 32 DAT. Results denote that severe drought significantly influences root proline and DPPH activity compared to a non-significant increase in leaves. In addition, a non-significant increase is observed in sugar (leaf and root), lipid peroxidase activity (leaf and root) with a non-significant decrease noted for starch content (leaf and root). Means denoted with different letters indicate significance at $p<0.05$.

identified in our study have been listed in the Supplementary Table S1.

Discussion

Drought causes morphological and physiological changes in plants. The drought response is primarily determined by the rate and extent to which water status in plants is hydraulically regulated (Skelton et al., 2015). Subsequently, this phenomenon mediates the duration and intensity of the physiological changes and the processes that underlie mortality. In our study, the significant decrease in SMC in drought-treated plants was primarily due to the lack of water supply (only 20% received). SMC decline also indicates a lack of nutrient uptake by *P. strobus* plants under drought condition. Similarly, several forest tree species have been reported to show low SMC and nutrient uptake under severe drought conditions (Chakhchar et al., 2018; Ji et al., 2021). Monitoring the SMC deficits can indicate potential impacts on *P. strobus* development and soil health, supporting the assessment of drought-tolerant, resilient, and vulnerable ecosystems. Leaf RWC is an important indicator of water status in plants as it relates to the balance between leaf water supply and transpiration rate (Tanentzap et al., 2015). Decline in RWC in *P. strobus* plants indicates a lower stomatal conductance and photosynthetic exchange under water deficit conditions. Supporting the RWC evidence, the lower chlorophyll content observed in leaves of drought-treated plants indicates an impact on chlorophyll abundance. Impacts on chlorophyll pigment, especially photosystem II, under drought conditions has been reported in various tree species (Batra et al., 2014; Li et al., 2020; Vastag et al., 2020; Javed et al., 2021). For instance, teak plants under severe drought exposure (20 days of water withholding) show a reduction in chlorophyll content and leaf RWC by 9.57% (Galeano et al., 2019).

Plants regulate their R/S ratios in response to the availability of substrates (mainly water) and to environmental changes. Our findings (non-significant decline in drought-treated plants) suggest that a drought-induced shift in R/S ratio can improve plant water uptake potential in a short window determined by both water and atmospheric parameters. Similar to our results, opposite effects of R/S water balance have been previously reported in two grass species (Gargallo-Garriga et al., 2014). An opposite metabolic activity in shoots and roots may account for the lack of large reductions in productivity during drought experiments at least for a short term (Gargallo-Garriga et al., 2014; Boudiar et al., 2020). An intra-specific variation in assimilate partitioning (water/soluble sugar) between roots and shoots has been found in wheat during drought stress (Fang et al., 2017; Mathew et al., 2019).

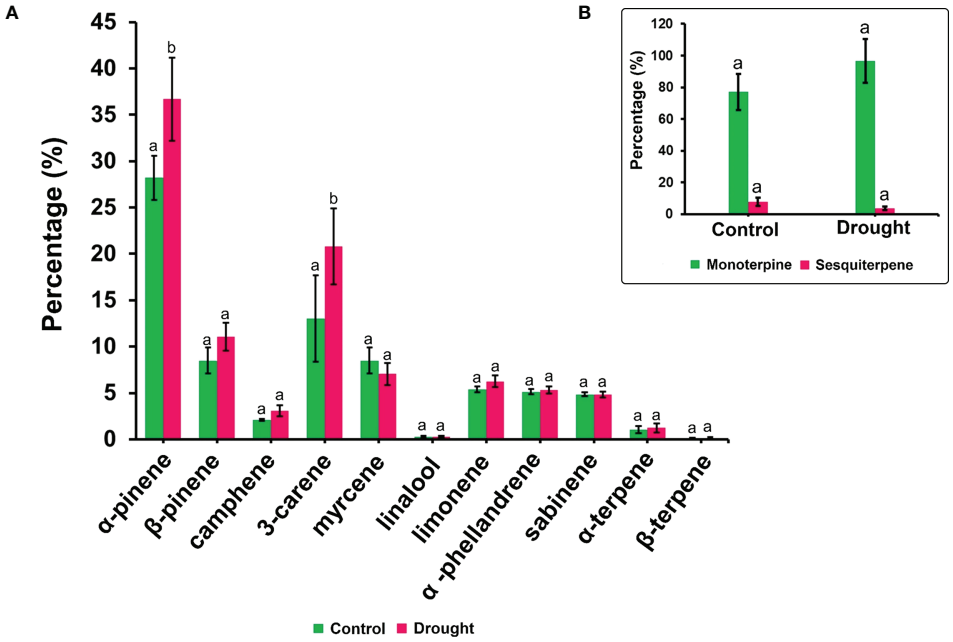


FIGURE 4
Volatile synthesis (VOC)-Monoterpenes. **(A)** major monoterpenes and their content in root samples **(B)** total accumulation of main monoterpenes and sesquiterpenes in root samples measured 32 DAT. Results indicate the influence of severe drought on the significant accumulation of two critical monoterpenes α-pinene and delta-3-carene apart from a non-significant increase for other critical monoterpenes like β-pinene, camphene and limonene. Significant accumulation of total monoterpene content is noted compared to drought treated seedling samples. Means denoted with different letters indicate significance at $p<0.05$.

Plants produce and accumulate compatible solutes to improve water absorption and maintain hydration of protoplasts under drought stress (Blum, 2017). In the present study, the accumulation of organic solutes, including soluble sugar and proline, indicates their role as osmoregulants to prevent leaf senescence and improve *P. strobus* plant performance under drought condition. The increase in proline level is in parallel with a low RWC in the leaves of drought-treated *P. strobus* plants. Several studies have suggested that proline accumulation in plants can be considered as a general response to abiotic stresses (Yaish, 2015; Ghosh et al., 2022). In contrast, soluble sugars may also act as osmoprotectants based on their substitution with water *via* hydrogen linkage and by establishing bonds with proteins and membranes and they provide protection against dehydration or peroxidation (Ahmad et al., 2020). Our results indicated that an increased proline concentration and accumulation of high concentration of soluble sugars in the leaves and roots protect *P. strobus* plants from intercellular oxidative damage. Proline has been recognized as a signaling molecule that activates ROS detoxification pathways (Anwar Hossain et al., 2014).

Notably, our findings support the hypothesis that drought stress decreases the starch concentration with an increase in soluble sugar concentration (Dai et al., 2018; Tsamir-Rimon et al., 2021). Severe drought treatment largely reduced photosynthetic carbon (C) assimilation as observed in the chlorophyll analysis (Figure 2). The restricted C assimilation affected the C supply chain and cannot satisfy the C demand of *P. strobus* plants for maintaining metabolism and growth. This resulted in depletion of internal C reservoirs of starch (Figure 4). Starch depletion under water deficit conditions, owing to depleted photosynthesis, has been also found across different species and tissues (Regier et al., 2009; Mitchell et al., 2013; Klein et al., 2014; Lloret et al., 2018). Similar to our results, the trends of starch depletion and increase in sugar levels have been previously observed in another Pinus species, Pinus radiata (Mitchell et al., 2013). Under drought treatment, NSCs buffer the asynchrony between C supply and growth, which decrease and increase the C demand needed to maintain a minimum level of plant respiration (Sperling et al., 2017; Ryhti et al., 2022). More importantly, we speculate that the starch depletion observed in our study may lead to mortality in P. strobus plants over long drought periods. Future studies should elucidate whether the duration of drought alone determines gross depletion of carbohydrates (starch) leading to mortality.

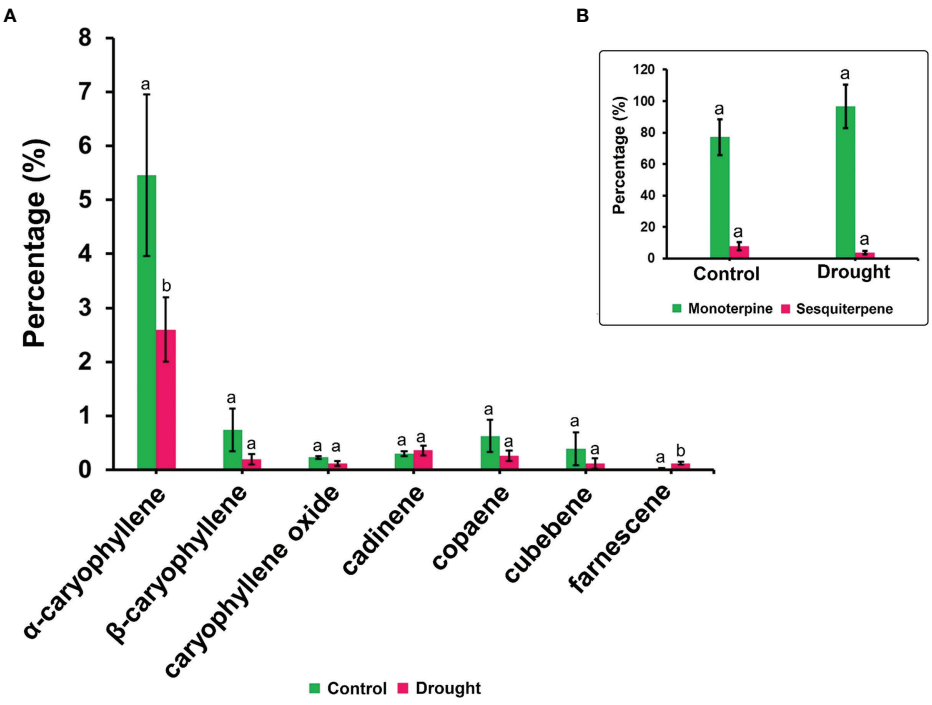


FIGURE 5
Volatile synthesis (VOC)-Sesquiterpenes. **(A)** list of sesquiterpenes and their content in root samples **(B)** total accumulation of main monoterpenes and sesquiterpenes in root samples measured 32 DAT. Results highlight the influence of severe drought on the decline in total sesquiterpene accumulation supported by a decrease in major sesquiterpenes like α-caryophyllene, β-caryophyllene and cadinene. Farnescene being the only sesquiterpene showing a non-significant increase in their content among drought treated seedling sample. Means denoted with different letters indicate significance at $p<0.05$.

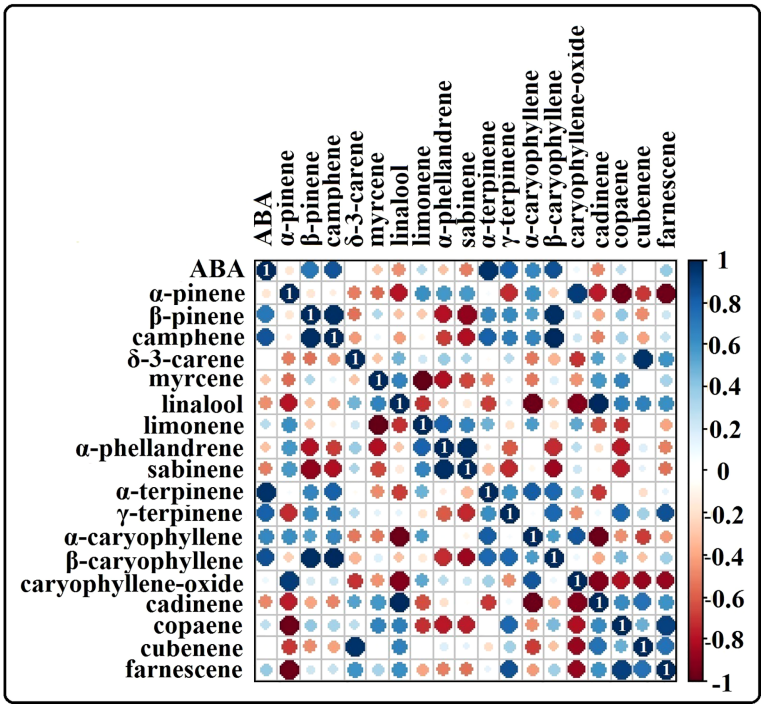


FIGURE 6
Heat map showing the correlation analysis of ABA content vs terpene content from our study. Positive correlation between ABA and the terpenes are shown in 'blue' and negative correlation between ABA and terpenes are shown in the color range 'red'. Results highlight a strong positive correlation between several monoterpenes like α-pinene, camphene, α-terpene, y-terpinene and ABA whereas negative/weak positive correlation is observed for several sesquiterpenes like caryophyllene oxide, cadinene, copaene, cubenene and farnescene in relation with ABA.

In recent years, several studies have investigated the signaling function of VOCs in the ecosystem (Vivaldo et al., 2017; Ninkovic et al., 2021). Our results showed that drought stress had a positive effect on the production of monoterpenes, as the levels were higher than those in control plants (Figure 4). The alternate C source (starch depletion) can contribute to monoterpene production under drought conditions, preventing these isoprenoids from being reduced (de Souza et al., 2018). The other possible reason may be the increase in soil temperature, which in turn favors monoterpene synthesis as the internal monoterpene synthesis respond to increase in temperature (Birami et al., 2021). Increase in leaf monoterpene emissions from *P. halepensis* and *Cistus albidus* has been attributed to monoterpene accumulation within leaves which is favored during drought periods (Turtola et al., 2003). Water stress induces a shift in terpene composition when water deficit exceeds 4 days (Ormeño et al., 2007). The patterns in monoterpene synthesis in P. strobus plants over prolonged water deficit conditions needs to be examined in future studies. Notably, monoterpene accumulation, especially α-pinene, in roots causes oxidative stress leading to growth inhibition (Singh et al., 2006). Therefore, future studies should investigate whether an increase in α-pinene synthesis leads to additional oxidative damage in P. strobus roots, thereby aggravating drought stress.

Reduced levels of sesquiterpenes in drought-treated plants might have been due to the shift in terpene composition as our study period exceeded a month. Our results suggested that sesquiterpenes may probably be replaced by monoterpenes when drought is prolonged, because drought can impede the cyclization of sesquiterpene precursors (Kopaczyk et al., 2020; Arizmendi et al., 2022). The increase in ABA content and the subsequent stomatal closure is also considered an important signaling event under drought stress across several species (Bharath et al., 2021; Rehman et al., 2021). The increase in root ABA content positively correlates with an increase in several monoterpene and negatively correlates with several sequiterpene content in our study. Although certain studies reported the link between ABA and isoprenoid synthesis under drought (Perreca et al., 2020), whether an increase in ABA content triggers monoterpene synthesis under drought stress remains to be studied. Drought stress has been found to decrease the accumulation of ABA via regulation of the methyl salicylate pathway (Jin et al., 2021). Notably, the production of isoprene and terpenoids is stimulated by jasmonic acid (JA) in plants (Tanaka et al., 2014). Interestingly, the JA and salicylic acid (SA)

responsive signalling cascades mediated by JASMONATE ZIM DOMAIN PROTEIN (JAZ) and MYC2 transcription factors can enhance the emission of constitutively emitted isoprene, monoterpenes and sesquiterpenes, which may upregulate stress-specific hormonal signaling (Yang et al., 2019; Dani and Loreto, 2022). Therefore, it will be interesting to study the crosstalk among phytohormones associated with the synthesis of root VOCs in P. strobus seedlings, especially the pathway existing between terpene synthesis and ABA response under water-deficit conditions. The analyzed correlation coefficient results provided novel insights on the internetwork among volatiles (terpenes) and plant hormone ABA under severe drought stress. Controlling water transpiration *via* stomata represents one of the main strategies for plants to increase drought tolerance. This movement is strictly regulated by various environmental stimuli, such as water status, light, and CO_2 concentration, as well as the endogenous factor, ABA (Daszkowska-Golec and Szarejko, 2013; Driesen et al., 2020). The significant increase in root ABA levels in our study denotes the signaling of roots to fasten the stomatal closure, thereby reducing the transpiration water loss.

Conclusion

Severe drought drastically affected the water transport from roots to leaves (early stomatal closure) and disrupted the chlorophyll content in P. strobus plants. The impaired chlorophyll functioning subsequently limited the C assimilation process because the intake of atmospheric C is reduced. Consequently, the production of energy (glucose) is reduced in P. strobus plants. Under severe drought, the soil temperature increases and prevents the invasion of soil microbes and P. strobus plants produced relatively higher amounts of root monoterpenes. However, the synthesis of isoprenes in plants requires a surplus of C, which is limited owing to water deficit conditions. Therefore, C for producing energy required for VOC production (monoterpenes) in P. strobus plants is obtained from the internal storage reservoir (starch). Since the monoterpene α-pinene can induce oxidative stress, we speculate that P. strobus plants may undergo both drought and oxidative stress. This in turn causes a significant increase in ABA and proline accumulation in roots. However, whether monoterpenes also signal the leaf stomatal closure via ABA is currently unknown. To maintain intact plant cells and reduce the oxidative damage, P. strobus plants produce additional osmolytes in the form of sugar and proline. Together, our results suggest that starch depletion is an indicator for plant mortality in P. strobus under prolonged exposure to severe drought conditions.

Data availability statement

The raw data supporting the conclusions of this article will be made available by the authors, without undue reservation.

Author contributions

UC and HK designed the experiment. UC performed the field, laboratory experiments and wrote the manuscript. SB and SK assisted with laboratory experiments. KK, CP, AH Y-SL assisted with field experiments. All authors contributed to the article and approved the submitted version.

Funding

This work was jointly supported by a grant from National Institute of Ecology (NIE), funded by the Ministry of Environment (MOE), Republic of Korea (NIE-B-2022-02) and basic science research program through National Research Foundation (NRF) funded by the Ministry of Education (2021R111A2044159), Republic of Korea.

Conflict of interest

The authors declare that the research was conducted in the absence of any commercial or financial relationships that could be construed as a potential conflict of interest.

Publisher's note

All claims expressed in this article are solely those of the authors and do not necessarily represent those of their affiliated organizations, or those of the publisher, the editors and the reviewers. Any product that may be evaluated in this article, or claim that may be made by its manufacturer, is not guaranteed or endorsed by the publisher.

Supplementary material

The Supplementary Material for this article can be found online at: https://www.frontiersin.org/articles/10.3389/fpls.2022.1030140/full#supplementary-material

References

Ahmad, F., Singh, A., and Kamal, A. (2020). Osmoprotective role of sugar in mitigating abiotic stress in plants. In Eds. A. Roychoudhury and D. K. Tripathi *Protective chemical agents in the amelioration of plant abiotic stress* Hoboken, New Jersey: Wiley, 53–70.

Anwar Hossain, M., Hoque, M. A., Burritt, D. J., and Fujita, M. (2014). *Proline protects plants against abiotic oxidative stress: Biochemical and molecular mechanisms in oxidative damage to plants*. Ed. P. Ahmad. (San Diego: Academic Press), 477–522.

Arizmendi, N., Alam, S. B., Azyat, K., Makeiff, D., Befus, A. D., and Kulka, M. (2022). The complexity of sesquiterpene chemistry dictates its pleiotropic biologic effects on inflammation. *Molecules* 27, 2450. doi: 10.3390/molecules27082450

Arnon, D. I. (1949). Copper enzymes in isolated chloroplasts. polyphenoloxidase in *Beta vulgaris*. *Plant Physiol.* 24, 1–15. doi: 10.1104/pp.24.1.1

Asbjornsen, H., Mcintire, C. D., Vadeboncoeur, M. A., Jennings, K. A., Coble, A. P., and Berry, Z. C. (2021). Sensitivity and threshold dynamics of *Pinus strobus* and *Quercus* spp. in response to experimental and naturally occurring severe droughts. *Tree Physiol.* 41, 1819–1835. doi: 10.1093/treephys/tpab056

Batra, N. G., Sharma, V., and Kumari, N. (2014). Drought-induced changes in chlorophyll fluorescence, photosynthetic pigments, and thylakoid membrane proteins of *Vigna radiata*. *J. Plant Interact.* 9, 712–721. doi: 10.1080/17429145.2014.905801

Bertamini, M., Grando, M. S., Zocca, P., Pedrotti, M., Lorenzi, S., and Cappellin, L. (2019). Linking monoterpenes and abiotic stress resistance in grapevines. *Bio Web Conf.* 13, 01003. doi: 10.1051/bioconf/20191301003

Bharath, P., Gahir, S., and Raghavendra, A. S. (2021). Abscisic acid-induced stomatal closure: An important component of plant defense against abiotic and biotic stress. *Front. Plant Sci.* 12, 615114. doi: 10.3389/fpls.2021.615114

Bhusal, N., Lee, M., Lee, H., Adhikari, A., Han, A. R., Han, A., et al. (2021). Evaluation of morphological, physiological, and biochemical traits for assessing drought resistance in eleven tree species. *Sci. Total. Environ.* 779, 146466. doi: 10.1016/j.scitotenv.2021.146466

Birami, B., Bamberger, I., Ghirardo, A., Grote, R., Arneth, A., Gaona-Colmán, E., et al. (2021). Heatwave frequency and seedling death alter stress-specific emissions of volatile organic compounds in Aleppo pine. *Oecologia* 197, 939–956. doi: 10.1007/s00442-021-04905-y

Bista, D. R., Heckathorn, S. A., Jayawardena, D. M., and Boldt, J. K. (2020). Effect of drought and carbon dioxide on nutrient uptake and levels of nutrient-uptake proteins in roots of barley. *Am. J. Bot.* 107, 1401–1409. doi: 10.1002/ajb2.1542

Blanch, J. S., Peñuelas, J., and Llusià, J. (2007). Sensitivity of terpene emissions to drought and fertilization in terpene-storing pinus halepensis and non-storing *Quercus ilex*. *Physiol. Plant* 131, 211–225. doi: 10.1111/j.1399-3054.2007.00944.x

Blum, A. (2017). Osmotic adjustment is a prime drought stress adaptive engine in support of plant production. *Plant Cell Environ.* 40, 4–10. doi: 10.1111/pce.12800

Boudiar, R., Casas, A. M., Gioia, T., Fiorani, F., Nagel, K. A., and Igartua, E. (2020). Effects of low water availability on root placement and shoot development in landraces and modern barley cultivars. *Agronomy* 10, 134. doi: 10.3390/agronomy10010134

Bradford, J. B., Shriver, R. K., Robles, M. D., Mccauley, L. A., Woolley, T. J., Andrews, C. A., et al. (2022). Tree mortality response to drought-density interactions suggests opportunities to enhance drought resistance. *J.Appl. Ecol.* 59, 549–559. doi: 10.1111/1365-2664.14073

Celiński, K., Bonikowski, R., Wojnicka-Półtorak, A., Chudzińska, E., and Maliński, T. (2015). Volatiles as chemosystematic markers for distinguishing closely related species within the *Pinus mugo* complex. *Chem. Biodivers.* 12, 1208–1213. doi: 10.1002/cbdv.201400253

Chakhchar, A., Chaguer, N., Ferradous, A., Filali-Maltouf, A., and El Modafar, C. (2018). Root system response in *Argania spinosa* plants under drought stress and recovery. *Plant Signal. Behav.* 13, e1489669. doi: 10.1080/15592324.2018.1489669

Chang, H., Son, J., Je Sun, M., Oh, C. Y., Cho, M., Kim, J., et al. (2021). Emission rates of biogenic volatile organic compunds (BVOCs) from various tree species in Korea (I). *J.Korean. Soc.For.Sci.* 110, 543–553. doi: 10.14578/jkfs.2021.110.4.543

Dai, Y., Wang, L., and Wan, X. (2018). Relative contributions of hydraulic dysfunction and carbohydrate depletion during tree mortality caused by drought. *AoB. Plants* 10, plx069. doi: 10.1093/aobpla/plx069

Dani, K. G. S., and Loreto, F. (2022). Plant volatiles as regulators of hormone homeostasis. *New Phytol.* 234, 804–812. doi: 10.1111/nph.18035

Dao, P. T. A., Hai, N., Nhan, N., Quan, T., and Mai, N. (2012). Study on DPPH free radical scavenging and lipid peroxidation inhibitory activities of vietnamese medicinal plants. *Nat. Prod. Sci.* 18, 1–7.

Daszkowska-Golec, A., and Szarejko, I. (2013). Open or close the gate – stomata action under the control of phytohormones in drought stress conditions. *Front. Plant Sci.* 4, 138. doi: 10.3389/fpls.2013.00138

Delory, B. M., Delaplace, P., Fauconnier, M.-L., and Du Jardin, P. (2016). Root-emitted volatile organic compounds: can they mediate belowground plant-plant interactions? *Plant Soil* 402, 1–26. doi: 10.1007/s11104-016-2823-3

de Souza, V. F., Niinemets, Ü., Rasulov, B., Vickers, C. E., Duvoisin Júnior, S., Araújo, W. L., et al. (2018). Alternative carbon sources for isoprene emission. *Trends Plant Sci.* 23, 1081–1101. doi: 10.1016/j.tplants.2018.09.012

dos Santos, T. B., Ribas, A. F., De Souza, S. G. H., Budzinski, I. G. F., and Domingues, D. S. (2022). Physiological responses to drought, salinity, and heat stress in plants: A review. *Stresses* 2, 113–135. doi: 10.3390/stresses2010009

Driesen, E., Van Den Ende, W., De Proft, M., and Saeys, W. (2020). Influence of environmental factors light, CO_2, temperature, and relative humidity on stomatal opening and development: A review. *Agronomy* 10, 1975. doi: 10.3390/agronomy10121975

Fang, Y., Du, Y., Wang, J., Wu, A., Qiao, S., Xu, B., et al. (2017). Moderate drought stress affected root growth and grain yield in old, modern and newly released cultivars of winter wheat. *Front. Plant Sci.* 8, 672. doi: 10.3389/fpls.2017.00672

Forlani, G., and Funck, D. (2020). A specific and sensitive enzymatic assay for the quantitation of l-proline. *Front. Plant Sci.* 11, 582026. doi: 10.3389/fpls.2020.582026

Galeano, E., Vasconcelos, T. S., Novais De Oliveira, P., and Carrer, H. (2019). Physiological and molecular responses to drought stress in teak (*Tectona grandis l.f.*). *PloS One* 14, e0221571. doi: 10.1371/journal.pone.0221571

Gargallo-Garriga, A., Sardans, J., Pérez-Trujillo, M., Rivas-Ubach, A., Oravec, M., Vecerova, K., et al. (2014). Opposite metabolic responses of shoots and roots to drought. *Sci. Rep.* 4, 6829. doi: 10.1038/srep06829

Gfeller, V., Huber, M., Förster, C., Huang, W., Köllner, T. G., and Erb, M. (2019). Root volatiles in plant–plant interactions I: High root sesquiterpene release is associated with increased germination and growth of plant neighbours. *Plant Cell Environ.* 42, 1950–1963. doi: 10.1111/pce.13532

Ghosh, U. K., Islam, M. N., Siddiqui, M. N., Cao, X., and Khan, M. A. R. (2022). Proline, a multifaceted signalling molecule in plant responses to abiotic stress: understanding the physiological mechanisms. *Plant Biol.* 24, 227–239. doi: 10.1111/plb.13363

Haas, J. C., Vergara, A., Serrano, A. R., Mishra, S., Hurry, V., and Street, N. R. (2021). Candidate regulators and target genes of drought stress in needles and roots of Norway spruce. *Tree Physiol.* 41, 1230–1246. doi: 10.1093/treephys/tpaa178

Javed, M., Iqbal, M., Bano, H., Hussain, N., Ghaffar, A., Zafar, Z. U., et al. (2021). Photosynthetic acclamatory response of panicum antidotale retz. populations to root zone desiccation stress. *Braz. J. Biol.* 84, e252735. doi: 10.1590/1519-6984.252735

Ji, W., and Ji, X. (2021). Comparative analysis of volatile terpenes and terpenoids in the leaves of pinus species-a potentially abundant renewable resource. *Molecules* 26, 5244. doi: 10.3390/molecules26175244

Ji, Y., Li, Y., Yao, N., Biswas, A., Zou, Y., Meng, Q., et al. (2021). The lagged effect and impact of soil moisture drought on terrestrial ecosystem water use efficiency. *Ecol. Indic.s* 133, 108349. doi: 10.1016/j.ecolind.2021.108349

Jin, J., Zhao, M., Gao, T., Jing, T., Zhang, N., Wang, J., et al. (2021). Amplification of early drought responses caused by volatile cues emitted from neighboring tea plants. *Hortic. Res.* 8, 243. doi: 10.1038/s41438-021-00704-x

Kim, C. J., Park, M. J., and Lee, J. H. (2014). Analysis of climate change impacts on the spatial and frequency patterns of drought using a potential drought hazard mapping approach. *Int. J.Climatol.* 34, 61–80. doi: 10.1002/joc.3666

Kleiber, A., Duan, Q., Jansen, K., Junker-Frohn, L., Kammerer, B., Rennenberg, H., et al. (2017). Drought effects on root and needle terpenoid content of a coastal and an interior Douglas fir provenance. *Tree Physiol.* 37, 1648–1658. doi: 10.1093/treephys/tpx113

Klein, T., Hoch, G., Yakir, D., and Korner, C.. (2014). Drought stress, growth andnonstructural carbohydrate dynamics of pine trees in a semi-arid forest. *Tree Physiol.* 34, 981–992.

Kopaczyk, J. M., Warguła, J., and Jelonek, T. (2020). The variability of terpenes in conifers under developmental and environmental stimuli. *Environ. Exp. Bot.* 180, 104197. doi: 10.1016/j.envexpbot.2020.104197

Korea Meteorological Administration. (2018). *Weather information* https://data.kma.go.kr/ data/grnd/selectAsosRltmList.do?pgmNo=36. (Accessed 25 April 2018).

Lackus, N. D., Lackner, S., Gershenzon, J., Unsicker, S. B., and Köllner, T. G. (2018). The occurrence and formation of monoterpenes in herbivore-damaged poplar roots. *Sci. Rep.* 8, 17936. doi: 10.1038/s41598-018-36302-6

Lee, H., Jeon, J., Kang, M., Cho, S., Park, J., Lee, M., et al. (2021a). The resilience of the carbon cycles of temperate coniferous and broadleaved forests to drought. *For. Ecol. Manage.* 491, 119178. doi: 10.1016/j.foreco.2021.119178

Lee, H., Lee, W. Y., and Kang, J. W. (2021b). Effects of elevated atmospheric CO2 on rhizosphere microbial community of *Pinus densiflora* (Korean red pine). *For. Sci.Technol.* 17, 16–22. doi: 10.1080/21580103.2020.1866089

Li, M. H., Jiang, Y., Wang, A., Li, X., Zhu, W., Yan, C. F., et al. (2018). Active summer carbon storage for winter persistence in trees at the cold alpine treeline. *Tree Physiol.* 38, 1345–1355. doi: 10.1093/treephys/tpy020

Liu, H., Li, X., Xiao, J., and Wang, S. (2012). A convenient method for simultaneous quantification of multiple phytohormones and metabolites: application in study of rice-bacterium interaction. *Plant Methods* 8, 2–2. doi: 10.1186/1746-4811-8-2

Li, J., West, J. B., Hart, A., Wegrzyn, J. L., Smith, M. A., Domec, J.-C., et al. (2021). Extensive variation in drought induced gene expression changes between loblolly pine genotypes. *Front.Genet.* 12, 661440. doi: 10.3389/fgene.2021.661440

Li, P., Zhu, Y., Song, X., and Song, F. (2020). Negative effects of long-term moderate salinity and short-term drought stress on the photosynthetic performance of *Hybrid pennisetum*. *Plant Physiol.Biochem.* 155, 93–104. doi: 10.1016/j.plaphy.2020.06.033

Lloret, F, Sapes, G, Rosas, T, Galiano, L, Saura-Mas, S, Sala, A, et al. (2018). Non-structural carbohydrate dynamics associated with drought-induceddie-off in woody species of a shrubland community. *Ann. Bot.* 121, 1383–1396.

Mathew, I., Shimelis, H., Mutema, M., Clulow, A., Zengeni, R., Mbava, N., et al. (2019). Selection of wheat genotypes for biomass allocation to improve drought tolerance and carbon sequestration into soils. *J. Agron.Crop. Sci.* 205, 385–400. doi: 10.1111/jac.12332

Mitchell, P. J., O'grady, A. P., Tissue, D. T., White, D. A., Ottenschlaeger, M. L., and Pinkard, E. A. (2013). Drought response strategies define the relative contributions of hydraulic dysfunction and carbohydrate depletion during tree mortality. *New Phytol.* 197, 862–872. doi: 10.1111/nph.12064

Moran, E., Lauder, J., Musser, C., Stathos, A., and Shu, M. (2017). The genetics of drought tolerance in conifers. *New Phytol.* 216, 1034–1048. doi: 10.1111/nph.14774

Nam, W. H., Hayes, M. J., Svoboda, M. D., Tadesse, T., and Wilhite, D. A. (2015). Drought hazard assessment in the context of climate change for south Korea. *Agric. Water Manage.* 160, 106–117. doi: 10.1016/j.agwat.2015.06.029

Ninkovic, V., Markovic, D., and Rensing, M. (2021). Plant volatiles as cues and signals in plant communication. *Plant Cell Environ.* 44, 1030–1043. doi: 10.1111/pce.13910

Ormeño, E., Mévy, J. P., Vila, B., Bousquet-Mélou, A., Greff, S., Bonin, G., et al. (2007). Water deficit stress induces different monoterpene and sesquiterpene emission changes in Mediterranean species. relationship between terpene emissions and plant water potential. *Chemosphere* 67, 276–284. doi: 10.1016/j.chemosphere.2006.10.029

Otaka, J., Komatsu, M., Miyazaki, Y., Futamura, Y., and Osada, H. (2017). Two new triterpenoids from the roots of pinus densiflora. *Biosci. Biotechnol. Biochem.* 81, 449–452. doi: 10.1080/09168451.2016.1263149

Perreca, E., Rohwer, J., González-Cabanelas, D., Loreto, F., Schmidt, A., Gershenzon, J., et al. (2020). Effect of drought on the methylerythritol 4-phosphate (MEP) pathway in the isoprene emitting conifer *Picea glauca*. *Front. Plant Sci.* 11, 546295. doi: 10.3389/fpls.2020.546295

Polle, A., Chen, S. L., Eckert, C., and Harfouche, A. (2019). Engineering drought resistance in forest trees. *Front. Plant Sci.* 9, 1875. doi: 10.3389/fpls.2018.01875

Possell, M., and Loreto, F. (2013). "The role of volatile organic compounds in plant resistance to abiotic stresses: Responses and mechanisms," in *Biology, controls and models of tree volatile organic compound emissions*. Eds. Ü. Niinemets and R. K. Monson (Dordrecht: Springer Netherlands), 209–235.

Quan, W., and Ding, G. (2017). Root tip structure and volatile organic compound responses to drought stress in masson pine (*Pinus massoniana* lamb.). *Acta Physiol. Plant* 39, 258. doi: 10.1007/s11738-017-2558-7

Regier, N, Streb, S, Cocozza, C, Schaub, M, Cherubini, P, Zeeman, SC, et al. (2009). Drought tolerance of two black poplar (Populus nigraL.) clones: contribution of carbohydrates and oxidative stress defence. *Plant, Cell Environ.* 32, 1724–1736.

Rehman, A., Azhar, M. T., Hinze, L., Qayyum, A., Li, H., Peng, Z., et al. (2021). Insight into abscisic acid perception and signaling to increase plant tolerance to abiotic stress. *J. Plant Interact.* 16, 222–237. doi: 10.1080/17429145.2021.1925759

Ryhti, K., Schiestl-Aalto, P., Tang, Y., Rinne-Garmston, K. T., Ding, Y., Pumpanen, J., et al. (2022). Effects of variable temperature and moisture conditions on respiration and nonstructural carbohydrate dynamics of tree roots. *Agr. For. Meteorol.* 323, 109040. doi: 10.1016/j.agrformet.2022.109040

Schenkel, D., Lemfack, M., Piechulla, B., and Splivallo, R. (2015). A meta-analysis approach for assessing the diversity and specificity of belowground root and microbial volatiles. *Front. Plant Sci.e* 6, 707. doi: 10.3389/fpls.2015.00707

Semerci, A., Semerci, H., Çalişkan, B., Çiçek, N., Ekmekçi, Y., and Mencuccini, M. (2017). Morphological and physiological responses to drought stress of European provenances of scots pine. *Eur. J. For. Res.* 136, 91–104. doi: 10.1007/s10342-016-1011-6

Sharma, E., Anand, G., and Kapoor, R. (2017). Terpenoids in plant and arbuscular mycorrhiza-reinforced defence against herbivorous insects. *Ann. Bot.* 119, 791–801. doi: 10.1093/aob/mcw263

Signori-Müller, C., Oliveira, R. S., Barros, F. V., Tavares, J. V., Gilpin, M., Diniz, F. C., et al. (2021). Non-structural carbohydrates mediate seasonal water stress across Amazon forests. *Nat. Commun.* 12, 2310. doi: 10.1038/s41467-021-22378-8

Singh, H. P., Batish, D. R., Kaur, S., Arora, K., and Kohli, R. K. (2006). α-pinene inhibits growth and induces oxidative stress in roots. *Ann. Bot.* 98, 1261–1269. doi: 10.1093/aob/mcl213

Skelton, R. P., West, A. G., and Dawson, T. E. (2015). Predicting plant vulnerability to drought in biodiverse regions using functional traits. *Proc. Natl. Acad. Sci. U.S.A.* 112, 5744–5749. doi: 10.1073/pnas.1503376112

Song, W., Lee, B., Cho, N., Jung, S., Kim, E.-S., and Lim, J.-H. (2020). Effects of drought stress and nitrogen fertilization on growth and physiological charecteristics of pinus densiflora seedlings under elevated temperature and CO_2 concentration. *Korean. J. Agric. For. Meteorol.* 22, 57–67. doi: 10.5532/KJAFM.2020.22.257

Sperling, O., Silva, L. C. R., Tixier, A., Théroux-Rancourt, G., and Zwieniecki, M. A. (2017). Temperature gradients assist carbohydrate allocation within trees. *Sci. Rep.* 7, 3265. doi: 10.1038/s41598-017-03608-w

Szmigielski, R., Cieslak, M., Rudziński, K. J., and Maciejewska, B. (2011). Identification of volatiles from pinus silvestris attractive for *Monochamus galloprovincialis* using a SPME-GC/MS platform. *Environ. Sci. pollut. Res. Int.* 19, 2860–2869. doi: 10.1007/s11356-012-0792-5

Tanaka, K., Taniguchi, S., Tamaoki, D., Yoshitomi, K., Akimitsu, K., and Gomi, K. (2014). Multiple roles of plant volatiles in jasmonate-induced defense response in rice. *Plant Signal. Beha.v.* 9, e29247. doi: 10.4161/psb.29247

Tanentzap, F. M., Stempel, A., and Ryser, P. (2015). Reliability of leaf relative water content (RWC) measurements after storage: consequences for *in situ* measurements. *Botany* 93, 535–541. doi: 10.1139/cjb-2015-0065

Tan, L., Fan, R., Sun, H., and Guo, S. (2021). Root foraging of birch and larch in heterogeneous soil nutrient patches under water deficit. *PloS One* 16, e0255848. doi: 10.1371/journal.pone.0255848

Tsamir-Rimon, M., Ben-Dor, S., Feldmesser, E., Oppenhimer-Shaanan, Y., David-Schwartz, R., Samach, A., et al. (2021). Rapid starch degradation in the wood of olive trees under heat and drought is permitted by three stress-specific beta amylases. *New Phytol.* 229, 1398–1414. doi: 10.1111/nph.16907

Turtola, S., Manninen, A.-M., Rikala, R., and Kainulainen, P. (2003). Drought stress alters the concentration of wood terpenoids in scots pine and Norway spruce seedlings. *J. Chem. Ecol.* 29, 1981–1995. doi: 10.1023/A:1025674116183

Ullah, A., Bano, A., and Khan, N. (2021). Climate change and salinity effects on crops and chemical communication between plants and plant growth promoting microorganisms under stress. *Front. Sustain. Food Syst.* 5, 618092. doi: 10.3389/fsufs.2021.618092

Vastag, E., Orlovic, S., Konopkova, A., Kurjak, D., Cocozza, C., Psidova, E., et al. (2020). *Magnolia grandiflora l.* shows better responses to drought than *Magnolia* × *soulangeana* in urban environment. *iForest. - Biogeosci. Forestry.* 13, 575–583. doi: 10.3832/ifor3596-013

Vijayaraghavareddy, P., Lekshmy, S. V., Struik, P. C., Makarla, U., Yin, X., and Sreeman, S. (2022). Production and scavenging of reactive oxygen species confer to differential sensitivity of rice and wheat to drought stress. *Crop Environ.* 1, 15–23. doi: 10.1016/j.crope.2022.03.010

Vivaldo, G., Masi, E., Taiti, C., Caldarelli, G., and Mancuso, S. (2017). The network of plants volatile organic compounds. *Sci. Rep.* 7, 11050. doi: 10.1038/s41598-017-10975-x

Xiang, Z., Cai, K., Liang, G., Zhou, S., Ge, Y., Zhang, J., et al. (2014). Analysis of volatile flavour components in flue-cured tobacco by headspace solid-phase microextraction combined with GC×GC-TOFMS. *Analytical. Methods* 6, 3300–3308. doi: 10.1039/c3ay41956h

Yaish, M. W. (2015). Proline accumulation is a general response to abiotic stress in the date palm tree (*Phoenix dactylifera l.*). *Genet. Mol. Res.* 14, 9943–9950. doi: 10.4238/2015.August.19.30

Yang, J., Duan, G., Li, C., Liu, L., Han, G., Zhang, Y., et al. (2019). The crosstalks between jasmonic acid and other plant hormone signaling highlight the involvement of jasmonic acid as a core component in plant response to biotic and abiotic stresses. *Front.Plant. Sci.* 10, 1349. doi: 10.3389/fpls.2019.01349

Yang, X., Zhao, J., Zheng, J., Leng, P.-S., Li, X., Hu, Z., et al. (2015). Analysis of floral scent emitted from syringa plants. *J.For.Res* 27, 273–281. doi: 10.1007/s11676-015-0156-3

Yang, Z., Zhou, B., Ge, X., Cao, Y., Brunner, I., Shi, J., et al. (2021). Species-specific responses of root morphology of three co-existing tree species to nutrient patches reflect their root foraging strategies. *Front.Plant. Sci.* 11, 618222. doi: 10.3389/fpls.2020.618222

Zhang, Y., Luan, Q., Jiang, J., and Li, Y. (2021). Prediction and utilization of malondialdehyde in exotic pine under drought stress using near-infrared spectroscopy. *Front. Plant Sci.* 12, 735275. doi: 10.3389/fpls.2021.735275

Zhang, H., Zhao, Y., and Zhu, J.-K. (2020). Thriving under stress: How plants balance growth and the stress response. *Dev. Cell* 55, 529–543. doi: 10.1016/j.devcel.2020.10.012

frontiers | Frontiers in Plant Science

TYPE Original Research
PUBLISHED 10 January 2023
DOI 10.3389/fpls.2022.1026421

Check for updates

OPEN ACCESS

EDITED BY
Muhammad Waseem,
Hainan University, China

REVIEWED BY
Sombir Rao,
Cornell University, United States
Muhammad Imran,
Tsinghua University, China

*CORRESPONDENCE
Youling Zeng
zeng_ylxju@126.com

SPECIALTY SECTION
This article was submitted to Plant Abiotic Stress, a section of the journal Frontiers in Plant Science

RECEIVED 23 August 2022
ACCEPTED 01 December 2022
PUBLISHED 10 January 2023

CITATION
Ji J, Zeng Y, Zhang S, Chen F, Hou X and Li Q (2023) The miR169b/NFYA1 module from the halophyte *Halostachys caspica* endows salt and drought tolerance in *Arabidopsis* through multi-pathways. *Front. Plant Sci.* 13:1026421. doi: 10.3389/fpls.2022.1026421

COPYRIGHT
© 2023 Ji, Zeng, Zhang, Chen, Hou and Li. This is an open-access article distributed under the terms of the Creative Commons Attribution License (CC BY). The use, distribution or reproduction in other forums is permitted, provided the original author(s) and the copyright owner(s) are credited and that the original publication in this journal is cited, in accordance with accepted academic practice. No use, distribution or reproduction is permitted which does not comply with these terms.

The miR169b/NFYA1 module from the halophyte *Halostachys caspica* endows salt and drought tolerance in *Arabidopsis* through multi-pathways

Jieyun Ji[1], Youling Zeng[1]*, Suwei Zhang[1], Fangyuan Chen[1], Xianfei Hou[2] and Qiang Li[2]

[1]Xinjiang Key Laboratory of Biological Resources and Genetic Engineering, College of Life Science and Technology, Xinjiang University, Urumqi, China, [2]Institute of Economic Crops, Xinjiang Academy of Agricultural Sciences, Urumqi, China

Salt and drought are the major abiotic stress factors plaguing plant growth, development and crop yields. Certain abiotic-stress tolerant plants have developed special mechanisms for adapting to adverse environments in the long process of evolution. Elucidating the molecular mechanisms by which they can exert resistance to abiotic stresses is beneficial for breeding new cultivars to guide agricultural production. *Halostachys caspica*, a perennial halophyte belonging to *Halostachys* in Amaranthaceae, is extremely tolerant to harsh environments, which is commonly grown in the saline-alkali arid desert area of Northwest, China. However, the molecular mechanism of stress tolerance is unclear. Nuclear Factor Y-A (NFYA) is a transcription factor that regulates the expression of downstream genes in plant response to adverse environments. It has also been reported that some members of the NFYA family are the main targets of miR169 in plants. In this study, we mainly focused on exploring the functions and preliminary mechanism of the miR169b/NFYA1 module from *H. caspica* to abiotic stress. The main results showed that RLM-RACE technology validated that *HcNFYA1* was targeted by HcmiR169b, qRT-PCR revealed that HcmiR169b was repressed and *HcNFYA1* was induced in the *H. caspica* branches under various abiotic stress as well ABA treatment and *Arabidopsis* stable transformation platform with molecular methods was applied to elucidate that the HcmiR169b/HcNFYA1 module conferred the salt and drought tolerance to plants by enhancing ABA synthesis and ABA signal transduction pathways, maintaining ROS homeostasis and the stability of cell membrane. *HcNFYA1* is expected to be a candidate gene to improve plant resistance to salt and drought stresses.

KEYWORDS

miR169b/NFYA1 module, salt stress, drought stress, *Halostachys caspica*, regulatory mechanism

Introduction

Environmental stresses such as drought and salinity significantly affect plant' s physiological processes, limit the distribution of plants, and reduce crop production (Bailey-Serres et al., 2019; Zhang et al., 2020). Plants have evolved interrelated regulatory pathways that enable them to respond promptly and adapt to various environmental stresses (Gong et al., 2020). The presence of critical factors in these pathways can enhance plant resistance to different stresses by maintaining the stability of cell membranes and increasing their ability to scavenge reactive oxygen species (ROS), which may be an appropriate target for crop improvement (Miller et al., 2010; Nadarajah, 2020; Zhang et al., 2022).

Due to global climate change, drought has become one of the serious stresses limiting crop yields (Gupta et al., 2020). During soil water deficits, osmotic stress causes plants to express genes, *NCEDs* and *ABAs*, involved in ABA synthesis, which increases the amount of ABA within the tissues (Waadt et al., 2022; Kuromori et al., 2022). When ABA is present, the ABA receptor proteins PYR/PYLs can bind to the protein phosphatase PP2Cs and inhibit their activities, and thereby derepress PP2Cs' inhibitory effect on the protein kinase SnRK2 (Sah et al., 2016). SnRK2s can phosphorylate transcription factors ABFs and ABI3/5 to activate ABA-responsive genes, which contain ABRE elements in the promoter and their proteins can provide plants with greater tolerance to osmotic stress through different mechanisms, including the closure of stomata (Hsu et al., 2021). Salt stress has also become a major factor reducing crop yields due to land salinization. As plants are exposed to high salt environments, they are poisoned by harmful ions (such as Na^+) in addition to osmotic stress, and it is widely known certain proteins (SOS, NHX) have been evolved to exclude Na^+ to the outside of cells and partition sodium ions into vacuoles (Zelm et al., 2020).

MicroRNA (miRNA) is a small non-coding RNA that regulates its complementary target genes by cleaving mRNA or inhibiting translation (Bartel, 2009; Yu et al., 2017). In plants, regulatory modules composed of miRNAs and their target genes play important roles in physiological and biochemical processes (Song et al., 2019; Samad et al., 2017; Pagano et al., 2021). miR169 is one of the largest miRNA families in plants, and its target genes mainly encode the transcription factor nuclear factor Y-A (NFYA) (Luan et al., 2014; Chaves-Sanjuan et al., 2021; Wang et al., 2022). NFYA proteins form trimers with NFYB/C and then bind to CCAAT elements in downstream gene promoters to influence gene expression (Laloum et al., 2013; Zanetti et al., 2017).

The miR169/NFYA module regulates plant growth and development (Luan et al., 2014; Chaves-Sanjuan et al., 2021; Wang et al., 2022). Overexpression of *miR169d* promoted early flowering by targeting *AtNFYA2*; overexpression of *AtNFYA8* was reported to delay flowering in *Arabidopsis thaliana* (Xu et al., 2014; Zhao et al., 2020). However, more studies have focused on the function of miR169/NFYA module in adversity stress (Li et al., 2008). The suppression of *Arabidopsis* miR169a/c expression led to an up-regulation of its target gene, *AtNFYA5*, resulting in drought resistance. *GmNFYA3*, the gene targeted by GmmiR169c in soybean (*Glycine max*), confers drought tolerance, while GmmiR169c reduced drought resistance in *Arabidopsis* by targeting the cleavage of *AtNFYA1/5* (Ni et al., 2013; Yu et al., 2019). Salt stress suppressed the expression of maize (*Zea mays*) ZmmiR169q, and up-regulated its target gene *ZmNFYA8*, finally enhancing salt tolerance in maize by attenuating ROS-induced toxicity (Xing et al., 2021). In contrast, tomato (*Solanum lycopersicum*) SlymiR169c and poplar (*Populus trichocarpa*) PtmiR169o enhanced the plant's drought resistance (Zhang et al., 2011; Jiao et al., 2021). The miR169/NFYA module in plants is not functionally conserved in response to abiotic stresses.

Halostachys caspica is a perennial shrub in Amaranthaceae, which can grow in the extremely arid and saline-alkali environments. In our previous study, the expression of miR169b was significantly different in the small RNA libraries of the *Halostachys caspica* roots under high salinity and *NFYA1* was the potential target of this miRNA using this species' transcriptome data by bioinformatic prediction. (Yang et al., 2015). However, the miR169b/NFYA1 module has not been studied, and its role has not still been elucidated in *H. caspica*. In this work, we first experimentally validated that *HcNFYA1* is the real target of HcmiR169b, and explored their expression patterns in *H. caspica* under various abiotic-stresses. The functions and regulatory mechanism of the HcmiR169b and HcNFYA1 module were investigated by generating *HcmiR169b*/*HcNFYA1* heterologously expressed *Arabidopsis thaliana*.

Materials and methods

H. caspica culture and stress treatments

H. caspica seeds were harvested from extremely saline-alkali and arid areas in the Gurbantunggut Desert in Xinjiang, China. Healthy seeds were sown in pots with the substrate (perlite: vermiculite: flower soil = 1:1:3) and cultivated under natural light and suitable temperature (25°C - 28°C). Eight-week-old *H. caspica* plants were exposed to 600 mM NaCl, 1000 mM mannitol, 0 °C freezing stress, 100 μM methyl viologen (MV) and 300 μM abscisic acid (ABA) for 0, 3 and 24 h, and assimilating branches were taken and put in liquid nitrogen for subsequent qRT-PCR assays.

Cloning and bioinformatics analysis of *HcmiR169b* precursor and *HcNFYA1*

The *HcmiR169b* mature sequence was obtained from a small RNA library derived from *H. caspica* roots (Yang et al., 2015).

The *HcmiR169b* precursor sequence was obtained through homologous cloning and 5'-RACE nested amplification using the *H. caspica* cDNA as template. Based on the EST sequence of *HcNFYA1* in the *H. caspica* transcriptome data, the full length of *HcNFYA1* gene was cloned from the *H.caspica* cDNA using the SMARTer RACE 5'/3' Kit (Takara, Japan).

Amino acid sequences of NFYA family members were downloaded from the PlantTFDB plant transcription factor database (http://planttfdb.gao-lab.org/index.php) (Jin et al., 2017). Multiple comparisons of amino acid sequences were performed using DNAMAN software (LynnonBiosoft, USA). Phylogenetic analysis was applied using the proximity method (1000 replicates) with MEGA 11 software (Mega Limited, New Zealand).

Validation of HcmiR169b cleavage site in *HcNFYA1* by RLM-RACE

As shown in the Supplementary Figure S1, the method in this study was modified according to the RNA ligase mediated (RLM)-cDNA end rapid amplification (RACE) technique developed by (Wang and Fang, 2015). T4 RNA ligase (Ambion, Canada) was used to add an adapter to the 3' hydroxyl end of *H. caspica* RNA. A specific primer (GSP) complementary to the adapter was used for reverse transcription to obtain cDNA with the adapter sequence. Two rounds of nested PCR amplification was carried based on the cDNA and the second round of amplification products were cloned into the pMD-19T vector for sequencing, and the sequencing results were analyzed to determine the cleavage site of *HcNFYA1* by HcmiR169b. The primers used in this study were listed in Supplementary Table S1.

Detection of gene expression by qRT-PCR

Total RNAs were extracted from plant samples by RNA prep pure Plant Kit (Tiangen, China). The stem-loop method was used for microRNA reverse transcription, with *HcU6* and *AtU6* serving as internal controls (Chen et al., 2005), and protein-coding genes were reverse-transcribed using One-Step gDNA Removal and cDNA Synthesis SuperMix (Transgen, China), with *HcUBQ10* and *Atactin* as internal controls (Zhang et al., 2015). qRT-PCR was performed in a CFX96 Touch Real-Time PCR System (Bio-Rad, USA) using a PerfectStart Green qPCR SuperMix (Transgen, China) with three biological replicates per sample. The relative expression of genes was calculated by $2^{-\Delta\Delta CT}$ comparison method (Livak and Schmittgen, 2001). The primers were shown in Supplementary Table S1.

Subcellular localization and transcriptional activation analysis of HcNFYA1

The *HcNFYA1* open reading frame (ORF) region was inserted into the plant expression vector pCAMBIA1301-1-GFP (Liu et al., 2009). HcNFYA1 was fused to GFP for expression and transformed into onion epidermal cells using the *Agrobacterium* GV3101-mediated transient transformation system. Onion epidermal cells were stained with DAPI and observed under a LSM800 Confocal Microscope (Zeiss, Germany).

The ORF region of *HcNFYA1* was constructed into the pGBKT7 vector containing the GAL4 DNA binding domain. The recombinant plasmid was transformed into the Y2H Gold yeast strain. Transformants were screened in SD/-Trp-His medium containing X-α-Gal and HcTOE3 was used as a positive control (Yin et al., 2021). The primers were listed in Supplementary Table S1.

Generation of transgenic *Arabidopsis* and stress treatment

The precursor sequence of *HcmiR169b* and the ORF region of *HcNFYA1* were constructed into plant expression vector pCAMBIA2300, and transformed into *Arabidopsis* wild type (Columbia) by inflorescence infection (Zhang et al., 2006). Positive lines were screened by kanamycin primarily. The selected T_3 generation transgene *Arabidopsis* lines with single copy were verified by genomic PCR and qRT-PCR.

Arabidopsis seeds were sterilized with sodium hypochlorite (10%) and 75% ethanol (90%) for 5 min and sown in 1/2 MS medium. After 3 days of vernalization at 4°C with a 16 h/8 h light/dark photoperiod, petri dishes with plants were put in the growing chamber at 22°C. After two weeks of growth, the plants were transferred to pots filled with the substrate (perlite: vermiculite: flower soil = 1:1:3) for cultivation.

Arabidopsis germination experiments were conducted in 1/2 MS medium containing NaCl (125 mM), mannitol (250 mM), and ABA (0.5 μM, 0.75 μM). The seed germination rates were recorded daily, and the cotyledon greening rates were measured after 7 days.

For the salt treatment, four-week-old *Arabidopsis* plants were irrigated with 300 mM NaCl for 7 days, photographed, dried at 80°C for 24 hours, and weighed for the dry weight (10 biological replicates). 300 mM NaCl-treated *Arabidopsis* leaves were collected for qRT-PCR (24 h) and measuring some physiological and biochemical parameters (3 d).

For the drought treatment, *Arabidopsis* plants were planted in pots containing the same substrate weight and re-watered for 3 days after stopping irrigation for 7 or 9 days. The plants were

photographed and counted for survival numbers (three independent experiments with 40 biological replicates each). *Arabidopsis* leaves were collected when irrigation was stopped for 5 days for physiological index testing. Leaves were taken for qRT-PCR analysis after 24 h of treatment when *Arabidopsis* was irrigated with 20% PEG6000.

Determination of physiological and biochemical indicators

Adult *Arabidopsis* leaves were submerged with 1 mg/mL of Evans blue, DAB, and NBT solution and stained for 2 h at 37°C in the dark. The leaves were placed in absolute alcohol at boiling temperature for 30 min to remove chlorophyll. 10 blades were run per treatment.

Whole *Arabidopsis* plants were soaked in 50 ml ultrapure water for 24 h. The solution conductivity (C1) was measured and the solution conductivity (C2) was measured again after boiling for 1 h using a Conductivity Meter (DSS-307, China). C1/C2×100% was calculated as the relative electrolyte leakage.

The measurements of chlorophyll, MDA, H_2O_2, O_2^- and proline contents as well as the detection of POD, APX and SOD enzyme activities were performed according to the manufacturer's instructions (Solarbio, China). Soluble protein content was determined using the BCA Soluble Protein Content Kit (Addison, China). The content of ABA was determined by ABA ELISA assay kit (Saipei, China). Per sample had three biological replicates for each treatment, and 0.1 g of *Arabidopsis* leaves were collected for each biological replicate.

Analysis of water loss and stomatal aperture of *Arabidopsis* leaves

Arabidopsis leaves were taken and placed in an area with good airflow. The initial fresh weight (W_0) and the fresh weight of the leaves were measured every 5-30 minutes (W_t), and 100%-W_t/W_0 was called as the water loss rate.

Arabidopsis leaves were immersed in stomatal opening buffer (5 mM MES, 10 mM KCl, 50 mM $CaCl_2$, pH 5.6) for 2 h, transferred to a solution containing 0 mM/300 mM mannitol or 0 μM/30 μM ABA for 2 h and then observed under a microscope for photographs. The aspect ratio was analyzed using Image J software (National Institutes of Health, USA). Three *Arabidopsis* leaves were run for each treatment, and at least 50 clear stomata in the field of view were obtained for each leaf.

Statistical analysis

SPSS Statistics 20 (IBM, USA) was employed for data analysis. All experiments were performed at least 3 times. Experimental data of gene expression in *H. caspica* and aspect ratio with *Arabidopsis* leaves for stomatal aperture analysis were assessed by Student's t-test (*p<0.05, **p<0.01, ***p<0.001, ****p<0.0001). All other data were assessed using Duncan's test (p<0.05).

Results

Expression patterns of miR169b and its targeted gene *NFYA1* in *Halostachys caspica* under abiotic stresses

HcNFYA1 was predicted to be targeted by HcmiR169b in our previous work (Yang et al., 2015). Here, RLM-RACE experiment was conducted to verify their targeting between HcmiR169b and *HcNFYA1* (Rhoades et al., 2002; Wu et al., 2012). The results of agarose gel electrophoresis were shown in the Supplementary Figure S2. The final products by sequencing indicated that HcmiR169b cleaves the 3'UTR region of *HcNFYA1* with 100% (6/6) efficiency (Figure 1A).

Eight-week-old *H. caspica* were exposed to salt (Figure 1B), drought (Figure 1C), cold (Figure 1D), and oxidative stress (Figure 1E) as well as exogenous hormone ABA (Figure 1F). After 3 and 24 hours of treatment, individual assimilating branches were extracted and used for qRT-PCR analysis. The results showed that the expressions of HcmiR169b and *HcNFYA1* presented a significant negative correlation, HcmiR169b was significantly inhibited and *HcNFYA1* was notably induced under different abiotic stress treatments. HcmiR169b and *HcNFYA1* appeared to respond to various abiotic stresses, including salt and drought stress; *HcNFYA1* might be controlled by HcmiR169b under these adverse conditions.

HcNFYA1 acts as a transcription factor

The coding sequence of *HcNFYA1* is 903 bp in length, and its encoded protein contains 300 amino acids. HcNFYA1 protein contained the binding sites for NFYB/C and CCAAT (Supplementary Figure S3A). Based on a phylogenetic analysis of conserved amino acids found in HcNFYA1 and members of the NFYA family of other plant species, including *Arabidopsis*, soybean, maize, rice, and *Beta vulgaris*, HcNFYA1 was clustered with BvNFYA1 (Supplementary Figure S3B).

To determine the subcellular localization of HcNFYA1, the HcNFYA1-GFP fusion protein was expressed in the onion epidermis using an *Agrobacterium*-mediated transient transformation system. Under laser confocal microscopy, the fluorescent signal of HcNFYA1-GFP overlapped with the 4-diamino-2-phenylindole (DAPI) signal were observed and appeared only in the nucleus (Figure 2A). This suggested that

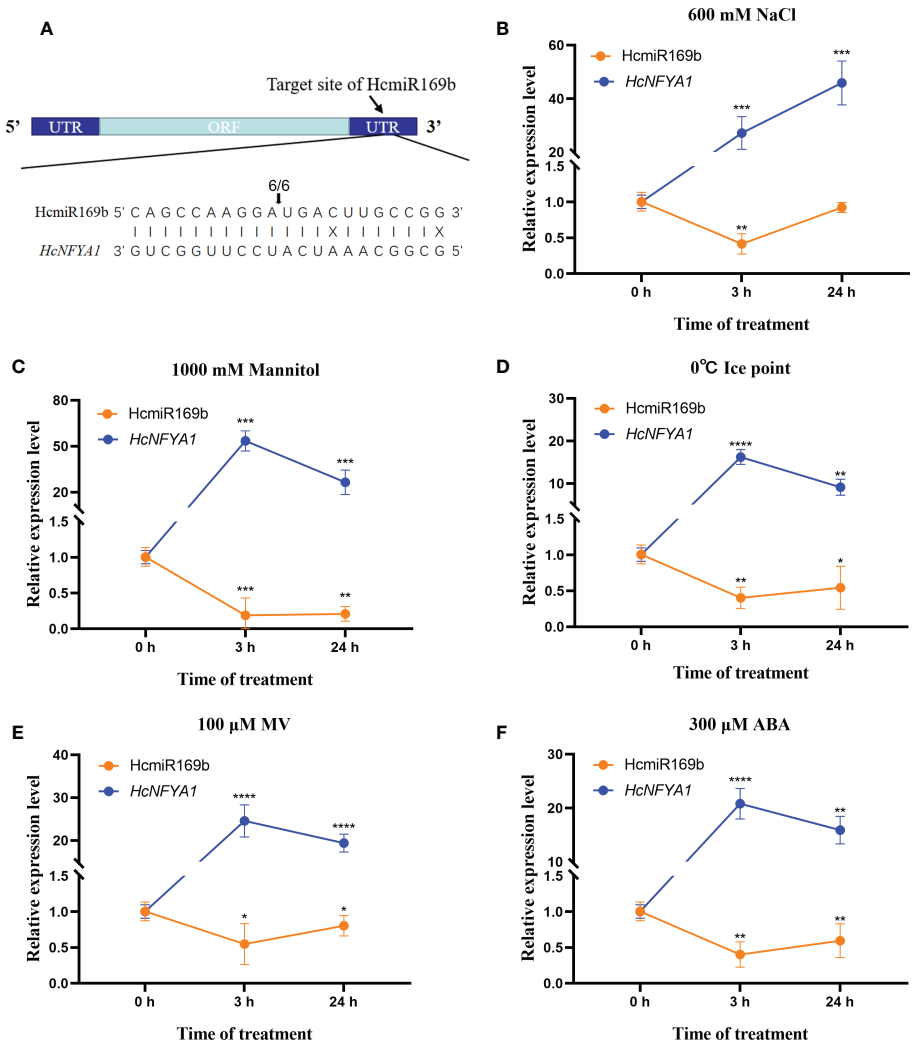


FIGURE 1
Targeting relationship between *Halostachys caspica* miR169b and *NFYA1* and the expression patterns of both genes under abiotic stress. **(A)** RLM-RACE identified the targeted cleavage of *HcNFYA1* by HcmiR169b. Arrows indicated specific cleavage site, and the number on the arrow indicated the number of independent clones for detecting the cleavage site. **(B-F)** The expression of mature miR169b and *NFYA1* in assimilating branches of *Halostachys caspica* under salt **(B)**, simulated drought **(C)**, cold **(D)**, oxidative stress **(E)** and exogenous hormone ABA **(F)**. *HcU6* and *HcUBQ10* were used as internal controls. All data were represented as the means ± SD of three biological replicates. Asterisks indicated significantly different transcriptional levels compared to 0 h (Student's t-test, *p<0.05, **p<0.01, ***p<0.001, ****p<0.0001).

HcNFYA1 was translated and then translocated into the nucleus to function.

To identify whether HcNFYA1 functions as a transcription factor. The ORF region of *HcNFYA1* was constructed into the yeast BD expression vector pGBKT7 and transformed into Y2H Gold cells. The HcNFYA1 protein, like the positive control (Yin et al., 2021), activated the expression of a downstream reporter gene, the protein encoded by this gene caused X-α-Gal to degrade and made transformed yeast show blue color (Figure 2B), indicating that HcNFYA1 had transcriptional activation activity.

Halostachys caspica miR169b/NFYA1 module affects the germination of *Arabidopsis* seeds under salt and drought stress

To elucidate the function of the HcmiR169b/HcNFYA1 module in abiotic stress, we generated 35S:*HcmiR169b* and 35S:*HcNFYA1* transgenic *Arabidopsis* homozygous lines with single copy by the methods of inflorescence infection and kanamycine screening. Based on the results of qRT-PCR assay for T_3 generation of transgenic plants, two individual

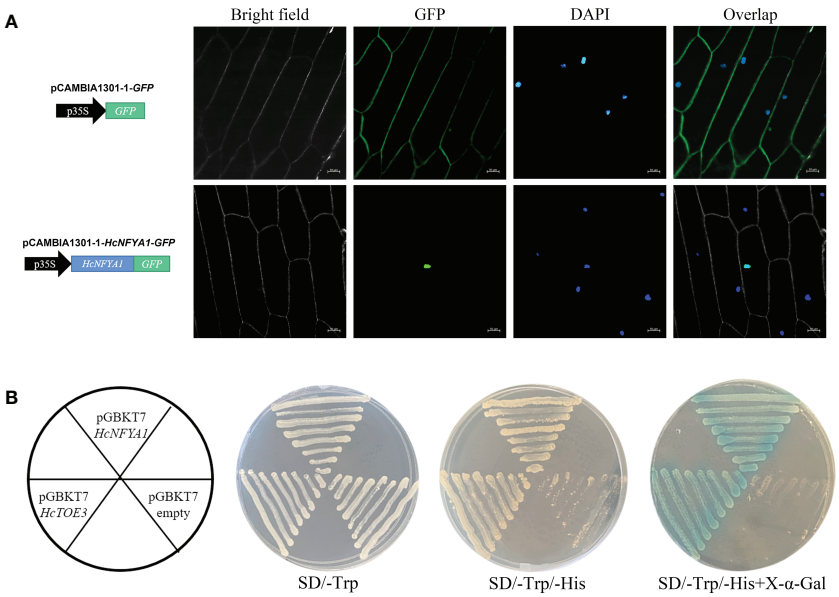


FIGURE 2
Characteristic analysis of transcription factor HcNFYA1. **(A)** Localization of HcNFYA1-GFP fusion protein in onion epidermal cells, DAPI was used as a nuclear marker. **(B)** Transcriptional activation analysis of HcNFYA1 in yeast expression system. HcTOE3 was used as a positive control.

transgenic lines (*HcmiR169b* OE5 and *HcmiR169b* OE11, *HcNFYA1* OE2 and *HcNFYA1* OE3) were selected for subsequent experiments; both of transgenic lines had high expressions for respectively transformed genes (Figure 3A, D). Because of the highly conserved mature sequences between HcmiR169b and AtmiR169b, a portion of AtmiR169b expression was also detected possibly (Supplementary Figure S4). The expressions of its predicted target gene *AtNFYA1/5* were reduced in 35S:*HcmiR169b Arabidopsis* by qRT-PCR assay (Figure 3B, C).

The seed germination was consistent between 35S:*HcmiR169b Arabidopsis* and WT on 1/2 MS medium (Supplementary Figure S5A). However, the germination rate of 35S:*HcmiR169b* seeds was lower when NaCl (125 mM) or mannitol (250 mM) was added to the medium in comparison with the WT (Supplementary Figure S5B, C), suggesting that HcmiR169b made *Arabidopsis* more sensitive to salt and drought stresses during the stage of seed germination. Compared with the WT, 35S:*HcNFYA1 Arabidopsis* seeds in 1/2 MS medium were exhibited slightly delayed germination (Supplementary Figure S5D). When NaCl or mannitol was added to the medium, the germination rate of 35S:*HcNFYA1 Arabidopsis* seeds was decreased compared to the WT (Supplementary Figure S5E, F). Overexpression of *HcNFYA1* inhibited *Arabidopsis* seed germination under salt- and drought-stressed conditions.

Halostachys caspica miR169b/NFYA1 module regulates salt tolerance in *Arabidopsis*

Under salt stress of 300 mM NaCl, 35S:*HcmiR169b Arabidopsis* grew smaller and the leaves wilted more severely than WT, whereas 35S:*HcNFYA1 Arabidopsis* grew larger, leaves wilted less (Figure 3E). In addition, under salt stress, the dry weight of aboveground parts (Figure 3F), chlorophyll (Figure 3G) and soluble protein (Figure 3H) contents were lower in 35S:*HcmiR169b Arabidopsis* and higher in 35S:*HcNFYA1 Arabidopsis*, compared to those in the WT. In conclusion, HcmiR169b negatively regulated salt tolerance in *Arabidopsis*, whereas HcNFYA1 was positive in regulating salt tolerance in *Arabidopsis*.

Halostachys caspica miR169b/NFYA1 module regulates drought tolerance in *Arabidopsis*

To examine the role of *Halostachys caspica* miR169b/NFYA1 in response to drought stress, four-week-old *Arabidopsis* were stopped from irrigation untill different phenotypes emerged among them. Almost 7 days after ceasing to irrigate, 35S:*HcmiR169b Arabidopsis* showed leaf drying, and its survival rate

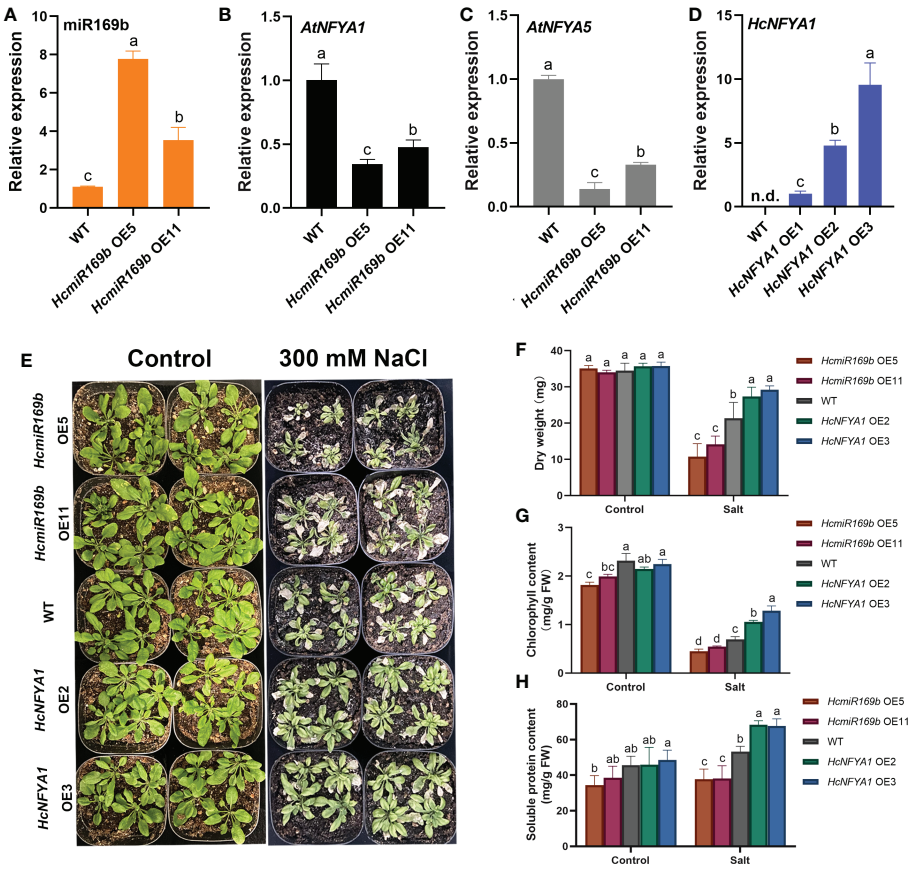


FIGURE 3
Functional analysis of *Halostachys caspica* miR169b/NFYA1 module under salt stress. **(A-C)** Relative expression of miR169b **(A)**, *AtNFYA1* **(B)** and *AtNFYA5* **(C)** in wild-type and *HcmiR169b* heterologous expressed *Arabidopsis*, the expression level of wild-type was adjusted to 1. **(D)** Relative expression of *HcNFYA1* in wild-type and *HcNFYA1* heterologous expressed *Arabidopsis*, adjusting the expression level of *HcNFYA1* OE1 to 1. **(E)** Phenotype of adult *Arabidopsis* under 300 mM NaCl stress for 7 d. **(F-H)** The aboveground dry weight **(F)**, chlorophyll content **(G)** and soluble protein content **(H)** of *Arabidopsis* under salt stress. Values for aboveground dry weight represented the means ± SD of 10 biological replicates, and values for other data represented the means ± SD of three biological replicates. Different letters indicated significant differences in the detected values of various types of *Arabidopsis* between treatments (Duncan's multiple range test, $p<0.05$).

after 3 days of rewatering was significantly lower than that of WT. Continuing with no irrigation for 9 days, 35S:*HcmiR169b Arabidopsis* leaves had completely dried out and wild-type *Arabidopsis* leaves were wilted, whereas 35S:*HcNFYA1 Arabidopsis* was still growing well. At this point, 3 days after rewatering, the survival rate of 35S:*HcmiR169b Arabidopsis* was already below 20%, 50% for wild-type *Arabidopsis*, and up to 80% for 35S:*HcNFYA1 Arabidopsis* (Figure 4A, B). Under drought stress, the drought-responding positive regulatory hormone ABA content was the highest in 35S:*HcNFYA1 Arabidopsis* and the lowest in 35S:*HcmiR169b* (Figure 4C). HcmiR169b appeared to be a negative regulator of drought resistance in *Arabidopsis*, whereas HcNFYA1 was a positive regulator.

Water loss was faster in detached leaves of 35S:*HcmiR169b Arabidopsis* and slower in leaves of 35S:*HcNFYA1 Arabidopsis* compared with WT (Figure 4D). In detached leaves of *Arabidopsis*, the rate of water loss was primarily dependent on the degree of stomatal opening. After treatment with 300 mM mannitol, 35S:*HcmiR169b Arabidopsis* had significantly more open stomata than WT, and 35S:*HcNFYA1 Arabidopsis* had more completely closed stomata than WT (Figure 4E-G). This suggested that the HcmiR169b/HcNFYA1 module may regulate drought tolerance in *Arabidopsis* through stomatal activity.

Halostachys caspica miR169b/NFYA1 module regulates the stability of plant cell membrane systems and resistance to oxidative stress

Adversity stress leads to disruption of plant cell membrane and ROS homeostasis. We monitored the integrity of cell membranes in various types of *Arabidopsis* under salt and drought stress based on the Evans blue staining (Figure 5A),

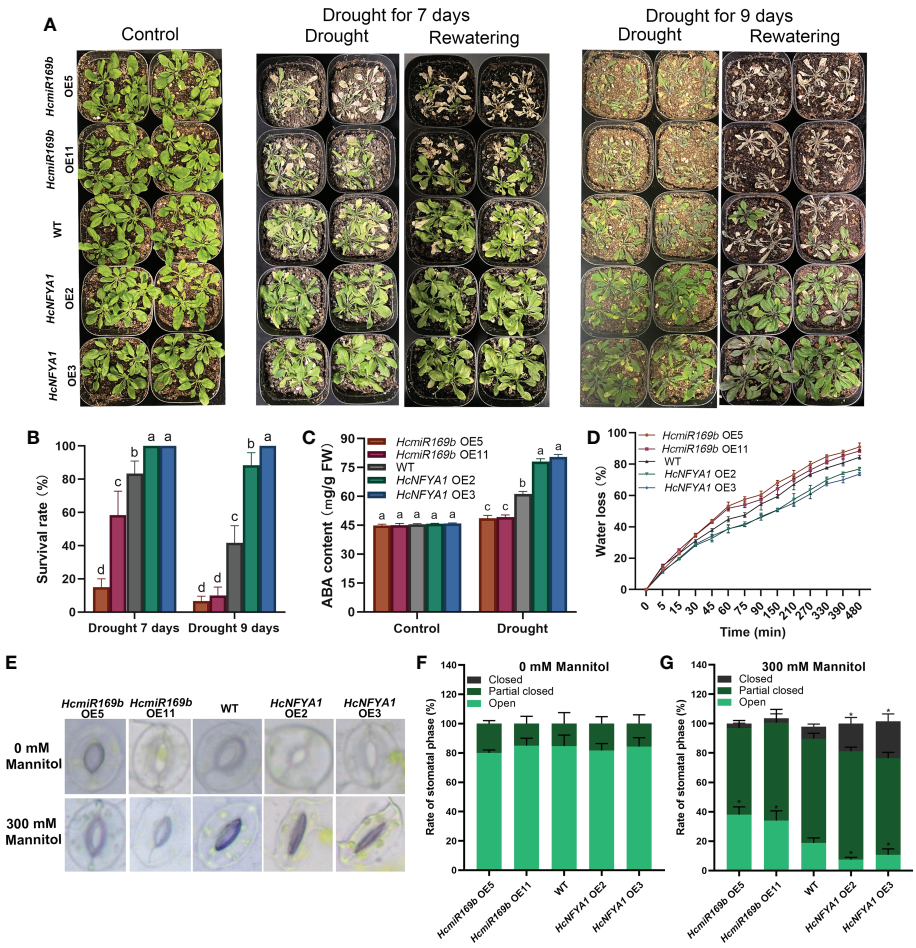


FIGURE 4
Functional analysis of *Halostachys caspica* miR169b/NFYA1 module under drought stress. **(A, B)** Phenotype **(A)** and survival **(B)** of adult *Arabidopsis* after 7 or 9 days of natual drought and 3 days of rewatering. **(C)** ABA content in *Arabidopsis* under control and drought stress. **(D)** Determination of water loss in detached leaves of *Arabidopsis*. **(E-G)** Stomatal apertures of *Arabidopsis* leaves under 0 and 300 mM mannitol (simulated drought) treatment were photographed **(E)** and the percentage of various stomata **(F, G)**. Data were shown as the means ± SD of three independent experiments. Different letters indicated significant differences in survival rate and ABA content of each type of *Arabidopsis* between treatments (Duncan's multiple range test, $p<0.05$), asterisk indicated a significant difference in the percentage of this stomatal type compared to WT (Student's t-test, $*p<0.05$).

electrolyte leakage (Figure 5D) and malondialdehyde (MDA) content (Figure 5E) assays. The results showed that 35S:*HcmiR169b Arabidopsis* cell membrane was more severely damaged compared to the WT, while 35S:*HcNFYA1 Arabidopsis* cell membrane integrity was better. Diaminobenzidine (DAB) and nitro-blue tetrazolium (NBT) staining (Figure 5B, C), H_2O_2 and O_2^- content (Figure 5F, G) measurements with leaves in various *Arabidopsis* were performed. The results showed that 35S:*HcmiR169b Arabidopsis* accumulated more ROS and 35S:*HcNFYA1 Arabidopsis* increased less ROS compared to the WT under salt and drought stress.

Proline (Pro)is used as an osmoregulatory substance to keep the osmotic pressure stability in plants and maintain the integrity of the cell membrane (Székely et al., 2008). The Pro content (Figure 5H) and the expression of its key synthetic enzyme gene *P5CS* (Figure 5L) were lower in 35S:*HcmiR169b Arabidopsis* than those in the WT under salt and drought stress, and the opposite results were obtained from 35S:*HcNFYA1 Arabidopsis*. Antioxidant enzymes play an important role in scavenging plant ROS species, so the activities of antioxidant enzymes (Figure 5I-K) and their transcription levels of relative synthetic enzyme genes (Figure 5M-O) were examined in *Arabidopsis*. Under salt and drought stress, 35S:*HcmiR169b Arabidopsis* had the lowest antioxidant enzyme activities and gene expression at both protein and RNA levels, whereas 35S:*HcNFYA1 Arabidopsis* had the highest antioxidant enzyme activities, and WT *Arabidopsis* was in the middle. Under the control conditions, there was no significant difference in physiological indices and gene

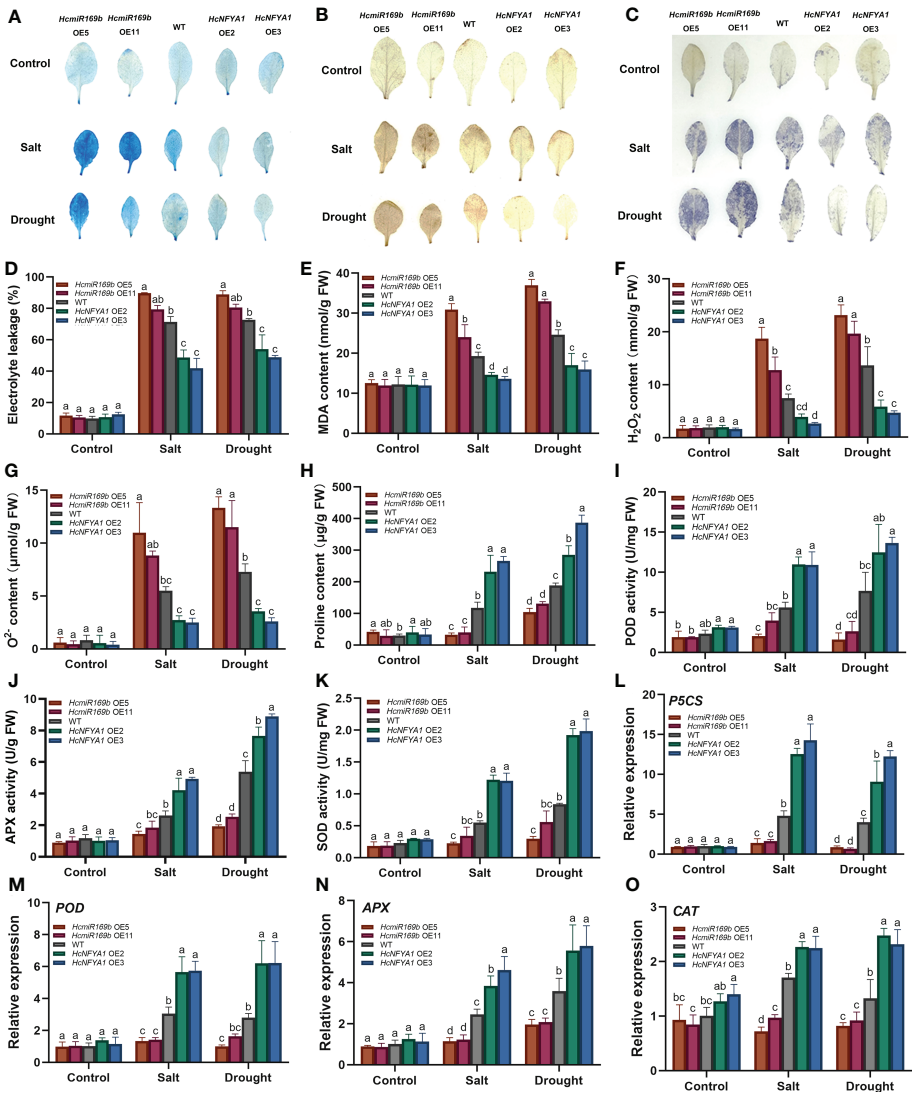


FIGURE 5
The performance of WT and two transgenic (*HcmiR169b*, *HcNFYA1* OE) *Arabidopsis* lines under salt and drought stress. **(A–C)** Evans blue **(A)**, DAB **(B)** and NBT **(C)** staining of adult *Arabidopsis* leaves under control, salt (300 mM NaCl) and drought (stop the irrigation) stress. **(D)** Electrolyte leakage assay. **(E-H)** MDA **(E)**, H_2O_2 **(F)**, O_2^- **(G)**, proline **(H)** contents. **(I–K)** POD **(I)**, APX **(J)**, SOD **(K)** enzyme activities. **(L–O)** Relative expression of *P5CS* **(L)**, *POD* **(M)**, *APX* **(N)**, *CAT* **(O)** genes. All data represented the means ± SD of three biological replicates. Different letters indicated significant differences in the detected values of various types of *Arabidopsis* between treatments (Duncan's multiple range test, $p<0.05$).

transcription levels between the transgenic (*HcmiR169b*, *HcNFYA1* OE) *Arabidopsis* and the WT.

Expression analysis of stress-responsive genes in *Halostachys caspica* miR169b/NFYA1 module

To investigate the regulatory mechanism in which the *Halostachys caspica* miR169b/NFYA1 module functions under salt and drought stress, we selected classical stress-responsive genes (*RD29A*, *LEA3*), salt stress-related genes (*SOS3*, *NHX1*), drought stress-related gene (*DREB2A*), ABA synthesis genes (*NCED3*, *ABA1*) and ABA signaling pathway positively regulatory genes (*ABF1*, *RAB18*, *ABI5*) for further analysis. Notably, in the controls, three genes, *LEA3*, *SOS3*, and *ABF1*, were significantly less expressed in 35S:*HcmiR169b Arabidopsis* and much more expressed in 35S:*HcNFYA1 Arabidopsis* than those in the WT, and all of them have CCAAT elements in their promoters (Figure 6B, C, J). Among them, *ABF1* was directly regulated by NFYA family members in soybean (Yu et al., 2021).

Under salt and drought stress conditions, all genes were significantly more expressed in 35S:*HcNFYA1 Arabidopsis* than those in the WT, and the opposite was observed in the 35S:*HcmiR169b Arabidopsis* (Figure 6). According to these results, HcNFYA1 can confer salt and drought tolerance to plants by activating downstream responsive genes; HcmiR169b reduced salt and drought resistance by silencing these pathways these genes involved in.

Halostachys caspica miR169b/NFYA1 module regulates plant response to exogenous hormone ABA

Exogenous hormone ABA reduces the seed germination rate of plants (Sah et al., 2016). To explore how the miR169b/NFYA1 module is involved in ABA signaling, the seeds of various types of *Arabidopsis* lines were sown on 1/2 MS medium containing 0, 0.5, and 0.75 μM ABA to observe their germination and cotyledon greening rates. Several types of *Arabidopsis* were capable of reaching 100% germination and cotyledon greening on ABA-free media; however, the germination rate and cotyledon greening rate of 35S:*HcmiR169b Arabidopsis* were significantly higher with exogenous hormone ABA treatments than without ABA treatment, while these growth parameters of 35S:*HcNFYA1 Arabidopsis* were significantly lower than WT (Figure 7A-H). ABA also induces the closure of plant stomata. Under 30 μM ABA treatment, stomatal closure in the leaves of 35S:*HcmiR169b Arabidopsis* was lower and stomatal closure of 35S:*HcNFYA1 Arabidopsis* was higher compared with WT (Figure 7I-K). Accordingly, HcmiR169b inhibited the ABA signaling pathway in *Arabidopsis*, while HcNFYA1 activated this pathway.

Discussion

Halostachys caspica grown in the saline-alkali arid land for a long history, has developed extreme resistance to harsh environments. We have reported that miRNAs play an

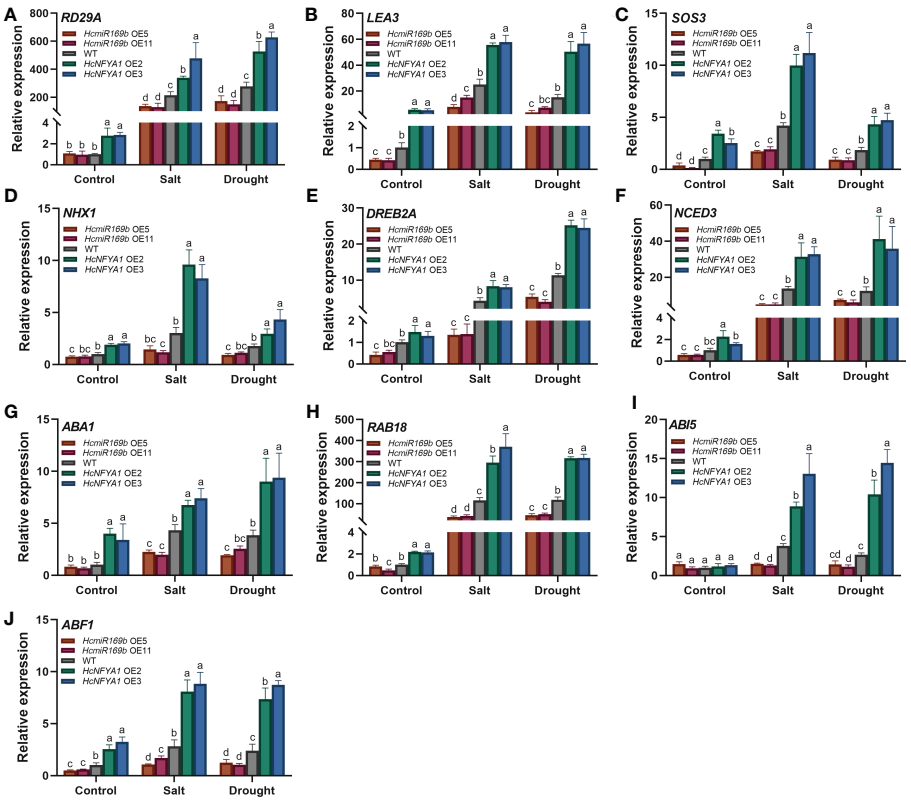


FIGURE 6
Expression of downstream stress-responsive genes in WT and two transgenic (*HcmiR169b*, *HcNFYA1* OE) *Arabidopsis* under salt and drought stress. **(A-J)** The relative expression levels of *RD29A* **(A)**, *LEA3* **(B)**, *SOS3* **(C)**, *NHX1* **(D)**, *DREB2A* **(E)**, *NCED3* **(F)**, *ABA1* **(G)**, *RAB18* **(H)**, *ABI5* **(I)** and *ABF1* **(J)** in adult *Arabidopsis* under the control, salt (300 mM NaCl) and drought (20% PEG6000) stress. All data represented the means ± SD of three biological replicates. Different letters indicated significant differences in the detected values of various types of *Arabidopsis* between treatments (Duncan's multiple range test, $p<0.05$).

essential role in stress tolerance in this species (Yang et al., 2015). Using the *Arabidopsis* stable transformation platform and molecular methods, we revealed such a resistance mechanism on abiotic stress—*Halostachys caspica* miR169b-targeted NFYA1 improves plant tolerance to salt and drought stresses through enhancing ABA synthesis and the associated signaling pathways, maintaining ROS homeostasis and the cell membrane integrity (Figure 8).

The miR169 family is the largest and most conserved miRNA family in plants. *NFYA*, targeted by miR169, has been validated in maize, soybean, and oilseed rape. In these species, miR169 expression are repressed by various stresses such as salt and drought; whereas the opposite pattern is observed for *NFYA* genes (Luan et al., 2014; Yu et al., 2019; Wang et al., 2022). Our present study validated that *HcNFYA1* is a true target of miR169b in *H. caspica* by RLM-RCE technology (Figure 1A). Under salt, drought stress and ABA treatment, HcmiR169b expression was inhibited, and its targeted gene *HcNFYA1* was significantly induced in *H. caspica* (Figure 1B-F). Thus, miR169/NFYA1 module may play an important role in plant's adaptation to adversity stresses.

It was reported that the AtmiR169a and GmmiR169c made *Arabidopsis* sensitive to drought stress in adulthood by negative regulating the drought-resistant regulator *AtNFYA5* (Li et al., 2008; Yu et al., 2019). Moreover, these two microRNA mature sequences differ from HcmiR169b by only two bases at the 3'

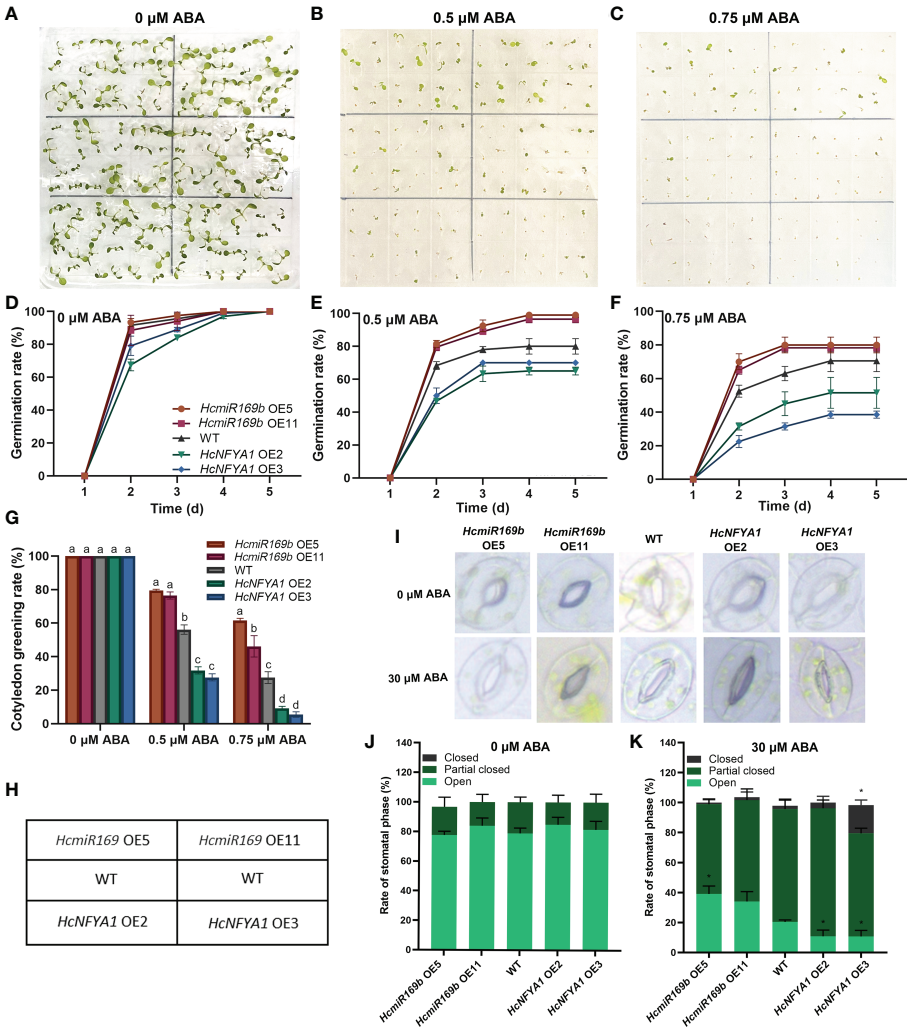


FIGURE 7
Halostachys caspica miR169b/NFYA1 module responds to the exogenous hormone ABA. **(A-G)** Seed germination phenotypes **(A–C)**, germination curves **(D-F)**, and cotyledon greening rate **(G)** of *Arabidopsis* under 0 μM, 0.5 μM, and 0.75 μM ABA treatments. **(H)** Layout designs of figure A-C. **(I-K)** Stomatal aperture photographs **(I)** and percentage of various stomata **(J, K)** of *Arabidopsis* leaves under 0 μM ABA and 30 μM ABA treatments. Data were shown as the means ± SD of three biological replicates. Different letters indicated significant differences in cotyledon greening rate of each type of *Arabidopsis* between treatments (Duncan's multiple range test, $p<0.05$), asterisk indicated a significant difference in the percentage of this stomatal type compared with WT (Student's t-test, $*p<0.05$).

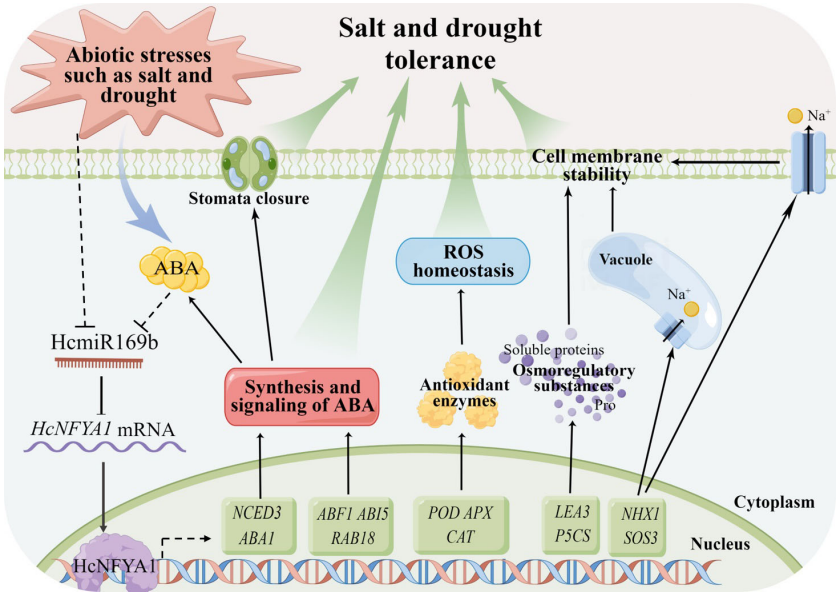


FIGURE 8
Halostachys caspica miR169b/NFYA1 module participates in the regulation network of plant tolerance to salt and drought stresses.

end. In our study, overexpression of HcmiR169b in *Arabidopsis* also reduced the expression of *AtNFYA5* and *AtNFYA1*, as shown in Figure 3B, C. Based on these results, we demonstrated that HcmiR169b conferred *Arabidopsis* sensitivity to salt and drought stress at both the germination and adult stages (Supplementary Figure S5A-C, Figure 3, 4).

As shown in the Supplementary Table S2, nine NFYA family members have been reported to contribute to plant resistance to salt and drought stress in *Arabidopsis*, soybean, poplar, maize, and rice. (Lee et al., 2015; Lian et al., 2018; Ma et al., 2020a; Ma et al., 2020b). However, the reported members are evolutionarily distant from HcNFYA1 except for AtNFYA1 (Supplementary Figure S3). AtNFYA1 inhibits the seed germination of *Arabidopsis* under salt stress by enhancing ABA signaling (Li et al., 2013); this ABA-mediated arrest of seed germination provides plants with an adaptive mechanism to improve survivals under stress conditions (Zhu, 2016). HcNFYA1 also enhanced ABA signaling (Figure 7) and stalled the seed germination of *Arabidopsis* under salt and drought stress (Supplementary Figure S5D-F). Nevertheless, once the plants reached adulthood, 35S:*HcNFYA1 Arabidopsis* exhibited greater tolerance to salt and drought than the WT and 35S:*HcmiR169b Arabidopsis* (Figure 3, 4).

In recent years, the miR169/NFYA module has received more attention, and its functions have been reported to respond to drought stress in oilseed rape and poplar, and to salinity stress in maize (Li et al., 2021; Jiao et al., 2021; Xing et al., 2021). In this study, we utilized the *Arabidopsis* stable transformation platform and molecular methods to elucidate the action mechanism of the *Halostachys caspica* miR169b/NFYA1 module to confer plant salt tolerance and drought resistance by multiple pathways, including (i) Synthesis and signaling transduction of ABA. Dry conditions and high salinity can cause plants to experience osmotic stress, and ABA is the most significant hormone accumulated in plant response to osmotic stress. To respond to osmotic stress, ABA induced leaf stomatal closure and other responses (Farooq et al., 2009). As shown in Figure 4C and Figure 6F, G, HcNFYA1 increased ABA content in transgenic *Arabidopsis* under salt and drought stress by activating the expression of *NCED3* and *ABA1*, the key genes for ABA synthesis (José et al., 2005; Ren et al., 2007). 35S:*HcNFYA1 Arabidopsis* increased sensitivity to ABA in comparison with the WT (Figure 7), because HcNFYA1 promoted the expression of *ABF1*, *ABI5*, and *RAB18* genes (Figure 6H-J), which are positively regulated by ABA signaling (Choi et al., 2000; Sonia et al., 2016). (ii) ROS homeostasis. ROS can be accumulated excessively under salt and drought stress, and plants have evolved antioxidant systems to scavenge reactive oxygen species and thus maintain ROS homeostasis (Apel and Hirt, 2004). For example, ZmmiR169q/NFYA8 conferred salt tolerance in maize by maintaining ROS homeostasis (Xing et al., 2021). 35S:*HcNFYA1 Arabidopsis* has higher antioxidant enzyme activities and more expressions of corresponding enzyme genes than those of WT and 35S:*HcmiR169b Arabidopsis* subjected to salt and drought stress (Figure 5I-K, M-O), resulting in less accumulation of reactive oxygen species than the WT (Figure 5B, C, F, G). This suggested that HcNFYA1 confers salt and drought tolerance by maintaining ROS

homeostasis. (iii) Cell membrane stability. When plants are exposed to salt and drought stress, the water potential within the cell becomes out of balance, causing cell membrane rupture (Farooq et al., 2009). In salt stress, HcNFYA1 regulated Na^+ transport by increasing the expression of genes such as *NHX1* and *SOS3* (Figure 6C, D), thus improving the stability of the membrane system (Shi et al., 2002; Barragán et al., 2012). HcNFYA1 also activated the expression of *LEA3* and *P5CS* to enhance the accumulation of soluble proteins and osmolytes in plants (Figure 3H, Figure 5H, L, Figure 6B), thus enhancing the osmotic adjustment ability and increasing the salt and drought resistance (Székely et al., 2008; Duan et al., 2012).

All together, our research indicates that under salt and drought stress, the expression of HcmiR169b and *HcNFYA1* in *Halostachys caspica* has a significantly negative relationship, HcmiR169b was repressed and *HcNFYA1* was increased. Transcription factor HcNFYA1 confers plant tolerance to salt and drought stresses through multiple pathways (Figure 8). These results enrich our understanding of the environmental adaptation mechanisms for the dominant plant *H. caspica* in extremely arid and saline environments and have crucial theoretical significance. However, application of the HcmiR169b/HcNFYA1 module to the molecular breeding of crops still requires a deeper understanding of their roles in plant growth and development.

Data availability statement

The original contributions presented in the study are included in the article/Supplementary Material. Further inquiries can be directed to the corresponding author.

Author contributions

JJ and YZ designed the experiments, analyzed the data, and wrote the manuscript. JJ, SZ, FC, XH, and QL performed the experiments. All authors contributed to the article and approved the submitted version.

Funding

This work was supported by the National Natural Science Foundation of China (No. 31760071), and the Graduate Science Research Innovation Project of Xinjiang Uygur Autonomous Region (No. XJ2021G085).

Acknowledgments

We greatly appreciate Dr. Chengxia La for providing us with qRT-PCR instrument and other experimental platforms in Institute of Economic Crops, Xinjiang Academy of Agricultural Sciences in helping us to promote work smoothly.

Conflict of interest

The authors declare that the research was conducted in the absence of any commercial or financial relationships that could be construed as a potential conflict of interest.

Publisher's note

All claims expressed in this article are solely those of the authors and do not necessarily represent those of their affiliated organizations, or those of the publisher, the editors and the reviewers. Any product that may be evaluated in this article, or claim that may be made by its manufacturer, is not guaranteed or endorsed by the publisher.

Supplementary material

The Supplementary Material for this article can be found online at: https://www.frontiersin.org/articles/10.3389/fpls.2022.1026421/full#supplementary-material

References

Apel, K., and Hirt, H. (2004). REACTIVE OXYGEN SPECIES: metabolism, oxidative stress, and signal transduction. *Annu. Rev. Plant Biol.* 55, 373–399. doi: 10.1146/annurev.arplant.55.031903.141701

Bailey-Serres, J., Parker, J. E., Ainsworth, E. A., Oldroyd, G. E. D., and Schroeder, J. I. (2019). Genetic strategies for improving crop yields. *Nature* 575, 109–118. doi: 10.1038/s41586-019-1679-0

Barragán, V., Leidi, E. O., Andrés, Z., Rubio, A., Luca, A. D., Fernández, J. A., et al. (2012). Ion exchangers NHX1 and NHX2 mediate active potassium uptake into vacuoles to regulate cell turgor and stomatal function in *Arabidopsis*. *Plant Cell* 24, 1127–1142. doi: 10.1105/tpc.111.095273

Bartel, D. P. (2009). MicroRNAs: Target recognition and regulatory functions. *Cell* 136, 215–233. doi: 10.1016/j.cell.2009.01.002

Chaves-Sanjuan, A., Gnesutta, N., Gobbini, A., Martignago, D., Bernardini, A., Fornara, F., et al. (2021). Structural determinants for NF-y subunit organization and NF-Y/DNA association in plants. *Plant J.* 105, 49–61. doi: 10.1111/tpj.15038

Chen, C., Ridzon, D. A., Broomer, A. J., Zhou, Z., Lee, D. H., Nguyen, J. T., et al. (2005). Real-time quantification of microRNAs by stem-loop RT-PCR. *Nucleic Acids Res.* 33, e179. doi: 10.1093/nar/gni178

Choi, H. I., Hong, J. H. E., Ha, J. O., Kang, J., and Kim, S. Y. (2000). ABFs, a family of ABA-responsive element binding factors. *J. Biol. Chem.* 275, 1723–1730. doi: 10.1074/jbc.275.3.1723

Duan, J., Cai, W., and Sunghun, P. (2012). *OsLEA3-2*, an abiotic stress induced gene of rice plays a key role in salt and drought tolerance. *PloS One* 7, e45117. doi: 10.1371/journal.pone.0045117

Farooq, M., Wahid, A., Kobayashi, N., Fujita, D., and Basra, S. M. A. (2009). Plant drought stress: effects, mechanisms and management. *Agron. Sus Dev.* 29, 185–212. doi: 10.1051/agro:2008021

Gong, Z. Z., Xiong, L. M., Shi, H. Z., Yang, S. H., Herrera-Estrella, L. R., Xu, G. H., et al. (2020). Plant abiotic stress response and nutrient use efficiency. *Sci. China Life Sci.* 63, 635–674. doi: 10.1007/s11427-020-1683-x

Gupta, A., Rico-Medina, A., and Caño-Delgado, A. I. (2020). The physiology of plant responses to drought. *Science* 368, 266–269. doi: 10.1126/science.aaz7614

Hsu, P. K., Dubeaux, G., Takahashi, Y., and Schroeder, J. I. (2021). Signaling mechanisms in abscisic acid-mediated stomatal closure. *Plant J.* 105, 307–321. doi: 10.1111/tpj.15067

Jiao, Z. Y., Lian, C.L., Han, S., Huang, M. B., Shen, C., Li, Q., et al. (2021). PtmiR169o plays a positive role in regulating drought tolerance and growth by targeting the *PtNF-YA6* gene in poplar. *Environ. Exp. Bot.* 189, 104549. doi: 10.1016/j.envexpbot.2021.104549

Jin, J. P., Tian, F., Yang, D. C., Meng, Y. Q., Kong, L., Luo, J. C., et al. (2017). PlantTFDB 4.0: toward a central hub for transcription factors and regulatory interactions in plants. *Nucleic Acids Res.* 45, 1040–1045. doi: 10.1093/nar/gkw982

José, M. B., Pedro, P., Miguel, G. G., Ramón, S., Pedro, L. R., María, R. P., et al. (2005). A mutational analysis of the *ABA1* gene of *Arabidopsis thaliana* highlights the involvement of ABA in vegetative development. *J. Ex Bot.* 56, 2071–2083. doi: 10.1093/jxb/eri206

Kuromori, T., Fujita, M., Takahashi, F., Yamaguchi-Shinozaki, K., and Shinozaki, K. (2022). Inter-tissue and inter-organ signaling in drought stress response and phenotyping of drought tolerance. *Plant J.* 109, 342–358. doi: 10.1111/tpj.15619

Laloum, T., De, M. S., Gamas, P., Baudin, M., and Niebel, A. (2013). CCAAT-box binding transcription factors in plants: Y so many? *Trends Plant Sci.* 18, 157–166. doi: 10.1016/j.tplants.2012.07.004

Lee, D. K., Kim, H. I., Jang, G., Chung, P. J., Jeong, J. S., Kim, Y. S., et al. (2015). The NF-YA transcription factor OsNF-YA7 confers drought stress tolerance of rice in an abscisic acid independent manner. *Plant Sci.* 241, 199–210. doi: 10.1016/j.plantsci.2015.10.006

Lian, C. L., Li, Q., Yao, K., Zhang, Y., Mrng, S., Yin, W. L., et al. (2018). *Populus trichocarpa* PtNF-YA9, a multifunctional transcription factor, regulates seed germination, abiotic stress, plant growth and development in *Arabidopsis*. *Front. Plant Sci.* 9, 954. doi: 10.3389/fpls.2018.00954

Li, J., Duan, Y. J., Sun, N. L., Wang, L., Feng, S. S., Fang, Y. J., et al. (2021). The miR169n-NF-YA8 regulation module involved in drought resistance in *Brassica napus* L. *Plant Sci.* 313, 111062. doi: 10.1016/j.plantsci.2021.111062

Li, Y. J., Fang, Y., Fu, Y. R., Huang, J. G., Wu, C. A., and Zhang, C. C. (2013). NFYA1 is involved in regulation of post germination growth arrest under salt stress in *Arabidopsis*. *PloS One* 8, e61289. doi: 10.1371/journal.pone.0061289

Li, W. X., Oono, Y., Zhu, J. H., He, X. J., Wu, J. M., Iida, K., et al. (2008). The *Arabidopsis* NFYA5 transcription factor is regulated transcriptionally and posttranscriptionally to promote drought resistance. *Plant Cell* 20, 2238–2251. doi: 10.1105/tpc.108.059444

Liu, L., Zhang, F. C., and Zeng, Y. L. (2009). Subcellular localization of Na^+/H^+ antiporter and H^+-PPase of *Kalidium foliatum*. *Act Bot. Boreal-Occident Sin.* 29, 463–468. doi: 1000-4025(2009)03-0463-06

Livak, J. Y., and Schmittgen, T. D. (2001). Analysis of relative gene expression data using real-time quantitative PCR and the $2^{-\Delta\Delta CT}$ method. *Methods* 25, 402–408. doi: 10.1006/meth.2001.1262

Luan, M. D., Xu, M. Y., Lu, Y. M., Zhang, Q. X., Zhang, L., Zhang, C. Y., et al. (2014). Family-wide survey of miR169s and *NF-YAs* and their expression profiles response to abiotic stress in maize roots. *PloS One* 9, e91369. doi: 10.1371/journal.pone.0091369

Ma, X. J., Fu, J. D., Tang, Y. M., Yu, T. F., Yin, Z. G., Chen, J., et al. (2020a). *GmNFYA13* improves salt and drought tolerance in transgenic soybean plants. *Front. Plant Sci.* 11, 587244. doi: 10.3389/fpls.2020.587244

Ma, X. J., Yu, T. F., Li, X. H., Cao, X. Y., Ma, J., Chen, J., et al. (2020b). Overexpression of *GmNFYA5* confers drought tolerance to transgenic *Arabidopsis* and soybean plants. *BMC Plant Biol.* 20, 123. doi: 10.1186/s12870-020-02337-z

Miller, G., Suzuki, N., Ciftci-Yilmaz, S., and Mittler, R. (2010). Reactive oxygen species homeostasis and signalling during drought and salinity stresses. *Plant Cell Environ.* 33, 453–467. doi: 10.1111/j.1365-3040.2009.02041.x

Nadarajah, K. K. (2020). ROS homeostasis in abiotic stress tolerance in plants. *Int. J. Mol. Sci.* 21, 5208. doi: 10.3390/ijms21155208

Ni, Z. Y., Hu, Z., Jiang, Q. Y., and Zhang, M. N. (2013). *GmNFYA3*, a target gene of miR169, is a positive regulator of plant tolerance to drought stress. *Plant Mol. Biol.* 82, 113–129. doi: 10.1007/s11103-013-0040-5

Pagano, L., Rossi, R., Paesano, L., and Marmiroli, M. (2021). miRNA regulation and stress adaptation in plants. *Environ. Exp. Bot.* 184, 104369. doi: 10.1016/j.envexpbot.2020.104369

Ren, H. B., Fan, J. Y., and Gao, Z. H. (2007). Roles of a sustained activation of *NCED3* and the synergistic regulation of ABA biosynthesis and catabolism in ABA signal production in *Arabidopsis*. *Chin. Sci. Bull.* 52, 484–491. doi: 10.1007/s11434-007-0072-9

Rhoades, M. W., Reinhart, B. J., Lim, L. P., Burge, C. B., Bartel, B., and Bartel, D. P. (2002). Prediction of plant microRNA targets. *Cell* 110, 513–520. doi: 10.1016/S0092-8674(02)00863-2

Sah, S. K., Reddy, K. R., and Li, J. X. (2016). Abscisic acid and abiotic stress tolerance in crop plants. *Front. Plant Sci.* 7, 571. doi: 10.3389/fpls.2016.00571

Samad, A. F.A., Sajad, M., Nazaruddin, N., Fauzi, I. A., Murad, A. M.A., Zainal, Z., et al. (2017). MicroRNA and transcription factor: key players in plant regulatory network. *Front. Plant Sci.* 8, 565. doi: 10.3389/fpls.2017.00565

Shi, H. Z., Quintero, F. J., Pardo, J. M., and Zhu, J. K. (2002). The putative plasma membrane Na^+/H^+ antiporter SOS1 controls long-distance na^+ transport in plants. *Plant Cell* 14, 465–477. doi: 10.1105/tpc.010371

Song, X. W., Li, Y., and Cao, X. F. (2019). MiRNAs and their regulatory roles in plant-environment interactions. *Annu. Rev. Plant Biol.* 70, 489–525. doi: 10.1146/annurev-arplant-050718-100334

Sonia, B., Sourabh, S., Anagh, R., and Ronita, N. C. (2016). ABI3 mediates dehydration stress recovery response in *Arabidopsis thaliana* by regulating expression of downstream genes. *Plant Sci.* 250, 125–140. doi: 10.1016/j.plantsci.2016.06.006

Székely, G., Abrahám, E., Cséplo, A., Rigó, G., Zsigmond, L., Csiszár, J., et al. (2008). Duplicated *P5CS* genes of *Arabidopsis* play distinct roles in stress regulation and developmental control of proline biosynthesis. *Plant J.* 53, 11–28. doi: 10.1111/j.1365-313X.2007.03318.x

Waadt, R., Seller, C. A., Hsu, P. K., Takahashi, Y., Munemasa, S., and Schroeder, J. I. (2022). Plant hormone regulation of abiotic stress responses. *Nat. Rev. Mol. Cell Biol.* 23, 680-694. doi: 10.1038/s41580-022-00479-6

Wang, C., and Fang, J. G. (2015). RLM-RACE, PPM-RACE, and qRT-PCR: an integrated strategy to accurately validate miRNA target genes. *Methods Mol. Biol.* 1296, 175–186. doi: 10.1007/978-1-4939-2547-6_16

Wang, J., Zhou, Z. S., Tao, Q., Chen, X. P., Shui, C., Ren, X. Y., et al. (2022). *Brassica napus* miR169 regulates *BnaNF-YA* in salinity, drought and ABA responses. *Enciron. Exp. Bot.* 199, 104882. doi: 10.1016/j.envexpbot.2022.104882

Wu, H. J., Ma, Y. K., Chen, T., Wang, M., and Wang, X. J. (2012). PsRobot: a web-based plant small RNA meta-analysis toolbox. *Nucleic Acids Res.* 40, W22–W28. doi: 10.1093/nar/gks554

Xing, L. J., Zhu, M., Luan, M. D., Zhang, M., Jin, L., Liu, Y. P., et al. (2021). miR169q and NUCLEAR FACTOR YA8 enhance salt tolerance by activating PEROXIDASE1 expression in response to ROS. *Plant Physiol.* 188, 608–623. doi: 10.1093/plphys/kiab498

Xu, M. Y., Zhang, L., Li, W. W., Hu, X. L., Wang, M. B., Fan, Y. L., et al. (2014). Stress-induced early flowering is mediated by miR169 in *Arabidopsis thaliana*. *J. Exp. Bot.* 65, 89–101. doi: 10.1093/jxb/ert353

Yang, R. R., Zeng, Y. L., Yi, X. Y., Zhao, L. J., and Zhang, Y. F. (2015). Small RNA deep sequencing reveals the important role of microRNAs in the halophyte *Halostachys caspica*. *Plant Biotechnol. J.* 13, 395–408. doi: 10.1111/pbi.12337

Yin, F. L., Zeng, Y. L., Ji, J. Y., Wang, P. J., Zhang, Y. F., and Li, W. H. (2021). The halophyte *Halostachys caspica* AP2/ERF transcription factor HcTOE3 positively regulates freezing tolerance in *Arabidopsis*. *Front. Plant Sci.* 12, 638788. doi: 10.3389/fpls.2021.638788

Yu, Y., Jia, T. R., and Chen, X. M. (2017). The "how' and "where' of plant microRNAs. *New Phytol.* 216, 1002–1017. doi: 10.1111/nph.14834

Yu, T. F., Liu, Y., Fu, J. D., Ma, J., Fang, Z. W., Chen, J., et al. (2021). The NF-Y-PYR module integrates the abscisic acid signal pathway to regulate plant stress tolerance. *Plant Biotechnol. J.* 19, 2589–2605. doi: 10.1111/pbi.13684

Yu, Y. H., Ni, Z. Y., Wang, Y., Wan, H. N., Hu, Z., Jiang, Q. Y., et al. (2019). Overexpression of soybean miR169c confers increased drought stress sensitivity in transgenic *Arabidopsis thaliana*. *Plant Sci.* 285, 68–78. doi: 10.1016/j.plantsci.2019.05.003

Zanetti, M. E., Rípodas, C., and Niebel, A. (2017). Plant NF-y transcription factors: Key players in plant-microbe interactions, root development and adaptation to stress. *Biochim. Biophys. Acta Gene Regul. Mech.* 1860, 645–654. doi: 10.1016/j.bbagrm.2016.11.007

Zelm, E. V., Zhang, Y. X., and Testerink, C. (2020). Salt tolerance mechanisms of plants. *Annu. Rev. Plant Biol.* 71, 403–433. doi: 10.1146/annurev-arplant-050718-100005

Zhang, X. R., Henriques, R., Lin, S. S., Niu, Q. W., and Chua, N. H. (2006). *Agrobacterium*-mediated transformation of *Arabidopsis thaliana* using the floral dip method. *Nat. Protoc.* 1, 641–646. doi: 10.1038/nprot.2006.97

Zhang, S. W., Zeng, Y. L., Yi, X. Y., and Zhang, Y. F. (2015). Selection of suitable reference genes for quantitative RT-PCR normalization in the halophyte *Halostachys caspica* under salt and drought stress. *Sci. Rep.* 6, 30363. doi: 10.1038/srep30363

Zhang, H. M., Zhao, Y., and Zhu, J. K. (2020). Thriving under stress: how plants balance growth and the stress response. *Cell* 55, 529–543. doi: 10.1016/j.devcel.2020.10.012

Zhang, H. M., Zhu, J. H., Gong, Z. Z., and Zhu, J. K. (2022). Abiotic stress responses in plants. *Nat. Rev. Genet.* 23, 104–119. doi: 10.1038/s41576-021-00413-0

Zhang, X. H., Zou, Z., Gong, P. J., Zhang, J. H., Ziaf, K., Li, H. X., et al. (2011). Over-expression of microRNA169 confers enhanced drought tolerance to tomato. *Biotechnol. Lett.* 33, 403–409. doi: 10.1007/s10529-010-0436-0

Zhao, H., Lin, K., Ma, L., Chen, Q. S., Gan, S., and Li, G. (2020). *Arabidopsis* NUCLEAR FACTOR y A8 inhibits the juvenile-to-adult transition by activating transcription of MIR156s. *J. Exp. Bot.* 71, 4890–4902. doi: 10.1093/jxb/eraa197

Zhu, J. K. (2016). Abiotic stress signaling and responses in plants. *Cell* 167, 313–324. doi: 10.1016/j.cell.2016.08.029

frontiers | Frontiers in Plant Science

TYPE Original Research
PUBLISHED 12 January 2023
DOI 10.3389/fpls.2022.1068649

Check for updates

OPEN ACCESS

EDITED BY
Muhammad Waseem,
Hainan University, China

REVIEWED BY
Akbar Hossain,
Bangladesh Wheat and Maize Research Institute, Bangladesh
Xiangnan Li,
Northeast Institute of Geography and Agroecology (CAS), China

*CORRESPONDENCE
Mohammad Javad Zarea
mj.zarea@ilam.ac.ir

SPECIALTY SECTION
This article was submitted to Plant Abiotic Stress, a section of the journal Frontiers in Plant Science

RECEIVED 13 October 2022
ACCEPTED 20 December 2022
PUBLISHED 12 January 2023

CITATION
Zarea MJ and Karimi N (2023) Grain yield and quality of wheat are improved through post-flowering foliar application of zinc and 6-benzylaminopurine under water deficit condition.
Front. Plant Sci. 13:1068649.
doi: 10.3389/fpls.2022.1068649

COPYRIGHT
© 2023 Zarea and Karimi. This is an open-access article distributed under the terms of the Creative Commons Attribution License (CC BY). The use, distribution or reproduction in other forums is permitted, provided the original author(s) and the copyright owner(s) are credited and that the original publication in this journal is cited, in accordance with accepted academic practice. No use, distribution or reproduction is permitted which does not comply with these terms.

Grain yield and quality of wheat are improved through post-flowering foliar application of zinc and 6- benzylaminopurine under water deficit condition

Mohammad Javad Zarea* and Nasrin Karimi

Department of Agronomy and Crop Breeding, Faculty of Agriculture, Ilam University, Ilam, Iran

Introduction: Zinc (Zn) as an essential micronutrient and cytokinin as phytohormone not only regulate plant growth but also play fundamental roles in plant tolerance against drought stress. Understating the function and the role of cytokinin in combined with an essential micronutrient, Zn, could improve the choice of a sustainable strategy for improvement of plant drought stress. The objective of this field research was to determine the effect of post-flowering foliar application of ZnSO4 and 6-benzylaminopurine (6-BAP) on grain yield and quality of winter wheat under water deficit condition.

Methods: Experiments were conducted under filed condition. Drought was imposed by with holding irrigation at the beginning of flowering till the signs of temporary wilting/leaf rolling appeared, after which all plots were irrigated to field capacity. The foliar treatment consisted of (1) foliar application of water, as control treatment; (2) foliar application of 10 g ha-1 6-BAP; (3) Foliar application of 20 g ha-1 6-BAP; (4) Foliar application of 10 g ha-1 6-BAP plus foliar application of 6 kg ha-1 ZnSO4 solution and (5) foliar application of 10 g ha-1 6-BAP plus foliar application of 6 kg ha-1 ZnSO4 solution 2 days before drought imposition. Data were collected on grain and straw yield, yield attributes, harvest index, flag leaf fresh matter and dry matter weight, TaCKX6-D1 expression, phytic acid content in grains, mycorrhiza colonization rate and succinate dehydrogenase (SD) activity.

Results: According to ANOVA, the factor 'Zn' significantly affected leaf relative water content ($p < 0.001$). Relative water content for plants foliar applied with 6-BAP was not statistically significant. Applying Zn increased yield, straw dry weight, and kernel weight relative to plants sprayed with water alone. Increased grain yield due to foliar application of Zn was associated with decrease in cytokinin oxidase/dehydrogenase (TaCKX) and increase in kernel weight. Results showed that the drought stress significantly decreased 1000-grain weight that was accompanied with over-expression of cytokinin oxidase/dehydrogenase (TaCKX). Foliar application of Zn increased the concentration of Zn in grains. The experimental data on the zinc content of grain indicated no significant difference between the 6-BAP at 10 mg L-1 and control treatment.

The phytate to Zn molar ratio was significantly affected by foliar applied Zn, but not significantly by applied 6-BAP. In the present study, SD activity of the hyphae of indigenous arbuscular mycorrhizal fungi (IAMF) associated with plant roots was also assayed. Results disclose that SD activity of IAMF was significantly affected by Zn treatments during grain filling stages.

Discussion: In summary, both foliar applied Zn and 6-BAP had the significant effects on all measured parameters in winter wheat. However, spike number, harvest index and mycorrhizal colonization rate were neither significantly affected by Zn nor 6- BAP. Foliar application of Zn at 0.6% (6 kg ha-1) and higher 6-BAP (20 mg L-1 m-2) promoted wheat growth and performances under imposed drought stress condition. Plant that only foliar sprayed with water showed higher level of TaCKX6-D1 expression as compared to Zn treated plants, indicating these plants were more affected by imposed drought relative to those plants treated with Zn. The results of this study provides evidence that a combination of Zn and 6-BAP could be an effective in improvement of drought tolerance of wheat and prevents grain yield from further reduction in terms of quality and quantity due to drought stress.

KEYWORDS

drought stress, Zn, cytokinin, TaCKX, yield, wheat, phytic acid

1 Introduction

Although the earth's climate has never been stable for thousands of years, but current global warming is unique in its speed and in its magnitude. During the last several decades, arid and semi-arid areas have experienced and extended drought. Farmers have been forced to rely on ground water, steadily drawing down the level of the water in the underlying aquifer. In Iran one-third of its wheat fields are irrigated and the rest are rain-fed, making most production reliant on rainfall. In semi-arid areas, most drought events are occurring during the winter wheat reproductive growth stage. Yu et al. (2018) studied the impact of droughts on winter wheat yield in eastern China. They concluded that drought during the flowering and filling stages had a significant negative effect on winter wheat yield. Drought occurring during anthesis has been reported to significantly decline the number of grains up to 50% (Saini and Westgate, 2000). According to Adil et al. (2022), the ZnO nanoparticles applied at the time of sowing had a positive effect on wheat yield under salt stress.

Remobilization of assimilates stored pre-anthesis and current assimilation determine grain formation and development in cereals such as wheat (Kobata et al., 1992; Inoue et al., 2004). Drought stress after anthesis (during grain filling) negatively restricts photosynthesis, leading to decline in contribution of current assimilates to the grain. Under drought conditions, there is a rapid decline in photosynthesis, limiting the contribution of current assimilates to the grain. However, drought occurring during grain filling increases the contribution of stem reserves stored pre-anthesis to grain (Yang et al., 2000). Under suitable conditions, contribution of stem reserves and assimilates derived from current photosynthates in final grain yield is 10% and 70 to 90%, respectively (Yang et al., 2000; Inoue et al., 2004). It must be noted that the photosynthates of flag leaf have an important role in grain filling, estimated 60% of the grain saccharides obtained from photosynthates in the flag leaf (Lei et al., 2022) that can be restricted by drought occurring during grain filling.

Zn is an essential micro-element with various roles in plant physiology, biochemical processes, activity of numerous enzymes, growth and development have been extensively studied (Cakmak, 2008; Cakmak et al., 2010; Rehman and Farooq, 2016; Rehman et al., 2018; Cakmak and Kutman, 2018; Karimi et al., 2021; Kaur and Garg, 2021; Liao et al., 2022; Sadeghizadeh and Zarea, 2022). Recently, the role of Zn in plant defense against herbivores and pathogens also reviewed by Cabot et al. (2019). However, the role and mechanisms by which Zn confers drought tolerance in plants has received less attention. The use of foliar application of mineral Zn has been shown to improve drought resistance in several crops. In a previous study, Ashkiani et al. (2020) pointed out the advantages of foliar application of zinc sulfate on seed oil yield of rapeseed under drought stress conditions. Rahmani et al. (2019) claimed that foliar application of Zn (1.2 kg ha^{-1}) significantly reduced

the adverse effect of drought on safflower. These authors attributed improved drought tolerance to higher accumulation of carbohydrate and proline. Yavas and Unay (2016) also showed a crucial role of Zn in resistance of wheat to drought stress. A similar observation was made by Pavia et al. (2019), who noted that application of $ZnSO_4$ heptahydrate solution through priming (0.4% Zn for 8 h) and foliar application (0.1% Zn) could enhanced photoprotection mechanisms in drought-stressed wheat. Sun et al. (2021) reported that the application of nano-ZnO (100 mg L^{-1}) mitigated the adverse effect of imposed drought stress in maize. Maize plants applied with nano-ZnO showed betterbetter stomatal movement, higher net photosynthetic rate and enhanced water use efficiency. Sun et al. (2020) reported that application of nano-ZnO (100 mg L^{-1}) activated the antioxidant enzyme system, resulting in increased tolerance to drought stress in in maize. This Similar with the observations of Wang et al. (2020) who found that nano-ZnO-primed wheat seed possessed more effective oxygen scavenging system. Ma et al. (2017) reported that zinc *via* increasing the transcription and activity of reactive oxygen species scavenging enzymes increased the concentration of antioxidant active substances. Improved antioxidant defense mechanisms due to foliar application of zinc at terminal growth have been also reported by Sattar et al. (2022) in drought induced wheat. In addition, it was reported that the foliar application of zinc increased grain yield and quality of wheat under drought stress condition (Sultana et al., 2018).

Actual big problem that is occurring in some countries is micronutrient deficiency. Zinc is involved in so many biochemical reactions in the body; it is a cofactor for numerous enzymes. Phytic acid is a chemical compound naturally found in grains such as cereal grains. That phytic acid serves as the main storage of phosphorus in the seeds. Phytic acid binds the zinc and it is going to create zinc deficiency. In a set of 330 breeding lines of wheat, Wen et al. (2022) reported that phytic acid ranged from 0.90 to 1.72% with a mean of 1.24%.

Cytokinins are plant hormones that have vital roles in various plant functions like root-shoot interactions, nucleic acid metabolism and cell division (Yang et al., 2016). Role of cytokinins in plants is important, particularly under stress (Hare et al., 1997). Recent research has focused on the effect of cytokinins in environmental stressesd improvement. Yang et al. (2016) reported that exogenous cytokinins improved winter wheat yield under heat stress. Liu and Huang (2002) found that heat stress tolerance was improved in creeping bent grass due to cytokinin application. This improvement was reported to be associated with an increase in antioxidant activities and decline in lipid peroxidation. Xu et al. (2011) claimed that treatment of broccoli florets with 6-benzylaminopurine inhibited chlorophyll degradation by decreasing in chlorophyllase levels. Cytokinin content in the grains was found by Yang et al. (2000) to be involved in grain filling percentage from early grain-filling stage till middle grain filling stage. According to Yang et al. (2003), cytokinins could affect the sink size of the grain in rice by mediating cell division in the endosperm. Endogenous cytokinins levels can be regulated by the enzyme so called cytokinin oxidase/dehydrogenase, CKO/CKX. Some studies claimed CKX genes that negatively regulated the levels of cytokinins have been reported to lead to improved crop yield and abiotic stresses tolerances (Arora and Sen, 2022). However, there is some evidences that indicate up regulation of this gene has also caused increased yield in rice.

The changing in cellular gene expression profiles is the major physiological response of plant to the environment stresses (Charfeddine et al., 2015). Cytokinin oxidase/dehydrogenase (CKX) by catalyzing the oxidation of side chain cleavage causes the degradation of cytokinins. This degradation is an irreversible reaction and results in inactivation of hormones. Thus cytokinin level in tissue is regulated by CKX activity. CKX through mediation in cytokinin concentration in tissue can control cytokinin-dependent processes (Schmülling et al., 2003). To date, CKX is found in various crops such as wheat, arabidopsis, maize, soybean and bean. Gao et al. (2019) reported that Zn content in rice seed was significantly affected by CKX expression. These authors reported that root-specific *Os*CKX4-overexpressing plants exhibited increased Zn nutrient and yield traits. Panda et al. (2018) attributed poor grain filling in rice to greater levels of *Os*CKX expression and lower cytokinin content. Li et al. (2018) reported a significant correlation between decreased *Ta*CKX2.2.1-3A expression and grain number. CKX-overexpressing has been shown to provoke drought and salinity tolerance (Werner et al., 2010; Nishiyama et al., 2011). There are several works indicated that cytokinin-deficient plants can better tolerate salt stress than wild type (Cortleven et al., 2019). The CKX genes have been reported to influence yield-related traits in wheat, barley and in rice (Szala et al., 2020).

Although the effectiveness of foliar application of Zn has been based on numerous studies, few studies have evaluated its effectiveness when combined with a plant growth promoting hormones like cytokinin. Therefore this study aimed to better understand how exposed winter wheat to drought stress response to foliar application of Zn in combination with 6-Benzylaminopurine (6-BAP). This current study investigated grain yield and yield components, cytokinin oxidase/dehydrogenase (TaCKX) gene expression, Zn concentration in grain, grain phytic acid: Zn molar ratios, mycorrhizal colonization rate and succinate dehydrogenase activity of mycorrhiza fungi responses in winter wheat to foliar application of Zn and 6-Benzylaminopurine (6-BAP) and their combination as well.

2 Materials and methods

2.1 Field experimental design

The experiment was conducted in 2021-2022 at a commercial wheat farm which is located in Dehgolan County, Kurdistan Province at 35˚17′N, 47 ° 22′E, West Iran. The experimental design was a 2 by 3 factorial combination of two levels of foliar spraying with Zn and 3 levels of foliar application of 6-benzylaminopurine (6-ABP) arranged in a randomized block design with three replicates. The levels of Zn factor were a single foliar spray of Zn as $ZnSO_4$ ×7 H_2O_2 at 0.5% concentration (v/v) and unsprayed control (0%). The second factor (6-PAB) consisted of three levels of foliar sprays of 6-BAP including 0 mg·L^{-1} as unsprayed control, 10 mg·L^{-1} and 20 mg·L^{-1}. Phosphorus from source of triple superphosphate and nitrogen as urea were spread evenly at the rate of 50 kg ha^{-1} and 100 kg N ha^{-1}, respectively, to the experimental field before sowing. Two levels of applied Zn, unsprayed control and foliar applied with 0.6% Zn, were designated as Zn0 and Zn0.6, respectively. The plot width was six 1.2-m rows by 6 m in length, attaining population rate of 130 plant m^{-2}. The previous crop was alfalfa. Winter wheat (*Triticum* aestivum, cv Pishgam, a bread-making variety) sowing was done in the fall. Winter wheat was grown in the fall (late-October). Wheat plants get established to the four- or five-leaf stage; they went into a dormancy period and then in mid-April started growing; get the stem elongation phase of rapid growth. Heading took place in early June. Harvest was done in mid-July. All plots received the same cultivation and agronomic management.

2.2 Drought imposition

Rainfall and supplemental water included water available for the crop. Monthly rainfall and average temperatures during the wheat growing season in this study is shown in Figure 1. Mean rainfall from grain filling to maturity was negligible. Rainfall from drought imposition (heading to maturity) totaled 0.1 mm. Total precipitation from planting to harvesting was 249.6 mm. Drought was imposed by withholding irrigation at the beginning of flowering for 27 days till the signs of temporary wilting/leaf rolling appeared, after which all plots were irrigated to field capacity. Rainfall and supplemental water included water available for the crop. Monthly rainfall and average temperatures during the wheat growing season in this study is shown in Figure 1.

2.3 Foliar application treatments

The treatment was as follows: (1) foliar application of water (1000 L ha^{-1}) as control treatment; (2) Foliar application of 10 g ha^{-1} 6-BAP at a rate of 1000 L ha^{-1} (10 mg L^{-1} m^{-2}); (3) Foliar application of 20 g ha^{-1} 6-BAP at a rate of 1000 L ha^{-1} (20 mg L^{-1} m^{-2}); (4) Foliar application of 10 g ha^{-1} 6-BAP plus foliar application of 6 kg ha^{-1} $ZnSO_4$ as a 0.6% (w/v) $ZnSO_4$ $7H_2O$ solution at a rate of 1000 L ha^{-1} and (5) foliar application of 10 g ha^{-1} 6-BAP plus foliar application of 6 kg ha^{-1} $ZnSO_4$ as a 0.6% (w/v) $ZnSO_4$ $7H_2O$ solution at a rate of 1000 L ha^{-1} 2 days before drought imposition at 7:00 P.M. Zn and 6-ABP were foliar applied using a hand sprayer with 2-L capacity. Plants were foliar sprayed one time. All solutions included Tween 20 at a final concentration of 0.2% (v/v) as a surfactant. Control plants were also foliar applied with water (1000 L ha^{-1}) plus 2 ml L^{-1} Tween 20. The application spray volume was 0.1 L^{-1} m^{-2}. To prepare 6-BAP stock solution, 100 mg of 6-BAP was dissolved in water using HCl (1%). 10 and 20 mg L-1 6-BAP were then prepared by diluting the prepared stock solution in water until the volume reaches 1 liter.

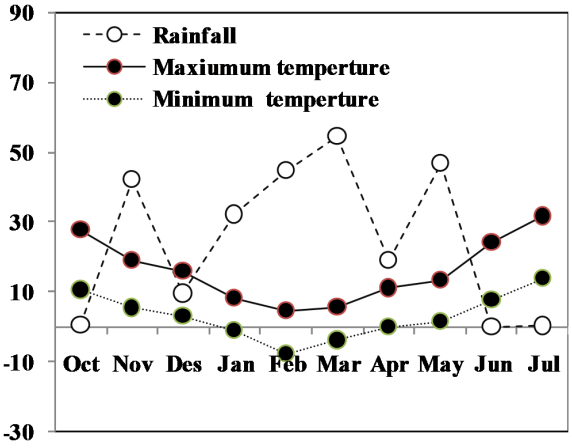


FIGURE 1
Monthly mean air maximum and minimum temperatures (°C) and rainfall (mm) totals during the whole growing season of winter.

2.4 Agronomic trait measurements

Data were collected on grain and straw yield, yield attributes (spike number $plant^{-1}$ and kernel number $spike^{-1}$ and 1000-kernel weight), harvest index, flag leaf fresh matter and dry matter weight, whole plant leaf fresh and dry weight and relative water content of flag leaf. To determine grain yield and straw yield, wheat was harvested at the end of spring (mid-July 2022) from a plot of 1 m^2, after avoiding borders on each side. At harvest, an area of 1 m^2 of each plot (a total 130 plants) was characterized for grain yield and above ground plant (straw yield). All samples were then dried until constant in weight. Grain yield was represented based on the adjusted moisture content of 120 g kg^{-1}. At wheat maturity, aboveground biomass (straw yield) was determined by hand harvesting at ground level from an area of 1 m^2. Spike number $plant^{-1}$ and kernel number

spike^{-1} were determined by counting the spikes and seeds on 3 plants and 3 spikes, respectively at harvest. To determine thousand-grain weight, 3 random spikes per plot were taken from 3 plants and hand shelled. Harvest index (HI) was calculated using the following equation:

$$HI\ (\%) = [grainweight]/[totaldryweightoftheabovegroundbiomass] \times 100 \quad (1)$$

Relative water content (RWC) as an important index of water status in plants was measured after drought imposition. RWC cogitate (reflects) the equilibrium (balance) between transpiration rate and water supply to the leaf tissue (Lugojan and Ciulca, 2011). Leaf relative water content was calculated according to the following formula:

$$Relativewatercontent\ (\%) = [freshweight - dryweight]/[turgidweight - dryweight] \times 100 \quad (2)$$

2.5 Zn and phytic acid content in grains

To determine the grain Zn concentration, Seed samples were first ground and then were digested in an acid (H_2O_2: HNO_3 at 3:10 v/v ratio). 0.2 g of dried grounded kernel samples was digested using concentrated acid HNO_3 and H_2O_2 mixture. Grain zinc concentration was then determined using a flame atomic absorption spectrophotometer. To measure phytic acid content in grain, the method reported by Liu et al. (2005) with some modification (Lu et al., 2020) was followed. Grain samples from each replicate were dried at 80°C for 48 h and were then grounded to fine powder. Phytic acid assay was conducted according to Liu et al. (2005) with modification. Grain sample (0.4 g) was placed into a 50 ml centrifuge tube and to it 10 ml 0.2 M HCl was added. Tubes were shaken for 2 h. Tubes were centrifuged at 12,000 rpm at room temperature for 10 min. The 2.5 ml of the aqueous phase (supernatant) was transferred into a new tube and to it 2 ml of 0.2% $FeCl_3$ solution was added. Samples were boiled in a bath for 30 min. After cooling, tubes were centrifuged again at 13,000 rpm for 15 min. Supernatant was discarded and the tube was washed twice with 5 ml distilled water. Afterwards, 3 ml of 1.5 M NaOH was added into the residue, vortexed for 2 min and then centrifuged at13,000 rpm for 10 min. Supernatant was discarded and 10 ml of 0.5 M HCl was added to dissolve the residue. Finally, deionized water was added to make the volume of 50 m. The indirect method previously described by Haug and Lantzsch (1983) was used to measure the phytate in the extract. Absorbance of the pink color that was developed by 2,20-bi-pyridine with un-reacted Fe^{3+} was recorded at 519 nm. The phytic acid to zinc molar ration was calculated according to the following formula:

$$PhytatetoZnmolarratio = [themoleofphytate\ (660.04\ gmol^{-1})]/[themolarofZn\ (65.4\ gmol^{-1}] \quad (3)$$

2.6 *Ta*CKX6-D1 expression

Expression level of *Ta*CKX6-D1 was determined in grain 7 days after anthesis. Total RNA were isolated from homogenized seed samples. The RNA was isolated using the RNX-Plus buffer. The manufacturer's instructions were followed for RNA isolation. Grains were first ground in liquid N and immediately transferred to a 2 ml tube, and to it 1 ml of ice cold RNX-Plus solution was immediately added. Shortly afterwards, tubes were vortexed for10 s and, then, were incubated at room temperature for 10 min in horizontal position. 200 µl of chloroform was added to the tubes and mixed thoroughly by shaking for 15s gently. Tubes were incubated on ice for 5 min. Tubes were then centrifuged at 12,000 rpm at 4°C for 15 min. The upper aqueous phase (supernatant) was transferred into a new RNase-free 1.5 ml tube and equal volume of Isopropanol was added and gently mixed. Tubes were incubated on ice for 15 min. Thereafter, tubes were centrifuged at 12,000 rpm at 4°C for 15 min. The supernatant was discarded and 1 ml of 75% Ethanol was added. Tubes were shortly vortexed to dislodge the pellet and then centrifuged at 4°C for 8 min at 7500 rpm. Supernatant was discarded and the pellet was dried at room temperature for a few minutes. Pellet was dissolved in 50µl of DEPC treated water. To help dissolve, tubes were placed in 55°C water bath for 10 min. The quality and quantity of total RNA were measured by using a NanoDrop. DNA contamination was eliminated by treating total RNA with DNase. cDNA was synthesized using a using Fermentas Nase Kit (Fermentas, Hanover, MD), according to the manufacturer's instructions and stored at -20°C. Semi-quantitative RT-PCR analysis was performance to evaluate the expression level of *Ta*CKX6-D1. The PCR amplification conditions for *Ta*CKX6 gene was as follows: 4 min at 95°C followed by 35 cycles of 30 s at 94°C, 10 s at 55°C and finally 45 s at 72°C, followed by 72°C for 7 min. To optimize the number of PCR cycles for semi-quantitative analysis, PCR products after 20, 25, 30 and 35 cycles were checked for visibility by running on 1.8% agarose gel. The 25 cycle was chosen and quantification was done in comparison to Tacyclophilin gene as reference genes. The primer pairs were designed using CKX6-D1 (Genbank accession: JQ797673). Designed primers were as follows: 5`ATCCATAAGCCTCTCACA ACAGT 3` as forward primer and 5`ACATCG GATCTAGCTTGTTCGT 3`as reverse primer, resulting product size of 170bp. The ΔΔCt method was used to calculate AQP gene expression (Pfaffl, 2001).

2.7 Mycorrhiza colonization rate and succinate dehydrogenase activity measurement

After 7 days of drought imposition, root samples were taken from 3 plants of each plot. Root samples were softened using 10% KOH solution. Root samples were boiled in KOH solutions for 15 min. Acidification of softened root samples were done with 1 M HCl solution. After Acidification roots were rinsed in distilled water. 0.02% Trypan blue was used to stain root samples. Root samples were simmering in this solution overnight. Excess stain was removed by 50% lactophenol for 2 h. To determine total root colonization rate, the grid line intersect method of McGonigle et al. (1990) was followed. Hyphae were observed through a grid placed in the microscope eyepiece. To assay succinate dehydrogenase activity (SDA), the method described by Hamel et al. (1990) and Kough et al. (1987) was followed to measure SDA. Roots were collected from three random chosen plants of each plot. Root samples were thoroughly washed with water on a fine sieve. Roots samples were then cut into 1 cm length and placed into 50 ml tub. 20 ml of prepared staining solution was added to the tube. Tubes were incubated at room temperature for 12 h. Staining solution contained 0.05 mM Tris buffer with pH of 7.4. Tris buffer contained Nitro Blue Tetrazolium salt (1 mg ml^{-1}), $MgCl_2$ (0.5 mM) and sodium succinate (0.25 M). After incubation, stained hyphae were rinsed with distilled water. Roots samples were prepared in polyvinyl alcohol (Hamel et al., 1990). Finally, evaluation of hyphal viability was detected under dark field microscopy.

2.8 Data analysis

Recorded data were analyzed (two-way ANOVA) with PROC procedure using SAS software package. When the *F*-test was significant the least significant differences test ($P = 0.05$) was used to determine differences among treatments.

3 Results

All plots received the same volume of applied water, cultivation and agronomic management. After that, all plants (all plots) underwent withholding irrigation at the beginning of flowering for 27 days till the signs of temporary wilting/leaf rolling appeared, after which all plots were irrigated to field capacity. The average grain yield of wheat under normal irrigation in selected farms near experimental site was 8.9 t ha^{-1}. In the current study average yield across foliar treatments was 4.83 t ha^{-1}.

3.1 Leaf fresh weight and dry weight

According to ANOVA, the factor 'Zn' significantly affected leaf relative water content ($p< 0.001$). Relative water content for plants foliar applied with 6-BAP was not statistically significant. Zn ×6-BAP had not significant effect on leaf relative water content (Table 1). After drought stress imposition, the rate of decreasing in relative water content of flag leaf was more in

TABLE 1 Effect of foliar applied Zn and 6-benzylaminopurine (6-BAP) on leaf relative water content, flag lea fresh weight and dry weight and total plant leaf fresh weight and dry weight.

Treatment	Relative water content	Flag leaf fresh wt.	Flag leaf dry wt.	Leaf fresh wt.	Leaf dry wt.
	%	g $leaf^{-1}$		g $plant^{-1}$	
Foliar Zn application (%)					
Zn0	65b	0.22b	0.11b	1.21b	0.60b
Zn0.6	72a	0.24a	0.13a	1.25a	0.65a
LSD (0.05)	2.53	0.013	0.012	0.032	0.062
Foliar 6-BAP (mg L^{-1})					
0	68a	0.23a	0.11a	1.22a	0.61a
10	68a	0.24a	0.11a	1.23a	0.62a
20	69a	0.24a	0.12a	1.24a	0.65a
LSD (0.05)	NS	NS	NS	NS	NS
Interaction					
Zn × 6-BAP	NS	NS	NS	NS	NS

NS no significant at 0.05 probability level. Means in a column followed by different lower case letters are significantly different at P < 0.05 according to Fisher's LSD test.

untreated plants than that of plants treated with Zn. Under post-anthesis drought stress, higher relative water content value (72%) was observed in Zn-foliar applied plants (Zn0.6) than those untreated plants (Zn0) (Table 1). Plants treated with Zn had a higher relative water content of 11.2% in relation to the untreated plants. The flag leaf fresh weight and dry weight were significantly affected by foliar applied Zn (Table 1). The flag leaf fresh weight and dry weight for plants foliar-applied with 6-BAP was not statistically significant. Zn × 6-BAP interaction was not significant for flag leaf fresh weight and dry weight. Plants foliar sprayed with Zn had higher flag leaf fresh weight (0.24 g leaf^{-1}) and flag leaf dry weight (0.13 g leaf^{-1}) than untreated plants. Results showed that foliar applied Zn resulted in higher flag leaf fresh weight (11.1%) and dry weight (16.7%) in comparison with unsprayed control. Leaf fresh weight and dry weight significantly affected by the factor 'Zn'. Foliar 6-BAP and Zn × 6-BAP interaction had no significant effect on the above mentioned traits. Leaf fresh weight (3%) and dry weight (7.9%) plant^{-1} were significantly higher for plants sprayed with Zn than that for unsprayed control plants (Table 1).

3.2 Yield, straw yield, harvest index and yield components

As shown in Table 2, the result of ANOVA indicated that the treatment Zn and 6-BAP and their interaction were significant for grain yield. Both foliar treatments (Zn and 6-BAP) had significant effect on yield (Table 3). As shown in Table 3, yield was 0.3 t ha^{-1} (6.58%) higher for Zn treatment (Zn0.6) than for the control (Zn0). Foliar spraying with Zn enhanced grain yield from 4.68 to 4.98 t ha^{-1} (Table 3). The grain yield obtained from 6-BAP (20 mg L^{-1}) foliar applied plants was higher than that in plants treated with 10 mg l^{-1} 6-BAP and unsprayed control plants (Table 3). Foliar applied 6-BAP at 20 mg l^{-1} increased yield up to 2.89 and 6% compared with 6-BAP at 10 mg l^{-1} and unsprayed control, respectively (Table 3). The yield response to foliar applied Zn plus 6-BAP was significantly positive (Figure 2A). Combination of Zn (0.6%) and 6-BAP at 20 mg l^{-1} resulted in highest grain yield (5.29 t ha^{-1}) (Figure 2A). According to ANOVA, the main effect of Zn on total dry matter yield (straw dry weight) was significant. The ANOVA for the data for the straw dry yield showed that the main effect of 6-bap and Zn

TABLE 2 Analysis of variance for the effect of foliar applied Zn and 6-benzylaminopurine (6-BAP) on grain yield.

Source	df	Means square	*F*-value	*P* > *F*
Zn	1	0.42782 **	18.65	0.0015
6-BAP	2	0.12277 *	5.35	0.0263
Zn × 6-BAP	2	0.14731 *	6.42	0.0161

*significant at 0.05 probability level.
**significant at 0.05 probability level.

TABLE 3 Main effect of foliar Zn and 6-Benzylaminopurine (6-BAP) on yield, straw dry weight, harvest index, and yield components of winter wheat.

Treatment	Grain yield	Straw dry wt.	Harvest index	Spike	Kernels	Kernels wt.
	T ha^{-1}		%	No. plant^{-1}	No spike^{-1}	Mg 1000-kernel^{-1}
Foliar Zn						
Zn0	4.68a	11.66b	40.27a	4.61a	21.13b	36.20b
Zn0.6	4.98b	11.96a	41.2a	4.51a	22.31a	36.89a
LSD (0.05)	0.15	0.28	NS	NS	0.59	0.26
Foliar 6-BAP (mg L^{-1})						
0	4.69b	11.72a	40.1a	4.56a	21.22b	36.34b
10	4.83ab	11.76a	40.59a	4.58a	21.66ab	36.51ab
20	4.97a	11.95a	41.61a	4.53a	22.29a	36.79a
LSD (0.05)	0.19	NS	NS	NS	0.72	0.32
Interaction						
Zn × 6-BAP	✳	NS	NS	NS	✳	✳

✳ significant at 0.05 probability level.
NS no significant at 0.05 probability level. Means in a column followed by different lower case letters are significantly different at P < 0.05 according to Fisher's LSD test.

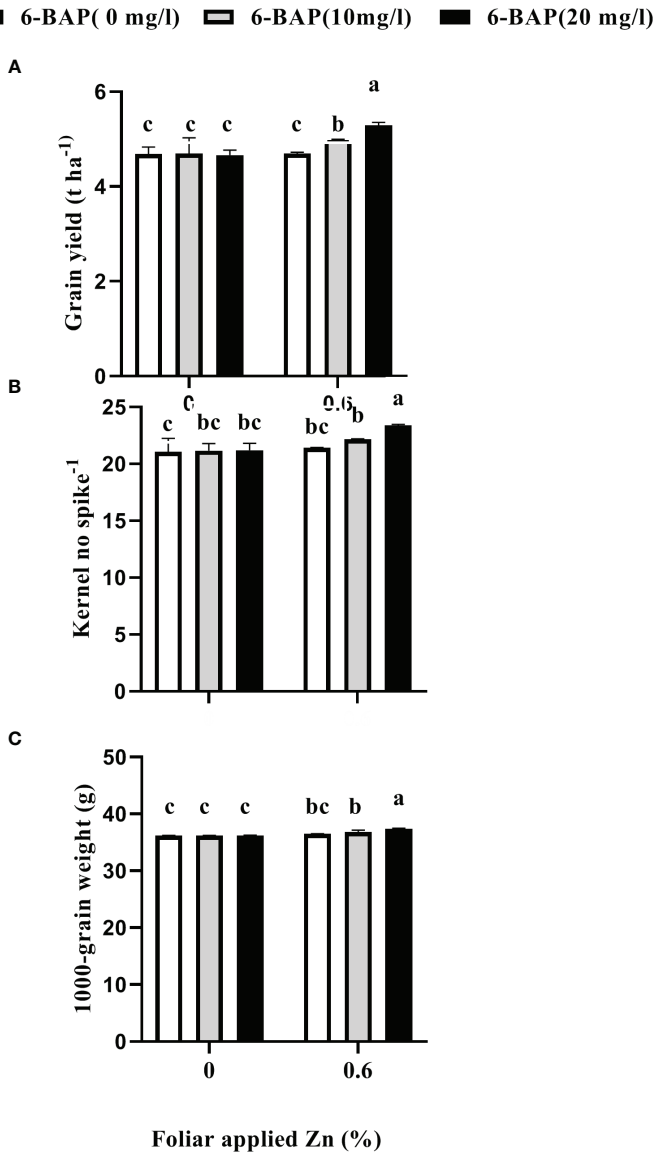


FIGURE 2
Effect of foliar applied Zn and 6-Benzylaminopurine (6-BAP) no grain yield **(A)**, kernel no spike-1 **(B)**, and 1000-kernel weight **(C)** of winter wheat under drought stress imposition. Different lowercase letters on the plots indicate significant differences ($P < 0.05$) among treatment means.

× 6-BAP interactions were not significant. Total straw dry weight was significantly increased by applied Zn by 0.29 t ha^{-1} (Table 3). Harvest index (%) and spike number plant^{-1} were not significantly affected by Zn, 6-BAP and their interaction (Table 2). Grain number per spike^{-1} was significantly affected by both foliar applied Zn and 6-BAP and their interaction as well (Table 3). As shown in Table 3, grain number per spike^{-1} of Zn treatment (22.31) was evidently higher than that of the untreated treatment (21.13). Foliar applied Zn increased number of seed spike^{-1} up to 5.5%. Plants sprayed with 20 mg L^{-1} 6-BAP had higher number of grain number per spike^{-1} than that of control treatment (Table 3). Foliar sprayed 20 mg L^{-1} 6-BAP increased grain number spike^{-1} up to 2.9% and 5% as compared with 10 mg L^{-1} applied 6-BAP and control treatment, respectively (Table 3). Plants foliar sprayed with Zn and treated with 20 mg L^{-1} 6-BAP (Zn + 6-BAP) gave the highest grain number spike^{-1} (Figure 2B). A significant grain weight (1000-kernel weight) response was found for foliar applied Zn and 6-BAP (Table 3). Thousand-grain weight was increased by 1.9% due to foliar applied Zn (Table 3). Foliar applied 20 mg l^{-1} 6-BAP enhanced thousand-grain weight up to 0.76% and 1.2% as compared to applied 6-BAP at 20 mg l^{-1} and unsprayed control, respectively (Table 3). There was significant Zn × 6-BAP interaction for grain weight. 1000-grain weight was the highest for plants foliar sprayed with Zn at 2% and 6-BAP at 20 mg l^{-1} (Figure 2C).

3.3 Zinc concentration and phytic acid/Zn molar ratio

Grain zinc content was significantly affected by foliar applied Zn and foliar 6-BAP application (Table 4). The Zn × 6-BAP interaction effect on kernel Zn concentration was not significant. As shown in Table 4, foliar applied 0.6% Zn (Zn0.6) increased kernel Zn concentration by 13.5% over in relation to the untreated plants (Zn0). The Zn concentration in kernel foliar sprayed with 6-BAP at 20 mg L^{-1} was higher than that of control treatment and 6-BAP at 10 mg L^{-1}. The experimental data on the zinc content of grain indicated no significant difference between the 6-BAP at 10 mg L^{-1} and control treatment. The phytate to Zn molar ratio was significantly affected by foliar applied Zn (Table 4). Plants foliar sprayed with 6% Zn had lower phytate to Zn molar ratio (29.1%) than that of control treatment. The phytate:Zn molar ratio was not significantly affected by foliar applied 6-BAP. There were no significant Zn × 6-BAP interaction effects for phytate to Zn molar ratio (Table 4).

3.4 CKX expression

Figure 3A shows the non-saturated gel image of the reverse transcription PCR ethidium bromide-stained agarose gels for gene expression of CKX. The intensity of the resulting band of RNA transcripts of CKX was visually higher in unsprayed plants. The main effect of foliar applied $ZnSO_4$ and 6-BAP significantly affected expression level of CKX in the kernel of winter wheat 5 days after drought stress imposition (Table 5). There was a significant effect of Zn + 6-BAP on CKX expression (Table 5). Plants foliar applied with Zn showed lower expression of CYTX transcripts compared to those unsprayed plants (Table 6). CKX expression transcripts were higher for those plants treated with 6-BAP (Table 6). The addition of 6-BAP to the foliar applied Zn, especially at 20 mg L^{-1}, resulted in lower expression of CYTX transcripts by 1.4-fold and 1.1-fold compared with following application of foliar 6-BAP (20 mg L^{-1}) alone and control treatment, respectively (Figure 3B).

3.5 Mycorrhizal colonization and succinate dehydrogenase activity

ANOVA indicated that mycorrhizal colonization percentage was influenced neither by foliar applied Zn nor 6-BAP and their interaction as well (Table 7). Succinate dehydrogenase activity (SDA) in roots of plants significantly affected by foliar applied Zn but not to applied 6-BAP (Table 7). Zn × 6-BAP interaction was not significant for SDA. Plants foliar applied with Zn exhibited higher SDA compared to untreated plants. At 4 days after drought imposition, plants sprayed with Zn solution performed higher levels of SDA (10.9%) in comparison with unsprayed control (Table 7). The effect of foliar applied Zn was not influenced by 6-BAP applied rate.

4 Discussion

Soil water shortage during grain filling under semi-arid and arid areas is becoming a major constraint in winter wheat production. Drought stress occurring at any stage of crop growth can lead to significant yield losses. However, in wheat, terminal drought is more devastating at reproductive phases (Farooq et al., 2017). Drought stress regularly occurs at the post-anthesis stage and leads to significant reduction in the growth and grain yield of wheat (Ullah et al., 2022). The adaption of a

TABLE 4 Impact of foliar applied Zn and 6-Benzylaminopurine (6-BAP) on grain Zn concentration and phytic acid to zinc mole ration.

Treatment	Zn concentration	Phytic acid : Zn
	mg kg^{-1}	
Foliar Zn (%)		
Zn0	26.5b	3.72a
Zn0.6	30.1a	2.88b
LSD (0.05)	0.86	0.28
Foliar 6-BAP (mg L^{-1})		
0	27.7b	3.51a
10	28.1b	3.26ab
20	29.3a	3.13ab
LSD (0.05)	1.05	NS

NS no significant at 0.05 probability level. Means in a column followed by different lower case letters are significantly different at $P < 0.05$ according to Fisher's LSD test.

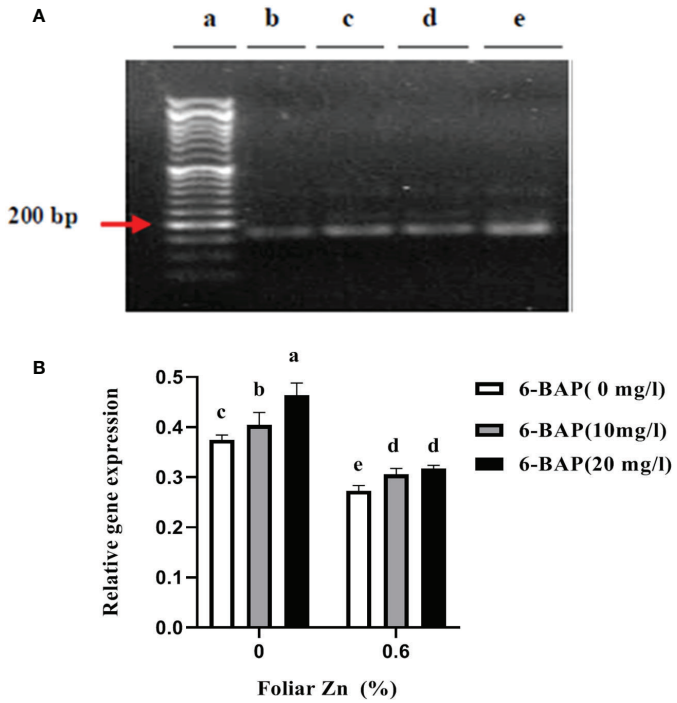


FIGURE 3
(A) Semi quantitative reverse transcription PCR visualization of CKX transcript encoding *Ta*CKX6-D1 expression in winter wheat under drought stress on 1.9% agarose gel. **(B)** Amplification at 25th cycles for transcript encoding *TA*CYTX. (a) Marker; (b) foliar applied Zn + 6-BAP (20 mg L-1); (c) foliar applied Zn + 6-BAP (10 mg L-1); (d) foliar applied Zn + 6-BAP (20 mg L-1) (e) unsprayed control treatment. Different lowercase letters on the plots indicate significant differences ($P < 0.05$) among treatment means.

TABLE 5 Analysis of variance for the effect of foliar applied Zn and 6-benzylaminopurine (6-BAP) on *Ta*CKX.

Source	df	Means square	*F*-value	*P* > *F*
Zn	1	0.06008	241.92	0.0001
6-BAP	2	0.00672	27.07	0.0001
Zn × 6-BAP	2	0.00105	4.23	0.0466

TABLE 6 Transcript expression analysis of *Ta*CKX6 using semi-quantitative RT-PCR.

Treatment	*Ta*CKX6
Foliar Zn application	
Zn0	0.41a
Zn0.6	0.29b
LSD (0.05)	0.016
Foliar 6-BAP application	
0 mg L^{-1}	0.32c
10 mg L^{-1}	0.35b
20 mg L^{-1}	0.39a
LSD (0.05)	0.02

Means in a column followed by different lower case letters are significantly different at $P < 0.05$ according to Fisher's LSD test.

plan to drought stress through nutrition and phytohormones management (foliar application) requires information regarding the effect of nutrient and plant hormone on any particular crop or environment. In the present investigation Zn and 6-BAP were foliar applied before drought imposition. The crop response to exogenous application of 6-ABP and foliar Zn may be dependent on the timing of the foliar application of Zn and phytohormone. We hypothesized that when Zn and 6-BAP being applied before drought stress imposition when plant water content is sufficient, applied Zn and 6-BAP may be better absorbed through stomata rather than Zn and 6-BAP sprayed on drought stressed plants. The results of this study indicated the beneficial effect of foliar application of Zn and 6-ABP on post anthesis drought-stressed wheat yield. However, in the current study, three recorded traits including number of spike $plant^{-1}$, harvest index and mycorrhizal colonization rate were significantly affected neither by applied Zn nor 6-ABP.

TABLE 7 Effect of foliar applied on mycorrhizal colonization (MC) percentage and Succinate dehydrogenase activity (SDA).

Treatment	MC	SDA
	%	%
Foliar Zn application (%)		
Zn0	36.2a	52.5b
Zn0.6	34.8a	58.3a
LSD (0.05)	NS	1.93
Foliar 6-BAP application (mg L^{-1})		
0	35.8a	55.1a
10	35.1a	55.2a
20	35.6a	56.0a
LSD (0.05)	NS	NS
Interaction		
Zn × 6-BAP	NS	NS

NS no significant at 0.05 probability level. Means in a column followed by different lower case letters are significantly different at $P < 0.05$ according to Fisher's LSD test.

In the present study, the number of spike $plant^{-1}$ was similar among all treatments. This could be because the final spike number per plant is mainly determined during vegetative growth stage. On the other hand, foliar treatments at the reproductive growth stage are late for the improvement in the final number of tiller (spike) set. In current study, application of Zn and 6-ABP was made at post-anthesis, when the spikes (tiller) were set. In current investigation, the harvest index was similar in all treatments. Harvest index is defined as the yield of grain divided by the total biological yield (stover + grain). In this study, grain yield was increased only by applied Zn. Similarly, straw yield was also enhanced due to foliar applied Zn. Therefore no significant difference in harvest index was observed among treatments. Mycorrhizal colonization rate was significantly similar in all foliar treatments, indicating non-significant effect of applied Zn and 6-BAP on this trait. This could be because foliar treatment during the grain filling stage is late for the increase in the mycorrhizal colonization rate.

4.1 Leaf relative water content and leaf fresh weight and dry weight

In the current study, relative water content of flag leaf and other plant leaves was greater in plants foliar sprayed with Zn. Sun et al. (2021) made similar observations about the improvement of water relations due to applied nano-ZnO. Other work (Sattar et al., 2022) showed a positive effect of Zn as foliar application on leaf water relative content in wheat. Foliar applied 6-ABP did not have a significant effect on the above mentioned recorded traits.

4.2 Zn effect on yield and yield components

In cereal such as wheat total grain yield is determined by yield components. In the present study, we observed drought imposed after anthesis markedly declined grain yield of untreated plants mainly due to less grain weight and number of grains. These results are in agreement with those of Anwar et al. (2021) who reported decreased grain yield in wheat was mainly due to less number of grains and grain weight. Grain yield is determined by its attributes, spike number $plant^{-1}$, grain no spike and kernel weight. Grain number $spike^{-1}$ and grain weight are major components of grain yield in winter wheat that are affected by various environmental factors like drought. Severe drought during anthesis could decrease grain yield up to 50% by reducing the number of grains (Saini and Westgate, 2000). The higher grain yield obtained in this study due to Zn application is associated with improved kernel no and kernel weight, suggesting that applying Zn positively affected these yield components. The results of this study, indicated the beneficial effect of foliar application of Zn on post anthesis drought-stressed wheat yield is in line with other studies reporting positive effects of foliar sprayed with Zn on crops, such as wheat (Yavas and Unay, 2016; Pavia et al., 2019; Anwar et al., 2021; Sattar et al., 2022), pak choi (Brassica rapa L.; Fatemi et al., 2021), safflower (Rahmani et al., 2019). There are investigations that elucidate the role of Zn as foliar spraying or seed priming on drought improvement in plants like wheat. Prior research has determined the adequate supply of Zn improved drought tolerance in wheat, sunflower, tomato, red cabbage and maize (Sun et al., 2020; Umair Hassan et al., 2020; Wang et al., 2020;

Sun et al., 2021). Plants foliar sprayed with Zn gave a higher yield of 300 kg ha^{-1} (6.58%) in comparison with control plants. Previous studies had indicated that foliar applying Zn is associated with positive yield response in wheat (Karim et al., 2012). In this study higher yield was associated with improved leaf water content, kernel no. $spike^{-1}$ and kernel weight. There are intensive studies on the positive role of Zn on wheat yield. However, sometimes winter wheat yield response to foliar Zn apparently has no significant effect on wheat yield. According to Wang et al. (2012), foliar application of 0.5% (w/v) $ZnSO_4$ H_2O solution at the beginning of stem elongation and flowering stage had no significantly positive effect on grain yield of wheat. These authors suggested that local soils are not Zn deficient. Karim et al. (2012) reported that, under drought condition, foliar applied Zn increased wheat grain yield up to 19%, whereas foliar applied Zn did not affect grain yield in the absence of drought . Overall, these findings suggest that the positive role of foliar Zn application depends on the soil condition and environmental constraint.

4.3 6-BAP effect on yield and yield components

In the present study, exogenous applied 6-BAP increased grain weight and kernel number per spike. Cytokinin has a stimulatory effect on cell division, grain weight and endosperm cell number (Panda et al., 2018). It has been reported that there is a positive correlation between endosperm cell number with grain filling and grain weigh (Panda et al., 2018). Yang et al. (2016) claimed that treated wheat plants with cytokinins had a positive effect on the number of spikelets on wheat. Similar to wheat, a positive relation between exogenous cytokinin applications with the number of spikelets has been also reported in rice (Panda et al., 2018). Our finding is in line with the finding of Zheng et al. (2016) that increased yield in wheat due to application of 6-BAP is related to increased grain number. However, these authors did not observe any significant effect of foliar application of 6-BAP on 1000-grain weight.

4.4 Zn ×6-BAP interaction effect on yield and yield components

In this investigation, straw dry weight, harvest index and number of spike $plant^{-1}$ were not significantly affected by Zn × 6-BAP interaction. However, grain yield and yield components (grain number and grain weight) were significantly influenced by foliar application of Zn × 6-BAP interaction. In current study, grain yield, yield components of grain number and grain weight in untreated plants were significantly lower as compared with plants sprayed with Zn + 6-BAP. The effect of foliar-Zn on grain yield was influenced by 6-BAP application. The increase in grain yield, grain weight and grain number $spike^{-1}$ resulting from foliar applied Zn was dependent on the 6-BAP concentration rate. Grain yield, grain number per spike, and grain weight increased as the concentration rate of 6-BAP was increased from 10 to 20 mg L^{-1}. This interaction indicated that grain yield, grain weight and grain number per spike were increased 12%, 11 and 3% by foliar applied 20 mg L^{-1} 6-BAP. Kernel weight and number of kernels per spike are the primary yield attributes of wheat (Holman et al., 2021). Kernel weight is the result of a regulated balance between sink (seed size) and source organ. We hypothesize that the exogenous applied 6-BAP before drought imposition may enhance the sink size (endosperm cell number). In the current study, foliar application of Zn decreased *Ta*CKX6-D1 expression and improved leaf water content that helped in improving yield and yield components of kernel weight and kernel number.

4.5 Grain Zn concentration and grain phytic acid:Zn molar ratios

In the present study, foliar Zinc application increased Zn concentration in grain by 13.5% compared to the control (Zn0) treatment. The translocation of foliar-applied Zn can be through trichomes and stomata (Domınguez et al., 2011; Wang et al., 2017). Wang et al. (2017) showed that foliar applied 0.3% Zn resulted in up to 95% increases in grain Zn concentration in winter wheat. Similarly, Yang et al. (2011) and Khampuang et al. (2020) reported that foliar application of Zn at early grain filling improved grain Zn concentration in wheat plants grown in low soil Zn condition. Yang et al. (2011) also found that foliar application of 0.3% of $ZnSO_4$ $7H_2O$ solution (1.5 kg ha^{-1}) at early grain filling resulted in an average increase of 64% Zn concentration compared to the no foliar Zn (control) treatment. In a field experiment conducted in Turkey during the 2003-2004 cropping season, Ozturka et al. (2006) reported that foliar Zn applications (0.68 kg ha^{-1}) in the form of $ZnSO_4$ $7H_2O$ on wheat plants increased grain Zn concentrations. 45% of the total absorbed Zn from the zinc applied to leaves has been reported to translocate from leaf into roots and other parts of shoots under Zn-deficient conditions. In the Zn-adequate plants, this proportion has been reported to be nearly 25% (Haslett et al., 2001; Erenoglu et al., 2002). Phytic acid can chelates micronutrients such as Zn and decrease absorption of it by monogastric animal and human. Humans cannot digest phytic acid because of the absence of enzyme phytase in their digestive tract (Brouns 2021).

To our knowledge, this is the first study that shows a positive effect of foliar-applied cytokinin on grain Zn concentrations. Increased Zn concentration in grain due to 6-BAP may be related to the enhancing of translocation of Zn from vegetative tissues into grain. Foliar-applied 6-BAP may affect translocation of Zn from vegetative tissues into grain. In the present study, foliar applied Zn had a significant effect on the grain phytic acid/Zn molar ratio. Foliar Zn decreased the phytic acid:Zn molar

ratio. According to a study reported, foliar applied Zn resulted in reduction of grain phytic acid:Zn molar ratios by 52.0% in winter wheat (Wang et al., 2017).

4.6 TaCKX6-D1 expression

Plants involved various mechanisms through by mitigate the adverse effect of drought stress. Modulation in endogenous levels of phytohormones is one of the strategy plant adapted to withstand drought stress. In this study, control plants and foliar 6-BAP treated plants had higher expression of CKX, while plants from Zn treatment had lower rate of CKX gene expression. Endogenous plant hormones are controlled by genes. Endogenous cytokinins levels can be regulated by the enzyme called cytokinin oxidase/dehydrogenase, CKO/CKX. Some studies claimed CKX genes that negatively regulated the levels of cytokinins has been reported to lead to improved crop yield and abiotic stresses tolerances (Arora and Sen, 2022). Therefore higher level expression of CKX gene in control plants might be because these plants were more affected by imposed drought relative to those plants treated with Zn. However, there is some evidences that indicate up regulation of this gene has also caused increased yield in rice. Several investigators (Ma et al., 2017; Sultana et al., 2018; Pavia et al., 2019; Ullah et al., 2019; Ashkiani et al., 2020; Sattar et al., 2022) have studied the role of Zn in improvement of drought tolerance in wheat. Lower CKX gene expression in developing seeds might to because foliar applied Zn could, to some extent, mitigate the adverse effect of the imposed drought. Plants sprayed with 6-BAP, especially with 20 mg L^{-1}, had higher expression levels of *Ta*CKX6-D1 in compared to control treatment (unsprayed plants). However, grain weight was higher in these plants sprayed with 6-BAP. We assumed that elevated endogenous concentration of cytokinin due to foliar sprayed 6-BAP had induced *Ta*CKX6-D1 gene expression. Cytokinin oxidase/dehydrogenase regulate the level of local in plant tissue (Li et al., 2018). We postulate that increased expression of CKX in response to exogenous applied 6-BAP is a strategically mechanism to improve plant tolerance to imposed drought. In *Arabidopsis ipt* mutants that had decreased cytokinin exhibited higher drought tolerance in comparison to wild type (Nishiyama et al., 2011). There are numerous studies indicating that cytokinin levels decreased in response to stress. However and in contrast to these investigations, other findings have shown that cytokinine was increased in response to drought stress (Zwack and Rashotte, 2015). Macková et al. (2013) reported that decreased cytokinin levels in tobacco plants were achieved by enhanced gene expression of CKX. Increased kernel weight in plants applied with 6-BAP may be related to prolonged active photosynthesis period during grain filling (Chen et al., 2010). Previous research has shown that cytokinin can regulate senescence and stay-green trait (Li et al., 2018). Yang et al. (2016) reported that exogenous cytokinins through improving stay-green increased the yield of winter wheat cultivars. The expression level of *Ta*CKX6-D1 was lower in plants sprayed with Zn (2% v/v) as compared with unsprayed plants. Plants treated with Zn had higher kernel weight and kernel number per spike. Ashikari et al. (2005) and Panda et al. (2018) reported that there was a negative relation between *Os*CKX2 and grain number in rice. Zhang et al. (2012) also reported an inverse correlation between *Ta*CKX6-D1 and 1000-grain weight in wheat. Szala et al. (2020) observed that grain yield and grain number were positively regulated by TaCKX8 but negatively by *Ta*CKX10. In the present study, plants foliar applied with Zn had higher leaf fresh and dry matter weight and leaf water content, postulating applied Zn could improve drought tolerance. In the present study, foliar Zn+6-BAP resulted in a significant negative increase in CKX gene expression. In the present study, foliar Zn+6-BAP resulted in a significant negative increase in CKX gene expression. On the other hand control plants and foliar 6-BAP treated plants had higher expression of CKX, while plants from Zn treatment had lower rate of CKX gene expression. Some studies claimed CKX genes that negatively regulated the levels of cytokinins have been reported to lead to improved crop yield and abiotic stress tolerances (Arora and Sen, 2022). Therefore higher level expression of CKX gene in control plants might be because these plants were more affected by imposed drought relative to those plants treated with Zn. However, there is some evidence that indicates up regulation of this gene has also caused increased yield in rice.

4.7 Mycorrhizal colonization and succinate dehydrogenase activity

The best of knowledge, the potential role of Zn and 6-Benzylaminopurine in improving mycorrhizal colonization and succinate dehydrogenase activity against terminal drought in wheat have never been studied. Neither Zn nor 6-Benzylaminopurine influenced mycorrhizal colonization. This might be because foliar treatment during the reproductive growth stage is late for the increasing in the mycorrhizal colonization rate. At 4 days after drought imposition, plants exogenously foliage applied with Zn solution performed higher levels of succinate dehydrogenase activity (10.9%) in comparison with unsprayed control. The literature search yields no previous research on the highlighting the effects of foliar applications of Zn on mycorrhizal colonization rate and succinate dehydrogenase activity to indicate the finding could occur. Sadeghizadeh and Zarea (2022) reported that applied Zn through seed priming led the succinate dehydrogenase activity of hyphae of *Serendipita indica* to increase in rice root. Amjad et al. (2021) reported that wheat performances in response to arbuscular mycorrhizal fungi (*Glumus intraradisis*) were more profound due to Zn application.

4.8 Conclusion

Arid- and semi-arid regions have been severely affected by long term deficit in precipitation. In these areas wheat experiences climate change, hot and dry weather and weather variability, becoming a major threat to winter wheat production. However this situation is not limited to wheat and other crops are negatively affected by this situation. Field research needs to be undertaken to investigate agronomic strategies that lead in alleviation of the adverse effect of drought stress. In summary, both foliar applied Zn and 6-BAP had the significant effects on all measured parameters in winter wheat. However, spike number, harvest index and mycorrhizal colonization rate were neither significantly affected by Zn nor 6-BAP. Foliar application of Zn at 0.6% (6 kg ha^{-1}) and higher 6-BAP (20 mg L^{-1} m^{-2}) promoted wheat growth and performances under imposed drought stress condition. Plant that only foliar sprayed with water showed higher level of *Ta*CKX6-D1 expression as compared to Zn treated plants, indicating these plants were more affected by imposed drought relative to those plants treated with Zn. Concentrations of Zn and phytates in grain need to be considered as well. This study investigated whether combined foliar application of Zn with cytokinin can improve winter wheat grain yield and quality. Zn (6 kg ha-1) combined with 6-Benzylaminopurine (20 mg L-1) gave the best results in terms of yield and yield quality. The results of this study provides evidence that a combination of Zn and 6-BAP could be an effective in improvement of drought tolerance of wheat and prevents grain yield from further reduction in terms of quality and quantity due to drought stress.

Data availability statement

The original contributions presented in the study are included in the article/Supplementary Material. Further inquiries can be directed to the corresponding author.

Author contributions

MZ contributed to the material preparation, performing the experiments, data collection and analysis, validation and writing- original draft preparation; NK assisted in carrying out the field research and data collection contributing. All authors contributed to the article and approved the submitted version.

Acknowledgments

We are grateful for financial support from Ilam University. We would like to thank editor and reviewers for their careful reading of our manuscript and their many insightful comments and suggestions on earlier drafts of the manuscript.

Conflict of interest

The authors declare that the research was conducted in the absence of any commercial or financial relationships that could be construed as a potential conflict of interest.

Publisher's note

All claims expressed in this article are solely those of the authors and do not necessarily represent those of their affiliated organizations, or those of the publisher, the editors and the reviewers. Any product that may be evaluated in this article, or claim that may be made by its manufacturer, is not guaranteed or endorsed by the publisher.

References

Adil, M., Bashir, S., Bashir, S., Aslam, Z., Ahmad, N., Younas, T., et al. (2022). Zinc oxide nanoparticles improved chlorophyll contents, physical parameters, and wheat yield under salt stress. *Front. Plant Sci.* 13. doi: 10.3389/fpls.2022.932861

Amjad, S. F., Mansoora, N., Din, I. U., Khalid Iqbal, R., Jatoi, G. H., Murtaza, G., et al. (2021). Application of zinc fertilizer and mycorrhizal inoculation on physiobiochemical parameters of wheat grown under waterstressed environment. *Sustainability* 13, 11007. doi: 10.3390/su131911007

Anwar, S., Khalilzadeh, R., Khan, S., Nisa, Z., Bashir, R., Pirzad, A., et al. (2021). Mitigation of drought stress and yield improvement in wheat by zinc foliar spray relates to enhanced water use efficiency and zinc contents. *Int. J. Plant Prod.* 15, 377–389. doi: 10.1007/s42106-021-00136-6.

Arora, K., and Sen, S. (2022). Cytokinin oxygenase/dehydrogenase inhibitors: An emerging tool in stress biotechnology employed for crop improvement. *Front. Genet.* 13. doi: 10.3389/fgene.2022.877510

Ashikari, M., Sakakibara, H., Lin, S., Yamamoto, T., Takashi, T., Nishimura, A., et al. (2005). Cytokinin oxidase regulates rice grain production. *Sci.* 309, 741–745. doi: 10.1126/science.1113373

Ashkiani, A., Sayfzadeh, S., Shirani Rad, A. H., Valadabadi, A., and Hadidi Masouleh, E. (2020). Effects of foliar zinc application on yield and oil quality of rapeseed genotypes under drought stress. *J. Plant Nutr.* 309, 741–745. doi: 10.1080/01904167.2020.1739299

Brouns, F. (2021). Phytic Acid and Whole Grains for Health Controversy. *Nutrients*. 14, 25. doi: 10.3390/nu14010025.

Cabot, C., Martos, S., Llugany, M., Gallego, B., Tolrà, R., and Poschenrieder, C. (2019). A role for zinc in plant defense against pathogens and herbivores. *Front. Plant Sci.* 10. doi: 10.3389/fpls.2019.01171

Cakmak, I. (2008). Enrichment of cereal grains with zinc: agronomic orgenetic biofortification? *Plant Soil* 302, 1–17. doi: 10.1007/s11104-007-9466-3

Cakmak, I., Kalayci, M., Kaya, Y., Torun, A. A., Aydin, N., Wang, Y., et al. (2010). Biofortification and localization of zinc in wheat grain. *J. Agric. Food Chem.* 58, 9092–9102. doi: 10.1021/jf101197h

Cakmak, I., and Kutman, U. B. (2018). Agronomic biofortification of cereals with zinc: a review. *E. J. Soil Sci.* 69, 172–180. doi: 10.1111/ejss.12437

Charfeddine, M., Bouaziz, D., Charfeddine, S., Hammami, A., Ellouz, O. N., and Bouzid, R. G. (2015). Overexpression of dehydration-responsive element-binding 1protein (DREB1) in transgenic *Solanum tuberosum* enhances tolerance to biotic stress. *Plant Biotechnol. Rep.* 9, 79–88. doi: 10.1007/s11816-015-0345-8

Chen, J. B., Liang, Y., Hu, X. Y., Wang, X. X., Tan, F. Q., Zhang, H. Q., et al. (2010). Physiological characterization of 'stay-green' wheat cultivars during the grain filling stage under field growing conditions. *Acta Physiol. Plant* 32, 875–882. doi: 10.1007/s11738-010-0475-0

Cortleven, A., Leuendorf, J. E., Frank, M., Pezzetta, D., Bolt, S., and Schmüulling, T. (2019). Cytokinin action in response to abiotic and biotic stresses in plants. *Plant Cell Environ.* 42, 998–1018. doi: 10.1111/pce.13494

Domınguez, E., Heredia-Guerrero, J. A., and Heredia, A. (2011). The biophysical design of plant cuticles, an overview. *New Phytol.* 189, 938–949. doi: 10.1111/j.1469-8137.2010.03553.x

Erenoglu, B., Nikolic, M., Romheld, V., and Cakmak, I. (2002). Uptake and transport of foliar applied zinc (^{65}Zn) in bread and durum wheat cultivars differing in zinc efficiency. *Plant Soil* 241, 251–257. doi: 10.1023/A:1016148925918

Fatemi, H., Zaghdoud, C., Nortes, P. A., Carvajal, M., and Martínez-Ballesta, M. D. C. (2020). Differential aquaporin response to distinct effects of two Zn concentrations after foliar application in pak choi *(Brassica rapa L.)* plants. *Agron.* 10, 450. doi: 10.3390/agronomy10030450

Farooq, M., Gogoi, N., Barthakur, S., Baroowa, B., Bharadwaj, N., Alghamdi, S. S., et al. (2017). Drought stress in grain legumes during reproduction and grain filling. *Agron. Crop Scie.* 203, 81–102. doi: 10.1111/jac.12169

Gao, S., Xiao, Y., Xu, F., Gao, X., Cao, S., Zhang, F., et al. (2019). Cytokinin-dependent regulatory module underlies the maintenance of zinc nutrition in rice. *New Phytol.* 224, 202–215. doi: 10.1111/nph.15962

Hamel, C., Fyles, H., and Smith, D. L. (1990). Measurement of development of endomycorrhizal mycelium using three different vital stains. *New Phytol.* 115, 297–302. doi: 10.1111/j.1469-8137.1990.tb00455.x

Hare, P. D., Cress, W. A., and Staden, J. V. (1997). The involvement of cytokinins in plant responses to environmental stress. *Plant Growth Regul.* 23, 79–103. doi: 10.1023/A:1005954525087

Haslett, B. S., Reid, R. J., and Rengel, Z. (2001). Zinc mobility in wheat: uptake and distribution of zinc applied to leaves or roots. *Ann. Bot.* 87, 379–386. doi: 10.1006/anbo.2000.1349

Haug, W., and Lantzsch, H. J. (1983). Sensitive method for the rapid determination of phytate in cereals and cereal products. *J. Sci. Food Agric.* 34, 1423–1426. doi: 10.1002/jsfa.2740341217

Holman, J. D., Haag, L. A., Schlegel, A. J., and Assefa, Y. (2021). Yield components of dryland winter wheat genotypes and response to seeding rate. *Agron. J.* 113, 1776–1791. doi: 10.1002/agj2.20607

Inoue, T., Inanaga, S., Sugimoto, Y., and Siddig, K. E. L. (2004). Contribution of pre-anthesis assimilates and current photosynthesis to grain yield, and their relationships to drought resistance in wheat cultivars grown under different soil moisture. *Photosynthetica* 42, 99–104. doi: 10.1023/B:PHOT.0000040576.52128.ed

Karimi, N., Goltapeh, E. M., Amini Mehnaz, S., and Zarea, M. J. (2021). Effect of *Azospirillum zeae* and seed priming with zinc, manganese and auxin on growth and yield parameters of wheat, under dryland farming. *Agric. Res.* 10, 44–55. doi: 10.1007/s40003-020-00480-5

Karim, M. R., Zhang, Y. Q., Zhao, R. R., Chen, X. P., Zhang, F. S., and Zou, C. Q. (2012). Alleviation of drought stress in winter wheat by late foliar application of zinc, boron, and manganese. *J. Plant Nutr. Soil Sci.* 175, 142–151. doi: 10.1002/jpln.201100141

Kaur, H., and Garg, N. (2021). Zinc toxicity in plants: a review. *Planta* 253, 129. doi: 10.1007/s00425-021-03642-z

Khampuang, K., Lordkaew, S., Dell, B., and Prom-u-thai, C. (2020). Foliar zinc application improved grain zincaccumulation and bioavailable zinc in unpolishedand polished rice. *Plant Prod. Sci.* 4, 94–102. doi: 10.1080/1343943X.2020.1797512

Kobata, T., Palta, J. A., and Turner, N.C. (1992). Rate of development of post anthesis water deficits and grain filling of spring wheat. *Crop Sci.* 32, 1238–1242. doi: 10.2135/cropsci1992.0011183X003200050035x

Kough, J. L., Gianinazzi-Pearson, V., and Gianinazzi, S. (1987). Depressed metabolic activity of vesicular-arbuscular mycorrhizal fungi after fungicide application. *New Phytol.* 106, 707–715. doi: 10.1111/j.1469-8137.1987.tb00171.x

Lei, L., Wu, D., Cui, C., Gao, X., Yao, Y., Dong, J., et al. (2022). Transcriptome analysis of early senescence in the post-anthesis flag leaf of wheat *(Triticum aestivum L.). Plants (Basel).* 11, 2593. doi: 10.3390/plants11192593.

Liao, F., Lilay, G. H., Castro, P. H., Azevedo, H., and Assunção, A. G. L. (2022). Regulation of the zinc deficiency response in the legume model medicago truncatula. *Front. Plant Sci.* 13. doi: 10.3389/fpls.2022.916168

Li, Y., Song, G., Gao, J., Zhang, S., Zhang, R., Li, W., et al. (2018). Enhancement of grain number per spike by RNA interference of cytokinin oxidase 2 gene in bread wheat. *Hereditas* 155, 33. doi: 10.1186/s41065-018-0071-7

Liu, Z. G., Cheng, F. M., and Zhang, G. P. (2005). Grain phytic acid content in japonica rice as affected by cultivar and environment and its relation to protein content. *Food Chem.* 89, 49–52. doi: 10.1016/j.foodchem.2004.01.081

Liu, X. Z., and Huang, B. R. (2002). Cytokinin effects on creeping bentgrass response to heat stress: II. leaf senescence and antioxidant metabolism. *Crop Sci.* 42, 466–472. doi: 10.2135/cropsci2002.4660

Lu, M., Cao, X., Pan, J., Gurajala, H. K., He, Z., Yang, X., et al. (2020). Genotypic variations in zinc accumulation and bioaccessibility among wheat (*Triticum aestivum* l.) genotypes under two different field conditions. *J. Cereal Sci.* 93, 102953. doi: 10.1016/j.jcs.2020.102953

Lugojan, C., and Ciulca, S. (2011). Evaluation of relative water content in winter wheat. *J. Hortic. Fores. Biotechnol.* 15, 173–177.

Ma, D., Sun, D., Wang, C., Ding, H., Qin, H., Hou, J., et al. (2017). Physiological responses and yield of wheat plants in zinc-mediated alleviation of drought stress. *Front. Plant Sci.* 8. doi: 10.3389/fpls.2017.00860

Macková, H., Hronková, M., Dobrá, J., Turečková, V., Novák, O., Lubovská, Z., et al. (2013). Enhanced drought and heat stress tolerance of tobacco plants with ectopically enhanced cytokinin oxidase/dehydrogenase gene expression. *J. Exp. Bot.* 64, 2805–2815. doi: 10.1093/jxb/ert131.

McGonigle, T. P., Miller, M. H., Evans, D. G., Fairchild, G. L., and Swan, J. A. (1990). A new method which gives an objective measure of colonization of roots by vesicular-arbuscular mycorrhizal fungi. *New Phytol.* 115, 495–501. doi: 10.1111/j.1469-8137.1990.tb00476.x

Nishiyama, R., Watanabe, Y., Fujita, Y., Le, D. T., Kojima, M., Werner, T., et al. (2011). Analysis ofcytokinin mutants and regulation of cytokinin metabolic genes revealsimportant regulatory roles of cytokinins in drought, salt and abscisicacid responses, and abscisic acid biosynthesis. *Plant Cell* 23, 2169–2183. doi: 10.1105/tpc.111.087395

Ozturka, L., Yazicia, M. A., Yucelb, C., Torunb, A., Cekicc, C., Bagcid, A., et al. (2006). Concentration and localization of zinc during seed development and germination in wheat. *Physiol. Plant* 128, 144–152. doi: 10.1111/j.1399-3054.2006.00737.x

Panda, B. B., Sekhar, S., Dash, S. K., Behera, L., and Shaw, B. P. (2018). Biochemical and molecular characterization of exogenous cytokinin application on grain filling in rice. *BMC Plant Biol.* 18, 89. doi: 10.1186/s12870-018-1279-4

Pavia, A., Roque, J., Rocha, L., Ferreira, H., Castro, C., Carvalho, A., et al. (2019). Zinc priming and foliar application enhances photoprotection mechanisms in drought-stressed wheat plants during anthesis. *Plant Physiol. Biochem.* 140, 27–42. doi: 10.1016/j.plaphy.2019.04.028

Pfaffl, M. W. (2001). A new mathematical model for relative quantification in real-time RT-PCR. *Nucleic Acids Res.* 29, e45. doi: 10.1093/nar/29.9.e45

Rahmani, F., Sayfzadeh, S., Jabbari, H., Valadabadi, S. A., and Masouleh, E. H. (2019). Alleviation of drought stress effects on safflower yield by foliar application of zinc. *Int. J. Plant Prod.* 13, 297–308. doi: 10.1007/s42106-019-00055-7

Rehman, A., and Farooq, M. (2016). Zinc seed coating improves the growth, grain yield and grain biofortification of bread wheat. *Acta Physiol. Plant* 38, 238. doi: 10.1007/s11738-016-2250-3

Rehman, A., Farooq, M., Ozturk, L., Asif, M., and Siddique, K. H. M. (2018). Zinc nutrition in wheat-based cropping systems. *Plant Soil* 422, 283–315. doi: 10.1007/s11104-017-3507-3

Sadeghizadeh, M., and Zarea, M. J. (2022). Effects of seed priming with zinc on germination, nursery seedling growth and paddy fields yield of two rice (*Oryza sativa* l.) cultivars. *J. Crop Sci. Biotechnol.* 25, 313–324. doi: 10.1007/s12892-021-00133-1

Saini, H. S., and Westgate, M. E. (2000). "Reproductive development in grain crops during drought," in *Advances in agronomy*, vol. 68 . Ed. D. L. Sparks (New York, NY: Academic Press), 59–96.

Sattar, A., Wang, X., Ul-Allah, S., Sher, A., Ijaz, M., Irfan, M., et al. (2022). Foliar application of zinc improves morpho-physiological and antioxidant defense mechanisms, and agronomic grain biofortification of wheat (*Triticum aestivum* l.) under water stress. *Saudi J. Biol. Sci.* 29, 1699–1706. doi: 10.1016/j.sjbs.2021.10.061

Schmülling, T., Werner, T., Riefler, M., Krupková, E., and y Manns, I. B. (2003). Structure and function of cytokinin oxidase/dehydrogenase genes of maize, rice, arabidopsis and other species. *J. Plant Res.* 116, 241–252. doi: 10.1007/s10265-003-0096-4

Sultana, S., Naser, H. M., Quddus, M. A., Shil, N. C., and Hossain, M. A. (2018). Effect of foliar application of iron and zinc on nutrient uptake and grain yield of wheat under different irrigation regimes. *Bangladesh J. Agril. Res.* 43, 395–406. doi: 10.3329/BJAR.V43I3.38388

Sun, L., Song, F., Guo, J., Zhu, X., Liu, S., Liu, F., et al. (2020). Nano-ZnO induced drought tolerance is associated with melatonin synthesis and metabolism in maize. *Int. J. Mol. Sci.* 21, 782. doi: 10.3390/ijms21030782

Sun, L., Song, F., Zhu, X., Liu, S., Liu, F., Wang, Y., et al. (2021). Nano-ZnO alleviates drought stress *via* modulating the plant water use and carbohydrate metabolism in maize. *Arch. Agron. Soil Sci.* 67, 245–259. doi: 10.1080/03650340.2020.1723003

Szala, K., Ogonowska, H., Lugowska, B., Zmijewska, B., Wyszynska, R., Dmochowska-Boguta, M., et al. (2020). Different sets of *Ta*CKX genes affect yield related traits in wheat plants grown in a controlled environment and in field conditions. *BMC Plant Biol.* 20, 496. doi: 10.1186/s12870-020-02713-9

Ullah, A., Tian, Z., Xu, L., Abid, M., Lei, K., Khanzada, A., et al. (2022). Improving the effects of drought priming against post-anthesis drought stress in wheat (*Triticum aestivum* l.) using nitrogen. *Front. Plant Sci.* 13. doi: 10.3389/fpls.2022.965996

Ullah, A., Romdhane, L., Rehman, A., and Farooq, M. (2019). Adequate zinc nutrition improves the tolerance against drought and heat stresses in chickpea. *Plant Physiol. Biochem.* 143, 11–18. doi: 10.1016/j.plaphy.2019.08.020.

Umair Hassan, M., Aamer, M., Umer Chattha, M., Haiying, T., Shahzad, B., Barbanti, L., et al. (2020). The critical role of zinc in plants facing the drought stress. *Agr.* 10, 396. doi: 10.3390/agriculture10090396

Wang, S., Li, M., Liu, K., Tian, X., Li, S., Chen, Y., et al. (2017). Effects of zn, macronutrients, andtheir interactions through foliar applications onwinter wheat grain nutritional quality. *PloS One* 12, e0181276. doi: 10.1371/journal.pone.0181276

Wang, Z., Li, H., Li, X., Xin, C., Si, J., et al. (2020). Nano-ZnO priming induces salt tolerance by promoting photosynthetic carbon assimilation in wheat. *Arch. Agron. Soil Sci.* 66, 1259–1273. doi: 10.1080/03650340.2019.1663508

Wang, J., Mao, H., Zhao, H., Huang, D., and Wang, Z. (2012). Different increases in maize and wheat grain zinc concentrations caused by soil and foliar applications of zinc in loess plateau, China. *Field Crop Re.* 135, 89–96. doi: 10.1016/j.fcr.2012.07.010

Wen, Z., Juliana, P., Dhugga, H. S., Pacheco, M., Martínez, U. I., Aguilar, A., et al. (2022). Genome-wide association study of phytic acid in wheat grain unravels markers for improving biofortification. *Front. Plant Sci.* 13. doi: 10.3389/fpls.2022.830147

Werner, T., Nehnevajova, E., Kollmer, I., Novak, O., Strnad, M., Kramer, U., et al. (2010). Root-specific reduction of cytokinin causesenhanced root growth, drought tolerance, and leaf mineral enrichmentin arabidopsis and tobacco. *Plant Cell* 22, 3905–3920. doi: 10.1105/tpc.109.072694

Xu, F., Yang, Z. F., Chen, X. H., Jin, P., Wang, X. L., and Zheng, Y. H. (2011). 6-benzylaminopurine delays senescence and enhances health-promoting compounds of harvested broccoli. *J. Agric. Food Chem.* 60, 234–240. doi: 10.1021/jf204088422148319

Yang, D.Q., Li, Y., Shi, Y., Cui, Z., et al. (2016). Exogenous cytokinins increase grain yield of winter wheat cultivars by improving stay-green characteristics under heat stress. *PloS One* 11, e0155437. doi: 10.1371/journal.pone.0155437

Yang, J. C., Peng, S. B., Visperas, R. M., Sanico, A. L., Zhu, Q. S., and Gu, S. L. (2000). Grain filling pattern and cytokinin content in the grains and roots of rice plants. *Plant Growth Regul.* 30, 261–270. doi: 10.1023/A:1006356125418

Yang, X. W., Tianx, H., Galew, J., Caoy, X., Lu X, C., and Zhaoa, Q. (2011). Effect of soil and foliar zinc application on ZincConcentration and bioavailability in wheat grain grown on potentially zinc-deficient soil. *Cereal Res. Commun.* 39, 535–543. doi: 10.1556/CRC.39.2011.4.8

Yang, J. C., Zhang, J. H., Wang, Z. Q., and Zhu, Q. S. (2003). Hormones in the grains in relation to sink strength and postanthesis development of spikelets in rice. *Plant Growth Regul.* 41, 185–195. doi: 10.1023/B:GROW.0000007503.95391.38

Yavas, I., and Unay, A. (2016). Effects of zinc and salicylic acid on wheat under drought stress. *J. Anim. Plant Scie.* 26, 1012–1018.

Yu, H., Zhang, Q., Sun, P., and Sung, C. (2018). Impact of droughts on winter wheat yield in different growth stages during 2001–2016 in Eastern China. *Int. J. Disaster Risk. Sci.* 9, 376–391. doi: 10.1007/s13753-018-0187-4

Zhang, L., Zhao, Y., Gao, L., Zhao, G., Zhou, R., Zhang, B., et al. (2012). TaCKX6-D1, the ortholog of rice OsCKX2, is associated with grain weight in hexaploid wheat. *New Phytol.* 195, 574–584. doi: 10.1111/j.1469-8137.2012.04194.x

Zheng, C., Zhu, Y., Wang, C., and Guo, T. (2016). Wheat grain yield increase in response to pre- anthesis foliar application of 6-benzylaminopurine is dependent on floret development. *PloS One* 11, e0156627. doi: 10.1371/journal.pone.0156627

Zwack, P. J., and Rashotte, A. M. (2015). Interactions between cytokinin signalling and abiotic stress responses. *J. Exp. Bot.* 66, 4863–4871. doi: 10.1093/jxb/erv172

frontiers | Frontiers in Plant Science

TYPE Original Research
PUBLISHED 13 January 2023
DOI 10.3389/fpls.2022.1050359

Check for updates

OPEN ACCESS

EDITED BY
Mehtab Muhammad Aslam,
The Chinese University of Hong Kong, China

REVIEWED BY
Rabia Shahid,
Hainan University, China
Abbu Zaid,
Govt. Degree College Doda, India

*CORRESPONDENCE
Guihua Li
Liguihua@gdaas.cn
Nasim Ahmad Yasin
nasimhort@gmail.com

SPECIALTY SECTION
This article was submitted to Plant Abiotic Stress, a section of the journal Frontiers in Plant Science

RECEIVED 21 September 2022
ACCEPTED 31 October 2022
PUBLISHED 13 January 2023

CITATION
Hussain S, Ahmed S, Akram W, Li G and Yasin NA (2023) Selenium seed priming enhanced the growth of salt-stressed *Brassica rapa* L. through improving plant nutrition and the antioxidant system.
Front. Plant Sci. 13:1050359.
doi: 10.3389/fpls.2022.1050359

COPYRIGHT
© 2023 Hussain, Ahmed, Akram, Li and Yasin. This is an open-access article distributed under the terms of the Creative Commons Attribution License (CC BY). The use, distribution or reproduction in other forums is permitted, provided the original author(s) and the copyright owner(s) are credited and that the original publication in this journal is cited, in accordance with accepted academic practice. No use, distribution or reproduction is permitted which does not comply with these terms.

Selenium seed priming enhanced the growth of salt-stressed *Brassica rapa* L. through improving plant nutrition and the antioxidant system

Saber Hussain[1,2], Shakil Ahmed[2], Waheed Akram[3], Guihua Li[1]* and Nasim Ahmad Yasin[1,4]*

[1]Guangdong Key Laboratory for New Technology Research of Vegetables/Vegetable Research Institute, Guangdong Academy of Agricultural Sciences, Guangzhou, China, [2]Institute of Botany, University of the Punjab, Lahore, Pakistan, [3]Department of Plant Pathology, Faculty of Agricultural Sciences, University of the Punjab, Lahore, Pakistan, [4]Senior Superintendent Gardner (SSG) Department, University of the Punjab, Lahore, Pakistan

Various abiotic stresses may affect the germination, growth, and yield of direct-seeded vegetable crops. Seed priming with effective antioxidant mediators may alleviate these environmental stresses by maintaining uniformity in seed germination and improving the subsequent health of developing seedlings. Salt-induced stress has become a limiting factor for the successful cultivation of *Brassica rapa* L., especially in Southeast Asian countries. The present study was performed to elucidate the efficacy of seed priming using selenium (Se) in mitigating salt-induced oxidative stress in turnip crops by reducing the uptake of Na^+. In this study, we administered three different levels of Se (Se-1, 75 µmol L^{-1}; Se-2, 100 µmol L^{-1}; and Se-3, 125 µmol L^{-1}) alone or in combination with NaCl (200 mM). Conspicuously, salinity and Se-2 modulated the expression levels of the antioxidant genes, including catalase (*CAT*), peroxidase (*POD*), superoxide dismutase (*SOD*), and ascorbate peroxidase (*APX*). The upregulated expression of stress-responsive genes alleviated salt stress by scavenging the higher reactive oxygen species (ROS) level. The stress ameliorative potential of Se (Se-2 = 100 µmol L^{-1}) enhanced the final seed germination percentage, photosynthetic content, and seedling biomass production up to 48%, 56%, and 51%, respectively, under stress. The advantageous effects of Se were attributed to the alleviation of salinity stress through the reduction of the levels of malondialdehyde (MDA), proline, and H_2O_2. Generally, treatment with Se-2 (100 µmo L^{-1}) was more effective in enhancing the growth attributes of *B. rapa* compared to Se-1 (75 µmo L^{-1}) and

Se-3 (125 μmo L^{-1}) under salt-stressed and non-stressed conditions. The findings of the current study advocate the application of the Se seed priming technique as an economical and eco-friendly approach for salt stress mitigation in crops grown under saline conditions.

KEYWORDS

antioxidant, gene expression, NaCl, seed priming, Se, turnip

Introduction

Selenium (Se) is an essential micronutrient required for the normal growth of plants subjected to several abiotic and biotic stresses (Kaur et al., 2022). However, a higher amount of this element may have harmful effects on the physiochemical activities of plants (Shafiq et al., 2019). Selenium may enter the food chain through the consumption of plant-based food items (Feng et al., 2021). Hence, it is important to study its effects and outcomes in living organisms. In the case of plants, Se triggers various metabolic activities by assisting in the biosynthesis of selenoenzymes. Selenoenzymes act as antioxidants and safeguard cellular membranes through the detoxification of reactive oxygen species (ROS) (Abou El-hamd and Ahmed, 2021). Nevertheless, the pro-oxidant activity of a higher concentration of Se causes oxidative damage and reduces plant growth (Galić et al., 2021). Similarly, different types of this element also induce varying effects on different plant tissues (Zulfiqar et al., 2022). Sulfur (S) and Se use similar S-transporter pathways in plants and form selenomethionine (SeMet) or selenocysteine (SeCys) (Hossain et al., 2021). The methylated form of Se is non-toxic for various plants (Sarwar et al., 2020).

It is a universal truth that conventional breeding techniques, as well as genetic engineering, may help in the development of cultivars with good germination potential and yield. However, these breeding techniques are time-consuming, while genetic engineering has become a contentious approach (Johnson and Puthur, 2021). To overcome such difficulties, plant genes of the abiotic stress-tolerant Brassicaceae family have been characterized during the last three decades and are being further exploited for the development of varieties with higher productivity (Zhu et al., 2021). The cost of genetic engineering and conventional breeding procedures for the development of stress-tolerant cultivars is a significant constraint to the success of these approaches. Therefore, economical and eco-friendly techniques are necessary to raise successful crops under extreme environmental conditions. Seed priming using different elements, including phytohormones, acids, salts, vitamins, and minerals, may induce stress tolerance in developing seedlings to help combat biotic and abiotic stresses (Alves et al., 2021; Zaid et al., 2022). However, determining the appropriate concentration and priming duration of the nutri-priming agents is crucial in enhancing seed vigor and alleviating plant stress (Kumar et al., 2020). Therefore, it is mandatory to observe the prior optimization of nutrients such as Se before their use as priming elements. Researchers have confirmed the beneficial effects of Se as a priming agent, yet there is a dearth of information on the application of this dynamic nutrient in the case of turnip stress alleviation under saline regimes.

Turnip (*Brassica rapa*) is a common horticultural crop cultivated worldwide. The seeds of this crop are used for the extraction of cooking oil and biofuel (Cartea et al., 2019). In contrast, the foliage and root of *B. rapa* are used as a vegetable. Moreover, the glucosinolates isolated from this plant have tremendous medicinal value in the treatment of various types of cancer (Paul et al., 2019). Unfortunately, the continuously increasing salinity has reduced the yield of this crop in salt-affected areas of the world.

Salinity is a common cause of abiotic stress in plants, which may cause 65% yield loss in crop plants (Esmaeili et al., 2021). Higher salt accumulation in arable land impedes the physiological and biochemical activities of plants by inducing salinity stress (Fariduddin et al., 2019). The increased uptake and translocation of sodium ions (Na^+) reduces the water uptake in plants, resulting in the induction of osmotic stress. Similarly, elevated levels of Na^+ reduce the uptake of essential plant mineral cations such as calcium (Ca^{2+}) and potassium (K^+) (Kapadia et al., 2021). Decreased levels of Ca^{2+} and K^+ cause the deterioration of cellular integrity and hamper plant growth (Alnusairi et al., 2021). In addition, higher levels of ROS induce oxidative damage in salt-stressed plants (Challabathula et al., 2022). Salinity stress spoils the photosynthetic machinery, impedes physiological progressions, including stomatal conductivity, and decreases the leaf area of plants (Ahanger et al., 2019).

Keeping in view the beneficial effects of Se seed priming in various crops, it was assumed that priming *B. rapa* seeds with this dynamic element could enhance seed germination and seedling growth by favoring the growth, related physiochemical activities, synthesis of photosynthetic pigments, and improvement of the antioxidant machinery under salt stress. The core objective of the

current study was to unravel the potential application of Se seed priming in regulating *B. rapa* germination and seedling growth under saline conditions. The priming-induced modulations of the physiological and metabolic characteristics of *B. rapa* seeds and seedlings were also explored and compared.

Methodology

Seed priming and growth conditions

The present research work was carried out in a laboratory at the Institute of Botany, University of the Punjab, Lahore, Pakistan. The experiments had a completely randomized design (RCBD), which included eight treatments and five replications. The treatments used Se as the seed priming agent administered at three concentration levels—75 μmo L^{-1} (Se-1), 100 μmo L^{-1} (Se-2), and 125 μmo L^{-1} (Se-3)—and one level of salt stress given as 200 mM NaCl, in accordance with Sogoni et al. (2021). Distilled water was used as the control. Uniform, healthy-looking seeds of *B. rapa* var. Purple Top White Globe, obtained from Ayub Agricultural Research Institute (AARI), Faisalabad, Pakistan, with 10% initial moisture content (dry weight basis), were surface sterilized by dipping them in a 0.5% solution of sodium hypochlorite for 3 min. The sterilized seeds were subsequently washed meticulously with distilled water. For Se pretreatment, air-dried seeds were soaked in the respective Se solution (75, 100, or 125 μmo L^{-1}) prepared by dissolving Na_2SeO_3 in distilled water. The glass flasks containing these seeds were placed in the dark overnight for 12 h at room temperature and aerated with an orbital shaker. The primed seeds were then removed from the flask and dried by placing them over two coats of sterile blotting papers. The seeds were then air-dried at room temperature. Afterward, nine seeds from each treatment were placed over two coats of sterile filter papers in 90-mm Petri plates. Subsequently, 10 ml NaCl solution (200 mM) was added to allocated Petri plates as the designated stress level, while distilled water was used in others. All Petri dishes were placed inside a growth chamber with a light intensity of 18 μmol photon m^{-2} s^{-1} (16-h light/8-h dark) at 25°C. Seeds showing at least ≥2 mm radical growth were considered germinated. Germination data were recorded after 5, 10, and 15 days.

The equation proposed by Ellis and Roberts (1981) was employed to analyze the germination percentage (final germination percentage, FGP) after 5, 10, and 15 days of sowing.

$$\text{FGP} = \frac{\text{No. of seeds germinated after 15 days}}{\text{Total number of seeds}} \times 100$$

The 15-day-old seedlings were then removed from the Petri plates, rinsed three times with distilled water, followed by surface drying by placing them over the blotting papers, and then immediately stored in liquid nitrogen for further examination.

Estimation of biomass production

The seedling length was analyzed using a scale, while fresh weight was measured using an electrical weight balance.

Quantification of total soluble sugar, total soluble protein, proline, and malondialdehyde contents

The content of total soluble sugar (TSS) in the seedlings was analyzed employing the anthrone technique developed by Irigoyen et al. (1992). Bradford's (1976) technique was followed to calculate the content of total soluble protein (TSP), while proline content was quantified using the method of Bates et al. (1973). For the estimation of the malondialdehyde (MDA) level, the extent of lipid peroxidation was measured using thiobarbituric acid (TBA), as illustrated by Heath and Packer (1968).

Estimation of chlorophyll content

The contents of chlorophyll a (Chl *a*), chlorophyll b (Chl *b*), carotenoids, and total chlorophyll from the prewashed fresh foliage samples were determined according to Lichtenthaler and Wellburn (1983). For this purpose, a 0.1-g shoot sample was homogenized with 20 ml of 80% acetone (*v*/*v*) and centrifuged at 10,000 × *g* for 3 min, then stored and covered on ice until use. Thereafter, the spectrophotometric value of the extract was observed at 663, 645, and 480 nm to calculate the Chl *a*, Chl *b*, and total chlorophyll contents, respectively. The carotenoids were extracted with 80% acetone and assessed according to Lichtenthaler (1987).

Estimation of α-amylase activity

After 15 days of incubation, the crude extract from the treated seedlings was prepared according to Sottirattanapan et al. (2017) by centrifugation at 10,000 × *g* for 10 min at 4°C. The activity of α-amylase from the supernatant was quantified according to the 3,5-dinitrosalicylic acid technique of Miller (1959) by observing the absorbance at 540 nm.

Quantification of Se content and Na uptake

The number of mineral nutrients, including Na and Se, was examined from the finely ground oven-dried plant samples. The Na content was estimated using a flame photometer (Baruah

et al., 1998). The technique developed by Thimmaiah (1999) was used to estimate the Se content.

Activity of antioxidant enzymes

A foliage sample (1 g) ground with liquid nitrogen was mixed with pre-chilled potassium phosphate buffer (50 mM) along with 1% (*w*/*v*) polyvinylpyrrolidone and 2 mM Na-EDTA (pH 7.0). The solution was centrifuged at 14,000 × *g* for 15 min at 4°C. The activities of antioxidant enzymes, including catalase (CAT), peroxidase (POD), and superoxide dismutase (SOD), were analyzed from the resulting supernatant using the methods of Chance and Maehly (1955); Aebi (1974), and Dhindsa et al. (1981), respectively.

RNA extraction and gene expression

Another independent experiment was conducted in which the freshly detached shoot sample of 15-day-old Se-2-treated *B. rapa* plants was immediately stored in liquid nitrogen. For the extraction of total RNA, the TransZol Up reagent (TransGen Biotech, Beijing, China) was used. RNA quality and quantity were analyzed using the Nanodrop 2000 spectrophotometer (Thermo Fisher Scientific, Waltham, MA, USA). For complementary DNA (cDNA) production, 2 µg RNA was transferred into the TransScript One-Step gDNA Removal and cDNA Synthesis SuperMix kit according to the manufacturer's instructions (TransGen Biotech, Beijing, China). Subsequently, a 1:10 dilution of cDNA was used for quantitative real-time PCR analysis with the TransStart Tip Green qPCR SuperMix (TransGen Biotech, Beijing, China) attached to a Roche LightCycler 480 thermal cycler instrument (384-well; Roche, Basel, Switzerland). The primers listed below were used to assess the expression levels of the *APX*, *SOD*, *POD*, and *CAT* genes (Zhang et al., 2020).

Primer sequences (5′–3′)

Genes	Forward	Reverse
SOD	TCACTGACAGCCAGATTCCTC	CCTGCGTTTCCAGTAGACAA
CAT	GCCGAACCCGAAAACAAA	GTCATCAAACATCCAGCACCA
APX	CCCATTCGGAACAATGAGGT	ACAGCCACAACACCAGCAAG
POD	CTCCCACCGTATCCTCG	CGTGCTGCTCAAAGTCG

Statistical analysis

The data obtained were presented as the average of five replicates. The influence of the different treatments was evaluated using analysis of variance *via* the general linear model process of Statistical Analysis System (SAS Statistix 8.1 software). Tukey's honestly significant difference test was used to analyze differences in the mean values of various treatments at a 5% significance level.

Results

Germination percentage and seedling growth

The results of the present study showed that, during seedling germination, salinity stress (200 mM NaCl) significantly inhibited *B. rapa* seed germination by 53% compared to seeds grown in the control condition (Table 1). However, Se pretreatment improved the FGP by 88% and 100% in the stressed and non-stressed conditions, respectively (Table 1). Of the three priming treatments, Se-2 (100 µmo L^{-1}) and Se-3 (125 µmo L^{-1}) were 100% more effective in restoring the FGP compared to Se-1 (75 µmo L^{-1}), which restored the FGP by 88% after 15 days of germination. Se-primed seedlings grown without NaCl stress showed a relatively enhanced seedling length (58%) compared to the control, indicating the positive influence of Se (Table 1). Salinity stress inhibited seedling length by 45% and 30% compared to the control at 10 and 15 days, respectively (Table 1). Seed priming with Se-2 enhanced the length of *B. rapa* seedlings by 33% when grown under NaCl stress conditions.

Biomass production

Salinity stress reduced the seedling biomass accumulation by 55% compared with non-NaCl stress (Table 1). When Se-primed seeds were grown under non-stressed conditions, these seedlings exhibited 52% and 18% significantly higher biomass production compared to the salt-stressed and non-stressed conditions, respectively (Table 1).

Chlorophyll content

Selenium seed priming, particularly Se-2 (100 µmo L^{-1}), showed beneficial effects on the biosynthesis of photosynthetic contents, with increases in Chl *a*, Chl *b*, carotenoids, and total chlorophyll of 28%, 34%, 62%, and 37%, respectively, in *B. rapa* seedlings developing under normal conditions (Table 2). Se-2-treated seedlings exhibited a significantly elevated photosynthetic content compared to seedlings grown in the NaCl-spiked and control conditions (Table 2).

TABLE 1 Influence of Se pretreatment on seed germination (in percent) and vegetative growth of *Brassica rapa* seedlings under saline conditions.

Treatments	FGP			Seedling length (cm)	Seedling fresh weight (g/plant)
	5 DAS (%)	10 DAS (%)	15 DAS (%)		
Control	30.55 ± 0.48f	100 ± 0.00a	100 ± 0.00a	8.94 ± 0.092b	0.87 ± 0.086a
NaCl	11.12 ± 0.25g	41.67 ± 0.40d	52.76 ± 0.21c	3.06 ± 0.092f	0.64 ± 0.05e
Se-1	44.45 ± 0.48e	86.12 ± 0.40bc	88.89 ± 0.41b	7.84 ± 0.23c	1.04 ± 0.05bc
Se-2	66.65 ± 0.28a	95.12 ± 0.25ab	100 ± 0.00a	13.02 ± 0.33a	1.66 ± 0.08a
Se-3	86.11 ± 0.62a	100 ± 0.00a	100 ± 0.00a	6.06 ± 0.12d	0.98 ± 0.07cd
NaCl+Se-1	55.56 ± 0.40d	77.76 ± 0.28c	88.89 ± 0.21b	5.6 ± 0.17de	0.96 ± 0.52cd
NaCl+Se-2	88.89 ± 0.25c	88.89 ± 0.25bc	100 ± 0.00a	9.7 ± 0.21b	1.2 ± 0.07b
NaCl+Se-3	77.78 ± 0.85b	94.45 ± 0.21b	100 ± 0.00a	4.7 ± 0.23e	0.83 ± 0.03d

Data presented are the mean ± SD of five replications. Different letters denote significant differences between treatments at $p \leq 0.05$. NaCl = 200 mM NaCl; Se-1 = 75 µmo L^{-1} Se; Se-2 = 100 µmo L^{-1} Se; Se-3 = 125 µmo L^{-1} Se.
FGP, final germination percentage; DAS, days after sowing; C, control.

Total soluble sugar, protein content, and α-amylase activity

With Se priming, significantly higher TSS and TSP contents up to 48% and 41%, respectively, were recorded compared to control seedlings grown without NaCl stress (Table 2). In addition, Se seed priming affected the TSS and TSP by 36% and 43%, respectively, under salinity stress. In particular, Se-2 improved the TSS and TSP contents by 48% and 45%, respectively, as opposed to NaCl-treated seedlings alone. The data from the current study depicted 75% higher activity of the α-amylase enzyme in Se-pretreated seedlings compared to non-Se-primed seedlings. The interactive effects of Se and NaCl resulted in a 33% increase in α-amylase activity compared to the control condition. Statistical analysis revealed that Se-2-treated plants significantly exhibited maximum α-amylase activity and soluble sugar content (33% and 21%, respectively) under both stressed and non-stressed conditions (Table 3).

Proline content

Salinity stress enhanced the biosynthesis of proline by 21% (Figure 1). Additional proline was synthesized in salt-stressed plants that received Se-2 pretreatment; generally, Se-2-treated seedlings exhibited 14% more proline content than those grown in the normal condition (Figure 1). The effect of Se treatment under the stress condition was observed between Se-2 and NaCl for proline synthesis in treated seedlings, which enhanced the level of proline in treated seedlings by 13% compared to the control condition.

Effect of Se on the H_2O_2 and MDA levels

Salt stress enhanced the H_2O_2 and MDA contents in *B. rapa* seedlings by 29% and 33%, respectively, compared to the control conditions. However, under salinity regimes, lower

TABLE 2 Influence of Se pretreatment on the photosynthetic pigments and total soluble protein of *Brassica rapa* seedlings under saline conditions.

Treatments	Chlorophyll *a* (mg g^{-1} FW)	Chlorophyll *b* (mg g^{-1} FW)	Total chlorophyll (mg g^{-1} FW)	Total soluble protein (mg g^{-1} FW)	Carotenoids (µg/g FW)
Control	0.93 ± 0.02d	1.02 ± 0.06d	0.97 ± 0.04e	1.98 ± 0.18cd	0.71 ± 0.05cd
NaCl	0.46 ± 0.06e	0.41 ± 0.06f	0.43 ± 0.24f	0.84 ± 0.40f	0.67 ± 0.13d
Se-1	2.63 ± 0.31b	2.21 ± 0.56b	2.42 ± 0.21b	2.40 ± 0.34b	0.20 ± 0.01e
Se-2	3.22 ± 0.28a	2.94 ± 0.49a	2.58 ± 0.14a	4.84 ± 0.21a	1.13 ± 0.22ab
Se-3	1.63 ± 0.40cd	1.19 ± 0.11c	1.41 ± 0.22d	1.53 ± 0.20e	1.22 ± 0.20a
NaCl+Se-1	1.51 ± 0.23cd	1.20 ± 0.24c	1.36 ± 0.15d	1.51 ± 0.30d	0.14 ± 0.01f
NaCl+Se-2	2.04 ± 0.34c	1.72 ± 0.39bc	1.89 ± 0.16c	1.92 ± 0.45c	1.14 ± 0.22ab
NaCl+Se-3	0.98 ± 0.03d	0.89 ± 0.06e	0.94 ± 0.04e	1.46 ± 0.16d	0.86 ± 0.21c

Data presented are the mean ± SD of five replications. Different letters denote significant differences between treatments at $p \leq 0.05$. NaCl = 200 mM NaCl; Se-1 = 75 µmo L^{-1} Se; Se-2 = 100 µmo L^{-1} Se; Se-3 = 125 µmo L^{-1} Se.
FW, fresh weight.

TABLE 3 Influence of Se pretreatment on total soluble sugar, α-amylase, and nutrient content of *Brassica rapa* seedlings under saline conditions.

Treatments	α-Amylase (U g^{-1} FW)	Total soluble sugar (mg g^{-1} FW)	Selenium (mg g^{-1} DW)	Na^+ (mg g^{-1} DW)
Control	4.51 ± 1.11b	1.68 ± 0.22d	0.41 ± 0.04c	12.81 ± 0.31de
NaCl	1.45 ± 0.12e	0.82 ± 0.05f	0.09 ± 0.12d	28.15 ± 0.41a
Se-1	3.6 ± 0.54c	3.48 ± 0.21b	0.85 ± 0.06a	8.34 ± 0.42ef
Se-2	5.98 ± 0.45a	4.26 ± 0.05a	0.96 ± 0.02a	6.42 ± 0.32f
Se-3	4.11 ± 0.14bc	2.42 ± 0.34c	0.74 ± 0.06ab	9.13 ± 1.00e
NaCl+Se-1	2.34 ± 0.55d	1.66 ± 0.26d	0.57 ± 0.14bc	21.36 ± 1.31b
NaCl+Se-2	4.34 ± 1.01bc	2.24 ± 0.57c	0.61 ± 0.02bc	13.48 ± 0.60d
NaCl+Se-3	3.23 ± 0.21c	1.22 ± 0.21e	0.48 ± 0.05c	14.68 ± 0.97c

Data presented are the mean ± SD of five replications. Different letters denote significant differences between treatments at $p \leq 0.05$. NaCl = 200 mM NaCl; Se-1 = 75 µmo L^{-1} Se; Se-2 = 100 µmo L^{-1} Se; Se-3 = 125 µmo L^{-1} Se.
FW, fresh weight; DW, dry weight.

levels of H_2O_2 and MDA were recorded in Se-treated seedlings in the order Se-2, Se-1, and Se-3 (Figure 1). An antagonistic effect was observed between Se-2 and NaCl regarding the biosynthesis of H_2O_2 and MDA, which decreased by 48% and 49%, respectively, compared to the normal condition (Figure 1). A significantly reduced level of MDA was depicted by Se-2-pretreated seedlings compared to control seedlings under salt stress conditions.

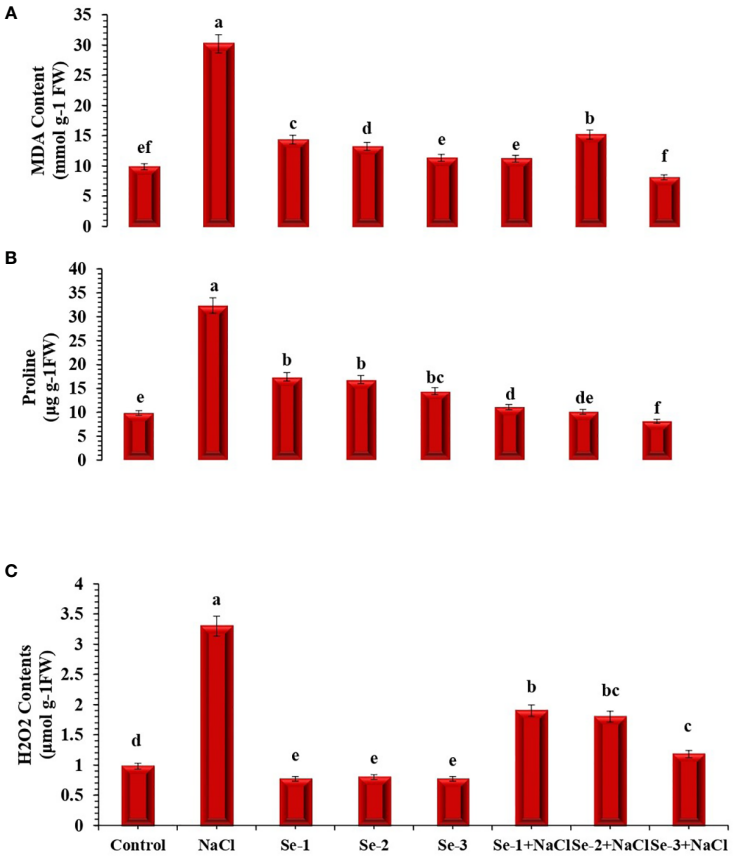


FIGURE 1
Influence of Se pretreatment on the non-enzymatic content of *Brassica rapa* seedlings under saline conditions. **(A)** Malondialdehyde (MDA). **(B)** Proline. **(C)** Hydrogen peroxide (H_2O_2). Data presented are the mean ± SD of five replications. *Different letters* denote significant differences between treatments at $p \leq 0.05$. *C*, control. *NaCl* = 200 mM NaCl; *Se-1* = 75 µmo L^{-1} Se; *Se-2* = 100 µmo L^{-1} Se; *Se-3* = 125 µmo L^{-1} Se.

Se-priming enhanced the Se content by reducing the Na uptake

Salt toxicity significantly decreased the uptake of Se by 21% compared to the control condition. Nevertheless, improved plant nutrition was observed in Se-primed seedlings in all conditions compared to salt-stressed seedlings not treated with Se. The current research revealed that Se-2 was the most effective treatment regarding Se uptake, which increased Se by 13% and reduced Na uptake by 17% in both the control and salinity-stressed *B. rapa* plants. Moreover, Se-2 significantly enhanced the uptake of Se in both stressed and non-stressed conditions by 11% and 14%, respectively, compared to the control condition (Table 3).

Activity of antioxidant enzymes

Higher SOD activity was observed in Se-2-treated *B. rapa* seedlings under both stressed and non-stressed conditions, which increased by 29% and 19% as compared to the control. When subjected to salinity stress, the Se-2-treated seedlings revealed an elevated SOD activity compared to the control under both stressed and non-stressed conditions (20% and 23%, respectively) (Figure 2). Se priming enhanced the

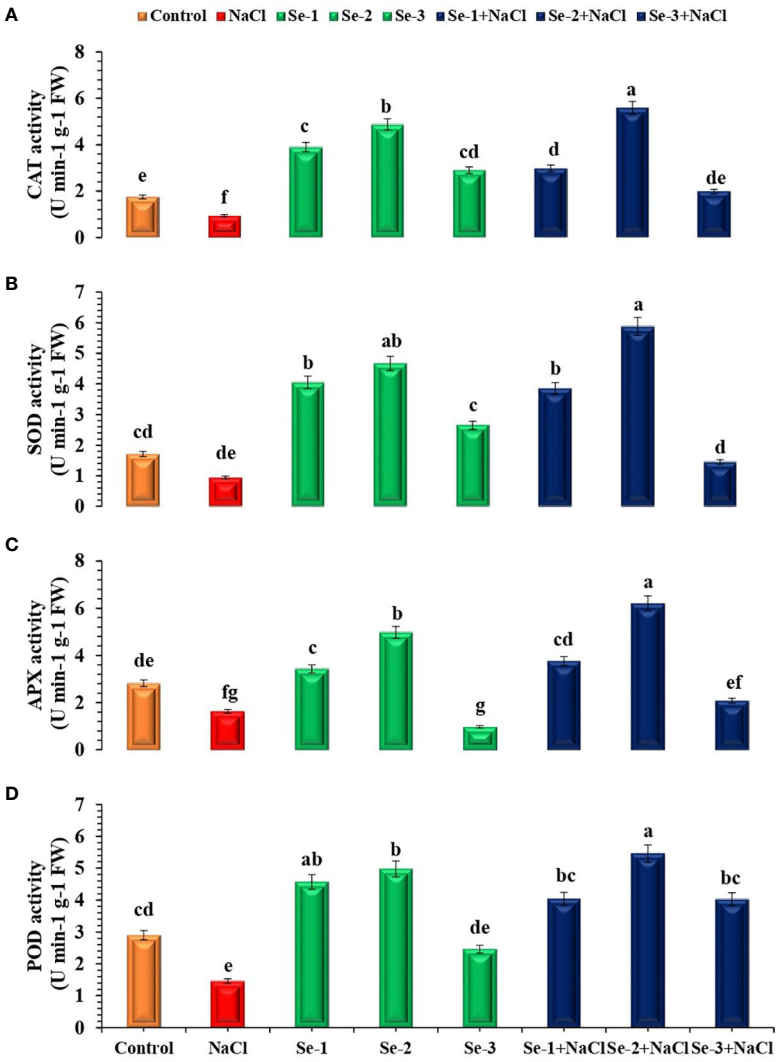


FIGURE 2
Influence of Se pretreatment on the antioxidant activity of *Brassica rapa* seedlings under saline conditions. **(A)** Catalase (CAT). **(B)** Superoxide dismutase (SOD). **(C)** Ascorbate peroxidase (APX). **(D)** Peroxidase (POD). Data presented are the mean ± SD of five replications. *Different letters* denote significant differences between treatments at $p \leq 0.05$. *C*, control. *NaCl* = 200 mM NaCl; *Se-1* = 75 µmo L^{-1} Se; *Se-2* = 100 µmo L^{-1} Se; *Se-3* = 125 µmo L^{-1} Se.

ascorbate peroxidase (APX) activity in treated seedlings by 26% compared to normal conditions. Moreover, Se-2-pretreated seedlings showed 30% and 24% augmented APX activity under stressed and non-stressed conditions, respectively, compared to the control (Figure 2). Priming with Se increased the activity of CAT by 35% and that of POD by 43% compared to the control condition. Statistical analysis revealed that Se-2-primed seeds exhibited 16% and 35% elevation of the activity of CAT in both stressed and non-stressed conditions, respectively, compared to the control condition. The same pattern was observed for POD in Se-treated seedlings grown in stressed and non-stressed conditions (Figure 2). In this case, Se-2-treated non-stressed and stressed seedlings demonstrated 34% and 18% higher POD activity, respectively, compared to the control condition.

Expression of antioxidant genes

Salinity and Se-2 treatment modulated the expression levels of the stress-responsive genes compared to the control condition. The transcript level of the *APX* gene was enhanced by about 1.6-fold with the administration of Se-2 to salt-stressed *B. rapa* plants. Salt-stressed plants that received Se-2 treatment exhibited a 2.96-fold higher expression of *APX* than that of control plants under saline conditions (Figure 3). The expression level of *CAT* was elevated by 4.2-fold in salt-stressed *B. rapa* plants compared to the control. Similarly, the transcript level of *CAT* increased by 3.98-fold in Se-2-treated plants subjected to salinity stress. Salt-treated plants demonstrated a 1.8-fold higher transcript level of *SOD* compared to the control. Similarly, the application of Se-2 upregulated the expression of *SOD* by 3.87-fold compared to control plants under saline regimes. It was also observed that the transcript level of *POD* was elevated by 2.9-fold when *B. rapa* plants were grown under salt stress compared to the control. Additionally, there was a 4.2-fold increase in gene expression in Se-2-treated plants under salt stress.

Discussion

Appropriate seed germination is one of the primary initial growth phases that determine the future growth, stand, and yield of crop plants, especially under biotic and abiotic stresses. The data of the current study revealed that salt stress significantly reduced the germination percentage and early seedling growth of *B. rapa*. Several other studies have demonstrated the harmful effects of salinity stress on seed germination and the growth of seedlings (Gamalero and Glick, 2022). Selenium is not regarded as a fundamental nutrient because minute concentrations of this element may have harmful or beneficial effects on the growth of different plant species (Ismael et al., 2019; Hasanuzzaman et al., 2020; Buturi et al., 2021). In this study, the application of Se to salt-stressed *B. rapa* through seed priming elucidated the versatile features of this element. Data from the present study showed that salinity severely affected seed germination. Similar results of salt stress on the seed germination of other plants have been reported by various researchers (Egamberdieva et al., 2019). However, in the current study, different concentrations of Se showed multifaceted results under optimal and stressed conditions. It was found that seed pretreatment with Se-2 solution (100 μmo L^{-1}) was more effective in alleviating salt stress and enhancing seed germination and seedling growth compared to the other two priming concentrations. A lower concentration of Se used for seed priming enhanced seed germination and seedling growth (Moulick et al., 2018). However, Se toxicity at a higher concentration induced negative effects, resulting in a decrease in the growth parameters (Çatav et al., 2022). In this study, the lower Se concentration (Se-1, 75 μmo L^{-1}) decreased salinity stress and improved growth under both stressed and non-stressed conditions (Table 1). The higher Se concentration (Se-2, 100 μmo L^{-1}) alleviated NaCl stress by improving the germination index, seedling length, and fresh weight in stressed plants; however, Se induced toxicity at the highest concentration (Se-3, 100 μmo L^{-1}), which decreased the germination index, seedling length, and fresh weight in non-stressed plants (Table 1). A lot of researchers have reported the interactive effects of Se and salt stress in hydroponic conditions. The results of these studies showed that the adverse effects of salt stress on the germination and growth of seedlings may be mitigated by seed priming with Se. Nevertheless, there is a dearth of knowledge describing the potential of seed pretreatment with various Se concentrations in alleviating salt stress in vegetable crops (Table 1). The experimental study results demonstrated the beneficial role of Se seed priming in the alleviation of salt stress, and we advocate using this strategy to prevail over salinity issues in arable areas.

The photo-oxidation reactivity triggered by salinity increased the biosynthesis of superoxide radicals and hydrogen peroxide (H_2O_2). The augmented synthesis of superoxide radicals and H_2O_2 decreased the chloroplast and thylakoid membranes, resulting in the degradation of the photosynthetic pigments, including Chl *a*, Chl *b*, carotenoids, and total chlorophyll (Rejeb, 2015). Additionally, the elevated activity of chlorophyllase and the cellular injuries under saline conditions caused chlorophyll deprivation and reduced the water content in plants (Aazami et al., 2021; Giordano et al., 2021). In the present research, the higher concentration of chlorophyll in Se-2-treated seedlings suggests the efficacy of Se in alleviating the degradation of Chl *a*, Chl *b*, carotenoids, and total chlorophyll by reducing the negative impacts of salt stress (Table 2). Earlier reports also illustrated that exogenously applied Se decreased the degradation of photosynthetic pigments in crops subjected to abiotic stresses (Andrade et al., 2018; Amin et al., 2020; Farooq et al., 2020).

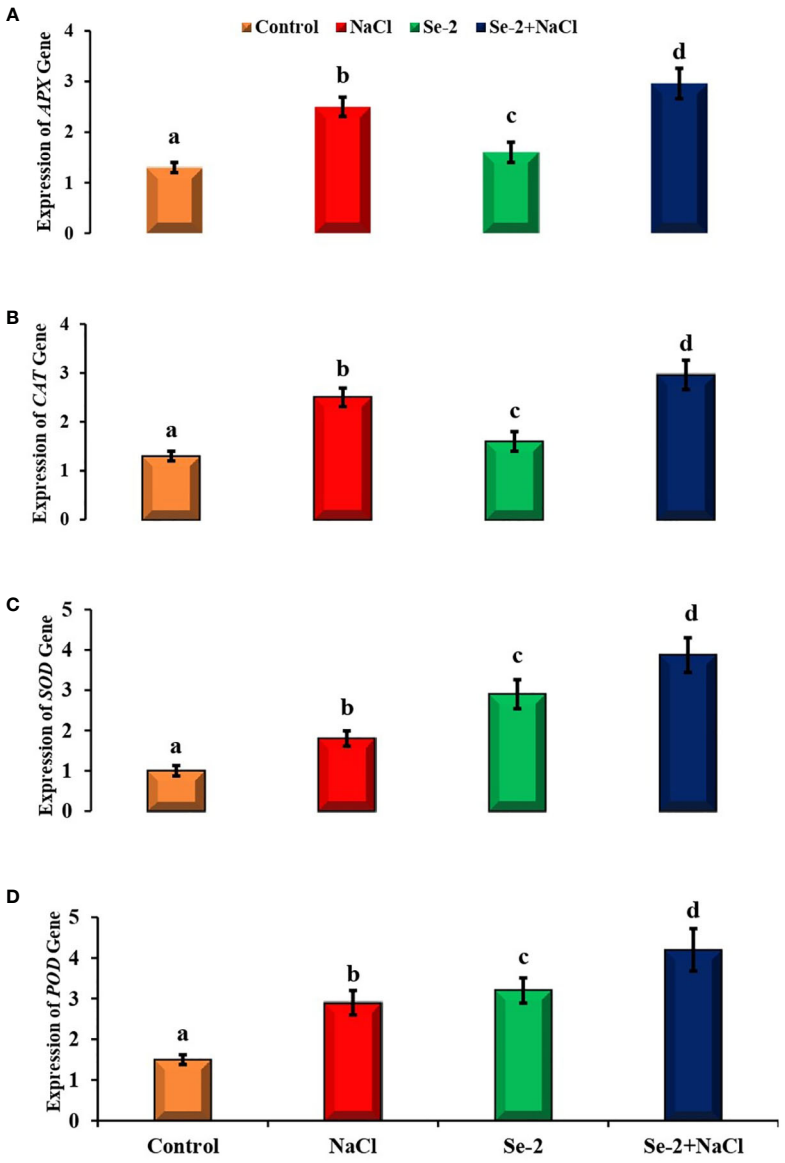


FIGURE 3
Quantitative real-time PCR analysis of the transcript levels of antioxidant defense-related genes in the shoots of turnip plants treated with Se and NaCl. **(A–D)** Relative expression of the *APX* **(A)**, *CAT* **(B)**, *SOD* **(C)**, and *POD* **(D)** genes. *Bars* represent the mean values of three independent experiments with standard errors. *Different letters* denote significant differences between treatments ($p \leq 0.05$). *C*, control. *NaCl* = 200 mM NaCl; *Se-2* = 100 µmo L^{-1} Se.

The findings of the present research exhibited improvements in the production of total soluble proteins and in the sugar content of Se-pretreated seedlings. The higher protein level in halotolerant plants under saline conditions reduces cellular damage and enables these plants to sustain membrane integrity (Singh and Jha, 2017). Selenium alters the metabolic activities of amino acids to augment protein synthesis by replacing the sulfur ions in sulfur, including amino acids such as cysteine and methionine (Ahmad et al., 2017; Yilmaz et al., 2018). Hence, it may be assumed that the modulated metabolism in Se-2-treated salt-stressed seedlings encouraged higher protein synthesis. Parallel to the results of the current study, Põldma et al. (2013) found an amplified concentration of total soluble protein in Se-treated plants subjected to salt stress. The results of the study showed that NaCl reduced the biosynthesis of TSS in stressed seedlings (Table 2), whereas Se pretreatment enhanced the synthesis of TSS. Nasibi et al. (2022) revealed that soluble sugars reduce the membrane osmotic potential and decrease water loss by binding to the membrane lipid bilayer. Sugars form hydrogen bonds with polar polypeptide residues and avert

protein deprivation (Zhang et al., 2021). The increased concentration of TSS in Se-treated seedlings decreased cellular damage by regulating a balance among the cellular vacuole, osmotic cytosol intensity, and external medium that uphold cell turgor (Kaur et al., 2021; Kumari et al., 2021). Our results also demonstrated higher activity of α-amylase and soluble sugar content in Se-primed seedlings (Table 3).

Plants enhance the synthesis of stress-responsive proline to decrease protein degradation, detoxify the augmented level of ROS, and maintain membrane integrity (Mohammadi and Roshandel, 2020). Several studies have confirmed the stress alleviation efficiency of this low-molecular-weight organic solute (Zhu et al., 2020). The results of the current study also showed higher proline accumulation in NaCl-stressed seedlings (Figure 1). Selenium application further enhanced proline accumulation in treated seedlings under stress. Stress alleviation through higher proline synthesis in Se-treated salted plants has been observed by El Moukhtari et al. (2020) and Umair et al. (2020) in *Phaseolus vulgaris* and *Breasica oleracae* crops, respectively. Proline is a stress biomarker that acts as an osmolyte to maintain cellular integrity and scavenge ROS (Kaur et al., 2021). Proteolysis and conservation of the proline precursors enhance the level of this osmoprotectant in plants subjected to salt stress (Kaur et al., 2021). The increased level of proline helps in the reduction of ROS and MDA levels in salt-stressed plants (Zhang et al., 2021). The higher Se content in Se-treated seedlings may have accomplished some basic functions of proline regarding the alleviation of salt stress. Ibrahim (2014) also found decreased proline content in Se-pretreated wheat plants under drought stress.

Salt stress enhances the biosynthesis of H_2O_2, which is the foundation of cellular contraction, apoptosis, DNA disintegration, and chromatin abridgment (Jeong et al., 2022). Enzymatic and non-enzymatic antioxidants assist in stress mitigation by scavenging the higher level of H_2O_2 (Danouche et al., 2020). In this study, Se-2 seed priming significantly decreased the levels of H_2O_2 in treated plants (Figure 1). The study results concerning the lower accumulation of H_2O_2 in Se-treated salt-stressed seedlings are in agreement with the findings of Rady et al. (2021) and Rehman et al. (2022). Similarly, salt-stressed *B. rapa* seedlings showed a higher MDA content than the control. Conversely, Se-2 pretreatment significantly lowered the MDA content in NaCl-stressed plants (Figure 1). The seedlings developed from Se-2-primed seeds exhibited decreased MDA levels compared to the non-Se-treated seedlings under salt stress, signifying the function of Se in reducing lipid peroxidation through improving the antioxidant system, which safeguarded the membrane integrity (Li et al., 2019; Soleymanzadeh et al., 2020). The present findings are also validated by other studies that showed that exogenous Se application decreased the MDA levels in other plant species under stress (Huang et al., 2018; Ulhassan et al., 2019).

The Na^+ ion content was lower in Se-primed seedlings compared to non-primed seedlings. It is assumed that a similar transporter is shared by Se and Na. Hence, the antagonistic relationship between Se and Na may have reduced the translocation of Na ions. Selenium reduced the Na^+ content in treated seedlings through binding it to the cell wall of the root (Habibi, 2017). The cysteine synthase enzyme converts the inorganic Se absorbed by the aleurone layer of seeds into organic Se (Hu et al., 2022). The results of this study revealed that the lower concentration of Se (75 μmo L^{-1}) effectively decreased the Na content in salt-stressed plants (Table 3). Some early studies have shown that the application of a lower concentration of inorganic Se easily converts into the organic forms of Se, such as SeMet and selenomethyl cysteine, which have antioxidant capacity and can alleviate plant stress (Wrobel et al., 2020; Gui et al., 2022).

Salt-induced oxidative stress augments ROS biosynthesis and impedes the root growth, shoot growth, and biomass production of plants. Antioxidant enzymes, including SOD, APX, CAT, and POD, alleviate oxidative damage by scavenging the higher level of ROS (Jahan et al., 2019; Moustafa-Farag et al., 2020). These enzymes protect plants from ROS-induced plasma membrane peroxidation (Sharma et al., 2020). The current study showed elevated SOD, APX, CAT, and POD activities in Se-2-treated salt-stressed seedlings. The findings of the current research are compatible with preceding studies showing that exogenously supplemented Se improved the activity of SOD, APX, CAT, and POD in salt-stressed seedlings (Sheikhalipour et al., 2021; Jabeen et al., 2021). Higher enzyme activity may have detoxified free radicals and decreased ROS-induced oxidative injury (Figure 2). El-Badri et al. (2022a) observed that exogenously applied Se upregulated the expression of stress-responsive antioxidant genes to mitigate salt stress in *B. napus* seedlings. Equally, Rossatto et al. (2017) reported that reverse transcription quantitative PCR (RT-qPCR) revealed higher expression levels of *CAT*, *APX*, and *SOD*, which detoxified ROS in rice plants to alleviate NaCl toxicity. Moreover, the data of the present research regarding the modulation of the expression levels of *POD*, *CAT*, *APX*, and *SOD* are in agreement with the findings of El-Badri et al. (2022b). They reported that modulations in the transcript levels of these antioxidant genes enhanced the activity of the respective antioxidant enzymes to induce salt tolerance by scavenging ROS in *B. napus* plants. The higher activity of these antioxidant enzymes converted H_2O_2 to H_2O. Hence, the higher water content observed in Se-2-treated seedlings may be a result of the upregulated activity and higher expression levels of these enzymes (Yaldiz and Camlica, 2021).

Conclusion

It may be concluded that Se pretreatment through seed priming at concentrations of 75 µmo L^{-1}, 100 µmo L^{-1}, and 125 µmo L^{-1} Se reduced the toxic effects of salinity stress associated with seed germination and seedling growth of *B. rapa* by reducing the Na uptake and improving the Se uptake, suppressing the oxidative damage, and by improving the antioxidant system and the expression levels of the genes involved in the antioxidant system of plants. Taken as a whole, this work provides insights toward our understanding and discovery of the specific morphophysiological and biochemical mechanisms behind Se-induced salinity stress tolerance in *B. rapa*. Conversely, additional research work is compulsory to determine the transcriptomic, metabolomics, genomics, and proteomics inflections related to salt stress alleviation in Se-treated *B. rapa* plants under field conditions.

Data availability statement

The original contributions presented in the study are included in the article/supplementary material. Further inquiries can be directed to the corresponding authors.

Author contributions

NY and SA conceived the idea for this study. SH and WA performed the experiments. SA, NY,GL and SH prepared the manuscript draft. SA,GL and NY reviewed and edited the final version. All authors contributed to the article and approved the submitted version.

Funding

This study was financially supported by the Guangdong Province Key Areas Research and Development Plan (Project No: 2022B0202110003); Guangdong Provincial special Fund for Modern Agriculture Industry Technology Innovation Teams (project nos. 2022KJ122 and 2023KJ122) and China Young Scientist Talent Program (project no. QN2022030024L).

Conflict of interest

The authors declare that the research was conducted in the absence of any commercial or financial relationships that could be construed as a potential conflict of interest.

Publisher's note

All claims expressed in this article are solely those of the authors and do not necessarily represent those of their affiliated organizations, or those of the publisher, the editors and the reviewers. Any product that may be evaluated in this article, or claim that may be made by its manufacturer, is not guaranteed or endorsed by the publisher.

References

Aazami, M. A., Rasouli, F., and Ebrahimzadeh, A. (2021). Oxidative damage, antioxidant mechanism, and gene expression in tomato responding to salinity stress under *in vitro* conditions and application of iron and zinc oxide nanoparticles on callus induction and plant regeneration. *BMC Plant Bio* 21 (1), 1–23. doi: 10.1186/s12870-021-03379-7

Abou El-hamd, N., and Ahmed, E. Z. (2021). Red kidney bean (*Phaseolus vulgaris* l.) germination and seedling growth as affected by selenium, nano-selenium, and sulfur. *J. Plant Physio. Patho.* 9:8, 261. doi: 10.3390/plant1000261

Aebi, H. (1974). "Catalase," in *Methods of enzymatic analysis* (Verlag Chemie: Academic press), 673–684. doi: 10.1016/b978-0-12-091302-2.50032-3

Ahanger, M. A., Qin, C., Begum, N., Maodong, Q., Dong, X. X., El-Esawi, M., et al. (2019). Nitrogen availability prevents the oxidative effects of salinity on wheat growth and photosynthesis by upregulating the antioxidants and osmolytes metabolism, and secondary metabolite accumulation. *BMC Plant Biol.* 19 (1), 1–12. doi: 10.1186/s12870-019-2085-3

Ahmad, S., Khan, H., Shahab, U., Rehman, S., Rafi, Z., Khan, M. Y., et al. (2017). Protein oxidation: an overview of metabolism of sulfur containing amino acid, cysteine. *Front. Bioscience-Scholar.* 9 (1), 71–87. Available at: https://agris.fao.org/agris-search/search.do?recordID=XE8182678.

Alnusairi, G. S., Mazrou, Y. S., Qari, S. H., Elkelish, A. A., Soliman, M. H., Eweis, M., et al. (2021). Exogenous nitric oxide reinforces photosynthetic efficiency, osmolyte, mineral uptake, antioxidant, expression of stress-responsive genes and ameliorates the effects of salinity stress in wheat. *Plants* 10 (8), 1693. doi: 10.3390/plants10081693

Alves, R. D. C., Rossatto, D. R., da Silva, J. D. S., Checchio, M. V., de Oliveira, K. R., Oliveira, F. D. A., et al. (2021). Seed priming with ascorbic acid enhances salt tolerance in micro-tom tomato plants by modifying the antioxidant defense system components. *Biocatalysis Agric. Biotechnol.* 31, 101927. doi: 10.1016/j.bcab.2021.101927

Amin, I., Banerjee, A., Zaid, A., Mir, M. A., Wani, S. H., Ahmed, N., et al. (2020). "Spectrum of physiological and molecular responses in plant salinity stress tolerance," in *Improving abiotic stress tolerance in plants* (Boca Raton, Florida: CRC Press), 1–12. doi: 10.1201/9780429027505-1

Andrade, F. R., da Silva, G. N., Guimarães, K. C., Barreto, H. B. F., de Souza, K. R. D., Guilherme, L. R. G., et al. (2018). Selenium protects rice plants from water deficit stress. *Ecotoxicol. Environ. Saf.* 164, 562–570. doi: 10.1016/j.ecoenv.2018.08.022

Baruah, M. K., Kotoky, P., and Borah, G. C. (1998). Gold in high sulphur Indian coals. *Fuel* 77 (15), 1867–1868. doi: 10.1016/s0016-2361(98)00082-9

Bates, L. S., Waldren, R. P., and Teare, I. D. (1973). Rapid determination of free proline for water-stress studies. *Plant Soil* 39 (1), 205–207. doi: 10.1007/bf00018060

Bradford, M. M. (1976). A rapid and sensitive method for the quantitation of microgram quantities of protein utilizing the principle of protein-dye binding. *Anal. Biochem.* 72 (1-2), 248–254. doi: 10.1016/0003-2697(76)90527-3

Buturi, C. V., Mauro, R. P., Fogliano, V., Leonardi, C., and Giuffrida, ,. F. (2021). Mineral biofortification of vegetables as a tool to improve human diet. *Foods* 10 (2), 223. doi: 10.3390/foods10020223

Cartea, E., De Haro-Bailón, A., Padilla, G., Obregón-Cano, S., del Rio-Celestino, M., and Ordás, A. (2019). Seed oil quality of *Brassica napus* and *Brassica rapa* germplasm from northwestern Spain. *Foods* 8 (8), 292. doi: 10.3390/foods8080292

Çatav, Ş.S., Köşkeroğlu, S., and Tuna, A. L. (2022). Selenium supplementation mitigates boron toxicity induced growth inhibition and oxidative damage in pepper plants. *South Afr. J. Bot.* 146, 375–382. doi: 10.1016/j.sajb.2021.11.013

Challabathula, D., Analin, B., Mohanan, A., and Bakka, K. (2022). Differential modulation of photosynthesis, ROS and antioxidant enzyme activities in stress-sensitive and-tolerant rice cultivars during salinity and drought upon restriction of COX and AOX pathways of mitochondrial oxidative electron transport. *J. Plant Physiol.* 268, 153583. doi: 10.1016/j.jplph.2021.153583

Chance, B., and Maehly, A. C. (1955). Assay of catalases and peroxidases. *Methods Enzymol.* 2, 764–775. doi: 10.1016/s0076-6879(55)02300-8

Danouche, M., El Ghachtouli, N., El Baouchi, A., and El Arroussi, H. (2020). Heavy metals phytoremediation using tolerant green microalgae: enzymatic and non-enzymatic antioxidant systems for the management of oxidative stress. *J. Environ. Chem. Eng.* 8 (5), 104460. doi: 10.1016/j.jece.2020.104460

Dhindsa, R. S., Plumb-Dhindsa, P., and Thorpe, T. A. (1981). Leaf senescence: correlated with increased levels of membrane permeability and lipid peroxidation, and decreased levels of superoxide dismutase and catalase. *J. Exp. Bot.* 32 (1), 93–101. doi: 10.1093/jxb/32.1.93

Egamberdieva, D., Wirth, S., Bellingrath-Kimura, S. D., Mishra, J., and Arora, N. K. (2019). Salt-tolerant plant growth promoting rhizobacteria for enhancing crop productivity of saline soils. *Front. Microbiol.* 10. doi: 10.3389/fmicb.2019.02791

El-Badri, A. M., Batool, M., Mohamed, I. A., Wang, Z., Wang, C., Tabl, K. M., et al. (2022a). Mitigation of the salinity stress in rapeseed (*Brassica napus* l.) productivity by exogenous applications of bio-selenium nanoparticles during the early seedling stage. *Environ. Pollut.* 310 (2), 119815. doi: 10.1016/j.envpol.2022.119815

El-Badri, A. M., Hashem, A. M., Batool, M., Sherif, A., Nishawy, E., Ayaad, M., et al. (2022b). Comparative efficacy of bio-selenium nanoparticles and sodium selenite on morpho-physiochemical attributes under normal and salt stress conditions, besides selenium detoxification pathways in brassica napus l. *J. nanobiotechnol.* 20 (1), 1–23. doi: 10.1186/s12951-022-01370-4

Ellis, R. H., and Roberts, E. H. (1981). The quantification of ageing and survival in orthodox seeds. *Seed Sci. Technol. (Netherlands)* 9 (2), 1–7. doi: 10.2841/s454

El Moukhtari, A., Cabassa-Hourton, C., Farissi, M., and Savouré, A. (2020). How does proline treatment promote salt stress tolerance during crop plant development? *Front. Plant Sci.* 11. doi: 10.3389/fpls.2020.01127

Esmaeili, N., Cai, Y., Tang, F., Zhu, X., Smith, J., Mishra, N., et al. (2021). Towards doubling fibre yield for cotton in the semiarid agricultural area by increasing tolerance to drought, heat and salinity simultaneously. *Plant Biotechnol. J.* 19 (3), 462–476. doi: 10.1111/pbi.13476

Fariduddin, Q., Zaid, A., and Mohammad, F. (2019). "Plant growth regulators and salt stress: mechanism of tolerance trade-off," in *Salt stress, microbes, and plant interactions: causes and solution* (Singapore: Springer), 91–111. doi: 10.1007/978-981-13-8801-9_4

Farooq, A., Bukhari, S. A., Akram, N. A., Ashraf, M., Wijaya, L., Alyemeni, M. N., et al. (2020). Exogenously applied ascorbic acid-mediated changes in osmoprotection and oxidative defense system enhanced water stress tolerance in different cultivars of safflower (*Carthamus tinctorious*L.). *Plants* 9 (1), 104. doi: 10.3390/plants9010104

Feng, R., Zhao, P., Zhu, Y., Yang, J., Wei, X., Yang, L., et al. (2021). Application of inorganic selenium to reduce accumulation and toxicity of heavy metals (metalloids) in plants: The main mechanisms, concerns, and risks. *Sci. Total Environ.* 771, 144776. doi: 10.1016/j.scitotenv.2020.144776

Galić, L., Špoljarević, M., Jakovac, E., Ravnjak, B., Teklić, T., Lisjak, M., et al. (2021). Selenium biofortification of soybean seeds influences physiological responses of seedlings to osmotic stress. *Plants* 10 (8), 1498. doi: 10.3390/plants10081498

Gamalero, E., and Glick, B. R. (2022). Recent advances in bacterial amelioration of plant drought and salt stress. *Biology* 11 (3), 437. doi: 10.3390/biology11030437

Giordano, M., Petropoulos, S. A., and Rouphael, Y. (2021). Response and defence mechanisms of vegetable crops against drought, heat and salinity stress. *Agriculture* 11 (5), 463. doi: 10.3390/agriculture11050463

Gui, J. Y., Rao, S., Gou, Y., Xu, F., and Cheng, S. (2022). Comparative study of the effects of selenium yeast and sodium selenite on selenium content and nutrient quality in broccoli florets (*Brassica oleracea* l. var. italica). *J. Sci. Food Agric.* 102 (4), 1707–1718. doi: 10.1002/jsfa.11511

Habibi, G. (2017). Selenium ameliorates salinity stress in petroselinum crispum by modulation of photosynthesis and by reducing shoot Na accumulation. *Russian J. Plant Physiol.* 64 (3), 368–374. doi: 10.1134/s1021443717030086

Hasanuzzaman, M., Bhuyan, M. B., Raza, A., Hawrylak-Nowak, B., Matraszek-Gawron, R., Al Mahmud, J., et al. (2020). Selenium in plants: Boon or bane? *Environ. Exp. Bot.* 178, 104170. doi: 10.1016/j.envexpbot.2020.104170

Heath, R. L., and Packer, L. (1968). Photoperoxidation in isolated chloroplasts: I. kinetics and stoichiometry of fatty acid peroxidation. *Arch. Biochem. biophysics* 125 (1), 189–198. doi: 10.1016/0003-9861(68)90654-1

Hossain, A., Skalicky, M., Brestic, M., Maitra, S., Sarkar, S., Ahmad, Z., et al. (2021). Selenium biofortification: roles, mechanisms, responses and prospects. *Molecules* 26 (4), 881. doi: 10.3390/molecules26040881

Huang, C., Qin, N., Sun, L., Yu, M., Hu, W., and Qi, Z. (2018). Selenium improves physiological parameters and alleviates oxidative stress in strawberry seedlings under low-temperature stress. *Int. J. Mol. Sci.* 19 (7), 1913. doi: 10.3390/ijms19071913

Hu, W., Su, Y., Zhou, J., Zhu, H., Guo, J., Huo, H., et al (2022). Foliar application of silicon and selenium improves the growth, yield and quality characteristics of cucumber in field conditions. *ScientiaHorticulturae* 294, 110776. doi: 10.1016/j.scienta.2021.110776

Ibrahim, H. M. (2014). Selenium pretreatment regulates the antioxidant defense system and reduces oxidative stress on drought-stressed wheat (*Triticum aestivum* l.) plants. *Asian J. Plant Sci.* 13 (3), 120–128. doi: 10.3923/ajps.2014.120.128

Irigoyen, J. J., Einerich, D. W., and Sánchez-Díaz, M. (1992). Water stress induced changes in concentrations of proline and total soluble sugars in nodulated alfalfa (*Medicago sativd*) plants. *Physiologia plantarum* 84 (1), 55–60. doi: 10.1111/j.1399-3054.1992.tb08764.x

Ismael, M. A., Elyamine, A. M., Moussa, M. G., Cai, M., Zhao, X., and Hu, C. (2019). Cadmium in plants: uptake, toxicity, and its interactions with selenium fertilizers. *Metallomics* 11 (2), 255–277. doi: 10.1039/c8mt00247a

Jabeen, Z., Fayyaz, H. A., Irshad, F., Hussain, N., Hassan, M. N., Li, J., et al. (2021). Sodium nitroprusside application improves morphological and physiological attributes of soybean (*Glycine max* l.) under salinity stress. *PLos One* 16 (4), e0248207. doi: 10.1371/journal.pone.0248207

Jahan, M. S., Wang, Y., Shu, S., Zhong, M., Chen, Z., Wu, J., et al. (2019). Exogenous salicylic acid increases the heat tolerance in tomato (*Solanum lycopersicum* l.) by enhancing photosynthesis efficiency and improving antioxidant defense system through scavenging of reactive oxygen species. *Scientia Hortic.* 247, 421–429. doi: 10.1016/j.scienta.2018.12.047

Jeong, M. J., Lim, D. S., Kim, S. O., Park, C., Leem, S. H., Lee, H., et al. (2022). Protection of oxidative stress-induced DNA damage and apoptosis by rosmarinic acid in murine myoblast C2C12 cells. *Biotechnol. Bioprocess Eng.* 27 (2), 171–182. doi: 10.1007/s12257-021-0248-1

Johnson, R., and Puthur, J. T. (2021). Seed priming as a cost effective technique for developing plants with cross tolerance to salinity stress. *Plant Physiol. Biochem.* 162, 247–257. doi: 10.1016/j.plaphy.2021.02.034

Kapadia, C., Sayyed, R. Z., El Enshasy, H. A., Vaidya, H., Sharma, D., Patel, N., et al. (2021). Halotolerant microbial consortia for sustainable mitigation of salinity stress, growth promotion, and mineral uptake in tomato plants and soil nutrient enrichment. *Sustainability* 13 (15), 8369. doi: 10.3390/su13158369

Kaur, H., Kaur, H., Kaur, H., and Srivastava, S. (2022). The beneficial roles of trace and ultratrace elements in plants. *Plant Growth Regul.* 98 (3), 1–18. doi: 10.1007/s10725-022-00837-6

Kaur, H., Manna, M., Thakur, T., Gautam, V., and Salvi, P. (2021). Imperative role of sugar signaling and transport during drought stress responses in plants. *Physiologia Plantarum* 171 (4), 833–848. doi: 10.1111/ppl.13364

Kumar, A., Droby, S., White, J. F., Singh, V. K., Singh, S. K., Zhimo, V. Y., et al. (2020). "Endophytes and seed priming: agricultural applications and future prospects," in *Microbial endophytes* (Sawston, Cambridge: Woodhead Publishing), 107–124. doi: 10.1016/b978-0-12-819654-0.00005-3

Kumari, S., Chhillar, H., Chopra, P., Khanna, R. R., and Khan, M. I. R. (2021). Potassium: A track to develop salinity tolerant plants. *Plant Physiol. Biochem.* 167, 1011–1023. doi: 10.1016/j.plaphy.2021.09.031

Lichtenthaler, H. K. (1987). "[34] chlorophylls and carotenoids: pigments of photosynthetic biomembranes," in *Methods in enzymology*, (New York: Academic Press) 148, 350–382. doi: 10.1016/0076-6879(87)48036-1

Lichtenthaler, H. K., and Wellburn, A. R. (1983). *Determinations of total carotenoids and chlorophylls a and b of leaf extracts in different solvents* (Bailrigg, Lancaster: University of Lancaster). doi: 10.1042/bst0110591

Li, J., Zhou, X., Wei, B., Cheng, S., Zhou, Q., and Ji, S. (2019). GABA application improves the mitochondrial antioxidant system and reduces peel browning in 'Nanguo'pears after removal fromcold storage. *Food Chem.* 297, 124903. doi: 10.1016/j.foodchem.2019.05.177

Miller, E. C. (1959). Technique for building amalgam restorations. *J. Prosthetic Dentistry* 9 (4), 652–667. doi: 10.1016/0022-3913(59)90138-6

Mohammadi, R., and Roshandel, P. (2020). Ameliorative effects of a static magnetic field on hyssop (*Hyssopus officinalis* l.) growth and phytochemical traits under water stress. *Bioelectromagnetics* 41 (6), 403–412. doi: 10.1002/bem.22278

Moulick, D., Santra, S. C., and Ghosh, D. (2018). Seed priming with Se mitigates as-induced phytotoxicity in rice seedlings by enhancing essential micronutrient uptake and translocation and reducing as translocation. *Environ. Sci. pollut. Res.* 25 (27), 26978–26991. doi: 10.1007/s11356-018-2711-x

Moustafa-Farag, M., Mohamed, H. I., Mahmoud, A., Elkelish, A., Misra, A. N., Guy, K. M., et al. (2020). Salicylic acid stimulates antioxidant defense and osmolyte metabolism to alleviate oxidative stress in watermelons under excess boron. *Plants* 9 (6), 724. doi: 10.3390/plants9060724

Nasibi, F., Aminian, F., Mohammadinejad, G., and Hassanshahian, M. (2022). Seed priming with selenium nanoparticle and plant growth promoting rhizobacteria improve seedling development of foxtail millet (Setaria italica) under salinity stress. *In Plant Growth Regulation*. doi: 10.21203/rs.3.rs-1809244/v1

Paul, S., Geng, C. A., Yang, T. H., Yang, Y. P., and Chen, J. J. (2019). Phytochemical and health-beneficial progress of turnip (*Brassica rapa*). *J. Food Sci.* 84 (1), 19–30. doi: 10.1111/1750-3841.14417

Põldma, P., Moor, U., Tõnutare, T., Herodes, K., and Rebane, ,. R. (2013). Selenium treatment under field conditions affects mineral nutrition, yield and antioxidant properties of bulb onion (*Allium cepa* l.). *Acta Sci. Pol. Hortorum. Cultus* 12 (6), 167–181. doi: 10.1080/01904167.2013.1952237

Rady, M. M., Desoky, E. S. M., Ahmed, S. M., Majrashi, A., Ali, E. F. , Arnaout, S. M., et al. (2021). Foliar nourishment with nano-selenium dioxide promotes physiology, biochemistry, antioxidant defenses, and salt tolerance in *Phaseolus vulgaris*. *Plants* 10 (6), 1189. doi: 10.3390/plants10061189

Rehman, S., Chattha, M. U., Khan, I., Mahmood, A., Hassan, M. U., Al-Huqail, A. A., et al. (2022). Exogenously applied trehalose augments cadmium stress tolerance and yield of mung bean (*Vigna radiata* l.) grown in soil and hydroponic systems through reducing cd uptake and enhancing photosynthetic efficiency and antioxidant defense systems. *Plants* 11 (6), 822. doi: 10.3390/plants11060822

Rejeb, K. B. (2015). *Involvement of reactive oxygen species (ros) in the regulation of antioxidant capacity and proline metabolism in arabidopsis thaliana under water stress (Doctoral dissertation, université Pierre et Marie curie-Paris VI; université de Tunis El-manar* (Faculté des Sciences de Tunis (Tunisie).

Rossatto, T., do Amaral, M. N., Benitez, L. C., Vighi, I. L., Braga, E. J. B., de Magalhães Júnior, A. M., et al. (2017). Gene expression and activity of antioxidant enzymes in rice plants, cv. BRS AG, under saline stress. *Physiol. Mol. Biol. Plants* 23 (4), 865–875. doi: 10.1007/s12298-017-0467-2

Sarwar, N., Akhtar, M., Kamran, M. A., Imran, M., Riaz, M. A., Kamran, K., et al. (2020). Selenium biofortification in food crops: Key mechanisms and future perspectives. *J. Food composition Anal.* 93, 103615. doi: 10.1016/j.jfca.2020.103615

Shafiq, S., Adeel, M., Raza, H., Iqbal, R., Ahmad, Z., Naeem, M., et al. (2019). Effects of foliar application of selenium in maize (*Zea mays* l.) under cadmium toxicity. *In Biol. Forum-An Int. J.* Vol. 11, No. 2, 27–37. doi: 10.1080/15588742.2019

Sharma, A., Soares, C., Sousa, B., Martins, M., Kumar, V., Shahzad, B., et al. (2020). Nitric oxide-mediated regulation of oxidative stress in plants under metal stress: a review on molecular and biochemical aspects. *Physiologia plantarum* 168 (2), 318–344. doi: 10.1111/ppl.13004

Sheikhalipour, M., Esmaielpour, B., Behnamian, M., Gohari, G., Giglou, M. T., Vachova, P., et al. (2021). Chitosan–selenium nanoparticle (Cs–Se NP) foliar spray alleviates salt stress in bitter melon. *Nanomaterials* 11 (3), 684. doi: 10.3390/nano11030684

Singh, R. P., and Jha, P. N. (2017). Analysis of fatty acid composition of PGPR klebsiella sp. SBP-8 and its role in ameliorating salt stress in wheat. *Symbiosis* 73 (3), 213–222. doi: 10.1007/s13199-017-0477-4

Sogoni, A., Jimoh, M. O., Kambizi, L., and Laubscher, C. P. (2021). The impact of salt stress on plant growth, mineral composition, and antioxidant activity in tetragonia decumbens mill.: An underutilized edible halophyte in south Africa. *Horticulturae* 7 (6), 140. doi: 10.3390/horticulturae7060140

Soleymanzadeh, R., Iranbakhsh, A., Habibi, G., and Ardebili, Z. O. (2020). Selenium nanoparticle protected strawberry against salt stress through modifications in salicylic acid, ion homeostasis, antioxidant machinery, and photosynthesis performance. *Acta BiologicaCracoviensia s. Botanica* 62 (1), 44–62. doi: 10.24425/abcsb.2019.127751

Sottirattanapan, P., Nantachai, K., Daduang, S., Funahashi, T., and Yamada, M. (2017). Purification and characterization of amylase from roots of paederia foetida Linn. *Biocatalysis Agric. Biotechnol.* 10, 329–335. doi: 10.1016/j.bcab.2017.04.012

Thimmaiah, S. K. (1999). *Standard methods of biochemical analysis* (New Delhi, India: Kalyani), 545.

Ulhassan, Z., Huang, Q., Gill, R. A., Ali, S., Mwamba, T. M., Ali, B., et al. (2019). Protective mechanisms of melatonin against selenium toxicity in brassica napus: insights into physiological traits, thiol biosynthesis and antioxidant machinery. *BMC Plant Biol.* 19 (1), 1–16. doi: 10.1186/s12870-019-2110-6

Umair, H. ,. M., Aamer, M., UmerChattha, M., Haiying, T., Shahzad, B., Barbanti, L., et al. (2020). The critical role of zinc in plants facing the drought stress. *Agriculture* 10 (9), 396. doi: 10.3390/agriculture10090396

Wrobel, K., Guerrero Esperanza, M., Yanez Barrientos, E., Corrales Escobosa, A. R., and Wrobel, K. (2020). Different approaches in metabolomic analysis of plants exposed to selenium: A comprehensive review. *Acta Physiologiae Plantarum* 42 (7), 1–20. doi: 10.1007/s11738-020-03113-0

Yaldiz, G., and Camlica, M. (2021). Selenium and salt interactions in sage (*Salvia officinalis* l.): Growth and yield, chemical content, ion uptake. *Ind. Crops Products* 171, 113855. doi: 10.1016/j.indcrop.2021.113855

Yilmaz, S., İlbaş, A.İ., Akbulut, M., and Çetin, A. (2018). Grain amino acid composition of barley (*Hordeum vulgare* l.) cultivars subjected to selenium doses. *Turkish J. Biochem.* 43 (3), 268–276. doi: 10.1515/tjb-2017-0027

Zaid, A., Mohammad, F., and Siddique, K. H. (2022). Salicylic acid priming regulates stomatal conductance, trichome density and improves cadmium stress tolerance in mentha arvensis l. *Front. Plant Sci.* 13. doi: 10.3389/fpls.2022.895427

Zhang, X., Zhang, Z., Guo, J., Ma, J., Xie, S., Zhao, Y., et al. (2021). Combination of multiple computational methods revealing specific sub-sectional recognition and hydrogen-bond dependent transportation of CKII peptide fragment in O-GlcNAc transferase. *Comput. Struct. Biotechnol. J.* 19, 2045–2056. doi: 10.1016/j.csbj.2021.04.009

Zhang, X., Zhang, L., Sun, Y., Zheng, S., Wang, J., and Zhang, T. (2020). Hydrogen peroxide is involved in strigolactone induced low temperature stress tolerance in rape seedlings (*Brassica rapa* l.). *Plant Physiol. Biochem.* 157, 402–415. doi: 10.1016/j.plaphy.2020.11.006

Zhu, Y., Jiang, X., Zhang, J., He, Y., Zhu, X., Zhou, X., et al. (2020). Silicon confers cucumber resistance to salinity stress through the regulation of proline and cytokinins. *Plant Physiol. Biochem.* 156, 209–220. doi: 10.1016/j.plaphy.2020.09.014

Zhu, Z. H., Sami, A., Xu, Q. Q., Wu, L. L., Zheng, W. Y., Chen, Z. P., et al. (2021). Effects of seed priming treatments on the germination and development of two rapeseed (*Brassica napus* l.) varieties under the co-influence of low temperature and drought. *PLos One* 16 (9), e0257236. doi: 10.1371/journal.pone.0257236

Zulfiqar, F., Nafees, M., Chen, J., Darras, A., Ferrante, A., Hancock, J. T., et al. (2022). Chemical priming enhances plant tolerance to salt stress. *Front. Plant Sci.* 13. doi: 10.3389/fpls.2022.946922

frontiers | Frontiers in Plant Science

TYPE Original Research
PUBLISHED 02 February 2023
DOI 10.3389/fpls.2023.1123080

Check for updates

OPEN ACCESS

EDITED BY
Muhammad Waseem,
Hainan University, China

REVIEWED BY
Rehana Sardar,
University of the Punjab, Pakistan
Basharat Ali,
University of the Punjab, Pakistan

*CORRESPONDENCE
Nadeem Hussain
nadeemhussain396@yahoo.com
Abdul Ghaffar
abdulghaffar467@yahoo.com

SPECIALTY SECTION
This article was submitted to Plant Abiotic Stress, a section of the journal Frontiers in Plant Science

RECEIVED 13 December 2022
ACCEPTED 18 January 2023
PUBLISHED 02 February 2023

CITATION
Ghaffar A, Hussain N, Ajaj R, Shahin SM, Bano H, Javed M, Khalid A, Yasmin M, Shah KH, Zaheer M, Iqbal M, Zafar ZU and Athar H-u-R (2023) Photosynthetic activity and metabolic profiling of bread wheat cultivars contrasting in drought tolerance.
Front. Plant Sci. 14:1123080.
doi: 10.3389/fpls.2023.1123080

COPYRIGHT
© 2023 Ghaffar, Hussain, Ajaj, Shahin, Bano, Javed, Khalid, Yasmin, Shah, Zaheer, Iqbal, Zafar and Athar. This is an open-access article distributed under the terms of the Creative Commons Attribution License (CC BY). The use, distribution or reproduction in other forums is permitted, provided the original author(s) and the copyright owner(s) are credited and that the original publication in this journal is cited, in accordance with accepted academic practice. No use, distribution or reproduction is permitted which does not comply with these terms.

Photosynthetic activity and metabolic profiling of bread wheat cultivars contrasting in drought tolerance

Abdul Ghaffar[1*], Nadeem Hussain[1*], Rahaf Ajaj[2], Suzan Marwan Shahin[3], Hussan Bano[4], Muhammad Javed[1,5], Ayesha Khalid[1], Memoona Yasmin[1], Kausar Hussain Shah[1], Muhammad Zaheer[1], Muhammad Iqbal[1,6], Zafar Ullah Zafar[1] and Habib-ur-Rehman Athar[1]

[1]Institute of Botany, Bahauddin Zakariya University, Multan, Pakistan, [2]Department of Environmental and Public Health, College of Health Sciences, Abu Dhabi University, Abu Dhabi, United Arab Emirates, [3]College of Arts and Science, Umm Al Quwain University, Umm Al Quwain, United Arab Emirates, [4]Department of Botany, The Women University, Multan, Pakistan, [5]Department of Botany, University of Education, Lahore, Pakistan, [6]Department of Botany, University of Okara, Okara, Pakistan

The rapid increase in population growth under changing climatic conditions causes drought stress, threatening world food security. The identification of physiological and biochemical traits acting as yield-limiting factors in diverse germplasm is pre-requisite for genetic improvement under water-deficit conditions. The major aim of the present study was the identification of drought-tolerant wheat cultivars with a novel source of drought tolerance from local wheat germplasm. The study was conducted to screen 40 local wheat cultivars against drought stress at different growth stages. Barani-83, Blue Silver, Pak-81, and Pasban-90 containing shoot and root fresh weight >60% of control and shoot and root dry weight >80% and 70% of control, respectively, P (% of control >80 in shoot and >88 in root), K^+ (>85% of control), and quantum yield of PSII > 90% of control under polyethylene glycol (PEG)-induced drought stress at seedling stage can be considered as tolerant, while more reduction in these parameters make FSD-08, Lasani-08, Punjab-96, and Sahar-06 as drought-sensitive cultivars. FSD-08 and Lasani-08 could not maintain growth and yield due to protoplasmic dehydration, decreased turgidity, cell enlargement, and cell division due to drought treatment at adult growth stage. Stability of leaf chlorophyll content (<20% decrease) reflects photosynthetic efficiency of tolerant cultivars, while ~30 µmol/g fwt concentration of proline, 100%–200% increase in free amino acids, and ~50% increase in accumulation of soluble sugars were associated with maintaining leaf water status by osmotic adjustment. Raw OJIP chlorophyll fluorescence curves revealed a decrease in fluorescence at O, J, I, and P steps in sensitive genotypes FSD-08 and Lasani-08, showing greater damage to photosynthetic machinery and greater decrease in JIP test parameters, performance index (PI_{ABS}), maximum quantum yield (Fv/Fm) associated with increase in Vj, absorption (ABS/RC), and dissipation per reaction center (DIo/RC) while a decrease in electron transport per reaction center (ETo/RC). During the present study, differential modifications in morpho-physiological, biochemical,

and photosynthetic attributes that alleviate the damaging effects of drought stress in locally grown wheat cultivars were analyzed. Selected tolerant cultivars could be explored in various breeding programs to produce new wheat genotypes with adaptive traits to withstand water stress.

KEYWORDS

drought stress, mineral nutrients, osmotic adjustment, *Triticum aestivum*, chlorophyll fluorescence, water relations

1 Introduction

Global wheat production is forecast at 783.8 million tons in 2022 (FAOSTAT, 2022). Global human population is expected to exceed 9 billion by 2050, requiring at least 60% increase in wheat yield (Sekher, 2022). The drought puts 22 million people at risk of starvation by September 2022, and it triggered global economic losses about 124 billion US $ from 1998 to 2017, according to a report from the United Nations World Food Programme (WFP and UNICEF, 2022). The percentage of vegetation affected by drought has more than doubled in the last 40 years, and it has affected more people worldwide than any other natural hazard. Up to 26% of the usable area of the earth is subjected to drought and approximately 12 million hectares (Mha) of land is lost each year due to drought worldwide (FAO et al., 2022). Out of the total 79.6 Mha land of Pakistan, 62 Mha is vulnerable to drought stress while about 27% of land under cultivation is facing drought stress (FAOSTAT, 2022). Drought resistance in crop plants includes avoidance and tolerance. In recent years, different strategies have been adopted to minimize the challenges associated with drought, such as supplemental irrigation, modern dry land farming, mulching, artificial precipitation, ground water recharge, and use of compatible and drought-tolerant genotypes. Breeding is one of the most efficient options to overcome drought stress through the development of new genotypes adapted to drought (Blum, 2016). Different morpho-physiological traits of wheat that are hampered under drought stress include plant height, leaf area, chlorophyll content, stomatal conductance, relative water content, osmotic potential, water potential, and photosynthesis, so the mechanism of damage can be understood by studying these attributes under drought stress (Ahmad et al., 2022; Chen et al., 2022a; Peršić et al., 2022). Reduced uptake of N, P, and K^+ was observed in plants under drought stress. Low N uptake under dry conditions affects leaf water relations, chlorophyll fluorescence, and other photosynthetic attributes restricting growth and yield (Sallam et al., 2019). Drought stress increases concentration of soluble sugars, proline, and anti-oxidant enzymes activities to combat reactive oxygen species (ROS) (Tefera et al., 2021). Reduction in protein content under drought stress may be due to protein hydrolysis or oxidative inhibition of protein synthesis (Ozturk et al., 2021). However, Halder et al. (2022) described that drought stress caused the accumulation of osmoprotectant proteins (dehydrins) in drought-tolerant wheat cultivars to protect plant cellular structures from drought-induced damages. These proteins are highly hydrophilic and impart drought stress tolerance by enhancing the water retention capacity, elevating chlorophyll content, maintaining photosynthetic machinery, activating ROS detoxification, and promoting the accumulation of compatible solutes (Riyazuddin et al., 2022)

Plants cannot utilize sufficient light energy under drought stress, so electron transport chain is disturbed, leading to the production of ROS, which damage thylakoid membranes (Zhu et al., 2021). The structural and functional activity of PSII can be evaluated by fast chlorophyll *a* fluorescence technique to screen drought-tolerant and drought-sensitive varieties of a particular plant species (Kalaji et al., 2018; Bashir et al., 2021; Li and Kim, 2021). Fluorescence transients from Fo (minimal fluorescence when all reaction centers are open) to Fm (maximum fluorescence when all reaction centers are closed) are called OJIP curves, which can be analyzed by JIP test and used to evaluate plant responses against drought stress (Tsimilli-Michael, 2020). The O–J phase tells about the PSII subunits connectivity and reduction in the acceptor side of PSII, J–I represents reduction in PQ pool, while the reduction in acceptor side of PSI is explained by the I–P phase (Hussain et al., 2022). Drought stress disturbs electron transfer at acceptor and donor sides of PSII, damages OEC activity, affects energetic connectivity among PSII subunits, and reduces electron transfer capacity and redox state of PSI (Zhou et al., 2019).

Plants use different mechanisms to combat drought stress such as completing life cycle before severe water stress (drought escape), conserving water by closing stomata and reducing leaf area (drought avoidance), and by osmotic adjustment (drought tolerance) (Qayyum et al., 2021). During osmotic adjustment, plants accumulate various organic and inorganic solutes (sugars, polyols, amino acids, etc.) under water-deficit conditions to maintain water status of plants and thus turgor potential to sustain photosynthesis (Zhang et al., 2022). There is little progress in developing drought-tolerant wheat cultivars due to limited knowledge about the mechanism of drought tolerance in crops, dramatic change in some physiological parameters in plants under drought stress, and genotype and environment interaction. It is suggested that information from morphological, physiological, biochemical, gene expression, genetic studies, and breeding must be integrated to understand complexity of drought tolerance in crops. Screening of available germplasm against drought stress is an important strategy in plants to cope up with the harmful effects of water deficit (Tefera et al., 2021). It is hypothesized that a novel source of drought tolerance is present in new local germplasm collection of wheat, which can be used for developing drought-tolerant wheat cultivars through selective breeding. However, pre-breeding requires a detailed characterization of germplasm. The current study was aimed to assess genotypic variability in physiological and

biochemical traits in new local germplasm collection of wheat, particularly those that are related to photosystem-II activity. The secondary objective of the study was to draw the relationship between studied traits and degree of drought tolerance. The selected cultivars having traits with high heritability and positive correlation with grain yield may be used as donors in breeding programs.

2 Materials and methods

2.1 Screening of germplasm against PEG-induced drought stress under hydroponic conditions

The study was conducted at Botanic Gardens, Bahauddin Zakariya University, Multan (30°15 N and 71°30 E). Germplasm of 40 wheat cultivars collected from Ayub Agriculture Research Institute (AARI) Faisalabad and Regional Agricultural Research Institute (RARI) Bahawalpur, Pakistan, was surface sterilized with 5% sodium hypochlorite solution for 5 min to avoid any fungal infection and washed thoroughly with distilled water. A total of 40 bowls of 24 × 24 × 10 cm (length × width × depth) size obtained from G.M. Scientific Store, Multan, Pakistan, were taken and divided into two groups of 20 bowls each (Supplementary Figure S1). Seeds of two varieties (10 of each) were sown in each bowl in two separate rows. One group of plants (control) was filled with Hoagland nutrient solution (Hoagland and Arnon, 1950) having 1-in. thick layer of plastic microbeads (inert polyethylene), while the treatment block was given 10% PEG-8000 solution in Hoagland solution to induce drought stress. The plants were harvested after 14 days of germination, and various parameters including shoot and root biomass (fresh and dry) and N, P, and K^+ contents were measured.

2.2 Appraisal of morpho-physiological attributes of selected wheat cultivars under drought stress at adult stage

The selected drought-tolerant (Barani-83, Blue silver, Pak-81, and Pasban-90) and drought-sensitive (FSD-08, Lasani-08, Punjab-96, and Sahar-06) cultivars were further grown till adult stage, and differences in morpho-physiological and yield responses between tolerant and sensitive cultivars were explored under water stress conditions. A total of 80 plastic pots each with a diameter of 28 cm were taken. Eight seeds of each variety were sown in a pot filled with 8 kg fertile and well-textured garden soil of 18% field capacity and 36% soil saturation. Ten days after sowing, four equidistantly placed and uniformly sized plants were left in each pot after thinning. The experiment was arranged in completely randomized design (CRD) with eight cultivars, two treatments (control and drought), and five replicates. Initially, all the pots were irrigated with tap water, but after 2 weeks of germination, half of the plants were subjected to drought stress by withholding water (pre-anthesis drought cycle) till wilting state becomes evident, while the other group of plants were irrigated continuously with tap water. At this stage, different morpho-physiological and biochemical parameters were measured. Two of the four plants were harvested, and the experiment continued till the end, and finally, yield attributes were determined.

2.3 Measurements

2.3.1 Growth attributes

Plant length was calculated by using a measuring tape from the soil surface to the tip of the longest spike. Flag leaf area was determined by the Muller (1991) formula, which is given as: flag leaf area = maximum length × maximum breadth × 0.74. Total chlorophyll content (SPAD) was estimated by using a portable chlorophyll meter SPAD 502 (Minolta, chlorophyll meter, SPAD-502, Japan) as proposed by Del Pozo et al. (2016). The middle part of the third mature leaf of each plant was used to measure the quantum yield (QY) of PSII by using handheld FluorPen (FP-100 MX-LM, Photon System Instruments, Czech Republic). A weak measuring light was used to measure Fo, and then, a saturated pulse of 3,000 μmol m^{-2} s^{-1} was applied to measure Fm. QY of PSII was calculated using the formula: QY = Fv/Fm = (Fm – Fo)/Fm.

Fresh weight of the shoot and root was noted with the help of electric balance (BSM-220.4, Hanchen, China) after separating the shoot from the root; then, plants were dried in an electric oven (UN-110, Memmert, Germany) at 75°C for 72 h, and dry biomass was noted.

2.3.2 Leaf water relations

The second leaf from the top was cut from the main tiller to measure the water potential of the leaf (Ψw) at early in the morning using a Scholander-type pressure chamber (Arimad-2, Japan) as described by Scholander et al. (1964). The same leaf was kept in a freezer at −20°C for a week and thawed by a glass rod to extract cell sap, which was used for measuring osmotic potential (Ψs) by an osmo-meter (Vapro, 5520, USA). Turgor potential (Ψp) was calculated from the difference in Ψw and Ψs by the formula as described by Nobel (1991), i.e., Ψp = Ψw − Ψs. Fresh leaf samples were weighed (Fw) and dipped in water in the dark for 24 h so that they become turgid, and their turgid weight (Tw) was noted. These leaves were then dried in an oven at 80°C for 48 h, and the dried weight (Dw) was noted. The formula that was used to determine relative water content as described by Jones and Turner (1978) is RWC (%) = [(Fw − Tw)/(Fw − Dw)] × 100.

2.3.3 Organic osmolytes

Fresh leaf sample (0.25 g) was ground in 3% sulfo-salicylic acid (5 ml) in a chilled pestle and mortar. The homogenate was filtered, and 2 ml was taken in a test tube in which 2 ml acid ninhydrin solution (1.25 g ninhydrin+20 ml of 6M orthophosphric acid+30 ml glacial acetic acid) and 2 ml glacial acetic acid were added and heated in a boiling water bath for 1 h at 100°C, and the reaction was terminated by cooling in ice bath. Four milliliters of toluene was added in the test tube, vortexed for 15–20 s, and allowed to stand, and then, the upper layer (chromophore) was taken. Absorbance was recorded at 520 nm using a spectrophotometer, and the concentration of proline was determined with the help of a standard curve (Bates

et al., 1973). Proteins were calculated using bovine serum albumin (BSA) calibration curve on fresh weight basis (Bradford, 1976), while the concentration of total free amino acids was measured following the Hamilton et al. (1943) protocol. Total soluble sugars were estimated by standard methods as proposed by Yemm and Willis (1954). In 0.2 g dried ground leaf sample taken in a test tube, 10 ml of 80% ethyl alcohol was added and shaken overnight. The supernatant was taken in plastic bottles after three to four times washing with water and then made the volume of each sample up to 50 ml with distilled water. A 0.3 ml extract was put in a test tube and 3 ml of anthrone solution added and heated for 10 min in a water bath and cooled, and absorbance was recorded at 625 nm by a UV spectrophotometer.

2.3.4 Mineral nutrients and malondialdehyde

The digestion mixture (Se, 0.42g; $Li_2SO_4.2H_2O_2$, 14g dissolved in 350 ml of H_2O_2 and 420 ml conc. H_2SO_4) was used for plant tissue digestion. A total of 100 mg of dried ground plant material was digested in 2 ml of digestion mixture, adding $HClO_4$ (0.5 ml) on a hot plate. The digested mixture was diluted to 50 ml with distilled water and filtered, and K^+ was measured by a flame photometer (Jenway, PFP-7) following the method of Allen et al. (1985). P contents were determined by a spectrophotometer (Jenway, 6850, UK), measuring absorption at 470 nm (Jackson, 1958). Leaf N contents were estimated according to Kjeldhal method (Bremner, 1965). Leaf lipid peroxidation can be estimated by measuring MDA content, adopting thCakmak and Horst (1991) method.

2.3.5 Yield-related parameters

The number of tillers per plant, number of spikelet per spike, and number of grains per spike were counted; spike length was measured by a measuring tape, while 100 grain weight and grain yield per plant were measured by using electric balance.

2.3.6 Fast chlorophyll *a* fluorescence transient (OJIP)

Chlorophyll *a* fluorescence was measured from the middle part of the third mature leaf of each plant (40 min after sunset to ensure dark adaptation of leaves and then exposed to strong actinic light of 3,000 µmol m^{-2} s^{-1}), with a handheld chlorophyll fluorescence meter (FluorPen FP-100 MX-LM, Photon System Instruments, Czech Republic) from 20 µs to 2 s. The data were recorded based on literature available on websites of chlorophyll fluorescence meter manufacturers using computer software FlourPen v 1.0.4.0. According to Strasser et al. (2004), the JIP test parameters used to measure energy distribution, flux ratios, and performance index include ABS/RC, TRo/RC, ETo/RC, and DIo/RC (absorption, trapped energy, electron transport, and dissipation energy flux per reaction center) and Fo, Fj, Fi, and Fm (minimum fluorescence, fluorescence intensity at J phase, fluorescence intensity at I phase, and maximum fluorescence). Fv, Vj, and Vi represent variable fluorescence, relative variable fluorescence at phase J, and relative variable fluorescence at phase I of the fluorescence transient curve. Fm/Fo = electron transport rate through PSII, Fv/Fo = ratio of photochemical to non-photochemical quantum efficiency, Fv/Fm = maximum quantum yield of primary photochemistry, while PI_{ABS} is the photosynthetic performance index on absorption basis. ΦPSII shows the effective quantum yield of PSII photochemistry, ΦDo explains maximum quantum yield of non-photochemical de-excitation, ΦEo represents quantum yield of electron transport, and ψo = ETo/TRo explains the yield of electron transport per trapped excitation.

2.4 Statistical analysis

The adult experimental plan was a two-factor factorial completely randomized design with eight cultivars, two treatments, and five replications. Data were analyzed by two-way analysis of variance (ANOVA) using the computer program CoStat (Version 6.303, USA). Means ± SE were compared with least significant difference (LSD) test at 5% level of significance by Snedecor and Cochran (1989). Graphical representation of data was performed by MS Excel software.

3 Results

3.1 Screening and selection of local wheat germplasm against drought stress at seedling stage

All the wheat cultivars showed significant ($p \leq 0.001$) reduction in shoot and root fresh and dry biomass and K^+ and P accumulation under water-deficit conditions. The extent of reduction in biomass and K^+ and P accumulation in the leaves and roots varied considerably in all wheat cultivars. The percentages of control values of shoot and root fresh and dry weight were maximum in four cultivars (Barani-83, Blue silver, Pak-81, and Pasban-90), while FSD-08, Lasani-08, Punjab-96, and Sahar-06 showed minimum percent of control values of shoot and root fresh and dry weight due to PEG-induced water stress (Figures 1A-D). Shoot and root K^+ concentration calculated on dry weight basis decreased under drought stress. Maximum percent of control or minimum decrease was observed in cultivar Barani-83 (97% of control of shoot and 83% of control of root), followed by Blue Silver, Pak-13, Pak-81, and Pasban-90. However, a maximum decrease or minimum percent of control was observed in FSD-08 (67% of control of the shoot and 65% of control of the root) followed by Lasani-08, Punjab-96, and Sahar-06 under drought stress conditions (Figures 2A, B). Shoot and root P concentration decreased in all the cultivars under drought stress. A maximum decrease was observed in FSD-08 (54% of control of shoot and 56% of control of root) and then come varieties Lasani-08 (56% of control of the shoot and root) followed by Punjab-96 and Sahar-06 under drought stress conditions. A minimum decrease was observed in Barani-83 with 85% and 89% of control of the shoot and root, respectively, followed by Blue Silver, Pak-81, and Pasban-90 under water scarce conditions (Figures 2C, D).

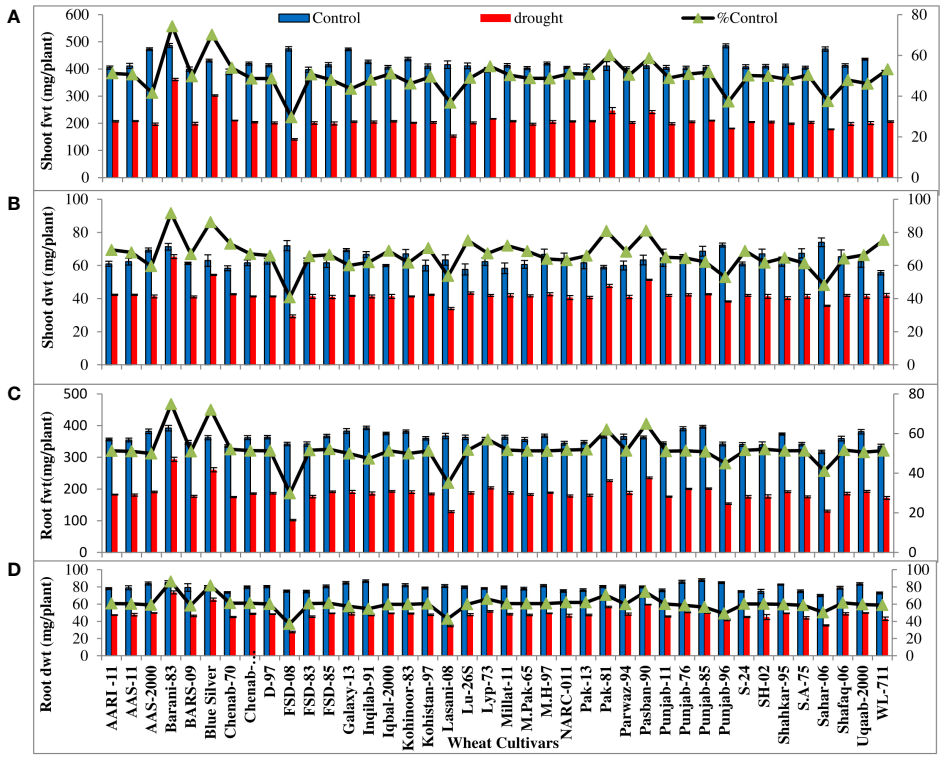


FIGURE 1
Shoot and root fresh and dry weights (mg/plant) of wheat seedlings, when plants of 40 local wheat cultivars were grown under normal or PEG-induced drought stress for 2 weeks. Means (± SE; n=5) are presented on the primary vertical axis, while % of the control values are presented on the secondary vertical axis. **(A)** Shoot fwt, **(B)** shoot dwt, **(C)** root fwt, and **(D)** root dwt.

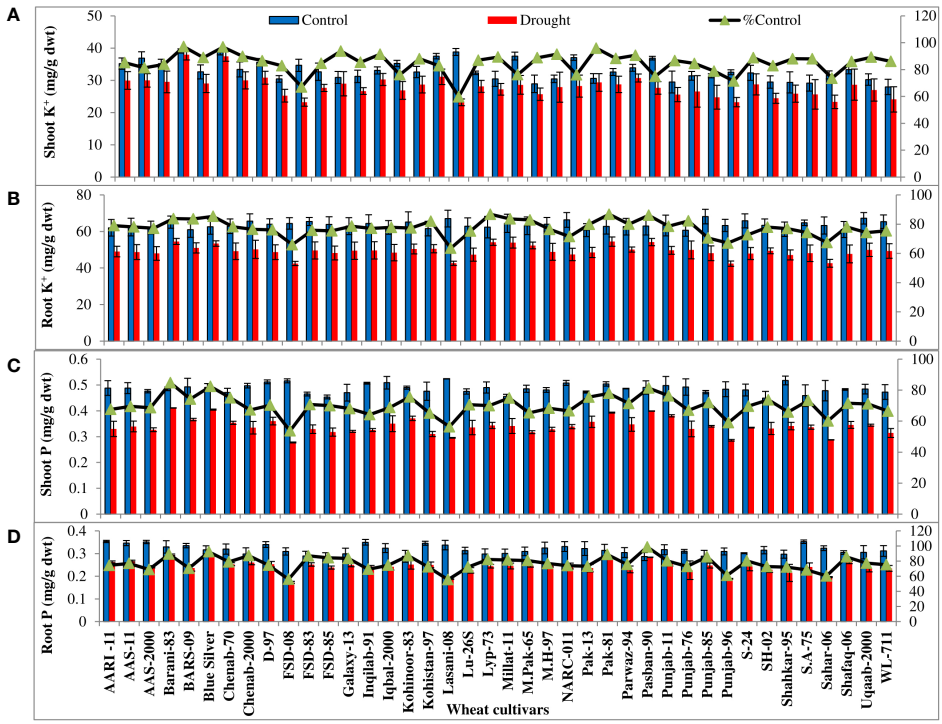


FIGURE 2
Shoot and root K^+ and P accumulation in wheat seedlings when plants of 40 local wheat cultivars were grown under normal or PEG-induced drought stress for 2 weeks. Means (± SE; n=5) are presented on the primary vertical axis, while percent of the control values is presented on the secondary vertical axis. **(A)** Shoot K^+, **(B)** root K^+, **(C)** shoot P, and **(D)** root P.

3.2 Assessment of differential morphological and physio-biochemical responses of selected wheat cultivars under drought stress

3.2.1 Shoot and root fresh and dry biomass, plant height, flag leaf area, quantum yield of PSII, and total chlorophyll content (SPAD)

Drought stress reduced shoot and root fresh and dry biomass significantly ($p \leq 0.001$) in all wheat cultivars (Table 1) examined in the present study. Less decrease was observed in fresh and dry biomass of the shoot and root in Barani-83 than Blue Silver, Pak-81, and Pasban-90; however, maximum decrease in FSD-08 followed by Lasani-08, Punjab-96, and Sahar-06 was found under drought stress (Figures 3A-D). ANOVA of the data showed significant ($p \leq 0.001$) decrease in plant height in all wheat cultivars under drought stress (Table 1). Differences among cultivars were also significant with respect to plant height; a lesser decrease (16%) in plant height in Pasban-90, while greater decrease in Pak-81 (17%), Blue Silver (20%), and Barani-83 (24%), respectively, was observed, whereas Sahar-06 showed maximum decrease (48%) in plant height, followed by Punjab-96 (37%), Lasani-08 (32%), and FSD-08 (28%), respectively, under water stress conditions (Figure 3E). Although the cultivars differed significantly based on flag leaf area, total chlorophyll contents, and quantum yield of PSII under drought stress (Table 1), the reduction in flag leaf area, total chlorophyll contents, and quantum yield of PSII was 85%, 35%, and 18%, respectively, in FSD-08; 81%, 28%, and 14%, respectively, in Lasani-08; and only 63%, 10%, and 4% in Barani-83; while 70%, 14%, and 6%, respectively, in Blue Silver was noted under the influence of water stress. The varieties Pak-81, Pasban-90, Punjab-96, and Sahar-06 show intermediate reduction in flag leaf area, total chlorophyll contents, and quantum yield under drought stress (Figures 3F-H).

3.2.2 Water relations parameters

ANOVA of the data explained significant ($p \leq 0.001$) decrease in all water relation parameters in all wheat cultivars on exposure to drought stress (Table 1). Drought stress reduced water potential (Ψ_w) in all wheat cultivars; however, a minimum decrease (87%) in Barani-83 while more in Blue Silver, Pak-81, and Pasban-90 was noted due to the effect of drought stress. A maximum decline in Ψ_w in FSD-08 (210%) followed by Lasani-08, Punjab-96, and Sahar-06 under drought conditions was observed (Figure 4A). As far as osmotic potential (Ψs) is concerned, Barani-83 showed a minimum decrease (39%) followed by Blue Silver, Pak-81, and Pasban-90, which shows more decrease in the respective order; however, genotype FSD-08 showed maximum decrease (53%), followed by Lasani-08, Punjab-96, and Sahar-06, showing more decrease, respectively, under drought stress conditions (Figure 4B). Drought stress caused minimum reduction (24%) in turgor potential (Ψp) in Barani-83 while maximum (55%) in cv. FSD-08 (Figure 4C). Reduction in relative water content (RWC) due to drought stress was only 3% in Barani-83 followed by Blue Silver, Pak-81, and Pasban-90 with 7%, 10%, and 15% decrease, respectively, as compared to control. A maximum decrease (24%) in RWC was seen in FSD-08 followed by Lasani-08, Punjab-96, and Sahar-06 with 20%, 16%, and 15% decrease, respectively, due to drought stress (Figure 4D).

3.2.3 Mineral nutrients and MDA

The percentage of N, P, and K^+ of the shoot was significantly ($p \leq 0.001$) reduced among the wheat cultivars under drought conditions (Table 1). The cultivars differed significantly in accumulation of mineral nutrients in leaves; a slightly less decrease in N in Barani-83 (18%), Blue Silver (28%), Pak-81(34%), and Pasban-90 (38%) was observed, while a decreasing order of N was 62%, 59%, 53%, and 46% in FSD-08, Lasani-08, Punjab-96, and Sahar-06 cultivars, respectively (Figure 5A). The percentage decrease in P was least (21%) in Barani-83 followed by Blue Silver (30%), Pak-81 (29%), and Pasban-90 (33%). The cv. FSD-08 retained the least P contents with 50% decrease, while Lasani-08, Punjab-96, and Sahar-06 cultivars exhibited 48%, 47%, and 41% decrease, respectively, under drought stress conditions and may be considered as drought-sensitive cultivars (Figure 5B). Maximum K^+ contents under drought conditions were retained by cv. Barani-83 and showed least reduction (20%), while Blue Silver, Pak-81, and Pasban-90 showed 28%, 38%, and 39% decrease, respectively. On the other hand, the maximum percent decrease was shown by FSD-08, i.e., 68% followed by Lasani-08, Punjab-96, and Sahar-06 varieties with 59%, 56%, and 47% decrease, respectively, due to water stress (Figure 5C). MDA contents represent a measure of lipid peroxidation by ROS. A significant increase in MDA concentration ($p \leq 0.001$) was observed in all wheat cultivars under the influence of drought stress (Table 1). Drought stress caused less damage to plasma membranes in Barani-83, Blue Silver, Pak-81, and Pasban-90, i.e., less lipid peroxidation as compared to FSD-08, Lasani-08, Punjab-96, and Sahar-06 wheat cultivars, which exhibit a significant increase in MDA contents (Figure 5D).

3.2.4 Organic osmolytes

Statistical results showed a significant ($p \leq 0.001$) (Table 1) increase in total soluble sugars, proline, and free amino acids while a decrease in total soluble proteins in response to drought stress in all wheat cultivars. Cultivars differed considerably in accumulation of total soluble sugars under drought stress. A maximum increase (48%) in total soluble sugars was noted in cv. Barani-83 due to drought stress as compared to its control, while Blue Silver, Pak-81, and Pasban-90 with 37%, 38%, and 35% increase, respectively, come next to it. The lowest increase was displayed by FSD-08, i.e., 20%, followed by Lasani-08, Punjab-96, and Sahar-06 cultivars with ~25%–31% increase on facing drought stress (Figure 6A). A positive correlation was found between the degree of drought tolerance and proline accumulation. Barani-83 accumulated maximum proline and can be considered as the most drought tolerant, while FSD-08 with least increase in accumulation of proline (94%) was considered as drought sensitive (Figure 6B). Total soluble protein concentration diminished, while those of total free amino acids increase significantly ($p \leq 0.001$) in all wheat cultivars under drought stress (Table 1). Barani-83, Blue Silver, Pak-81, and Pasban-90 exhibited decrease in total soluble proteins from ~14%–28%, while FSD-08, Lasani-08, Punjab-96, and Sahar-06 wheat cultivars showed greater decrease, i.e., 52%, 42%, 37%, and 33%, respectively, under dry conditions. Cultivars showing

10.3389/fpls.2023.1123080

TABLE 1 Mean squares from ANOVA of the data for growth parameters, water relation parameters, mineral nutrients, MDA, organic osmolytes, and yield attributes of eight wheat (*Triticum aestivum* L.) cultivars subjected to drought stress at adult growth stage.

Source of variation	Df	Shoot fwt	Shoot dwt	Root fwt	Root dwt	Plant height
Genotypes (G)	7	200.907***	2.552***	0.024***	6.170***	615.563***
Drought (D)	1	13,728.2***	138.811***	6.882***	0.360***	13,936.5***
G × D	7	169.643***	2.476***	0.0112***	7.654***	274.972***
Error	64	30.276	0.603	0.00224	1.247	11.168
Total	79					
Source of variation	Df	Flag leaf area	Chlorophyll content (SPAD)	Quantum yield of PSII	Water potential	Osmotic potential
Genotypes (G)	7	78.082*	17.859**	0.002***	0.0488***	0.0122***
Drought (D)	1	18,960.85***	2,117.5***	0.217***	18.509***	0.0107***
G × D	7	128.551***	26.298***	0.002***	0.0816***	0.0107**
Error	64	28.491	4.425	2.52e−4	0.00469	0.00273
Total	79					
Source of variation	Df	Turgor potential	Relative water content	Shoot N	Shoot P	Shoot K^+
Genotypes (G)	7	0.0268***	88.928***	0.731***	0.601***	27.118***
Drought (D)	1	2.126***	2491.2***	53.203***	60.302***	1,465.01***
G × D	7	0.0182***	88.179***	0.943***	0.530***	7.2577*
Error	64	0.00321	2.0042	0.0335	0.0322	3.0043
Total	79					
Source of variation	Df	MDA	Total soluble sugars	Proline	Total soluble proteins	Total free amino acids
Genotypes (G)	7	6.651***	48.115***	103.742***	0.343***	40.364***
Drought (D)	1	468.262***	6,505.436***	3,430.401***	19.080***	1,967.57***
G × D	7	2.400ns	55.377***	105.0595***	0.411***	46.0643***
Error	64	1.341	8.0432	1.221	0.0218	0.900
Total	79					
Source of variation	Df	Grain yield/plant	100 grain weight	No. of grains/spike	No. of spikelets/spike	Spike length
Genotypes (G)	7	44.206***	0.723***	93.707***	23.771***	2.0416**
Drought (D)	1	3,614.4***	28.043***	3,380***	744.2***	533.028***
G × D	7	61.813***	0.381***	27.142ns	10.142**	0.906ns
Error	64	2.116	0.0932	17.15	3.025	0.517
Total	79					
Source of variation	Df	No. of tillers/plant				
Genotypes (G)	7	15.783***				
Drought (D)	1	1,015.312***				
G x D	7	3.369ns				

(Continued)

TABLE 1 Continued

Source of variation	Df	No. of tillers/ plant				
Genotypes (G)	7	15.783***				
Drought (D)	1	1,015.312***				
G x D	7	3.369ns				
Error	64	1.962				
Total	79					

*, **, *** significant at 0.05, 0.01, and 0.001 probability levels, respectively.
ns, non-significant; Df, degree of freedom.

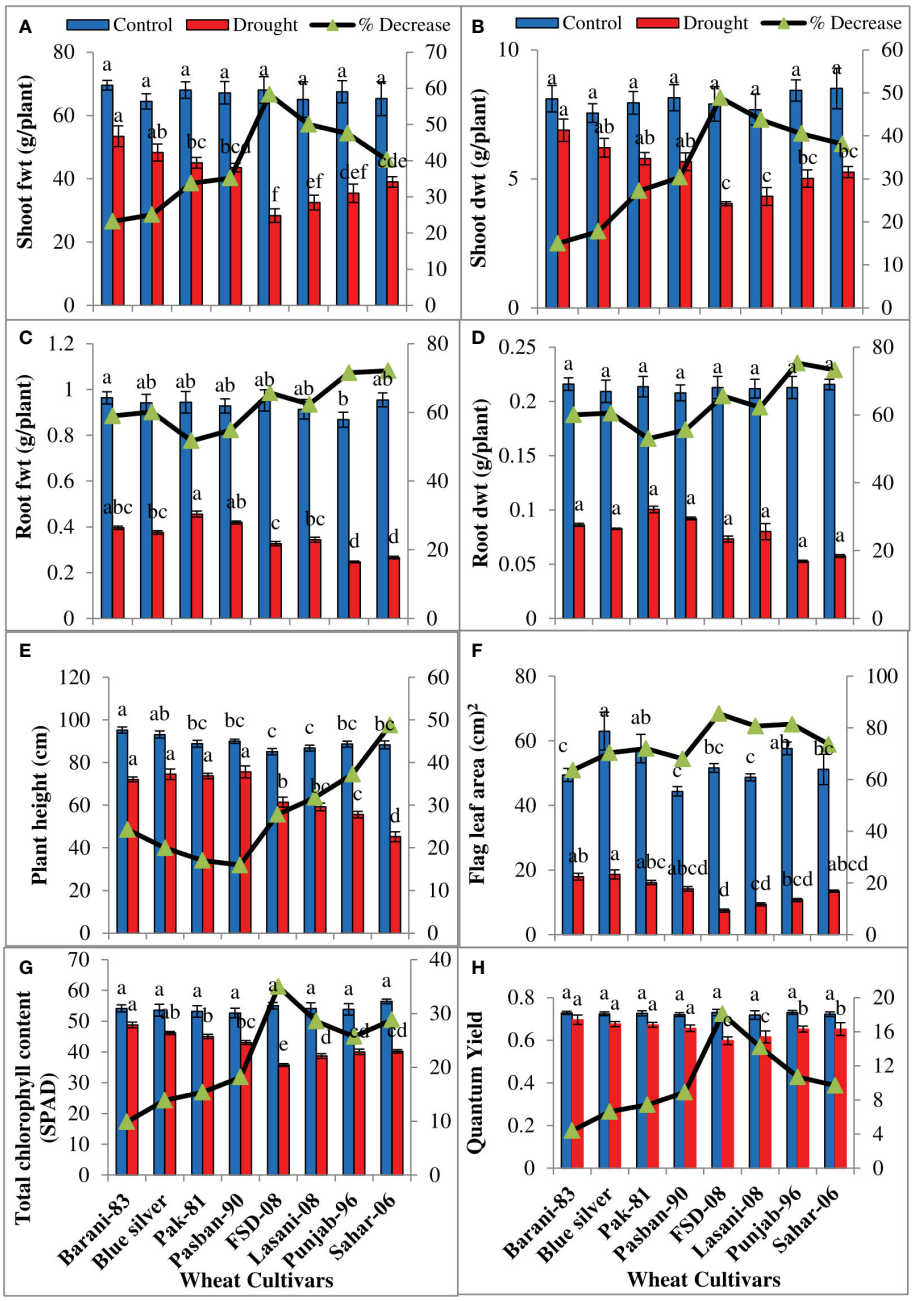


FIGURE 3
Growth attributes of selected wheat cultivars subjected to control or drought stress at adult stage. Means (± SE; n=5) are presented on the primary vertical axis, while percent decrease value is presented on the secondary vertical axis. Different letters represent significant differences among cultivars at $p < 0.05$ according to LSD test. **(A)** Shoot fresh weight, **(B)** shoot dry weight, **(C)** root fresh weight, **(D)** root dry weight, **(E)** plant height, **(F)** flag leaf area, **(G)** total chlorophyll content (SPAD), and **(H)** quantum yield of PSII.

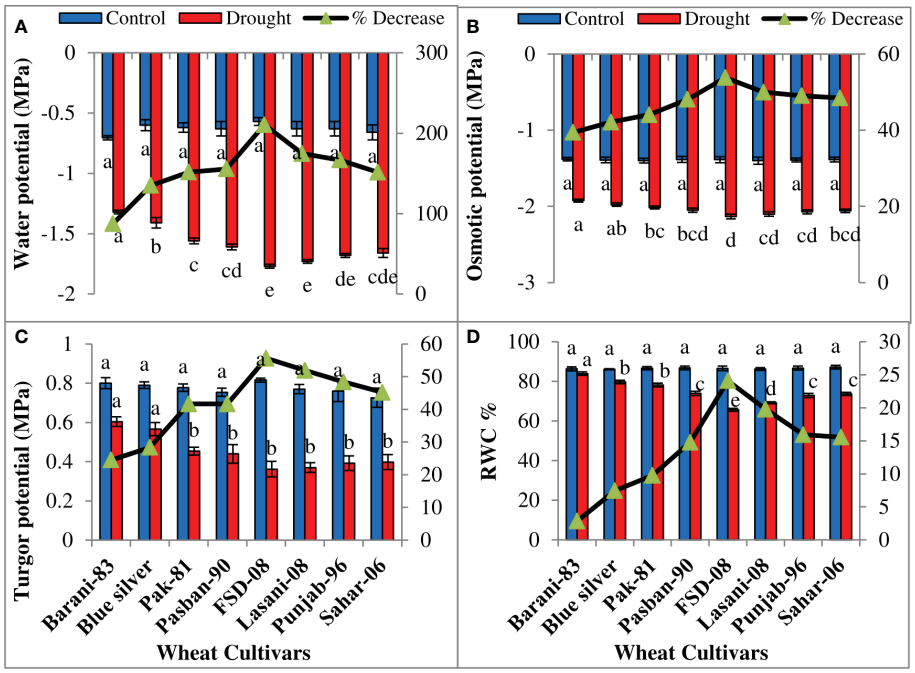


FIGURE 4
Water relations attributes of selected wheat cultivars subjected to control or drought stress at adult stage. Means (± SE; n=5) are presented on the primary vertical axis, while percent decrease value is presented on the secondary vertical axis. Different letters represent significant differences among cultivars at $p < 0.05$ according to LSD test. **(A)** Water potential, **(B)** osmotic potential, **(C)** turgor potential, and **(D)** % relative water content.

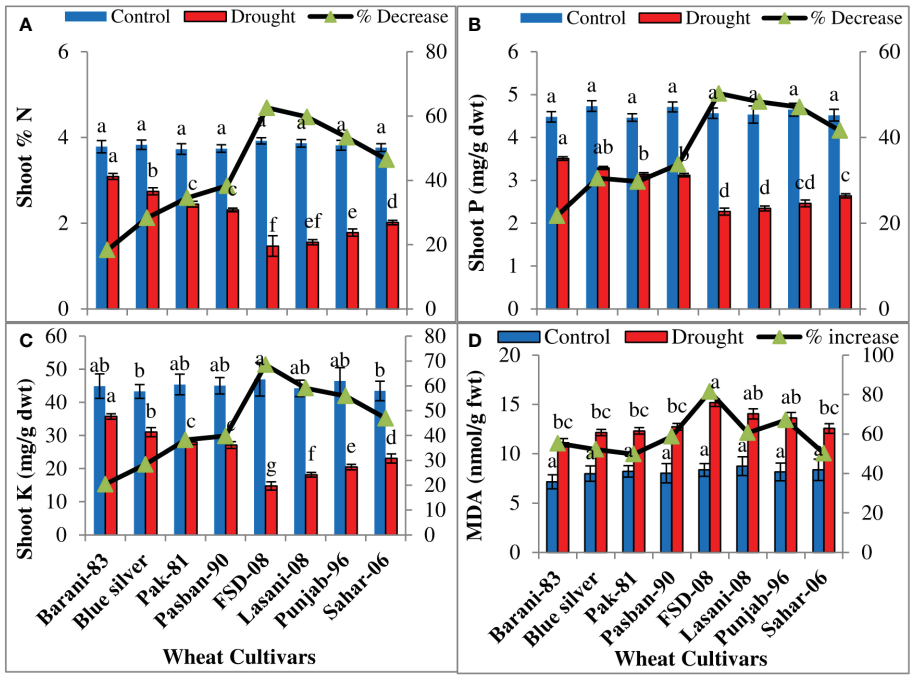


FIGURE 5
Accumulation of mineral nutrients and MDA in selected wheat cultivars subjected to control or drought stress at adult stage. Means (± SE; n=5) are presented on the primary vertical axis, while percent decrease value is presented on the secondary vertical axis. Different letters represent significant differences among cultivars at $p < 0.05$ according to LSD test. **(A)** Shoot N, **(B)** shoot P, **(C)** shoot K^+, and **(D)** MDA.

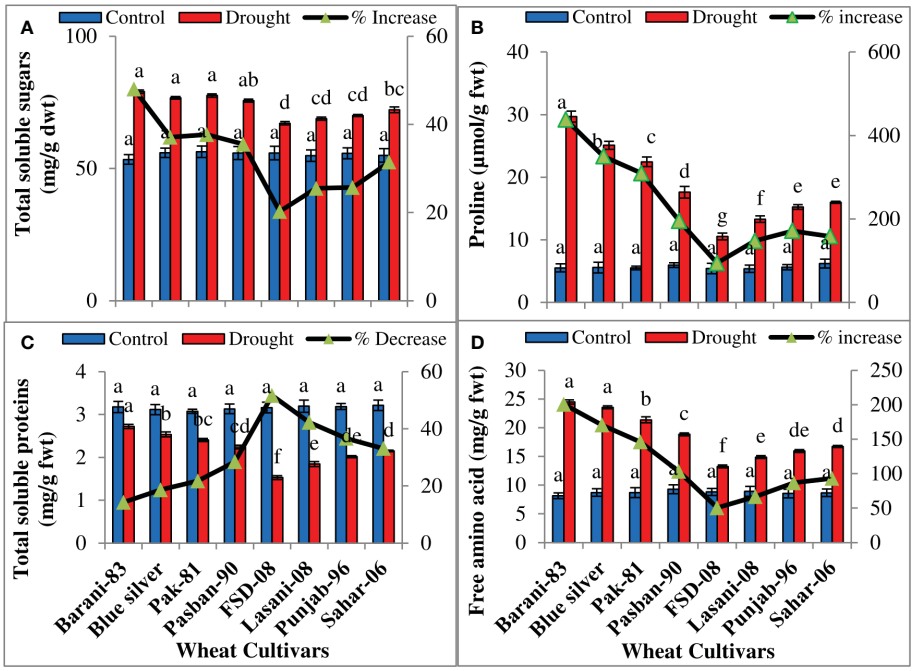


FIGURE 6
Accumulation of organic osmolytes in selected wheat cultivars subjected to control or drought stress at adult stage. Means (± SE; n=5) are presented on the primary vertical axis, while percent increase/decrease value is presented on the secondary vertical axis. Different letters represent significant differences among cultivars at $p < 0.05$ according to LSD test. **(A)** Total soluble sugars, **(B)** proline, **(C)** total soluble proteins, and **(D)** free amino acids.

greater decrease in protein contents have greater increase in total free amino acids contents (Figures 6C, D).

3.2.5 Yield attributes

Analysis of variance of the data showed significant ($p \leq 0.001$) decrease in all yield parameters under water deficiency (Table 1). Under drought conditions, the highest grain yield (g/plant) with minimum decrease (24%) was recorded in Barani-83 followed by Blue Silver, Pak-81, and Pasban-90 with ~34%–45% decrease and may be considered as drought resistant, while the least grain yield was shown by FSD-08 with 76% decrease, followed by Lasani-08, Punjab-96, and Sahar-06 with 69%, 63%, and 57% decrease, respectively, and are thought to be drought-sensitive cultivars (Figure 7A). Similarly, a lesser decrease in 100-grain weight (g) was observed in Barani-83, Blue Silver, Pak-81, and Pasban-90, while a greater decrease was observed in FSD-08, i.e., 45%, followed by Lasani-08 (34%), Punjab-96 (31%), and Sahar-06 (30%) as depicted in Figure 7B. The number of grains per spike in Barani-83 decreased much less under drought stress followed by Blue Silver, Pak-81, and Pasban-90, however, a greater reduction was found in FSD-08 followed by Lasani-08, Punjab-96, and Sahar-06 (Figure 7C). The production potential of wheat is indicated by the number of spikelets per spike, which is adversely affected by drought stress in all wheat cultivars studied. Barani-83 with the least decrease (12%) in the number of spikelets per spike is followed by Blue Silver, Pak-81, and Pasban-90, whereas FSD-08 exhibited 43% decrease in the number of spikelets per spike, Lasani-08, Punjab-96, and Sahar-06 come after it (Figure 7D). The maximum length of spike was attained by the well-watered crop, which was substantially reduced under dry conditions. It was found that Barani-83 exhibited minimum percent reduction (23%) in spike length, while FSD-08 showed maximum percent reduction in spike length (36%) when plants faced water stress environment. The other cultivars were intermediate in reducing spike length on exposure to drought stress (Figure 7E). The number of fertile tillers per plant is an important indicator of plant yield, which is substantially decreased in all cultivars due to drought stress. Minimum percent reduction (44%) was shown by Barani-83 followed by Blue Silver, Pak-81, and Pasban-90 with 48%, 49%, and 51% decrease in the number of fertile tillers per plant, respectively. However, the maximum decrease (76%) was displayed by FSD-08 followed by Lasani-08, Punjab-96, and Sahar-06 with 71%, 60%, and 56% decrease, respectively, under drought stress (Figure 7F).

3.2.6 Chlorophyll *a* fluorescence transient

Chlorophyll *a* fluorescence transients (Ft) measured by JIP test explain that no considerable change in typical OJIP kinetics was observed in cv. Blue Silver, while a small decrease in chlorophyll fluorescence in cv. Barani-83 was found at I and P steps; however, in cvs. FSD-08 and Lasani-08, a greater decrease in fluorescence was observed at J, I, and P steps as clearly seen from Figures 8A-D. Kinetic differences between double normalized drought stressed and control plants for chlorophyll *a* fluorescence values over a time range of 20–300 µs (between O and K steps) is called ΔV_{OK} or L-band, which expresses uncoupling of OEC. Its increased value in FSD-08, Lasani-08, and Blue Silver indicated uncoupling of OEC with core protein of PSII, while in Barani-83, no such L-band was observed (Figure 9A). ΔV_{OJ} (K-band) represents kinetic differences between double-normalized drought stressed and control plants over a time range of 20–2,000 µs (between O and J steps) and expresses OEC activity. FSD-08 and Lasani-08 showed positive K-band values, while Blue

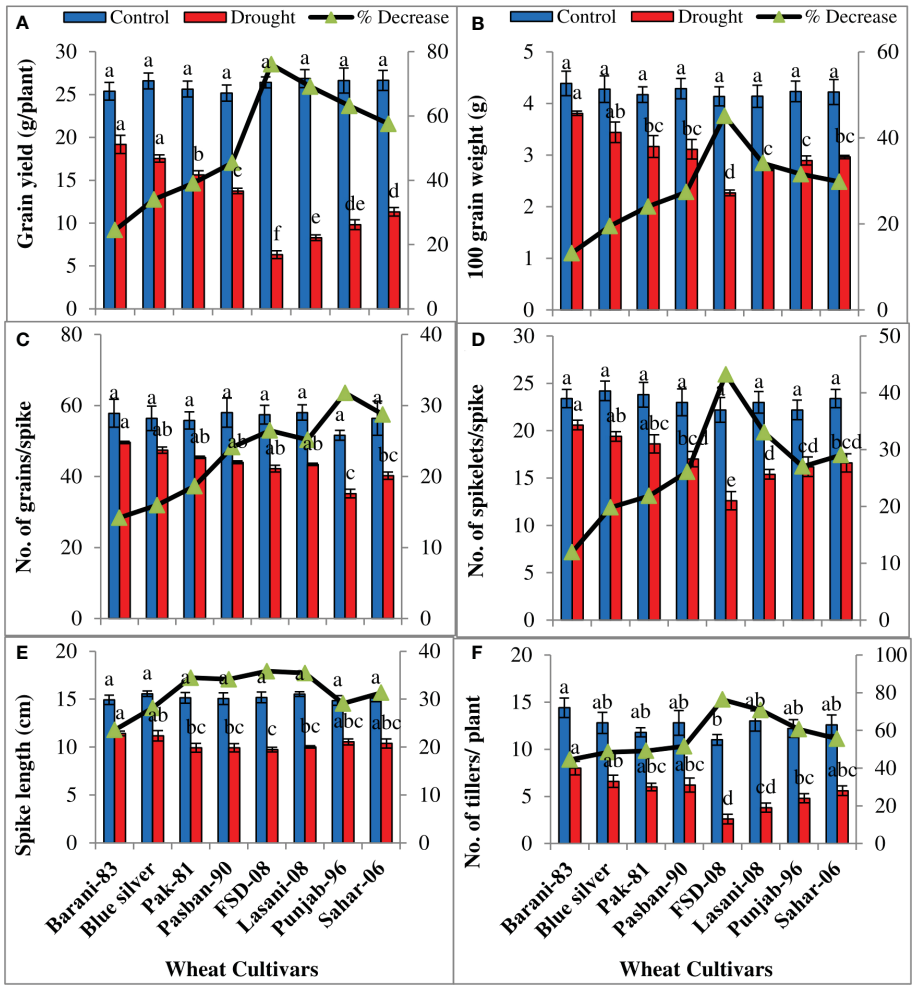


FIGURE 7
Yield attributes of selected wheat cultivars subjected to control or drought stress at adult stage. Means (± SE; n=5) are presented on the primary vertical axis, while percent decrease value is presented on secondary vertical axis. Different letters represent significant differences among cultivars at $p < 0.05$ according to LSD test. **(A)** Grain yield, **(B)** 100 grain weight, **(C)** number of grains/spike, **(D)** number of spikelets/spike, **(E)** spike length, and **(F)** number of tillers/plant.

Silver and Barani-83 showed negative values (Figure 9B). Fo and Fj values in cvs. FSD-08 and Lasani-08 significantly increased, whereas they remained unchanged in cvs. Blue Silver and Barani-83 under drought stress (Figure 10). A greater decrease in Fi, Fm, and Fv in FSD-08 and Lasani-08 as compared to Blue Silver and Barani-83 was observed under dry conditions. The relative variable chlorophyll fluorescence at J (Vj) was significantly higher in cvs. FSD-08 and Lasani-08 than that of cvs. Blue Silver and Barani-83 (Figure 10). The functional status of PSII is represented by various chlorophyll fluorescence ratios (Fm/Fo, Fv/Fo, and Fv/Fm). Under water scarcity, a greater decrease in all of these ratios was found in cvs. FSD-08 and Lasani-08 as compared to those of cvs. Blue Silver and Barani-83 (Figure 10). The quantum efficiency of primary photochemistry (ΦPo), trapped energy (Ψo), and electron transport (ΦEo) was greatly decreased in FSD-08 and Lasani-08, while a lesser decrease in these values in cvs. Blue Silver and Barani-83 was observed under water-deficient conditions (Figure 10). Increase in energy fluxes for absorption (ABS/RC), trapping (TRo/RC), and heat dissipation (DIo/RC) was observed in drought-stressed plants of cvs. FSD-08 and Lasani-08, whereas the energy fluxes for electron transport (ETo/RC) decreased due to imposition of drought stress (Figure 10). A greater decrease in PI_{ABS} (performance index of PSII) due to drought stress was observed in cvs. FSD-08 and Lasani-08 than that of cvs. Blue Silver and Barani-83 (Figure 10).

4 Discussion

Drought-induced osmotic stress at vegetative, flowering, or grain filling stage adversely affects crop production. In the present study, PEG treatment decreased shoot and root fresh and dry weight of seedlings in all wheat cultivars (Supplementary Figure S2) as observed previously by Peršić et al. (2022) that morpho-physiological and biochemical traits of seedlings shoot and root are greatly affected by PEG-induced drought stress reducing growth. Different growth parameters (plant height, length of roots, and fresh and dry matter weight), number of branches, and plant yield in *Cleome amblyocarp* are significantly decreased due to increasing levels of water stress (Shahin et al., 2018a). Reduction in growth attributes such as fresh and dry biomass and RWC in *Brassica napus* was observed by Chen

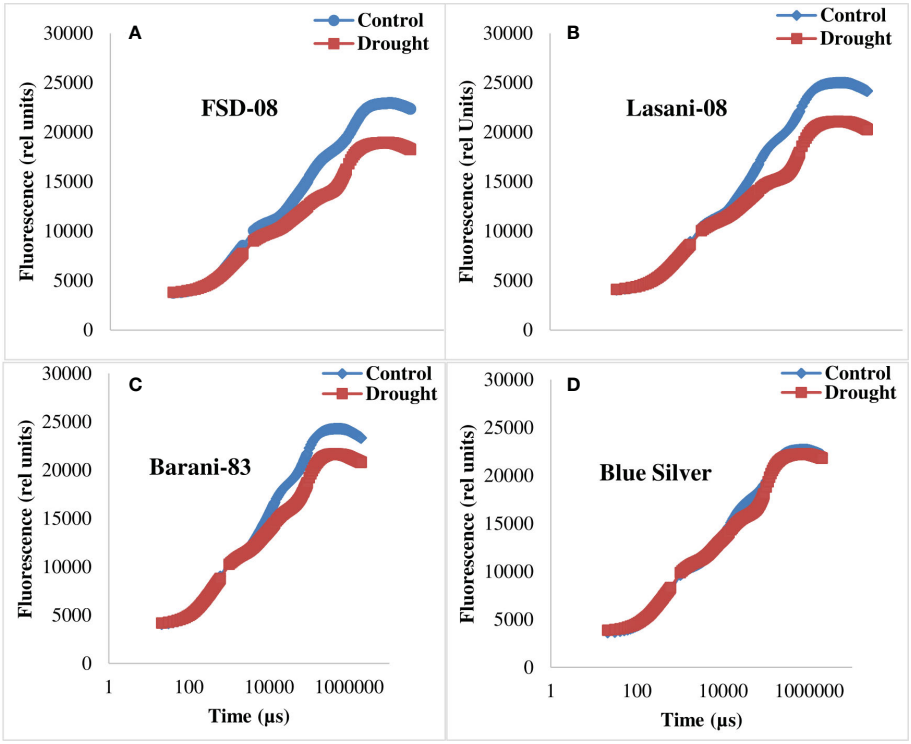


FIGURE 8
Raw OJIP chlorophyll *a* fluorescence curves (Ft) of the four selected wheat cultivars when plants were subjected to control or drought stress at adult stage. **(A)** FSD-08, **(B)** Lasani-08, **(C)** Barani-83, and **(D)** Blue Silver.

et al. (2022b). Our results indicated that water stress led to a decline in shoot and root fresh and dry weights, with FSD-08 as the most affected and sensitive cultivar in contrast to Barani-83, the least affected and most tolerant variety under drought stress conditions (Figures 3A-D). Previously, it was observed that drought stress destroys photosynthetic pigments, disturbs PSII activity, and reduces stomatal conduction, influx of CO_2, and its fixation by Calvin cycle enzymes (Ashraf and Harris, 2013). In present studies, the decrease in plant height and leaf area under drought stress (Figures 3E, F) might be due to protoplasmic dehydration, which in turn decreases turgidity, cell enlargement, and cell division. A reduction in plant height and leaf area due to the decrease in cell elongation under drought stress was observed by Shahin et al. (2018b). Drought-linked decline in chlorophyll contents was due to greater activity of chlorophyllase enzyme or destruction of thylakoid membrane; as a result, photosynthetic performance in the form of quantum yield is also reduced (Shen et al., 2020). Drought-tolerant wheat cultivars in this experiment have higher leaf chlorophyll content and quantum yield of PSII than sensitive genotypes (Figures 3G, H) producing high yield under drought stress, indicating a positive correlation between chlorophyll content, quantum yield of PSII, and crop yield, in accordance with findings of Chowdhury et al. (2021) and Bano et al. (2021) that drought-tolerant wheat cultivars have greater chlorophyll content and quantum yield.

Wasaya et al. (2021) noted a reduction in spike length, number of grains per spike, and grain weight under drought stress in wheat cultivars, while a reduction in the number of tillers per plant, number of spikelet per spike, and number of grains per spike was observed by Panhwar et al. (2021). The results obtained from the present research suggest that Barani-83, Blue Silver, Pak-81, and Pasban-90 showed better response towards drought conditions, while FSD-08, Lasani-08, Punjab-96, and Sahar-06 cultivars showed poor performance in terms of yield attributes such as the decline in grain yield and 100 grain weight under water shortage is due to reduced production of photo-assimilates and their reduced absorption by sink while the reduction in the number of grains per spike was due to loss of pollen viability as explained in earlier studies by Chowdhury et al. (2021).

Plant water status is measured in terms of RWC, which reflects metabolic activities of plant tissues (Chowdhury et al., 2021). A reduction in RWC was found in all wheat cultivars under drought stress; less reduction in tolerant cultivars (Barani-83 and Blue Silver) while more in sensitive cultivars (FSD-08 and Lasani-08) were found in the present study. These results are in agreement with the previous studies by Belay et al. (2021) who found less reduction in RWC in drought-tolerant wheat cultivars under water-deficit conditions. The decrease in RWC might be due to reduced water uptake and greater loss of water from leaves, which reduces leaf turgor potential, inhibits cell elongation and cell division, and ultimately reduces growth and yield (Camaille et al., 2021). Under such conditions, plants modify their osmotic potential by lowering the water potential in a process called osmotic adjustment, which is carried out by accumulation of suitable solutes like soluble sugars, proline, free amino acids, soluble proteins, and glycine-betaine that increase the tolerance to all types of environmental stresses (Ashraf and Foolad, 2007). The conservation of desirable cellular turgidity under water scarcity permits the plant to keep its physio-metabolic functions such as opening of stomata, photosynthesis, cell expansion, and other developmental processes

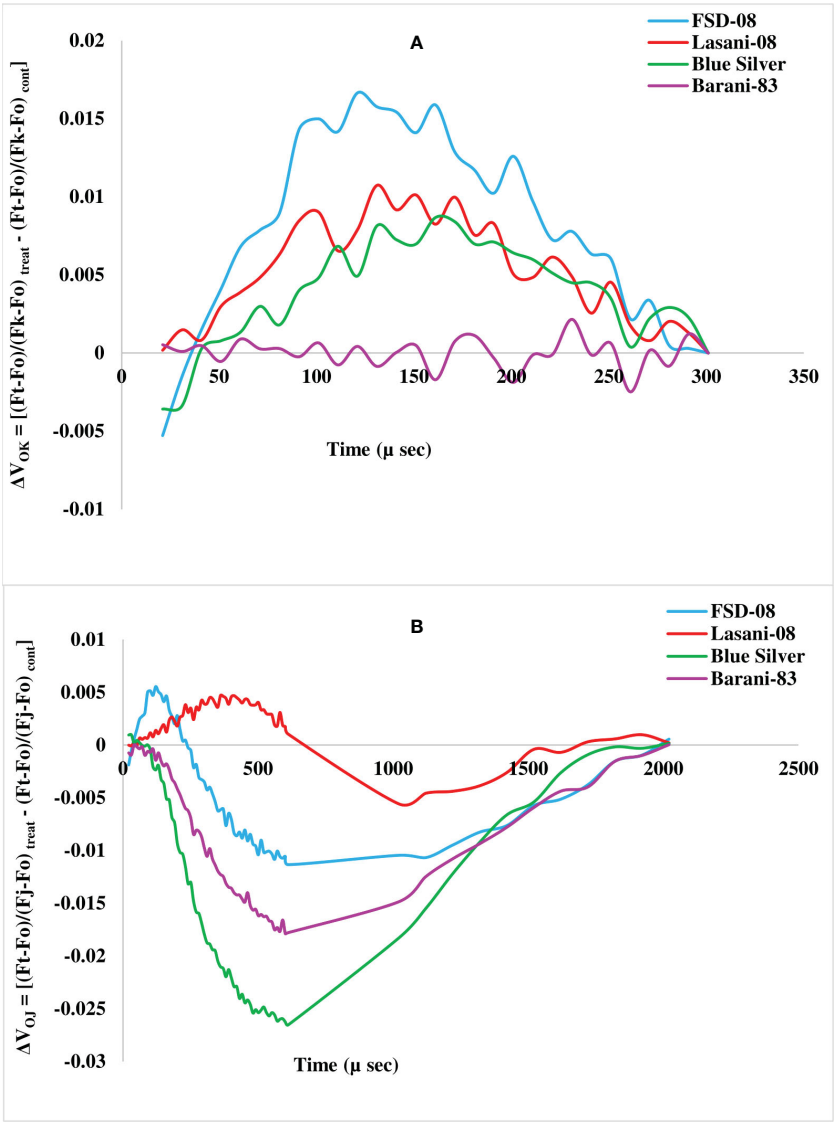


FIGURE 9
Kinetic differences of four selected wheat cultivars subjected to control or drought stress at adult stage. **(A)** Double normalized between Fo and Fk (L-band). **(B)** Double normalized between Fo and Fj (K band).

at optimum level (Serraj and Sinclair, 2002). Cultivars recognized as drought tolerant during the present study maintained water status by accumulation of total soluble sugars, proline, and amino acids (Figures 6A, B, D). Different studies have already explained that accumulation of osmo-protectants like soluble sugars, soluble proteins, and proline in leaves is involved in maintaining plant water status under stress conditions (Gontia-Mishra et al., 2016; Blum, 2017; Qayyum et al., 2021). Increase in proline production under drought stress is needed to supply energy for growth and survival to tolerate plants against drought stress (Shahin et al., 2018b). A greater concentration of proline plays an important role in osmotic adjustment, ROS scavenging, and stabilizing cellular components (Hussain et al., 2021). In wheat, the soluble sugars play the most important role in osmotic adjustment during drought stress (Camaille et al., 2021).

Drought-tolerant cultivars Barani-83, Blue Silver, Pak-81, and Pasban-90 showed greater amounts of N, P, and K^+ accumulated in the leaves as compared to FSD-08, Lasani-08, Punjab-96, and Sahar-06 cultivars under drought stress; previously, it was observed that plants exposed to drought stress have low N content in comparison to well-watered plants as found for rice and wheat due to restricted movement of N and P in the soil and less absorption by roots (Sun et al., 2012). Severe drought reduces N and P contents in leaves of wheat, canola, and soybean plants (Ashraf and Foolad, 2013). Noman et al. (2018) observed reduced levels of K, P, and Ca^{2+} in roots and shoots of wheat plants under drought stress. Oxidative stress refers to generation of ROS in response to drought stress due to shifting of Calvin cycle to photorespiration, which causes lipid peroxidation, chlorophyll etiolation, protein oxidation, and damage to cellular organelles, DNA, and RNA (Abedi and Pakniyat, 2010). Our experimental results are also in accordance with Outoukarte et al. (2019), who reported that enhanced lipid peroxidation and more ROS result in loss of membranes ability to control the rate of ion movement into and out of cells, an indication of plasma membrane

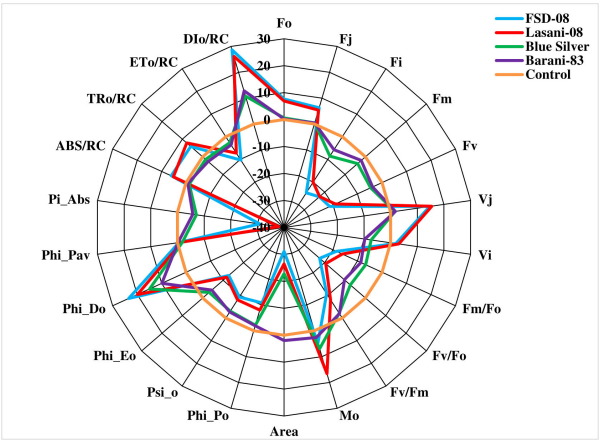


FIGURE 10
Radar plot of selected JIP test parameters showing changes in chlorophyll *a* fluorescence transients (normalized to control as reference) of four selected wheat cultivars subjected to drought stress at adult growth stage.

damage as revealed by increased MDA content, osmotic stress, and reduced N, P, and K status of drought-sensitive wheat cultivars (FSD-08, Lasani-08, Punjab-96, and Sahar-06) that ultimately affect their final yield.

The effects of drought stress on the shape of raw OJIP curves (Ft) show that Fo and Fj under drought stress were significantly increased, while Fi and Fm were markedly reduced in cvs. FSD-08 and Lasani-08 (Figures 8A-D). However, all these fluorescence attributes either remained unchanged or slightly changed in cvs. Blue Silver and Barani-83 due to water stress, which suggests only minor structural damage to PSII at both donor and acceptor end of PSII in these cultivars and can be considered as drought tolerant. Sensitive cvs. FSD-08 and Lasani-08 exhibited increased Fo and decreased energy trapping capacity of PSII, while decreased Fm may be attributed to inactive reaction centers. Damage to oxygen-evolving complex (OEC) reducing Fv values and increasing Vj is an indication of lowering PSII ability to reduce plastoquinone in these cultivars. Similar findings in mung bean were observed by Bano et al. (2021). L-band expresses uncoupling of OEC; its increased value in FSD-08, Lasani-08, and Blue Silver indicated uncoupling of OEC with core protein of PSII, while in Barani-83, no such L-band was observed (Figure 9A). Negative K-band values for Blue Silver and Barani-83 show that plants maintain antenna complex and PSII reaction center under the influence of drought stress (Figure 9B), while its positive values for cvs. FSD-08 and Lasani-08 show reduced OEC performance due to disturbance in electron flow from OEC to PSII reaction center in accordance with the previous studies, which explain that K-step gives information about the destruction of OEC (Guo et al., 2020). Many studies explain that double normalized differential chlorophyll *a* fluorescence kinetics such as L- and K-bands indicate drought tolerance potential in plants (Brestic and Zivcak, 2013; Kalaji et al., 2018; Zhou et al., 2019). Drought stress caused minor changes in Fv/Fm in cvs. Blue Silver and Barani-83, which suggest no photoinhibition, while the decrease in PSII efficiency of cvs. FSD-08 and Lasani-08 was mainly due to photoinhibition with greater decrease in Fv/Fm. The results are supported by the findings of Flexas et al. (2009) and Lawlor and Tezara (2009). The quantum yields of primary photochemistry (ΦPo) and the electron transfer from QA to PQ (ΦEo) are slightly affected in drought-tolerant cultivars (Blue Silver and Barani-83), while a greater decrease was observed in cvs. FSD-08 and Lasani-08. However, quantum yield for heat dissipation (ΦDo) increased only in drought-sensitive cultivars FSD-08 and Lasani-08. Fv/Fm and PI_{ABS} are important screening tools to investigate photosynthetic efficiency and effects of abiotic stresses on PSII in different plants. PI_{ABS} depends upon the concentration of active reaction centers of chlorophyll, efficiency of energy trapping, and electron transport from PSII to the plastoquinone pool (Botyanszka et al., 2020). Water stress increased the energy fluxes of absorption (ABS/RC), trapping (TRo/RC), and electron transport (ETo/RC) in FSD-08 and Lasani-08, while it decreased those in Blue Silver and Barani-83 cultivars. Strasser et al. (2000) explained that effective antenna size and absorbed energy are reduced in drought-tolerant cultivars, whereas drought-sensitive cultivars were unable to regulate the antenna size, so active reaction centers of PSII are damaged due to over-excitation. The absorbed energy by antenna proteins is dissipated as heat (DIo/RC) (Figure 10).

5 Conclusions

A great genetic variability was found among wheat cultivars in the present study. Based on maintaining growth, photosynthetic pigments, and RWC and good osmotic adjustment by accumulating proline, total soluble sugars, and proteins under water stress, Barani-83 and Blue silver were considered the most drought tolerant, while based on disruption of photosynthetic pigments and poor management of water status, FSD-08 and Lasani-08 were ranked as drought-sensitive cultivars. Chlorophyll *a* fluorescence transients confirmed better efficiency of photosystem II in tolerant cultivars (Barani-83 and Blue Silver) due to greater dissipation (DIo/RC) of absorbed energy (ABS/RC) and downregulation of electron transport per reaction center (ETo/RC) to prevent photosystem-II from photooxidative damage. Greater PSII stability and functional activity in drought-tolerant cultivars (Barani-83 and Blue Silver) was evident with greater performance index (PI_{ABS}) and greater quantum yield (Fv/Fm) of PSII.

Data availability statement

The original contributions presented in the study are included in the article/Supplementary Material. Further inquiries can be directed to the corresponding authors.

Author contributions

Conceptualization and designing the experiments, H-u-RA, RA, ZUZ, and SS. Execution of experiments, NH, AG, ZUZ, HB, AK, and MY. Data analysis, NH, MJ, RA, MI, SN, SS, and MZ. Data validation, H-u-RA. First draft writing, NH, AG, and KS. Supervision of the experiment, H-u-RA and ZUZ. Review and editing of the manuscript, H-u-RA, RA, SS, MJ, MI, AK, HB, and MZ. Proofing of the manuscript, H-u-RA, SN, SS, and RA.

Providing resources and funding acquisition, RA and SS. All authors contributed to the article and approved the submitted version.

Acknowledgments

The research work is a part of PhD study of Abdul Ghaffar. The authors are thankful to all who contributed in making this research study possible.

Conflict of interest

The authors declare that the research was conducted in the absence of any commercial or financial relationships that could be construed as a potential conflict of interest.

Publisher's note

All claims expressed in this article are solely those of the authors and do not necessarily represent those of their affiliated organizations, or those of the publisher, the editors and the reviewers. Any product that may be evaluated in this article, or claim that may be made by its manufacturer, is not guaranteed or endorsed by the publisher.

Supplementary material

The Supplementary Material for this article can be found online at: https://www.frontiersin.org/articles/10.3389/fpls.2023.1123080/full#supplementary-material

References

Abedi, T., and Pakniyat, H. (2010). Antioxidant enzymes changes in response to drought stress in ten cultivars of oilseed rape (Brassica napus l.). *Czech J. Genet. Plant Breed.* 46, 27–34. doi: 10.17221/67/2009-CJGPB

Ahmad, A., Aslam, Z., Javed, T., Hussain, S., Raza, A., Shabbir, R., et al. (2022). Screening of wheat (Triticum aestivum l.) genotypes for drought tolerance through agronomic and physiological response. *Agronomy* 12, 287. doi: 10.3390/agronomy12020287

Allen, S., Dobrenz, A., Schonhorst, M., and Stoner, J. (1985). Heritability of NaCl tolerance in germinating alfalfa seeds 1. *Agron. J.* 77, 99–101. doi: 10.2134/agronj1985.00021962007700010023x

Ashraf, M., and Foolad, M. R. (2007). Roles of glycine betaine and proline in improving plant abiotic stress resistance. *Environ. Exp. Bot.* 59, 206–216. doi: 10.1016/j.envexpbot.2005.12.006

Ashraf, M., and Foolad, M. R. (2013). Crop breeding for salt tolerance in the era of molecular markers and marker-assisted selection. *Plant Breed.* 132, 10–20. doi: 10.1111/pbr.12000

Ashraf, M., and Harris, P. J. (2013). Photosynthesis under stressful environments: an overview. *Photosynthetica* 51, 163–190. doi: 10.1007/s11099-013-0021-6

Bano, H., Athar, H. U. R., Zafar, Z. U., Kalaji, H. M., and Ashraf, M. (2021). Linking changes in chlorophyll a fluorescence with drought stress susceptibility in mung bean [Vigna radiata (L.) wilczek]. *Physiol. Plantarum* 172, 1244–1254. doi: 10.1111/ppl.13327

Bashir, N., Athar, H.-U.-R., Kalaji, H. M., Wróbel, J., Mahmood, S., Zafar, Z. U., et al. (2021). Is photoprotection of PSII one of the key mechanisms for drought tolerance in maize? *Int. J. Mol. Sci.* 22, 13490. doi: 10.3390/ijms222413490

Bates, L. S., Waldren, R. P., and Teare, I. (1973). Rapid determination of free proline for water-stress studies. *Plant Soil* 39, 205–207. doi: 10.1007/BF00018060

Belay, G. A., Zhang, Z., and Xu, P. (2021). Physio-morphological and biochemical trait-based evaluation of Ethiopian and Chinese wheat germplasm for drought tolerance at the seedling stage. *Sustainability* 13, 4605. doi: 10.3390/su13094605

Blum, A. (2016). Stress, strain, signaling, and adaptation–not just a matter of definition. *J. Exp. Bot.* 67, 562–565. doi: 10.1093/jxb/erv497

Blum, A. (2017). Osmotic adjustment is a prime drought stress adaptive engine in support of plant production. *Plant Cell Environ.* 40, 4–10. doi: 10.1111/pce.12800

Botyanszka, L., Zivcak, M., Chovancek, E., Sytar, O., Barek, V., Hauptvogel, P., et al. (2020). Chlorophyll fluorescence kinetics may be useful to identify early drought and irrigation effects on photosynthetic apparatus in field-grown wheat. *Agronomy* 10, 1275. doi: 10.3390/agronomy10091275

Bradford, M. M. (1976). A rapid and sensitive method for the quantitation of microgram quantities of protein utilizing the principle of protein-dye binding. *Analytical Biochem.* 72, 248–254. doi: 10.1016/0003-2697(76)90527-3

Bremner, J. M. (1965). "Organic nitrogen in soils," in *Soil nitrogen*. Eds. W. V. Bartholomew and F. E. Clark (USA: The American Society of Agronomy, Inc).

Brestic, M., and Zivcak, M. (2013). "PSII fluorescence techniques for measurement of drought and high temperature stress signal in crop plants: protocols and applications," in *Molecular stress physiology of plants* (Springer, India: Springer). doi: 10.1007/978-81-322-0807-5_4

Cakmak, I., and Horst, W. J. (1991). Effect of aluminium on lipid peroxidation, superoxide dismutase, catalase, and peroxidase activities in root tips of soybean (*Glycine max*). *Physiol. Plantarum* 83, 463–468. doi: 10.1111/j.1399-3054.1991.tb00121.x

Camaille, M., Fabre, N., Clément, C., and Ait Barka, E. (2021). Advances in wheat physiology in response to drought and the role of plant growth promoting rhizobacteria to trigger drought tolerance. *Microorganisms* 9, 687. doi: 10.3390/microorganisms9040687

Chen, W., Miao, Y., Ayyaz, A., Hannan, F., Huang, Q., Ulhassan, Z., et al. (2022b). Purple stem brassica napus exhibits higher photosynthetic efficiency, antioxidant potential and anthocyanin biosynthesis related gene expression against drought stress. *Front. Plant Sci.* 2606. doi: 10.3389/fpls.2022.936696

Chen, F., Wang, H., Zhao, F., Wang, R., Qi, Y., Zhang, K., et al. (2022a). The response mechanism and threshold of spring wheat to rapid drought. *Atmosphere* 13, 596. doi: 10.3390/atmos13040596

Chowdhury, M. K., Hasan, M., Bahadur, M., Islam, M. R., Hakim, M. A., Iqbal, M. A., et al. (2021). Evaluation of drought tolerance of some wheat (Triticum aestivum l.) genotypes through phenology, growth, and physiological indices. *Agronomy* 11, 1792. doi: 10.3390/agronomy11091792

Del Pozo, A., Yáñez, A., Matus, I. A., Tapia, G., Castillo, D., Sanchez-Jardón, L., et al. (2016). Physiological traits associated with wheat yield potential and performance under water-stress in a Mediterranean environment. *Front. Plant Sci.* 7, 987. doi: 10.3389/fpls.2016.00987

FAOSTAT (2022) *License: CC BY-NC-SA 3.0 IGO*. Available at: https://www.fao.org/faostat/en/#data/QCL/visualize.

FAO, UNICEF 2022, WFP and WHO (2022). *The state of food security and nutrition in the world 2022. repurposing food and agricultural policies to make healthy diets more affordable* (Rome: FAO. FAO, Rome).

Flexas, J., Barón, M., Bota, J., Ducruet, J.-M., Gallé, A., Galmés, J., et al. (2009). Photosynthesis limitations during water stress acclimation and recovery in the drought-adapted vitis hybrid Richter-110 (V. berlandieri× v. rupestris). *J. Exp. Bot.* 60, 2361–2377. doi: 10.1093/jxb/erp069

Gontia-Mishra, I., Sapre, S., Sharma, A., and Tiwari, S. (2016). Amelioration of drought tolerance in wheat by the interaction of plant growth-promoting rhizobacteria. *Plant Biol.* 18, 992–1000. doi: 10.1111/plb.12505

Guo, Y., Lu, Y., Goltsev, V., Strasser, R. J., Kalaji, H. M., Wang, H., et al. (2020). Comparative effect of tenuazonic acid, diuron, bentazone, dibromothymoquinone and methyl viologen on the kinetics of chl a fluorescence rise OJIP and the MR820 signal. *Plant Physiol. Biochem.* 156, 39–48. doi: 10.1016/j.plaphy.2020.08.044

Halder, T., Choudhary, M., Liu, H., Chen, Y., Yan, G., and Siddique, K. H. (2022). Wheat proteomics for abiotic stress tolerance and root system architecture: Current status and future prospects. *Proteomes* 10, 17. doi: 10.3390/proteomes10020017

Hamilton, P. B., Van Slyke, D. D., and Lemish, S. (1943). The gasometric determination of free amino acids in blood filtrates by the ninhydrin-carbon dioxide method. *J. Biol. Chem.* 150, 231–250. doi: 10.1016/S0021-9258(18)51268-0

Hoagland, D. R., and Arnon, D. I. (1950). ". the water-culture method for growing plants without soil," in *Circular*, vol. 347. (Berkeley, USA: College of Agriculture, University of California).

Hussain, N., Ghaffar, A., Zafar, Z. U., Javed, M., Shah, K. H., Noreen, S., et al. (2021). Identification of novel source of salt tolerance in local bread wheat germplasm using morpho-physiological and biochemical attributes. *Sci. Rep.* 11, 1–12. doi: 10.1038/s41598-021-90280-w

Hussain, N., Sohail, Y., Shakeel, N., Javed, M., Bano, H., Gul, H. S., et al. (2022). Role of mineral nutrients, antioxidants, osmotic adjustment and PSII stability in salt tolerance of contrasting wheat genotypes. *Sci. Rep.* 12, 1–13. doi: 10.1038/s41598-022-16922-9

Jackson, M. (1958). *Soil chemical analysis Englewood cliffs* (New Jersey, USA: NT Prentice Hall Inc).

Jones, M. M., and Turner, N. C. (1978). Osmotic adjustment in leaves of sorghum in response to water deficits. *Plant Physiol.* 61, 122–126. doi: 10.1104/pp.61.1.122

Kalaji, H. M., Račková, L., Paganová, V., Swoczyna, T., Rusinowski, S., and Sitko, K. (2018). Can chlorophyll-a fluorescence parameters be used as bio-indicators to distinguish between drought and salinity stress in tilia cordata mill? *Environ. Exp. Bot.* 152, 149–157. doi: 10.1016/j.envexpbot.2017.11.001

Lawlor, D. W., and Tezara, W. (2009). Causes of decreased photosynthetic rate and metabolic capacity in water-deficient leaf cells: a critical evaluation of mechanisms and integration of processes. *Ann. Bot.* 103, 561–579. doi: 10.1093/aob/mcn244

Li, M., and Kim, C. (2021). Chloroplast ROS and stress signaling. *Plant Commun.*, 3(1), 100264. doi: 10.1016/j.xplc.2021.100264

Muller, J. (1991). Determining leaf surface area by means of a wheat osmoregulation water use: the challenge. *Agric. Meteorol.* 14, 311–320. doi: 10.25081/jpsp.2019.v5.3700

Nobel, P. (1991). *Physicochemical and environmental plant physiology* (New York, NY: Academic Press).

Noman, A., Ali, Q., Naseem, J., Javed, M. T., Kanwal, H., Islam, W., et al. (2018). Sugar beet extract acts as a natural bio-stimulant for physio-biochemical attributes in water stressed wheat (Triticum aestivum l.). *Acta Physiol. Plantarum* 40, 1–17. doi: 10.1007/s11738-018-2681-0

Outoukarte, I., El Keroumi, A., Dihazi, A., and Naamani, K. (2019). Use of morpho-physiological parameters and biochemical markers to select drought tolerant genotypes of durum wheat. *J. Plant Stress Physiol.*, 01–07. doi: 10.25081/jpsp.2019.v5.3700

Ozturk, M., Unal Turkyilmaz, B., García-Caparrós, P., Khursheed, A., Gul, A., and Hasanuzzaman, M. (2021). Osmoregulation and its actions during the drought stress in plants. *Physiol. Plantarum* 172, 1321–1335. doi: 10.1111/ppl.13297

Panhwar, N. A., Mierzwa-Hersztek, M., Baloch, G. M., Soomro, Z. A., Sial, M. A., Demiraj, E., et al. (2021). Water stress affects the some morpho-physiological traits of twenty wheat (Triticum aestivum l.) genotypes under field condition. *Sustainability* 13, 13736. doi: 10.3390/su132413736

Peršić, V., Ament, A., Drezner, G., and Cesar, V. (2022). PEG-induced physiological drought for screening winter wheat genotypes sensitivity–integrated biochemical and chlorophyll a fluorescence analysis. *Front. Plant Sci.* 13. doi: 10.3389/fpls.2022.987702

Qayyum, A., Al Ayoubi, S., Sher, A., Bibi, Y., Ahmad, S., Shen, Z., et al. (2021). Improvement in drought tolerance in bread wheat is related to an improvement in osmolyte production, antioxidant enzyme activities, and gaseous exchange. *Saudi J. Biol. Sci.* 28, 5238–5249. doi: 10.1016/j.sjbs.2021.05.040

Riyazuddin, R., Nisha, N., Singh, K., Verma, R., and Gupta, R. (2022). Involvement of dehydrin proteins in mitigating the negative effects of drought stress in plants. *Plant Cell Rep.* 41, 519–533. doi: 10.1007/s00299-021-02720-6

Sallam, A., Alqudah, A. M., Dawood, M. F., Baenziger, P. S., and Börner, A. (2019). Drought stress tolerance in wheat and barley: advances in physiology, breeding and genetics research. *Int. J. Mol. Sci.* 20, 3137. doi: 10.3390/ijms20133137

Scholander, P. F., Hammel, H., Hemmingsen, E., and Bradstreet, E. (1964). Hydrostatic pressure and osmotic potential in leaves of mangroves and some other plants. *Proc. Natl. Acad. Sci. United States America* 52, 119. doi: 10.1073/pnas.52.1.119

Sekher, T. (2022) in *World Population Day-2022 Symposium & Launch of United Nations World Population Prospects-2022, Conference Proceedings Columbia University*.

Serraj, R., and Sinclair, T. (2002). Osmolyte accumulation: can it really help increase crop yield under drought conditions? *Plant Cell Environ.* 25, 333–341. doi: 0.1046/j.1365-3040.2002.00754.x

Shahin, S., Kurup, S., Cheruth, J., Lennartz, F., and Salem, M. (2018b). Growth, yield, and physiological responses of cleome amblyocarpa barr. & murb. under varied irrigation levels in sandy soils. *J. Food Agric. Environ.* 16, 124–134. doi: 10.1234/4.2018.5508

Shahin, S., Kurup, S., Cheruth, A.-J., and Salem, M. (2018a). Chemical composition of cleome amblyocarpa barr. & murb. essential oils under different irrigation levels in sandy soils with antioxidant activity. *J. Essential Oil Bearing Plants* 21, 1235–1256. doi: 10.1080/0972060X.2018.1512422

Shen, J., Guo, M.-J., Wang, Y.-G., Yuan, X.-Y., Wen, Y.-Y., Song, X.-E., et al. (2020). Humic acid improves the physiological and photosynthetic characteristics of millet seedlings under drought stress. *Plant Signaling Behav.* 15, 1774212. doi: 10.1080/15592324.2020.1774212

Snedecor, G. W., and Cochran, W. G. (1989). *Statistical methods. eight edition* (Ames, Iowa: Iowa state University press).

Strasser, R. J., Srivastava, A., and Tsimilli-Michael, M. (2000). "The fluorescence transient as a tool to characterize and screen photosynthetic samples," in *Probing Photosynthesis: Mechanism, Regulation and Adaptation* eds M. Yunus, U. Pathre and P. Mohanty (London, UK: CRC Press, Taylor and Francis Group) 445–483.

Strasser, R. J., Tsimilli-Michael, M., and Srivastava, A. (2004). "Analysis of the chlorophyll a fluorescence transient," in *Chlorophyll a fluorescence* (New York, USA: Springer).

Sun, M., Gao, Z.-Q., Yang, Z.-P., and He, L.-H. (2012). Absorption and accumulation characteristics of nitrogen in different wheat cultivars under irrigated and dryland conditions. *Aust. J. Crop Sci.* 6, 613. doi: 10.3316/informit.362102772665611

Tefera, A., Kebede, M., Tadesse, K., and Getahun, T. (2021). Morphological, physiological, and biochemical characterization of drought-tolerant wheat (Triticum spp.) varieties. *Int. J. Agron.* 2021, 1–12. doi: 10.1155/2021/8811749

Tsimilli-Michael, M. (2020). Special issue in honour of Prof. reto j. strasser–revisiting JIP-test: An educative review on concepts, assumptions, approximations, definitions and terminology. *Photosynthetica* 58, 275–292. doi: 10.32615/ps.2019.150

Wasaya, A., Manzoor, S., Yasir, T. A., Sarwar, N., Mubeen, K., Ismail, I. A., et al. (2021). Evaluation of fourteen bread wheat (Triticum aestivum l.) genotypes by observing gas exchange parameters, relative water and chlorophyll content, and yield attributes under drought stress. *Sustainability* 13, 4799. doi: 10.3390/su13094799

WFP and UNICEF (2022). *The state of food security and nutrition in the world 2022* (Rome, Italy: FAO).

Yemm, E., and Willis, A. (1954). The estimation of carbohydrates in plant extracts by anthrone. *Biochem. J.* 57, 508–514. doi: 10.1042/bj0570508

Zhang, X., Yang, H., and Du, T. (2022). Osmotic adjustment of tomato under mild soil salinity can enhance drought resistance. *Environ. Exp. Bot.* 202, 105004. doi: 10.1016/j.envexpbot.2022.105004

Zhou, R., Kan, X., Chen, J., Hua, H., Li, Y., Ren, J., et al. (2019). Drought-induced changes in photosynthetic electron transport in maize probed by prompt fluorescence, delayed fluorescence, P700 and cyclic electron flow signals. *Environ. Exp. Bot.* 158, 51–62. doi: 10.1016/j.envexpbot.2018.11.005

Zhu, J., Cai, D., Wang, J., Cao, J., Wen, Y., He, J., et al. (2021). Physiological and anatomical changes in two rapeseed (Brassica napus l.) genotypes under drought stress conditions. *Oil Crop Sci.* 6, 97–104. doi: 10.1016/j.ocsci.2021.04.003

frontiers | Frontiers in Plant Science

TYPE Original Research
PUBLISHED 02 February 2023
DOI 10.3389/fpls.2023.1061845

Check for updates

OPEN ACCESS

EDITED BY
Mehtab Muhammad Aslam,
The Chinese University of Hong Kong, China

REVIEWED BY
Hongchun Xiong,
Institute of Crop Sciences (CAAS), China
Gautam Saripalli,
University of Maryland, College Park, United States

*CORRESPONDENCE
Matías Schierenbeck
schierenbeck@ipk-gatersleben.de;
m_schierenbeck@hotmail.com
Ahmad M. Alqudah
aalqudah@qu.edu.qa;
ahqudah@gmail.com

SPECIALTY SECTION
This article was submitted to Plant Abiotic Stress, a section of the journal Frontiers in Plant Science

RECEIVED 05 October 2022
ACCEPTED 09 January 2023
PUBLISHED 02 February 2023

CITATION
Schierenbeck M, Alqudah AM, Thabet SG, Lohwasser U, Simón MR and Börner A (2023) Association mapping unravels the genetics controlling seedling drought stress tolerance in winter wheat. *Front. Plant Sci.* 14:1061845. doi: 10.3389/fpls.2023.1061845

COPYRIGHT
© 2023 Schierenbeck, Alqudah, Thabet, Lohwasser, Simón and Börner. This is an open-access article distributed under the terms of the Creative Commons Attribution License (CC BY). The use, distribution or reproduction in other forums is permitted, provided the original author(s) and the copyright owner(s) are credited and that the original publication in this journal is cited, in accordance with accepted academic practice. No use, distribution or reproduction is permitted which does not comply with these terms.

Association mapping unravels the genetics controlling seedling drought stress tolerance in winter wheat

Matías Schierenbeck[1,2,3]*, Ahmad M. Alqudah[4]*, Samar G. Thabet[5], Ulrike Lohwasser[1], María Rosa Simón[2,3] and Andreas Börner[1]

[1]Genebank Department, Leibniz Institute of Plant Genetics and Crop Plant Research (IPK), OT Gatersleben, Seeland, Germany, [2]Cereals, Faculty of Agricultural Sciences and Forestry, National University of La Plata, La Plata, Argentina, [3]CONICET CCT La Plata, La Plata, Argentina, [4]Biological Science Program, Department of Biological and Environmental Sciences, College of Art and Science, Qatar University, Doha, Qatar, [5]Department of Botany, Faculty of Science, Fayoum University, Fayoum, Egypt

Drought is a major constraint in wheat (*Triticum aestivum L.*) grain yield. The present work aimed to identify quantitative trait nucleotides (QTNs)/ candidate genes influencing drought tolerance-related traits at the seedling stage in 261 accessions of a diverse winter wheat panel. Seeds from three consecutive years were exposed to polyethylene glycol 12% (PEG-6000) and a control treatment (distilled water). The Farm-CPU method was used for the association analysis with 17,093 polymorphic SNPs. PEG treatment reduced shoot length (SL) (-36.3%) and root length (RL) (-11.3%) compared with control treatments, while the coleoptile length (CL) was increased by 11% under drought conditions, suggesting that it might be considered as an indicator of stress-tolerance. Interestingly, we revealed 70 stable QTN across 17 chromosomes. Eight QTNs related to more than one trait were detected on chromosomes 1B, 2A (2), 2B, 2D, 4B, 7A, and 7B and located nearby or inside candidate genes within the linkage disequilibrium (LD) interval. For instance, the QTN on chromosome 2D is located inside the gene TraesCS2D02G133900 that controls the variation of CL_S and SL_C. The allelic variation at the candidate genes showed significant influence on the associated traits, demonstrating their role in controlling the natural variation of multi-traits of drought stress tolerance. The gene expression of these candidate genes under different stress conditions validates their biological role in stress tolerance. Our findings offer insight into understanding the genetic factors and diverse mechanisms in response to water shortage conditions that are important for wheat improvement and adaptation at early developmental stages.

KEYWORDS

drought tolerance, seedling, winter wheat, GWAS, candidate genes, PEG, FarmCPU, breeding

1 Introduction

Globally, wheat is the main source of vegetable protein for humanity and provides around 20% of global calories for human consumption. It is considered a primary food staple in Europe, North Africa, Middle East and is growing in popularity in Asia (Food and Agriculture Organization, 2014). In wheat, Daryanto et al. (2016) reported that drought is a major yield-limiting factor worldwide, a situation that will increase in the future due to global climate change and uncertainties in precipitation patterns. Based on this problem, increasing the area sown in regions unsuitable for crop production due to early drought stress is one of the strategies for enhancing worldwide wheat production and meeting global demand (Thabet et al., 2018; Thabet et al., 2020). Faced with these scenarios, it is critical to identify the genetic factors determining different ecophysiological attributes related to abiotic stresses in order to accelerate the rate of genetic gain of the crop.

Due to the importance of rapid leaf area development, early seedling growth is a critical stage for wheat establishment (Ma et al., 2020; Maulana et al., 2020). Despite the great number of results achieved in basic and applied research, the genetic and physiological background of drought tolerance is still insufficiently known (Sallam et al., 2019; Thabet and Alqudah, 2019; Mahpara et al., 2022). Reporting candidate genes associated with drought tolerance traits and proving their functions is one of the major challenges facing genetics today and could become a key factor to increase global wheat production. The QTL (quantitative trait loci) mapping approach is a fundamental tool for the genetic dissection of agronomical traits (Muqaddasi et al., 2017; Alqudah et al., 2020; Schierenbeck et al., 2021), grain yield-related traits (Sukumaran et al., 2018), biotic stresses (Maccaferri et al., 2016) and abiotic stress tolerance (Landjeva et al., 2008; Lin et al., 2019). Plant response to polyethylene glycol (PEG) is comparable to that induced by drought in its early stages, causing a reduction in germination and seedling growth (Liu et al., 2006; Landjeva et al., 2008; Kido et al., 2016; Ayalew et al., 2018; Lin et al., 2019; Mahpara et al., 2022). Selection for higher coleoptile (Rebetzke et al., 2014; Ma et al., 2020), shoot (Reynolds et al., 2000; Landjeva et al., 2008) and root length (Ayalew et al., 2018) in early drought conditions has been reported as important strategies for increasing water shortage tolerance.

Recent studies reported several QTLs under drought conditions during post-flowering (Li et al., 2015; Sukumaran et al., 2018), while fewer efforts were documented for early crop stages under stress conditions (Maulana et al., 2020; Sallam et al., 2022). QTNs (quantitative trait nucleotides) or MTAs (marker-trait associations) related to coleoptile length on several chromosomes (Rebetzke et al., 2014; Ma et al., 2020), shoot length on 1A, 2B, 3A, 4B, 5A, 7A (Maulana et al., 2020; Maulana et al., 2021), root length on 2B, 2D, 3B, 4A, 4B, 5D, 5B and 6D (Kadam et al., 2012; Maccaferri et al., 2016; Ayalew et al., 2019; Xu et al., 2021) were documented previously. Moreover, Thabet et al. (2018) reported several significant SNPs associated with barley germination parameters and seedling related-traits when exposed to 20% PEG. Maulana et al. (2020) reported multiple significant QTN (quantitative trait nucleotides) related to early drought tolerance that was responsible for the shoot length growth under such abiotic conditions. Despite this, new efforts are necessary to evaluate different wheat accessions and environmental conditions to improve seedling drought tolerance as well as grain yield potential.

Several studies identified a number of promising candidates that had potential roles in drought stress tolerance in cereal plants, including wheat. In rice, high expression of *DEEPER ROOTING 1* (*DRO1*) increases the root angle and deep rooting enhancing grain yield under drought-affected soils (Uga et al., 2013). Consistent with the findings in rice, (Kulkarni et al., 2017) reported three copies of *DRO1* orthologs in the wheat genome. Overexpression of wheat Zinc Finger Proteins (ZFPs) in roots, *TaZFP34* gene, improved root-to-shoot ratio due to a decrease in shoot elongation while maintaining root growth during drought stress (Chang et al., 2016).

Therefore, the primary aim of the present study is to report MTAs controlling drought tolerance at the early growth stage in a recently described wheat panel constituted of 261 genotypes. For this purpose, the accessions were characterized for three years by the ability to maintain the root, coleoptiles, and shoot growth under PEG osmotic stress and further analyzed with 17,093 valid SNPs through a GWAS scan. Potential candidate genes controlling the studied traits under stress conditions had been detected and discussed in the current study. Our findings are a valuable resource for breeding new varieties carrying stress tolerance alleles and understanding the genetic mechanisms related.

2 Materials and methods

2.1 Plant phenotyping

To examine how large the natural variation in studied traits is related to seedling growth under control and induced drought conditions, a wheat panel comprising 261 accessions was tested. Detailed information about these panels was described by Schierenbeck et al. (2021).

Experiments were performed at IPK Gatersleben (Germany) using seeds grown under field conditions and harvested in 2016, 2017, and 2018. To induce drought stress (S), twenty seeds per accession were placed on filter paper humidified with PEG 6000 (12%) and grown in chamber conditions at 21°C in the dark for 3 days, and subsequently by 5 days at a 12-h photoperiod as suggested by Landjeva et al. (2008). Distilled water was used for control treatment [Control (C)]. After eight days, the shoot length (SL), coleoptile length (CL), root length (RL), and root/shoot length ratio (RSR) were recorded on ten seedlings per genotype. A tolerance index (TI) was defined for the four traits as the relation between the mean value obtained under stress and control conditions. In total, three replications were performed.

2.1.1 Phenotypic data analysis

GenStat 19 software was used for the analysis of variance (ANOVA) and broad-sense heritability (H^2) calculations:

$$H^2 = \sigma g^2 / \left(\frac{\sigma gy^2}{y} + \frac{\sigma e^2}{ry} \right)$$

where the mean squares for accessions (σg^2), genotype × environment interaction (σgy^2), and residual error (σe^2), and y represents years and r (replicates). MVApp v2.0 (Julkowska et al., 2019) were used for correlations boxplot calculations.

The restricted maximum likelihood (REML) algorithm was applied and Best Linear Unbiased Estimators (BLUEs) for each treatment were calculated (BLUE-C and BLUE-S) using nlme package in R (Pinheiro et al., 2022).

2.2 Quantitative trait nucleotide analysis

2.2.1 Genotyping and GWAS study

The panel was genotyped by Trait Genetics GmbH using the 90K iSELECT chip (Wang et al., 2014) generating 17,093 SNPs after filtering markers with >10% missing data and MAF <5%. Markers were mapped according to their physical position based on IWGSC RefSeq v1.1 (http://www.wheatgenome.org) and then used to determine the population structure, linkage disequilibrium (LD) and for GWAS scan as described in Schierenbeck et al. (2021). The genome-wide pairwise estimates of LD were calculated as a squared correlation between pairs of polymorphic SNPs (r^2) for the whole genome using GenStat 18 (VSN International, 2015). Finally, LD decay patterns were visualized as the plot for the LD estimated the (r^2) vs. the distance between pairs of polymorphic SNPs (Mbp) using R-package GGPLOT2 (Wickham, 2016). The average genome-wide LD decay at $r^2 = 0.2$ (approximately 2.0 Mbp).

GWAS has performed by testing different statistical models in GAPIT 3 (R). The Farm-CPU model was chosen because it prevents model overfitting explained by a reduction in false-negative and false-positive associations (Bhatta et al., 2019; Schierenbeck et al., 2021; Wang & Zhang, 2021). The detected associations above the threshold of -log10 (p)≥3 in at least two environments were considered significant quantitative trait nucleotide (QTN) (Quan et al., 2021). A QTN was given to each significant SNP marker, and a quantitative nucleotide region (QNR) was given to the genomic regions (Gaur et al., 2022). For the highly associated QNR, LD block for specific physical distance including the strongest associated QTNs was calculated to define the physical interval of the associated QNR and then used for candidate gene detection (Alqudah et al., 2020).

2.2.2 Candidate gene analysis

Those stable and highly significant QTNs were analyzed to detect those high-confidence candidate genes related, using RefSeq annotation v1.1 (http://www.wheatgenome.org). Gene Annotation description (GO and Interpros) was reported using the Wheat Mine platform (https://urgi.versailles.inra.fr/WheatMine/begin.do).

RNA-Seq expression derived from the Wheat Expression Browser (http://www.wheat-expression.com/) was utilized for gene expression analysis of the multi-traits candidate genes. We also used the OPEN-ACCESS version of Genevestigator to check which gene is up or down expressed under drought and drought simulated by PEG from the expression and transcriptomes database (Hruz et al., 2008).

3 Results

3.1 Population structure and SNP coverage

As reported in our previous paper (Schierenbeck et al., 2021), the winter wheat panel clustered into three groups based on their continent of origin: 146 accessions derived from Eastern Europe-Western Asia (55.6%), 66 genotypes from Central-Northern Europe (25.2%) and 42 North-American accessions (16%). Regarding the SNP coverage, genome B showed the highest with 8,809 SNPs (51.5%), genome A was covered by 38.6% (6,595 SNPs) and D genome showed the lowest (9.9%) (Schierenbeck et al., 2021).

3.2 Phenotypic data analysis

The years, treatments, genotypes, *Treatments* × *Year* (except CL), and *Year* × *Treatments* × *Genotypes* interactions significantly influenced seedling growth parameters (Table 1). Drought treatment generates important reductions in growth parameters such as RL and SL, but an increase in CL and RSR. Table S2 indicates a summary as well as the main results. For tolerance index, significant differences were reported in the four variables (Table S1).

All variables analyzed under both growth conditions showed high broad-sense heritability ranging from 0.89 to 0.97 (control) and 0.87 to 0.97 under stress conditions (Table 1), while lower H^2 was detected for TI variables (Table S1).

Compared to the control treatment, PEG treatments reduced SL by 36.3% and RL by 11.3% in wheat seedlings. In contrast, increases of 11% in CL were reported under drought. For CL, values across the three years varied from 2.00 to 4.47 cm in control conditions (BLUE-C) and 2.11 to 4.77 cm under drought stress (BLUE-S). The SL values ranged from 7.01 to 15.31 cm (BLUE-C) and 3.77 to 9.96 cm under PEG stress (BLUE-S). Variations in RL in control conditions fluctuated between 16.06 to 20.91 cm, while values from 13.79 to 19.50 cm were detected under drought conditions (BLUE-S). For RSR, BLUE-C values varied from 1.198 to 2.551 and 1.713 to 4.336 under drought stress. Variations of BLUEs values for CL, SL, RL, and RSR across years and summary statistics are indicated in Table S2. Variations among accessions across years under control and stress conditions as well as BLUEs values are shown in Figure 1.

Highly significant correlations between CL and SL were reported under control (0.71) and drought conditions (0.56). Negative correlations were reported between CL and RSR, showing values of -0.72 (control) and -0.61 (drought). Non-significant correlations were detected for CL and RL, -0.06 for control, and -0.12 under drought. The SL and RL presented positive correlations for control (0.18) and stress (0.27), while negative associations were reported for SL-RSR under control (-0.92) and stress experiments (-0.87) (Figure 2).

The diverse origins of the genotypes presented a differential response in the traits evaluated under control and stress conditions. Wheat accessions from Eastern Europe-Western Asia showed higher coleoptile and shoot lengths under control (3.19 cm and 12.63 cm,

TABLE 1 Means square and p-value (ANOVA) of coleoptile length, shoot length, root length and root:shoot length in an experiment with two drought treatments evaluated on 261 wheat genotypes during 3 years.

Source of variation	D.F.	Coleoptile Length (CL)	Shoot Length (SL)	Root length (RL)	Root/Shoot ratio (RSR)
Years (Y)	2	78.55 (<0.001)	171.6 (0.006)	157.3 (0.005)	11.0 (0.022)
Error A	4	0.56	7.42	6.28	0.97
Treatment (T)	1	138.4 (<0.001)	21907 (<0.001)	5272 (<0.001)	486.2 (<0.001)
Y × T	2	0.19 (0.268)	48.17 (<0.001)	59.2 (<0.001)	1.92 (0.029)
Error B	6	0.11	0.99	1.06	0.28
Genotype (G)	260	2.98 (<0.001)	22.93 (<0.001)	8.41 (<0.001)	1.09 (<0.001)
Y × G	516	0.11 (<0.001)	1.48 (<0.001)	1.58 (<0.001)	0.06 (<0.001)
T × G	260	0.12 (<0.001)	2.74 (<0.001)	1.21 (<0.001)	0.12 (<0.001)
Y × T × G	516	0.05 (<0.001)	0.68 (<0.001)	0.90 (<0.001)	0.039 (<0.001)
Error C	3104	0.023	0.22	0.41	0.01
Total	4673				
H^2		0.98 (C) 0.97 (S)	0.97 (C) 0.94 (S)	0.89 (C) 0.87 (S)	0.98 (C) 0.95 (S)

H2, broad-sense heritability. ** indicate significance P<0.001; * P<0.05; ns (no significance) Control (C), Stress (S).

respectively) and stress conditions (3.57 cm and 8.08 cm, respectively) compared to those from Central and Northern Europe for CL (3.04 cm under control and 3.36 cm under stress) and SL (11.36 cm under control and 7.13 cm under stress). The North American cultivars showed intermediate values (Figure 3).

3.3 Genome-wide association mapping analysis

The FARM-CPU model showed 70 stable QTNs in at least two environments (-log10>3; p<0.001) related to wheat seedling growth under control and drought stress across 17 chromosomes. These QTNs were reported on chromosomes 1A (1), 1B (6), 2A (4), 2B (9), 2D (2), 3A (2), 4A (1), 4B (3), 4D (2), 5A (9), 5B (2), 5D (1), 6A (2), 6B (4), 6D (1), 7A (13) and 7B (8) (Figures 4A–C and Table S3).

For CL under controlled conditions, ten QTNs were identified on 1B (1), 2A (1), 2B (1), 2D (1), 4B (2), 5A (1), 6B (1), 6D (1) and 7A (1) (Figures 4A, B). The most significant QTNs were IAAV971 on chromosome 4B, RAC875_c25839_225 on chromosome 6D and Kukri_c44587_130 on chromosome 1B. The phenotypic variation explained by QTNs (R^2) ranged between 0.63 and 2.40% (Table S3). Under stress conditions (CL_S) seven, QTNs were found on 1B, 2A (2), 2D, 4B, 4D and 7A. Highly significant associations were reported for this trait in IAAV971 on 4B, IAAV6312 located on chromosome 2D and Kukri_c44587_130 on 1B. The R^2 for this trait oscillated between 0.53 to 3.40%. For their part, one MTA was detected for CL_TI, BS00082219_51 on Chromosome 5A (Figure 4C).

Eleven QTNs were detected for RL under control conditions were localized on 5B, 7A (7) and 7B (3) (Figures 4A, B). BobWhite_c24096_57 on chromosome 7A, BS00089942_51 on chromosome 7B, and Tdurum_contig65330_190 on chromosome 5B. All showed a positive response to this trait (Table S3). The phenotypic variation explained by QTNs ranged between 0.08 and 3.27%. Under stress conditions, three stable QTNs were detected for RL: wsnp_Ra_c33358_42248399 on 6B, Kukri_c860_353 on 7A, and Kukri_rep_c72909_657 on 7B. R^2 for the trait ranged between 0.48 and 2.07%. One QTN was related to the RL tolerance index (Figure 4C). Kukri_rep_c72909_657 and located on chromosome 7B.

Twenty-two QTNs were detected for SL (8 for SL_C, 2 for SL_S and 12 for SL_TI) (Figures 4A–C). For SL_C, QTNs were reported on chromosomes 2A (2), 4B, 4D, 5A, 6A, and 6B (2). QTNs such as wsnp_Ex_rep_c66270_64420584 on 2A, IAAV971 on 4B, wsnp_Ex_c3620_6612231 on 5A and BobWhite_c22827_193 on 6B showed the most significant associations with this trait (R^2 between 0.6-2.16%). Under stress conditions (SL_S), wsnp_Ex_rep_c67036_65492436 on 1B and Kukri_c20822_1029 on 4B were documented. Twelve QTNs linked with the SL tolerance index were found on chromosomes 4A (1), 5A (5), 7A (3) and 7B (3). The most significant were Ex_c7626_444 on 4A, wsnp_JD_rep_c61843_39601402 on 5A, BS00061911_51 on 7A and wsnp_Ra_rep_c69221_66574260 on 5A. The phenotypic variation (R^2) ranged between 0.65 and 4.06% (Table S3).

The RSR under control conditions showed 11 QTNs on 1B (2), 2A, 2B (2), 2D, 3A (2), 4B, 5A as well as 5B. The QTNs Kukri_c66451_128 on 1B, BS00060686_51 on 1B, BS00039422_51 on 2A, BobWhite_c2570_682 on 3A, Kukri_c18258_440 on 3A, *IAAV971* on 4B and Tdurum_contig17712_200 on 5A were the most significant ones. Under stress conditions (RSR_S), six QTNs were reported on chromosomes 1A, 2A, 2B (2), 4B and 5D. Highly significant associations were reported for GENE-4120_155 on 1A, RAC875_c52458_454 on 2A, BS00001140_51 on 2B; IAAV3303 on 2B and IAAV971 on 4B. Eight QTNs were detected for RSR_TI located on chromosomes 1B (2), 2B (5), and 6A (1). The most significant, such as tplb0034e07_1869, tplb0034e07_718, GENE-1442_78, Excalibur_c42248_663 and Kukri_rep_c108293_98 were reported on chromosome 2B (Table S3).

Moreover, eight multitraits QTNs across seven chromosomes were detected under control and stress treatments. These QTNs were detected on 1B (Kukri_c44587_130 related to CL-C and CL-S), 2A (RAC875_c52458_454 for CL-C/RSR-S/SL-C and RFL_Contig2656_871

10.3389/fpls.2023.1061845

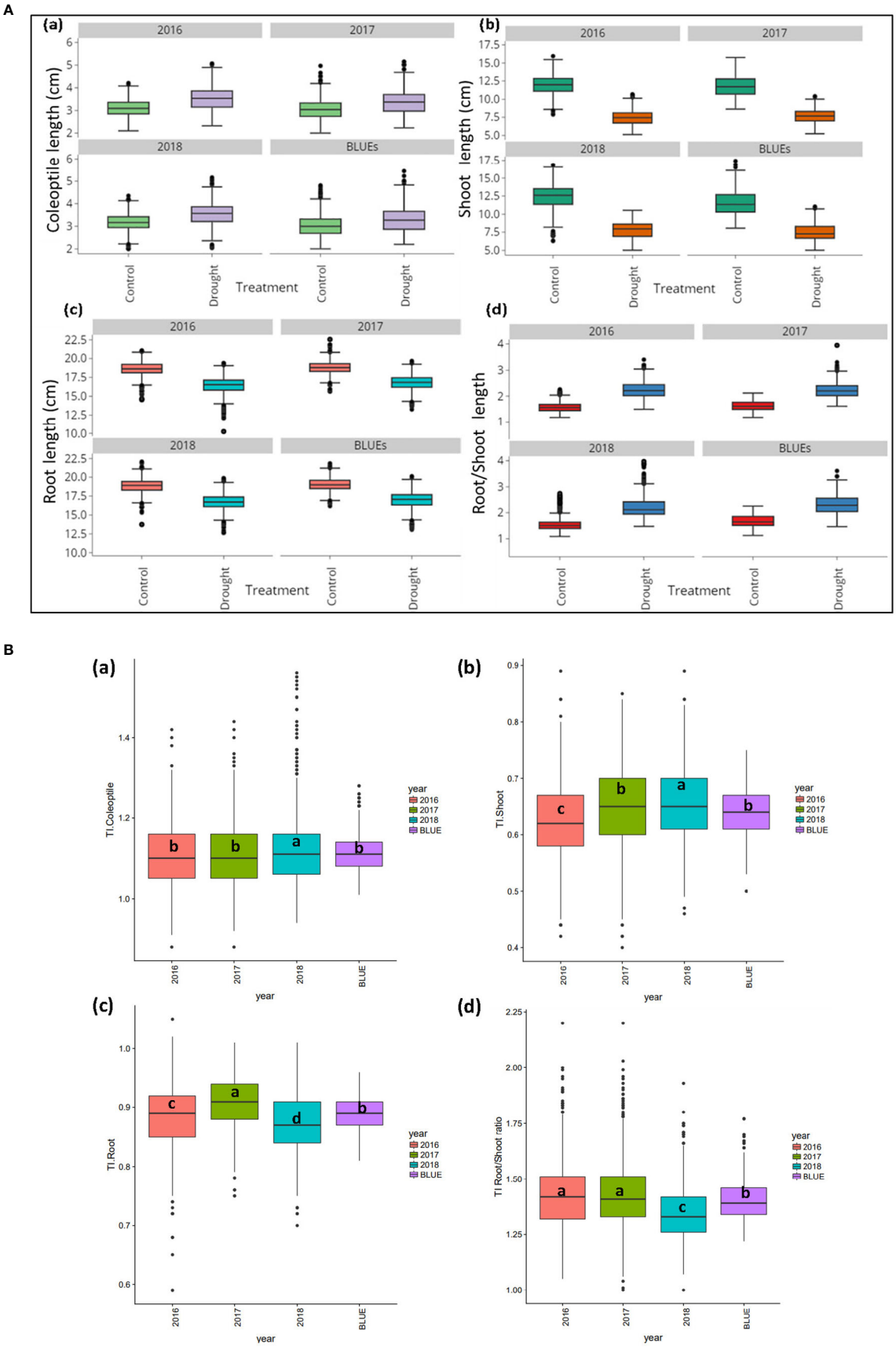


FIGURE 1
(A) Boxplot for real values for three years and BLUEs values for a) Coleoptile length (cm), b) Shoot length (cm) (c) Root length (cm), and d) Root/Shoot ratio in 261 winter wheat genotypes under control and drought stress. **(B)**. Boxplot for three years and BLUEs values for a) Coleoptile length tolerance index, b) Shoot length tolerance index c) Root length tolerance index and d) Root/Shoot ratio tolerance index in 261 winter wheat genotypes.

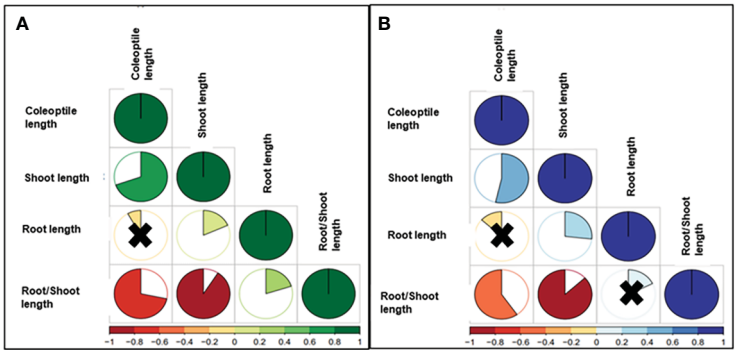


FIGURE 2
Pearson Correlation Coefficients of BLUEs values of the studied traits between **(A)** control and **(B)** drought in wheat genotypes. The degree of significance for all correlations was P<0.001. The color reflects the strength of the correlation. Black crosses indicate non-significant correlations.

for CL-C/CL-S), 2B (BS00001140_51 for RSR-C and RSR-S), 2D (IAAV6312 for CL_C and CL_S), 4B (IAAV971 for CL-C/CL-S/RSR-C/RSR-S/SL-C), 7A (BS00068033_51 for CL_S and SL_TI) and 7B (Kukri_rep_c72909_657 for RL_S and RL_TI) (Tables 2, S3).

3.4 Candidate genes underlying wheat seedling growth under control and PEG stress

Based upon GWAS outputs, we identified eight plausible candidate genes that are associated with two or more traits related to seedling growth under drought and control conditions. On chromosome 1B, the QTN Kukri_c44587_130 inside the *TraesCS1B02G480400* gene is located at a position 687794252-687799812 bp that harbor the CL phenotypic variation under both treatments. This CG is annotated as Zinc finger, CCCH-type superfamily that might be linked to biotic/abiotic stress tolerance in different species, including wheat (Figures S1A, B). For this QTN, accessions carrying the A allele showed longer coleoptiles under control and stress conditions (Figure S1C). The QTN RAC875_c52458_454 on chromosome 2A is located inside the gene *TraesCS2A02G442700* at position 692754161-692757947 bp and controls the variation of CL_S, RSR_S, and SL_C. Our candidate encodes a helix-loop-helix DNA-binding domain superfamily that pertain to the helix–loop–helix transcription factors (bHLH), playing a key part in regulating plant growth and development under various environmental stress conditions (Figures S2A–C). Genotypes carrying T alleles showed higher CL and SL under drought stress. A QTN (RFL_Contig2656_871) on chromosome 2A inside the candidate *TraesCS2A02G543900* at position (753538593-753541916 bp)

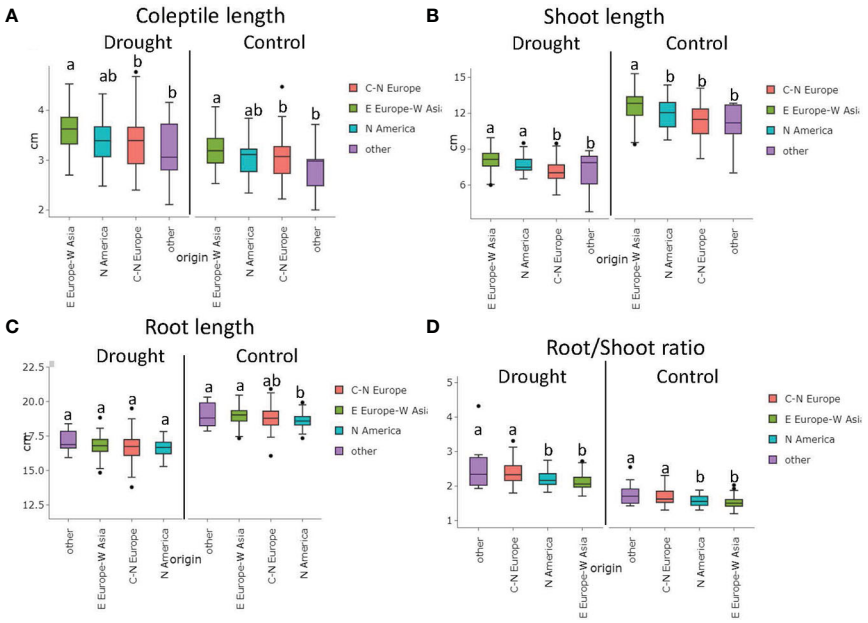


FIGURE 3
Variation on seedlings Coleoptile length **(A)**, Shoot length **(B)**, Root length **(C)**, and Root/Shoot Ratio **(D)** under control and drought stress based on genotype origin (BLUEs values). C-N Europe (Central-Northern Europe); E Europe- W Asia (Eastern Europe-Western Asia); N America (North America). Matching letters at thesame treatment are not statistically different (LSD p ≤ 0.05).

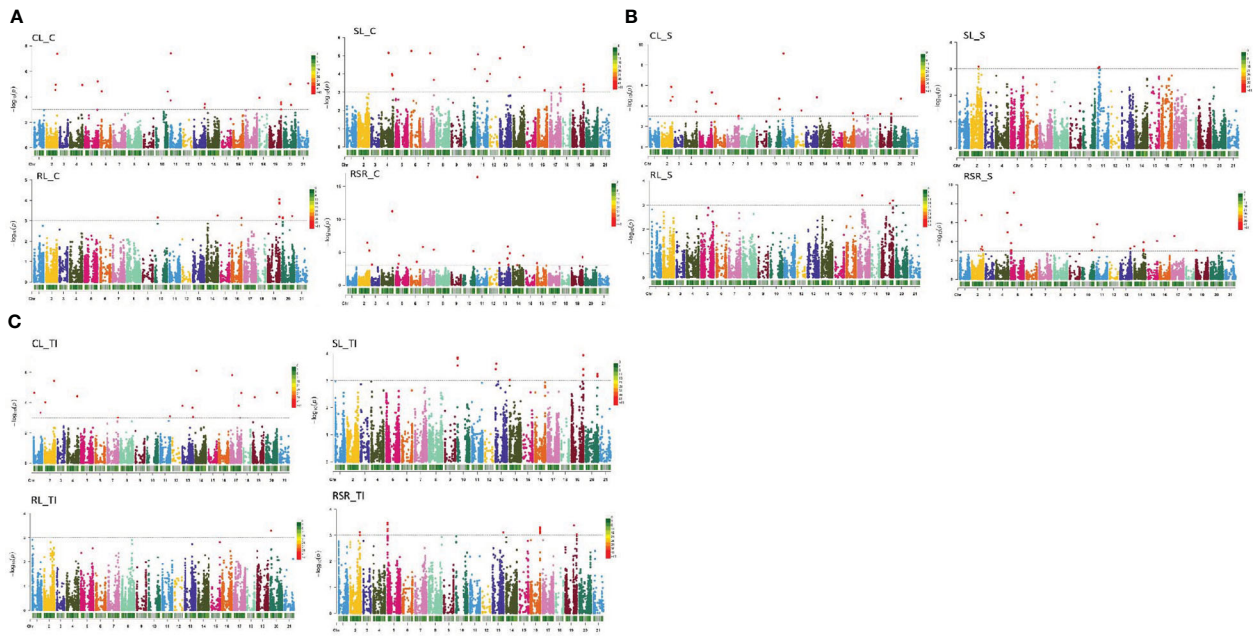


FIGURE 4
(A) Manhattan plots showing significant QTN (quantitative trait nucleotides) in 261 winter wheat genotypes used for seedling growth parameters (CL, SL, RL and RSR) under control conditions. Significant QTNs are indicated with red dots (P<0.001; -log10>3). **(B)** Manhattan plots showing significant QTN (quantitative trait nucleotides) in 261 winter wheat genotypes used for seedling growth parameters (CL, SL, RL and RSR) under stress conditions. Significant QTNs are indicated with red dots (P<0.001; -log10>3). **(C)** Manhattan plots showing significant QTN (quantitative trait nucleotides) in 261 winter wheat genotypes used for seedling growth tolerance index (CL, SL, RL and RSR). Significant QTNs are indicated with red dots (P<0.001; -log10>3).

controls the phenotypic variation of CL under both treatments and is annotated as a protein kinase-like domain superfamily (Figures S3A, B). The allelic effect for this QTN showed longer CL under both conditions for genotypes carrying the A allele (Figure S3C). The BS00001140_51 QTN was found inside the *TraesCS2B02G203900* gene (position 183315109-183318519 bp) on chromosome 2B associated to RSR under both control and drought conditions, and was annotated as CBS domain (Figures S4A–C). Another QTN (IAAV6312) on chromosome 2D is located within the *TraesCS2D02G133900* gene (position 78764128-78767414 bp) for CL under both conditions and encodes a ribosomal protein S9 that is involved in protein biosynthesis and regulates seed germination and seedling responses to drought stress (Figures S5A, B). For this QTN, genotypes carrying C allele showed longer coleoptiles under control and drought conditions (Figure S5C). Inside the *TraesCS4B02G051900* gene, a QTN (IAAV971) is located on chromosome 4B (position 40746325-40753688 bp) and controls the variation of CL, RSR under both treatments, and SL_C. This gene encodes the ATP-binding cassette (ABC) transporters mentioned as key contributors in diverse biological processes in different plant species, including phytohormones transportation, tolerance to a wide range of stresses as well as growth and development. (Figures 5A and 4B). For this QTN, allelic effects showed longer SL_C and CL under both conditions, for genotypes carrying the C allele (Figure 5C). Markedly, the BS00068033_51 QTN on chromosome 7A is located within the candidate *TraesCS7A02G545300* (position 721411549-721417543 bp) for CL_S and SL_TI related-traits. This candidate is annotated as auxin response factor 2 which belongs to phytohormones that are involved in stem cell systems and meristems maintenance and development (Figures S6A–C). Finally, the QTN (Kukri_rep_c72909_657) on chromosome 7B within the *TraesCS7B02G047100* gene (position 46343243-46351992 bp) for RL_S and RL_TI was identified (Figures S7A, B). Moreover, accessions carrying the G allele showed a positive effect on drought tolerance for coleoptile and root length compared to accessions carrying the A allele (Figure S7C).

The expression analysis of the eight multi-traits CG in contrasting growth conditions showed a wide range of gene expression. In that sense, all candidate genes presented a higher expression under 12%PEG compared with control and other stress conditions (Figure 6A). The genes *TraesCS2A02G543900*, *TraesCS2D02G133900*, and *TraesCS1B02G480400* showed the highest expression under drought stress PEG6000 while genes *TraesCS2A02G442700*, *TraesCS2B02G203900*, *TraesCS4B02G051900*, *TraesCS7A02G545300* and *TraesCS7B02G047100* showed an intermediate expression under the same conditions (Figure 6A). Based on the Genevestigator database, *TraesCS2B02G203900* was upregulated under simulated drought by PEG while *TraesCS2A02G543900* was downregulated in leaves and roots under PEG 6000 stress conditions (Figure 6B).

4 Discussion

4.1 Variability in seedling growth parameters

The detection of elements related to drought stress tolerance in the seedling stage is of major importance increasing the adaptation and accelerating the grain yield potential in environments where early droughts impose a primary constraint (Lin et al., 2019; Thabet and Alqudah, 2019). Despite the high number of identified QTN related to drought stress tolerance in post-flowering stages, studies regarding seedling growth-related traits under stress conditions are scarce or have been carried out only partially (Maulana et al., 2020). New efforts

TABLE 2 Distribution of pleiotropic loci or QTN (quantitative trait nucleotides) and candidate genes associated with two or more traits related to seedling growth under drought and control conditions.

Chr	Marker/Synonym	Trait/Effect/-LOG10 (p-value range	Marker Position (bp) and alleles	Candidate gene-Genomic location (bp)	Annotation (GO and InterPro)
1B	**Kukri_c44587_130 (IWB45466)**	**CL_C (+0.066-0.094 cm) -LOG10 = 4.83-6.98 CL_S (+0.091-0.132 cm) -LOG10 = 5.45-7.51**	**687795568.687795666 (171,31 cM) A-G**	***TraesCS1B02G480400*** **(687794252-687799812)**	metal ion binding (molecular function) IPR036855 Zinc finger, CCCH-type superfamily
2AL	**RAC875_c52458_454 (IWB58832)**	**CL_S (-0.064/-0.081 cm) -LOG10 = 3.57-4.24 RSR_S (+0.047-0.092) -LOG10 = 3.20-6.02 SL_C (-0.199/-0.233 cm) -LOG10 = 3.75-4.04**	**692755001.692755101 (115,13 cM) C-T**	***TraesCS2A02G442700*** **(692754161-692757947)**	protein dimerization activity (molecular function) IPR036638 Helix-loop-helix DNA-binding domain superfamily
2AL	**RFL_Contig2656_871 (IWB64018)**	**CL_C (-0.089/-0.104 cm) -LOG10 = 4.39-6.09 CL_S (-0.098/-0.156) -LOG10 = 3.91-6.19**	**753540747.753540847 (148,78 cM) A-G**	***TraesCS2A02G543900*** **(753538593-753541916)**	methionine biosynthetic process IPR011009 Protein kinase-like domain superfamily
2B	**BS00001140_51 (IWB5784)**	**RSR_C (-0.049/-0.072) -LOG10 = 3.23-3.76 RSR_S (-0.127/-0.221) -LOG10 = 3.62-9.64**	**183315442.183315542 (95,82 cM) A-G**	***TraesCS2B02G203900*** **(183315109-183318519)**	IPR000644, CBS domain
2D	**IAAV6312 (IWB35183)**	**CL_C (+0.055/0.063 cm) -LOG10 = 3.49-3.68 CL_S (+0.064/0.184 cm) -LOG10 = 3.68-7.55**	**78765708.78765908 (42,37 cM) A-C**	***TraesCS2D02G133900*** **(78764128-78767414)**	IPR000754 Ribosomal protein S9
4BS	**IAAV971 (IWB35611)**	**CL_C (-0.143/-0.209 cm) -LOG10 = 10.71-12.48 CL_S (-0.124/-0.249 cm) -LOG10 = 4.75-11.38 RSR_C (+0.070/0.095) -LOG10 = 8.41-16.48 RSR_S (+0.073/0.100) -LOG10 = 4.66-7.98 SL_C (-0.374/-0.621 cm) -LOG10 = 5.66-7.38**	**40752368.40752568 (57,48 cM) C-T**	***TraesCS4B02G051900*** **(40746325-40753688)**	protein kinase ATP binding IPR011009 Protein kinase-like domain superfamily
7AL	**BS00068033_51 (IWB10213)**	**CL_S (+0.075-0.088 cm) -LOG10 = 3.37-4.20 SL_TI (-0.012/-0.017) -LOG10 = 3.19-3.44**	**721417450.721417550 (212,66 cM) A-C**	***TraesCS7A02G545300*** **(721411549-721417543)**	auxin response factor 2
7B	**Kukri_rep_c72909_657 (IWB50233)**	**RL_S (+0.267-0.430 cm) -LOG10 = 3.05-4.09 RL_TI (+0.009-0.016) -LOG10 = 3.27-3.82**	**46351467.46351567 (53,75 cM) A-G**	***TraesCS7B02G047100*** **(46343243-46351992)**	IPR029005 LIM-domain binding protein/ SEUSS

cM (centimorgan); Effect: Allelic effect in units (+- centimeters); Coleoptile Length (CL); Shoot Length (SL); Root length (RL); Root/Shoot ratio (RSR); C (control); S (Stress).

are necessary to explore worldwide wheat accessions across different conditions in order to identify the genetic basis of seedling drought tolerance and potentially enhance the MAS in breeding programs.

Our study explores the power of the FARM-CPU model to identify stable quantitative nucleotide regions (QNRs) associated with wheat seedling's growth parameters in a recently reported wheat panel across three years. We reported extensive phenotypic variation as well as a high correlation among environments under stress and control conditions. The high heritability reported for all treatments (0.87–0.97) showed the utility of the set for breeding programs focused on drought stress tolerance in early crop stages as well as seedling growth habits for deep sowing. Consistent with our findings, Wei and Qi (1997) reported a highly significant correlation between CL and tolerance index under water shortage conditions, suggesting that coleoptile length might be used for drought-tolerance selection in early developmental stages in wheat breeding programs. For their part, Rauf et al. (2007) documented a significant and positive correlation between germination rate, CL, SL, and RL under control and PEG conditions. Moreover, the wide phenotypic variation of the panel provides more valuable inference in relation to Bi-parental populations, RILs, or DH lines due to a greater allelic diversity (Gupta et al., 2017; Sallam et al., 2019). Seedling´s growth parameters revealed significant discrepancies between genotypes origin. Higher CL, SL, and a lower RSR under both conditions were detected in Eastern Europe-Western Asia, while fewer differences were detected in root length.

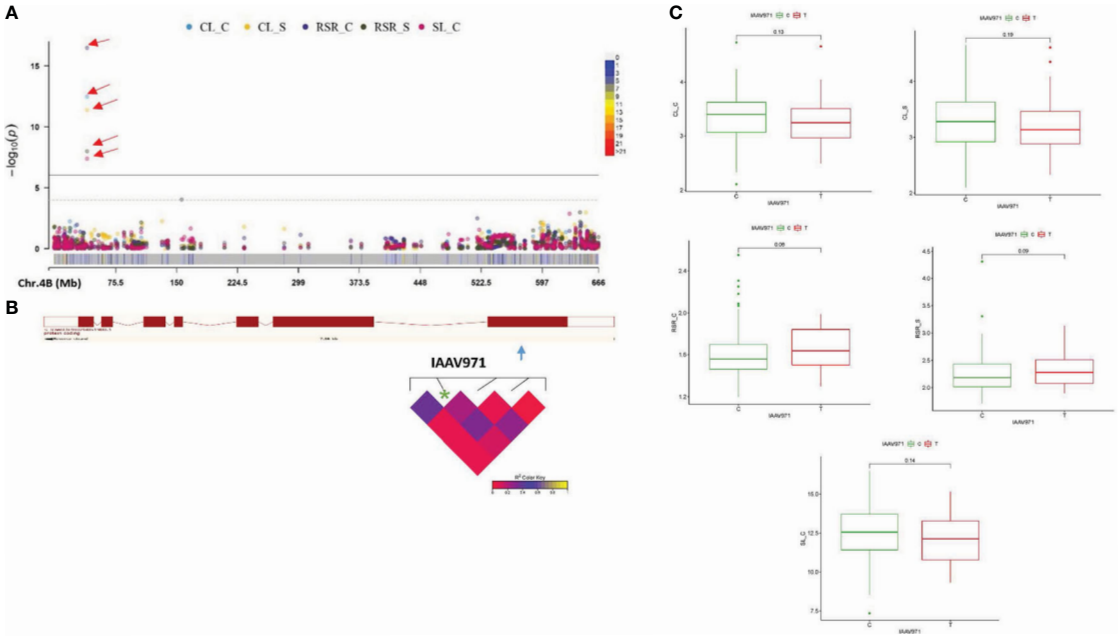


FIGURE 5
A Manhattan plots showing significant QTN (quantitative trait nucleotides) in 261 winter wheat genotypes for seedling growth parameters under (C) control and (S) drought stress **(A)** (CL_C, CL_S, RSR_C, RSR_S, and SL_C): CL, coleoptile length; RSR, root to shoot ratio; and SL, shoot length. Multitraits QTNs are indicated as ($P<0.001$; $-\log_{10}> 3$). **(B)** the structure of the TraesCS4B02G051900 gene with the position of the co-located QTN on 4B (40746325-40753688 bp) and the linkage disequilibrium (LD) interval, and **(C)** QTN -gene haplotype analysis.

4.2 QTN linked with seedling growth under PEG stress and control conditions

Our analysis reported QTNs related to drought stress tolerance in wheat seedlings across 17 chromosomes. These QTNs were stable across at least two environments, providing highly significant associations that can be used in further analysis.

Variations in CL from 2 to 4.47 cm under control and 2.11 to 4.77 cm under PEG stress conditions were documented. In total, 18 QTNs related to CL on chromosomes 1B (2), 2A (3), 2B, 2D (2), 4B (3), 4D, 5A, 6B, 6D, and 7A (2) were reported. Previous studies identified twelve significant QTLs on chromosomes 4B and 4D for coleoptile length in four wheat cultivars and explained 49% of the phenotypic variance (Rebetzke et al., 2007). Our findings agree with Yu and Bai (2010) that detected six significant QTLs for CL on chromosomes 1B, 3D, 4DS, 4DL, 5AS, and 5B, and some of them were also related to plant height in Chinese wheat landraces. Altogether, the colocalization of several QTLs across different chromosomes on the wheat genome suggested their potential roles in MAS programs.

Variations in SL from 7.01 to 15.31 cm (control) and 3.77 to 9.96 cm under PEG stress were reported. On chromosomes 1B, 2A (2), 4B (2), 4D, 5A, 6A, and 6B (2), ten QTNs related to SL were documented. Similarly, previous studies had reported some QTNs related to seedling growth parameters under early drought. For instance, five QTNs (*QSLDS.nri-2B, QSLDS.nri-3A*, and three *QSLDS.nri-4B*) were reported for shoot length at positions 153 cM, 68 cM, and 30-33 cM, respectively, as responsible for the variation of shoot length under drought condition (Maulana et al., 2020).

RL varied between 16.06 and 20.91 cm (control) and 13.79 to 19.50 cm under PEG conditions. Moreover, 14 QTNs were detected for RL under control and stress conditions. These markers were localized on chromosomes 5B, 6B, 7A (8), and 7B (4).In the same manner, Khalid et al. (2018) reported three QTN located on chromosome 7B between 122 to 128cM position, two related to root biomass (*QFRW.nust-7B*) that explained 59% of the phenotypic variance, and other for RL (*QRL.nust-7B*) under water-limited conditions. Moreover, Liu et al. (2012) explored nine QTNs for a doubled haploid wheat population related to the root morphological traits, including root length on chromosome 3B at the interval Xgwm644.2–P6901.2 under different water regimes. Using two related recombinant inbred line (RIL) populations in wheat, Zhang et al. (2013) detected two QTNs for root length under both control and drought stress located on chromosomes 1A, 4A, and 6B. A main-effect QTL from Weimai 8, with positive additive effects, was located between *Xswes131.3* and *Xswes131.4* on chromosome 6B under both water conditions.

We reported 17 QTNs associated with root/shoot ratio located on ten chromosomes (1A, 1B, 2A, 2B, 2D, 3A, 4B, 5A, 5B, and 5D). Genotypic variation for this trait ranged from 1.198 to 2.551 (control) and 1.713 to 4.336 under drought stress. Other authors reported QTLs related to this trait that increased RSR by reducing SL and maintaining RL during drought stress (Chang et al., 2016).

In total, 22 QTNs related to the tolerance index of parameters related to seedling growth were documented (1 for CL_TI, 12 for SL_TI, 1 for RL_TI, and 8 for RSR_TI) across seven chromosomes (1B, 2B, 4A, 5A, 6A, 7A, and 7B). Our results agree with Ayalew et al. (2017) who detected four root length QTLs on chromosome 1AS, 3AL, and 7BL with a total phenotypic variation of 47% under drought stress. Further, two root dry-weight QTLs with 10 and 15% of phenotypic variation were mapped to chromosomes 4 and 5AL

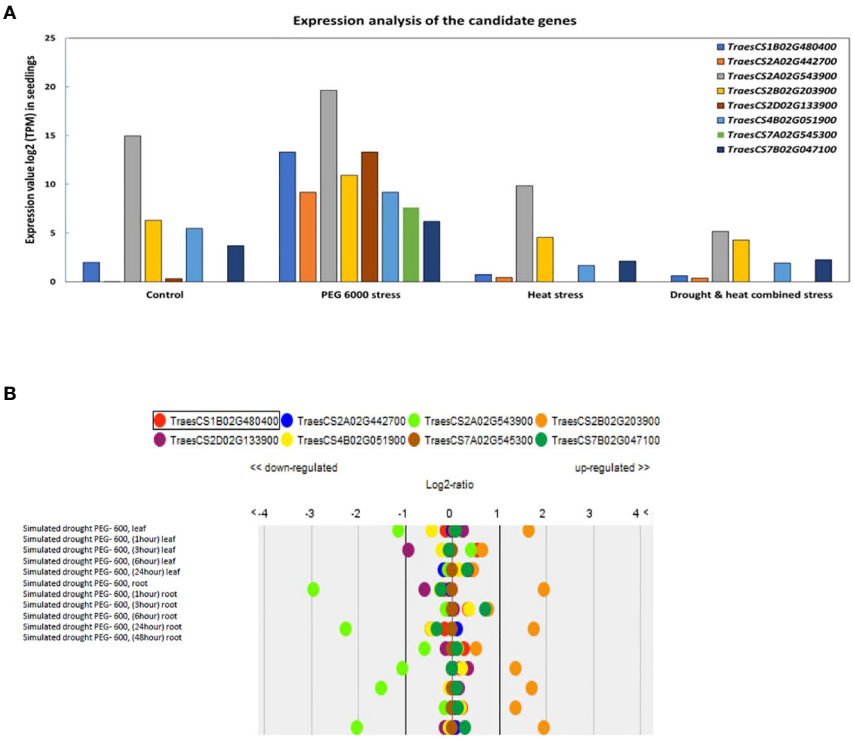


FIGURE 6
(A) Expression value log2 TPM (Transcripts Per Kilobase Million) of candidate genes in wheat seedlings after eight days under different stress conditions.
(B) Up and down regulation under control and drought simulated by PEG from the expression and transcriptomes database.

under stress conditions. Taken these results together, Ayalew et al. (2017) reported that two major drought-responsive alleles were displayed in a diverse panel of wheat genotypes that caused long root length under PEG-induced drought stress.

4.3 Candidate genes underlying drought stress tolerance

Based upon GWAS outputs, we identified eight plausible candidate genes that are associated with two or more seedling growth parameters under early drought stress and control conditions as well as high gene expression under different stress conditions. On chromosome 1B, the QTN (Kukri_c44587_130) inside *TraesCS1B02G480400* influence the CL growth under controlled and 12%PEG stress conditions. This gene is annotated as CCCH-type Zinc (Zn) finger protein that belongs to zinc finger proteins which is involved in plant biotic and abiotic stress tolerance in various plant species. In wheat, the overexpression of *TaZnFP* has been associated with an enhancement in abiotic tolerance, particularly drought (Min et al., 2013). Our candidate provides a basis for exploring the molecular mechanisms by which zinc finger proteins play a specific role in drought tolerance.

The QTN (RAC875_c52458_454) on chromosome 2A is located inside the gene *TraesCS2A02G442700* and controls the variation of CL_S, RSR_S, and SL_C. Our candidate encodes the helix-loop-helix DNA-binding domain superfamily that plays a key role in growth and development under abiotic stress conditions (Duek and Fankhauser, 2005; Groszmann et al., 2010). In wheat, Liu et al. (2020) reported that the transcription factor TabHLH49 is related to the dehydrin *WZY2* gene expression and enhances drought stress resistance. Moreover, Wang et al. (2019) reported that the *TabHLH* expression levels were upregulated in response to drought stress conditions in multiple wheat organs.

On chromosome 2B, the BS00001140_51 marker was found inside the *TraesCS2B02G203900* gene for RSR under both control and drought, annotated as the CBS domain. This gene which encodes for CBS domain-containing proteins (CDCPs), was identified to be associated with tolerance to multiple plant stresses (Kumar et al., 2018). Moreover, Wang et al. (2010) detected that the CBS domain-containing protein gene *TaCDCP1* from wheat was upregulated and participated in the signal transmission pathways in response to drought stress. In rice under drought conditions, some CDCP genes (*OsCBSX9* and *OsCBSCBS4*) presented an increase in expression levels (Tomar et al., 2022). Understanding CBS domain signaling pathways are critical in breeding programs aimed at developing crop varieties more resistant to various environmental stresses, including drought.

Another QTN (IAAV6312) marker on chromosome 2D is located within the *TraesCS2D02G133900* gene for CL under both conditions and encodes as ribosomal protein S9. Previous reports detected an upregulation of the 40S and 60S ribosomal proteins in citrus when exposed to PEG-induced osmotic stress (Ziogas et al., 2015). In maize, most hub proteins such as 50S Ribosomal protein L2 (rpl2-A) were involved in protein biosynthesis through regulation of seed germination and seedling responses to drought stress (Yang et al., 2014). Therefore, it can be speculated that this gene is involved in

drought stress responses, possibly through modulating plant growth and performance at the early developmental stage.

Inside the *TraesCS4B02G051900* gene, a QTN (IAAV971) located on chromosome 4B controls the variation of CL, RSR under both treatments, and SL_C. This gene encodes a ATP-binding cassette transporters (ABC) that is driven by ATP hydrolysis and acts as key contributors to diverse biological processes in different plant species, including growth, development, transport of phytohormones, stomatal closure, tolerance to biotic and abiotic stresses, etc (Dahuja et al., 2021). ABC transporters play a role *via* regulating the auxin and other phytohormones distribution inside the different organs and meristems (Lewis et al., 2007; Borghi et al., 2015). Under drought stress, Kuromori et al. (2014) and Krattinger et al. (2019) reported that the ABA transportation between the cytosol and the apoplast is regulated by the ABC transporters during the seed germination stage. For their part, *AtPDR12*/*ABCG40* ABC transporter play a role as ABA uptake transporter in the plasma membrane and further required for early stomatal closure during water-limited conditions (Kang et al., 2010). Our candidate gene can be considered to develop early drought-tolerant genotypes in wheat breeding programs.

Markedly, the BS00068033_51 marker on chromosome 7A is located within the candidate *TraesCS7A02G545300* for CL_S and SL_TI related-traits. This candidate is annotated as auxin response factor 2 which belongs to phytohormones that control the development and maintenance of plant meristems and stem cell systems (Friml et al., 2003; Kirschner et al., 2018). Phytohormones, including GA, cytokinin (Gordon et al., 2009), ethylene, ABA, brassinosteroids and strigolactones are key in the regulation of root and shoot differentiation (Marchant et al., 1999; Reinhardt et al., 2003). In maize (Ruzicka et al., 2009), rice (Yang et al., 2017) and *Arabidopsis* (Mussig et al., 2003), a reduction in RL and meristem size has been reported under high auxin concentrations. Thus, lower auxin concentrations are involved in regulating root growth in wheat (Kirschner et al., 2018). Altogether, this gene is a key regulator of root system architecture in wheat *via* modulating root length in response to drought stress conditions.

5 Conclusions

Via the novel FarmCPU method and using 17,093 valid SNPs, we reported 70 stable QTNs across 17 chromosomes associated with seedling growth parameters under control and drought stress conditions. Moreover, eight QTNs that are physically inside eight novel multi-traits candidate genes located on seven chromosomes showed high expression values in wheat seedlings under control and different stress conditions. Our findings offer insight into understanding the genetic factors and diverse mechanisms in response to water shortage conditions that are important for wheat improvement and adaptation at early developmental stages. New efforts should be made to explore the association between the CG functions with their effects on seedling growth under different sowing environments and dates as well as the effects of the genes on drought conditions imposed in later crop stages.

Data availability statement

The original contributions presented in the study are included in the article/Supplementary Material. The genotypic data of 90K gene-associated SNPs used in this study was published in https://pubmed.ncbi.nlm.nih.gov/24646323/. Further inquiries can be directed to the corresponding authors.

Author contributions

MS and AB designed the research. MS, ST, and AA analyzed data with help from MRS and UL. AB provided genotypic resources. MS, ST and AA wrote the manuscript with contributions from all co-authors. All authors contributed to the article and approved the submitted version.

Funding

IPK Gatersleben core funding supported this study. Costs for open access publishing were partially funded by the Deutsche Forschungsgemeinschaft (DFG, German Research Foundation, grant 491250510).

Acknowledgments

MS appreciates the support received from Alexander von Humboldt Foundation (Georg Forster Fellowship), Leibniz-DAAD Fellowship and Bayer Foundation (Jeff Schell Scholarship).

Conflict of interest

The authors declare that the research was conducted in the absence of any commercial or financial relationships that could be construed as a potential conflict of interest.

Publisher's note

All claims expressed in this article are solely those of the authors and do not necessarily represent those of their affiliated organizations, or those of the publisher, the editors and the reviewers. Any product that may be evaluated in this article, or claim that may be made by its manufacturer, is not guaranteed or endorsed by the publisher.

Supplementary material

The Supplementary Material for this article can be found online at: https://www.frontiersin.org/articles/10.3389/fpls.2023.1061845/full#supplementary-material

References

Alqudah, A. M., Sallam, A., Baenziger, P. S., and Börner, A. (2020). GWAS: Fast-forwarding gene identification and characterization in temperate cereals: lessons from barley–a review. *J. Adv. Res.* 22, 119–135. doi: 10.1016/j.jare.2019.10.013

Ayalew, H., Liu, H., Börner, A., Kobiljski, B., Liu, C., and Yan, G. (2018). Genome-wide association mapping of major root length QTLs under PEG induced water stress in wheat. *Front. Plant Sci.* 9, 1759. doi: 10.3389/fpls.2018.01759

Ayalew, H., Liu, H., and Yan, G. (2017). Identification and validation of root length QTLs for water stress resistance in hexaploid wheat (Titicum aestivum l.). *Euphytica* 213, 126. doi: 10.1007/s10681-017-1914-4

Bhatta, M., Shamanin, V., Shepelev, S., Baenziger, P. S., Pozherukova, V., Pototskaya, I., et al. (2019). Marker-trait associations for enhancing agronomic performance, disease resistance, and grain quality in synthetic and bread wheat accessions in Western Siberia. *G3: Genes Genomes Genet.* 9 (12), 4209–4222. doi: 10.1534/g3.119.400811

Borghi, L., Kang, J., Ko, D., Lee, Y., and Martinoia, E. (2015). The role of ABCG-type ABC transporters in phytohormone transport. *Biochem. Soc. Trans.* 43, 924–930. doi: 10.1042/BST20150106

Chang, H., Chen, D., Kam, J., Richardson, T., Drenth, J., Guo, X., et al. (2016). Abiotic stress upregulated TaZFP34 represses the expression of type-b response regulator and SHY2 genes and enhances root to shoot ratio in wheat. *Plant Sci.* 252, 88–102. doi: 10.1016/j.plantsci.2016.07.011

Dahuja, A., Kumar, R. R., Sakhare, A., Watts, A., Singh, B., Goswami, S., et al. (2021). Role of ATP-binding cassette transporters in maintaining plant homeostasis under abiotic and biotic stresses. *Physiologia Plantarum* 171, 785–801. doi: 10.1111/ppl.13302

Daryanto, S., Wang, L., and Jacinthe, P. A. (2016). Global synthesis of drought effects on maize and wheat production. *PloS one*, 11(5), e0156362.

Duek, P. D., and Fankhauser, C. (2005). bHLH class transcription factors take centre stage in phytochrome signalling. *Trends Plant Sci.* 10, 51–54. doi: 10.1016/j.tplants.2004.12.005

Food and Agriculture Organization. (2014). Available online: http://www.fao.org/resources/infographics/infographics-details/es/c/240943/ (accessed on 29 december 2022).

Friml, J., Vieten, A., Sauer, M., Weijers, D., Schwarz, H., Hamann, T., et al. (2003). Efflux-dependent auxin gradients establish the apical-basal axis of arabidopsis. *Nature* 426, 147–153. doi: 10.1038/nature02085

Gaur, A., Jindal, Y., Singh, V., Tiwari, R., Kumar, D., Kaushik, D., et al. (2022). GWAS to identify novel QTNs for WSCs accumulation in wheat peduncle under different water regimes. *Front. Plant Sci.* 13, 825687. doi: 10.3389/fpls.2022.825687

Gordon, S. P., Chickarmane, V. S., Ohno, C., and Meyerowitz, E. M. (2009). Multiple feedback loops through cytokinin signaling control stem cell number within the arabidopsis shoot meristem. *Proc. Natl. Acad. Sci. United States America* 106, 16529–16534. doi: 10.1073/pnas.0908122106

Groszmann, M., Bylstra, Y., Lampugnani, E. R., and Smyth, D. R. (2010). Regulation of tissue-specific expression of SPATULA, a bHLH gene involved in carpel development, seedling germination, and lateral organ growth in arabidopsis. *J. Exp. Bot.* 61, 1495–1508. doi: 10.1093/jxb/erq015

Gupta, P. K., Balyan, H. S., and Gahlaut, V. (2017). QTL analysis for drought tolerance in wheat: present status and future possibilities. *Agronomy* 7 (1), 5. doi: 10.3390/agronomy7010005

Hruz, T., Laule, O., Szabo, G., Wessendorp, F., Bleuler, S., Oertle, L., et al. (2008). Genevestigator V3: A reference expression database for the meta-analysis of transcriptomes. *Adv. Bioinf.* 2008, 420747. doi: 10.1155/2008/420747

Julkowska, M. M., Saade, S., Agarwal, G., Gao, G., Pailles, Y., Morton, M., et al. (2019). MVApp–multivariate analysis application for streamlined data analysis and curation. *Plant Physiol.* 180 (3), 1261–1276. doi: 10.1104/pp.19.00235

Kadam, S., Singh, K., Shukla, S., Goel, S., Vikram, P., Pawar, V., et al. (2012). Genomic associations for drought tolerance on the short arm of wheat chromosome 4B. *Funct. Integr. Genomics* 12 (3), 447–464. doi: 10.1007/s10142-012-0276-1

Kang, J., Hwang, J.-U., Lee, M., Kim, Y.-Y., Assmann, S. M., Martinoia, E., et al. (2010). PDR-type ABC transporter mediates cellular uptake of the phytohormone abscisic acid. *Proc. Nat. Acad. Sci.* 107, 2355–2360. doi: 10.1073/pnas.0909222107

Khalid, M., Gul, A., Amir, R., Ali, M., Afzal, F., Quraishi, U. M., et al. (2018). QTL mapping for seedling morphology under drought stress in wheat cross synthetic (W7984)/Opata. *Plant Genet. Resources: Characterization Utilization* 16, 359–366. doi: 10.1017/S1479262118000023

Kido, É.A., Ferreira-Neto, J. R. C., Pandolfi, V., de Melo Souza, A. C., and Benko-Iseppon, A. M. (2016). "Drought stress tolerance in plants: Insights from transcriptomic studies," in *Drought stress tolerance in plants*, vol. Vol 2. (Cham, Switzerland: Springer), 153–185.

Kirschner, G. K., Stahl, Y., Imani, J., von Korff, M., and Simon, R. (2018). Fluorescent reporter lines for auxin and cytokinin signalling in barley (Hordeum vulgare). *PLos One* 13, e0196086. doi: 10.1371/journal.pone.0196086

Krattinger, S. G., Kang, J., Bräunlich, S., Boni, R., Chauhan, H., Selter, L. L., et al. (2019). Abscisic acid is a substrate of the ABC transporter encoded by the durable wheat disease resistance gene Lr34. *New Phytologist* 223 (2), 853–866. doi: 10.1111/nph.15815

Kulkarni, M., Soolanayakanahally, R., Ogawa, S., Uga, Y., Selvaraj, M. G., and Kagale, S. (2017). Drought response in wheat: Key genes and regulatory mechanisms controlling root system architecture and transpiration efficiency. *Front. Chem.* 5, 106. doi: 10.3389/fchem.2017.00106

Kumar, R., Subba, A., Kaur, C., Ariyadasa, T. U., Sharan, A., Pareek, A., et al. (2018). OsCBSCBSPB4 is a two cystathionine-β-Synthase domain-containing protein from rice that functions in abiotic stress tolerance. *Curr. Genomics* 19, 50–59. doi: 10.2174/1389202918666170228141706

Kuromori, T., Sugimoto, E., and Shinozaki, K. (2014). Intertissue signal transfer of abscisic acid from vascular cells to guard cells plant physiol. *Plant Physiol.* 164 (4), 1587–1592. doi: 10.1104/pp.114.235556

Landjeva, S., Neumann, K., Lohwasser, U., and Börner, A. (2008). Molecular mapping of genomic regions associated withwheat seedling growth under osmotic stress. *Biol. Plantarum* 52 (2), 259–266. doi: 10.1007/s10535-008-0056-x

Lewis, D. R., Miller, N. D., Splitt, B. L., Wu, G., and Spalding, E. P. (2007). Separating the roles of acropetal and basipetal auxin transport on gravitropism with mutations in two arabidopsis multidrug resistance-like ABC transporter genes. *Plant Cell* 19, 1838–1850. doi: 10.1105/tpc.107.051599

Lin, Y., Yi, X., Tang, S., Chen, W., Wu, F., Yang, X., et al. (2019). Dissection of phenotypic and genetic variation of drought-related traits in diverse Chinese wheat landraces. *Plant Genome* 12, 190025. doi: 10.3835/plantgenome2019.03.0025

Liu, X.-L., Li, R., Chang, X.-p., and Jing, R. J. E. (2012). Mapping QTLs for seedling root traits in a doubled haploid wheat population under different water regimes. *Euphytica* 189 (1), 51–66. doi: 10.1007/s10681-012-0690-4

Liu, H., Ying, Y., Liu, D., Wang, X., and Zhang, L. (2020). Transcription factor TabHLH49 positively regulates dehydrin WZY2 gene expression and enhances drought stress tolerance in wheat. *BMC Plant Biol.* 20 (1), 1-10. doi: 10.1186/s12870-020-02474-5

Liu, W. J., Yuan, S., Zhang, N. H., Lei, T., Duan, H. G., Liang, H. G., et al. (2006). Effect of water stress on photosystem 2 in two wheat cultivars. *Biol. Plantarum* 50 (4), 597–602. doi: 10.1007/s10535-006-0094-1

Li, X., Xia, X., Xiao, Y., He, Z., Wang, D., Trethowan, R., et al. (2015). QTL mapping for plant height and yield components in common wheat under water-limited and full irrigation environments. *Crop Pasture Sci.* 66 (7), 660–670. doi: 10.1071/CP14236

Maccaferri, M., El-Feki, W., Nazemi, G., Salvi, S., Canè, M. A., Colalongo, M. C., et al. (2016). Prioritizing quantitative trait loci for root system architecture in tetraploid wheat. *J. Exp. Bot.* 67 (4), 1161–1178. doi: 10.1093/jxb/erw039

Mahpara, S., Zainab, A., Ullah, R., Kausar, S., Bilal, M., Latif, M. I., et al. (2022). The impact of PEG-induced drought stress on seed germination and seedling growth of different bread wheat (Triticum aestivum l.) genotypes. *PLos One* 17 (2), e0262937. doi: 10.1371/journal.pone.0262937

Ma, J., Lin, Y., Tang, S., Duan, S., Wang, Q., Wu, F., et al. (2020). A genome-wide association study of coleoptile length in different Chinese wheat landraces. *Front. Plant Sci.* 11, 677. doi: 10.3389/fpls.2020.00677

Marchant, A., Kargul, J., May, S. T., Muller, P., Delbarre, A., Perrot-Rechenmann, C., et al. (1999). AUX1 regulates root gravitropism in arabidopsis by facilitating auxin uptake within root apical tissues. *EMBO J.* 18, 2066–2073. doi: 10.1093/emboj/18.8.2066

Maulana, F., Huang, W., Anderson, J. D., Kumssa, T. T., and Ma, X. F. (2021). Genome-wide association mapping of seedling vigor and regrowth vigor in winter wheat. *Crops* 1 (3), 153–165. doi: 10.3390/crops1030015

Maulana, F., Huang, W., Anderson, J. D., and Ma, X.-F. (2020). Genome-wide association mapping of seedling drought tolerance in winter wheat. *Frontiers in Plant Science* 11. doi: 10.3389/fpls.2020.573786

Min, D. H., Zhao, Y., Huo, D.-Y., Li, L.-C., Chen, M., Xu, Z.-S., et al. (2013). Isolation and identification of a wheat gene encoding a zinc finger protein (TaZnFP) responsive to abiotic stresses. *Acta Physiologiae Plantarum* 35 (5), 1597-1604. doi: 10.1007/s11738-012-1202-9

Muqaddasi, Q. H., Brassac, J., Börner, A., Pillen, K., and Röder, M. S. (2017). Genetic architecture of anther extrusion in spring and winter wheat. *Front. Plant Sci.* 8, 754. doi: 10.3389/fpls.2017.00754

Mussig, C., Shin, G. H., and Altmann, T. (2003). Brassinosteroids promote root growth in arabidopsis. *Plant Physiol.* 133, 1261–1271. doi: 10.1104/pp.103.028662

Pinheiro, J., Bates, D.R Core Team (2022). Nlme: Linear and nonlinear mixed effects models. R package version 3.1-159.

Quan, X., Liu, J., Zhang, N., Xie, C., Li, H., Xia, X., et al. (2021). Genome-wide association study uncover the genetic architecture of salt tolerance-related traits in common wheat (Triticum aestivum l.). *Front. Genet.* 12, 563. doi: 10.3389/fgene.2021.663941

Rauf, M., Munir, M., ul Hassan, M., Ahmad, M., and Afzal, M. (2007). Performance of wheat genotypes under osmotic stress at germination and early seedling growth stage. *Afr. J. Biotechnol.* 6 (8).

Rebetzke, G. J., Ellis, M. H., Bonnett, D. G., and Richards, R. A. (2007). Molecular mapping of genes for coleoptile growth in bread wheat (Triticum aestivum l.). *Theor. Appl. Genet.* 114, 1173–1183. doi: 10.1007/s00122-007-0509-1

Rebetzke, G. J., Verbyla, A. P., Verbyla, K. L., Morell, M. K., and Cavanagh, C. R. (2014). Use of a large multiparent wheat mapping population in genomic dissection of coleoptile and seedling growth. *Plant Biotechnol. J.* 12 (2), 219–230. doi: 10.1111/pbi.12130

Reinhardt, D., Pesce, E. R., Stieger, P., Mandel, T., Baltensperger, K., Bennett, M., et al. (2003). Regulation of phyllotaxis by polar auxin transport. *Nature* 426, 255–260. doi: 10.1038/nature02081

Reynolds, M. P., Skovmand, B., Trethowan, R. M., and Pfeiffer, W. H. (2000). "Evaluating a conceptual model for drought tolerance," in *Molecular approaches for the genetic improvement of cereals for stable production in water-limited environments*. Eds. J. M. Ribaut and D. Poland TMolecular Approaches for the Genetic Improvement of Cereals for Stable Production in Water-Limited Environments. A Strategic Planning Workshop: El Batan, Texcoco (Mexico); 21-25 Jun 1999 49–53. (No. CIS-2516. CIMMYT.). Centro Internacional de Mejoramiento de Maiz y Trigo (CIMMYT), Mexico DF (Mexico)..

Ruzicka, K., Simaskova, M., Duclercq, J., Petrasek, J., Zazimalova, E., Simon, S., et al. (2009). Cytokinin regulates root meristem activity *via* modulation of the polar auxin transport. *Proc. Natl. Acad. Sci. U.S.A.* 106, 4284–4289. doi: 10.1073/pnas.0900060106

Sallam, A., Alqudah, A. M., Dawood, M. F. A., Baenziger, P. S., and Börner, A. (2019). Drought stress tolerance in wheat and barley: Advances in physiology, breeding and genetics research. *Int. J. Mol. Sci.* 20 (13), 3137. doi: 10.3390/ijms20133137

Sallam, A., Eltaher, S., Alqudah, A. M., Belamkar, V., and Baenziger, P. S. (2022). Combined GWAS and QTL mapping revealed candidate genes and SNP network controlling recovery and tolerance traits associated with drought tolerance in seedling winter wheat. *Genomics* 114 (3), 110358. doi: 10.1016/j.ygeno.2022.110358

Schierenbeck, M., Alqudah, A. M., Lohwasser, U., Tarawneh, R. A., Simón, M. R., and Börner, A. (2021). Genetic dissection of grain architecture-related traits in a winter wheat population. *BMC Plant Biol.* 21 (1), 1–14. doi: 10.1186/s12870-021-03183-3

Sukumaran, S., Reynolds, M. P., and Sansaloni, C. (2018). Genome-wide association analyses identify QTL hotspots for yield and component traits in durum wheat grown under yield potential, drought, and heat stress environments. *Front. Plant Sci.* 9, 81. doi: 10.3389/fpls.2018.00081

Thabet, S. G., and Alqudah, A. M. (2019). *Crops and drought* (Chichester: John Wiley & Sons, Ltd), pp 1–pp 8. eLS. doi: 10.1002/9780470015902.a0025265

Thabet, S. G., Moursi, Y. S., Karam, M. A., Börner, A., and Alqudah, A. M. (2020). Natural variation uncovers candidate genes for barley spikelet number and grain yield under drought stress. *Genes* 11 (5), 533. doi: 10.3390/genes11050533

Thabet, S. G., Moursi, Y. S., Karam, M. A., Graner, A., and Alqudah, A. M. (2018). Genetic basis of drought tolerance during seed germination in barley. *PLos One* 13, e0206682. doi: 10.1371/journal.pone.0206682

Tomar, S., Subba, A., Bala, M., Singh, A. K., Pareek, A., and Singla-Pareek, S. L. (2022). Genetic conservation of CBS domain containing protein family in oryza species and their association with abiotic stress responses. *Int. J. Mol. Sci.* 23 (3), 1687. doi: 10.3390/ijms23031687

Uga, Y., Sugimoto, K., Ogawa, S., Rane, J., Ishitani, M., Hara, N., et al. (2013). Control of root system architecture by DEEPER ROOTING 1 increases rice yield under drought conditions. *Nat. Genet.* 45, 1097–1102. doi: 10.1038/ng.2725

VSN International (2015). *Genstat for windows. 18th Edition* (Hemel Hempstead, UK: VSN International Ltd.).

Wang, X.-M., Sun, Y.-F., Liu, Bo, Wang, X.-J., Xu, L.-Q., Xu, X.-M., et al. (2010). Cloning and expression analysis of a CBS domain containing protein gene TaCDCP1 from wheat. *Acta Crops* 36 (12), 2091–2098. doi: 10.3724/SP.J.1006.2010.02091

Wang, S., Wong, D., Forrest, K., Allen, A., Chao, S., Huang, B. E., et al. (2014). Characterization of polyploid wheat genomic diversity using a high-density 90 000 single nucleotide polymorphism array. *Plant Biotechnol. J.* 12 (6), 787–796. doi: 10.1111/pbi.12183

Wang, L., Xiang, L., Hong, J., Xie, Z., and Li, B. (2019). Genome-wide analysis of bHLH transcription factor family reveals their involvement in biotic and abiotic stress responses in wheat (Triticum aestivum l.). *3 Biotech.* 9, 236–236. doi: 10.1007/s13205-019-1742-4

Wang, J., and Zhang, Z. (2021). GAPIT version 3: boosting power and accuracy for genomic association and prediction. *Genomics Proteomics Bioinf* 19 (4), 629-640. doi: 10.1016/j.gpb.2021.08.005

Wei, W., and Qi, Z. (1997). Studies on coleoptile length as criterion of appraising drought resistance in wheat. *Zuo wu xue bao* 23 (4), 459–467.

Wickham, H. (2016). "Data analysis," in *ggplot2* (Cham: Springer), 189–201.

Xu, F., Chen, S., Yang, X., Zhou, S., Wang, J., Zhang, Z., et al. (2021). Genome-wide association study on root traits under different growing environments in wheat (Triticum aestivum l.). *Front. Genet.* 12, 976. doi: 10.3389/fgene.2021.646712

Yang, L., Jiang, T., Fountain, J. C., Scully, B. T., Lee, R. D., Kemerait, R. C., et al. (2014). Protein profiles reveal diverse responsive signaling pathways in kernels of two maize inbred lines with contrasting drought sensitivity. *Int. J. Mol. Sci.* 15, 18892–18918. doi: 10.3390/ijms151018892

Yang, J., Yuan, Z., Meng, Q., Huang, G., Perin, C., Bureau, C., et al. (2017). Dynamic regulation of auxin response during rice development revealed by newly established hormone biosensor markers. *Front. Plant Sci.* 8, 256. doi: 10.3389/fpls.2017.00256

Yu, J.-B., and Bai, G.-H. (2010). Mapping quantitative trait loci for long coleoptile in Chinese wheat landrace wangshuibai. *Crop Sci.* 50 (1), 43–50. doi: 10.2135/cropsci2009.02.0065

Zhang, H., Cui, F., Wang, L., Li, J., Ding, A., Zhao, C., et al. (2013). Conditional and unconditional QTL mapping of drought-tolerance-related traits of wheat seedling using two related RIL populations. *J. Genet.* 92, 213–231. doi: 10.1007/s12041-013-0253-z

Ziogas, V., Tanou, G., Belghazi, M., Filippou, P., Fotopoulos, V., Grigorios, D., et al. (2015). Roles of sodium hydrosulfide and sodium nitroprusside as priming molecules during drought acclimation in citrus plants. *Plant Mol. Biol.* 89, 433–450. doi: 10.1007/s11103-015-0379-x

frontiers | Frontiers in Plant Science

TYPE Review
PUBLISHED 06 February 2023
DOI 10.3389/fpls.2022.1074395

Check for updates

OPEN ACCESS

EDITED BY
Muhammad Waseem,
Hainan University, China

REVIEWED BY
Samar Gamal Thabet,
Fayoum University, Egypt
Prafull Salvi,
National Agri-Food Biotechnology Institute, India

*CORRESPONDENCE
Utlwang Batlang
ubatlang@buan.ac.bw

SPECIALTY SECTION
This article was submitted to Plant Abiotic Stress, a section of the journal Frontiers in Plant Science

RECEIVED 19 October 2022
ACCEPTED 25 November 2022
PUBLISHED 06 February 2023

CITATION
Malambane G, Madumane K, Sewelo LT and Batlang U (2023) Drought stress tolerance mechanisms and their potential common indicators to salinity, insights from the wild watermelon *(Citrullus lanatus):* A review.
Front. Plant Sci. 13:1074395.
doi: 10.3389/fpls.2022.1074395

COPYRIGHT
© 2023 Malambane, Madumane, Sewelo and Batlang. This is an open-access article distributed under the terms of the Creative Commons Attribution License (CC BY). The use, distribution or reproduction in other forums is permitted, provided the original author(s) and the copyright owner(s) are credited and that the original publication in this journal is cited, in accordance with accepted academic practice. No use, distribution or reproduction is permitted which does not comply with these terms.

Drought stress tolerance mechanisms and their potential common indicators to salinity, insights from the wild watermelon *(Citrullus lanatus):* A review

Goitseone Malambane, Kelebogile Madumane, Lesego T. Sewelo and Utlwang Batlang*

Department of Crop and Soil Sciences, Botswana University of Agriculture and Natural Resources, Gaborone, Botswana

Climate change has escalated the effect of drought on crop production as it has negatively altered the environmental condition. Wild watermelon grows abundantly in the Kgalagadi desert even though the environment is characterized by minimal rainfall, high temperatures and intense sunshine during growing season. This area is also characterized by sandy soils with low water holding capacity, thus bringing about drought stress. Drought stress affects crop productivity through its effects on development and physiological functions as dictated by molecular responses. Not only one or two physiological process or genes are responsible for drought tolerance, but a combination of various factors do work together to aid crop tolerance mechanism. Various studies have shown that wild watermelon possess superior qualities that aid its survival in unfavorable conditions. These mechanisms include resilient root growth, timely stomatal closure, chlorophyll fluorescence quenching under water deficit as key physiological responses. At biochemical and molecular level, the crop responds through citrulline accumulation and expression of genes associated with drought tolerance in this species and other plants. Previous salinity stress studies involving other plants have identified citrulline accumulation and expression of some of these genes (chloroplast APX, Type-2 metallothionein), to be associated with tolerance. Emerging evidence indicates that the upstream of functional genes are the transcription factor that regulates drought and salinity stress responses as well as adaptation. In this review we discuss the drought tolerance mechanisms in watermelons and some of its common indicators to salinity at physiological, biochemical and molecular level.

KEYWORDS

climate change, root growth, stomatal closure, chloroplast-APX, citrulline, DRIP1, RAN GTPase, type-2 metallothionein (MT)

Introduction

Climate change, which is characterized by high temperatures, erratic and unreliable rainfalls as well as an increase of desert margins has become a common phenomenon in the arid and semi-arid regions of the world. These factors and their interactions bring about undesirable environmental conditions that affect agriculture and most importantly crop productivity. Drought and salinity stress has been attributed to a combination of several factors but generally it is notable when there is a reduction of available water in the soil, and atmospheric conditions that cause loss of water by transpiration for a period of time (Jaleel et al., 2009; Takahashi et al., 2020). Drought and salinity affects crops from morphological to molecular level in varying levels, these effects can be observed at any phenological stage (Farooq et al., 2008; Sheoran et al., 2022). Crop productivity is highly affected by drought and salinity stress reasons being that the ability of plants in utilization of light energy to carry out photosynthesis is also highly influenced by accessibility to moisture. One of the physiological processes that are highly affected by these abiotic stresses is the photosynthesis which is essential in both plant growth, development, and productivity.

Climate model predictions show that the adverse effects such as drought are not going to soften up but rather get worse over a period of time, with the sub-Saharan region proving to be highly affected (Walter et al., 2011; Brown et al., 2012) thus becoming important to unravel the morphology, physiology and genetic makeup of crops from areas experiencing natural drought (Hussain et al., 2015). A case in point is the xerophyte wild water melon *(Citrullus lanatus)*, found in the Kalahari desert of southern Africa, where it is known to withstand extended periods compared to other C3 species. Drought stress tolerance occurs in almost all plants, but its extent varies from species to species and even within similar species great variation can be observed (Niinemets, 2015; Gorim and Vandenberg, 2017; Iseki et al., 2018). A significant difference in phenotypic and transcriptional regulation of genes during drought between wild plants and domesticated plants has been noted by Akashi et al. (2008); Iseki et al. (2018); Rosero et al. (2020). This then suggests that wild species have better mechanisms in dealing with abiotic as compared to their cultivated relatives (Ghorecha et al., 2017; Iseki et al., 2018), thus making them important to study and harness their tolerance mechanisms this also applies to cultivated sensitive crops. Therefore, this review aims at consolidating findings on mechanisms that aid one of the drought tolerant wild species (wild watermelon) that survive and produce well in the harsh Kalahari Desert conditions.

The wild watermelon

Wild watermelon referred to as the wild cousin or the ancestor of the cultivated watermelon inhabits the Kalahari Desert which is in the western part of Botswana. The crop grows very well in this arid and hostile environments, however unsuitable for the cultivated watermelon, under above normal temperature and low rainfall. The soils are mostly sandy with low water holding capacity and less plant available nutrient required for growth. According to Gibson (1996) and Yokota et al. (2002), annual precipitation is about 200 mm, restricted to spring and summer during which annual plants thrive, but get exposed and suffer severe drought which is mostly survived by the wild watermelon.

Unlike its cultivated cousin, the fruits of wild watermelon are less palatable, not sweet, and the internal color is mostly white to creamy color and at times yellowish. The mature fruit has a similar size as the cultivated watermelon. However, a review by Mtumtum (2012) reported wild watermelons are edible and used in different forms, its leaves, flowers, and young fruit can be cooked as green vegetables. The seeds can be roasted and consumed as they are considered a delicacy. It contains relatively the same amount of water as cultivated watermelon; thus, it has become an important crop of the Kalahari Desert for it is a valuable source of water for the indigenous people and their livestock (Zulu and Modi, 2010). It is also an important part of cropping systems as the crop has been found to reduce the frequency of weeding and production costs by acting as a live mulch when grown as minor with other crops.

The crop survival in these extreme conditions of the desert suggests it to be drought tolerant, thus making it an important crop to study drought response mechanisms. Several studies on this matter relative to the mechanisms in aiding crop drought tolerance have been conducted. Further, the partial sequencing and isolation, characterization, as well as documentation for some of the important genes has been done and the information is available to be used in further studies. Furthermore, the species can be used as a model to elucidate the function of genes implicated in drought and salinity stress responses ultimately leading to enhancement of stress tolerance in cucurbit crops through genetic manipulation. Most importantly, the wild watermelon is an adaptable crop for addressing food security in the face of climate change.

Morpho-physiological responses to environmental stress

Resilient root growth under water deficit

Roots are a very important part of a plant during its growth and adaptation to stress especially the moisture deficit stress. Firstly, they are the anchors for every plant; and they also play an important role and are responsible for the nutrient, water uptake from the soil and sensing drought stress. The root growth evolution influenced by adaptation to the local environment is closely related with the plant phenotype, growth medium

properties and the availability of moisture, temperature, and nutrients of the medium (Bao et al., 2014). The type of root varies with the crop species and its growth, development and intensity is influenced by environmental information (Malamy, 2005). The water absorption of various plants under environmental stress is influenced by various root features like the primary root length, and number of lateral roots. In the case of the wild watermelon, under drought stress the plant expresses it xerophytic characteristic by extending its geophyte-type root system into deep ground water. However, even when the root extension is restricted by growing in a pot the plant could still withstand severe drought showing that its tolerance. (Yokota et al., 2002).

The root system has been known to have a great effect on how plants adapt and respond to environmental stress including drought and salinity (Wasaya et al., 2018; Comas et al., 2013; Karahara and Horie, 2021; An et al., 2003) and the special characters aiding the roots to help plants better adapt to moisture stress are plasticity (Lynch, 2007) and the plasticity is controlled by genetic components triggered by abiotic stress and holds a great potential in stabilizing productivity under suboptimal conditions (Zhu et al., 2011; Gifford et al., 2013).

Several molecular mechanisms have been suggested and confirmed to be responsible for root plasticity when tolerant crops are subjected to abiotic stresses. Several quantitative trait loci has been found to be responsible for the longitudinal and latitudinal growth of roots to access deeper and wider moisture in mitigation effects of salinity and drought stress. DEEPER ROOTING 1 (DRO1), SURFACE ROOTING (SRO1), AUXIN RESPONSE FACTOR 7 (ARF7), HIGH-AFFINITY K^+ TRANSPORTERS (HKT1) and CYCLOPHILIN (CYP) have been documented to be responsible in developing deeper and lateral rooting in various crops like rice (Singh et al., 2021; Uga et al., 2013), maize (Feng et al., 2022) and Arabidopsis (Guseman et al., 2017) thus suggesting an active role in the plants tolerance and avoidance to abiotic stress. Several other factors like QTLs and like qRT9 (Li et al., 2015), qTLRN, qLLRN (Niones et al., 2015) transcription factors like NACs (Thao et al., 2013), MYB (Zhao P. et al., 2019), NFY Family (Yang et al., 2022), has been suggested to play a significant role in the root architecture of plants during drought stress. Further molecular mechanisms playing an active role in the root morphological characteristics of various plants are documented in Table 1.

In wild water melons, the optimization of the root architecture to maximize use of deep water has been noted as an advantageous trait, as growing in drought stress condition a vigorous root growth was observed (Akashi et al., 2016a). In studying the root structure of wild watermelon Yoshimura et al. (2008) found out that when exposed to moisture stress, the root development is significantly an indication of triggered drought avoidance mechanisms aiding access to moisture in deeper soils (Figure 1). The good rooting pattern, densities and hydraulic conductance of the wild watermelon has been attributed to superior ability to access deeper water thus aiding its drought tolerance mechanisms (Smith, 2006), while the tap root and the semi-taproot that grows deeper as well as the root system that is spreading has also shown to contribute immensely to the tolerance mechanisms of wild watermelon (Condon and Hall, 1997). A proteome analysis on the root of wild watermelon exposed to drought stress revealed increased expressions levels of proteins associated with root morphogenesis and primary metabolism and these correlated with the enhanced root development (Yoshimura et al., 2008). These traits of the wild watermelon points to established drought tolerance mechanisms aiding the crop to survive under the harsh environmental conditions.

To study the root roles in the tolerance mechanism of the wild watermelon, Kajikawa et al. (2010) further developed a transgenic root hair system to better understand the root physiology and drought stress and the effects after exposure to stress, substantial growth under stressful osmotic conditions as compared to the cultivated watermelon which had their roots growth highly inhibited has since been observed. The role of the resilient wild watermelon root was also observed when Seymen et al. (2021) used wild watermelon rootstock in grafting of cultivated watermelon. When exposed to moisture stress conditions, the grafted plant showed superior tolerance to the stressful conditions as compared to un-grafted plants and that has been attributed to the role of the rootstock's roots.

The root morphology and physiology also aids plants to sustainable growth under salt stress; importantly the plasticity of roots have been noted to be instrumental in aiding plants to tolerate salinity (Arif et al., 2019). It has been noted that the plasticity assists plants by preventing accumulation of salts in roots thus allowing normal uptake of moisture from the soils (Schleiff and Muscolo, 2011). Li et al. (2014) also noted that changes in root morphology as a critical factor for plants in tolerating salt stress. This was ascertained as a higher root biomass and root length was observed in *Suaeda salsa* (Wang et al., 2021), *Robinia pseudoacacia* (Mao et al., 2016*) and Jerusalem artichoke* (Yang et al., 2016) as a salinity tolerance mechanisms. The rapid growth of root hairs has been positively identified to contribute to the increase in root densities thus aiding the tolerance mechanisms in plants exposed to saline soils (Arif et al., 2019). This phenomenon is only observed in salt tolerant plants as susceptible species have shown a contrasting response when exposed to saline conditions. Chang et al. (2019) observed that when three rice plants were exposed to saline soils, they recorded a significant reduction in root biomass and length as the intensity on the salinity increased. Several other salinity susceptible plant species also showed similar reduced root morphology when exposed to saline conditions (Ashraf et al., 2005; Arif et al., 2016). Cultivated watermelon has been recorded to be salt sensitive and thus attempts to improve the crop has primarily focused on the use of salt tolerant roots stocks to graft the crop. Watermelon showed great resistance to salinity when grafted to the salt tolerant species which develop a well-

TABLE 1 Molecular mechanisms involved in plant tolerance against salinity and drought stresses.

Name	Molecular class	Abiotic stress	Function/Plant trait	Plant species	Reference
DEEPER ROOTING 1 (DRO1)	QTL	Drought and salinity	Regulation of root architecture	*Triticum aestivum, oryza sativa*	Kulkarni et al. (2017)
SIMILAR TO RCD ONE (SRO1)	QTL	Drought and salinity	Seedling growth, regulates ROS and Cellular redox homeostasis	*Solanum lycopersicum*	Liu et al. (2014)
qRT9	QTL	Drought and salinity stress	Root Architecture (root thickness and length)	*Oryza sativa*	Li et al. (2015)
Total Lateral root Number (qTLRN), L-type Lateral Root Number (qLLRN)	QTL	Drought	Root architecture Lateral root growth	*Oryza sativa*	Niones et al. (2015)
(Auxin Response Factor) ARF	TF	Cold, Drought and salinity	Lateral root development, leaf expansion senescence, fruit development	*Elaeis guineensis*	Jin et al. (2022)
Myeloblastosis (MYB)	TF	Drought and salinity	Cuticle development, stomatal aperture, ABA signaling	Watermelon (*Citrullus lanatus L.*) *Arabidopsis thaliana*	Xu et al. (2018) Wang et al. (2021)
Nuclear factor Y (NFYs)	TF	Drought and salinity	Maintaining stable relative water content (RWC)	Watermelon (*Citrullus lanatus L.*) *Arachis Hypogaea L.*	Yang et al. (2017) Wan et al. (2021)
9-*cis*-epoxycarotenoid dioxygenase (NCED)	TF	Drought and salinity	Inhibiting Al+ toxicity, Stomatal aperture	Watermelon (*Citrullus lanatus L.*) *Citrus limonia*	Li et al. (2012) Gavassi et al. (2021)
NAM, ATAF and CUC (NAC families)	TF	Drought and salinity	Cell division, leaf senescence, formation of secondary wall	Watermelon (*Citrullus lanatus L.*) *Glycine max, Oryza sativa*	Song et al. (2020) Shao et al. (2015)
Basic leucine zipper motif (bZIP)	TF	Drought and salinity	Vascular development in roots, leaf and root development	*Oryza sativa*	Yang et al. (2019)
basic Helix-Loop-helix (bHLH)	TF	Drought and salinity	Light signaling transduction, Plant growth, Metabolite biosynthesis	Melon (*Cucumis melo*) *Myrothamnus flabellifolius Welw, Populus euphratica Olivier*	Tan et al. (2021) Guo et al. (2021)
WRKY	TF	Drought and salinity	Leaf senescence, development, and secondary metabolites synthesis	Watermelon (*Citrullus lanatus L.*) Sweet potato *(Ipomoea batatas)* and Rice *(Oryza sativa)*	Yang et al. (2018) Jiang et al. (2017)
Dehydration Responsive Element Binding (DREB)	TF	Drought and salinity	Signal transduction	*Arabidopsis thaliana* and soybean (*Glycine max*)	Niu et al. (2020)
Abscisic Stress induced Ripening (ASR)	Functional Protein	Drought and salinity	Modulating stomatal aperture, fruit ripening	*Oryza sativa*	Park et al. (2020)
High-affinity K+ (HKT)	Functional Protein	Salinity	Na+ removal from the xylem	Pumpkin (*Cucurbita moschata)* *Glycine max*, *Sorghum bicolor*	Sun et al. (2018) Li et al. (2019)
Cyclophilin (CYP)	Functional Protein	Drought and salinity	Cellular signaling, maintaining ion homeostasis, protein degradation and apoptosis	*Oryza sativa, Brassica rapa*	Olejnik et al. (2021)
Drought-Induced Peptide (DRIP)	Functional Protein	Drought and salinity	Accumulation of osmoprotectants	Wild watermelon (*Citrullus lanatus L.*)	Yokota et al. (2002)
CLAVATA3/ Embryo Surrounding region (CLE)	Functional Protein	Drought	Stomatal aperture	*Arabidopsis thaliana*	Zhang et al. (2019)
C-TERMINALLY ENCODED PEPTIDE (CEP)	Functional Protein	Drought and salinity	Tunes auxin signaling, lateral root growth	*Arabidopsis thaliana*	Smith et al. (2020)
Heat Shock Proteins (HSPs)	Functional Protein	Drought and salinity	Protect the Photosystems and thylakoid membrane	Wild watermelon (*Citrullus lanatus L.*)	Akashi et al. (2011)

(Continued)

TABLE 1 Continued

Name	Molecular class	Abiotic stress	Function/Plant trait	Plant species	Reference
				Rice *(Oryza sativa)* and Wheat (*Triticum aestivum*)	Mishra et al. (2018)
Late Embryogenesis Abundant (LEA)	Functional Protein	Drought and salinity	Stabilizing water homeostasis and ROS Scavenger	Wild watermelon (*Citrullus lanatus L.*) Potato (*Solanum tuberosum*	Akashi et al. (2008) Chen et al. (2019)
Dehydrins	Functional Proteins	Drought and salinity	Chaperons, chelators, free radical scavenging	Watermelon (*Citrullus lanatus L.*) *Arabidopsis thaliana* and Rice *(Oryza sativa)*	Lee et al. (2017) Tiwari and Chakrabarty (2021)
GTPase	Functional Proteins	Drought and salinity	Root hair development, pollen growth, hormonal signal transmission	Wild watermelon (*Citrullus lanatus L.*) Wheat (*Triticum aestivum*)	Akashi et al. (2016a) Choudhury et al. (2021)
Trehalose-6-phosphate synthase (TPS)	Functional Protein	Drought and salinity	ROS Scavenging, regulating Intracellular K+ /Na+ balance	Watermelon (*Citrullus lanatus*)	Yuan et al. (2022a) Yuan et al. (2022b)
Aquaporins	Functional Proteins	Drought and salinity	Regulated water transport and stomatal aperture	Watermelon (*Citrullus lanatus*)	Raturi et al. (2022)
Thaumatin-like protein (TLP)	Functional Protein	Drought and salinity	Immune response, stomatal aperture	Watermelon (*Citrullus lanatus*)	Ram et al. (2022)
Metallothionein (MT)	Functional Proteins	Drought and salinity	Root growth, transpiration rate, stomatal aperture, accumulation of compatible solutes	Wild watermelon (*Citrullus lanatus L.*) *Arabidopsis thaliana*	Akashi et al. (2004) Patankar et al. (2019)

Some mechanisms have already been documented to play an important role in wild watermelon tolerance mechanisms while the rest are potential molecular mechanisms behind the morphological and physiological tolerance mechanisms in wild watermelon. Quantitative trait Loci, (QTL); Transcription Factors, (TF).

established root biomass that aided the grafted plants to accumulate less salt ions thus water uptake was not limited (Yan et al., 2018: Zhu et al., 2018; Kuşvuran et al., 2021). This shows that improvement into the root system (be it morphological, physiological or molecular) will enhance the salinity tolerance of cultivated watermelon. With the wild watermelon showing a good establishment of root plasticity under other abiotic stress, it thus presents a potential model to understand the roots response of this and related species in stress tolerance studies.

Timely stomatal closure response to drought stress

Under normal circumstances gaseous exchange in plants is facilitated by the stomatal aperture; whereby the opening allows for CO_2 to be taken in for the process of photosynthesis while O_2 is taken out as a by-product. Stomatal opening responds to several environmental and physiological factors, such as; light, leaf-to-air vapor pressure deficit, drought and salinity stress (Farquhar and Sharkey, 1982). Plant responses to salinity and drought are often similar. The first phase of salinity stress is the osmotic effect, which is quite similar to that of drought stress (Yildiz et al., 2020). The presence of excess salts in soil causes osmotic stress formation by limiting water availability of plant with roots. In a similar way, osmotic stress is induced by low water potential that results from an actual lack of water in an environment, due to low precipitation (drought). In both cases plants cannot uptake sufficient water for normal growth and development and common stress related signal transduction pathways are activated.

Closure of stomata has been noted as a first response of plant to osmotic stress (Munns and Tester, 2008) and this is highly dependent on the plant species, where tolerant species will have a mechanism of controlling the stomata to allow partial gaseous exchange to facilitate the photosynthesis process (Pirasteh-Anosheh et al., 2016). Under drought stress where soil moisture is limited and/or high atmospheric evaporative demand, partial or complete stomatal closure allows plants to maintain a favorable water balance while limiting the carbon gain. Salinity-generating stress also results in stomatal regulation, an important strategy that enables plants to cope with NaCl-induced osmotic and ionic stresses (Orzechowska et al., 2021). Plants exposed to salinity close their stomata to protect against water loss. The opening is limited by the soil and atmospheric moisture content because during moisture deficit the stomata tends to reduce their opening as an established form

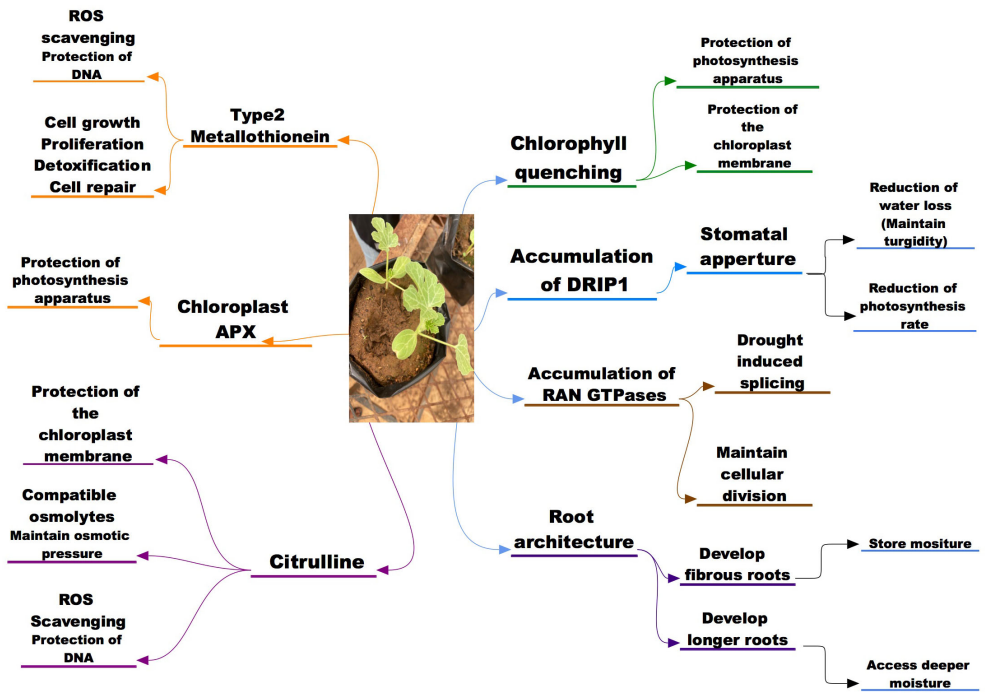


FIGURE 1
A schematic representation of the morphological, physiological and molecular potential indicators to drought and salinity stress tolerance in wild watermelon.

of first line of defense mechanism (Mansfield and Atkinson, 1990; Cornic and Massacci, 1996; Singh and Reddy, 2011; Hou et al., 2016). In doing so, excessive loss of leaf moisture and desiccation is avoided, thus protecting the cell structure and metabolisms. Stomatal closure plays an important role in protecting the most sensitive photosynthesis apparatus of the plant thus enabling the plant to survive/regenerate post the stress period (Martin-StPaul et al., 2017). Therefore, when the stomatal and non-stomatal limitations to photosynthesis are compared, the stomatal closure outweighs the later in plant growth and survival under stress conditions (Escalona et al., 2000; Tissue et al., 2005).

The response time of stomata during the critical period is very important in the survival of plants during drought and salinity stress, the quicker the plants respond, the better position they are in avoiding stress effects. This has been associated with the ability to withstand drought in *phaseolus* (Markhart, 1985) cowpea (Laffray and Louguet, 1990), sorghum (Tsuji et al., 2013), soybean (Hossain et al., 2015) and woody species (Yan et al., 2017); salinity in maize (Neto et al., 2004), Cotton (Janagoudar, 2007), sorghum (Duarado et al., 2022), *Eruca sativa* (Hniličková et al., 2017). This was attributed to stomatal closure as a form of salinity stress coping mechanism. The stomatal response can take several forms depending on the species and drought tolerance. Stomata can completely be closed under severe drought stress, and this is closely dependent on plant species, as tolerant species tend to control status of their stomata to allow carbon fixation and photosynthesis as well as improving water use efficiency (Laffray and Louguet, 1990; Pirasteh-Anosheh et al., 2016).

Stomatal aperture is highly regulated by the accumulation of the ABA. Several molecular mechanisms were found to play in the ABA-mediated stomatal aperture by triggering the ABA synthesis under drought stress (Daszkowska-Golec and Szarejko, 2013). Stress and ripening (ASR) gene family has been documented to play a significant role in the opening and closing of stomatas during abiotic stresses (Li et al., 2017) with several studies confirming the role in stomatal aperture. Other gene families like NCED (Sussmilch et al., 2017; Gavassi et al., 2021) and RAB have also been documented to play an important part in stomatal aperture during environmental stresses. Transcription factors like MYB (Oh et al., 2011; Simeoni et al., 2022) and Cyclophilin CYP (Liu et al., 2021; Olejnik et al., 2021), NAC (Du et al., 2014; Negi et al., 2018) and NFY (Guochao et al., 2017; Yu et al., 2021) families have been found to play a significant role in the ABA induced stomatal aperture

In comparison with cultivated watermelon, the wild watermelon has shown a different response pattern in stomatal closure when exposed to moisture deficit. The wild watermelon showed a rather quick stomatal response as observed by a

reduced internal CO_2 and dropped to almost zero in the earlier stages of moisture deficit; a same observation was made when the wild watermelon was compared to other crops in the citrullus family (Nanasato et al., 2010; Sanda et al., 2011; Mo et al., 2015; Malambane, 2018a). The stomatal closure of the wild watermelon response was observed within 3 days of moisture stress induction while the cultivated watermelon and cucumber took longer period for the internal CO_2 levels to drop. The wild watermelon internal CO_2 dropped to almost zero within 5 days post stress and was quicker as compared to the cultivated watermelon that took longer for the internal CO_2 to approach zero level. The timely stomatal closure of the wild watermelon results in lower internal CO_2 which then results in significantly reduction of the photosynthesis activity, and this can be thought to contribute to the survival of the plant as the energy is focused mostly in maintaining the plant under drought stress (Figure 1). The stomatal response of the wild watermelon to drought has shown similar trends as stomatal response to salinity in other crop species like melon, bottle gourd, pumpkins, luffa studied by Modarelli et al., 2020) and Arabidopsis thaliana (Orzechowska et al., 2021) thus the timely stomatal closure can be considered an important tolerance mechanisms for the wild watermelon during both drought and possibly for salinity stress too. However, in terms of salinity tolerance, precise physiological mechanisms need to be established in addition to safe guarding photosynthetic machinery through stomatal closure.

Protection of photosynthesis apparatus through chlorophyll fluorescence quenching

Stomatal closure as a response to abiotic stress usually results in a decrease in CO_2 supply to mesophyll cells and subsequently to the photosynthesis process. When drought is severe, this will be lead to a decrease in the rate of ATP and NADPH consumption for CO_2 assimilation (Baker and Rosenquist, 2004). In most sensitive plant species this would result in decreases in the rate of linear electron transport and consequently in operating efficiency of the most sensitive photosystem II (Φ_{PSII}) or the efficiency at which light absorbed by PSII antennae is used for reduction (QA reduction). In a similar manner, severe salt stress decreases pigment content and activity of photosynthetic electron transport (ΦPSII, qP), inhibits conversion (Fv/Fm) of light energy, and destroys cell membrane structure in plants (Jia et al., 2019). Chlorophyll (Chl) is an important pigment that reflects plant photosynthetic capacity and decrease in its content may be attributed to increased degradation and inhibited synthesis of the pigment. The loss of Chl is usually accompanied by inactivation of photochemical reactions, especially those mediated by PSII in plants exposed to salt stress and all this impact photosynthesis. Under drought and salinity stress, excess light energy absorbed by chlorophyll can cause irreversible damaged to PSII lead to cell death if not safely dissipated (quenched). This quenching acts as a protective mechanism that prevents the formation and accumulation of reactive oxygen species (ROS) induced by excessive reduction of the primary acceptor of PSII (Demmig-Adams and Adams, 2006; Zivcak et al., 2014). Quenching analysis allows for the separation of the contributions of photochemical and non-photochemical processes in the quenching of variable fluorescence, by inducing a temporary closure of all PSII reaction centers by a strong saturating light pulse (Baker, 2008). The decrease in fluorescence due to photochemistry is named photochemical quenching and the most useful parameter derived from quenching analysis is the measure of the efficiency of PSII (Φ_{PSII}) and quenching, qP indicates the proportion of open PSII reaction centers (Maxwell and Johnson, 2000) while the non-photochemical quenching (NPQ) represents the rapid and reversible thermal dissipation (heat loss) of absorbed light energy in the PSII antenna (Horton and Ruban, 2005). NPQ is believed to quench about 90% of the excitation energy in the PSII, has a mechanism that induce dehydration and this mechanism is thought to highly contribute to the high tolerance of some plants against severe dehydration caused by drought and salinity (Komura et al., 2010).

When comparing various genotypes of cotton under well-watered conditions, Zakhidov et al. (2016) found out that the stressed plants displayed higher values of Φ_{PSII} and most important in the drought tolerant lines the values were even higher by about 15% suggesting that chlorophyll fluorescence quenching efficiency is higher in tolerant species. When *Ginkgo biloba L.* seedlings were exposed to salinity stress, the results shows that maximum (Fv/Fm) and actual (ΦPSII) quantum yields of photosystem II (PSII) decreased gradually in the higher concentrations salt treatments and stability of the membrane system are greatly affected (Zhao H. et al., 2019) indicates the aggravation of the PSII reaction center at greater stress levels (Lu and Zhang, 2000; Percival, 2005), and this corresponds with diminished photosynthesis (Percival and Sheriffs, 2002; Kalaji et al., 2011). An analysis of whether chlorophyll fluorescence quenching performance was affected by the environment by Sanda et al. (2011); Malambane et al. (2021) showed that the wild watermelon NPQ and Φ_{PSII} values were higher when compared to the cultivated watermelon either in stressed or unstressed conditions in the two varying environments. This increase can be associated with the protection of the PSII from damage by the reduced rate of electron entry into the PSII. This suggests that the photochemical and non-photochemical quenching capacity of wild watermelon supersedes that of the cultivated relatives in any condition, thus suggesting a better response of the wild relative to drought stress. The superior quenching of the wild watermelon was associated with the photosynthesis pathway as Nanasato et al. (2010) observed that wild watermelon as a C_3 plant performed better than the

C_4 plants under drought stress. This was further ascertained by Guidi et al. (2019) who concluded that C_4 plants species are inferior when subjected to other abiotic stressors such as drought with respect to photo-inhibition. Even though the C_4 plants have a good acclimation potential, it has been reported that in most cases they lag behind the C_3 plants in acclimation responses (Sage and McKown, 2006) and one of the reasons attested to the quick acclimation of the C_3 plants is their system which allows photosynthetic plasticity to be concentrated at the cellular level rather than at tissue level. In studying temperature acclimation and temperature adaptation (Yamori et al., 2014) observed that the C_3 plants had a greater ability for temperature acclimation across broad range of temperatures as compared to the CAM and C_4 plants. ATP synthase has been documented as an important bioenergetic engine for all organisms, however the role of these important enzymes in the response to environmental fluctuations has been under study and some studies have shown potential involvement in drought and salinity stress tolerance (Zhang et al., 2008; Michaletti et al., 2018; Liu et al., 2021). When exposed to drought stress, wild watermelon levels of showed a photosynthetic activity decrease by approximately 50% as compared to the control plants (Kohzuma et al., 2009). The decrease was then associated with the photoprotection brought about by rapid increase of the qE which then suggested that the expression of ATP Synthase is an important part in the plant's acclimatization to environmental stress in wild watermelon (Hoshiyasu et al., 2013). When wild watermelon was exposed to high light under drought stress, the qE dramatically increase was observed by (Kohzuma et al., 2008) and this was attributed to the mechanisms that stabilizes the thylakoid pH. The protection mechanisms have further been explained in Dietz et al. (2001) where it was stated that this decrease in the ATPase subunits is important in over acidification of the thylakoid membrane thus protecting the photosynthesis apparatus.

Even though the protection of the photosystems by fluorescence quenching has been strongly suggested as one mechanisms for plants survival under drought stress, this can be suggested to be in response to light stress but less of moisture stress. Salinity stress imposes similar effects to plants as moisture stress because they all contribute to osmotic stress. But studies relating salinity stresses to PSII phytochemistry are conflicting and still inconclusive with some showing salinity inhibiting PSII activity while others showing PSII unaffected by the salinity stress. When comparing saline sensitive Arabidopsis to the tolerant Thellugiella, Stepien and Johnson, (2009) showed contrasting responses in the photosynthetic apparatus with Thellugiela inducing an alternative apparatus that aided it to tolerate salinity better that sensitive Arabidopsis. Exposure of the *Suaeda salsa* to saline environment showed no effect on any of the chlorophyll fluorescence parameters (Lu et al., 2003) this then suggests that in saline tolerant species there is no or limited changes in the PSII photochemistry thus suggesting the quenching mechanism to play a lesser important role in the plants salinity tolerance mechanism.

Citrulline accumulation as an osmo-protectant

Citrulline is a non-protein amino acid first identified from the juice of watermelon, *Citrullus lanatus* and found to also occur in other cucurbitaceous fruits. However, it ubiquitous in animals, bacteria, fungi, and plants (Joshi and Fernie, 2017). Exposure of plants to abiotic stress disrupts the electron transport chains resulting in the accumulation of ROS, which can lead to cellular damage and in response citrulline and other amino acids are produced to act as more potent ROS-scavengers or antioxidants, which can protect DNA and metabolic enzymes from oxidative damage (Akashi et al., 2001; Verslues and Juenger, 2011). Citrulline is biosynthesized from arginine synthesis pathway *via* the nitric oxide synthase as signaling mechanisms with several enzymes are involved. Three key enzymes that are involved in the synthesis of citrulline are NO synthase (NOS), ornithine carbamoyltransferase (OCT), which produces Cit, and argininosuccinate synthetase (ASS), which converts it into argininosuccinate (Anwar et al., 2021).

Watermelons and other plants have been documented to accumulate citrulline in response to osmotic (Dasgan et al., 2009; Cao et al., 2017), salinity (Kuşvuran et al., 2013) and drought stress (Kawasaki et al., 2000; Garg et al., 2016; Khan et al., 2019; Song et al., 2020). In cultivated watermelon a study by Song et al. (2020) reported a rapid accumulation of citrulline and related metabolites in the vegetative tissues due to drought stress. The study concluded that the metabolic pathways associated with citrulline synthesis and catabolism is regulated in the vegetative tissues of watermelon and its functional significance during drought stress. In previous study, Akashi et al. (2016b) revealed that spatial and developmental patterns of citrulline accumulation in wild watermelon during drought were largely different from those of the antioxidant lycopene, total proteins, and soluble sugars (glucose, fructose, and sucrose); thus, suggesting the accumulation may be regulated in a different manner from other nutrients during development. Wild watermelon has been found to primarily accumulate citrulline, and then glutamate and arginine, in place of proline and glycine betaine (Kawasaki et al., 2000). When compared to other compatible solutes like mannitol, proline and glycine betaine in wild watermelon leaves, citrulline had a much higher hydroxyl radical scavenging activity (Akashi et al., 2001). Osmolyte compatibility results from the absence of its interactions with substrates and cofactors, and the nonperturbing or its favorable effects on macromolecular-solvent interactions. It is likely that citrulline as an osmolyte accumulates in cells under drought and salinity and balance the osmotic difference between the cell's surroundings and the cytosol.

A much quicker response to salinity stress was observed in tolerant melons as compared to the sensitive ones where citrulline accumulation was observed 4 days earlier in tolerant species as compared to sensitive (Dasgan et al., 2009). In another study, Kusvuran et al. (2013) reported that citrulline is an important biochemical indicator in tolerance to salinity stress as salt tolerant melon genotypes accumulated more citrulline than the salt sensitive melon genotypes, suggesting that citrulline overproduction might be a consequence of adaptation to high saline and drought conditions. Despite the fact that citrulline accumulates in watermelon and other cucurbits in response to oxidative stress, (Akashi et al., 2001) reported that wild watermelon overproduced gamma-aminobutyric acid (GABA), proline and glutamine, not citrulline when it was subjected to saline conditions and the reasons for that metabolic salt response remains to be explained. However, citrulline was reported as the most efficient ROS scavenger compared to proline, mannitol and glycine betaine and effectively protecting DNA and metabolic enzymes from oxidative damage (Figure 1). Song et al. (2020) noted that the increased levels of citrulline protects the DNA cleavage and metabolic enzymes damage caused by ROS attacks, thus aiding the abiotic stress tolerance mechanisms of wild watermelon. Positive correlations have been found between citrulline accumulation and salinity drought stress tolerance in watermelons (Kusvuran et al., 2013). Salt tolerant melons (*Cucumis melo* L) genotypes have also been found to accumulate more citrulline in their leaves than sensitive (Dasgan et al., 2009). Furthermore, transgenic approaches have demonstrated a positive association between increased citrulline accumulation and drought and salt stress tolerance in Arabidopsis (Kalamaki et al., 2009a; Massange-Sánchez et al., 2016). Therefore, these accumulation and functionality of citrulline suggest it to be a key player in drought and potentially salinity tolerance mechanism in wild water melon and other crops.

Protection of chloroplast through accumulation of ascorbate peroxidase

Reactive oxygen species (ROS) are produced in normal manner as a signaling mechanism during plant growth, but when they are exposed to unfavorable environmental conditions their production is increased. Under drought stress closure of stomata and consequent decrease in CO_2 concentration in the leaf mesophyll results in the accumulation of NADPH in the chloroplasts. Under such conditions, O_2 acts as an alternative electron acceptor resulting in the generation of ROS (Sminorff, 1993). High levels of ROS in plant cells are toxic to enzymes, proteins, lipids, and DNA resulting in death, thus it is important for plants to quench this toxic levels of ROS. Transcriptome studies have shown increased abundance of response genes to oxidative stress due to drought in maize (Kakumanu et al., 2012), Arabidopsis (Desikan et al., 2001; Baxter et al., 2007) Rice (Zhang et al., 2017a) and tobacco (Zhang et al., 2017b). In addition to the non-enzymatic, the mechanisms that plants use to quench these ROS are the enzymatic antioxidant which are capable of quenching the ROS and bringing them to tolerable levels.

One major important enzymatic antioxidant is the Ascorbate Peroxidase (APX) (EC 1.11.1.11) which belongs to the class I heme-peroxidase (Asada, 1992; Lazzarotto et al., 2011). The APX exists in various isoforms classified according to their subcellular locality and they are; soluble isoforms found in cytosol (cAPX), mitochondria (mitAPX) and chloroplast stroma (sAPX), while membrane-bound isoforms are found in microbody (including peroxisome and glyoxisome) (mAPX) and chloroplast thylakoids (tAPX) (Shigeoka et al., 2002; Caverzan et al., 2012). The sAPX and tAPX are collectively referred to as the chloroplast APX (chlAPX) as they are found in the leaf chloroplast membranes. Several studies have pointed out that APX plays a key role in various plant abiotic stress response and recovery post stress exposure (Fini et al., 2012; Kausar et al., 2012; Zarei et al., 2012). Of the different isoforms of APX, the chloroplast APX gene expression was shown to be stimulated earlier in the tolerant cowpea cultivars under drought (D'Arcy-Lameta et al., 2006), thus suggesting that the chloroplast APX (chlAPX) responds first during drought stress protection. One characteristic of the chlAPX is that it is extremely sensitive to H_2O_2 under low-level ascorbate (Miyake and Asada, 1996). In most plants the cAPX showed high accumulation during drought stress (Yoshimura et al., 1998), leading to suggestions that cAPX might be one of the initial targets of oxidative injuries in plant leaves under drought (Shikanai et al., 1998).

However, this tendency was in contrast in wild watermelon as chlAPX accumulation was higher compared to other isoforms during drought stress period while the change in cAPX was non-significant throughout the experimental period (Nanasato et al., 2010). The up-regulation of the chlAPX was also observed in the domesticated watermelon thus suggesting that the behavior is common for the *Citrullus* family. While this response of chlAPX in watermelon has not been conclusively correlated with drought tolerance, the pattern is similar to other factors that contribute to the drought tolerance in wild watermelon. Malambane et al. (2018b) further reported chlAPX 3 folds enzymatic activity as compared to that of cAPX cytosolic in wild watermelon under drought stress, thus confirming its importance during drought stress in wild watermelon. The accumulation pattern of the chloroplastic APX in wild watermelon when exposed to the moisture deficit suggests that it contributes to the tolerance mechanisms of the plants to drought stress by quenching the radicals thus protecting the photosynthesis apparatus of the plant (Figure 1). Nanasato et al. (2015) observed that the biochemical process that is involved in the *cyt b* 561-ascorbate oxidase redox chain was significantly fortified in wild watermelon during exposure to drought stress (moisture

deficit and excess light). These results led to them proposing that this redox chain plays an important role in dissipating excess light thus aiding the crop to withstand the drought conditions.

Salinity stress creates ion imbalance and induces physiological drought like conditions by limiting the amount of water available to the plant, leading to lipid peroxidation and the production of ROS (Pandey et al., 2017). Under saline conditions, APX provides salinity tolerance at different levels to the affected plants (Sofo et al., 2015), thus APX is involved in the homeostasis of ascorbate, detoxification of H_2O_2, and the balancing of intracellular ROS messenger network (Diaz-Vivancos et al., 2013; Hernandez et al., 2001). Shalata et al. (2001) reported that during saline conditions, pea chloroplast APXs behaved differently, with sAPX increasing and tAPX decreasing gradually, while tAPX from tomato expressed in tobacco provided increased tolerance to salt and osmotic stress. In another study, Weisany et al. (2021) reported that APX transcripts in soybean increased due to salinity stress, while (Lin and Pu, 2010) documented that differential accumulation of APX transcripts with higher levels in tolerant genotypes were shown in sweet potato plants differing in their level of sensitivity to salt stress. The expression of cAPX, Mapx and chlAPX after exposure to 450mM NaCl in sweet potatoes plants was reported to be tissue specific and dependent on salt stress duration (Lin and Pu, 2010). Further, a cAPX from *Arabidopsis* in transgenic tobacco increased salt, drought, and PEG tolerance, and tomato plants over expressing pea cAPX were reported to be tolerant to salinity stress (Badawi et al., 2004; Wang et al., 2005). In comparison, over-expression of an APX from *Puccinellia tenuiflora* in Arabidopsis increased its tolerance to 175mM NaCl in addition to protection to lipid peroxidation, suggesting that APX provides salinity tolerance (Guan et al., 2015). Additionally, when analyzing for response of major antioxidant enzymes transcripts for different developmental stages in salt stressed rice, cAPX was up-regulated in 11-day-old seedlings, while in 6-week-old plants salt had no significant on this gene (Menezes-Benavente et al., 2004). The differences might be due to differences in cultivars, plant age and growth conditions (Tátrai et al., 2016).

Molecular responses

Expression of small signaling peptides and responsive proteins

Small signaling peptides play important roles in coordinating the intercellular communication in multicellular organisms (Yokota et al., 2002; Wang et al., 2016). These peptides have been found to play a role in wide-range of plant developmental and physiological processes (Feirs et al., 2005; Yaginuma et al., 2011; Song et al., 2013; Czyzewicz et al., 2015) and response against unfavorable stimuli (Lay and Anderson, 2005; Chen et al., 2019). The most common peptides associated with regulating against moisture stress are DRIP, CLE, IDA, PSK, CEP5 peptides while those regulating salinity responses are CAPE, RALF, AtPEP3 Peptides (Kim et al., 2021), and when exposed to osmotic stress these peptides have shown a similar accumulation pattern as a response mechanism of crops (Figure 2). Association of the response pattern of these peptides has been associated with several response factors of plants ABA accumulation and stomatal closure (McLachlan et al., 2018; Takahashi et al., 2018; Qu et al., 2019) in response to osmotic stress caused by either moisture or salinity. For instance, an AtMYB44 transcription factor involved in ABA-dependent and independent signaling pathways regulate stress adaptation and confer plant tolerance to salt stress (Nguyen and Cheong, 2018). Other transcription factors (AP2-EREBP, bZIP, bHLH, MYB, NAC, OFP, TCP, and WRKY) that are known to be acting in a similar manner through ABA signaling were recently determined by an RNA-Seq transcriptome analysis to be responsive and potentially contributing to salinity tolerance in water melons (Zhu et al., 2022). A transcriptome analysis of watermelon roots under osmotic stress revealed several response genes like Treahalose phosphate synthase (TPS) and Treahalose phosphate phosphatases (TPP) genes which were upregulated hence being suggested to aid plants tolerance mechanisms (Yang et al., 2016). In another transcriptome analysis study by Song et al., 2020, several differentially expressed genes were documented under osmotic and salinity stress with members of the ERF, WRKY, NAC, bHLH and MYB been over-represented suggesting their high active role in the tolerance mechanisms of watermelon seedlings. Yuan et al. (2022b) observed that genes involved plant hormone signal transduction, carbohydrate biosynthesis pathways were highly active in facilitating the tolerance mechanisms of watermelon seedlings against salinity stress. In another study by Zhang et al. (2020) it was found that overexpression of a MYB (SlMYB102) transcription factor in tomato *(Solanum Lycopersicon)* conferred salinity tolerance through increased upregulation of salinity stress related genes, increased the K+/Na+ ratio and the activity of active oxygen scavenging enzymes (SOD, POD, CAT, APX) and accumulation of the non-enzymatic antioxidants (ASA and GSH). These findings suggest that the response of watermelon to salt stress could be through a complex gene regulatory network, and MYB transcription factors may play an important role in salt tolerance by regulating downstream corresponding genes and the antioxidant systems.

One group of peptides that are highly expressed in the drought tolerant wild watermelon when exposed to drought and salinity stress is the drought-induced peptide (DRIP) (Figure 2). Yokota et al. (2002) exposed the watermelon cultivars and observed that DRIP-1 was induced in a similar manner in tolerance species response to either drought or salinity stress, thus suggesting it is highly involved in the tolerance mechanisms for the two stresses. A study on wild

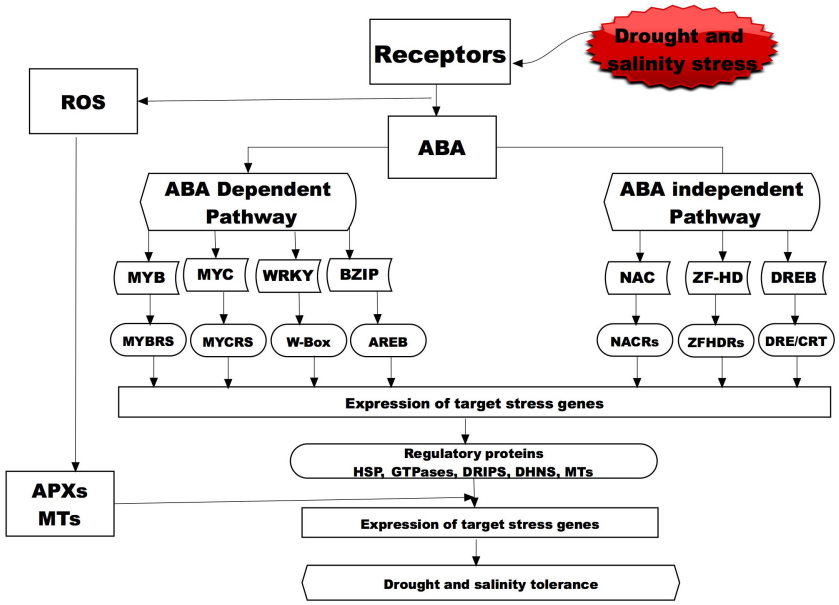


FIGURE 2
A representative diagram showing the molecular signaling for drought and salinity stress in plant through the ABA-dependent and independent pathways. Bolded and broken boxes show the molecular mechanisms that have been studied and presented in this review for the wild water melon drought tolerance and potential salinity tolerance indicators. Abscisic acid, (ABA; Myeloblastosis oncogene, (MYB); Myelocytomatosis oncogene, (MYC); WRKY Basic Leucine Zipper, (BZIP); NAC (NAM, ATAF and CUC) Zinc-finger homeodomain, (ZF-HD); Dehydration responsive element binding proteins, (DREB); MYB recognition site, (MYBRs); MYC recognition site, (MYCRs); ABA-responsive element binding protein, (AREB); NAC recognition site, (NARC); ZFHDR, cis-acting element/C-repeat DRE/CRT; Heat shock Proteins, (HSP); Drought induced proteins, (DRIP); ascorbate peroxidase, (APX); metallothionein, (MT); DHN, (Dehydrins).

watermelon leaves under severe drought stress revealed new peptides (DRIP-1 to DRIP-6), with the two isoforms of DRIP-1 showing an abundant accumulation as compared to the other DRIPs (Kawasaki et al., 2000). This accumulation pattern of the peptides was not observed in the control plants and the DRIP-1 isoforms in the watermelon leaves was associated with the accumulation of drought tolerance amino acids like arginine, glutamate and citrulline which have shown to play a critical role in ornithine synthesis. An analysis of proteins on the wild watermelon leaves exposed to moisture deficit for three days showed higher accumulation of DRIP-1, which was 5 times higher compared to the domesticated watermelon (Yokota et al., 2002). Similarly Roy et al. (2009) observed several new DRIPs accumulation in tomato leaves exposed to moisture stress as compared to the control plants. The role of small peptides in salinity stress has also being studied and that peptide *AtPep13* (Nakaminami et al., 2018) and *BoPROPEPs* (Wang et al., 2022) was actively involved in the tolerance against salinity as they naturally increased when plants were exposed to salt stress. Zhou et al. (2022) observed that a small peptide (*PIP3*) played a significant role in salinity tolerance of Arabidopsis thaliana when mutant with PIP3 knocked out exhibited salt sensitivity as compared to the wild types.

Ornithine effects on aiding drought and salinity tolerance on plants have been studied and documented (Kalamaki et al., 2009b; Anwar et al., 2018; Hussein et al., 2019; Çavuşoğlu and Çavuşoğlu, 2021). Arginine and ornithine are also used for the synthesis of polyamines and some alkaloids in plants (Urbano-Gámez et al., 2020). The activity of small peptide protein and contribution to drought and salinity tolerance could be through polyamines and alkaloids. Strong antioxidant activity of these secondary metabolites suggests that they could be acting downstream of the peptide proteins as protectants against ROS.

Proteins are known to be involved in various signaling and acting as key transcriptional activators for living organisms when exposed to different environments (Fotovat et al., 2017; Priya et al., 2019). Study of proteomics in elucidating the response mechanisms of plants to environmental stress has had significant results, thus a continued use to evaluate other climatic resilient plants like wild watermelon is of continued importance. A proteomic analysis of wild watermelon after exposure to drought stress revealed several drought related proteins to be highly expressed (Akashi et al., 2011). A total of 23 stress induced and 6 stress repressed proteins were positively identified and of these were mostly the heat shock proteins (HSPs). The HSPs has extensively been proven to play an important part in living organisms when exposed to various

biotic and abiotic stresses (Ruibal et al., 2013; Haq and Shakeel, 2020; Guo et al., 2020; Tian et al., 2021). Another proteomic study on wild watermelon by Si et al. (2009) revealed different expression of drought response related proteins when exposed to moisture stress with HSPs recording a high accumulation only four days when the crops were exposed to stress, while the NAC was highly expressed in the shoots as compared to the low expression observed in the roots when exposed to moisture stress. Several other proteins revealed varying expressions on either roots or shoots when exposed to moisture stress thus showing their active participation during drought response in wild watermelon. The role of response proteins in wild watermelon acclimatization to stress was further suggested by Li et al. (2018) who observed that the DEGs encoding late embryogenesis abundant (LEA) proteins, dehydrin, and heat shock proteins (HSPs) were highly expressed during drought stress.

These proteins that are highly associated with drought stress tolerance in wild watermelon and other crops have also shown to be active in tolerance to salinity stress (Figure 2). An analysis of the expressed proteins on wheat that was exposed to salinity revealed upregulation of several HSPs thus suggesting potential involvement in the salinity tolerance mechanism (Khateeb et al., 2020). To further ascertain the potential involvement of the HSPs in salinity tolerance mechanism, two HSP were isolated and overexpressed in rice and the results showed transgenic plants to have superior tolerance to both drought and salinity stress as compared to the wild type (Zou et al., 2021). A transcriptome analysis into the salt tolerance and sensitive willow genotypes recorded a total of 39 genes encoding for HSPs and all of these genes were upregulated under salinity stress and it was concluded that this small HSPs played in important role in response to salinity stress (Sui and Wang, 2020). However, some HSPs such as the watermelon ClHSP22.8 (He et al., 2021) could be key players in salinity tolerance and in water melons as negative regulators *via* ABA-dependent as well as independent and other signaling pathways. The involvement of these small HSPs in both drought and salinity stress are potential key players in the survival of plants under the two abiotic stresses. The body of knowledge accumulated so far has shown that HSPs play an important role wild watermelon tolerance to drought stress it can then be postulated that this HSPs could also contribute to the salinity stress when the plant is exposed to such as the two stresses could manifest through osmotic stress.

Expression of GTPase

Small guanosine triphosphate (GTPases)-binding proteins are tightly regulated molecular switches in signal transduction. These are a group of independent superfamily within the class of regulatory GTP hydrolases and are proteins that are capable of controlling a number of important processes and they possess a common structurally conserved GTP-binding domain (Bourne et al., 1990; Nilsson et al., 2002; Liu and Huang, 2009). The super family comprises of four families (RAN, ARF, RAB, ROP) that are conserved across eukaryotes; where RAN has been implicated in nucleocytoplasmic transport, RNA synthesis, processing and export and cell cycle checkpoint control (Scheffzek et al., 1995; Rush et al., 1996; Khuperkar et al., 2015) and ROP being involved in actin dynamics regulation, which controls polar growth and root hair development (Luo et al., 2006) and in salt tolerance signal pathways in plants (Yang, 2002).

Even though the functions of GTPase in animals and yeast have been well characterized and documented, the same cannot be said about plants. With the few reports available, the RAN GTPases involvement in mitosis; cell division and proliferation has been suggested. Rose and Meier (2001) suggested that a domain unique to plant RANGAP (the RAN GTPase activating protein) is responsible for its target on the plant nuclear rim. Transcriptome studies have also revealed drought enrichment of GTPases in maize ovary tissues with respect to drought induced splicing (Kakumanu et al., 2012), regulating of stomatal opening (Wang et al., 2017), conferring maximum ABA sensitivity (Lee and Seo, 2019) in Arabidopsis, found to trigger innate immunity in rice (Kawano et al., 2010). When Ran GTPase was overexpressed in Arabidopsis and Rice, the transgenic plants showed distinct phenotypes like increased number of tillers, weak apical dominance, excess rosette leaves and abnormal root growth suggesting the involvement of RAN GTPase in cell proliferation (Wang et al., 2006; Xu and Cai, 2014);. A transgenic approach demonstrated that plants overexpressing RAN genes had enhanced cold (Xu et al., 2016) and osmotic stress tolerance (Akashi et al., 2016a) as transgenic plants maintained cell division under stress conditions. In another study, a Rop protein, OsRacB, which acts as an accessory regulatory component in salt stress responses was identified (Christensen, 2003) and it expression studied in rice. Transgenic rice treated with salinity stress grew much better than the control, suggesting that overexpression of OsRacB in rice partly improve salinity tolerance, as had been shown in tobacco (Luo et al., 2006).

In wild watermelon one of the distinct features during drought is in the root growth that can reach up-to 2-3 meters down the sandy soils in search of the little conserved moisture. This extensive root growth can be thought to be stimulated by the RAN GTPase during drought, as shown in the significant induction of the RAN GTPase during analysis of root proteome of wild watermelon in the early stages of the crop under drought stress (Yoshimura et al., 2008). When grown under PEG induced drought stress the roots of wild watermelon were significantly different from the domesticated watermelon in both length, hairy roots development and dry mass as the wild watermelon recorded 2-3 folds increases showing an extensive growth in wild

watermelon root seedlings (Akashi et al., 2016a). Further, an overexpression of the CLRan on Arabidopsis resulted in increased root growth on both stressed and unstressed plants as compared to the wild types. A screening of the mRNA and protein abundance of the CLRan1 and CLRan2 displayed an incremental abundance of the RAN in the roots of the wild watermelon under drought stress as compared to the control. This thus suggests that the RAN GTPase is involved in the cell proliferation and this function is useful root development in wild watermelon thus playing a significant role when it comes to drought tolerance. These results thus further shows the involvement of small GTPases in both drought and salinity stress in plants. In response to salinity levels the grafted watermelon seedlings expressed several differentially expressed proteins and notably ATP synthase beta subunit was one of the protein highly expressed thus suggesting its role in the tolerance mechanisms against salinity stress (Yang et al., 2012).

Expression of Metallothionein (MT) as a protectant

The Metallothioneins (MTs) are low molecular mass (7-10kDa) proteins, which have a higher percentage of cysteine amino acids in the sequence (Liu et al., 2014). These proteins have long been discovered and isolated from horse kidneys as cadmium-binding proteins (Margoshes and Vallee, 1957). Their expression has been documented in plant responses to oxidative stress, where they act as protective factors by protecting cells through scavenging of stress induced ROS (Ruttkay-Nedecky et al., 2013). The MTs are directly involved in the removal of ROS enhancing the protection against cellular injury (Nzengue et al., 2012) and also act as an antioxidant for ROS-induced cellular injury (Chiaverini and De Ley, 2010). The ROS accumulate to toxic levels during drought stress conditions (Malambane, 2018a).

When plants are exposed to abiotic stress a usual increase in expression of the MT gene is observed, thus it has been concluded that the gene is important in tolerance mechanisms as it is associated with cell growth and proliferation, detoxification and cellular repair while maintaining the cellular homeostasis through ROS scavenging (Kumar et al., 2012). Overexpression of the MT gene from date palm (Patankar et al., 2019) and *Suaeda salsa*, (Jin et al., 2017) conferred drought and salinity tolerance in yeast and Arabidopsis. The transgenic plants accumulated less Na+ and maintained a high K+/Na+ ratio, which could be attributed to the role of the transgene on transporters such as HKT (Patankar et al., 2019). Further Soda et al. (2016) observed that metallothionein strongly interacts with other proteins like cytoskeleton to improve abiotic (drought and salinity) in diverse plant species. This was further confirmed by Mekawy et al. (2018) and Kumar et al. (2012) in which overexpressing *Os*MT-3a and *Os*MT-1e-P showed an improved tolerance to the NaCl stress by scavenging ROS in rice, *E.coli* and tobacco.

An analysis of wild watermelon under moisture stress showed a number of up-regulated genes in the leaf, and among the up-regulated genes was the Type 2 MT designated as *Cl*MT2 (*Citrullus lanatus* metallothionein Type-2) (Akashi et al., 2004). The effects of *Cl*MT2 on protecting genomic DNA under moisture stress were investigated and the results showed that the DNA degradation was significantly suppressed by the *Cl*MT2 in a dose dependent manner (Akashi et al., 2004). These then suggest that the up-regulation of the *Cl*MT2 in the leaves aid the plants tolerance mechanisms through DNA protection by ROS scavenging when exposed to drought stress (Figure 2). This upregulation of the *Cl*MT in wild watermelon could suggest that the crop has a strong chance in withstanding salinity stress through the ROS scavenging thus protecting the internal cellular mechanisms for the plants.

Conclusions and future perspectives

Drought stress is well documented to be a major factor in crop production and studies have shown that crops need a combination of factors to mitigate the effects of drought stress. Various studies on wild watermelon and other crops show that a combination of physiological, biochemical factors responses operating concert are responsible for drought tolerance. Figure 2 illustrates the concerted morphological, physiological, and molecular traits that the watermelon has developed to aid the drought tolerance mechanisms. The responses are resilient root growth and timely stomatal closure, accumulation of citrulline and expression of genes associated with drought stress in watermelons and many other crops and model species. The mechanisms presented here can also be studied on other species with promising drought tolerance mechanisms and be compared to those of the wild watermelon. However, the mechanisms presented in this review might not be all that contributes to tolerance of the crop, thus more studies are needed for the species to be considered as a model reference crop for drought tolerance and related studies. With limited studies on the salinity tolerance on wild watermelon and relatives, this review then aimed to associate the mechanisms for drought tolerance to the potential the plant might have in tolerating salinity. We have observed through other studies that the mechanisms wild watermelon has shown as drought tolerance are also similar mechanisms other plant species confer in salinity stress. Thus it can be concluded that wild watermelon through the drought tolerance mechanism can also double up as salinity tolerance but this need to be conferred through a scientific research focusing on citrulline accumulation, its biosynthesis genes, APX and ROS scavenging responses to the two stresses.

Drought and salinity stress research involving watermelon at molecular level revealed established transcription factors for tolerance in others species. The transcription factors; AP2-ERBP, bZIP, MYB, NAC, WRKY and their downstream target

genes, together regulons, have gained attention on their account of their role in drought and salinity tolerance pathways in plants. These are also presented in Figure 2 as ABA-depended and independent responsive to drought and salinity stress. A recent trancriptome study by Zhu et al. (2022) revealed that in addition to these, the OFP and TCP family of transcription factors responded to salinity stream in watermelons. A growing body of evidence suggests that OFP and TCP transcription factors participate in drought and salinity stress pathways in other plants (Danisman, 2016; Wang et al., 2020). Further other small signaling proteins like the Aquaporins whose primary role has been suggested as to maintain the water homeostasis in living cells thus playing and important role in moisture related stresses by maintaining the cells osmotic potential (Vera-Estrella, 2004; Afzal et al., 2016). In their role against drought and salinity stresses, it has been suggested that the Aquaporins regulated changes in the root, stem and leaf hydraulic conductivity, plant water usage in response to stress (Vandeleur et al., 2009; Vandeleur et al., 2014; Sade and Moshelion, 2017). Similarly, an observation where an up regulation of *ClAQP* was observed under salinity and drought stress and also during fruit development of the cultivated watermelon and cucumis melo (Wang et al., 2016; Kuşvuran et al., 2021; Lopez-Zaplana et al., 2022) suggesting the involvement of the aquaporins in tolerance mechanisms of the citrullus species. Another important protectant that has been documented to play an important role in drought and salinity stress is the trehalose that is suggested to play an important role in regulation of stomatal aperture, regulation of plant water use, osmolyte protectants and acting as an energy source thus aiding the tolerance mechanisms of plants. This protectant mechanism has also been observed in the cultivated watermelon (Yuan et al., 2022a; Yuan et al., 2022b) where it aided the crop to survive against the drought and salinity stresses. Other important molecular mechanisms that has shown potential to play an important role in the tolerance mechanisms of citrullus species is the Thaumatin-like protein (TLP) that has been documented to be actively involved in responses abiotic stresses in watermelon (Ram et al., 2022). All these potential tolerance mechanisms as observed in cultivated watermelon could thus suggest a much more pronounced expression and role in the more tolerant wild watermelon. Thus, this calls for their attention on their role and that of their target genes, to establish new regulons common in drought and salinity stress in wild watermelon. Having identified the transcription factors transcriptome analyses, their validation for drought and salinity stress tolerance can be done in water melons through transgenesis, Virus-induced gene silencing (VIGS), RNA interference, clustered regularly interspaced short palindromic repeat (CRISPR) genome editing system. Application of these techniques will be enable high throughput drought and salinity tolerance gene discovery pathways enabled by availability of its genetic transformation protocols, genome sequence of 20 accessions representing three different *C. Lanatus* subspecies (subsp. *Vulgaris*, subsp. *Mucosospermus and* subsp. *Lanatus)* (Guo et al., 2012). The identified transcription factors can be used to develop drought and salinity tolerant transgenic plants across three subspecies and other crops. Furthermore, and owing to the availability of transcriptome and metabolomic analysis resources in water melons, elucidation of dynamic coordination of drought and salinity responsive transcription factors in interacting pathways and their specific integration in the cellular network will provide new opportunities for the engineering of plant tolerance to these stresses.

Author contributions

GM conceptualized the research and wrote the manuscript; KM and LS conducted the literature review; UB conceptualized, supervised the research and reviewed the manuscript. All authors contributed to the article and approved the submitted version.

Funding

This work was financially supported by the Botswana University of Agriculture and Natural Resources Graduate Scholarship to KM and LS and The World Academy of Sciences Seed Grant for New African Principal Investigators to GM (SG-NAPI4500454040).

Conflict of interest

The authors declare that the research was conducted in the absence of any commercial or financial relationships that could be construed as a potential conflict of interest.

Publisher's note

All claims expressed in this article are solely those of the authors and do not necessarily represent those of their affiliated organizations, or those of the publisher, the editors and the reviewers. Any product that may be evaluated in this article, or claim that may be made by its manufacturer, is not guaranteed or endorsed by the publisher.

References

Afzal, Z., Howton, T. C., Sun, Y., and Mukhtar, M. S. (2016). The roles of aquaporins in plant stress responses. *J. Dev. Biol.* 4, 9. doi: 10.3390/jdb4010009

Akashi, K., Mifune, Y., Morita, K., Ishitsuka, S., Tsujimoto, H., and Ishihara, T. (2016b). Spatial accumulation pattern of citrulline and other nutrients in immature and mature watermelon fruits. *J. Sci. Food Agric.* 97, 479–487. doi: 10.1002/jsfa.7749

Akashi, K., Miyake, C., and Yokota, A. (2001). Citrulline, a novel compatible solute in drought tolerant wild watermelon leaves, is an efficient hydroxyl radical scavenger. *FEBS Lett.* 508, 438–442. doi: 10.1016/S0014-5793(01)03123-4

Akashi, K., Nishimura, N., Ishida, Y., and Yokota, A. (2004). Potent hydroxyl radical-scavenging activity of drought-induced type-2 metallothionein in wild watermelon. *Biochem. Biophys. Res. Commun.* 323, 72–78. doi: 10.1016/j.bbrc.2004.08.056

Akashi, K., Yoshida, K., Kuwano, M., Kajikawa, M., Yoshimura, K., Hoshiyasu, S., et al. (2011). Dynamic changes in the leaf proteome of a C3 xerophyte, citrullus lanatus (wild watermelon), in response to water deficit. *Planta* 233, 947–960. doi: 10.1007/s00425-010-1341-4

Akashi, K., Yoshimura, K., Kajikawa, M., Hanada, K., Kosaka, R., Kato, A., et al. (2016a). Potential involvement of drought-induced ran GTPase CLRan1 in root growth enhancement in a xerophyte wild watermelon. *Biosci Biotechnol. Biochem.* 80, 1907–1916. doi: 10.1080/09168451.2016.1191328

Akashi, K., Yoshimura, K., Nanasato, Y., Takahara, K., Munekage, Y., and Yokota, A. (2008). Wild plant resources for studying molecular mechanisms of drought/strong light stress tolerance. *Plant Biotechnol.* 25, 257–263. doi: 10.5511/plantbiotechnology.25.257

An, P., Inanaga, S., Li, X., Shimizu, H., and Tanimoto, E. (2003). Root characteristics in salt tolerance. *Root Res.* 12, 125–132. doi: 10.3117/rootres.12.125

Anwar, S., Ali, M. A., and Inselsbacher, E. (2021). Phenotypic analysis of arabidopsis thaliana arginine-deficient mutants. *Pure Appl. Biol. (PAB)* 11, 302–314. doi: 10.19045/bspab.2022.110032

Anwar, A., She, M., Wang, K., Riaz, B., and Ye, X. (2018). Biological roles of ornithine aminotransferase (OAT) in plant stress tolerance: Present progress and future perspectives. *Int. J. Mol. Sci.* 19, 3681. doi: 10.3390/ijms19113681

Arif, M. R., Islam, M. T., and Robin, A. H. K. (2019). Salinity stress alters root morphology and root hair traits in brassica napus. *Plants (Basel)* 8, 192. doi: 10.3390/plants8070192

Arif, H. K. B., Matthew, C., Uddin, M. J., and Bayazid, K. N. (2016). Salinity-induced reduction in root surface area and changes in major root and shoot traits at the phytomer level in wheat. *J. Exp. Bot.* 67, 3719–3729. doi: 10.1093/jxb/erw064

Asada, K. (1992). Ascorbate peroxidase - a hydrogen peroxide-scavenging enzyme in plants. *Physiologia Plantarum* 85, 235–241. doi: 10.1111/j.1399-3054.1992.tb04728.x

Ashraf, M. Y., Akhtar, K., Sarwar, G., and Ashraf, M. (2005). "Role of the rooting system in salt tolerance potential of different guar accessions," in *Agronomy for sustainable development*, vol. 25. (Springer Verlag/EDP Sciences/INRA), 243–249.

Baker, N. R. (2008). Chlorophyll fluorescence: a probe of photosynthesis *in vivo*. *Annu. Rev. Plant Biol.* 59, 89–113. doi: 10.1146/annurev.arplant.59.032607.092759

Badawi, G. H., Kawano, N., Yamauchi, Y., Shimada, E., Sasaki, R., Kubo, A., et al (2004). Over-expression of ascorbate peroxidase in tobacco chloroplasts enhances the tolerance to salt stress and water deficit. *Physiol Plant.* 121, 231–238. doi: 10.1111/j.0031-9317.2004.00308.x

Baker, N. R., and Rosenquist, E. (2004). Applications of chlorophyll flourescemce can improve crop production strategies: An examination of future possibilities. *J. Exp. Bot.* 55, 1607–1621. doi: 10.1093/jxb/erh196

Bao, Y., Aggarwal, P., Robbins, N. E.II, Sturrock, C. J., Thompson, M. C., Tan, H. Q., et al. (2014). Plant roots use a patterning mechanism to position lateral root branches toward available water. *PNAS* 111, 9319–9324. doi: 10.1073/pnas.1400966111

Baxter, C. J., Redestig, H., Schauer, N., Repsilber, D., Patil, K. R., Nielsen, J., et al. (2007). The metabolic response of heterophic arabidopsis cells to oxidative stress. *Plant Physiol.* 143, 312–325. doi: 10.1104/pp.106.090431

Bourne, H. R., Sanders, D. A., and McCormick, F. (1990). The GTPase superfamily: a conserved switch for diverse cell functions. *Nature* 348, 125–132. doi: 10.1038/348125a0

Brown, C., Ghile, Y., Laverty, M., and Li, K. (2012). Decision scaling: Linking bottom-up vulnerability analysis with climate projections in the water sector. *Water Resour. Res.* 48, W09537. doi: 10.1029/2011WR011212

Cao, D., Lutz, A., Hill, C. B., Callahan, D. L., and Roessner, U. (2017). A quantitative profiling method of phytohormones and other metabolites applied to barley roots subjected to salinity stress. *Front. Plant Sci.* 7, 2070. doi: 10.3389/fpls.2016.02070

Caverzan, A., Passaia, G., Rosa, S. B., Ribeiro, C. W., Lazzarotto, F., and Margis-pinheiro, M. (2012). Plant response to stresses: Role of ascorbate peroxidase in the antioxidant protection. *Genet. Mol. Biol.* 35, 1011–1019. doi: 10.1590/S1415-47572012000600016

Çavuşoğlu, K., and Çavuşoğlu, D. (2021). Role of l-ornithine in mitigation of salt stress in allium cepa l. *Bangladesh J. Bot.* 50, 1165–1171. doi: 10.3329/bjb.v50i4.57085

Chang, J., Cheong, B. E., Natera, S., and Roessner, U. (2019). Morphological and metabolic responses to salt stress of rice (Oryza sativa l.) cultivars which differ in salinity tolerance. *Plant Physiol. Biochem.* 144, 427–435. doi: 10.1016/j.plaphy.2019.10.017

Chen, Y. L., Fan, K. T., Hung, S. C., and Chen, Y. T. (2019). The role of peptides cleaved from proteins precursors in eliciting plants stress reactions. *New Phytol.* 6, 2267–2282.

Chen, Y., Li, C., Zhang, B., Yi, J., Yang, Y., Kong, C., et al. (2019). The role of the late embryogenesis-abundant (LEA) protein family in development and the abiotic stress response: A comprehensive expression analysis of potato (Solanum tuberosum). *Genes (Basel)* 10, 148. doi: 10.3390/genes10020148

Chiaverini, N., and De Ley, M. (2010). Protective effect of metallothionein on oxidative stress-induced DNA damage. *Free Radicals Res.* 44, 605–613. doi: 10.3109/10715761003692511

Choudhury, S., Mansi,, Muthusamy, S. K., Padaria, J. C., and Dalal, M. (2021). Genome-wide identification of ran GTPase family genes from wheat (T. aestivum) and their expression profile during developmental stages and abiotic stress conditions. *Funct. Integr. Genomics* 21, 239–250. doi: 10.1007/s10142-021-00773-0

Christensen, T. M., Vejlupkova, Z., Sharma, K. Y., Arthur, K. M., Spatafora, W. J., Albright, A. C., et al. (2003). Conserved subgroups and developmental regulation in the monocot rop gene family. *Plant Physiol.* 133, 1791–1808. doi: 10.1104/pp.103.029900

Comas, L. H., Becker, S. R., Cruz, V. M. V., Byrne, P. F., and Dierig, D. A. (2013). Root traits contributing to plant productivity under drought. *Front. Plant Sci.* 4, 442. doi: 10.3389/fpls.2013.00442

Condon, A. G., and Hall, A. E. (1997). 3-adaptation to diverse environments; variations in water-use efficiency within crop species. *Environ. Sci.* (Academic Press), 79–116. doi: 10.1016/B978-012378260-1/50004-X

Cornic, G., and Massacci, A. (1996). "Leaf photosynthesis under drought stress," in *Photosynthesis and the environment*. Ed. N. R. Baker (The Netherlands: Kluwer Academic Publishers).

Czyzewicz, N., Shi, C. L., Vu, L. D., Van De Cotte, B., Hodgman, C., and Butenko, M. A. (2015). Modulation of arabidopsis and monocot root architecture by CLAVATA3/EMBRYO SURROUNDING REGION 26 peptide. *J. Exp. Bot.* 66, 5229–5243. doi: 10.1093/jxb/erv360

Danisman, S. (2016). TCP Transcription factors at the interface between environmental challenges and the plant's growth responses. *Front. Plant Sci.* 7, 1930. doi: 10.3389/fpls.2016.01930

D'Arcy-Lameta, A., Ferrari-Iliou, R., Contour-Ansel, D., Pham-Thi, A. T., and Zuily-Fodil, Y. (2006). Isolation and characterization of four ascorbate peroxidase cDNAs responsive to water deficit in cowpea leaves. *Ann. Bot.* 97, 133–140. doi: 10.1093/aob/mcj010

Dasgan, H. Y., Kusvuran, S., Abak, K., Leport, L., Larher, F., and Bouchereau, A. (2009). The relationship between citrulline accumulation and salt tolerance during the vegetative growth of melon (Cucumis melo l.). *Plant Soil Environ.* 55, 51–57. doi: 10.17221/316-PSE

Daszkowska-Golec, A., and Szarejko., I. (2013). Open or close the gate – stomata action under the control of phytohormones in drought stress conditions. *Front. Plant Sci.* 4, 138. doi: 10.3389/fpls.2013.00138

Demmig-Adams, B., and Adams, W. W. (2006). Photoprotection in an ecological context: the remarkable complexity of thermal energy dissipation. *New Phytol* 172, 11–21. doi: 10.1111/j.1469-8137.2006.01835.x

Desikan, R., H.-Mackerness, S. A., Hancock, J. T., and Steven, J. N. (2001). Regulation of the arabidopsis transcriptome by oxidative stress. *Plant Physiol.* 127, 159–172. doi: 10.1104/pp.127.1.159

Diaz-Vivancos, P., Barba-Espín, G., and Hernández, J. A. (2013). Elucidating hormonal/ROS networks during seed germination: insights and perspectives. *Plant Cell Rep.* 32, 1491–502. doi: 10.1007/s00299-013-1473-7

Dietz, K. J., Tavakoli, N., Kluge, C., Mimura, T., Sharma, S. S., Harris, G. C., et al. (2001). Significance of the V-type ATPase for the adaptation to stressful growth conditions and its regulation on the molecular and biochemical level. *J. Exp. Bot.* 52, 1969–1980. doi: 10.1093/jexbot/52.363.1969

Du, M., Zhai, Q., Deng, L., Li, S., Li, H., Yan, L., et al. (2014). Closely related NAC transcription factors of tomato differentially regulate stomatal closure and reopening during pathogen attack. *Plant Cell* 26, 3167–3184. doi: 10.1105/tpc.114.128272

Dourado, P. R. M., de Souza, E. R., Santos, M. A. D., Lins, C. M. T., Monteiro, D. R., Paulino, M. K.S. S., et al (2022). Stomatal Regulation and Osmotic Adjustment in Sorghum in Response to Salinity. *Agriculture* 12, 658. doi: 10.3390/agriculture12050658

Escalona, J. M., Flexas, J., and Medrano, H. (2000). Stomatal and non-stomatal limitations to photosynthesis under water stress in field-grown grapevines. *Aust. J. Plant Physiol.* 27, 87–87. doi: 10.1071/PP99019_CO

Farooq, M., Wahid, A., Kobayashi, N., Fujita, D., and Basra, S. M. A. (2008). Plant drought stress: effects, mechanisms and management. *Agron. Sustain. Dev.* 29, 185–212. doi: 10.1051/agro:2008021

Farquhar, G. D., and Sharkey, T. D. (1982). Stomatal conductance and photosynthesis. *Annu. Rev. Plants Biol.* 61, 561–591. doi: 10.1146/annurev.pp.33.060182.001533

Feirs, M., Golemiec, E., Xu, J., van der Geest, L., Heidstra, R., Stiekema, W., et al. (2005). The 14-amino acids CLV3, CLE19, and CLE40 peptides trigger consumption of the root meristems in arabidopsis through a CLAVATA-dependent pathway. *Plant Cell* 17, 2542–2553. doi: 10.1105/tpc.105.034009

Feng, X., Jia, L., Cai, Y., Guan, H., Zheng, D., Zhang, W., et al. (2022). ABA inducible DEEPER ROOTING 1 improves adaptation of maize to water deficiency. *Plant Biotechnol. J.* 20, 2077–2088. doi: 10.1111/pbi.13889

Fini, A., Guidi, L., Ferrini, F., Brunetti, C., di Ferdinando, M., Biricolti, S., et al. (2012). Drought stress has contrasting effects on antioxidant enzymes activity and phenylpropanoid biosynthesis in fraxinus ornus leaves: An excess light stress affair? *J. Plant Physiol.* 169, 929–939. doi: 10.1016/j.jplph.2012.02.014

Fotovat, R., Alikhani, M., Valizadeh, M., Mirzaei, M., and Salekdeh, G. H. (2017). A proteomics approach to discover drought tolerance proteins in wheat pollen grain at meiosis stage. *Protein Peptides Lett.* 24, 26–36. doi: 10.2174/0929866523666161130143446

Garg, R., Shankar, R., Thakkar, B., Kudapa, H., Krishnamurthy, L., Mantri, N., et al. (2016). Transcriptome analyses reveal genotype- and developmental stage-specific molecular responses to drought and salinity stresses in chickpea. *Sci. Rep.* 6, 19228. doi: 10.1038/srep19228

Gavassi, M. A., Silva, G. S., Santiago, G. M., Thompson, A. J., Macleod, K., Oliveira, P. M. R., et al. (2021). NCED expression is related to increased ABA biosynthesis and stomatal closure under aluminum stress. *Environ. Exp. Bot.* 185, 104404. doi: 10.1016/j.envexpbot.2021.104404

Ghorecha, V., Zheng, Y., Liu, L., Sunkar, R., and Krishnayya, N. S. R. (2017). MicroRNA dynamics in a wild and cultivated species of convolvulaceae exposed to drought stress. *Physiol. Mol. Biol. Plants* 23, 291–300. doi: 10.1007/s12298-017-0426-y

Gibson, A. C. (1996). Origins of desert structural adaptations. In: Structure-function relations of warm desert plants. *Adaptations of desert organisms*. Berlin, Heidelberg: Springer. doi: 10.1007/978-3-642-60979-4_7

Gifford, M. L., Banta, J. A., Katari, M. S., Hulsmans, J., Chen, L., Ristova, D., et al. (2013). Plasticity regulators modulate specific root traits in discrete nitrogen environments. *PloS Genet.* 9, e1003760. doi: 10.1371/journal.pgen.1003760

Gorim, L. Y., and Vandenberg, A. (2017). Evaluation of wild lentil species as genetic resources to improve drought tolerance in cultivated lentil. *Front. Plant Sci.* 8, 1129. doi: 10.3389/fpls.2017.01129

Guan, Q., Wang, Z., Wang, X., Takano, T., and Liu, S. (2015). A peroxisomal APX from Puccinellia tenuiflora improves the abiotic stress tolerance of transgenic Arabidopsis thaliana through decreasing of H2O2 accumulation. *J Plant Physiol.* 175, 183–191. doi: 10.1016/j.jplph.2014.10.020

Guidi, L., Lo Piccolo, E., and Landi, M. (2019). Chlorophyll fluorescence, photoinhibition and abiotic stress: Does it make any difference the fact to be a C3 or C4 species? *Front. Plant Sci.* 10, 174. doi: 10.3389/fpls.2019.00174

Guochao, X., Congming, L., Ruofang, Z., and Jiming, J. (2017). Overexpression of StNF-YB3.1 reduces photosynthetic capacity and tuber production, and promotes ABA-mediated stomatal closure in potato (Solanum tuberosum l.). *Plant Sci.* 261, 50–59. doi: 10.1016/j.plantsci.2017.04.015

Guo, J., Sun, B., He, H., Zhang, Y., Tian, H., and Wang, B. (2021). Current understanding of bHLH transcription factors in plant abiotic stress tolerance. *Int. J. Mol. Sci.* 22, 4921. doi: 10.3390/ijms22094921

Guo, L. M., Li, J., He, J., Liu, H., and Zhang, H. (2020). A class I cytosolic HSP20 of rice enhances heat and salt tolerance in different organisms. *Sci Rep* 10, 1383. doi: 10.1038/s41598-020-58395-8

Guo, S., Zhang, J., Sun, H., Salse, J., Lucas, W.J., Zhang, H., et al (2012). The draft genome of watermelon (Citrullus lanatus) and resequencing of 20 diverse accessions. *Nat. Genet.* 45, 51–58. doi: 10.1038/ng.2470

Guseman, J. M., Webb, K., Srinivasan, C., and Dardick, C. (2017). DRO1 influences root system architecture in arabidopsis and prunus species. *Plant J.* 89, 1093–1105. doi: 10.1111/tpj.13470

Haq, N. U., and Shakeel, S. N. (2020). HSPs under Abiotic Stresses. In S. Fahad, S. Saud, Y. Chen, C. Wu and D. Wang (Eds.), *Abiotic Stress in Plants*. London: IntechOpen. doi: 10.5772/intechopen.93787

He, Y., Yao, Y., Li, L., Li, Y., Gao, J., and Fan, M. (2021). A heat-shock 20 protein isolated from watermelon (ClHSP22.8) negatively regulates the response of arabidopsis to salt stress *via* multiple signaling pathways. *Peer J.* 9, e10524. doi: 10.7717/peerj.10524

Hernández, J. A., Ferrer, M. A., Jiménez, A., Barceló, A. R., and Sevilla, F. (2001). Antioxidant systems and O2.-/H2O2 production in the apoplast of pea leaves. Its relation with salt-induced necrotic lesions in minor veins. *Plant Physiol.* 127, 817–831. doi: 10.1104/pp.010188

Hniličková, H., Hnilička, F., Martinkova, J., and Kraus, K. (2017). Effects of salt stress on water status, photosynthesis and chlorophyll fluorescence of rocket. *Plant Soil Environ.* 63, 362–367. doi: 10.17221/398/2017-PSE

Horton, P., and Ruban, A. V. (2005). Molecular design of the photosystem II light-harvesting antenna: photosynthesis and photoprotection. *J. Exp. Bot.* 56, 365–373. doi: 10.1093/jxb/eri023

Hoshiyasu, S., Kohzuma, K., Yoshida, K., Fujiwara, M., Fukao, Y., Yokota, A., et al. (2013). Potential involvement of n-terminal acetylation in the quantitative regulation of the " subunit of chloroplast ATP synthase under drought stress. *Biosci Biotechnol. Biochem.* 77, 998–1007. doi: 10.1271/bbb.120945

Hossain, M. D. M., Hon-Ming, L., and Zhang, J. (2015). Responses in gas exchange and water status between drought-tolerant and -susceptible soybean genotypes with ABA application. *Crop J.* 3, 500–506. doi: 10.1016/j.cj.2015.09.001

Hou, W., Sun, A. H., Chen, H. L., Yang, F. S., Pan, J. L., and Guan, M. Y. (2016). Effects of chilling and high temperatures on photosynthesis and chlorophyll fluorescence in leaves of watermelon seedlings. *Biol. Plantarum* 1, 148–154. doi: 10.1007/s10535-015-0575-1

Hussain, M. I., Dionyssia-Angeliki, L., Farooq, M., Nikoloudakis, N., and Khalid, N. (2015). Salt and drought stresses in safflower: a review. *Agron. Sustain. Dev.* 36, 4. doi: 10.1007/s13593-015-0344-8

Hussein, H. B. A., Mekki, B. B., E.Abd El-Sadek, M., and Ebd El Lateef, E. (2019). Effect of l-ornithine application on improving drought tolerance in sugar beet plants. *Heliyon* 5, e02631. doi: 10.1016/j.heliyon.2019.e02631

Iseki, K., Takahashi, Y., Muto, C., Naito, K., and Tomooka, N. (2018). Diversity of drought tolerance in the genus vigna. *Front. Plant Sci.* 9, 729. doi: 10.3389/fpls.2018.00729

Jaleel, C. A., Manivannan, P., Wahid, A., Farooq, M., Somasundaram, R., and Panneerselvam, R. (2009). Drought stress in plants: a review on morphological characteristics and pigments composition. *Int. J. Agric. Biol.* 11, 100–105.

Janagoudar, B. S. (2007). Salinity induced changes in stomatal response, bio-physical parameters, solute accumulation and growth in cotton (Gossypium spp.) The World Cotton Research Conference-4 September 10-14, 2007. Texas, USA: Lubbock Memorial Civic Center.

Jia, M., Li, D., Colombo, R., Wang, Y., Wang, X., Cheng, T., et al. (2019). Quantifying chlorophyll fluorescence parameters from hyperspectral reflectance at the leaf scale under various nitrogen treatment regimes in winter wheat. *Remote Sens.* 11, 2838. doi: 10.3390/rs11232838

Jiang, J., Ma, S., Ye, N., Jiang, M., Cao, J., and Zhang, J. (2017). WRKY transcription factors in plant responses to stresses. *J. Integrated Plant Biol.* 59, 86–101. doi: 10.1111/jipb.12513

Jin, S., Xu, C., Li, G., Sun, D., Li, Y., Wang, X., et al. (2017). Functional characterization of a type 2 metallothionein gene, SsMT2, from alkaline tolerant suaeda salsa. *Sci. Rep.* 7, 17914. doi: 10.1038/s41598-017-18263-4

Jin, L., Yarra, R., Zhou, L., and Cao, H. (2022). The auxin response factor (ARF) gene family in oil palm (Elaeis guineensis jacq.): Genome-wide identification and their expression profiling under abiotic stresses. *Protoplasma* 259, 47–60. doi: 10.1007/s00709-021-01639-9

Joshi, V., and Fernie, A. R. (2017). Citrulline metabolism in plants. *Amino Acids* 49, 1543–1559. doi: 10.1007/s00726-017-2468-4

Kajikawa, M., Morikawa, K., Abe, Y., Yokota, A., and Akashi, K. (2010). Establishment of a transgenic hairy root system in wild and domesticated watermelon (Citrullus lanatus) for studying root vigor under drought. *Plant Cell Rep.* 29, 771–778. doi: 10.1007/s00299-010-0863-3

Kakumanu, A., Ambavaram, M. M. R., Klumas, C., Krishnan, A., Batlang, U., Myers, E., et al. (2012). Effects of drought on gene expression in maize reproductive and leaf meristem tissue revealed by RNA-seq. *Plant Physiol.* 160, 846–867. doi: 10.1104/pp.112.200444

Kalaji, H. M., Govindjee, B. K., Kościelniak, J., and Żuk-Golaszewska, K. (2011). Effects of salt stress on photosystem II efficiency and CO2 assimilation of two Syrian barley landraces. *Environ. Exp. Bot.* 73, 64–72. doi: 10.1016/j.envexpbot.2010.10.009

Kalamaki, M. S., Alexandrou, D., Lazari, D., Merkouropoulos, G., Fotopoulos, V., Pateraki, I., et al. (2009b). Over-expression of a tomato n-acetyl-L-glutamate synthase gene (SlNAGS1) in arabidopsis thaliana results in high ornithine levels and increased tolerance in salt and drought stresses. *J. Exp. Bot.* 60, 1859–1871. doi: 10.1093/jxb/erp072

Kalamaki, M. S., Merkouropoulos, G., and Kanellis, A. K. (2009a). Can ornithine accumulation modulate abiotic stress tolerance in arabidopsis? *Plant Signal Behav.* 4, 1099–1111. doi: 10.4161/psb.4.11.9873

Kausar, R., Hossain, Z., Makino, T., and Komatsu, S. (2012). Characterization of ascorbate peroxidase in soybean under flooding and drought stresses. *Mol. Biol. Rep.* 39, 10573–10579. doi: 10.1007/s11033-012-1945-9

Kawano, Y., Chen, L., and Shimamoto, K. (2010). The function of rac small GTPase and associated proteins in rice innate immunity. *Rice* 3, 112–121. doi: 10.1007/s12284-010-9049-4

Kawasaki, S., Miyake, C., Kohchi, T., Fujii, S., Uchida, M., and Yokota, A. (2000). Responses of wild watermelon to drought stress: accumulation of an ArgE homologue and citrulline in leaves during water deficits. *Plant Cell Physiol.* 41, 864–873. doi: 10.1093/pcp/pcd005

Karahara, I., and Horie, T. (2021). Functions and structure of roots and their contributions to salinity tolerance in plants. *Breed Sci.* 71 (1), 89–108. doi: 10.1270/jsbbs.20123

Khan, N., Bano, A., Rahman, M. A., Guo, J., Kang, Z., and Babar, M. A. (2019). Comparative physiological and metabolic analysis reveals a complex mechanism involved in drought tolerance in chickpea (Cicer arietinum l.) induced by PGPR and PGRs. *Sci. Rep.* 9, 2097. doi: 10.1038/s41598-019-38702-8

Khateeb, W., Muhaidat, R., Alahmed, S., Al Zoubi, M. S., Al-Batayneh, K. M., El-Oqlah, A., et al. (2020). Heat shock proteins gene expression and physiological responses in durum wheat (Triticum durum) under salt stress. *Physiol Mol Biol Plants*. 26, 1599–1608. doi: 10.1007/s12298-020-00850-x

Khuperkar, D., Helen, M., Magre, I., and Joseph, J. (2015). Inter-cellular transport of ran GTPase. *PloS One* 10, e0125506. doi: 10.1371/journal.pone.0125506

Kim, J. S., Jeon, B. W., and Kim, J. (2021). Signaling Peptides Regulating Abiotic Stress Responses in Plants. *Front. Plant Sci.* 12, 704490. doi: 10.3389/fpls.2021.704490

Kohzuma, K., Akashi, K., Munekage, Y. N., Sanda, S., Hisabori, T., and Yokota, A. (2008). "Preferential decay of the CF1-e subunit induces thylakoid uncoupling in wild watermelon under drought stress," in *Photosynthesis. energy from the sun: 14th international congress on photosynthesis*. Eds. J. F. Allen, E. Gantt, J. H. Golbeck and B. Osmond (Springer), 617–621.

Kohzuma, K., Cruz, J. A., Akashi, K., Hoshiyasu, S., Munekage, Y. N., Yokota, A., et al. (2009). The long-term responses of the photosynthetic proton circuit to drought. *Plant Cell Environ.* 32, 209–219. doi: 10.1111/j.1365-3040.2008.01912.x

Komura, M., Yamagishi, A., Shibata, Y., Iwasaki, I., and Itoh, S. (2010). Mechanism of strong quenching of photosystem II chlorophyll fluorescence under drought stress in a lichen, physciella melanchla, studied by subpicosecond fluorescence spectroscopy, biochimica et biophysica acta (BBA). *Bioenergetics* 1797, 331–338. doi: 10.1016/j.bbabio.2009.11.007

Kulkarni, M., Soolanayakanahally, R., Ogawa, S., Uga, Y., Selvaraj, M. G., and Kagale, S. (2017). Drought response in wheat: Key genes and regulatory mechanisms controlling root system architecture and transpiration efficiency. *Frontier Chem.* 5, 106. doi: 10.3389/fchem.2017.00106

Kumar, G., Kushwaha, H. R., Panjabi-Sabharwal, V., Kumari, S., Joshi, R., Mittal, S., et al. (2012). Clustered metallothionein genes are co-regulated in rice and ectopic expression of OsMT1e-p conferes multiple abiotic stress tolerance in tobacco *via* ROS scavenging. *BMC Plant Biol.* 12, 107. doi: 10.1186/1471-2229-12-107

Kuşvuran, Ş, Kaya, E., and Ellialtıoğlu, Ş. (2021). Role of Grafting in Tolerance to Salt Stress in Melon (Cucumis melo L.) Plants: Ion regulation and antioxidant defense systems. *Biotechnol. Stud.* 30, 22–32. doi: 10.38042/biotechstudies.932376

Kuşvuran, S., Dasgan, H. Y., and Abak, K. (2013). Citrulline is an important biochemical indicator in tolerance to saline and drought stresses in melon. *Sci. World J.* 2013, 253414. doi: 10.1155/2013/253414

Laffray, D., and Louguet, P. (1990). Stomatal response and drought resistance. *Bull. la Société botanique france. Actualités Botaniques* 137, 47–60. doi: 10.1080/01811789.1990.10826986

Lay, F. T., and Anderson, M. A. (2005). Defensins- components of the innate immune systems in plants. *Curr. Protein Peptides Sci.* 6, 85–101. doi: 10.2174/1389203053027575

Lazzarotto, F., Teixeira, F. K., Rosa, S. B., Dunand, C., Fernandes, C. L., de Vasconcelos Fontenele, A., et al. (2011). Ascorbate peroxidase-related (APx-r) is a new heme-containing protein functionally associated with ascorbate peroxidase but evolutionarily divergent. *New Phytol.* 191, 234–250. doi: 10.1111/j.1469-8137.2011.03659.x

Lee, S. C., Lee, W. K., Ali, A., Kumar, M., Yang, T. J., and Song, K. (2017). Genome-wide identification of the dehydrin genes in the cucurbitaceae species. *Plant Breed. Biotechnol.* 5, 282–292. doi: 10.9787/PBB.2017.5.4.282

Lee, H. G., and Seo, P. J. (2019). MYB96 recruits the HDA15 protein to suppress negative regulators of ABA signaling in arabidopsis. *Nat. Commun.* 10, 1713. doi: 10.1038/s41467-019-09417-1

Li, J., Han, Y., Liu, L., Chen, Y., Du, Y., Zhang, J., et al. (2015). Qrt9, a quantitative trait locus controlling root thickness and root length in upland rice. *J. Exp. Bot.* 66, 2723–2732. doi: 10.1093/jxb/erv076

Li, Q., Li, P., Sun, L., Wang, Y., Ji, K., Sun, Y., et al. (2012). Expression analysis of β-glucosidase genes that regulate abscisic acid homeostasis during watermelon (Citrullus lanatus) development and under stress conditions. *J. Plant Physiol.* 169, 78–85. doi: 10.1016/j.jplph.2011.08.005

Li, H. B., Ma, Q. H., Li, H. G., Zhang, F. S., Rengel, Z., and Shen, J. B. (2014). Root morphological responses to localized nutrient supply differ among crop species with contrasting root traits. *Plant Soil* 376, 151–163. doi: 10.1007/s11104-013-1965-9

Li, J., Li, Y., Yin, Z., Jiang, J., Zhang, M., Guo, X., et al. (2017). OsASR5 enhances drought tolerance through a stomatal closure pathway associated with ABA and H2 O2 signalling in rice. *Plant Biotechnol J.* 15, 183–196. doi: 10.1111/pbi.12601

Li, H., Mo, Y., Cui, Q., Yang, X., Guo, Y., Wei, C., et al. (2018). Transcriptomic and physiological analyses reveal drought adaptation strategies in drought-tolerant and -susceptible watermelon genotypes. *Plant Sci.* 18, 30747–30747. doi: 10.1016/j.plantsci.2018.10.016

Lin, K. H., and Pu, S. F. (2010). Tissue and genotype specific ascorbate peroxidase expression in sweet potato in response to salt stress. *Biol Plantarum* 54, 664–670.

Liu, K., and Huang, Y. (2009). RanGTPase: A key regulator of nucleo-cytoplasmic trafficking. *Mol. Cell Pharamacol.* 1, 148–156. doi: 10.4255/mcpharmacol.09.19

Liu, S., Liu, S., Wang, M., Meng, C., Wang, M., and Xia, G. (2014). A wheat SIMILAR TO RCD-ONE gene enhances seedling growth and abiotic stress resistance by modulating redox homeostasis and maintaining genomic integrity. *Plant Cell* 26, 164–180. doi: 10.1105/tpc.113.118687

Liu, H., Shen, J., Yuan, C., Lu, D., Acharya, B. R., Wang, M., et al. (2021). The cyclophilin ROC3 regulates ABA-induced stomatal closure and the drought stress response of arabidopsis thaliana. *Front. Plant Sci.* 107, 713-736. doi: 10.3389/fpls.2021.668792

Liu, Y., Wu, H., Kou, L., Liu, X., Zhang, J., Guo, Y., et al. (2014). Two metallothionein genes in oxya chinensis: Molecular characteristics, expression patterns and roles in heavy metal stress. *PloS One* 9, e112759. doi: 10.1371/journal.pone.0112759

Li, H., Xu, G., Yang, C., Yang, L., and Liang, Z. (2019). Genome-wide identification and expression analysis of HKT transcription factor under salt stress in nine plant species. *Ecotoxicol. Environ. Saf.* 171, 435–442. doi: 10.1016/j.ecoenv.2019.01.008

Lopez-Zaplana, A., Martinez-Garcia, N., Carvajal, M., and Bárzana, G. (2022). Relationships between aquaporins gene expression and nutrient concentrations in melon plants (Cucumis melo l.) during typical abiotic stresses. *Environ. Exp. Bot.* 195, 104759. doi: 10.1016/j.envexpbot.2021.104759

Luo, M., Gu, S. H., Zhao, S. H., Zhang, F., and Wu, N. H. (2006). Rice GTPase OsRacB: potential accessory factor in plant salt-stress signaling. *Acta Biochim. Biophys. Sin.* 38, 393–402. doi: 10.1111/j.1745-7270.2006.00172.x

Lu, C., and Zhang, J. (2000). Role of light in theresponse of PSII photochemistry to salt stress inthe cyanobacterium spirulina platensis. *J. Exp. Bot.* 51, 911–917. doi: 10.1093/jxb/51.346.911

Lu, C., Qiu, N., Wang, B., and Zhang, J. (2003). Salinity treatment shows no effects on photosystem II photochemistry, but increases the resistance of photosystem II to heat stress in halophyte Suaeda salsa. *J. Exp. Bot.* 54, 851–860. doi: 10.1093/jxb/erg080

Lynch, J. P. (2007). Roots of the second green revolution. *Aust. J. Bot.* 55, 493–512. doi: 10.1071/BT06118

Malambane, G. (2018a). *Research on drought physiology, molecular responses, and development of biotechnology tools for the drought-tolerant wild watermelon (Citrullus lanatus acc.101117-1)* (Tottori University, Japan: PhD Thesis).

Malambane, G., Batlang, U., Ramolekwa, K., Tsujimoto, H., and Akashi, K. (2021). Growth chamber and field evaluation of physiological factors of two watermelon genotypes. *Plant Stress* 2, 100017. doi: 10.1016/j.stress.2021.100017

Malambane, G., Tsujimoto, H., and Akashi, K. (2018b). The cDNA structures and expression profile of the ascorbate peroxidase family during drought stress in wild watermelon. *J. Agric. Sci.* 8, 56–72. doi: 10.5539/jas.v10n8p56

Malamy, J. C. (2005). Intrinsic and environmental response pathways that regulate root system architecture. *Plant Cell Environ.* 28, 67–77. doi: 10.1111/j.1365-3040.2005.01306.x

Mansfield, T. J., and Atkinson, C. J. (1990). "Stomatal behaviour in water stressed plants," in *Stress responses in plants: Adaptation and acclimation mechanisms*. Eds. R. G. Alscher and J. R. Cumming (New York: Wiley-Liss), 241–264.

Mao, P., Zhang, Y., Cao, B., Guo, L., Shao, H., Cao, Z., et al. (2016). Effects of salt stress on eco-physiological characteristics in robinia pseudoacacia based on salt-soil rhizosphere. *Sci. Total Environ.* 568, 118–123. doi: 10.1016/j.scitotenv.2016.06.012

Margoshes, M., and Vallee, B. L. (1957). A cadminium protein from equine kidney cortex. *J. Am. Chemist Soc.* 79, 4813–4814. doi: 10.1021/ja01574a064

Murkhart, A. H. (1985). Comparative water relations of phaseolus vulgaris l. and phaseolus acutinifolius Gray. *Plant Physiol.* 77, 113–117. doi: 10.1104/pp.77.1.113

Martin-StPaul, N., Delzon, S., and Cochard, H. (2017). Plant resistance to drought depend on the timely stomatal closure. *Ecol. Lett.* 20, 1437–1442. doi: 10.1111/ele.12851

Massange-Sánchez, J. A., Palmeros-Suárez, P. A., Espitia-Rangel, E., Rodríguez-Arévalo, I., Sánchez-Segura, L., Martínez-Gallardo, N. A., et al. (2016). Overexpression of grain amaranth (Amaranthus hypochondriacus) AhERF or AhDOF transcription factors in arabidopsis thaliana increases water deficit- and salt-stress tolerance, respectively, via contrasting stress amelioration mechanisms. *PloS One* 11, 164280. doi: 10.1371/journal.pone.0164280

Maxwell, K., and Johnson, G. N. (2000). Chlorophyll fluorescence - a practical guide. *J. Exp. Bot.* 51, 659–668. doi: 10.1093/jexbot/51.345.659

McLachlan, D. H., Pridgeon, A. J., and Hetherington, A. M. (2018). How arabidopsis talks to itself about its water supply. *Mol. Cell* 70, 991–992. doi: 10.1016/j.molcel.2018.06.011

Mekawy, A. A.M., Assaha, D. V.M., Munehiro, R., Kohnishi, E., Nagaoka, T., Ueda, A., et al. (2018). Characterization of type 3 metallothionein-like gene (OsMT-3a) from rice, revealed its ability to confer tolerance to salinity and heavy metal stresses. *Environmental and Experimental Botany* 147, 157–166. doi: 10.1016/j.envexpbot.2017.12.002

Menezes-Benavente, L., Kernodle, S. P., Margis-Pinheiro, M., and Scandalios, J. G. (2004). Salt-induced antioxidant metabolism defenses in maize (Zea mays L.) seedlings. *Redox Rep*. 9, 29–36. doi: 10.1179/135100004225003888

Michaletti, A., Naghavi, M. R., Toorchi, M., Zolla, L., and Rinalducci, S. (2018). Metabolomics and proteomics reveal drought-stress responses of leaf tissues from spring-wheat. *Sci. Rep.* 8, 5710. doi: 10.1038/s41598-018-24012-y

Mishra, D., Shekhar, S., Singh, D., Chakraborty, S., and Chakraborty, N. (2018). "Heat shock proteins and abiotic stress tolerance in plants," in *Regulation of heat shock protein responses. heat shock proteins*, vol. 13 . Eds. A. Asea and P. Kaur (Cham: Springer).

Miyake, C., and Asada, K. (1996). Inactivation mechanism of ascorbate peroxidase at low concentrations of ascorbate; hydrogen peroxide decomposes compound I of ascorbate peroxidase. *Plant Cell Physiol.* 37, 423–430. doi: 10.1093/oxfordjournals.pcp.a028963

Modarelli, G. C., Rouphael, Y., De Pascale, S., Öztekin, G. B., Tüzel, Y., Orsini, F., et al. (2020). Appraisal of salt tolerance under greenhouse conditions of a cucurbitaceae genetic repository of potential rootstocks and scions. *Agronomy* 10, 967. doi: 10.3390/agronomy10070967

Mo, Y., Yang, R., Liu, L., Gu, X., Yang, X., Wang, Y., et al. (2015). Growth, photosynthesis and adaptive responses of wild and domesticated watermelon genotypes to drought stress and subsequent re-watering. *Plant Growth Regulators* 79, 229–241. doi: 10.1007/s10725-015-0128-9

Mtumtum, N. P. (2012). *Performance of wild watermelon (Citrullus lanatus l.) in response to population density and mulch* (University of Kwazulu-Natal, Pietermaritzburg, RSA: MSc Thesis, School of Agricultural, Earth and Environmental Sciences).

Munns, R., and Tester, M. (2008). Mechanisms of salinity tolerance. *The Annual of Plant Biology*. 59, 651–681. doi: 10.1146/annurev.arplant.59.032607.092911

Nakaminami, K., Okamoto, K., Higuchi-Takeuchi, M., Yoshizumi, T., Yamaguchi, Y., Fukao, Y., et al. (2018). AtPep3 is a hormone-like peptide that plays a role in the salinity stress tolerance of plants. *Proc. Natl. Acad. Sci.* 115, 5810–5815. doi: 10.1073/pnas.1719491115

Nanasato, Y., Akashi, K., and Yokota, A. (2015). Co-Expression of cytochrome b561 and ascorbate oxidase in leaves of wild watermelon under drought and high light conditions. *Plant Cell Physiol.* 46, 1515–1524. doi: 10.1093/pcp/pci164

Nanasato, Y., Miyake, C., Takahara, K., Kohzuma, K., Munekage, Y. N., Yokota, A., et al. (2010). "Mechanisms of drought and high light stress tolerance studied in a xerophyte, citrullus lanatus (wild watermelon)," in *The chloroplast. advances in photosynthesis and respiration (Vol. 31). basics and applications*. Ed. C. A. Rebeiz, et al (Dordrecht, Netherlands: Springer), 363–377.

Negi, S., Tak, H., and Ganapathi, T. R. (2018). A banana NAC transcription factor (MusaSNAC1) impart drought tolerance by modulating stomatal closure and H2O2 content. *Plant Mol. Biol.* 96, 457–471. doi: 10.1007/s11103-018-0710-4

Neto, A. A., Prisco, J. T., Eneas-Filho, J., Feitosa de Lacerda, C., and Silva, J. V. (2004). Effects of salt stress onplant growth, stomatal response and solute accumulation on different maize genotpes. *Brazillian J. Plant Physiol.* 16, 31–38. doi: 10.1590/S1677-04202004000100005

Nguyen, N. H., and Cheong, J. (2018). H2A.Z-containing nucleosomes are evicted to activate AtMYB44 transcription in response to salt stress. *Biochem. Biophys. Res. Commun.* 499, 1039–1043. doi: 10.1016/j.bbrc.2018.04.048

Niinemets, Ü. (2015). Uncovering the hidden facets of drought stress: secondary metabolites make the difference. *Tree Physiol.* 36, 129–132. doi: 10.1093/treephys/tpv128

Nilsson, J., Weis, K., and Kjems, J. J. (2002). The c-terminal extension of the small GTPase ran is essential for defining the GDP-bound form. *Mol. Biol.* 318, 583–593. doi: 10.1016/S0022-2836(02)00040-2

Niones, J. M., Inukai, Y., Suralta, R. R., and Yamauchi, A. (2015). QTL associated with lateral root plasticity in response to soil moisture fluctuation stress in rice. *Plant Soil* 391, 63–75. doi: 10.1007/s11104-015-2404-x

Niu, X., Luo, T., Zhao, H., Su, Y., Ji, W., and Li, H. (2020). Identification of wheat DREB genes and functional characterization of TaDREB3 in response to abiotic stresses. *Gene* 740, 144514. doi: 10.1016/j.gene.2020.144514

Nzengue, Y., Steiman, R., Rachidi, W., Favier, A., and Guiraud, P. (2012). Oxidative stress induced by cadimium in the C6 cell line: role of copper and zinc. *Biol. Trace Elements Res.* 146, 410–419. doi: 10.1007/s12011-011-9265-9

Oh, J. E., Kwon, Y., Kim, J. H., Noh, H., Hong, S. W., and Lee, H. (2011). A dual role for MYB60 in stomatal regulation and root growth of arabidopsis thaliana under drought stress. *Plant Mol. Biol.* 77, 91–103. doi: 10.1007/s11103-011-9796-7

Olejnik, P., Mądrzak, C. J., and Nuc, K. (2021). Cyclophilins and their functions in abiotic stress and plant–microbe interactions. *Biomolecules* 11, 1390. doi: 10.3390/biom11091390

Orzechowska, A., Trtílek, M., Tokarz, K. M., Szymańska, R., Niewiadomska, E., Rozpądek, P., et al. (2021). Thermal analysis of stomatal response under salinity and high light. *Int. J. Mol. Sci.* 22, 4663. doi: 10.3390/ijms22094663

Pandey, S., Fartyal, D., Agarwal, A., Shukla, T., James, D., Kaul, T., et al. (2017). Abiotic Stress Tolerance in Plants: Myriad Roles of Ascorbate Peroxidase. *Front. Plant Sci.* 8, 581. doi: 10.3389/fpls.2017.00581

Park, S. I., Kim, J. J., Shin, S. Y., Kim, Y. S., and Yoon, H. S. (2020). ASR enhances environmental stress tolerance and improves grain yield by modulating stomatal closure in rice. *Front. Plant Sci.* 10, 1752. doi: 10.3389/fpls.2019.01752

Patankar, H. V., Al-Harrasi, I., Al Kharusi, L., Jana, G. A., Al-Yahyai, R., Sunkar, R., et al. (2019). Overexpression of a metallothionein 2A gene from date palm confers abiotic stress tolerance to yeast and arabidopsis thaliana. *Int. J. Mol. Sci.* 20, 2871. doi: 10.3390/ijms20122871

Percival, G. C. (2005). The use of chlorophyll fluorescence to identify chemical and environmental stress in leaf tissue of three oak (Quercus) species. *J. Arboric* 31, 215–227. doi: 10.48044/jauf.2005.028

Percival, G. C., and Sheriffs, C. N. (2002). Identification of drought-tolerant woody perennials using chlorophyll fluorescence. *J. Arboric* 28, 215–223.

Pirasteh-Anosheh, H., Saed-Moucheshi, A., Pakniyat, H., and Pessarakli, M. (2016). "Stomatal responses to drought stress," in *Water stress and crop plants: a sustainable approach* (Chichester: Wiley).

Priya, M., Dhanker, O. P., Siddique, K. H. M., HanumanthaRao, B., Nair, R. M., Pandey, S., et al. (2019). Drought and heat stress-related proteins: an update about their functional relevance in imparting stress tolerance in agricultural crops. *Theor. Appl. Genet.* 132, 1607–1638. doi: 10.1007/s00122-019-03331-2

Qu, X., Cao, B., Kang, J., Wang, X., Han, X., Jiang, W., et al. (2019). Fine-tuning stomatal movement through small signaling peptides. *Front. Plant Sci.* 10, 69. doi: 10.3389/fpls.2019.00069

Ram, C., Danish, S., Kesawat, M. S., Panwar, B. S., Verma, M., Arya, L., et al. (2022). Genome-wide comprehensive characterization and expression analysis of TLP gene family revealed its responses to hormonal and abiotic stresses in watermelon (Citrullus lanatus). *Gene* 844, 146818. doi: 10.1016/j.gene.2022.146818

Raturi, G., Kumawat, S., Mandlik, R., Duhan, D., Thakral, V., Sudhakaran, S., et al (2022). Deciphering the role of aquaporins under different abiotic stress conditions in watermelon (Citrullus lanatus). *J. Plant Growth Regulation*. doi: 10.1007/s00344-022-10776-1

Rose, A., and Meier, I. (2001). A domain unique to plant RanGAP is responsible for its targeting to the plant nuclear rim. *PNAS* 98, 15377–15382. doi: 10.1073/pnas.261459698

Rosero, A., Granda, L., Berdugo-Cely, J. A., Šamajová, O., Šamaj, J., and Cerkal, R. (2020). A dual strategy of breeding for drought tolerance and introducing drought-tolerant, underutilized crops into production systems to enhance their resilience to water deficiency. *Plants (Basel)* 9, 1263. doi: 10.3390/plants9101263

Roy, R., Agrawal, V., and Gupta, S. C. (2009). Comparison of drought-induced polypeptides and ion leakage in three tomato cultivars. *Biol. Plantarum* 53, 685–690. doi: 10.1007/s10535-009-0123-y

Ruibal, C., Castro, A., Carballo, V., Szabados, L., and Vidal, S. (2013). Recovery from heat, salt and osmotic stress in Physcomitrella patens requires a functional small heat shock protein PpHsp16.4. *BMC Plant Biol* 13, 174. doi: 10.1186/1471-2229-13-174

Rush, M. G., Drivas, G., and D'Eustachio, P. (1996). The small nuclear GTPase ran: how much does it run? *Bioessays* 18, 103–112. doi: 10.1002/bies.950180206

Ruttkay-Nedecky, B., Nejdl, N., Gumulec, J., and Zitka, O. (2013). The role of metallothionein in oxidative stress. *Int. J. Mol. Sci.* 14, 6044–6066. doi: 10.3390/ijms14036044

Sade, N., and Moshelion, M. (2017). "Plant aquaporins and abiotic stress," in *Plant aquaporins. signaling and communication in plants*. Eds. F. Chaumont and S. Tyerman (Cham: Springer).

Sage, R. F., and McKown, A. D. (2006). Is C4 phoptosynthesis less phenotypically plastic than C3 photosynthesis? *J. Exp. Bot.* 57, 303–317. doi: 10.1093/jxb/erj040

Sanda, S., Yoshida, K., Kuwano, M., Kawamura, T., Nakajima, M., Akashi, K., et al. (2011). Responses of the photosynthetic electron transport system to excess light energy caused by water deficit in wild watermelon. *Physiol. Plant* 142, 247–264. doi: 10.1111/j.1399-3054.2011.01473.x

Scheffzek, K., Klebe, C., Fritz-Wolf, K., Kabsch, W., and Wittinghofer, A. (1995). Crystal structure of the nuclear ras-related protein ran in its GDP-bound form. *Nature* 374, 378–381. doi: 10.1038/374378a0

Schleiff, U., and Muscolo, A. (2011). Fresh look at plant salt tolerance as affected by dynamics at the soil/root-interface using leek and rape as model crops. *Eur. J. Plant Sci. Biotechnol.* 5, 27–32. doi: 10.13140/2.1.4383.4249

Seymen, M., Yavuz, D., Ercan, M., Akbulut, M., Çoklar, H., Kurtar, E. S., et al. (2021). Effect of wild watermelon rootstocks and water stress on chemical properties of watermelon fruit. *Horticulture Environment Biotechnol.* 62, 411–422. doi: 10.1007/S13580-020-00329-4

Shalata, A., Mittova, V., Volokita, M., Guy, M., and Tal, M. (2001). Response of the cultivated tomato and its wild salt-tolerant relative Lycopersicon pennellii to salt-dependent oxidative stress: The root antioxidative system. *Physiol Plant.* 112, 487–494. doi: 10.1034/j.1399-054.2001.1120405.x

Shao, H., Wang, H., and Tang, X. (2015). NAC transcription factors in plant multiple abiotic stress responses: progress and prospects. *Front. Plant Sci.* 6, 902. doi: 10.3389/fpls.2015.00902

Sheoran, S., Kaur, Y., Kumar, S., Shukla, S., Rakshit, S., and Kumar, R. (2022). Recent advances for drought stress tolerance in maize (Zea mays l.): Present status and future prospects. *Front. Plant Sci.* 13, 872566. doi: 10.3389/fpls.2022.872566

Shigeoka, S., Ishikawa, T., Tamoi, M., Miyagawa, Y., Takeda, T., Yabuta, Y., et al. (2002). Regulation and function of the ascorbate peroxidase isoenzymes. *J. Exp. Bot.* 53, 1305–1319. doi: 10.1093/jexbot/53.372.1305

Shikanai, T., Takeda, T., Yamauchi, H., Sano, S., Tomizawa, K., Yokota, A., et al. (1998). Inhibition of ascorbate peroxidase under oxidative stress in tobacco having bacterial catalase in chloroplasts. *FEBS Lett.* 428, 47–51. doi: 10.1016/S0014-5793(98)00483-9

Simeoni, F., Skirycz, A., Simoni, L., Castorina, G., Souza, L. P., Fernie, A. R., et al. (2022). The AtMYB60 transcription factor regulates stomatal opening by modulating oxylipin synthesis in guard cells. *Sci. Rep.* 12 (1), 533. doi: 10.1038/s41598-021-04433-y

Singh, B. K., Ramkumar, M. K., Dalal, M., Singh, A., Solanke, A. U., Singh, N. K., et al. (2021). Allele mining for a drought responsive gene DRO1determining root growth angle in donors of drought tolerance in rice (Oryza sativa l.). *Physiol. Mol. Biol. Plants* 27, 523–534. doi: 10.1007/s12298-021-00950-2

Singh, S. K., and Reddy, K. R. (2011). Regulation of photosynthesis, fluorescence, stomatal conductance and water-use efficiency of cowpea (Vigna unguiculata [L.] walp.) under drought. *J. Photochem. Photobiol.* 105, 40–50. doi: 10.1016/j.jphotobiol.2011.07.001

Si, Y., Zhang, C., Meng, S., and Dane, F. (2009). Gene expression changes in response to drought stress in citrullus colocynthis. *Plant Cell Rep.* 28, 997–1009. doi: 10.1007/s00299-009-0703-5

Sminorff, N. (1993). The role of active oxygen in the response of plants to water deficit and desiccation. *New Phytol* 125, 27–58. doi: 10.1111/j.1469-8137.1993.tb03863.x

Smith, B. (2006). *The farming book* (Pietermaritzburg: University of Kwazulu-Natal Press).

Smith, S., Zhu, S., Joos, L., Roberts, I., Nikonorova, N., Vu, L. D., et al. (2020). The CEP5 peptide promotes abiotic stress tolerance, as revealed by quantitative proteomics, and attenuates the AUX/IAA equilibrium in arabidopsis. *Mol. Cell Proteomics* 19, 1248–1262. doi: 10.1074/mcp.RA119.001826

Soda, N., Sharan, A., Gupta, B., Singla-Pareek, S. L., and Pareek, A. (2016). Evidence for nuclear interaction of a cytoskeleton protein (OsIFL) with metallothionein and its role in salinity stress tolerance. *Sci Rep* 6, 34762. doi: 10.1038/srep34762

Sofo, A., Scopa, A., Nuzzaci, M., and Vitti, A. (2015). Ascorbate Peroxidase and Catalase Activities and Their Genetic Regulation in Plants Subjected to Drought and Salinity Stresses. *Int J Mol Sci.* 16, 13561–13578. doi: 10.3390/ijms160613561

Song, X. F., Guo, P., Ren, S. C., Xu, T. T., and Liu, C. M. (2013). Antigonistic peptide technology for functional dissection of CLV3/ESR genes in arabidopsis. *Plant Cell Physiol.* 161, 1076–1085. doi: 10.1104/pp.112.211029

Song, Q., Joshi, M., DiPiazza, J., and Joshi, V. (2020). Functional relevance of citrulline in the vegetative tissues of watermelon during abiotic stresses. *Front. Plant Sci.* 11, 512. doi: 10.3389/fpls.2020.00512

Song, Q., Joshi, M., and Joshi, V. (2020). Transcriptomic analysis of short-term salt stress response in watermelon seedlings. *Int. J. Mol. Sci.* 21, 6036. doi: 10.3390/ijms21176036

Stepien, P., and Johnson, G. N. (2009). Contrasting responses of photosynthesis to salt stress in the glycophyte Arabidopsis and the halophyte thellungiella: role of the plastid terminal oxidase as an alternative electron sink. *Plant Physiol.* 149, 1154–65. doi: 10.1104/pp.108.132407

Sui, D., and Wang, B. (2020). Transcriptome analysis reveals complex defensive mechanisms in salt-tolerant and salt-sensetive shrub willow genotypes under salinity stress. *International journal of genomics*. 6870157. doi: 10.1155/2020/6870157

Sun, J., Cao, H., Cheng, J., He, X., Sohail, H., Niu, M., et al. (2018). Pumpkin CmHKT1;1 controls shoot na+ accumulation *via* limiting na+ transport from rootstock to scion in grafted cucumber. *Int. J. Mol. Sci.* 19, 2648. doi: 10.3390/ijms19092648

Sussmilch, F. C., Brodribb, T. J., and McAdam, S. A. M. (2017). Up-regulation of NCED3 and ABA biosynthesis occur within minutes of a decrease in leaf turgor but AHK1 is not required. *J. Exp. Bot.* 68, 2913–2918. doi: 10.1093/jxb/erx124

Takahashi, F., Kuromori, T., Urano, K., Yamaguchi-Shinozaki, K., and Shinozaki, K. (2020). Drought stress responses and resistance in plants: From cellular responses to long- distance intercellular communication. *Front. Plant Sci.* 11, 556972. doi: 10.3389/fpls.2020.556972

Takahashi, F., Suzuki, T., Osakabe, U., Betsuyaku, S., Kondo, Y., Dohmae, N., et al. (2018). A small peptide modulates stomatal control *via* abscisic acid in long-distance signaling. *Nature* 556, 235–238. doi: 10.1038/s41586-018-0009-2

Tan, C., Qiao, H., Ma, M., Wang, X., Tian, Y., Bai, S., et al. (2021). Genome-wide identification and characterization of melon bHLH transcription factors in regulation of fruit development. *Plants* 10, 2721. doi: 10.3390/plants10122721

Tátrai, Z. A., Sanoubar, R., Pluhár, Z., Mancarella, S., Orsini, F., and Gianquinto, G. (2016). Morphological and Physiological Plant Responses to Drought Stress in Thymus citriodorus. *International Journal of Agronomy* 2016, 4165750. doi: 10.1155/2016/4165750

Thao, N. P., Thu, N. B. A., Hoang, X. L. T., Ha, C. V., and Tran, L. S. P. (2013). Differential expression analysis of a subset of drought-responsive GmNAC genes in two soybean cultivars differing in drought tolerance. *Int. J. Mol. Sci.* 14, 23828–23841. doi: 10.3390/ijms141223828

Tian, F., Hu, X. L., Yao, T., Yang, X., Chen, J. G., Lu, M. Z., et al (2021). Recent Advances in the Roles of HSFs and HSPs in Heat Stress Response in Woody Plants. *Front. Plant Sci.* 12, 704905. doi: 10.3389/fpls.2021.704905

Tissue, D. T., Griffin, K. L., Turnbull, M. H., and Whitehead, D. (2005). Stomatal and non-stomatal limitations to photosynthesis in four tree species in a temperate rainforest dominated by dacrydium cupressinum in new Zealand. *Tree Physiol.* 25, 447–456. doi: 10.1093/treephys/25.4.447

Tiwari, P., and Chakrabarty, D. (2021). Dehydrin in the past four decades: From chaperones to transcription co-regulators in regulating abiotic stress response. *Curr. Res. Biotechnol.* 3, 249–259. doi: 10.1016/j.crbiot.2021.07.005

Tsuji, W., Ali, M., Inanaga, S., et al. (2013). Growth and gas exchange of three sorghum cultivars under drought stress. *Biol. Plantarum* 46, 583–587. doi: 10.1023/A:1024875814296

Uga, Y., Sugimoto, K., Ogawa, S., Rane, J., Ishitani, M., Hara, N., et al. (2013). Control of root system architecture by DEEPER ROOTING 1 increases rice yield under drought conditions. *Nat. Genet.* 45, 1097–1102. doi: 10.1038/ng.2725

Urbano-Gámez, J. A., El-Azaz, J., Ávila, C., de la Torre, F. N., and Cánovas, F. M. (2020). Enzymes involved in the biosynthesis of arginine from ornithine in maritime pine (Pinus pinaster ait.). *Plants (Basel)* 9, 1271. doi: 10.3390/plants9101271

Vandeleur, R. K., Mayo, G., Shelden, M. C., Gilliham, M., Kaiser, B. N., and Tyerman, S. D. (2009). The role of plasma membrane intrinsic protein aquaporins in water transport through roots: diurnal and drought stress responses reveal different strategies between isohydric and anisohydric cultivars of grapevine. *Plant Physiol.* 149, 445–460. doi: 10.1104/pp.108.128645

Vandeleur, R. K., Sullivan, W., Athman, A., Jordans, C., Gilliham, M., Kaiser, B. N., et al. (2014). Rapid shoot-to-root signalling regulates root hydraulic conductance *via* aquaporins. *Plant Cell Environ.* 37, 520–538. doi: 10.1111/pce.12175

Vera-Estrella, R. (2004). Novel regulation of aquaporins during osmotic stress. *Plant Physiol.* 135, 2318–2329. doi: 10.1104/pp.104.044891

Verslues, P. E., and Juenger, T. E. (2011). Drought, metabolites, and arabdopsis natural variaton: a promising combination for understanding adaptation to water-limited environments. *Curr. Opin. Plant Biol.* 14, 240–245. doi: 10.1016/j.pbi.2011.04.006

Walter, J., Nagy, L., Hein, R., Rasscher, U., Beikerkuhnlein, C., Willner, E., et al. (2011). Do plants remember drought? hints towards a drought-memory in grasses. *Environ. Exp. Bot.* 71, 34–40. doi: 10.1016/j.envexpbot.2010.10.020

Wang, A., Guo, J., Wang, S., Zhang, Y., Lu, F., Duan, J., et al. (2022). BoPEP4, a c-terminally encoded plant elicitor peptide from broccoli, plays a role in salinity stress tolerance. *Int. J. Mol. Sci.* 23, 3090. doi: 10.3390/ijms23063090

Wang, W., Liu, Z., Bao, L. J., Zhang, S. S., Zhang, C. G., Li, X., et al. (2017). The RopGEF2-ROP7/ROP2 pathway activated by phyB suppresses red light-induced stomatal opening. *Plant Physiol.* 174, 717–731. doi: 10.1104/pp.16.01727

Wang, X., Niu, Y., and Zheng, Y. (2021). Multiple functions of MYB transcription factors in abiotic stress responses. *Int. J. Mol. Sci.* 22, 6125. doi: 10.3390/ijms22116125

Wang, X., Xu, Y., Han, Y., Bao, S., Du, J., Yuan, M., et al. (2006). Overexpression of RAN1 in rice and arabidopsis alters primodial meristem, mitotics progress and sensitivity to auxin. *Plant Physiol.* 140, 91–101. doi: 10.1104/pp.105.071670

Wang, L. M., Zhang, L. D., Chen, J. B., Huang, D. F., and Zhang, Y. D. (2016). Physiological analysis and transcriptome comparison of two muskmelon (Cucumis melo l.) cultivars in response to salt stress. *Genet. Mol. Res.* 15, gmr.15038738.

Wang, D., Zhichen Cao, Z., Wang, W., Zhu, W., Xiaocong Hao, X., Fang, Z., et al. (2020). Genome-wide characterization of OFP family genes in wheat (Triticum aestivum l.) reveals that TaOPF29a-a promotes drought tolerance. *BioMed. Res. Int.* 2020, 9708324. doi: 10.1155/2020/9708324

Wan, Q., Luo, L., Zhang, X., Lv Y.m Zhu, S., Kong, L., Wan, Y., et al. (2021). Genome-wide identification and abiotic stress response pattern analysis of NF-y gene family in peanut (Arachis hypogaea l.). *Trop. Plant Biol.* 14, 329–344. doi: 10.1007/s12042-021-09295-2

Wang, Y., Wisniewski, M., Meilan, R., Cui, M., Webb, R., and Fuchigami, L. (2005). Overexpression of cytosolic ascorbate peroxidase in tomato (Lycopersicon esculentumin tomato (Lycopersicon esculentumin tomato (L.) confers tolerance to chilling and salt stress. *J.J.J ASHS* 130, 167–173.

Wasaya, A., Zhang, X., Fang, Q., and Yan, Z. (2018). Root phenotyping for drought tolerance: A review. *Agronomy* 8, 241. doi: 10.3390/agronomy8110241

Weisany, W., Sohrabi, Y., Heidari, G., Siosemardeh, A., and Ghassemi-Golezani, K. (2021). Changes in antioxidant enzymes activity and plant performance by salinity stress and zinc application in soybean (Glycine max L.). *Plant. Omics.* 5, 60–67.

Xu, P., and Cai, W. (2014). RAN1 is involved in plant cold resistance and development in rice (Oryza sativa). *J. Exp. Bot.* 65, 3277–3287. doi: 10.1093/jxb/eru178

Xu, Q., He, J., Dong, J., Hou, X., and Zhang, X. (2018). Genomic survey and expression profiling of the MYB gene family in watermelon. *Hortic. Plant J.* 4, 1–15. doi: 10.1016/j.hpj.2017.12.001

Xu, P., Zang, A., Chen, H., and Cai, W. (2016). The small G protein AtRAN1 regulates vegetative growth and stress tolerance in arabidopsis thaliana. *PloS One* 11, e0154787. doi: 10.1371/journal.pone.0154787

Yaginuma, H., Hirakawa, Y., kondo, Y., Ohashi-Ito, K., and Fukuda, H. (2011). A novel function of the TDIF-related peptides: promotion of axillary bud formation. *Plant Cell Physiol.* 52, 1354–1364. doi: 10.1093/pcp/pcr081

Yamori, W., Hikosaka, K., and Way, D. A. (2014). Temperature response of photosynthesis in C3, C4 and CAM plants: temperature acclimation and temperature adaptation. *Photosynthesis Res.* 119, 101–117. doi: 10.1007/s11120-013-9874-6

Yang, Z. (2002). Small GTPases: versatile signalling switches in plants. *Plant Cell* 14, S375–S388. doi: 10.1105/tpc.001065

Yang, H., Hu, J. X., Long, X. H., Liu, Z. P., and Rengel, Z. (2016). Salinity altered root distribution and increased diversity of bacterial communities in the rhizosphere soil of Jerusalem artichoke. *Sci. Rep.* 6, 20687. doi: 10.1038/srep20687

Yang, X., Li, H., Yang, Y., Wang, Y., Mo, Y., and Zhang, R. (2018). Identification and expression analyses of WRKY genes reveal their involvement in growth and abiotic stress response in watermelon (Citrullus lanatus). *PloS One* 13, e0191308. doi: 10.1371/journal.pone.0191308

Yang, Y., Mo, Y., Yang, X., Zhang, H., Wang, Y., Li, H., et al. (2016). Transcriptome profiling of watermelon root in response to short-term osmotic stress. *PloS One* 11 (11), e0166314. doi: 10.1371/journal.pone.0166314

Yang, Y., Wang, L., Tian, J., Li, J., Sun, J., He, L., et al. (2012). Proteomic study participating the enhancement of growth and salt tolerance of bottle gourd rootstock-grafted watermelon seedlings. *Plant Physiol. Biochem.* 58, 54–65. doi: 10.1016/j.plaphy.2012.05.026

Yang, S., Xu, K., Chen, S., Li, T., Xia, H., Chen, L., et al. (2019). A stress-responsive bZIP transcription factor OsbZIP62 improves drought and oxidative tolerance in rice. *BMC Plant Biol.* 19, 260. doi: 10.1186/s12870-019-1872-1

Yang, J., Zhu, J., and Yang, Y. (2017). Genome-wide identification and expression analysis of NF-y transcription factor families in watermelon (Citrullus lanatus). *J. Plant Growth Regulators* 36, 590–607. doi: 10.1007/s00344-017-9670-1

Yang, Y., Wang, B., Wang, J., He, C., Zhang, D., Li, P., et al. (2022). Transcription factors ZmNF-YA1 and ZmNF-YB16 regulate plant growth and drought tolerance in maize. *Plant Physiol.* 190, 1506–1525. doi: 10.1093/plphys/kiac340

Yan, Y., Wang, S., Wei, M., Gong, B., and Shi, Q. (2018). Effect of different rootstocks on the salt stress tolerance in watermelon seedlings. *Hortic. Plant J.* 4, 239–249. doi: 10.1016/j.hpj.2018.08.003

Yan, W., Zheng, S., Zhong, Y., and Shangguan, Z. (2017). Contrasting dynamics of leaf potential and gas exchange during progressive drought cycles and recovery in amorpha fruticosa and robinia pseudoacacia. *Sci. Rep.* 7, 4470. doi: 10.1038/s41598-017-04760-z

Yildiz, M., Poyraz, İ., Çavdar, A., Özgen, Y., and Beyaz, R. (2020). Plant Responses to Salt Stress. In (Ed.), *Plant Breeding - Current and Future Views*. IntechOpen. doi: 10.5772/intechopen.93920

Yokota, A., Kawasaki, S., Iwano, M., Nakamura, C., Miyake, C., and Akashi, K. (2002). Citrulline and DRIP-1 protein (ArgE homologue) in drought tolerance of wild watermelon. *Ann. Bot.* 89, 825–832. doi: 10.1093/aob/mcf074

Yoshimura, K., Ishikawa, T., Nakamura, Y., Tamoi, M., Takeda, T., Tada, T., et al. (1998). Comparative study on recombinant chloroplastic and cytosolic ascorbate peroxidase isozymes of spinach. *Arch. Biochem. Biophys.* 353, 55–63. doi: 10.1006/abbi.1997.0612

Yoshimura, K., Masuda, A., Kuwano, M., Yokota, A., and Akashi, K. (2008). Programmed proteome response for drought avoidance/tolerance in the root of a C3 xerophyte (wild watermelon) under water deficits. *Plant Cell Physiol.* 49, 226–241. doi: 10.1093/pcp/pcm180

Yuan, G., Liu, J., An, G., Li, W., Si, W., Sun, D., et al. (2022a). Genome-wide identification and characterization of the trehalose-6-Phosphate synthetase (TPS) gene family in watermelon (Citrullus lanatus) and their transcriptional responses to salt stress. *Int. J. Mol. Sci.* 23, 276. doi: 10.3390/ijms23010276

Yuan, G., Sun, D., An, G., Li, W., Si, W., Liu, J., et al. (2022b). Transcriptomic and metabolomic analysis of the effects of exogenous trehalose on salt tolerance in watermelon (Citrullus lanatus). *Cells* 11, 2338. doi: 10.3390/cells11152338

Yu, C., Yan, M., Dong, H., Luo, J., Ke, Y., Guo, A., et al. (2021). Maize bHLH55 functions positively in salt tolerance through modulation of AsA biosynthesis by directly regulating GDP-mannose pathway genes. *Plant Sci.* 302, 110676. doi: 10.1016/j.plantsci.2020.110676

Zakhidov, E., Nematov, S., and Kuvondikov, V. (2016). "Monitoring of the drought tolerance of various cotton genotypes using chlorophyll fluorescence," in *Applied photosynthesis*. Ed. M. M Najafpour. London: IntechOpen Limited.

Zarei, S., Ehsanpour, A. A., and Abbaspour, J. (2012). The role of over-expression of P5CS gene on proline, catalase, ascorbate peroxidase activity and lipid peroxidation of transgenic tobacco (Nicotiana tabacum l.) plant under *in vitro* drought stress. *J. Cell. Mol. Res.* 4, 43–49. doi: 10.22067/jcmr.v4i1.18249

Zhang, X., Chen, L., Shi, Q., and Ren, Z. (2020). SlMYB102, an R2R3-type MYB gene, confers salt tolerance in transgenic tomato. *Plant Sci.* 291, 110356. doi: 10.1016/j.plantsci.2019.110356

Zhang, X., Liu, S., and Takano, T. (2008). Overexpression of a mitochondrial ATP synthase small subunit gene (AtMtATP6) confers tolerance to several abiotic stresses in saccharomyces cerevisiae and arabidopsis thaliana. *Biotechnol. Lett.* 30, 1289–1294. doi: 10.1007/s10529-008-9685-6

Zhang, L., Shi, X., Zhang, Y., Wang, J., Yang, J., Ishida, T., et al. (2019). CLE9 peptide-induced stomatal closure is mediated by abscisic acid, hydrogen peroxide, and nitric oxide in arabidopsis thaliana. *Plant Cell Environ.* 42, 1033–1044. doi: 10.1111/pce.13475

Zhang, G., Zhang, M., Zhao, Z., Ren, Y., Li, Q., and Wang, W. (2017b). Wheat TaPUB1 modulates plant drought stress resistance by improving antioxidant capability. *Sci. Rep.* 7, 7549. doi: 10.1038/s41598-017-08181-w

Zhang, H., Zhao, Y., and Zhou, D. X. (2017a). Rice NAD+-dependent histone deacetylase OsSRT1 represses glycolysis and regulates the moonlighting function of

GAPDH as a transcriptional activator of glycolytic genes. *Nucleic Acids Res.* 45, 12241–12255. doi: 10.1093/nar/gkx825

Zhao, P., Hou, S., Guo, X., Jia, J., Yang, W., Liu, Z., et al. (2019). A MYB-related transcription factor from sheepgrass, LcMYB2, promotes seed germination and root growth under drought stress. *BMC Plant Biol.* 19, 564. doi: 10.1186/s12870-019-2159-2

Zhao, H., Liang, H., Chu, Y., Sun, C., Wei, N., Yang, M., et al. (2019). Effects of salt stress on chlorophyll fluorescence and the antioxidant system in gimkgo biloba l. *Seedlings. Hortic. Sci.* 54, 2125–2133. doi: 10.21273/HORTSCI14432-19

Zhou, H., Xiao, F., Zheng, Y., Liu, G., Zhuang, Y., Wang, Z., et al. (2022). PAMP-INDUCED SECRETED PEPTIDE 3 modulates salt tolerance through RECEPTOR-LIKE KINASE 7 in plants. *Plant Cell* 34, 927–944. doi: 10.1093/plcell/koab292

Zhu, J., Ingram, P. A., Benfey, P. N., and Elich, T. (2011). From lab to field, new approaches to phenotyping root system architecture. *Curr. Opin. Plant Biol.* 14, 310–317. doi: 10.1016/j.pbi.2011.03.020

Zhu, Y., Yuan, G., Gao, B., An, G., Li, W., Si, W., et al. (2022). Comparative transcriptome profiling provides insights into plant salt tolerance in watermelon (Citrullus lanatus). *Life* 12, 1033. doi: 10.3390/life12071033

Zhu, H., Zhao, S., Lu, X., He, N., Gao, L., Dou, J., et al. (2018). Genome duplication improves the resistance of watermelon root to salt stress. *Plant Physiol. Biochem.* 133, 11–21. doi: 10.1016/j.plaphy.2018.10.019

Zivcak, M., Kalaji, H. M., Shao, H. B., Olsovska, K., and Brestic, M. (2014). Photosynthetic proton and electron transport in wheat leaves under prolonged moderate drought stress. *J. Photochem. Photobiol.* 137, 107–115. doi: 10.1016/j.jphotobiol.2014.01.007

Zulu, N. S., and Modi, A. T. (2010). A preliminary study to determine water stress tolerance in wild melon (Citrulus lanatus l.). *South Afr. J. Plant Soil* 27, 334–336. doi: 10.1080/02571862.2010.10640004

Zou, J., Liu, C., Liu, A., Zou, D., and Chen, X. (2021). Overexpression of OsHsp17.0 and OsHsp23.7 enhances drought and salt tolerance in rice. *J Plant Physiol.* 2169, 628–35. doi: 10.1016/j.jplph.2011.12.014

frontiers | Frontiers in Plant Science

TYPE Original Research
PUBLISHED 14 February 2023
DOI 10.3389/fpls.2023.1118011

Check for updates

OPEN ACCESS

EDITED BY
PingWu Liu,
Hainan University, China

REVIEWED BY
Rehana Sardar,
University of the Punjab, Pakistan
Samar Gamal Thabet,
Fayoum University, Egypt

*CORRESPONDENCE
Chunlai Zhang
chunlaiz@hotmail.com

SPECIALTY SECTION
This article was submitted to Plant Abiotic Stress, a section of the journal Frontiers in Plant Science

RECEIVED 07 December 2022
ACCEPTED 06 January 2023
PUBLISHED 14 February 2023

CITATION
Zou C, Guo Z, Zhao S, Chen J, Zhang C and Han H (2023) Genome-wide analysis of long non-coding RNAs in sugar beet (*Beta vulgaris* L.) under drought stress. *Front. Plant Sci.* 14:1118011. doi: 10.3389/fpls.2023.1118011

COPYRIGHT
© 2023 Zou, Guo, Zhao, Chen, Zhang and Han. This is an open-access article distributed under the terms of the Creative Commons Attribution License (CC BY). The use, distribution or reproduction in other forums is permitted, provided the original author(s) and the copyright owner(s) are credited and that the original publication in this journal is cited, in accordance with accepted academic practice. No use, distribution or reproduction is permitted which does not comply with these terms.

Genome-wide analysis of long non-coding RNAs in sugar beet (*Beta vulgaris* L.) under drought stress

Chunlei Zou, Zhiqiang Guo, Shanshan Zhao, Jishuai Chen, Chunlai Zhang* and Haoran Han

College of Agriculture, Shanxi Agricultural University, Taigu, China

Drought stress is one of the most severe abiotic stresses that restrict global crop production. Long non-coding RNAs (lncRNAs) have been proved to play a key role in response to drought stress. However, genome-wide identification and characterization of drought-responsive lncRNAs in sugar beet is still lacking. Thus, the present study focused on analyzing lncRNAs in sugar beet under drought stress. We identified 32017 reliable lncRNAs in sugar beet by strand-specific high-throughput sequencing. A total of 386 differentially expressed lncRNAs (DElncRNAs) were found under drought stress. The most significantly upregulated and downregulated lncRNAs were TCONS_00055787 (upregulated by more than 6000 fold) and TCONS_00038334 (downregulated by more than 18000 fold), respectively. Quantitative real-time PCR results exhibited a high concordance with RNA sequencing data, which conformed that the expression patterns of lncRNAs based on RNA sequencing were highly reliable. In addition, we predicted 2353 and 9041 transcripts that were estimated to be the cis- and trans-target genes of the drought-responsive lncRNAs. As revealed by Gene Ontology (GO) and Kyoto Encyclopedia of Genes and Genomes (KEGG) analysis, the target genes of DElncRNAs were significantly enriched in organelle subcompartment, thylakoid, endopeptidase activity, catalytic activity, developmental process, lipid metabolic process, RNA polymerase activity, transferase activity, flavonoid biosynthesis and several other terms associated with abiotic stress tolerance. Moreover, 42 DElncRNAs were predicted as potential miRNA target mimics. LncRNAs have important effects on plant adaptation to drought conditions through the interaction with protein-encoding genes. The present study leads to greater insights into lncRNA biology and offers candidate regulators for improving the drought tolerance of sugar beet cultivars at the genetic level.

KEYWORDS

drought, *Beta vulgaris* L., long non-coding RNA, target gene, flavonoid biosynthesis, target mimic

Introduction

Drought is a most common abiotic stress restricting crop yield and quality in the world. Due to global climate change caused by the greenhouse effect, both the frequency and magnitude of drought are increasing (Naz et al., 2022). Drought stress can induce adverse reactions in plants, such as osmotic imbalance, membrane system damage, and reductions in respiration and the photosynthetic rate, which not only hinder the growth and metabolism of plants at all stages but also reduce the quality and yield of crop (Liu et al., 2020). Drought response in plants is complicated and may occur at the cellular, molecular and physiological levels (Giordano et al., 2016). Similar to other abiotic stress responses, drought response is related to multi-gene interactions within diverse pathways. During drought stress, several regulatory and functional genes undergo differential expression (referred to as differentially expressed genes (DEGs)) in plants, thereby forming complex signaling networks and affecting various biochemical and physiological responses (Wang et al., 2021). For instance, water deficiency can limit plant photosynthetic functions because of decreased leaf expansion, photosynthetic impairment, and decreased Calvin cycle enzyme activities, including phosphoenolpyruvate and Rubisco carboxylase (Bota et al., 2004). Under normal environmental conditions, the production and elimination of reactive oxygen species (ROS) in plant cells are in a dynamic balance. When plants are stimulated by drought stress, this balance is destroyed, resulting in a significant increase of ROS. ROS can target several organelles, like chloroplasts, peroxisomes, and mitochondria. This may result in cell membrane instability, senescence, or plant death (Ma et al., 2013). Hormonal modulation also represents a critical factor that induces water deficiency resistance in plants (Merlaen et al., 2020). Therefore, plants can achieve drought adaption by modulate several pathways, among which noncoding RNAs play essential roles (Chen et al., 2021b).

Noncoding RNAs (ncRNAs) are a class of RNA molecules that do not encode proteins and have catalytic activity, and are widely present in various organisms. Based on structure, ncRNAs can be divided into linear ncRNAs (linear-ncRNAs) and circular ncRNAs (circRNAs). Linear ncRNAs include microRNAs (miRNAs) and long noncoding RNAs (lncRNAs) (Mattick, 2009). LncRNA is a type of ncRNA that is over 200 bp long and plays widespread roles in virtually every plant biological processes (Wang et al., 2018). RNA-sequencing (RNA-seq) is an important approach in transcriptome research, which has helped to identify lncRNAs in several crops and model plants, like *Arabidopsis* (Severing et al., 2018), wheat (Lu et al., 2020), rice (Huang et al., 2021) and *Medicago truncatula* (Pecrix et al., 2018). Particularly, numerous stress-responsive lncRNAs have been identified in rice. They have been suggested to regulate anti-pathogen immunity (Ming et al., 2017) and responses to abiotic stresses like drought (Li et al., 2019a), salinity (Khemka and Singh, 2017), nutrient deficiency (Shin et al., 2018), and heavy metal resistance (Tang et al., 2019).

Numerous lncRNAs acting as endogenous miRNA target mimics (eTMs) have been detected in plants. Typically, lnc_253 and lnc_973 are the possible eTMs for miR156e in cotton under salt stress (Deng et al., 2018). Besides, lncRNA23468 plays the role of ceRNA in tomatoes for regulating NBSLRR genes through the decoy of miR482b with *Phytophthora infestans* (Jiang et al., 2019). LncRNA_1231 is responsible for sequestering miR156b in the flowering period of pigeon pea in a target-mimicry manner, thereby inducing flower-specific SPL-12 transcription factor (TF) up-regulation and modulating flower growth (Das et al., 2020). LncRNA39026 is an eTM for miR168a, which decoys miRNAs for increasing SlAGO1 expression, thereby promoting *Phytophthora infestans* tolerance (Cui et al., 2020). In Cassava, linRNA159 and linRNA340 are the target mimics for miR164 and miR169, respectively, under cold stress (Li et al., 2017). LncRNAs can competitively bind to miR398 while regulating CSD1 expression in winter wheat, thus, improving cold tolerance (Lu et al., 2020). Nonetheless, a few lncRNAs have been characterized experimentally and functionally so far.

Sugar beet (*Beta vulgaris* L.) is an important industrial crop that greatly contributes to the global sugar supply. Sugar beet can acclimate to various abiotic stresses, like salinity, drought, heat, or cold (Zou et al., 2021; Taleghani et al., 2022). In sugar beet, drought acclimation makes it possible to develop drought resistance *via* biochemical/physiological changes (Li et al., 2019b; Alkahtani et al., 2021). Drought response in sugar beet is potentially associated with the expression of protein-coding genes including *BvHb2* (Gisbert et al., 2020). Nonetheless, the roles of lncRNAs in drought-challenged sugar beet remains largely unclear. Therefore, this study aims to explore the role of lncRNAs in sugar beet drought resistance and identify drought-responsive lncRNAs. Therefore, we analyzed lncRNAs from sugar beet leaves under drought condition using high-throughput sequencing technology and bioinformatic approaches. Then the lncRNAs-miRNAs-mRNAs regulatory network related to drought stress response of sugar beet were screened, and quantitative real-time PCR was performed to investigate the expression patterns of drought-related lncRNAs in sugar beet. The results of this study will provide a basis for the next step analysis of the regulatory functions of lncRNAs related to drought resistance in sugar beet.

Material and methods

Plant materials and treatments

Sugar beet seeds (KWS9147) were germinated within pots in a greenhouse at 25°C, 80% relative humidity, and 16 h/8 h (day/night) photoperiod. Pot soil was gained from farmland in Taigu, Shanxi. The soil characteristics were as follows: 69.8 mg/kg alkali-hydro nitrogen, 44.7 mg/kg available phosphorus, 244.8 mg/kg available potassium and 15.6 g/kg organic matter.

After emergence, all seedlings were watered to 70% of soil water holding capacity (SWHC) with daily watering, before being subjected to drought stress. At the stage of fully expanding four leaves, the sugar beet seedlings were divided into two groups: (1) well-watered (CK) and (2) drought stress (DR). For the seedlings in the CK group, soil moisture was maintained at 70% of SWHC. Whereas, seedlings in DR group were unwatered for 8 days down to 30% of SWHC, and markedly curled leaves were observed. Then the respective samples were harvested, leaf cuttings were obtained and immediately preserved in liquid nitrogen under -80°C. Ten plants were set in every replicate, and altogether three separate replicates were established.

Determination of soluble sugar content, peroxidase activity, and salicylic acid content

Leaf soluble sugar content and peroxidase (POD) activity of sugar beet were determined according to the reports of DuBois et al. (2002) and Patra and Mishra (1979), respectively. Salicylic acid (SA) content was measured by the method of Yalpani et al. (1993). Leaves of sugar beet were ground into a fine powder within liquid nitrogen, and approximately 0.50 g samples were collected for subsequent experiments. Methanol was utilized twice for SA extraction. The samples were centrifuged to collect the supernatant, which was divided into two equivalent portions. Thereafter, solvent evaporation till dryness was conducted with the nitrogen stream. One portion was added with 5% trichloroacetic acid (TCA) for SA extraction thrice in the ethyl acetate: cyclopentane: isopropanol (100:99:1, v/v/v). For determining SA, the other portion was added with β-glucosidase (40 U, SIGMA) contained within acetate buffer (0.1 M, pH 5.2), followed by 90-min incubation under 37°C. Later, 5% TCA was added, and SA extract was obtained according to the previous description. Following solvent evaporation, a mobile phase consisting of 0.5 mM EDTA and 0.2 M acetate buffer (pH 5.0) was introduced for dissolving the dry residue, followed by analysis through HPLC and fluorometry using the WATERS Company chromatograph (Milford, Ma, USA) with the 2475 Multi-λ Fluorescence Detector and 2699 Separation Module Alliance. Spherisorb ODS2 WATERS Company column (4.6 × 10 mm, 3 μm) was employed for chromatographic separation. The emission and excitation wavelengths were set at 405 and 295 nm, respectively.

RNA extraction

Total RNAs were collected from each sample using TRIzol reagent (Invitrogen, Carlsbad, CA, USA), followed by treatment with DNase I (Takara Bio, Dalian, China) to remove contaminating genomic DNA (gDNA). The DNase I-treated total RNA was then incubated with RNase R (3 U/μg, Epicentre, Madison, WI, USA) at 37°C for a 1-h period. Finally, Bioanalyzer 2100 system (Agilent Technologies, CA, USA) and RNA Nano 6000 Assay Kit were employed for assessing RNA quantity and purity. After passing the quality detection, RNAs were used to construct libraries.

Library construction and RNA sequencing

Total RNA (1 μg/sample) served as input material for preparing the lncRNA library. NEBNext®Multiplex Small RNA Library Prep Set for Illumina® (NEB, USA) was utilized for obtaining strand-specific libraries following specific protocols. Later, index codes were added for attributing the sequences to diverse samples. After removing ribosome RNA (rRNA), total RNA was fragmented with divalent cations in NEBNext First Strand Synthesis Reaction Buffer (5X) by increasing temperature. M-MuLV Reverse Transcriptase (RNase H-) and random hexamer primers were used to prepare first-strand cDNA, while RNase H and DNA Polymerase I were utilized for synthesizing second-strand cDNA. Here, dUTP was used rather than dTTP. The rest overhangs were later transfected in blunt ends by polymerase/exonuclease activities. Following the 3'-end adenylation of DNA fragments, they were hybridized through ligation by NEBNext Adaptor containing the hairpin loop structure. 250-300 bp cDNA fragments were selected, and the AMPure XP system (Beckman Coulter, Beverly, USA) was used for purifying the library fragments. After adaptor ligation and size screening, second-strand cDNA was digested with USER Enzyme (NEB, USA) for a 15-min period at 37°C and later for a 5-min period at 95°C before PCR. Index (X) Primer, Universal PCR primers, and Phusion High-Fidelity DNA polymerase were used for the PCR. When the libraries were constructed, they were first quantified *via* Qubit2.0 Fluorometer, followed by dilution till 1.5 ng/μl as well as by detection of library insert size with Agilent 2100 bioanalyzer. When an expected insert size was obtained, we conducted qRT-PCR for the accurate quantification of effective library content (>2 nM) to ensure library quality. For clustering from libraries of acceptable quality, the TruSeq PE Cluster Kit V3-cBot- HS (Illumina) was used. Finally, the Illumina Novaseq 6000 was used for sequencing (Novogene Co., Ltd, China).

Identification of lncRNA

Raw reads (fastq format) processing was accomplished by adopting in-house Perl scripts. Thereafter, reads containing poly-N, adapter, or those of low quality, were eliminated for obtaining clean data (clean reads). Meanwhile, Q20, Q30, and GC content for all the raw data were determined, followed by the selection of a specific length range for downstream analyses.

The original sequencing data's clean reads were checked for quality control and compared to the reference genome sequence using HISAT2 (Kim et al., 2015). The genome of *Beta vulgaris* L. RefBeet-1.2.2 (ensemble, release-54) was used as the reference genome (http://plants.ensembl.org/Beta_vulgaris/Info/Index). StringTie software was used to assemble the results for comparison and to obtain mapped reads (Pertea et al., 2015). To look for unannotated transcription regions, the mapped reads were spliced together and compared to the original genome annotations. Sequences encoding short peptides with fewer than 50 amino acid residues or containing only a single exon were discarded in order to find new transcripts and genes for the species.

The identification of lncRNAs was divided into two stages: basic screening and potential coding-ability screening. The basic screening procedure included selecting (1) transcripts with class_code of "i","x", "u", "o", and "e"; (2) transcripts with ≥ 200-bp length and exon numbers ≥ 2; and (3) transcripts with FPKM ≥ 0.1. We used four different software programs designed to screen for coding ability: the CPC, CNCI, and PFAM protein domain analysis tools. We created a Venn diagram to visually display the results of the three analyses, and the same data identified within the three datasets was used for subsequent lncRNA analysis.

Analysis of differentially expressed lncRNAs (DElncRNAs) and mRNAs (DEmRNAs)

Fold change (FC) and P-values are the screening criteria used to declare differential expression in the process of detecting differential-

expression genes. FC is the ratio of expression levels between two samples (groups), and FC and *P*-value are calculated using R-packet DESeq. When screening lncRNA, the standard values that indicate significance are |log2 (FC)|≥ 2 and $P < 0.05$. The screening criteria for mRNA were |log2 (FC)|≥ 2 and FDR < 0.05. (we also adjusted mRNA data based on a false discovery rate [FDR]). String Tie was used to calculate the FPKM (fragments per kilobase of transcript per million fragments mapped) value to assess lncRNA and mRNA expression levels (Trapnell et al., 2010). The differentially expressed lncRNAs and mRNAs were then analyzed using hierarchical cluster analysis.

Prediction and functional annotations of the target genes of DElncRNAs

The positional relationship between lncRNA and target genes is used to predict lncRNA cis-target genes. Using a Perl script, we identified adjacent genes within 100 kb upstream and downstream of lncRNA as cis-target genes (Zhang et al., 2020). Trans-target genes interact with lncRNA *via* base complementary pairing, and they were predicted using lncTar, a target gene prediction tool (Li et al., 2015).

We used the R package topGO (Ashburner et al., 2000) to perform GO analysis of lncRNA target genes (http://www.geneontology.org/) for functional annotation of differential genes. The KOBAS software was used to determine the level of statistical enrichment of lncRNA target genes in the KEGG pathway (Mao et al., 2005).

Quantitative real-time PCR (qRT-PCR)

By using M-MLV Reverse Transcription Kit (Takara, Dalian, China), we collected total RNA for preparing cDNA through reverse transcription. Supplementary Table S1 explains the primers utilized (Sangon Biotechnology, Shanghai, China). miRcute SYBR Green MasterMix and SYBR GreenMaster Mix (Tiangen, Beijing, China) were adopted for qRT-PCR that was carried out using LineGene 9600 Plus qRT-PCR detection system (BIOER., Hangzhou, China). $2^{-\Delta\Delta Ct}$ approach was used in data calculation relative to the housekeeping gene of sugar beet *Actin*. The qRT-PCR assay was carried out thrice, and the data were represented as mean ± standard error (SE).

miRNA target mimicry prediction

Because lncRNAs can act as miRNA target mimics. The lncRNA sequences were submitted to TargetFinder and psRobot software for matching against the sugar beet miRNA database in order to identify lncRNAs that are targeted by miRNAs based on free energy and score value (Fahlgren and Carrington, 2010; Wu et al., 2012).

ceRNA network construction and analysis

CeRNAs were screened by the ceRNA-score principle (Das et al., 2014; Shu et al., 2019). The criteria were lncRNAs and mRNAs with the same numbers of miRNAs greater than three, $p < 0.05$, and FDR value < 0.1. FDR was calculated by correcting *p*-values using the p.adjust function in R. Then, all of the differentially-expressed lncRNA-miRNA and miRNA-mRNA relationship pairs were gained. Finally, the relationship pairs with negative correlation between miRNAs and their targets and positive correlation between miRNAs targets were selected, and these relationship pairs were combined to obtain ceRNA network. The Cytoscape 3.9.1 software was used to visualize the data.

Results

Differences in morphological parameters between two treatments

To examine the impacts of drought stress on the physiological characteristics of sugar beet, we measured soluble sugar content, POD activity, and SA content in leaves harvested in CK and DR-treated plants. As indicated in Figures 1A–C, drought stress significantly raised the above-mentioned physiological features. Based on such physiological differences, we contend that there were great differences at the genetic level, including lncRNAs and mRNAs in drought-challenged sugar beet.

Basic data statistics

Six cDNA libraries (CK1, CK2, CK3 and DR1, DR2, DR3) were constructed. Overall, 93775816, 107421550, 97896732, 106448750, 88929524, and 90913022 raw reads were obtained in CK1, CK2, CK3, DR1, DR2, and DR3 libraries, respectively (Table 1). After trimming adapters and filtering out low quality reads, 92758786 (CK1), 106281556 (CK2), 96751372 (CK3), 105457050 (DR1), 88200802 (DR2) and 89932544 (DR3) clean reads were remained and used for further analysis. The Q20 values of clean reads were greater than 96%, the Q30 values of all samples were greater than 89%, and the GC contents were greater than 40%. This suggested that the clean reads were of high quality. We mapped a total of 66308676, 74969665, 69822100, 79273072, 58164384, and 65396407 clean reads from CK1, CK2, CK3, DR1, DR2, and DR3 libraries, respectively, against the reference genome.

LncRNAs identification in sugar beet

LncRNAs were screened by complementary base pairing, while the non-coding transcripts were screened by CPC, PFAM, and CNCI. Altogether, 44722 lncRNAs were discovered from the six cDNA libraries, including 41722 from CPC, 39620 from PFAM, and 33484 from CNCI (Figure 2A). Each of the three methods identified the same 32017 lncRNAs and so these were considered as novel lncRNAs. Among these novel lncRNAs, 74.9% were located in intergene regions, so we classified them as lincRNA. They occupied a dominant proportion in the novel lncRNAs. Sense-lncRNAs and antisense-lncRNAs, respectively occupied 3.2% and 22.0% of the new lncRNAs (Figure 2B). Most lncRNAs (88.5%) had short-length (< 1000 nucleotides, nt), 7.9% had medium-length (1000-2000 nt),

10.3389/fpls.2023.1118011

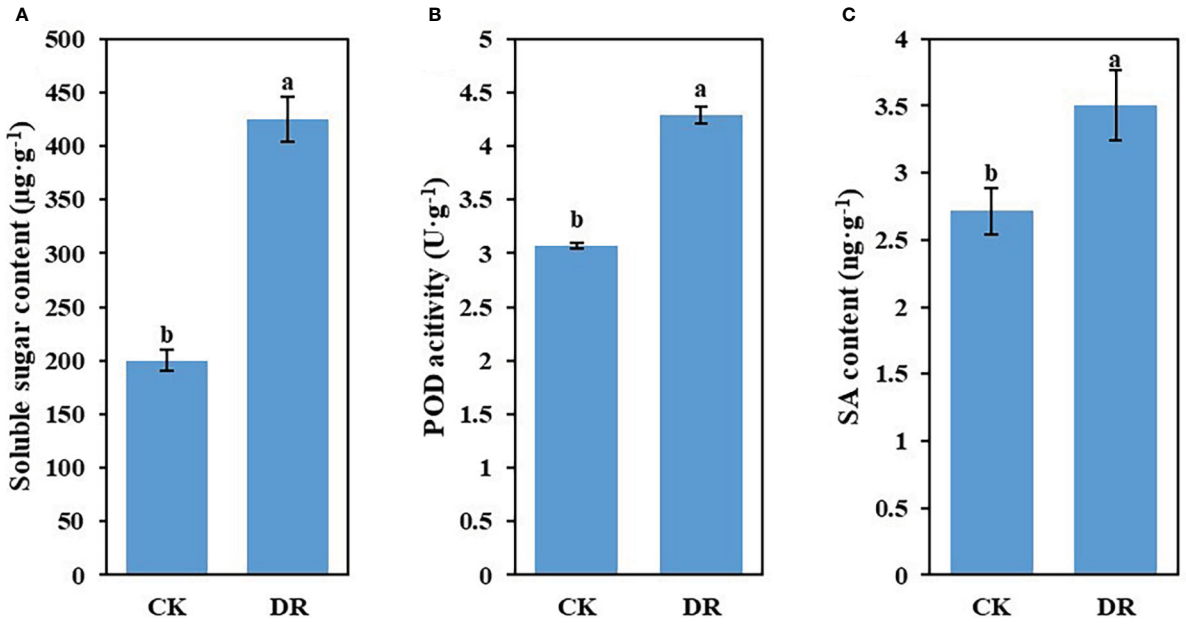


FIGURE 1
Effect of drought stress on the physiological characteristics of sugar beet. **(A)** Soluble sugar level. **(B)** POD activity. **(C)** SA level. Results are represented by means ± SE.

while only 3.6% had long-length (> 2000 nt) (Figure 2C). As indicated in Figure 2D, 96.7% of lncRNAs contained less than two exons. Typically, lncRNAs were associated with the features of small exon number and short transcript length. The box plot displayed the overall distribution of lncRNAs expression levels, of which most had FPKM values between 1 to 10 (Figure 2E). As shown in Figure 2F, 21853 lncRNAs were simultaneously found in both CK and DR groups, while 8224 and 1895 lncRNAs were uniquely found in CK and DR groups, respectively.

Analysis of drought-responsive lncRNAs and mRNAs

As revealed by sequencing analysis, lncRNAs conforming to $p < 0.05$ and $\log_2$ (foldchange, FC) ≥ 1 showed significant up-regulation. In contrast, those conforming to $p < 0.05$ and $\log_2$ (FC) ≤ −1 showed significant down-regulation. Based on the statistical analyses, there were altogether 386 drought-responsive DElncRNAs, including 170 with significant up-regulation and 216 with down-regulation (Figure 3A). The clustering analysis for DElncRNAs was displayed in Figure 3C. The most significantly upregulated lncRNA was TCONS_00055787 (upregulated by more than 6000 fold), followed by TCONS_00103111 and TCONS_00085517. Conversely, the most significantly downregulated lncRNA was TCONS_00038334 (downregulated by more than 18000 fold), followed by TCONS_00004463 and TCONS_00080695 (Supplementary Table S2). Furthermore, 1723 DEmRNAs (Figures 3B, D) (640 upregulated and 1083 downregulated) were identified in the DR group compared to the CK group.

To confirm lncRNA expression levels based on RNA-seq, qRT-PCR was conducted to analyze levels of nine random DElncRNAs.

TABLE 1 RNA-seq data of six samples.

Samples	CK1	CK2	CK3	DR1	DR2	DR3
Raw reads	93775816	107421550	97896732	106448750	88929524	90913022
Clean reads	92758786	106281556	96751372	105457050	88200802	89932544
Raw bases (G)	14.07	16.11	14.68	15.97	13.34	13.64
Clean bases (G)	13.91	15.94	14.51	15.82	13.23	13.49
Error rate (%)	0.03	0.03	0.03	0.03	0.03	0.03
Q20 (%)	96.97	96.61	96.92	97.07	96.34	96.73
Q30 (%)	91.61	90.87	91.40	91.86	89.96	91.00
GC content (%)	40.88	40.82	41.00	40.21	41.14	40.99
Total mapped reads	66308676 (71.49%)	74969665 (70.54%)	69822100 (72.17%)	79273072 (75.17%)	58164384 (65.95%)	65396407 (72.72%)

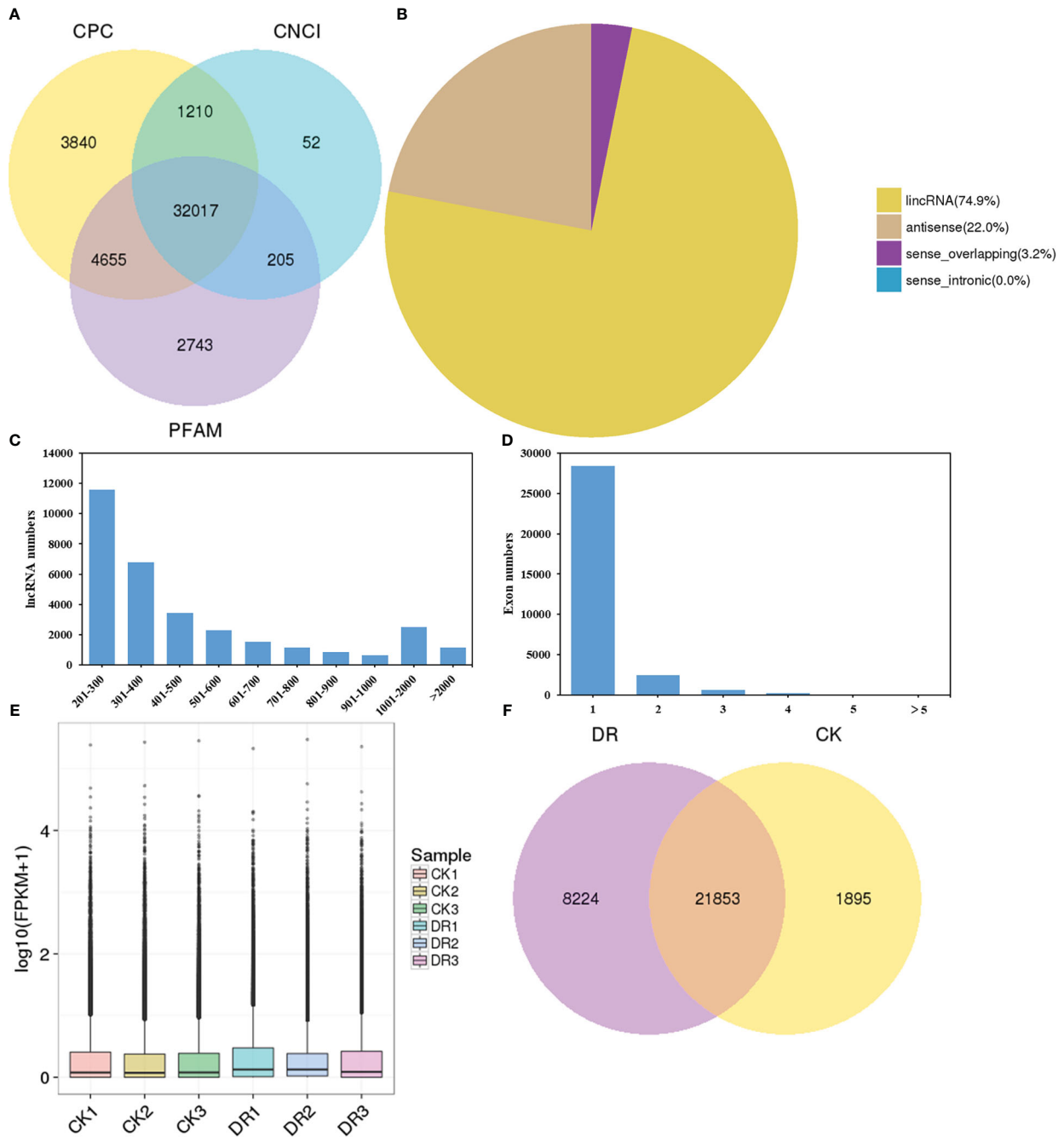


FIGURE 2
Prime features of lncRNA. **(A)** Venn diagram plot based on CPC, PFAM, and CNCI analyses. **(B)** Diagram showing lncRNA categories. **(C)** lncRNA length distribution. **(D)** Distribution of exon numbers in lncRNAs. **(E)** lncRNAs levels. **(F)** Venn diagram presenting shared and unique lncRNAs under CK and DR conditions.

Based on the sequencing, these lncRNAs included six down-regulated (TCONS_00025138, TCONS_00068434, TCONS_00110624, TCONS_00025136, TCONS_00045655 and TCONS_00020934) and three up-regulated (TCONS_00078442, TCONS_00030892 and TCONS_00049699) lncRNAs. As a result, the expression patterns of lncRNAs detected by qRT-PCR were highly consistent with those based on RNA sequencing (Figure 4), indicating high reliability of lncRNA expression profiles obtained by RNA-seq.

Predicted target genes for drought-responsive lncRNAs

LncRNA can regulate the expression of its adjacent genes and also act on further genes through base complementary pairing. We predicted 2532 lncRNA cis-target genes within 100 kb upstream and downstream of 386 DElncRNAs (Supplementary Table S3). According to the principle of base complementary pairing,

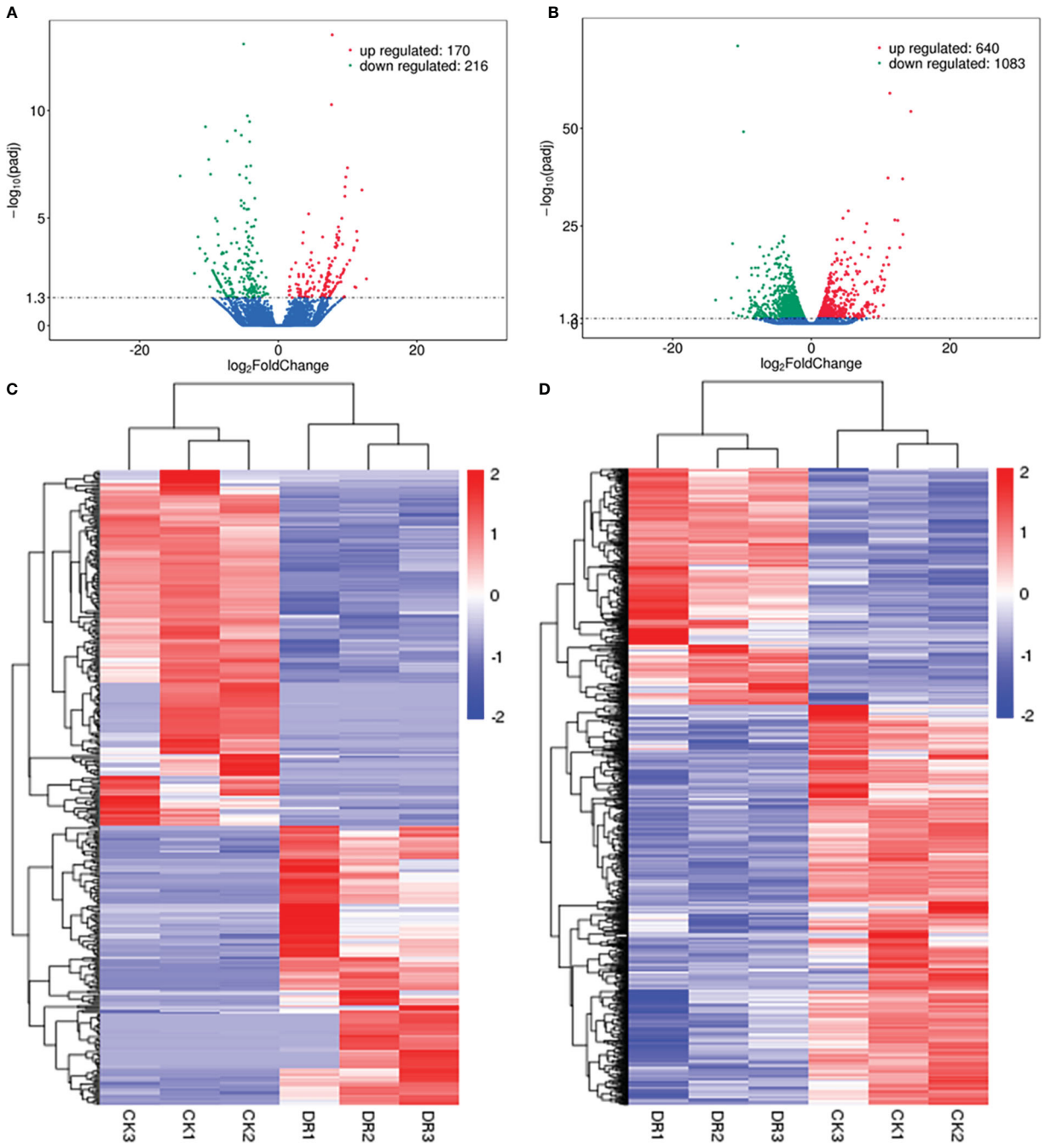


FIGURE 3
Analysis of DElncRNAs. **(A)** Volcano plot showing DElncRNAs. **(B)** Volcano plot showing DEmRNAs. **(C)** Heatmap for the DElncRNAs. **(D)** Heatmap for the DEmRNAs.

we predicted 9041 lncRNA trans-target genes (Supplementary Table S4). Concerning the target gene numbers in each lncRNA, many lncRNAs contained multiple target genes. For instance, TCONS_00068434 had five cis-target genes (*BVRB_7g163400*, *BVRB_7g163410*, *BVRB_7g163380*, *BVRB_7g163390*, and *BVRB_7g163420*) and 322 trans-target genes (including *BVRB_6g136680*, *BVRB_2g028320*, and *BVRB_2g039860*). As shown in Figure 4, TCONS_00025138, TCONS_00068434, TCONS_00110624, TCONS_00025136, TCONS_00045655, TCONS_00020934,TCONS_00078442, TCONS_00030892, and TCONS_00049699 shared an identical trend of expression with corresponding target genes *BVRB_6g136190*, *BVRB_009610*, *BVRB_6g136680*, *BVRB_6g127660*, *BVRB_5g118060*, *BVRB_9g204220*, *BVRB_3g057080*, *BVRB_5g099960*, and *BVRB_2g026490*, respectively. Moreover, many of these target genes were predicted to encode a variety of proteins, like squamosa promoter-binding-like protein 6 (*BVRB_6 g136190*, targeted by TCONS_00025138), 1-aminocyclopropane-1-carboxylate oxidase 1 (*BVRB_9g204220*, targeted by TCONS_00110624) and receptor-like protein EIX2 (*BVRB_3g057080*, targeted by TCONS_00110811). Our above findings indicated that DElncRNAs might regulate different biological processes to adapt to drought conditions.

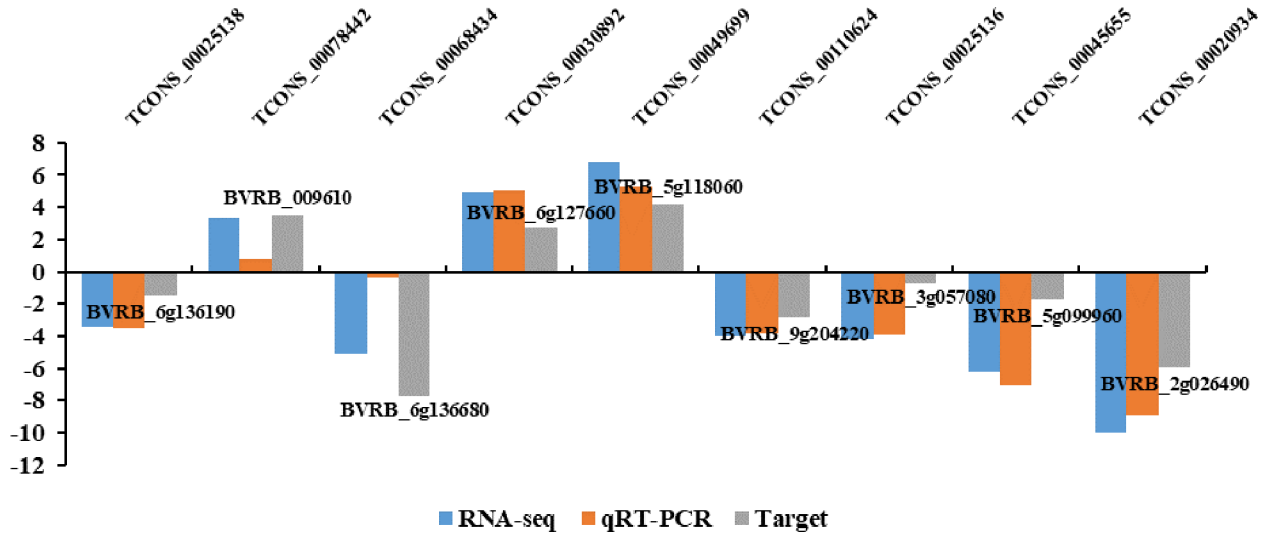


FIGURE 4
qRT-PCR verification for the nine lncRNAs and their target genes.

GO and KEGG analyses for potential target genes of DElncRNAs

For delineating the biological functions, the predicted target genes of the drought-responsive lncRNAs were sorted into GO term categories. As a result, cis-target genes were categorized into 1663, 375 and 812 GO terms in biological process, cellular component and molecular function, respectively (Supplementary Table S5), whereas trans-target genes were clustered into 2303, 546 and 1225 GO terms in biological process, cellular component and molecular function, respectively (Supplementary Table S6). For the BP category, organelle organization and phosphorus metabolic process were the most highly represented terms for cis- and trans-target genes, respectively, suggesting some functional role of cell organs and phosphorin in drought response (Figure 5). In the CC category, cis-target genes related to the organelle sub-compartment, and trans-target genes corresponding to the thylakoid and thylakoid parts were most abundant. Endopeptidase activity for cis-target genes and catalytic activity for trans-target genes were most significantly enriched in the MF category, which indicated that enzymatic reaction played an important role in sugar beet drought response. Meanwhile, the target genes were also found to be enriched in other stress related terms, including developmental process, lipid metabolic process, RNA polymerase activity, and transferase activity.

The results of KEGG analysis for cis- and trans-target genes for drought-responsive lncRNAs were presented in Supplementary Tables S7 andS8. And the 20 most significantly enriched KEGG pathways were displayed in Figure 6. The top four KEGG pathways included linoleic acid metabolism, glucosinolate biosynthesis, flavonoid biosynthesis, and zeatin biosynthesis for cis-target genes (Supplementary Table S7; Figure 6A), while for trans-target genes, these were carbon fixation in photosynthetic organisms, flavonoid biosynthesis, tyrosine metabolism, and photosynthesis (Supplementary Table S7; Figure 6B). Among them, the most heavily enriched pathways were linoleic acid metabolism and flavonoid biosynthesis (Figure 6). Our observations suggested that these processes play critical roles in drought response. Furthermore, carbon fixation in photosynthetic organisms and photosynthesis were significantly affected when sugar beet plants were subjected to drought condition, suggesting that drought stress significantly inhibited photosynthetic carbon assimilation in sugar beet plants. Flavonoid was found to be a significant determinant of drought tolerance in Arabidopsis (Li et al., 2022). Similarly, our findings also indicated that the application of flavonoid biosynthesis may help to alleviate drought stress in sugar beet plants.

Flavonoids are the important elements in abiotic stress resistance in plants (Kovinich and Durkin, 2018; Shah and Smith, 2020; Li et al., 2022). Flavonoid biosynthesis pathway is illustrated in Figure 7A. In this study, we identified two genes associated with the flavonoid biosynthesis pathway targeted by drought-responsive lncRNAs: *BVRB_1g007170* encoding dihydroflavonol 4-reductase (EC1.1.1.219) (targeted by TCONS_00009457), and *BVRB_1g016280* encoding flavanone 3-dioxygenase (EC1.14.11.9) (targeted by TCONS_00088109). Chalcone synthase represents a critical enzyme for flavonoid synthesis (Chen et al., 2021c). The two genes, *BVRB_6g151690* and *BVRB_6g152260* encoding chalcone synthase, were estimated as the targets of TCONS_00055970 and TCONS_00056083, respectively.These results indicated that the target genes of DElncRNAs may play critical roles in the biosynthesis of flavonoids during drought stress in sugar beet.

Photosynthetic carbon fixation provides mass and energy sources for various life activities in plants, including stress resistance. In the present study, we predicted several target genes of DElncRNAs related to carbon fixation in photosynthetic organisms (Figure 7B). Fructose-1,6-bisphosphatase plays a key role in gluconeogenesis and photosynthetic assimilate sucrose synthesis (Andrew et al., 2017). In our present study, both *BVRB_1g011460* and *BVRB_5g111310*, targeted by TCONS_00057113, encoded fructose-1,6-bisphosphatase (EC3.1.3.37). Malate dehydrogenase is involved in many critical metabolic processes in plants, like glycolysis and

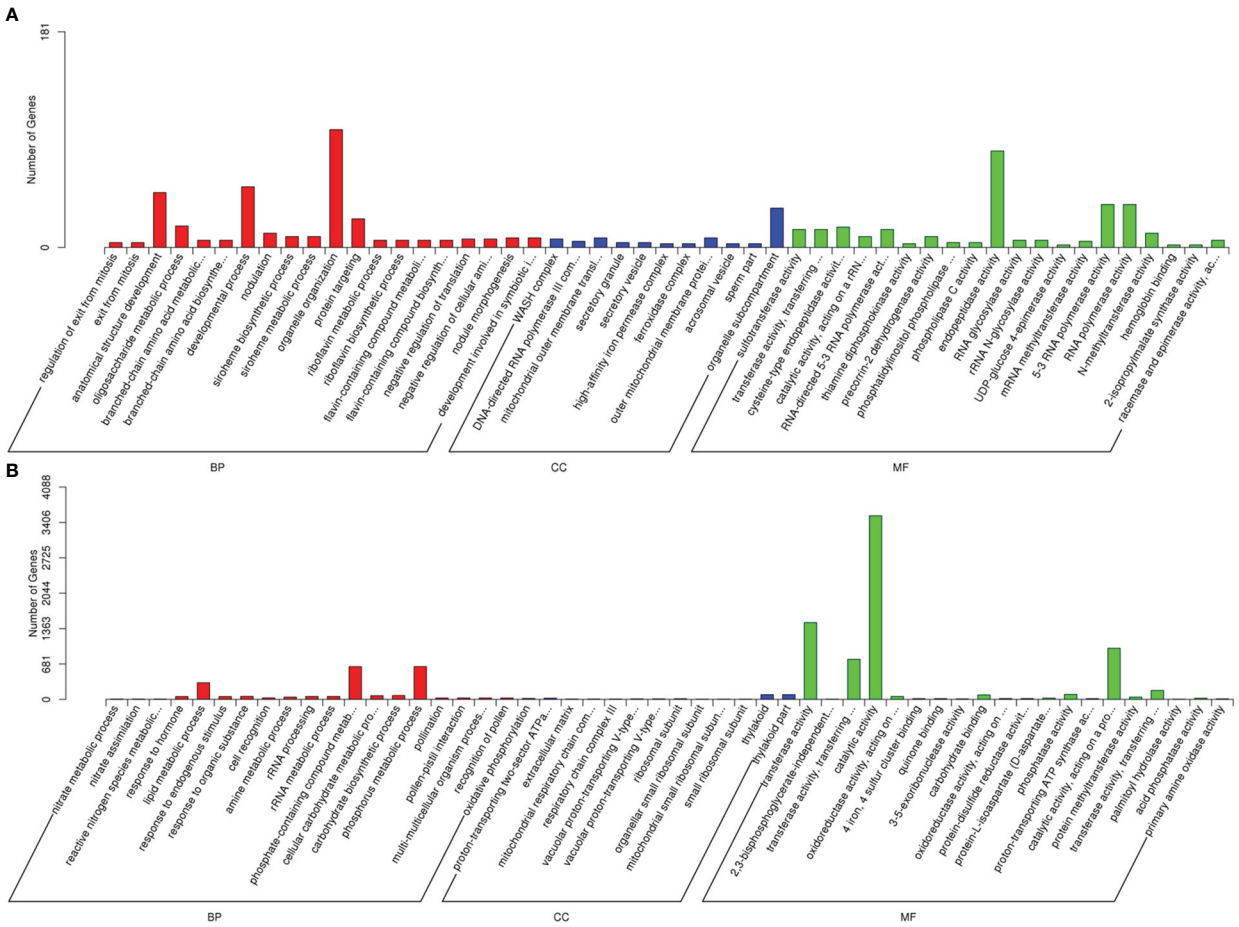


FIGURE 5
GO classification for the predicted target genes of DElncRNAs. **(A)** Go terms for cis-target genes. **(B)** Go terms for trans-target genes.

photosynthesis (Eprintsev and Gataullina, 2018). Three malate dehydrogenase (1.1.1.37) genes *BVRB_5g124340*, *BVRB_3g049020* and *BVRB_6g137210* were targeted by TCONS_00072169, TCONS_00034128 and TCONS_00002455, respectively. These results suggested that photosynthetic carbon assimilation was critically restrained under drought conditions in sugar beet plants.

Functional prediction of DElncRNAs acting as miRNA target mimics

LncRNAs can also act as miRNA mimics, disrupting miRNA regulation. Like miRNA-mRNA interactions, lncRNA can be degraded by the corresponding miRNA to reduce its effect on the target mRNA. We used Target Finder and psRobot to predict lncRNAs that could be miRNA target mimics based on free energy, score values, and other filtering conditions. In this study, 1756 distinct lncRNAs were predicted to be potential target mimics of 45 miRNAs, with 42 of those 1756 lncRNAs being DElncRNAs (Supplementary Table S9). Multiple DElncRNAs can be targeted by a miRNA, and a miRNA can be targeted by multiple DElncRNAs. For example, the miRNA ath-miR167a-5p targeted 5 DElncRNAs (TCONS_00034119, TCONS_00105108, TCONS_00023171, TCONS_00023940, and TCONS_00100201), and the lncRNA TCONS_00001191 was one common target mimicry of two miRNAs (ath-miR164a and ath-miR164c-5p). Therefore, lncRNAs may have a significant impact on miRNA function.

Construction of ceRNA network related to drought resistance

The lncRNA-mRNA-miRNA network was built to evaluate the lncRNA-associated ceRNA interaction landscape in drought-stressed sugar beet. The lncRNA-mRNA interaction was first discovered using the Pearson correlation coefficient of the expression value. Following that, ceRNAs were filtered using the ceRNA score, which was defined as the number of microRNA response elements (MREs) shared by mRNAs and lncRNAs divided by the total number of lncRNA MREs. Both mRNAs and lncRNAs are targeted for a given lncRNA-miRNA-mRNA triplet. We further filtered the 9 DElncRNAs and 10 DEmRNAs in drought response through literature mining and functional annotation. Based on the selected mRNAs implicated in drought response, we constructed a network of 24 lncRNA-miRNA-

10.3389/fpls.2023.1118011

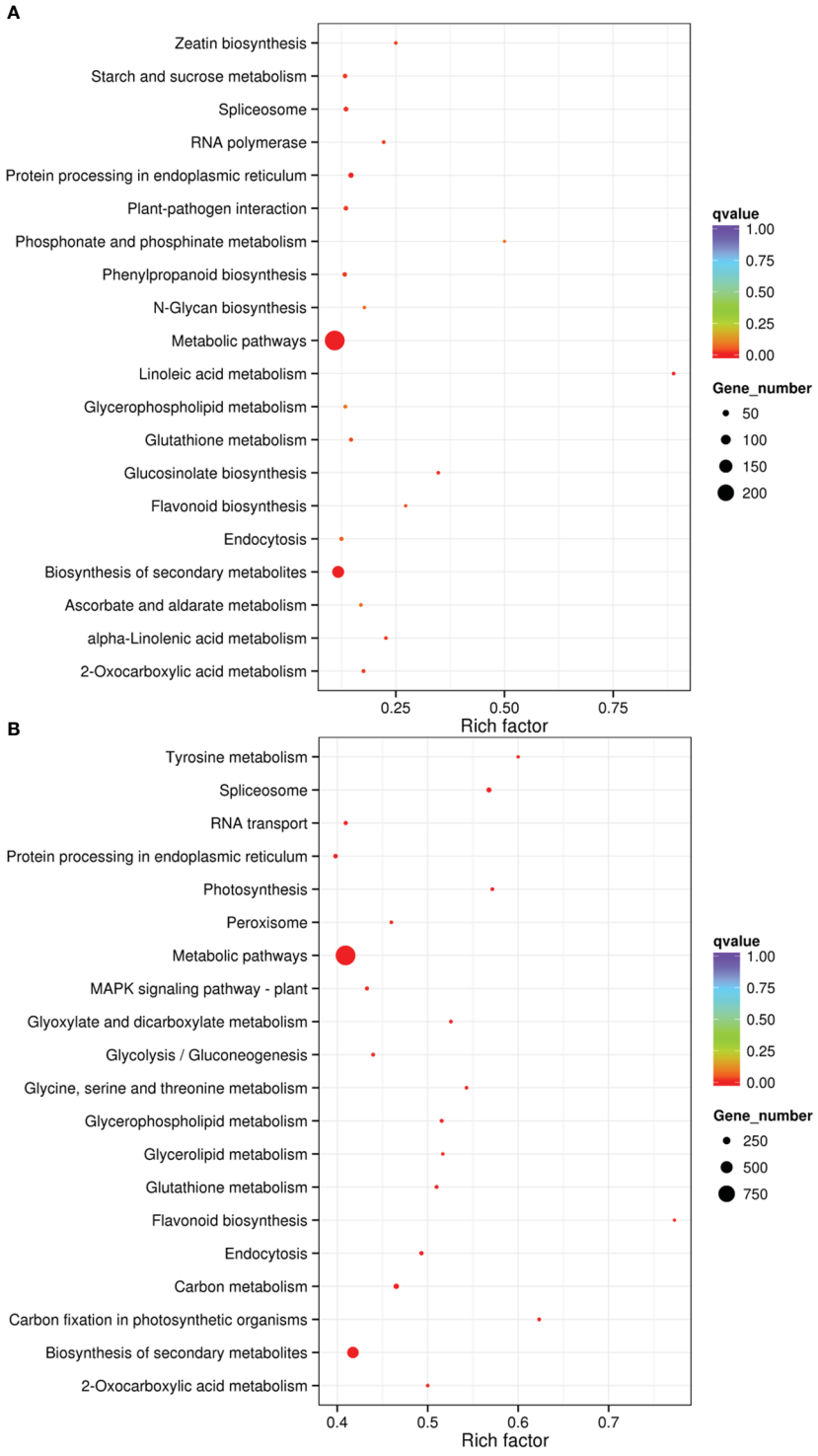


FIGURE 6
KEGG analysis of the predicted target genes for DElncRNAs. **(A)** KEGG pathways for cis- target genes. **(B)** KEGG pathways for trans-target genes.

mRNA triplets, including 9 lncRNA, 7 miRNAs and 10 mRNAs (Figure 8). In this network, one target gene *BVRB_8g197060* was annotated as protein phosphatase 2C and cyclic nucleotide-binding/kinase domain-containing protein based on NCBI nucleotide sequence annotations. *BVRB_6g136050* was annotated as splicing factor-like protein 1. These two target genes with several DElncRNAs were targeted by ath-miR159c and ath-miR157d, respectively.

Discussion

LncRNA, a type of ncRNA, has been extensively reported in animals, plants and fungi (Zhang et al., 2016). Numerous lncRNAs have been detected in plants; however, their functions remain largely unclear. In particular, the understanding of its role in drought stress is limited. In order to explore the function of lncRNA in drought stress,

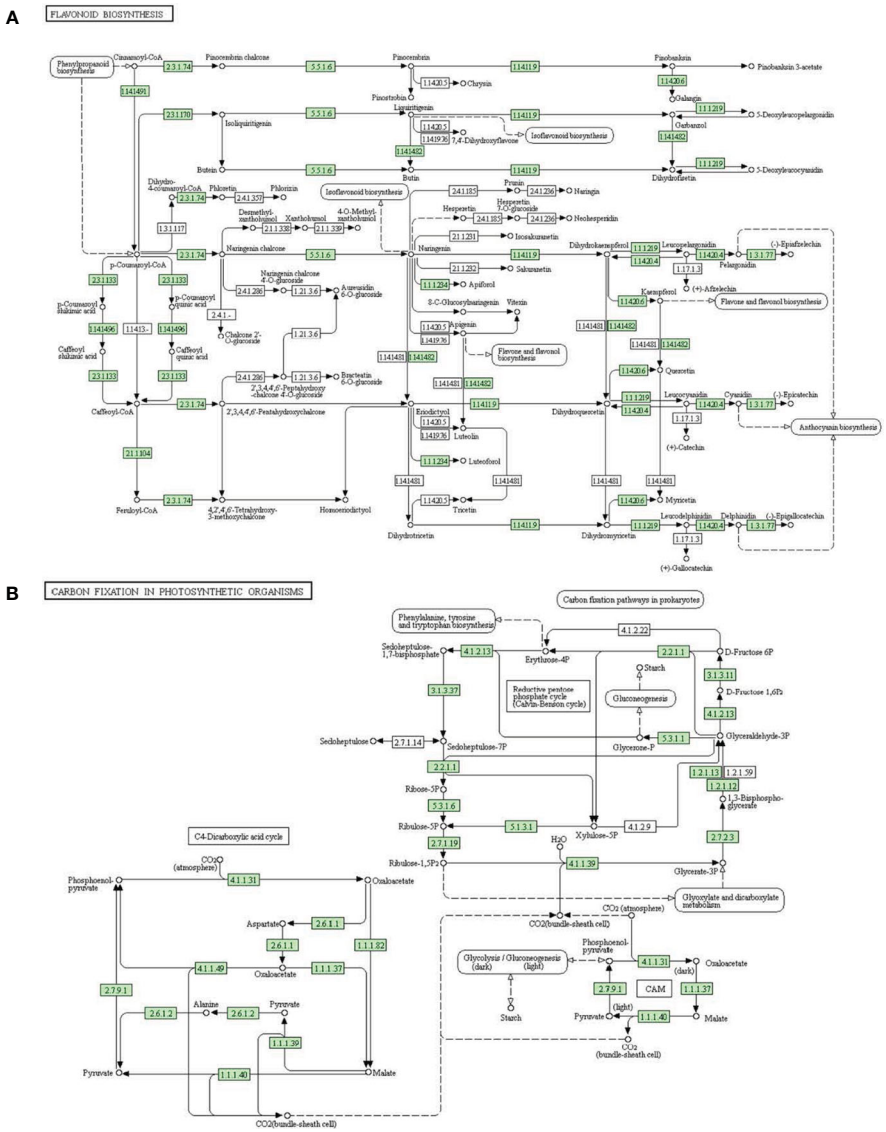


FIGURE 7
Targets of DElncRNAs in two enriched pathways. **(A)** Flavonoid biosynthesis pathway. **(B)** Carbon fixation in photosynthetic organisms pathway.

we used high-throughput sequencing technology to analyze the lncRNA transcriptome in sugar beet cultivar KWS9147 on a genome-wide scale. A total of 32017 lncRNAs were identified in the leaves of sugar beet (Figure 2F), which indicated that lncRNA may take part in the regulation of various life activities of sugar beet. Consistent with previous studies (Li et al., 2014; Zhu et al., 2015), most of the novel lncRNAs identified in the present study were located in the intergenic regions (Figure 2B), indicating that the type of novel lncRNAs were long intergenic non-coding RNAs (lincRNAs). In addition, lncRNA had short transcript length as well as low exon number (Figures 2C, D), which is in line with previous results (Chen et al., 2021a; Xu et al., 2021).

The decreasing water resource has been attributed as the major factor restricting global crop yield and quality. Various responsive mechanisms have evolved in plants to release damage resulting from abiotic stresses (Zhu, 2002). Many protein-encoding genes were found to exert important roles in regulating the response to abiotic stress in plants, like *DREB1A/CBF3* and *SOS1* (Jaglo et al., 1998; Liu et al., 1998; Qiu et al., 2002). Additionally, lncRNAs have been identified as powerful approaches in plants for enhancing their abiotic stress tolerance (Liu and Zhu, 2014). Liu et al. (2012) identified 6484 lincRNAs, among which 1832 responded to salinity, cold, drought, and abscisic acid. Wang et al. (2017) identified 10,785 lncRNAs in legume model species *Medicago truncatula*, including 224 responsive to phosphate deficiency in roots and 358 in leaves. So far, lncRNAs related to drought-responsive modulation were extensively investigated in maize (Zhang et al., 2014), cotton (Lu et al., 2016), *Arabidopsis* (Qin et al., 2017), cultivated rice (Yuan et al., 2018), cassava (Li et al., 2017), and wheat (Cagirici et al., 2017), suggesting a universal role of lncRNAs in drought response in diverse plant species. In the present study, we detected specific and common lncRNAs in control and drought-treated samples of sugar beet for investigating the potential lncRNA functions during drought stress (Figure 2F). Compared with the control group, 386 DElncRNAs were found in sugar beet under drought stress, of which 170 were up-regulated and 216 were down-regulated (Figure 3A). Moreover, The

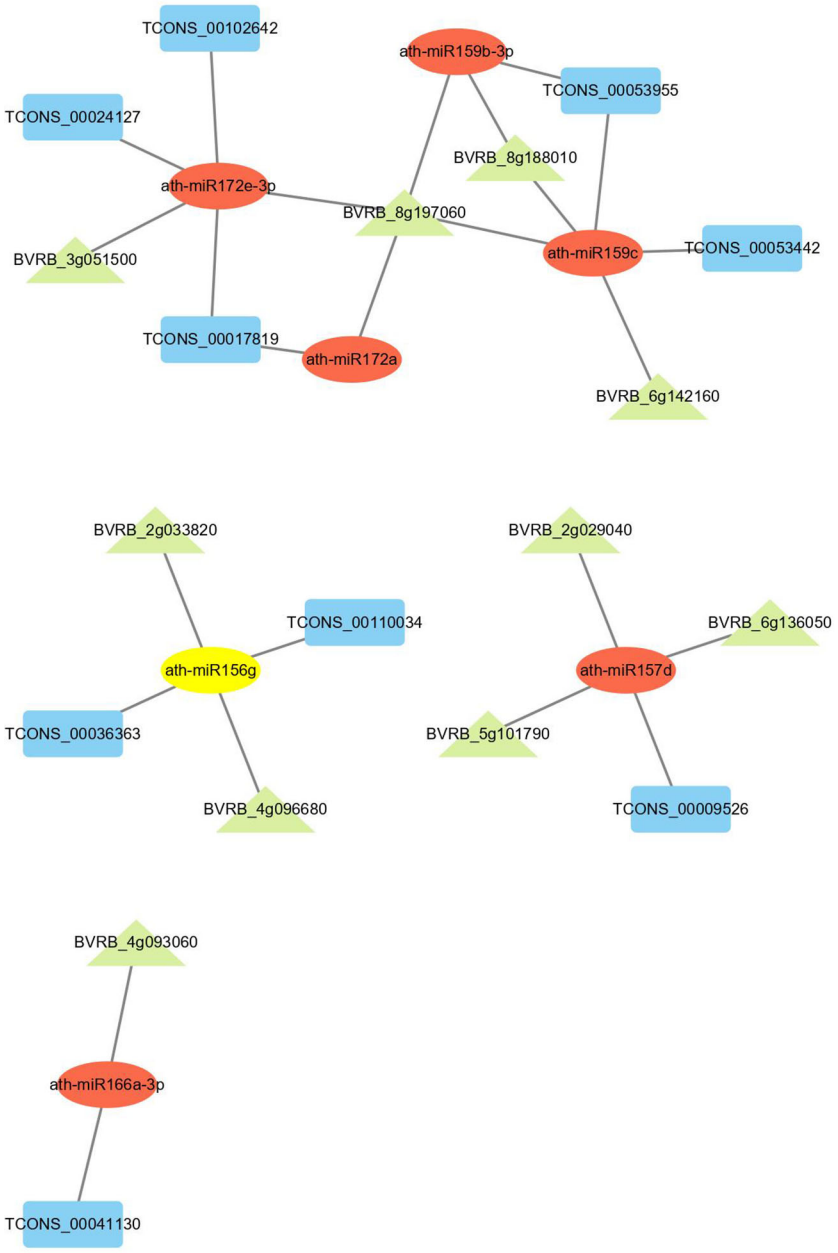


FIGURE 8
CeRNA network in sugar beet under drought stress. Rectangle, ellipse and triangle nodes represent lncRNAs, miRNAs and mRNAs, respectively. The edges represented the competing interactions among them.

most significantly upregulated lncRNAs TCONS_00055787 was upregulated by more than 6000 fold (Supplementary Table S2), which implied that this lncRNA may play a vital role in sugar beet drougt response.

Meanwhile, 2532 and 9041 transcripts were predicted as the candidate cis- and trans-target genes of drought-responsive lncRNAs, respectively (Supplementary Tables S3 and S4). In plants, promoter-binding-like proteins and receptor-like proteins have been reported to be involved in abiotic stress responses (Wei et al., 2015; Thabet et al., 2021; Rahim et al., 2022). In the present study, several candidate target genes encoded various proteins including squamosa promoter-binding-like protein 6 (*BVRB_6g136190*, targeted by TCONS_00025138), 1-aminocyclopropane-1-carboxylate oxidase 1 (*BVRB_9g204220*, targeted by TCONS_00110624) as well as receptor-like protein EIX2 (*BVRB_3g057080*, targeted by TCONS_00110811). These results suggested that the three DElncRNAs (TCONS_00025138, TCONS_00110624 and TCONS_00110811) may exert important roles in drought stress response of sugar beet by regulating the expression of genes encoding promoter-binding-like proteins and receptor-like proteins.

GO enrichment and KEGG pathway analyses of lncRNAs target genes can help us to understand the functions of lncRNAs more effectively (Muhammad et al., 2022). Oxido-reduction plays a key role in plant abiotic stress responses (Ali et al., 2021). Endopeptidase, catalytic, and transferase activity is closely associated with oxido-reduction (Douglas, 2008). According to GO enrichment analysis, the

target genes for drought-responsive lncRNAs were significantly enriched in organelle sub-compartments, thylakoids, endopeptidase activity, catalytic activity, developmental process, lipid metabolic process, RNA polymerase activity, and transferase activity (Figure 5). This phenomenon indicated that lncRNAs may be involved in drought resistance by modulating target genes controlling oxidoreductase activity, which was in accordance the report of Huang et al. (2014). Plant flavonoids also play important roles in abiotic/biotic stress responses (Baskar et al., 2018). According to KEGG pathway analysis on the target genes for DElncRNAs, the most significantly enriched pathway was involved in flavonoid biosynthesis (Figure 6). In the flavonoid biosynthesis pathway, several target genes of drought-responsive lncRNAs were related to dihydroflavonol 4-reductase and flavanone 3-dioxygenase (Figure 7A), implying that lncRNAs may participate in regulating flavonoid biosynthesis to relieve the damage to sugar beet seedlings under drought conditions. Photosynthetic carbon metabolism lays a material foundation for various life activities in the plants (Lawlor and Cornic, 2002). In the present study, one of most enriched pathway was photosynthetic carbon fixation (Figure 6). In the photosynthetic carbon fixation pathway, some target genes of DElncRNAs encoded fructose-1,6-bisphosphatase and malate dehydrogenase (Figure 7B), which are both involved in photosynthesis (Eprintsev and Gataullina, 2018; Andrew et al., 2017). This result proved that lncRNA could enhance the drought tolerance of sugar beet by affecting photosynthetic carbon metabolism.

MiRNAs and lncRNAs are important transcripts in gene regulation, and lncRNAs may interact with miRNAs as precursors or target mimics (Qiu et al., 2019). Chen et al. (2016) identified 9 intergenic lncRNAs as precursors of 11 known miRNAs in poplar under nitrogen deficiency. Deng et al. (2018) speculated that lnc_973 and lnc_253 regulate the expression of ghr-miR399 and ghr-156e in *Gossypium hirsutum* as a target mimic under salt stress. In the present study, 42 DElncRNAs were predicted as target mimics of several miRNAs (Supplementary Table S9), suggesting that lncRNAs were also important for miRNA-mediated regulation under drought stress.

Researchers discovered that lncRNA can function as ceRNA to inhibit miRNA function and compete with other miRNA targets (Salmena et al., 2011). There have been no studies on ceRNA in sugar beets so far. We created a ceRNA network for sugar beet in response to drought stress for the first time using transcriptome sequencing data (Figure 8). *BVRB_8g197060* was identified as a protein phosphatase 2C and cyclic nucleotide-binding/kinase domain-containing protein in our network, while *BVRB_6g136050* was identified as a splicing factor-like protein 1. These drought-responsive genes, along with several DElncRNAs, formed a ceRNA network that was targeted by miRNAs such as ath-miR159c and ath-miR157d (Figure 8). According to the report of Kobi et al. (2010), *SGN-U567133* represents a novel class of miR159 targets in plants, raising the possibility that post-transcriptional regulation by Sl-miR159 is required for normal tomato development. The expression of potato GAMyb-like genes, which are responsible for drought stress, was negatively regulated by Stu-miR159s (Yang et al., 2014). Growth and development are inhibited in drought-stressed plants (Quiroga et al., 2020). MiR157 was associated with the development in some sorts of plants (Zhou et al., 2021). These findings suggested that lncRNAs may regulate growth, development, and stress tolerance of sugar beet under drought conditions by sponging ath-miR159c and ath-mi157d.

To our knowledge, the current work is the first to report the systemic retrieval, characterization and analysis of lncRNAs isolated from drought-challenged sugar beet plants using high-throughput sequencing. From the results of the present study, we conclude that lncRNAs play important roles on sugar beet adaptation to drought conditions through the interaction with protein-encoding genes. Our findings provide newfound information regarding the potential role of lncRNAs in response to drought stress, further research is required to elucidate the molecular mechanisms of significantly dysregulated lncRNAs.

Data availability statement

The datasets presented in this study can be found in online repositories. The names of the repository/repositories and accession number(s) can be found below: https://www.ncbi.nlm.nih.gov/, GSE205413.

Author contributions

CZo: Investigation, writing, review and editing. ZG, SZ, and JC: Investigation. CZh: Conceptualization, Writing - review & editing. HH: Investigation. All authors contributed to the article and approved the submitted version.

Funding

This work was supported by Doctoral Research Starting Project at Shanxi Agricultural University (2021BQ21), Award Scientific Program for Excellent Doctors in Shanxi Province (SXBYKY2021073) and Natural Science Foundation of China (31971994).

Conflict of interest

The authors declare that the research was conducted in the absence of any commercial or financial relationships that could be construed as a potential conflict of interest.

Publisher's note

All claims expressed in this article are solely those of the authors and do not necessarily represent those of their affiliated organizations, or those of the publisher, the editors and the reviewers. Any product that may be evaluated in this article, or claim that may be made by its manufacturer, is not guaranteed or endorsed by the publisher.

Supplementary material

The Supplementary Material for this article can be found online at: https://www.frontiersin.org/articles/10.3389/fpls.2023.1118011/full#supplementary-material

References

Ali, H. E., Janina, M., Asis, H., Bernhard, M. S., David, N., Björn, U., et al. (2021). Plant PhysioSpace: A robust tool to compare stress response across plant species. *Plant Physiol.* 187, 1795–1811.

Alkahtani, M., Hafez, Y., Attia, K., Rashwan, E., Husnan, L., AlGwaiz, H., et al. (2021). Evaluation of silicon and proline application on the oxidative machinery in drought-stressed sugar beet. *Antioxidants* 10, 398.

Andrew, J. S., Patricia, E. L., Philip, A. D., Lauren, R. H., Tracy, L., Stefan, T., et al. (2017). Simultaneous stimulation of sedoheptulose 1,7-bisphosphatase, fructose 1,6-bisphophate aldolase and the photorespiratory glycine decarboxylase-h protein increases CO2 assimilation, vegetative biomass and seed yield in arabidopsis. *Plant Biotechnol. J.* 15, 805–816.

Ashburner, M., Ball, C., Blake, J., Botstein, D., Butler, H., Cherry, J., et al. (2000). Gene ontology: Tool for the unification of biology. the gene ontology consortium. *Nat. Genet.* 1, 25–29.

Baskar, V., Rajendran, V., and Ramalingam, S. (2018). Flavonoids (antioxidants systems) in higher plants and their response to stresses. *Antioxidants Antioxidant Enzymes Higher Plants* pp, 253–268.

Bota, J., Medrano, H., and Flexas, J. (2004) Is photosynthesis limited by decreased rubisco activity and RuBP content under progressive water stress? *New Phytol.* 162, 671–681. doi: 10.1111/j.1469-8137.2004.01056.x

Cagirici, H., Alptekin, B., and Budak, H. (2017). RNA Sequencing and co-expressed long non-coding RNA in modern and wild wheats. *Sci. Rep.* 7, 10670.

Chen, K., Huang, Y., Liu, C., Liang, Y., and Li, M. (2021b). Transcriptome profile analysis of arabidopsis reveals the drought stress-induced long non-coding RNAs associated with photosynthesis, chlorophyll synthesis, fatty acid synthesis and degradation. *Front. Plant Sci.* 12, 643182.

Chen, M., Wang, C., Bao, H., Chen, H., and Wang, Y. (2016). Genome-wide identification and characterization of novel lncRNAs in populus under nitrogen deficiency. *Mol. Genet. Genomics* 291, 1663–1680.

Chen, Q., Zhang, R., Li, D., and Wang, F. (2021c). Transcriptomic and coexpression network analyses revealed pine chalcone synthase genes associated with pine wood nematode infection. *Int. J. Mol. Sci.* 22, 11195.

Chen, J., Zhong, Y., and Qi, X. (2021a). LncRNA TCONS_00021861 is functionally associated with drought tolerance in rice (Oryza sativa l.) *via* competing endogenous RNA regulation. *BMC Plant Biol.* 21, 410.

Cui, J., Jiang, N., Hou, X., Wu, S., Zhang, Q., Meng, J., et al. (2020). Genome-wide identification of lncRNAs and analysis of ceRNA networks during tomato resistance to phytophthora infestans. *Phytopathology* 110, 456–464.

Das, S., Ghosal, S., Sen, R., and Chakrabarti, J. (2014). lnCeDB: Database of human long noncoding RNA acting as competing endogenous RNA. *PloS One* 9, e98965.

Das, A., Saxena, S., Kumar, K., Tribhuvan, K., Singh, N., and Gaikwad, K. (2020). Non-coding RNAs having strong positive interaction with mRNAs reveal their regulatory nature during flowering in a wild relative of pigeonpea (Cajanus scarabaeoides). *Mol. Biol. Rep.* 47, 3305–3317.

Deng, F., Zhang, X., Wang, W., Yuan, R., and Shen, F. (2018). Identification of gossypium hirsutum long non-coding RNAs (lncRNAs) under salt stress. *BMC Plant Biol.* 18, 23.

Douglas, R. C. (2008). Plastocyanin-ferredoxin oxidoreduction and endosymbiotic gene transfer. *Photosynthesis Res.* 97, 245–253.

DuBois, M., Hamilton, J. K., Rebers, P., and Smith, F. (2002). Calorimetric dubois method for determination of sugar and related substances. *Analytical Chem.* 28, 350–356.

Eprintsev, A., and Gataullina, M. (2018). Isolation, purification, and properties of peroxisomal malate dehydrogenase from maize mesophyll. *Appl. Biochem. Microbiol.* 54, 320–323.

Fahlgren, N., and Carrington, J. C. (2010). miRNA target prediction in plants. *Methods Mol. Biol.* 592, 51–57.

Giordano, D., Provenzano, S., Ferrandino, A., Vitali, M., Pagliarani, C., Roman, F., et al. (2016). Characterization of a multifunctional caffeoyl-CoA O-methyltransferase activated in grape berries upon drought stress. *Plant Physiol. Biochem.* 101, 23–32.

Gisbert, C., Timoneda Monfort, A., Porcel, R., Ros, R., and Mulet, J. (2020). Overexpression of BvHb2, a class 2 non-symbiotic hemoglobin from sugar beet, confers drought-induced withering resistance and alters iron content in tomato. *Agronomy* 10, 1754.

Huang, X., Zhang, H., Wang, Q., Guo, R., Wei, L., Song, H., et al. (2021). Genome-wide identification and characterization of long non-coding RNAs involved in flag leaf senescence of rice. *Plant Mol. Biol.* 105, 655–684.

Huang, L., Zhang, F., Wang, W., Zhou, Y., Fu, B., and Li, Z. (2014). Comparative transcriptome sequencing of tolerant rice introgression line and its parents in response to drought stress. *BMC Genomics* 15, 1026.

Jaglo, K., Gilmour, S., Zarka, D., Schabenberger, O., and Thomashow, M. (1998). Arabidopsis CBF1 overexpression induces COR genes and enhances freezing tolerance. *Science* 280, 104–106.

Jiang, N., Cui, J., Shi, Y., Yang, G., Zhou, X., Hou, X., et al. (2019). Tomato lncRNA23468 functions as a competing endogenous RNA to modulate NBS-LRR genes by decoying miR482b in the tomato-phytophthora infestans interaction. *Horticulture Res.* 6, 28.

Khemka, N., and Singh, U. (2017). PLncPRO for prediction of long non-coding RNAs (lncRNAs) in plants and its application for discovery of abiotic stress-responsive lncRNAs in rice and chickpea. *Nucleic Acids Res.* 45, e183.

Kim, D., Langmead, B., and Salzberg, S. L. (2015). HISAT: A fast spliced aligner with low memory requirements. *Nat. Methods* 12, 357–360.

Kobi, B., Anat, H., Ran, S., Moshe, L., Naomi, O., Tzahi, A., et al. (2010). Identification and characterization of a novel miR159 target not related to MYB in tomato. *Planta* 232, 1009–1022.

Kovinich, N., and Durkin, P. (2018). Hormone deficient mutants have distinct flavonoid proportion fingerprints in response to abiotic stress. *Plant Signaling Behav.* 13, 1–5.

Lawlor, D., and Cornic, G. (2002). Photosynthetic carbon assimilation and associated metabolism in relation to water deficits in higher plants. *Plant Cell Environ.* 25, 275–294.

Li, L., Eichten, S. R., Shimizu, R., Petsch, K., Yeh, C. T., Wu, W., et al. (2014). Genome-wide discovery and characterization of maize long non-coding RNAs. *Genome Biol.* 15, R40.

Li, B., Fan, R. N., Fan, Y. T., Liu, R. N., Zhang, H., Chen, T. T., et al. (2022). The flavonoid biosynthesis regulator PFG3 confers drought stress tolerance in plants by promoting flavonoid accumulation. *Environ. Exp. Bot.* 196, 104792.

Li, Y., Liu, N., Fan, H., Su, J., Fei, C., Wang, K., et al. (2019b). Effects of deficit irrigation on photosynthesis, photosynthate allocation, and water use efficiency of sugar beet. *Agric. Water Manage.* 223, 105701.

Li, J., Ma, W., Zeng, P., Wang, J., Geng, B., Yang, J., et al. (2015). LncTar: a tool for predicting the RNA targets of long noncoding RNAs. *Briefings Bioinf.* 16, 806–812.

Liu, J., Jung, C., Xu, J., Wang, H., Deng, S., Bernad, L., et al. (2012). Genome-wide analysis uncovers regulation of long intergenic noncoding RNAs in arabidopsis. *Plant Cell* 24, 4333–4345.

Liu, Q., Kasuga, M., Sakuma, Y., Abe, H., Miura, S., Yamaguchi-Shinozaki, K., et al. (1998). Two transcription factors, DREB1 and DREB2, with an EREBP/AP2 DNA binding domain separate two cellular signal transduction pathways in drought- and low-temperature-responsive gene expression, respectively, in arabidopsis. *Plant Cell* 10, 1391–1406.

Liu, Y., Zhang, M., Meng, Z., Wang, B., and Chen, M. (2020). Research progress on the roles of cytokinin in plant response to stress. *Int. J. Mol. Sci.* 21, 6574.

Liu, R., and Zhu, J. K. (2014). Non-coding RNAs as potent tools for crop improvement. *Natl. Sci. Rev.* 1, 186–189.

Li, P., Yang, H., Wang, L., Liu, H., Huo, H., Zhang, C., et al. (2019a). Physiological and transcriptome analyses reveal short-term responses and formation of memory under drought stress in rice. *Front. Genet.* 8, 10.

Li, S., Yu, X., Lei, N., Cheng, Z., Zhao, P., He, Y., et al. (2017). Genome-wide identification and functional prediction of cold and/or drought-responsive lncRNAs in cassava. *Sci. Rep.* 7, 45981.

Lu, X., Chen, X., Mu, M., Wang, J., Wang, X., Wang, D., et al. (2016). Genome-wide analysis of long noncoding RNAs and their responses to drought stress in cotton (Gossypium hirsutum l.). *PloS One* 11, e0156723.

Lu, Q., Guo, F., Xu, Q., and Cang, J. (2020). LncRNA improves cold resistance of winter wheat by interacting with miR398. *Funct. Plant Biol.* 47, 544–557.

Mao, X., Cai, T., Olyarchuk, J. G., and Wei, L. (2005). Automated genome annotation and pathway identification using the KEGG orthology (KO) as a controlled vocabulary. *Bioinformatics* 21, 3787–3793.

Mattick, J. (2009). The genetic signatures of noncoding RNAs. *PloS Genet.* 5, e1000459.

Ma, C., Wang, Z., Kong, B., and Lin, T. (2013). Exogenous trehalose differentially modulate antioxidant defense system in wheat callus during water deficit and subsequent recovery. *Plant Growth Regul.* 70, 275–285.

Merlaen, B., De Keyser, E., and Van Labeke, M. C. (2020). The jasmonic acid pathway, rather than abscisic acid, may partly explain contrasting stomatal responses in two strawberry cultivars under osmotic stress. *Plant Physiol. Biochem.* 151, 21–33.

Ming, Z., Zhang, M., Xing, L., Li, W., Jiang, H., Wang, L., et al. (2017). Transcriptomic analysis of long non-coding RNAs and coding genes uncovers a complex regulatory network that is involved in maize seed development. *Genes* 8, 274. doi: 10.3390/genes8100274

Muhammad, W., Yang, X. X., Mehtab, M. A., Li, M. N., Zhu, L., Chen, S. S., et al. (2022). Genome-wide identification of long non-coding RNAs in two contrasting rapeseed (Brassica napus l.) genotypes subjected to cold stress. *Environ. Exp. Bot.* 201, 104969. doi: 10.1016/j.envexpbot.2022.104969

Naz, H., Aisha Akram, N., Ashraf, M., Ingo Hefft, D., and Latief Jan, B. (2022). Leaf extract of neem (Azadirachta indica) alleviates adverse effects of drought in quinoa (Chenopodium quinoa willd.) plants through alterations in biochemical attributes and antioxidants. *Saudi J. Biol. Sci.* 29, 1367–1374.

Patra, H., and Mishra, D. (1979). Pyrophosphatase, peroxidase and polyphenoloxidase activities during leaf development and senescence. *Plant Physiol.* 63, 318–323.

Pecrix, Y., Staton, S., Sallet, E., Lelandais-Brière, C., Moreau, S., Carrere, S., et al. (2018). Whole-genome landscape of medicago truncatula symbiotic genes. *Nat. Plants* 4, 1017–1025.

Pertea, M., Pertea, G. M., Antonescu, C. M., Chang, T. C., Mendell, J. T., and Salzberg, S. L. (2015). StringTie enables improved reconstruction of a transcriptome from RNA-seq reads. *Nat. Biotechnol.* 33, 290–295.

Qin, T., Zhao, H., Cui, P., Albesher, N., and Xiong, L. (2017). A nucleus-localized long non-coding RNA enhances drought and salt stress tolerance. *Plant Physiol.* 175, 00574.02017.

Qiu, Q., Guo, Y., Dietrich, M., Schumaker, K., and Zhu, J. K. (2002). Regulation of SOS1, a plasma membrane Na+/H+ exchanger in arabidopsis thaliana, by SOS2 and SOS3. *Proc. Natl. Acad. Sci. United States America* 99, 8436–8441. doi: 10.1073/pnas.122224699

Qiu, C. W., Zhao, J., Chen, Q., and Wu, F. (2019). Genome-wide characterization of drought stress responsive long non-coding RNAs in Tibetan wild barley. *Environ. Exp. Bot.* 164, 124–134.

Quiroga, G., Erice, G., Aroca, R., Zamarreño, A., Garcia-Mina, J., and Ruiz-Lozano, J. (2020). Radial water transport in arbuscular mycorrhizal maize plants under drought stress conditions is affected by indole-acetic acid (IAA) application. *J. Plant Physiol.* 246-247, 153115.

Rahim, A. A., Uzair, M., Rehman, N., Rehman, O. U., Zahra, N., and Khan, M. R. (2022). Genome-wide identification and characterization of receptor-like protein kinase 1 (RPK1) gene family in triticum aestivum under drought stress. *Front. Genet.* 13, 912251.

Salmena, L., Poliseno, L., Tay, Y., Kats, L., and Pandolfi, P. (2011). A ceRNA hypothesis: The rosetta stone of a hidden RNA language? *Cell* 146, 353–358.

Severing, E., Faino, L., Jamge, S., Busscher, M., Kuijer-Zhang, Y., Bellinazzo, F., et al. (2018). Arabidopsis thaliana ambient temperature responsive lncRNAs. *BMC Plant Biol.* 18, 145.

Shah, A., and Smith, D. L. (2020). Flavonoids in agriculture: Chemistry and roles in, biotic and abiotic stress responses, and microbial associations. *Agronomy* 10, 1209.

Shin, S. Y., Jeong, J., Lim, J. Y., Kim, T., Park, J., Kim, J. J., et al. (2018). Transcriptomic analyses of rice (Oryza sativa) genes and non-coding RNAs under nitrogen starvation using multiple omics technologies. *BMC Genomics* 19, 532.

Shu, X., Dong, Z., Zhang, M., and Shu, S. (2019). Integrated analysis identifying long non-coding RNAs (lncRNAs) for competing endogenous RNAs (ceRNAs) network-regulated palatal shelf fusion in the development of mouse cleft palate. *Ann. Trans. Med.* 7, 762.

Taleghani, D., Rajabi, A., Sadeghzadeh Hemayati, S., and Saremirad, A. (2022). Improvement and selection for drought-tolerant sugar beet (Beta vulgaris l.) pollinator lines. *Results Eng.* 13, 100367.

Tang, Z., Xu, M., Ito, H., Cai, J., Ma, X., Qin, J., et al. (2019). Deciphering the non-coding RNA-level response to arsenic stress in rice (Oryza sativa). *Plant Signaling Behav.* 14, 1–11.

Thabet, S. G., Moursi, Y. S., Sallam, A., Karam, M. A., and Alqudah, A. M. (2021). Genetic associations uncover candidate SNP markers and genes associated with salt tolerance during seedling developmental phase in barley. *Environ. Exp. Bot.* 188, 104499.

Trapnell, C., Williams, B. A., Pertea, G., Mortazavi, A., Kwan, G., van Baren, M. J., et al. (2010). Transcript assembly and quantification by RNA-seq reveals unannotated transcripts and isoform switching during cell differentiation. *Nat. Biotechnol.* 28, 511–515.

Wang, Y., Luo, X., Sun, F., Hu, J., Zha, X., Su, W., et al. (2018). Overexpressing lncRNA LAIR increases grain yield and regulates neighbouring gene cluster expression in rice. *Nat. Commun.* 9, 3516.

Wang, W. N., Min, Z., Wu, J. R., Liu, B. C., Xu, X. L., Fang, Y. L., et al. (2021). Physiological and transcriptomic analysis of Cabernet sauvginon (Vitis vinifera l.) reveals the alleviating effect of exogenous strigolactones on the response of grapevine to drought stress. *Plant Physiol. Biochem.* 167, 400–409.

Wang, T., Zhao, M., Zhang, X., Liu, M., Yang, C., Chen, Y., et al. (2017). Novel phosphate deficiency-responsive long non-coding RNAs in the legume model plant medicago truncatula. *J. Exp. Bot.* 68, 5937–5948.

Wei, L., Deng, X. G., Zhu, T., Zheng, T., Li, P. X., Wu, J. Q., et al. (2015). Ethylene is involved in brassinosteroids induced alternative respiratory pathway in cucumber (Cucumis sativus l.) seedlings response to abiotic stress. *Front. Plant Sci.* 6, 385. doi: 10.1146/annurev.arplant.55.031903.141701

Wu, H. J., Ma, Y. K., Tong, C., Wang, M., and Wang, X. J. (2012). PsRobot: A web-based plant small RNA meta-analysis toolbox. *Nucleic Acids Res.* 40, W22–W28.

Xu, Y. C., Zhang, J., Zhang, D. Y., Nan, Y. H., Ge, S., and Guo, Y. L. (2021). Identification of long noncoding natural antisense transcripts (lncNATs) correlated with drought stress response in wild rice (Oryza nivara). *BMC Genomics* 22, 424.

Yalpani, N., León, J., Lawton, M. A., and Raskin, I. (1993). Pathway of salicylic acid biosynthesis in healthy and virus-inoculated tobacco. *Plant Physiol.* 103, 315–321.

Yang, J., Zhang, N., Mi, X., Wu, L., Ma, R., Zhu, X., et al. (2014). Identification of miR159s and their target genes and expression analysis under drought stress in potato. *Comput. Biol. Chem.* 53, 204–213.

Yuan, J., Li, J., Yang, Y., Tan, C., Zhu, Y., Hu, L., et al. (2018). Stress-responsive regulation of long non-coding RNA polyadenylation in oryza sativa. *Plant J.* 93, 814–827.

Zhang, G., Duan, A. G., Zhang, J., and He, C. Y. (2016). Genome-wide analysis of long non-coding RNAs at the mature stage of sea buckthorn (Hippophae rhamnoides Linn) fruit. *Gene* 596, 130–136.

Zhang, W., Han, Z., Guo, Q., Liu, Y., Zheng, Y., Wu, F., et al. (2014). Identification of maize long non-coding RNAs responsive to drought stress. *PloS One* 9, e98958.

Zhang, T., Liang, Q., Li, C., Fu, S., Kundu, J., Zhou, X., et al. (2020). Transcriptome analysis of rice reveals the lncRNA–mRNA regulatory network in response to rice black-streaked dwarf virus infection. *Viruses* 12, 951.

Zhou, Q., Shi, J. W., Li, Z. N., Zhang, S. S., Zhang, S. T., Zhang, J. Q., et al. (2021). miR156/157 targets SPLs to regulate flowering transition, plant architecture and flower organ size in petunia. *Plant And Cell Physiol.* 62, 839–857.

Zhu, J. K. (2002). Salt and drought stress signal transduction in plants. *Annu. Rev. Plant Biol.* 53, 247–273.

Zhu, B. Z., Yang, Y. F., Li, R., Fu, D. Q., Wen, L. W., Luo, Y. B., et al. (2015). RNA Sequencing and functional analysis implicate the regulatory role of long non-coding RNAs in tomato fruit ripening. *J. Exp. Bot.* 66, 4483–4495.

Zou, C. L., Wang, Y. B., Wang, B., Liu, D., Liu, L., Li, C. F., et al. (2021). Small RNA sequencing in sugar beet under alkaline stress. *Sugar Tech* 23, 57–64.

frontiers | Frontiers in Plant Science

TYPE Original Research
PUBLISHED 20 February 2023
DOI 10.3389/fpls.2023.1090366

Check for updates

OPEN ACCESS

EDITED BY
Muhammad Waseem,
Hainan University, China

REVIEWED BY
Samar Gamal Thabet,
Fayoum University, Egypt
Umashankar Chandrasekaran,
Seoul National University, Republic of Korea

*CORRESPONDENCE
Gui-Lian Mao
fransis-0327@163.com

SPECIALTY SECTION
This article was submitted to Plant Abiotic Stress, a section of the journal Frontiers in Plant Science

RECEIVED 05 November 2022
ACCEPTED 30 January 2023
PUBLISHED 20 February 2023

CITATION
Yao X-C, Meng L-F, Zhao W-L and Mao G-L (2023) Changes in the morphology traits, anatomical structure of the leaves and transcriptome in *Lycium barbarum* L. under salt stress. *Front. Plant Sci.* 14:1090366. doi: 10.3389/fpls.2023.1090366

COPYRIGHT
© 2023 Yao, Meng, Zhao and Mao. This is an open-access article distributed under the terms of the Creative Commons Attribution License (CC BY). The use, distribution or reproduction in other forums is permitted, provided the original author(s) and the copyright owner(s) are credited and that the original publication in this journal is cited, in accordance with accepted academic practice. No use, distribution or reproduction is permitted which does not comply with these terms.

Changes in the morphology traits, anatomical structure of the leaves and transcriptome in *Lycium barbarum* L. under salt stress

Xiao-Cui Yao, Li-Fang Meng, Wang-Li Zhao and Gui-Lian Mao*

School of Life Sciences, Ningxia University, Yinchuan, China

Salt stress directly affects the growth of plants. The limitation of leaf grow is among the earliest visible effects of salt stress. However, the regulation mechanism of salt treatments on leaf shape has not been fully elucidated. We measured the morphological traits and anatomical structure. In combination with transcriptome analysis, we analyzed differentially expressed genes (DEGs) and verified the RNA-seq data by qRT-PCR. Finally, we analyzed correlation between leaf microstructure parameters and expansin genes. We show that the leaf thickness, the width, and the leaf length significantly increased at elevated salt concentrations after salt stress for 7 days. Low salt mainly promoted the increase in leaves length and width, but high salt concentration accelerated the leaf thickness. The anatomical structure results indicated that palisade mesophyll tissues contribute more to leaf thickness than spongy mesophyll tissues, which possibly contributed to the increase in leaf expansion and thickness. Moreover, a total of 3,572 DEGs were identified by RNA-seq. Notably, six of the DEGs among 92 identified genes concentrated on cell wall synthesis or modification were involved in cell wall loosening proteins. More importantly, we demonstrated that there was a strong positive correlation between the upregulated *EXLA2* gene and the thickness of the palisade tissue in *L. barbarum* leaves. These results suggested that salt stress possibly induced the expression of *EXLA2* gene, which in turn increased the thickness of *L. barbarum* leaves by promoting the longitudinal expansion of cells of the palisade tissue. This study lays a solid knowledge for revealing the underlying molecular mechanisms of leaf thickening in *L. barbarum* in response to salt stresses.

KEYWORDS

***Lycium barbarum* L., salt stress, expansin, transcriptome, leaf thickness**

1 Introduction

Soil salinization is a global environmental problem affecting the composition of ecosystems. The increasing number of salinized soils is a consequence of salinity in global warming, the evaporation rate, and over-cultivation, which has become a serious problem (Tang et al., 2015). This phenomenon of soil salinity is gradually aggravated in the future, as a

result of poor-quality irrigation water, over-applicated fertilizer, and so on. Therefore, the salt tolerance mechanism of plants, especially halophytes, faced with salt is becoming imperative to elucidate at the morphology, physiology, biochemistry, and molecular level (Lv et al., 2019). Plant leaf, as the main vegetative organ for photosynthesis and transpiration, shows one of the earliest visible effects of salinity. The restriction of leaf growth is usually considered as an important parameter to evaluate plant tolerance to salt stress (Chen et al, 2014; Avestan et al., 2021). Leaf structure is the key to evaluate leaf growth. Navarro et al. observed that the anatomical changes in *Arbutus unedo* leaves under salt stress (0, 52, and 105 mM NaCl) showed that the cell size of the second layer of palisade cells significantly increased in parallel with the levels of salinity compared with control plants (Navarro et al., 2007). Leaf growth is affected by the time and space of expansion and mesophyll cell division. Moreover, leaf thickness increases with leaf expansion, along with changes in the size and longitudinal number of mesophyll cells (Hu et al., 2022). Another research found that the leaves of cucumber seedlings became smaller and thicker in response to salt stress (Yan et al., 2020). Meanwhile, the thickness of palisade tissue, sponge tissue, and the leaf structure became loose and disordered, and the intercellular space of mesophylls was thinner under salt stress. This would be explained by salt stress promoting cell division but inhibiting lateral expansion of leaf cells (Yuan et al., 2015). As for halophytes, the rapid thickening of the leaves has been often associated with a delay in the development, but longer survival of individual leaves under saline conditions (Zeng et al., 2018). However, the precise mechanisms of leaf thickening are still understood much less.

According to the "acid growth" theory, all authors are at a consensus that auxin-mediated acidification of the leaf apoplast induces leaf growth, which results in increased cell wall extensibility (Rayle and Cleland, 1970; Neves-Piestun and Bernstein, 2001; Spartz et al., 2016; Höfte and Voxeur, 2017; Polak and Karcz, 2021). The pH around the growing plant cells spans from 4.0 to 5.5, which is also the range in which acidification activates expansion activity (Geilfus and Mühling, 2011; 2012; Cosgrove, 2017). It is noteworthy that the plant cell wall will produce appropriate responses to adapt to salt stress. In order to tolerate salt stress, the plant can alter the expression of expansin genes in the cell wall. Expansins, as one of the important factors in mediating acid-induced leaf growth, are proteins of the four subfamilies, including α-expansin (EXPA), β-expansin (EXPB), expansin-like A (EXLA), and expansin-like B (EXLB), located in the cell wall (Marowa et al., 2016). They are involved in regulating plant abiotic stress tolerance and development by facilitating cell wall expansion in a pH-dependent manner (Chen et al., 2018). In addition, expansin proteins are involved in various developmental processes such as root growth (Liu et al, 2021b; Wang et al., 2019), plant growth (Li et al., 2022a; Marowa et al., 2020), leaf growth (İncili et al., 2022), stem growth (Santiago et al., 2018), stomatal aperture regulation (Wei et al., 2011), fruit ripening and softening (Valenzuela-Riffo et al., 2020; Chen et al., 2022), and salt stress response (Chalekaei et al., 2021; İncili et al., 2022). The activity of expansin correlates with the mRNA level of the target genes, and the transcription of expansin is regulated by the growth environment (Lee and Kende, 2001; Kuluev et al., 2017; Mu et al., 2021). Although expansin was reported to respond to abiotic stress in various species, it regulates the leaf structure of *L. barbarum* to coordinate with the leaf expansion and leaf thickening under salt stress is yet unclear.

Lycium barbarum L. is the only halophytic plant of the *Lycium* group in Solanaceae family. As a saline plant, *L. barbarum* exhibits remarkable adaptability for cultivation in saline and non-salinized soils (Li et al., 2022b). Previous studies in Ningxia *L. barbarum* have focused on ion transport and homeostasis, osmotic regulation (Yuan et al., 2016; Li et al., 2022b), and photosynthesis (Ma et al., 2021). However, the physiological and molecular mechanism behind its leaf morphological changes is still elusive. The aim of this study was to characterize the mechanism of leaf growth response to salt treatment in *L. barbarum*. The growth and microstructural and transcriptomic changes in the leaves of *L. barbarum* seedlings in response to different concentrations of NaCl stress for 7 days were investigated. This study improves our understanding of salt tolerance mechanism in *L. barbarum* leaves and provide an important information to explore the measurement for improvements of salt–alkali lands.

2 Materials and methods

2.1 Plant material, growth conditions, and salt treatment

The seeds of *L. barbarum* L. (Cultivar Ningqi 10) were immersed into 1% gibberellin for 30 min, followed by 10 min of disinfection with 0.1% potassium permanganate, then were grown in soil (nutrient soil:perlite:vermiculite = 3:1:1) in an artificial climate chamber (16 h light at 24°C/6 h night at 20°C). After the seedlings had grown two cotyledons, they were transferred to Hoagland's nutrient solution for hydroponic growth; solutions were refreshed every 3 days. When seedlings reached the 10-leaf stage, salt stress was started by adding different concentrations of NaCl (0, 100, and 200 mmol·L^{-1}) to the nutrient solution for additional 7 days. Leaves for transcriptome analysis and RNA isolation were frozen in liquid nitrogen and stored at −80°C.

2.2 Leaf microscopic analysis

Five replicate leaves of each treatment were selected to measure leaf thickness, leaf length, and leaf width after 7 days of different NaCl treatments. For anatomical characterization, 1–1.5-mm-thick leaves containing main veins were cut and collected and fixed overnight in 50% formalin–acetic acid–alcohol (FAA) solution as previously described (Moll et al., 2002). The leaf segments were dehydrated with a graded alcohol concentrations and embedded in paraffin. The sections were cut at 10 μm using an optical microtome, stained with toluidine blue for 2–5 min, rinsed with distilled water, and then placed in xylene for 10 min. The leaf microstructure was examined with a microscope. Additionally, leaf thickness was quantified with a microscope (Nikon Eclipse E100, JPN) using a calibrated scale bar provided by CaseViewer software.

2.3 Determination of leaf water content and water retention

Lycium barbarum leaves treated with salt for 7 days were rinsed with distilled water, quickly drained with surface water and weighed (FW), then dried to a constant weight (DW) in an oven at 65°C. The water content and dry fresh weight specific gravity of the leaves were calculated by the following equations:

Water content % = (FW − DW)/FW_0 × 100%

Dry fresh weight specific gravity = FW/DW

The water-retaining capacity of the leaves was measured by weighing the initial fresh weight of the leaf (FW_0), then placing it on a filter paper and measuring the fresh weight (FW_0); then, the fresh weight (FW) was first measured every 2 min to every 20 min at the next 10 min for 2 h and constantly weighed (DW) in a blast furnace at 65°C. The water retention capacity was evaluated by the following formula:

Water-retaining capacity (WRC)% = (FW-DW)/(FW_0-DW) × 100%

2.4 RNA extraction and transcriptome sequencing

Total RNA was extracted from plant root samples of *L. barbarum* treated with 0, 100, and 200 mM NaCl solution using column RNA isolation kit (Qiagen, Hilden, Germany) according to the manufacturer's protocol. The RNA quality and integrity were analyzed using a NanoDrop 2000 Ultra-microspectrophotometer (Agilent Technologies, Santa Clara, CA, USA). Additionally, sequencing libraries were generated using NEBNext®Ultra™ RNA Library Prep Kit for Illumina® (NEB, USA) following the manufacturer's recommendations, and index codes were added to attribute sequences to each sample. The library preparations were sequenced on an Illumina Hiseq 2000 platform based on the manufacturer's instructions. The sequence data have been submitted to the NCBI Sequence Read Archive (https://www.ncbi.nlm.nih.gov/sra) under BioProject accession number PRJNA902940.

2.5 Transcriptome *de novo* assembly

The RNA sample of each repeat was separately sequenced. Clean data were acquired by removing spliced sequences, low-quality reads, and erroneous reads, which was assembled using Trinity software to obtain unigene sequences. *De novo* assembly and comprehensive sequence library construction were carried out with pooled clean datasets of nine samples. DIAMOND software was used to compare unigene sequences to COG, GO, KEGG, KOG, Pfam, Swiss-Prot, TrEMBL, eggnog, and NR databases, finding proteins with the highest sequence similarity to a given transcript and searching for their functional annotation. A typical cutoff e-value was set $<1.0\times10^{-5}$. Unigenes for the final annotation information was obtained using the HMMER parameter E-value ≤ $1e^{-10}$, and BLAST parameter E-value ≤ $1e^{-5}$ GO annotations were performed using the BLAST2GO (http://www.geneontology.org/) program.

2.6 DEGs analysis and functional enrichment

To assay differentially expressed genes (DEGs) between different samples, the transcripts per million (TPM) reads method was used to calculate the expression level of each transcript. Quantification of gene abundance was made with RSEM (http://deweylab.biostat.wisc.edu/rsem/). DEG analysis was performed using DESeq2 (http://www.bioconductor.org/packages/release/bioc/html/DESeq.html) software with Q-values ≤ 0.05, where DEGs with |log2FC|>1 and Q-values ≤ 0.05 were considered as significant. There were three test groups, namely, G0 (A1_A2_A3_versus_B1_B2_B3), G1 (A1_A2_A3_versus_C1_C2_C3), and G2(B1_B2_B3_versus_C1_C2_C3), that we set. In addition, functional enrichment analysis was performed on DEGs, including GO functional enrichment analysis and KEGG pathway analysis. The metabolic pathways that met this threshold were defined as those significantly enriched in DEGs, using a threshold of Q-value < 0.05 in GO terms and metabolic pathways compared to the whole transcriptome.

2.7 DEG validation by qRT-PCR analysis

Total RNA was extracted from plant roots under control and salt stress conditions using the RNAeasy Plant Mini Kit (Qiagen, Hilden, Germany). RNA purity and concentration were analyzed using a Nano Drop 2000 ultra-microspectrophotometer (Agilent Technologies, Santa Clara, CA, USA). cDNA was reversed by using TIAN Script II cDNA (Tian Gen, CHN). The quantitative real-time PCR (qRT-PCR) was performed using SYBR Green qPCR SuperMix (Tian Gen,CHN). The constitutively expressed gene actin of *L. barbarum* was used as the interreference. Primer Express 3.0 (Premier Biosoft, USA) software was used to design the primer sequences for fluorescence quantitative analysis of actin and genes involved in expansion proteins (Table 1). Each experiment was repeated at least three times, and the reaction conditions were 95°C for 3 min and 39 cycles at 95°C for 10 s, 58°C for 20s, and 72°C for 30 s. The $2^{-\Delta\Delta Ct}$ method was used to calculate the relative expression of differential genes.

2.8 Statistical analysis

All data were replicated at least three times, presented as mean ± standard error (SE), and analyzed by IBM SPSS Statistics 24 software, followed by Duncan's multiple range test at 0.05 and 0.01 level. One-way analysis of variance (ANOVA) was used for comparison between groups.

3 Results

3.1 Salinity stresses promoted the growth of leaf

Plant tolerance to salt stress was assessed by comparing changes in plant growth and leaf biomass (leaf thickness, leaf length, and leaf width). As shown in Figures 1, 2, after 7 days of 100 mmol·L^{-1} NaCl, the leaves were visibly larger and healthier compared to the control

TABLE 1 Primers used for quantitative real-time PCR analysis.

Primers	Sequence (5′→3′)	*Tm* (°C)	Purpose
EXLA2-F	TTTCTAGTGCTTCTGCCCTTCAG	59	qRT-PCR analysis
EXLA2-R	AAAGCCGATTGCTAAATTTCCA	59	
EXPA8-F	CCTCTCCAGCACTTTGATTTAGC	58	
EXPA8-R	TCCAGCTTTGTATTTGGCAATTT	59	
EXPA3-F	TGGCAATCAAACGCAGTCTTA	58	
EXPA3-R	GAGCGATGGTCACTAGCTTTGAC	59	
EXPA15-F	TGGTCACAGCTACCAATTTTTGC	60	
EXPA15-R	CACCAGCCCCCTGCTTTAT	59	
EXPA16-F	CCTAACGACAATGGAGGATGGT	59	
EXPA1f 6-R	GGCATGGCAAGGTCGAAA	59	
EXPA10-F	TGGCAAAACAACGCTTACCTT	58	
EXPA10-R	CCATCGCCTGTGGTAACCTT	59	
Actin-F	CTCACTGAAGCACCTCTC	51	Reference genes
Actin-R	ACGACCACTAGCATACAAG	51	

group. The length, width, and thickness of leaves increased by 27.31%, 36.44%, and 11.54%, respectively. This shows that it has a stimulating effect on leaf lateral direction expansion under 100 mmol·L^{-1} NaCl. Notably, 200 mmol·L^{-1} NaCl insignificantly increased the leaf thickness (up to 26.97%, $p < 0.05$) rather than the length (3.13%, $p < 0.05$) and the width (9.19%, $p < 0.05$) of *L. barbarum* leaves compared with the control group.

3.2 Salt stress induced the alteration of water content and retention of leaf

The tissue water content (TWC) and the ratio of fresh weight to dry weight (FW/DW) of the leaves were measured after 7 days salt treatments. A total of 100 mmol·L^{-1} NaCl treatment significantly prompted the increase in TWC and the ratio of FW/DW ($p<0.05$), which increased by 36.44% and 21.71% compared to the control, respectively (Figures 3A, B). However, both decreased under 200 mmol·L^{-1} NaCl stress. Meanwhile, WRC of the leaf decreased with increasing treatment concentration (Figure 3C). The WRC with 200 mmol·L^{-1} NaCl was markedly lower than that of other treatments. These results indicate that moderate salt (100 mmol·L^{-1}) could reduce the rate of water loss and increase the water retention of leaves.

3.3 Salinity stresses effected microstructure changes in leaf mesophyll cells

As shown in Figure 4, the upper and lower epidermis thicknesses were essentially affected when exposed to salt treatments. The tightly

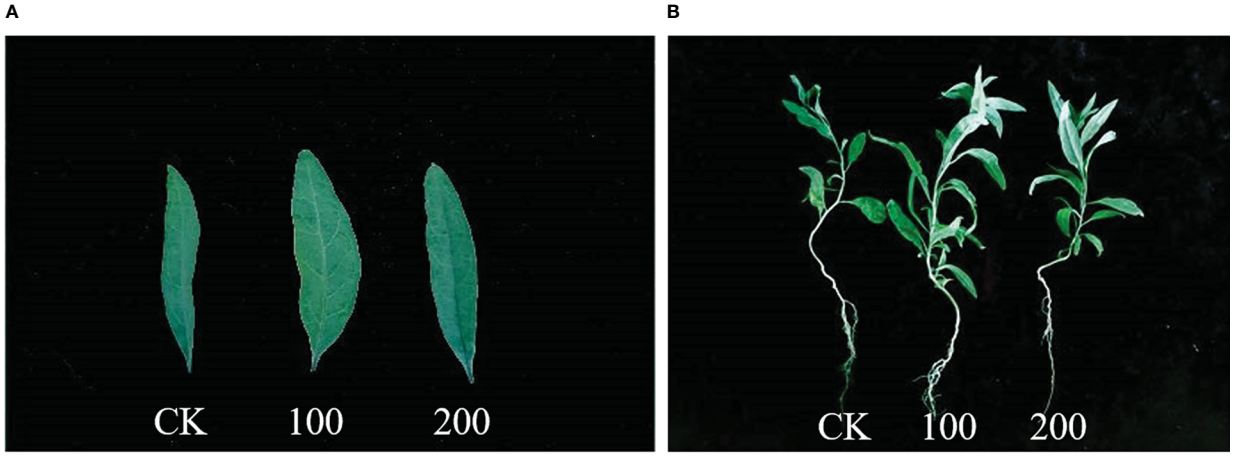


FIGURE 1
Phenotype of seedlings treated with different concentrations of salt for 7 days. **(A)** Leaf blade phenotype. **(B)** Whole plant phenotype. CK, 0 mmol·L^{-1}. 100, 100 mmol·L^{-1}. 200, 200 mmol·L^{-1}.

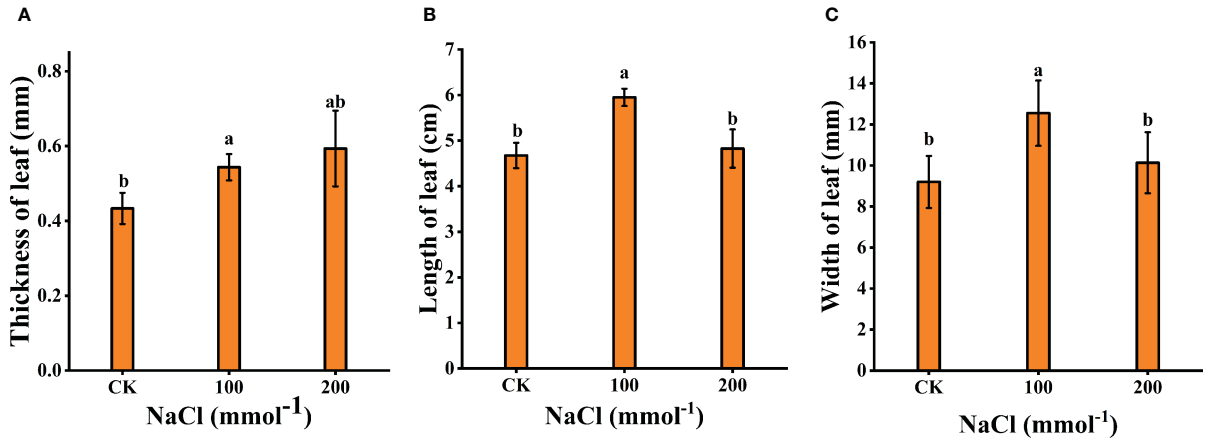


FIGURE 2
Effects of different salt concentrations on the growth of young seedlings in *Lycium barbarum* L. **(A)** Thickness of leaf. **(B)** Length of leaf. **(C)** Width of leaf. Data were analyzed by a Student's t-test; a $p<0.05$ was considered as statistically significant.

arranged mesophyll cells of *L. barbarum* leaf was found under salt stress. A larger cell density of the palisade tissue and a smaller cell size of the spongy tissue were observed. More striking was the difference in the palisade tissue; salt stress resulted in a large thickness increase especially in 200 mmol·L^{-1} NaCl treatment. Palisade tissue width was greatest at 100 mmol·L^{-1} NaCl (49.70% increased, compared with the control plants, $p<0.05$). Nonetheless, the spongy tissue thickness and palisade tissue width in salt stress showed first an increase (up to 52.56% and 49.70% under 100mmol·L^{-1} NaCl, compared with the control group, $p<0.05$) and then a decrease, which resulted in the highest ratio of palisade tissue and spongy tissue thickness (37.88%, $p<0.05$) adding 100 mmol·L^{-1} NaCl. The variation in CTR in salt treatment was consistent with that in the spongy tissue thickness. No significant difference in SR was observed under salt stress. These results indicate that NaCl stress has a significant effect on the epidermal and cellular tissue thickness of the leaves, especially 200 mmol·L^{-1} NaCl treatment. Likewise, salt stress altered the leaf vein anatomy. The main vein thickness and the vascular bundle thickness under salt stress were consistent with that in the spongy tissue thickness, increasing by 16.43% and 26.81% compared with that without salt treatment, respectively. Meanwhile, a significant increase was found in MV cell size, phloem thickness, xylem thickness, parenchyma thickness, and xylem to phloem thickness ratio with the increase in the concentration of NaCl (Table 2).

3.4 Transcriptome sequencing analysis

We selected three treatments with three biological replicates of *L. barbarum* leaves as material for RNA-seq sequencing analysis. After filtering and screening, clean data were obtained. We had performed sequence assembly with Trinity software. To reduce redundance in gene expression analysis, we saved only the longest transcript of each contig and defined them as unigenes. As shown in Table 3, a total of 90,489 unigenes were assembled, with an N50 of 1,493 unigenes. Among the assembled unigenes, approximately 38.58% ranged from

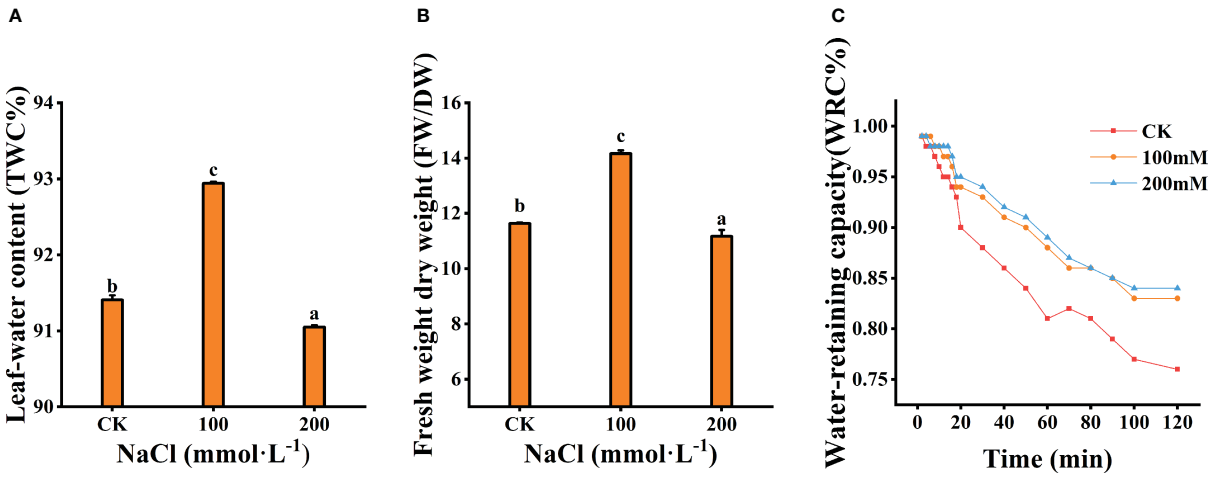


FIGURE 3
Effects of different salt concentrations on the water content and water-retaining capacity of the leaves. **(A)** Leaf-water content. **(B)** Fresh weight dry weight. **(C)** Water-retaining capacity. Data were analyzed by a Student's t-test; a $p<0.05$ was considered as statistically significant.

200 to 300 bp, whereas 23.61% ranged from 300 to 500 bp, and approximately 17.68% ranged from 500 to 1,000 bp. The unigenes between 1,000 and 2,000 bp accounted for 10.53% of all unigenes. The length of the other 9.59% of unigenes exceeded 2,000 bp. Table 4 shows that 57.69 Gb of clean data was obtained, with each sample reaching 6.03 Gb of clean data. The percentage of Q30 base was more than 92.78%; the proportion of GC was approximately 43%. These results indicated that the sequencing quality was good for the next stage of analysis. The clean data from each sample was compared to the assembled Transcript or Unigene library. The mapped ratio of clean data to transcripts ranged from 77.15% to 77.97% Table 5. The result showed that the data were reliable and could be used for subsequent analysis.

Based on genes expression in each sample, the unigene sequence was compared with the Nr, Swiss-Prot, COG, KOG, eggNOG4.5, and KEGG databases using DIAMOND software, and the KEGG Orthotogy results were obtained using KOBAS. InterProScan used the database integrated with InterPro to analyze the GO orthogonal results of the new gene. After predicting the amino acid sequence of unigene, the annotation information of unigene was obtained compared with the Pfam database by the HMMER software. Table 6 shows that TrEMBL and NR databases had the most unigenes with 32,966 (36.43%) and 32,899 (36.36%), respectively, followed by eggNOG database with 27,087 (29.93%), GO database with 25,592 (28.28%), Pfam database with 20,773 (22.96%), KEGG database with 20,621 (22.79%), and Swissprot database with 19,008 (21.01%), with the least being the KOG and COG databases with 17,075 (18.87%) and 7,530 (8.32%) unigenes, respectively. The distribution of annotated e-values based on the NR database showed that a large number of unigenes (50.88%) were less than $1E^{-50}$ (Figure 5A). When compared with the NR database, they were comparable to *Solanum tuberosum* (15.90%), *Nicotiana attenuata* (12.19%), *Nicotiana capsicum* (11.82%), *Nicotiana tomentosiformis*

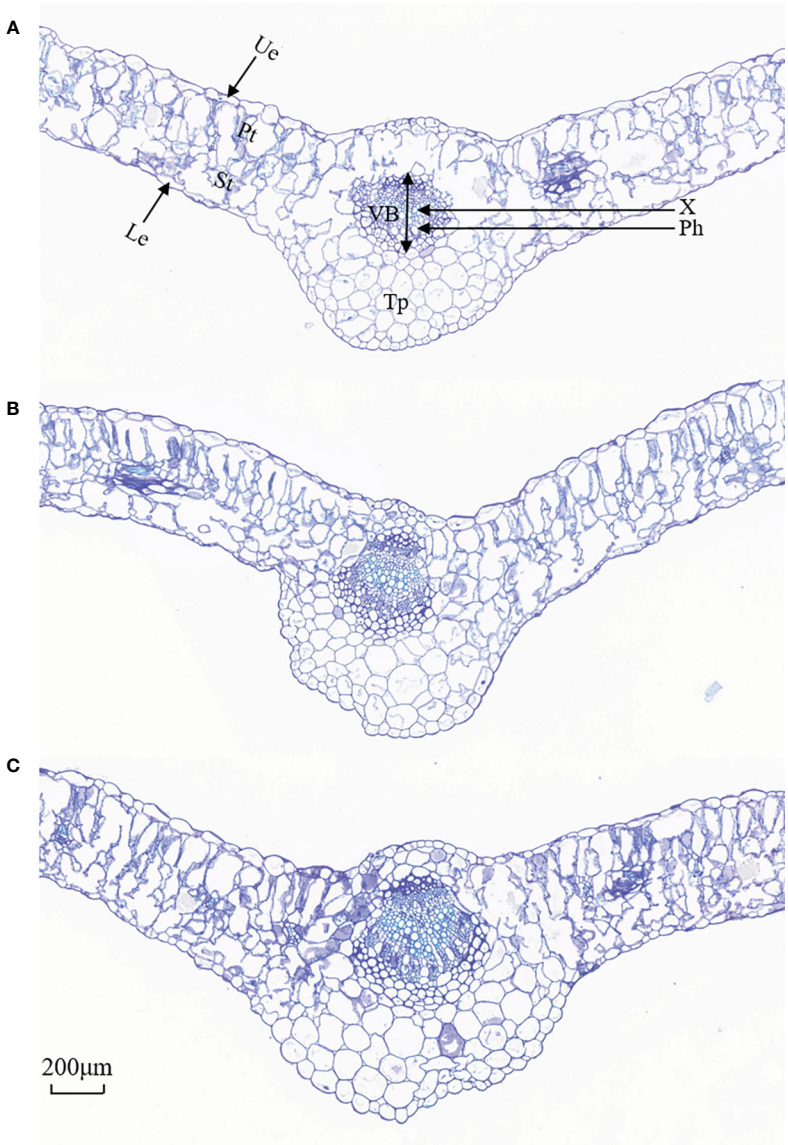


FIGURE 4
Representative images of cross-sectional structure of *Lycium barbarum* L. leaves (10×). **(A)** CK (0 mmol·L^{-1}). **(B)** 100 mmol·L^{-1}. **(C)** 200 mmol·L^{-1}. Ue, upper epidermal; Le, lower epidermis; Pt, palisade tissue; St, spongy tissue; VB, vascular bundle; X, xylem; Ph, phloem; Tp, thick parenchyma (thick angles and parenchyma).

TABLE 2 Anatomical structure parameters of leaves treated with different concentrations of *Lycium barbarum* L..

Determining quota	CK	100 mmol·L^{-1}	200 mmol·L^{-1}
Ue thickness / (μm)	24.85±11.08 a	30.12±8.78 a	32.35±6.68 a
Le thickness / (μm)	14.77±4.02 ab	15.70±3.37 b	21.91±3.91 a
Leaf thickness / (μm)	279.26±13.58 b	279.67±7.89 b	307.63±15.25 a
Pt thickness / (μm)	126.87±35.84 b	134.88±11.05 ab	154.60±26.75 a
St thickness / (μm)	80.73±9.85 b	123.16±21.70 a	99.96±8.23 c
Pt / St	0.66±0.11 b	0.91±0.10 a	0.66±0.08 b
CTR / (%)	28.82±2.29 c	43.88±6.668 a	32.46±1.25 b
SR / (%)	44.98±10.61 a	48.18±2.88 a	49.99±6.48 a
MV thickness / (μm)	596.12±4.51 b	591.14±14.81 b	694.06±20.8 a
VB thickness / (μm)	159.52±21.68 b	158.92±8.86 b	202.28±20.06 a
Ph thickness / (μm)	43.62±9.37 b	59±3.53 a	64.48±4.32 a
X thickness / (μm)	38.5±2.48 c	55.36±4.29 b	76.28±19.92 a
TP thickness / (μm)	274.44±24.05 c	300.26±25.61 ab	325.92±22.07 a
X / Ph	0.9±0.13 c	0.94±0.11 ab	1.17±0.24 a

Ue, Upper epidermal. Le, Lower epidermis. Pt, Palisade tissue. St, Spongy tissue. CTR, Tightness. SR, Looseness. MV, Medium vein. VB, Vascular Bundle. Ph, Phloem. X, Xylem. Tp, Thick parenchyma (thick angles and parenchyma).

TABLE 3 Statistical table of assembly results.

Demo Unigenes Length	Total Number	Percentage / (%)
200-300	34,910	38.58
300-500	21,367	23.61
500-1000	16,001	17.68
1000-2000	9,530	10.53
2000+	8,681	9.59
Total Number	90,489	
Total Length	69,653,536	
N50 Length	1,493	
Mean Length	7,697,458,918	

TABLE 4 Sequencing data of samples.

BMK-ID	Read Number	Base Number	GC Content / (%)	%≥Q30 / (%)
A1	21,648,604	6,471,704,060	43.25	93.82
A2	21,190,866	6,337,830,914	43.05	93.82
A3	21,234,550	6,347,845,140	43.09	94.09
B1	20,172,028	6,031,803,682	43.10	93.60
B2	21,043,998	6,294,939,350	43.34	94.01
B3	21,051,791	6,296,242,170	43.00	94.24
C1	21,956,133	6,566,957,692	42.81	94.06
C2	22,924,909	6,853,761,104	42.72	93.76
C3	21,692,405	6,486,272,634	42.78	92.78

TABLE 5 Comparison of sequencing data and assembly results.

BMK-ID	Clean Reads	Mapped Reads	Mapped Ratio/(%)
A1	21,648,604	16,845,746	77.81
A2	21,190,866	16,499,302	77.86
A3	21,234,550	16,554,069	77.96
B1	20,172,028	15,670,161	77.68
B2	21,043,998	16,409,029	77.97
B3	21,051,791	16,388,219	77.85
C1	21,956,133	16,939,895	77.15
C2	22,924,909	17,727,299	77.33
C3	21,692,405	16,833,582	77.60

(7.22%), *Nicotiana sylvestris* (6.62%), *Nicotiana tabacum* (6.59%), *Solanum pennellii* (4.48%), *Solanum lycopersicum* (4.32%), *Capsicum baccatum* (4.28%), and *Tripterygium wilfordii* (4.26%), which had higher homology (Figure 5B).

Principal component analysis (PCA) showed high similarity between biological replicates of the same group under different salt conditions (Figure 6A). Pearson correlation coefficient was used as an important indicator to evaluate the correlation between the gene expression in the nine samples. In this study, the biological replicates of the different treatments clustered together illustrate the reliability of the test (Figure 6B).

3.5 DEGs analysis and functional enrichment

A total of 3,572 DEGs were identified with salt treatments and without treatment(log2FC) ≥ 1 and p-value < 0.05). Among them, 1,542 DEGs were detected containing 634 downregulated and 908 upregulated genes, respectively, in G0_*vs*_G1 (Figure 7A). In G0_*vs*_G2, there were 2,492 DEGs containing 1,134 downregulated and 1,358 upregulated genes. Of the DEGs (1305) in G1_*vs*_G2, 597 upregulated and 708 downregulated genes were identified. Compared with the control group, the number of up- and downregulated DEGs increased with increasing salt treatment concentration. Notably, total DEGs were successfully annotated into nine public databases; among them, TrEMBL and NR databases were the most involved in annotated DEGs (Figure 7B). Figure 8 shows that a ternary Venn diagram was constructed based on a comparison of all DEGs in the salt treatment group with those in the control group, which had 442 unique DEGs in G0_*vs*_G1, 978 unique DEGs in G0_*vs*_G2, and 478 unique DEGs in G1_*vs*_G2. There are 93 DEGs in common among the three groups.

GO and KEGG analysis were performed to obtained the functional formation of DEGs. The GO items were enriched into three types, namely, biological process (BP), cellular component (CC), and molecular function (MF). The BP was mainly enriched in metabolic process, cellular process, and single-organism process; the CC was mainly enriched in the cell, cell part, and membrane, while binding, catalytic activity, and nucleic acid binding transcription factor activity were mostly enriched in MF (Figure 9). KEGG enrichment analysis showed (Figure 10) that 1,016 DEGs were annotated to 127 metabolic pathways. The over-presented pathways were phytohormone signal transduction pathway, the plant pathogen interaction pathway, and plant MAPK signaling pathway.

3.6 Candidate of the cell-wall-related DEGs response to salt stress

A total of 92 DEGs related to cell wall synthesis or modification were identified (Table 7), including xyloglucan endotransglucosylase/

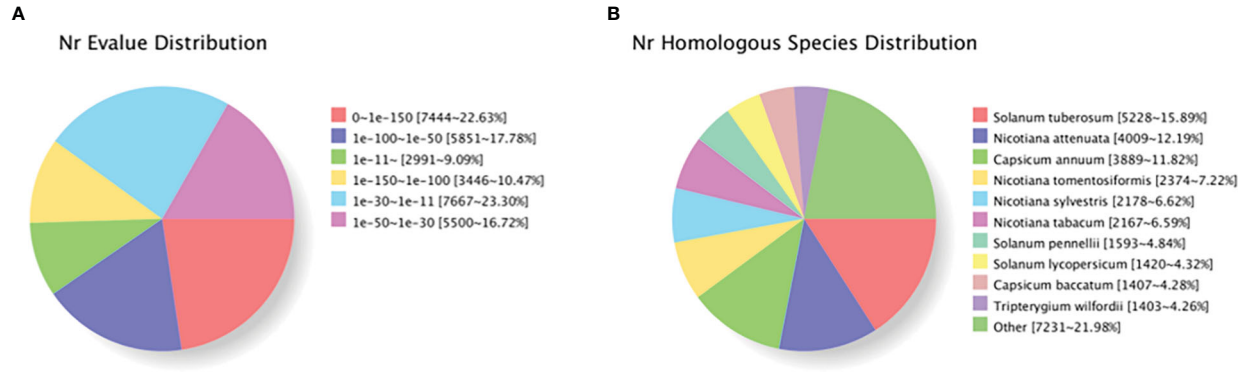


FIGURE 5
Characteristics of homology search of individual plants of *Lycium barbarum* L. using NCBI non-redundant (Nr) database. **(A)** Distribution of E-value for unique sequence blast hit with cutoff E-value of $1E^{-5}$. **(B)** Species distribution in each single-phase top BLAST with cutoff E-value of $1E^{-5}$.

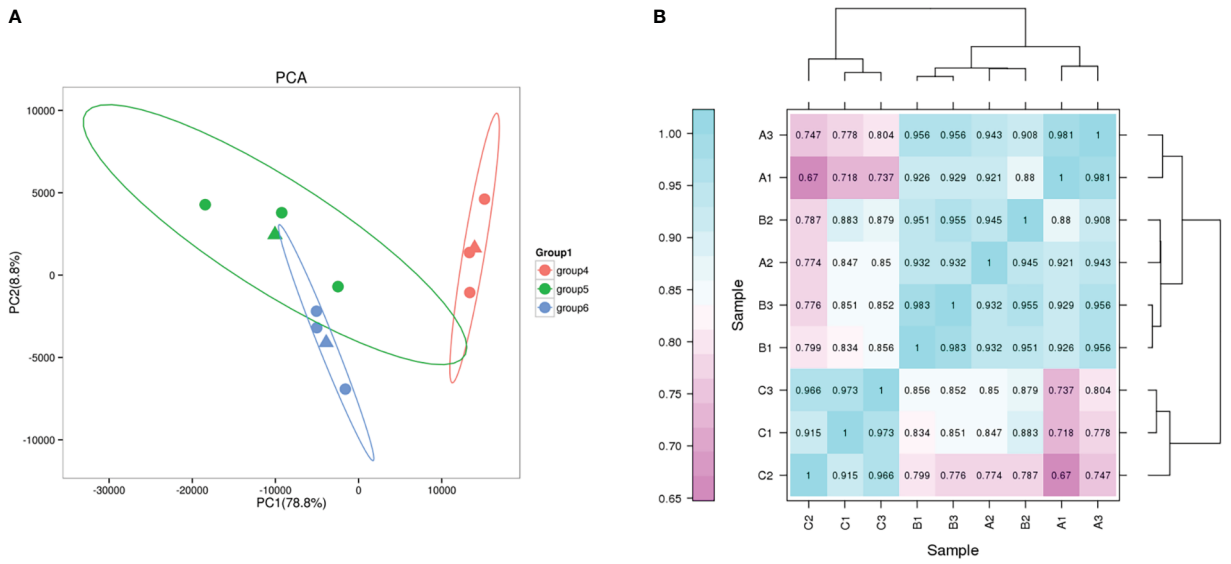


FIGURE 6
PCA and correlation analysis. **(A)** PCA plot of transcriptome profiles from different conditions. group4, G2; group5, G0; group6, G1. **(B)** Correlation analysis between different samples.

hydrolase protein, cellulose synthase, and expansin, which were mostly upregulated in leaves stressed with 200 mmol·L^{-1} NaCl. Expansins, however, were downregulated in salt stress except for the upregulated expansin-like A2 (*EXLA2*) gene.

3.7 Validation of RNA-seq data by qRT-PCR

Based on the DEGs of plants under salt stress, six genes related to the expansin proteins (*EXLA2*, *EXPA8*, *EXPA3*, *EXPA15*, *EXPA16*, and *EXPA10*) were selected for quantitative RNA-Seq and qRT-PCR. As shown in Figure 11, *EXLA2* gene expression was upregulated both in 100 mmol·L^{-1} and 200 mmol·L^{-1} NaCl. The 100 mmol·L^{-1} NaCl induced the upregulated expression of *EXPA8* and *EXPA10* by increasing 20.37% and 69.48%, respectively ($p < 0.05$), but downregulated under 200 mmol·L^{-1} NaCl, which decreased by 57.04% and 70.12%, respectively ($p < 0.05$), whereas the expression of *EXPA3*, *EXPA15*, and *EXPA16* gene was a downregulated response to salt stress. The transcriptome data were in generally agreement with qRT-PCR, indicating that the RNA-seq data were valid and reliable.

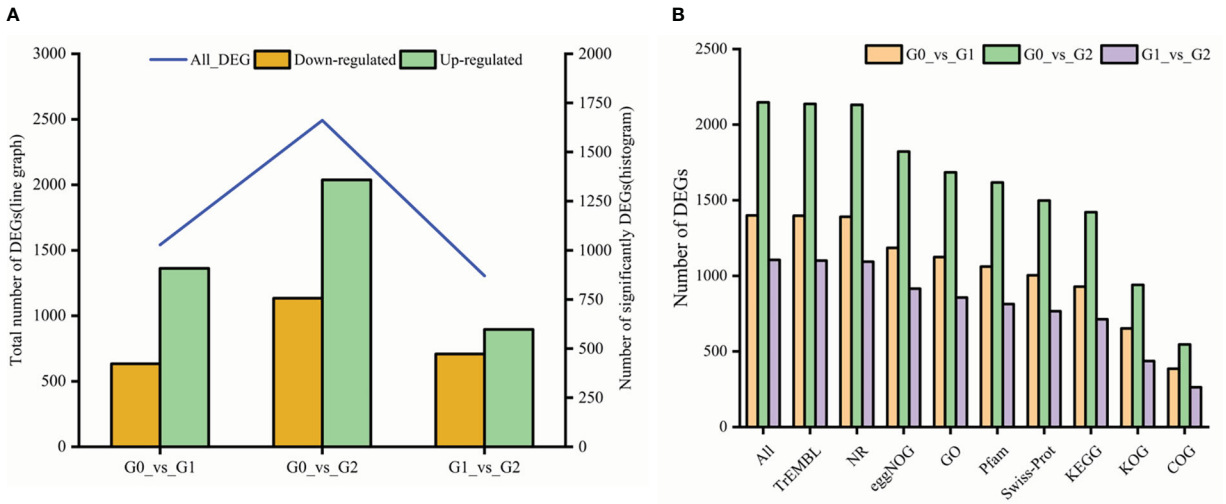


FIGURE 7
The number of differentially expressed genes (DEGs) and their functional annotations to seven public databases. **(A)** The number of DEGs were upregulated or downregulated in three groups. **(B)** All represent a total number of genes annotated in at least one the public database: TrEMBL, Translation of EMBL; NR, non-redundant nucleotide sequences; eggNOG, A database of orthologous groups of genes; GO, Gene Ontology; Pfam, Protein families; Swissprot, Swiss-Protein; KEGG, Kyoto Encyclopedia of Genes and Genomes; KOG, Eukaryotic Orthologous Groups and COG, Clusters of Orthologous Groups of proteins.

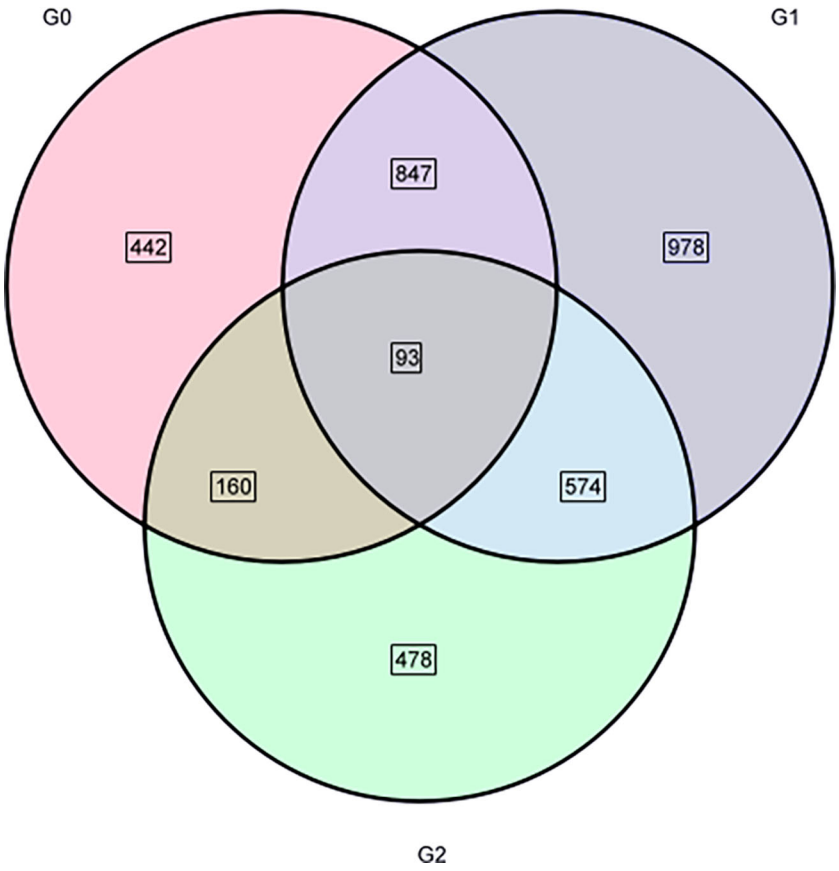


FIGURE 8
Venn diagram of the three groups of DEGs.

3.8 Correlation analysis between leaf microstructure parameters and expansin genes

There was a positive relation between salt treatment concentration and xylem and thick parenchyma ($p<0.05$) between upper epidermal thickness and firmness of cell and phloem ($p<0.05$), between lower epidermal and the ratio of xylem to phloem ($p<0.05$), and between palisade tissue thickness and expression of *EXLA2* gene. There was a positive relationship between leaf thickness and main vein thickness and vascular bundle ($p<0.05$) but a negatively correlation with *EXPA16* gene expression ($p<0.05$) (Figure 12).

4 Discussion

Salt stress can result in the total physiological metabolic level changes in plants, which ultimately cause alternation of plant phenotype. The changes in morphological characteristics in responses to salt stress in plants are considered important for evaluating salt tolerance, of which leaves growth is the most (Zhao et al., 2021). However, how the leaf growth processes vary relative to the three length, width, and thickness of *L. barbarum* is rarely studied under salt stress. A study of two goji species found improved growth at a moderate salinity (100 and 200 mM NaCl) compared with the control (Li et al., 2022b). In this study, according to the phenotype growth of *L. barbarum*, we found that low concentrations of salt (100 mmol·L^{-1} NaCl) treatment significantly promote the leaves growth of *L. barbarum* by increasing the leaves length and width determined by cell division. Low concentrations of salt stress promote the leaf growth of *L. barbarum* mainly due to long-term adaptations to salt-stressed environments, which already have a variety of heritable adaptive traits that allow them to show some degree of resilience to salt-stressed environments and have developed a high tolerance to salinity (Mohammed et al., 2021; Palchetti et al., 2021). More importantly, leaves were thicker in high salt compared to low salt in contrast to the leaf length and width. As we all know, leaves development contains cell division and cell expansion processes (Gonzalez et al., 2012; Kalve et al., 2014), which contribute to differences in leaf area in response to salt stress. It indicated that low salt induced the width and length of *L. barbarum* leaves by promoting expansion rates in longitudinal and lateral direction (Kalve et al, 2014). As for plant leaf, a certain thickness is required and worth maintaining for whole plant functioning. In this study, the leaf thickness of *L. barbarum* gradually increased with increasing salt treatment concentration; especially, there was visible thickening on the leaf thickness of *L. barbarum*, and retention of the leaves was enhanced under 200 mmol·L^{-1} NaCl treatment. Many studies have indicated that the plant tissues with strong plasticity such as leaves first undergo morphological changes under salt stress (Gómez-Bellot et al., 2015; Acosta-Motos et al., 2015a; Acosta-Motos et al., 2015b). These plants generally retain water and improve water availability by leaf thickening under salt stress to improve their salt

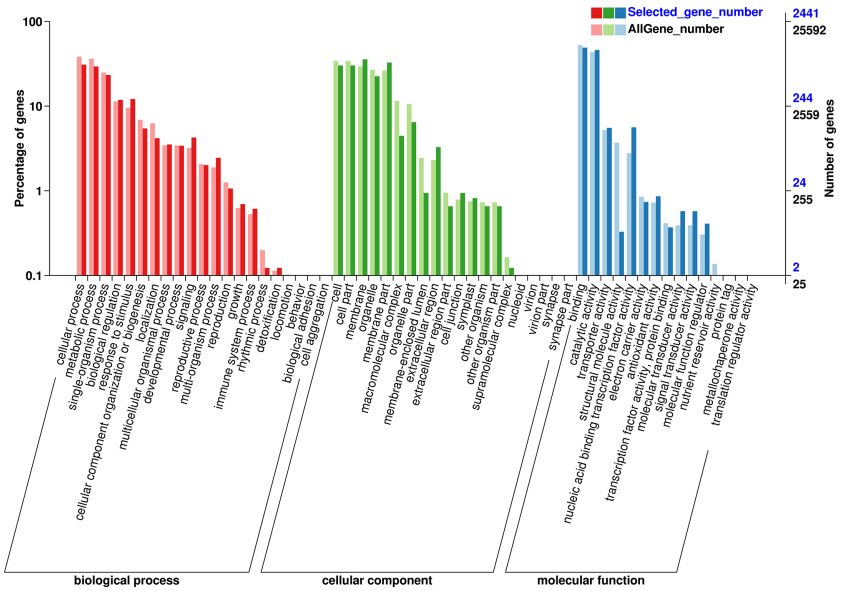


FIGURE 9
Gene ontology (GO) enrichment analysis of DEGs. GO classified as BP, CC, and MF.

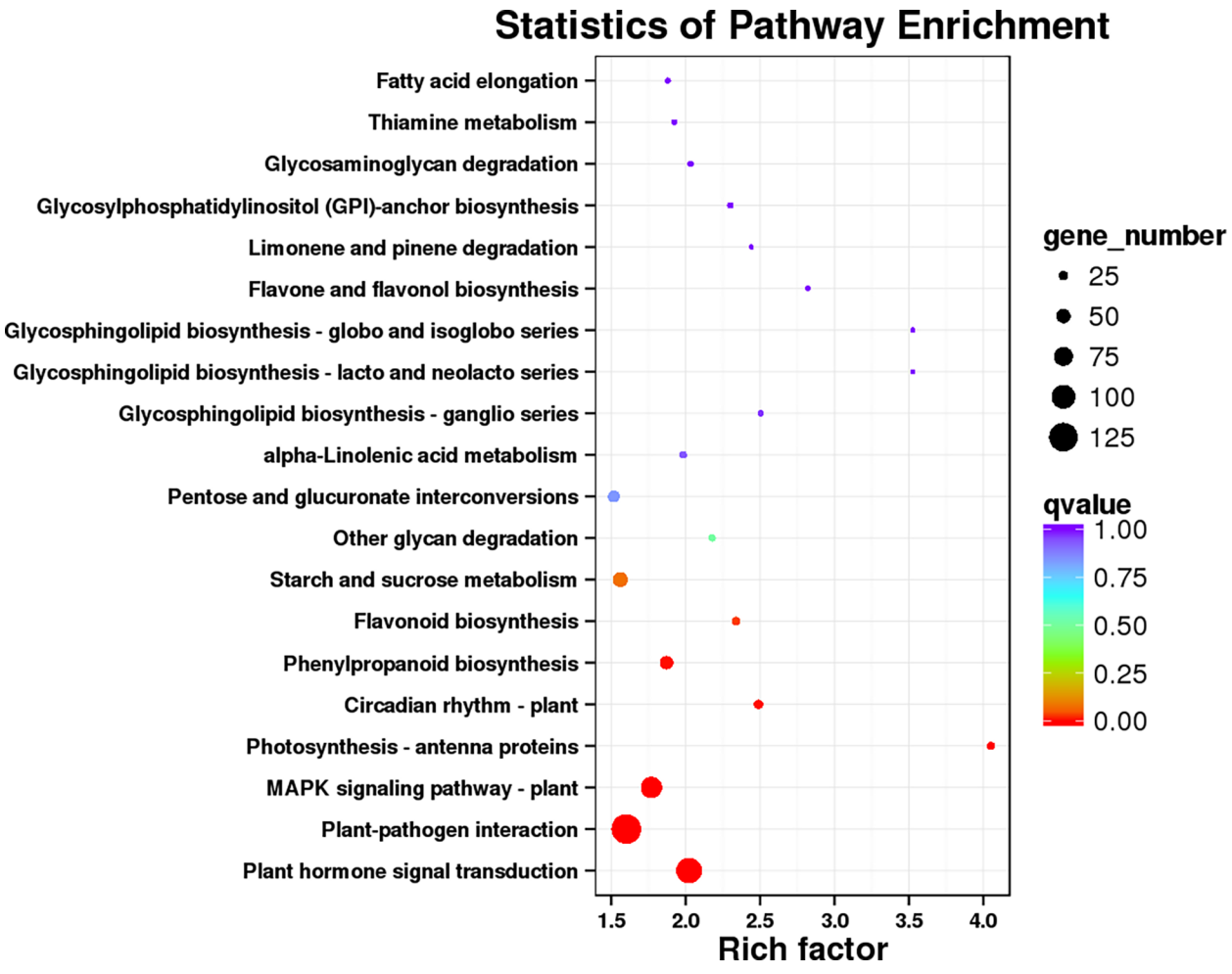


FIGURE 10
The database of KEGG enrichment analysis of DEGs.

TABLE 6 Numbers of annotated differentially expressed genes (DEG).

Anno_Database	Annotated_Number	300<=length<1000	length>=1000
COG_Annotation	7,530	1,663	4,634
GO_Annotation	25,592	8,161	12,098
KEGG_Annotation	20,621	6,222	10,555
KOG_Annotation	17,075	4,800	8,552
Pfam_Annotation	20,773	5,754	11,713
Swissprot_Annotation	19,008	5,516	10,376
TrEMBL_Annotation	32,966	11,179	14,943
eggNOG_Annotation	27,087	8,842	13,017
NR_Annotation	32,899	11,024	14,856
All_Annotated	34,988	11,770	15,030

tolerance. In this study, the leaf thickness of *L. barbarum* gradually increased with increasing salt treatment concentration; especially, the leaf thickness of *L. barbarum* was visibly thickened, and retention of the leaves was enhanced under 200 mmol·L^{-1} NaCl treatment. To a certain extent, the thickening of the leaves reduces the evaporation of water from the leaves, and the water retention capacity of the leaves increases accordingly. These results indicated that *L. barbarum* could conserve water and prevent the water transport efficiency by increasing the ability of water storage under salt stress, which is considered as an important adaptive strategy to improve their salt tolerance to halophytes (Longstreth and Nobel, 1979; Zeng et al., 2018).

In the anatomical structure of *L. barbarum* leaves, we found that the thickness of the upper and lower epidermis is significantly increased, and there were closer and more neatly arranged epidermal cells under salt stress, which were consistent with the previous research in *Arbutus unedo* leaves (Navarro et al., 2007). The palisade mesophyll tissues contribute more to leaf thickness than spongy mesophyll tissues (Table 2). Large thickness of the palisade tissue was observed when NaCl was added; the increase in the thickness of the palisade tissue can promote the synthesis of organic matter to maintain the normal metabolism of plants, thereby reducing the damage caused by salt stress (Shen et al., 2022). Palisade tissue width in salt stress increased with 100 mol L^{-1} NaCl, which indicated that low salt facilitated cell expansion. In turn, cell expansion decided leaf growth (Gonzalez et al, 2012). It could be found that the thickening of leaves was caused by the longitudinal expansion of the palisade tissue and cells with salt application; the cells expanded toward the periphery with the leaf expansion. This was consistent with the research in which the thickening of the leaves was caused by the elongation of the palisade tissue in the response of *Myrtus communis* L. and *Eugenia myrtifolia* L. salt stress (Acosta-Motos et al., 2015a; Acosta-Motos et al., 2015b). It indicated that the leaf thickening of *L. barbarum* under salt stress was caused by the volume expansion of various cells in the leaves toward various dimensions. This phenomenon lays a structural foundation for the storage of nutrients in leaves to salt stress tolerance. In addition, salt stress also could produce different effects on plant leaf vein *via* the xylem area, which was reported in *Iperata cylindrica* (L.) Raeuschel as well (Hameed et al., 2009). The present study found that under the salt stress, the leaf vein thickness of *L. barbarum* increased in response to high salt treatment (200 mmol·L^{-1}), indicating that *L. barbarum* could improve their ability to absorb water and nutrients and reduce water loss, thus increasing the relative water content of plants by increasing the thickness of phloem and xylem and the size of vascular bundles under salt stress (Li, 2022).

What is the underlying molecular mechanism of significant morphological changes in leaves by genes regulation in *L. barbarum* under salt stress? We identified 90,489 genes that were expressed among the leaves of *L. barbarum* through high-throughput Illumina sequencing, from which 3,572 DEGs were gained by GO enrichment; KEGG pathways enrichment analysis showed that salt stress induced the expression of 92 DEGs mostly upregulated and involved in cell wall synthesis or modification (Table 7). Plant cell walls are mainly composed of hemicellulose, cellulose, pectin, and so on (Kong et al, 2018). Among them, CESA is the key enzyme involved in cellulose synthesis (Turner and Kumar, 2018), xyloglucan and glucomannan in hemicellulose synthesis (Kumar et al., 2018), and PME and PAE in pectin synthesis (Kumar et al., 2018). Furthermore, XTH and expansin are key enzymes involved in cell wall loosening to promote cell elongation (Kumar et al., 2018). We found that most of these genes were unregulated, which protected plant cells from salt hurt *via* regulation of the metabolic process of the plant cell wall (CW) (Table 7). Previous studies have reported that salt stress has complicated effects on the expression of cell-wall-related genes (Qin et al., 2021). As a main component of cell wall, expansin plays a vital role in plant to abiotic stress tolerance by mediating cell wall expansion (Liu et al., 2021a; Sampedro and Cosgrove, 2005). In this study, we identified six DEGs related to expansin, and the expression of *EXLA2* gene was upregulated with the increase in salt stress. Abuqamar et al. determined the expression of *AtEXLA2* in response to salt stress. *AtEXLA2* was upregulated to salt, which indicates that plant responses to salinity stress can regulate *AtEXLA2* expression (Abuqamar et al., 2013). In addition, we hypothesized that the unregulated expression of *EXLA2* gene was related to the leaf thickening of *L. barbarum* in response to salt stress. It was observed

10.3389/fpls.2023.1090366

TABLE 7 Cell wall biosynthesis/modification related DEGs.

ID	G0_vs_G1	G0_vs_G2	G1_vs_G2	gene	family
c33306.graph_c0	normal	normal	down	XTH6	xyloglucan endotransglucosylase/hydrolase dsprotein
c41322.graph_c0	normal	Up	up	XTH15	
c51681.graph_c0	up	normal	normal	XTH8	
c56789.graph_c2	normal	Up	normal	XTH	
c59110.graph_c1	up	Up	normal	XTH	
c61562.graph_c0	up	Up	normal	XTH9	
c62703.graph_c1	up	Up	normal	XTH30	
c64658.graph_c0	normal	Up	up	XTH8	
c66853.graph_c0	up	Up	normal	XTH27	
c66916.graph_c1	up	Up	normal	XTH22	
c67790.graph_c1	up	normal	down	XTH27	
c68064.graph_c1	down	down	normal	XTH31	
c69153.graph_c0	normal	Up	up	XTH23	
c66690.graph_c2	normal	Up	up	XTH	
c66690.graph_c6	normal	Up	up	XTH	
c68053.graph_c3	normal	Up	up	CSLC4	Xyloglucan glycosyltransferase
c69088.graph_c0	up	Up	down	WAK2	Wall-associated receptor kinase
c48003.graph_c2	normal	Up	normal	GAE6	UDP-glucuronate 4-epimerase
c62137.graph_c0	up	normal	normal	GAE6	
c66557.graph_c4	up	Up	normal	GAE6	
c70710.graph_c0	normal	Up	normal	GAE1	
c56198.graph_c1	normal	Up	normal	MUR4	UDP-arabinose 4-epimerase
c59089.graph_c0	normal	normal	down	GUX1	UDP-glucuronate
c62425.graph_c0	normal	Up	normal	UGD3	UDP-glucose 6-dehydrogenase
c64302.graph_c0	normal	Up	normal	UGD3	
c54084.graph_c0	normal	down	down	TBL28	trichome birefringence-like
c56452.graph_c1	normal	down	down	TBL36	
c62826.graph_c0	up	Up	normal	TBL39	
c41860.graph_c0	normal	normal	down	SUS6	Sucrose synthase
c41860.graph_c1	normal	normal	down	SUS6	
c69754.graph_c1	normal	down	normal	SBT3.4	Subtilisin-like
c69836.graph_c1	normal	down	down	LRK10	Rust resistance kinase
c58120.graph_c0	normal	down	down	At2g20870	Putative cell wall protein
c69469.graph_c1	up	normal	normal	PR5K	PR5-like receptor kinase
c68705.graph_c3	up	normal	normal	PGIP2	Polygalacturonase inhibitor
c41672.graph_c0	up	Up	normal	PME41	pectinesterase
c53737.graph_c0	down	normal	up	PECS-2.1	
c57833.graph_c0	normal	normal	down	PME29	
c62749.graph_c0	normal	normal	down	PME22	
c65008.graph_c2	up	normal	normal	PME	

(Continued)

TABLE 7 Continued

ID	G0_vs_G1	G0_vs_G2	G1_vs_G2	gene	family
c63704.graph_c0	up	normal	normal	PAE12	Pectin acetylesterase
c69320.graph_c1	up	normal	normal	PAE8	
c70062.graph_c0	down	down	normal	PAE11	
c53520.graph_c0	normal	normal	down	ERECTA	LRR receptor-like serine/threonine-protein kinase
c61237.graph_c1	normal	down	down	IRK	
c65748.graph_c2	up	normal	down	RGI3	
c65916.graph_c0	up	Up	normal	At1g74360	
c61801.graph_c0	normal	down	down	RPK2	
c68769.graph_c1	up	Up	normal	RGI3	
c69760.graph_c3	normal	Up	normal	At1g56140	
c62971.graph_c0	normal	down	normal	PXC1	Leucine-rich repeat receptor-like protein
c69459.graph_c5	up	Up	up	At5g35370	G-type lectin S-receptor-like serine/threonine-protein
c60817.graph_c0	up	Up	normal	RCOM_0530710	Glycosyl transferase family
c70219.graph_c0	up	normal	normal	GRP-1	Glycine-rich cell wall structural protein
c57498.graph_c0	normal	normal	down	CSLA2	Glucomannan 4-beta-mannosyltransferase
c57498.graph_c1	normal	normal	down	CSLA2	
c65626.graph_c4	up	Up	normal	CSLA9	
c68899.graph_c1	normal	normal	down	CSLA9	
c70541.graph_c0	normal	normal	down	CSLA9	
c50767.graph_c1	up	Up	normal	GATL9	Galacturonosyltransferase-like
c54030.graph_c0	up	Up	normal	GATL1	
c62099.graph_c0	normal	normal	down	GAUT12	Galacturonosyltransferase
c67662.graph_c0	normal	Up	normal	GAUT5	
c63141.graph_c0	up	Up	normal	FLA9	Fasciclin-like arabinogalactan protein
c49912.graph_c0	normal	normal	down	EXPA10	Expansin
c51480.graph_c0	normal	down	down	EXPA3	
c55782.graph_c0	normal	down	down	EXPA8	
c56797.graph_c0	normal	down	normal	EXPA3	
c59033.graph_c0	normal	down	–	EXPA1	
c59033.graph_c1	normal	down	down	EXPA15	
c60996.graph_c0	normal	down	–	EXPA15	
c68991.graph_c1	up	Up	normal	EXL2	EXORDIUM-like
c62854.graph_c1	normal	Up	normal	CHN48	Endochitinase
c41993.graph_c0	down	down	normal	DFRA	Dihydroflavonol 4-reductase
c54143.graph_c1	down	normal	normal	SNL6	Cinnamoyl-CoA reductase-like
c54042.graph_c0	normal	down	normal	CSP41B	Chloroplast stem-loop binding
c57123.graph_c0	normal	–	down	CSLD5	
c57123.graph_c1	up	–	down	CSLD5	
c62228.graph_c0	down	normal	normal	CSLG3	
c66029.graph_c0	normal	up	up	CSLD3	

(Continued)

TABLE 7 Continued

ID	G0_vs_G1	G0_vs_G2	G1_vs_G2	gene	family
c69291.graph_c0	normal	down	normal	CSLG2	
c69518.graph_c2	normal	up	normal	CSLE6	
c69518.graph_c3	normal	up	normal	CSLE6	
c69555.graph_c2	normal	up	up	CSLD3	
c59403.graph_c2	up	up	normal	CESA1	Cellulose synthase
c61874.graph_c0	normal	normal	down	CESA4	
c40836.graph_c0	down	normal	normal	C/VIF1	Cell wall / vacuolar inhibitor of fructosidase
c60331.graph_c0	normal	up	up	C/VIF2	
c64996.graph_c0	normal	normal	down	CDC2C	Cell division control protein
c63747.graph_c0	up	up	normal	CALS12	Callose synthase
c62512.graph_c0	normal	normal	down	IRX9	Beta-1,4-xylosyltransferase
c66442.graph_c2	normal	up	normal	RHM1	UDP-glucose 4,6-dehydratase

All the data in the table |log2FC| > 1 and Q value ≤0.05.

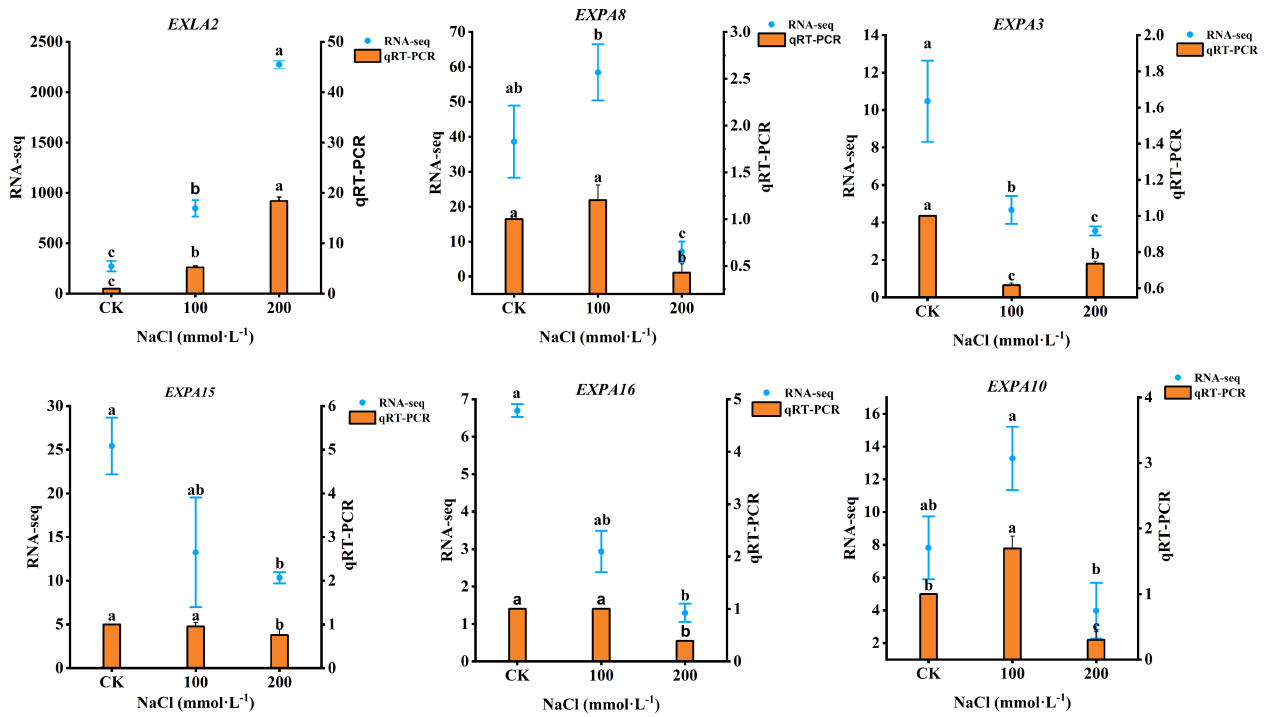


FIGURE 11
qRT-PCR results showing the mRNA expression level of six genes. Data were analyzed by a Student's t-test; a $p<0.05$ was considered as statistically significant.

in the microstructure that salt concentration promoted leaf thickening due to the enlargement of palisade tissue and cells, which associated with changes in the cell wall composition. To prove our hypothesis, in this regard, we correlated leaf microstructure with gene expression analysis of expansion. Correlation analysis showed that the expression of *EXLA2* gene was positively correlated with palisade tissue thickness. Previous studies showed that a certain concentration of salt stress can promote the activity of tonoplast H^+-ATPase and plasma membrane H^+-ATPase in *Arabidopsis thaliana* and *L. barbarum* cell membranes, acidify the cell wall by pumping out protons from the cell membrane, and promote the activation of expansin (Bulle et al., 2016). In this study, our hypothetical idea was further reinforced, namely, high expression of *EXLA2* gene induced response to salt stress, comparted excess salt ions into the cell wall with succulent tissue by proton pump H^+-ATPase, promoted the thickness of palisade tissue and cells, which made thickened leaves to adapt to salt stress (Abuqamar et al., 2013). In addition, the other expansions including *EXPA3*, *EXPA8*, *EXPA15*, *EXPA16*, and *EXPA10* genes were all downregulated in response to

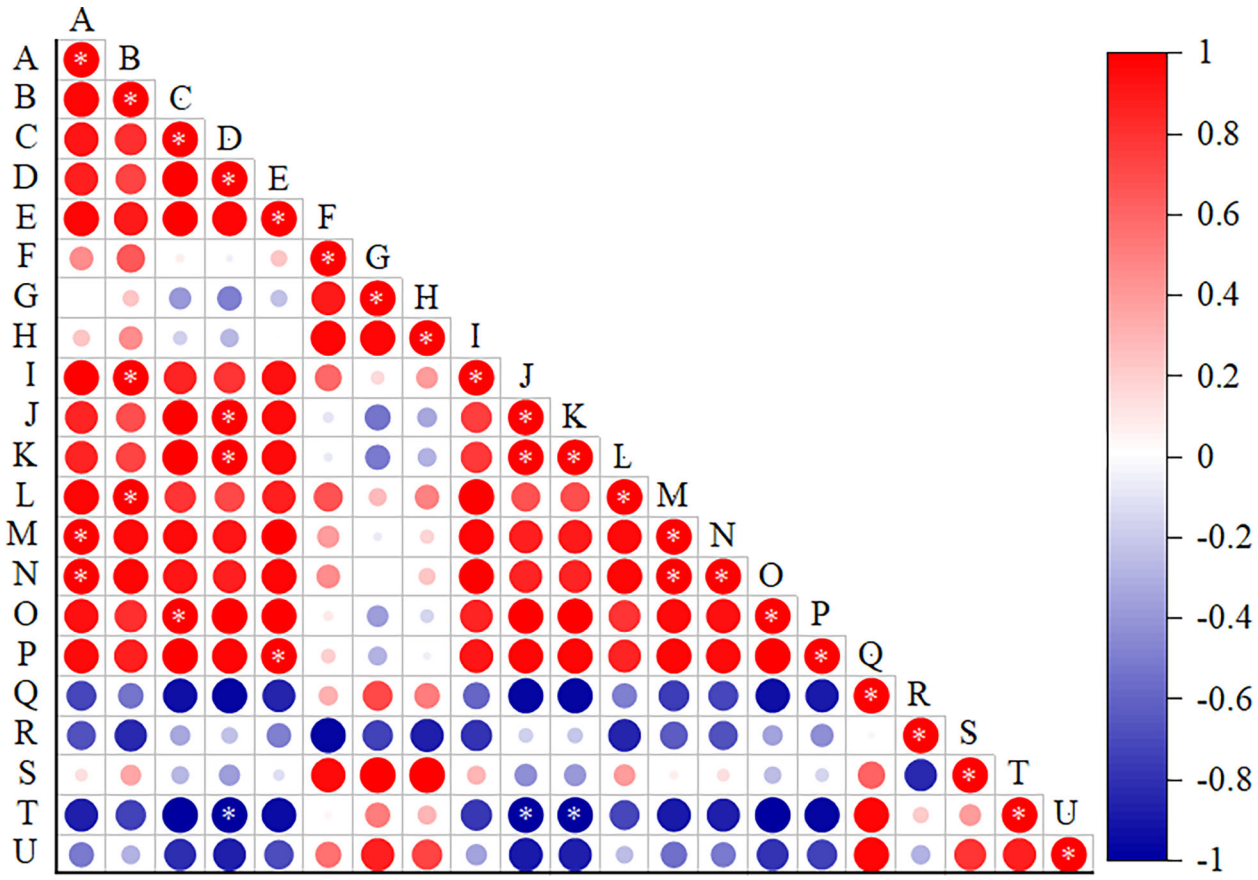


FIGURE 12
Correlation analysis of the leaf microstructural indicators and expansin genes. **(A)** Salt concentration, **(B)** Ue thickness, **(C)** Le thickness, **(D)** leaf thickness, **(E)** Pt thickness, **(F)** St thickness, **(G)** Pt/St, **(H)** CTR, **(I)** SR, **(J)** MV thickness, **(K)** VB thickness, **(L)** Ph thickness, **(M)** X thickness, **(N)** TP thickness, **(O)** X/Ph, and **(P–U)** expression levels of *EXLA2*, *EXPA8*, *EXPA3*, *EXPA15*, *EXPA16*, and *EXPA10*. Data were analyzed by a Student's t-test; a $p<0.05$ was considered as statistically significant.

200 mmol·L^{-1} NaCl stress. It properly implied that high NaCl stress inhibited the expression of these genes, indicating that different expansin genes have different functions faced salt stress. These results will inform our further research into the potential molecular mechanisms of leaf thickening in *L. barbarum* in response to salt stress.

5 Conclusion

Low concentrations of salt (100 mmol·L^{-1}NaCl) treatment significantly promote the leaves growth of *L. barbarum* by increasing the leaves length and width. In the country, high salt stress promoted the thickening of the leaves, increased leaves thickness, reduced water loss, and increased the water retention capacity of the leaves. The palisade mesophyll tissues contribute more to leaf expansion and thickness. Additionally, high salt treatment induced the thickness of leaves main vein, phloem and xylem thickness, vascular bundle size, and parenchyma thickness, which improve their ability to absorb water and nutrients and reduces water loss. Transcriptome analysis further revealed the expression of multiple expansin-related DEGs in *L. barbarum* leaves treated with different salt concentrations for 7 days. There were six expansin proteins that were screened; the expression of *EXLA2* gene was upregulated with the increase in salt stress, which promoted the expansion of palisade tissue cells, thereby increasing the leaf thickness. Therefore, further study is needed to define functions of *EXLA2* gene in the future. Our study thus provided information for further understanding the molecular mechanism and salt tolerance of *L. barbarum* by leaf thickening.

Data availability statement

The original contributions presented in the study are publicly available. This data can be found here: NCBI, PRJNA902940.

Author contributions

X-CY: conceptualization, formal analysis, data curation, investigation, methodology, software, and writing—original draft. L-FM: conceptualization, data curation, formal analysis, investigation, methodology, software, and writing—original draft. W-LZ: validation.

G-LM: conceptualization, supervision, funding acquisition, project administration, resources, and writing—review and editing. All authors contributed to the article and approved the submitted version.

Funding

This study was supported by grant of National Natural Science Foundation of China (NSFC) (32260408) and National key research and development program of China (2021YFD1900600).

Acknowledgments

We would like to thank Mr. Yan Long Li from Ningxia Academy of Agricultural and Forestry Science for his assistance in gene sequence of qRT-PCR.

Conflict of interest

The authors declare that they have no known competing financial interests or personal relationships that could have appeared to influence the work reported in this paper.

Publisher's note

All claims expressed in this article are solely those of the authors and do not necessarily represent those of their affiliated organizations, or those of the publisher, the editors and the reviewers. Any product that may be evaluated in this article, or claim that may be made by its manufacturer, is not guaranteed or endorsed by the publisher.

References

Abuqamar, S., Ajeb, S., Sham, A., Enan, M. R., and Iratni, R. (2013). A mutation in the expansin-like A2 gene enhances resistance to necrotrophic fungi and hypersensitivity to abiotic stress in arabidopsis thaliana. *Mol. Plant Pathol.* 14 (8), 813–827. doi: 10.1111/mpp.12049

Acosta-Motos, J. R., Diaz-Vivancos, P., Álvarez, S., Fernández-García, N., Sánchez-Blanco, M. J., and Hernández, J. A. (2015a). NaCl-Induced physiological and biochemical adaptative mechanisms in the ornamental *Myrtus communis* l. plants. *J. Plant Physiol.* 183, 41–51. doi: 10.1016/j.jplph.2015.05.005

Acosta-Motos, J. R., Diaz-Vivancos, P., Álvarez, S., Fernández-García, N., Sanchez-Blanco, M. J., and Hernández, J. A. (2015b). Physiological and biochemical mechanisms of the ornamental *Eugenia myrtifolia* l. plants for coping with NaCl stress and recovery. *Planta.* 242 (4), 829–846. doi: 10.1007/s00425-015-2315-3

Avestan, S., Ghasemnezhad, M., Esfahani, M., and Barker, A. V. (2021). Effects of nanosilicon dioxide on leaf anatomy, chlorophyll fluorescence, and mineral element composition of strawberry under salinity stress. *J. Plant Nutr.* 44 (20), 3005–3019. doi: 10.1080/01904167.2021.1936036

Bulle, M., Yarra, R., and Abbagani, S. (2016). Enhanced salinity stress tolerance in transgenic chilli pepper (*Capsicum annuum* l.) plants overexpressing the wheat antiporter (*TaNHX2*) gene. *Mol. Breeding.* 36 (4). doi: 10.1007/s11032-016-0451-5

Chalekaei, M., Abbasi, A., Yousefi, S., and Dadashiet, D. (2021). Over-expression of *AtEXPB2* alleviates salt stress damage in transgenic tobacco plants. *Russ J. Plant Physiol.* 68, 274–285. doi: 10.1134/S1021443721020035

Chen, M., Mishra, S., Heckathorn, S. A., Frantz, J. M., and Krause, C. (2014). Proteomic analysis of arabidopsis thaliana leaves in response to acute boron deficiency and toxicity reveals effects on photosynthesis, carbohydrate metabolism, and protein synthesis. *J. Plant Physiol.* 171, 235–242. doi: 10.1016/j.jplph.2013.07.008

Chen, Y. H., Xie, B., An, X. H., Ma, R. P., Zhao, D. Y., Cheng, C. G., et al. (2022). Overexpression of the apple expansin-like gene *MdEXLB1* accelerates the softening of fruit texture in tomato. *J. Integr. Agric.* 21 (12), 3578–88. doi: 10.1016/j.jia.2022.08.030

Chen, L. J., Zou, W. S., Fei, C. Y., Wu, G., Li, X. Y., Lin, H. H., et al. (2018). α-expansin *EXPA4* positively regulates abiotic stress tolerance but negatively regulates pathogen resistance in nicotiana tabacum. *Plant Cell Physiol.* 59 (11), 2317–2330. doi: 10.1093/pcp/pcy155

Cosgrove, D. J. (2017). Diffuse growth of plant cell walls. *Plant Physiol.* 176 (1), 16–27. doi: 10.1104/pp.17.01541

Geilfus, C.-M., and Mühling, K. H. (2011). Transient alkalinization in the leaf apoplast of vicia faba l. depends on NaCl stress intensity: An *in situ* ratio imaging study. *Plant Cell Environ.* 35 (3), 578–587. doi: 10.1111/j.1365-3040.2011.02437

Geilfus, C.-M., and Mühling, K.-H. (2012). Ratiometric monitoring of transient apoplastic alkalinizations in the leaf apoplast of living vicia faba plants: Chloride primes and PM-H^+-ATPase shapes NaCl-induced systemic alkalinizations. *New Phytologist.* 197 (4), 1117–1129. doi: 10.1111/nph.12046

Gómez-Bellot, M. J., Nortes, P. A., Ortuño, M. F., Romero, C., Fernández-García, N., and Sánchez-Blanco, M. J. (2015). Influence of arbuscular mycorrhizal fungi and treated wastewater on water relations and leaf structure alterations of *Viburnum tinus* l. plants during both saline and recovery periods. *J. Plant Physiol.* 188, 96–105. doi: 10.1016/j.jplph.2015.09.007

Gonzalez, N., Vanhaeren, H., and Inzé, D. (2012). Leaf size control: complex coordination of cell division and expansion. *Trends Plant Sci.* 17 (6), 332–340. doi: 10.1016/j.tplants.2012.02.003

Hameed, M., Ashraf, M., and Naz, N. (2009). Anatomical adaptations to salinity in cogon grass [Imperata cylindrica (L.) raeuschel] from the salt range, Pakistan. *Plant Soil.* 322, 229–238. doi: 10.1007/s11104-009-9911-6

Höfte, H., and Voxeur, A. (2017). Plant cell walls. *Curr. Biol.* 27 (17), 865–870. doi: 10.1016/j.cub.2017.05.025

Hu, W. S., Lu, Z. F., Gu, H. H., Ye, X. L., Liu, X. K., Cong, R. H., et al. (2022). Potassium availability influences the mesophyll structure to coordinate the conductance of CO_2 and H_2O during leaf expansion. *Plant Cell Environment.* 45 (10), 2987–3000. doi: 10.1111/pce.14405

İncili, Ç.Y., Arslan, B., Çelik, E. N. Y., Ulu, F., Horuz, E., Baloglu, M. C., et al. (2022). Comparative bioinformatics analysis and abiotic stress responses of expansin proteins in cucurbitaceae members: watermelon and melon. *Protoplasma.* 1–19. doi: 10.1007/s00709-022-01793-8

Kalve, S., Fotschki, J., Beeckman, T., Vissenberg, K., and Beemster, G. T. (2014). Three-dimensional patterns of cell division and expansion throughout the development of *Arabidopsis thaliana* leaves. *J. Experimental Botany* 65, 22, 6385–6397. doi: 10.1093/jxb/eru358

Kong, Y., O'Neill, M., and Zhou, G. (2018). Plant cell walls: Isolation and monosaccharide composition analysis. *Methods Mol. Biol.* 1744, 313–319. doi: 10.1007/978-1-4939-7672-0-25

Kuluev, B. R., Knyazev, A. V., Mikhaylova, E. V., and Chemeris, A. V. (2017). The role of expansin genes *PtrEXPA3* and *PnEXPA3* in the regulation of leaf growth in poplar. *Russ J. Genet.* 53, 651–660. doi: 10.1134/s1022795417060084

Kumar, M., Mishra, L., Carr, P., Pilling, M., Gardner, P., Mansfield, S. D., et al. (2018). Exploiting CELLULOSE SYNTHASE (CESA) class specificity to probe cellulose microfibril biosynthesis. *Plant Physiol.* 177 (1), 151–167. doi: 10.1104/pp.18.00263

Lee, Y., and Kende, H. (2001). Expression of beta-expansins is correlated with internodal elongation in deepwater rice. *Plant Physiol* 127 (2), 645–654.

Li, J., Liu, Z., Gao, C., Miao, Y., and Cui, K. (2022a). Overexpression of *DsEXLA2* gene from dendrocalamus sinicus accelerates the plant growth rate of arabidopsis. *Phytochemistry.* 199, 113178. doi: 10.1016/j.phytochem.2022.113178

Li, W. N., Rao, S. P., Du, C., Li, P., Dai, G. L., and Chen, J. H. (2022b). Strategies used by two goji species, lycium ruthenicum and lycium barbarum, to defend against salt stress. *Scientia Hortic.* 306, 111430. doi: 10.1016/j.scienta.2022.111430

Liu, C., Fu, M., Guo, F., and Wu, C. (2021a). Genome-wide identification of expansin gene family in barley and drought-related expansins identification based on RNA-seq. *Genetica* 149 (5-6), 283–297. doi: 10.1007/s10709-021-00136-4

Liu, W., Xu, L., Lin, H., and Cao, J. (2021b). Two expansin genes, *AtEXPA4* and *AtEXPB5*, are redundantly required for pollen tube growth and *AtEXPA4* is involved in primary root elongation in arabidopsis thaliana. *Genes.* 12 (2), 249. doi: 10.3390/genes12020249

Longstreth, D. J., and Nobel, P. S. (1979). Salinity effects on leaf anatomy: Consequences for photosynthesis. *Plant Physiol.* 63 (4), 700–3. doi: 10.1104/pp.63.4.700

Lv, B., Wu, Q., Wang, A., Li, Q., Dong, Q., Yang, J., et al. (2019). A WRKY transcription factor, FtWRKY46, from tartary buckwheat improves salt tolerance in transgenic arabidopsis thaliana. *Plant Physiol. Biochem.* 147, 43–53. doi: 10.1016/j.plaphy.2019.12.004

Ma, Y., Xie, Y., Ha, R., Cao, B., and Song, L. (2021). Effects of elevated CO_2 on photosynthetic accumulation, sucrose metabolism-related enzymes, and genes

identification in goji berry (*Lycium barbarum* l.). *Front. Plant Sci.* 12. doi: 10.3389/fpls.2021.643555

Marowa, P., Ding, A., and Kong, Y. (2016). Expansins: roles in plant growth and potential applications in crop improvement. *Plant Cell Rep.* 35 (5), 949–965. doi: 10.1007/s00299-016-1948-4

Marowa, P., Ding, A., Xu, Z., and Kong, Y. (2020). Overexpression of *NtEXPA11* modulates plant growth and development and enhances stress tolerance in tobacco. *Plant Physiol. Biochem.* 151, 477–485. doi: 10.1016/j.plaphy.2020.03.033

Mohammed, H. A., Ali, H. M., Qureshi, K. A., Alsharidah, M., Kandil, Y. I., Said, R., et al. (2021). Comparative phytochemical profile and biological activity of four major medicinal halophytes from qassim flora. *Plants (Basel)* 10 (10), 2208. doi: 10.3390/plants10102208

Moll, S., Anke, S., Kahmann, U., Hänsch, R., Hartmann, T., and Ober, D. (2002). Cell-specific expression of homospermidine synthase, the entry enzyme of the pyrrolizidine alkaloid pathway in Senecio vernalis, in comparison with its ancestor, deoxyhypusine synthase. *Plant Physiol.* 130 (1), 47–57. doi: 10.1104/pp.004259.

Mu, Q., Li, X., Luo, J., Pan, Q., Li, Y., and Gu, T. (2021). Characterization of expansin genes and their transcriptional regulation by histone modifications in strawberry. *Planta* 254 (2), 21. doi: 10.1007/s00425-021-03665-6

Navarro, A., Bañón, S., Olmos, E., and Sánchez-Blanco, M. J. (2007). Effects of sodium chloride on water potential components, hydraulic conductivity, gas exchange and leaf ultrastructure of arbutus unedo plants. *Plant Sci.* 172, 473–480. doi: 10.1016/j.plantsci.2006.10.006

Neves-Piestun, B. G., and Bernstein, N. (2001). Salinity-induced inhibition of leaf elongation in maize is not mediated by changes in cell wall acidification capacity. *Plant Physiol.* 32 (2), 141–152. doi: 10.1104/pp.125.3.1419

Palchetti, M. V., Reginato, M., Llanes, A., Hornbacher, J., Papenbrock, J., Barboza, G. E., et al. (2021). New insights into the salt tolerance of the extreme halophytic species *Lycium humile* (Lycieae, solanaceae). *Plant Physiol. Biochem.* 163, 166–177. doi: 10.1016/j.plaphy.2021.03.054

Polak, M., and Karcz, W. (2021). Some new methodological and conceptual aspects of the "Acid growth theory" for the auxin action in maize (*Zea mays* l.) coleoptile segments: Do acid- and auxin-induced rapid growth differ in their mechanisms. *Int. J. Mol. Sci.* 22 (5), 2317. doi: 10.3390/ijms22052317

Qin, C., Ahanger, M. A., Lin, B., Huang, Z., Zhou, J., Ahmed, N., et al. (2021). Comparative transcriptome analysis reveals the regulatory effects of acetylcholine on salt tolerance of nicotiana benthamiana. *Phytochemistry* 181, 112582. doi: 10.1016/j.phytochem.2020.112582

Rayle, D. L., and Cleland, R. (1970). Enhancement of wall loosening and elongation by acid solutions. *Plant Physiol.* 46 (2), 250–253. doi: 10.1104/pp.46.2.250

Sampedro, J., and Cosgrove, D. J. (2005). The expansin superfamily. *Genome Biol.* 6 (12), 242. doi: 10.1186/gb-2005-6-12-242

Santiago, T. R., Pereira, V. M., de Souza, W. R., Steindorff, A. S., Cunha, B. A. D. B., Gaspar, M., et al. (2018). Genome-wide identification, characterization and expression profile analysis of expansins gene family in sugarcane (*Saccharum* spp.). *PLoS One.* 13 (1), e0191081. doi: 10.1371/journal.pone.0191081.

Shen, Z., Cheng, X., Li, X., Deng, X., Dong, X., Wang, S., et al. (2022). Effects of silicon application on leaf structure and physiological characteristics of glycyrrhiza uralensis fisch. and glycyrrhiza inflata bat. under salt treatment. *BMC Plant Biol.* 22 (1), 390. doi: 10.1186/s12870-022-03783-7

Spartz, A. K., Lor, V. S., Ren, H., Olszewski, N. E., Miller, N. D., Wu, G., et al. (2016). Constitutive expression of arabidopsis SMALL AUXIN UP RNA19 (SAUR19) in tomato confers auxin-independent hypocotyl elongation. *Plant Physiol.* 173 (2), 1453–1462. doi: 10.1104/pp.16.01514

Tang, X. L., Mu, X. M., Shao, H. B., Wang, H. Y., and Brestic, M. (2015). Global plant-responding mechanisms to salt stress: Physiological and molecular levels and implications in biotechnology. *Crit. Rev. Biotechnol.* 35 (4), 425–437. doi: 10.3109/07388551.2014.889080

Turner, S., and Kumar, M. (2018). Cellulose synthase complex organization and cellulose microfibril structure. *Philos. Trans. A Math Phys. Eng. Sci.* 376 (2112). doi: 10.1098/rsta.2017.0048

Valenzuela-Riffo, F., Parra-Palma, C., Ramos, P., and Morales-Quintana, L. (2020). Molecular and structural insights into *FaEXPA5*, an alpha-expansin protein related with cell wall disassembly during ripening of strawberry fruit. *Plant Physiol. Biochem.* 154, 581–589. doi: 10.1016/j.plaphy.2020.06.010

Wang, Y.-H., Que, F., Wang, G.-L., Hao, J.-N., Li, T., Xu, Z.-S., et al. (2019). iTRAQ-based quantitative proteomics and transcriptomics provide insights into the importance of expansins during root development in carrot. *Front. Genet.* 10. doi: 10.3389/fgene.2019.00247

Wei, P.-C., Zhang, X.-Q., Zhao, P., and Wang, X.-C. (2011). Regulation of stomatal opening by the guard cell expansin *AtEXPA1*. *Plant Signaling Behavior.* 6 (5), 740–742. doi: 10.4161/psb.6.5.15144

Yan, Y., Sun, M., Li, Y., Wang, J., He, C., and Yu, X. (2020). The CsGPA1-CsAQPs module is essential for salt tolerance of cucumb er seedlings. *Plant Cell Rep.* 39 (10), 1301–1316. doi: 10.1007/s00299-020-02565-5

Yuan, H. J., Liu, K., Wang, C. M., Xie, H. C., Li, H. J., and Jia, H. Z. (2016). The differences between two cultivars of lycium barbarum in osmotic stress tolerance and salt tolerance. *Pratacultural Sci.* 10 (4), 681–690. doi: 10.11829/j.issn 1001-0629. 2015-0526

Yuan, Y. H., Zhong, M., Shu, S., Du, N. S., He, L. Z., Yuan, L. Y., et al. (2015). Effects of exogenous putrescine on leaf anatomy and carbohydrate metabolism in cucumber (*Cucumis sativus* l.) under salt stress. *J. Plant Growth Regulation.* 34, 451–464. doi: 10.1007/s00344-015-9480-2

Zeng, F., Shabala, S., Maksimović, J. D., Maksimović, V., Bonales-Alatorre, E., Shabala, L., et al. (2018). Revealing mechanisms of salinity tissue tolerance in succulent halophytes: A case study for carpobrotus rossi. *Plant Cell Environ.* 41 (11), 2654–2667. doi: 10.1111/pce.13391

Zhao, S. S., Zhang, Q. K., Liu, M. Y., Zhou, H. P., Ma, C. L., and Wang, P. P. (2021). Regulation of plant responses to salt stress. *Int. J. Mol. Sci.* 22 (9), 4609. doi: 10.3390/ijms22094609

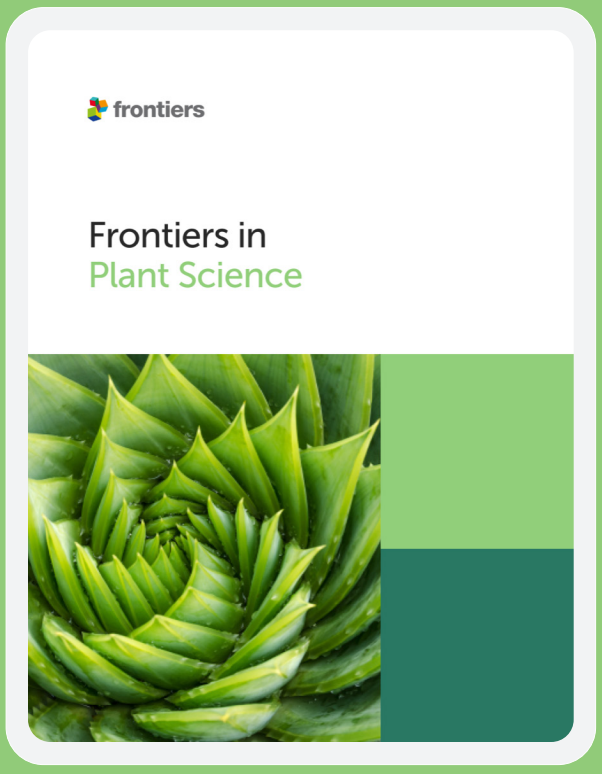
Frontiers in
Plant Science

Cultivates the science of plant biology and its applications

The most cited plant science journal, which advances our understanding of plant biology for sustainable food security, functional ecosystems and human health.

Discover the latest Research Topics

See more →



Frontiers

Avenue du Tribunal-Fédéral 34
1005 Lausanne, Switzerland
frontiersin.org

Contact us

+41 (0)21 510 17 00
frontiersin.org/about/contact